

New Technologies for Urban Safety of Mega Cities in Asia

*9-10 December 2007
Dhaka, Bangladesh*

Edited by

*Mehedi Ahmed Ansari
and
Kawin Worakanchana*

Co-Organized by

*Bangladesh Network Office for Urban Safety (BNUS),
BUET, Dhaka, Bangladesh*

&

*International Center for Urban Safety Engineering (ICUS)
Institute of Industrial Science
The University of Tokyo, Japan*

NEW TECHNOLOGIES FOR URBAN SAFETY OF MEGA CITIES IN ASIA

MEHIDI AHMED ANSARY
Chairman Organizing Committee
USMCA2007

ICUS Report No 27, April, 2008

PREFACE

In almost all Mega Cities in Asia, due to the rapid economic growth and development, many high-rise buildings and complex infrastructure systems have been constructed in recent decades. Of prime concern is the high concentration of population, haphazard land development and commercial activities taking place in these cities. Other critical issues that are associated with the rapid urbanization include: environmental problems, supply of water, gas and power, sanitation, transportation, etc. It is therefore reasonable to postulate that the consequences of even a moderate level of natural event in the form of cyclone, earthquake, torrential flood, tornado, tsunami, etc. may be enormous in these cities. For instance, the recent Sumatra Earthquake and associated tsunami of December 2004 and October 2005 Kashmir Earthquake caused severe damage and a massive loss of life in the region. Urban safety of mega cities in Asia has therefore naturally become a prime concern for the architects, engineers, planners and policymakers. It also poses a real challenge to them alike due to its multi-dimensional nature, which covers areas from structural design, maintenance and rehabilitation to disaster mitigation and risk assessment.

Recent development of various advanced technologies has provided motivation to focus on devising new methodologies for sustainable development of Asian mega cities with adequate safety and security. With this realization and recognition of the importance of using advanced tools in urban safety, the International Centre for Urban Safety Engineering was established at the Institute of Industrial Science, The University of Tokyo, and has taken the lead in organizing this series of symposia in the Asian region. After the successful completion of the earlier symposia in Thailand, Japan, India, Singapore and again in Thailand in 2002, 2003, 2004, 2005 and 2006, respectively, the present sixth symposium is being jointly organized by BNUS, BUET, Bangladesh and ICUS, IIS, The University of Tokyo, Japan. The symposium is sponsored by the Foundation for the Promotion of Industrial Science, Japan, Center of Excellence, The University of Tokyo and CEGIS, Bangladesh. It is also nominally supported by the Embassy of Japan, Bangladesh.

Focus of this symposium is to help local and regional officials and experts involved in safety and security practice to enhance their knowledge by effectively disseminating information on new technologies for urban safety. It will provide a platform for developing and strengthening a network among the Asian researchers and practitioners for future collaboration in diverse areas related to urban safety. To accomplish these objectives, the symposium will have two keynote sessions and ten parallel sessions on *Safety Assessment and Monitoring of Existing Infrastructure, Advanced Technologies for Assessment of Urban Safety, Maintenance, Retrofitting and Rehabilitation of Structures, Design and Assessment of Structures for Seismic, and Impact Loads, Disaster Management, Tsunamis, Flood and Environmental Risk Assessment and Urban Road Safety*. These sessions will present more than seventy technical papers including two keynote and five plenary papers.

I would like to take this opportunity to thank the Steering, Technical and Organizing Committees as well as the Symposium Secretariat and ICUS staffs for their time and effort in putting this symposium together. Special thanks are due to the authors of technical papers, participants and all others who took time out of their schedules to contribute to the success of this symposium. I would also like to thank the sponsors for their generous support and contribution.

Table of Contents

	<i>Page</i>
Opening Session	
SECTION 1 Keynote Lectures	
The World Seismic Safety Initiative-What We Do and Do not Do? <i>(Keynote Lecture)</i> <i>Tsuneo Katayama</i>	1
Forensic Diagnosis of Underwater Slope failure in Jamuna River <i>(Keynote Lecture)</i> <i>Kenji Ishihara, Yoshimichi Tsukamoto</i>	11
Distress in the Tarmac at Newly Opened Suvarnabhumi Airport <i>(Keynote Lecture)</i> <i>Worsak Kanok-Nukulchai</i>	41
Safety Problems Related to Deterioration of Concrete Structures <i>(Keynote Lecture)</i> <i>Taketo Uomoto</i>	51
Proposal of a Sustainable Tsunami Disaster Mitigation System for the Indian Ocean Region <i>(Keynote Lecture)</i> <i>Kimiro Meguro, Masasuke Takashima</i>	61
Technical Sessions	
SECTION 2 Safety Assessment and Monitoring of Existing Infrastructure 1	
Digital Chi-Chi City on Google Earth as Post-Earthquake Recovery Digital Archive <i>Osamu Murao, Atsushi Miyamoto</i>	67
Visual Screening Methods for Earthquake Vulnerability Assessment <i>A. B. Afifa Imtiaz, Mahfuza Shamim, Ashutosh Sutra Dhar, Mehedi Ahmed Ansary, Mohammad Zobair, Md. Zakaria Ahmad</i>	79
Numerical and Experimental Study of Structures with Soft Stories <i>Himadree Roy, Iftekhar Anam</i>	91
Seismic Vulnerability Assessment of RC Building of Dhaka City <i>Mohammad Sajedul Hug, Mohammad Rafat Sadat, Mohammad Salahuddin Rizvi, Md. Nafiul Haque, Mehedi Ahmed Ansary</i>	103
Assessment of Cyclone Shelters in Cox's Bazar against Earthquake Hazard <i>Rajan Saha, Ashutosh Sutradhar, Mehedi Ahmed Ansary</i>	113
Partially Encased Composite Columns: An Innovative Composite Structural System <i>Mahbuba Begum</i>	127

SECTION 3 Advanced Technologies for Assessment of Urban Safety 1

A Study on Effect of Land-Use Control along Active Faults in Japan <i>Miho Yoshimura Ohara, Kimiro Meguro</i>	139
Application of Geophysical Imaging in Subsurface Characterization for Urban Safety from Earthquake – A Case Study from Dhaka Mega City, Bangladesh <i>Aftab Alam Khan, Muhammad Shahadat Hossain</i>	147
Estimation of Risk Due to Earthquake Hazard in Ap, India an it Based Approach <i>Md. Ziya Ur Rahman Siddiqui, Ranjeet Joshi, Ramancharla Pradeep Kumar</i>	161
Model Test measuring Earth Pressure Acting on Buried Structure Due to Differential Settlement <i>Reiko Kuwano, Toshiyuki Horii, Hidetoshi Kohashi</i>	173
Landslide Hazard Aalysis for Urban Areas Using Raster Data Set <i>Md. Zahid Hasan Siddiquee, Monsur Ahmed, Rubel Das</i>	183
Seismic Microzonation of Cox’s Bazar Bangladesh <i>A. B. Afifa Imtiaz, Mehedi Ahmed Ansary, Ashutosh Sutra Dhar</i>	191

SECTION 4 Maintenance, Retrofitting and Rehabilitation of Structures

Influence of Re-curing Condition on Damage and Recovery of Mortar Exposed to Fire <i>Michael Henry, Yoshitaka Kato</i>	201
Strategic Maintenance of Port and Harbor Concrete Structures Based on Life-Cycle Management <i>Hiroshi Yokota, Mitsuyasu Iwanami, Toru Yamaji, Ema Kato</i>	211
Variation of Corrosion Characterization of Reinforcing Bar in Existing RC Structure <i>Ema Kato, Mitsuyasu Iwanami, Hiroshi Yokota, Takumi Shimomura</i>	221
Evaluation of the Seismic Vulnerability of Bangladeshi RC Building using Non-Destructive Testing <i>Syed Zillur Rahman, Mehedi Ahmed Ansary, MA Noor, Rajan Saha, Hisashi Kanada, Miho Yoshimura, Kimiro Meguro, Taketo Uomoto</i>	231
Ductility of Concrete Structures with Lateral Confinement and Compression Reinforcement <i>Md. Shah Aziz Akand, Iftekhar Anam</i>	243

SECTION 5 Design and Assessment of Structures for Seismic and Impact Loads

Residual Seismic Capacity Estimation of RC Frames with Unreinforced Concrete Block Infill <i>Ho Choi, Yoshiaki Nakano</i>	253
The Effect of Infills on the Dynamic Behavior of RC Frames <i>Samy Muhammad Reza, Raquib Ahsan, Mehedi Ahmed Ansary</i>	265

Analysis of Axial Vibration of Piles in Layered Soil and Application to Batter Pile Foundations	275
<i>Raquib Ahsan, Jorgen Johansen, Kazuo Konagai, Hidetaki Tanaka</i>	
Seismic Assessment of Pile Founded Khilgaon Flyover Mahbuba Begum	287
<i>Mohammad Moslem Uddin, Mehedi A. Ansary, Tahsin R. Hossain, Munaz A. Noor</i>	
Proposal of a Methodology to Design PP-band Meshes to Retrofit Low Earthquake Resistant Unreinforced Masonry Houses	297
<i>Paola Mayorca, Kimiro Meguro</i>	
Modeling Nonlinear Stress-Strain Relations of Materials	307
<i>Md. Raquibul Hossain, Mohammed Saiful Alam Siddiquee, Syed Ishtiaq Ahmed</i>	

SECTION 6 Disaster Management 1

Enhancement on Disaster Prevention and Mitigation in Kaohsiung City	311
<i>Tai-Ping Chang</i>	
Models of a Technical Platform for Emergency Management	321
<i>Weng Wenguo</i>	
The State-of-the-Art of Information Technology on Disaster Prevention and Mitigation in Taiwan Urban Area	333
<i>Kai-Lin Hsu</i>	
Experimental Study of Fire Propagation in a Compartment with Different Approaching Wind Conditions	343
<i>Hong Huang, Ryoza Ooka, Naian Liu, Linhe Zhang, Zhihua Deng, Shinsuke Kato</i>	

SECTION 7 Tsunamis, Flood and Environmental Risk Assessment

Protective Measures of Flood Embankment along the Jamura River in Bangladesh	357
<i>Md. Musur Rahman, Mohammad Asad Hussain, Md. Motaher Hossain, Maminul Haque Sarker and Mohammad Nazim Uddin</i>	
Developing an Universal Water Resource Assessment Model for Sustainable Water Security	367
<i>Akiyuki Kawasaki, Srikantha Herath, Kimiro Meguro</i>	
Application of Remote sensing and GIS techniques in Water induced Disaster Management: A case Study of Bangladesh	375
<i>Md. Shahabul Islam, Md. Mafizur Rahman, Kul Prathuchai</i>	
Climatic Perturbation and Flood Risk in Coastal Cities: A Comparative Study in South and South East Asia	385
<i>Dushmanta Dutta</i>	
Spontaneous Urbanization of Dhaka City and Water Logging as a Consequence	397
<i>Umma Tamima, Md. Sohel Reza Amin</i>	

SECTION 8 Advanced Technologies for Assessment of Urban Safety 2

- Study on the Potential of Tree Shape Classification by Using the Simulated LIDAR Data and a Tree Crown Model** 409
Takahiro Endo, Yoshifumi Yasuoka
- LIDAR: A Technology of New Era** 417
Mohammad Abdul Quader, MD. Zahid Hasan Siddiquee, Ruble Das
- Management of Building Energy Consumption and Renewable Energy Supply in the Ecological Communities Using GIS** 425
Md. Zahid Hassan Siddiquee, Ursula Eicker, Dietrich Schroder
- Comparative Analysis and Monitoring of Urban Heat Island Intensity in Asian Mega Cities by MODIS** 435
Wataru Takeuchi, Kawin Worakanchana, Yoshifumi Yasuoka, Vibarad Phonekeo
- Numerical Simulation of Atmospheric Pollution over Kanto area using the MM5/CMAQ Model “Simulation of Ozone Concentration between Two Different Weather Days”** 441
M. V. Khiem, H. Hayami, H. Huang, R. Ooka

SECTION 9 Safety Assessment and Monitoring of Existing Infrastructure 2

- Automatic and Real-Time Bridge Health Monitoring for Heavy Traffic Routes** 453
Sanae Miyazaki, Yuji Ishikawa, Takahide Okubo, Kimihiko Izumi, Eiichi Sasaki, Chitoshi Miki
- 3-D Applied Element Method for PP-Band Retrofitted Masonry** 461
Worakanchan Kawin, Paola Mayoca, Ramesh Guragain, Sathiparan Navaratnaraj, Kimiro Meguro
- Structural Health Assessment of Infrastructure: The Bangladesh Perspective** 473
Rais Ahmad, M. Kabirul Islam, M. Zakaria Ahmed, Tribikram Kundu
- Investigation for Promoting Seismic Retrofit of Critical Facilities-A Case Study of Wakayama City** 483
R Amano, Takeyuki Ebi, SShogo Hayashi, Kimiro Meguro, Kouji Uematsu, Kazuhisa Fujita
- Fragility Analysis of Reinforced Concrete Frame Structures** 499
MA Noor and M Yasin
- Flood in Bangladesh with Focuses on 2007 Flood** 509
Md. Aynual Kabir

SECTION 10 Disaster Management 2

- A Study for Improving Total Disaster Reduction Ability of Nursery Schools and Kindergartens** 521
Mariko Abe, Kimiro Meguro

School Earthquake Safety Program (SESP) in Old Dhaka, Bangladesh <i>Israt Jahan, Mehedi Ahmed Ansary</i>	529
Vulnerability Risk Areas of Bangladesh due to Multiple Natural Hazards <i>M.S. Akther, Mehedi Ahmed Ansary</i>	541
Proposal of Intensity Scales for Different Natural Hazards in Bangladesh <i>M.S. Akther, Mehedi Ahmed Ansary</i>	555
Some Emerging Hazards in Metropolitan Cities of Bangladesh <i>KM Maniruzzaman, MA Rahman</i>	573
Earthquake Preparedness Helps to Combat Urban Disasters <i>Wahida Bashir Ahmed</i>	579
Earthquake preparedness Combined with Community Efforts <i>Md. Faiz Shah</i>	585
Socio-Economic and Environmental Aspects of Disaster Risk Reduction Management for Sustainable Development in Bangladesh <i>Murshed Ahmed</i>	591

SECTION 11 Urban Road Safety

Urban Road Safety: Effective Rescue of Accident Victims Using GIS Technology <i>Md Mazharul Hoque, Kazi Md Shifun Newaz, S M Sohel Mahmud, Sabreena Anowar Armana Sabiha Hung</i>	607
Comparative Analysis of On-Street Parking Management Practices in Different Countries <i>Shinji Tanaka, Masao Kuwahara</i>	621
Public Transport in Bangkok: A Case of the Passenger Vans <i>Shinya Hanoka, Supaporn Kaewko Leopairojna</i>	631
Evaluation of Effectiveness of Pedestrian Overpasses in Dhaka Metropolitan <i>Md. Mizanur Rahman, Muhammad Ashikul Islam, Md. Kamrul Hasan Rizvi</i>	643
Road Traffic Accidents and Injuries: A Serious Safety Concern in Urban Areas of Bangladesh <i>Md. Mazharul Hoque, Chowdhury Kawsar Arefin Siddiqui, Tahera Anjuman, Sabreena Anowar, Shahnewaz Hasanat-E-Rabbi</i>	653

Photograph



USMCA2007 Group Photo



Welcome board



Registration



ICUS booth at symposium



Opening ceremony



Prof. J. R. Choudhury



Prof. A. M. M. Safiullah



HE Masayuki Inoue



Prof. Mehedi A. Ansary



Mourning ceremony



Prof. Tsuneo Katayama



Prof. Kimiro Meguro



Mr. Tapan Chowdhury



Prof. Kenji Ishihara



Prof. Worsak Kanok-Nukulchai



*Signing MOU Ceremony
between ICUS and AIT*



Dr. Ryozo Ooka



Dr. Yoshitaka Kato



Banquet



Banquet



Banquet



Prof. Hiroshi Yokota



Dr. Wataru Takeuchi



Dr. Ema Kato



Young-researcher-award awardees



BNUS office in BUET



Delegates from symposium visiting civil engineering department at BUET



Delegates from symposium visiting BUET



Group Photo at BUET

Opening Session

THE WORLD SEISMIC SAFETY INITIATIVE – WHAT WE DO AND DO NOT DO

TSUNEO KATAYAMA
Tokyo Denki University, Tokyo, Japan
katayama@cck.dendai.ac.jp

ABSTRACT

The World Seismic Safety Initiative (WSSI) was established in 1992 following the decisions made by the International Association for Earthquake Engineering (IAEE) during the 10th World Conference on Earthquake Engineering (10WCEE) in Madrid in support of the United Nations' "International Decade for Natural Disaster Reduction (IDNDR)." IDNDR was a brainchild of earthquake engineering professionals, because its original concept was presented in 1984 by Dr. Frank Press in his Keynote Speech during 7WCEE in San Francisco.

Although IAEE endorsed the idea and recommended its prompt implementation, there had been difficulties for IAEE to take any definite actions because of its structural weakness. The proposal of the Decade, however, gained the attention of academic institutions and associations worldwide, and, in December 1987, a United Nations (UN) General Assembly Resolution declared the 1990's as the UN's IDNDR (1990-2000) to promote internationally coordinated efforts to reduce losses caused by natural disasters, especially in developing countries.

WSSI was incorporated in Singapore in May 1995 as a non-profit public benefit company, and is operated by its international Board of 15 Directors. Since its foundation, WSSI has been actively working to make concrete measures to mitigate losses caused by earthquakes especially in the Asian developing region. WSSI tries to make visible outcomes, however small they may be, because disasters respect our actions, not our words.

WSSI holds High Level Meetings to help raise public and government awareness of earthquake risk in the decision-making sector. We carry out a project to facilitate the redistribution of seismometers to be replaced in the U.S. to developing countries. Awards have so far been given to Armenia, India, China (2 places), and Bangladesh with a total number of about 400 such seismometers.

WSSI is not a funding agency. WSSI tries to trigger local high efforts, build on and encourage local resources, and to help identify and prioritize local actions. We also attempt to assist in adding credibility to local efforts.

1. PRE-HISTORY

More than 20 years have passed since we heard Frank Press' keynote address in San Francisco during the eighth World Conference on Earthquake Engineering (8WCEE) in 1984. He proposed in his speech an idea of establishing the International Decade for Hazard Reduction in which all nations join forces to reduce the consequences of natural disasters. He emphasized what better way to start the new millennium than a world better organized to reduce suffering from natural disasters.

Researchers are often simple-minded. IAEE endorsed the idea and recommended its prompt implementation without realizing difficulties to be met once the idea would materialize. During the following four years until earthquake engineers met again in Japan for the WCEE, no progress or any efforts to make progresses had been made among earthquake engineers and scientists.

The biggest change for me, however, was that I had been appointed to be Secretary General of IAEE. The International Decade for Natural Disaster Reduction (IDNDR) was to be inaugurated in 1990 as an official UN project. We knew that IDNDR was our brainchild. IAEE again adopted a resolution, and urged Secretary General to take some actions to support this very worthy project. All that IAEE did, however, was to establish a small IDNDR committee. People often ironically say there is no crisis to which academics will not respond with a committee or a workshop.

The IAEE was established in 1963 to promote international cooperation among scientists and engineers in the field of earthquake engineers with its Central Office in Japan. The members of IAEE are national or regional organizations. There are about 55 members in the Association. Although IAEE is very visible through the World Conference on Earthquake Engineering (WCEE) held every four years, its administration is not well organized, and until very recently there were no dues for member countries. The WCEE is held by the sole responsibility of its inviting member country. Most of important businesses are managed through the General Assembly of Delegates and the Executive Committee Meeting, both held during WCEE.

Creation of the committee turned out to be only superficial, and it took three years to organize a small meeting in Tokyo in October 1991. The meeting was an occasion of harsh self examination. The meeting resolved that IAEE should make any structural changes that will facilitate its ability to promote the earthquake engineering program for the Decade, and that it should prepare a working paper on the IAEE's role in the Decade so that discussions would be made during 10WCEE scheduled in Madrid in 1992.

The 10th WCEE was held in Madrid in July 1992. During this Conference, it was everybody understands that, unless a special initiative is established with the capacity of gathering people and funds, the possibility for IAEE to have a significant impact on IDNDR was remote. IAEE

decided to form the World Seismic Safety Initiative (WSSI) as a new undertaking of IAEE in support of IDNDR with the goals to disseminate state-of-the-art earthquake engineering information throughout the world, to incorporate experience and research findings into recommended practices and codes in earthquake-prone countries, and to advance engineering knowledge through problem-focused research. Our understanding is that disasters respect our actions, not our words. The first Board of Directors Meeting of WSSI was held in Tokyo in September, 1993.

WSSI was incorporated in Singapore in May 1995 as a non-profit public benefit company under the name, "World Seismic Safety Initiative Ltd." Incorporation was necessary for liability and fund-raising reasons. The non-profit terms of incorporation are favorable to tax status. As of October 2007, WSSI is operated by its international Board of 15 Directors. Seven Directors are from Asia, 4 from North America, 2 from New Zealand, and 2 from Europe. The present Chairman is Haresh C. Shah. The Directors meet in Singapore at least once a year.

2. BANGKOK WORKSHOPS

In January 1993, the Scientific and Technical Committee (STC) of IDNDR was held in New Delhi, India. Prof. Shah and Katayama attended this meeting and proposed WSSI as a new IDNDR project. WSSI was officially approved as an International and Regional IDNDR project.

Immediately following the STC in India, WSSI held a workshop, "Seismic Risk Management for Countries of the Asia Pacific Region" in early February 1993 in Bangkok as its first initiative. The Asia Pacific region historically has experienced extensive economic and human losses from earthquakes (You only have to remember the recent damaging earthquakes in Iran and Pakistan, and the devastating Tsunamis in the Indian Ocean.) The region in recent decades, however, has been going through major urbanization and economic development.

It was thought, therefore, most appropriate for WSSI to compile a status of earthquake mitigation policies and plans in place in the countries of the Asia Pacific region. We invited about 30 participants from 19 countries to a golf club in a suburb of Bangkok. Participants from developing countries were invited. There were participants from such countries as Bangladesh, Brunei, Malaysia, Myanmar, Nepal, Pakistan, Thailand, and Vietnam. Undisturbed by the noise from the city of Bangkok, all of us freely and sincerely discussed the dilemma we faced. The challenge was to find the right combinations of actions that would mitigate the earthquake risk through integrated strategy, consistent with the available resources of these countries and aspirations of their citizens.

This first modest but definitive step of WSSI turned out to be a great success beyond any expectations. We strongly felt that WSSI was not going

to be another paper organization, and that we could make a dent in managing earthquake risk in developing countries.

Participants reported on the state-of-the-art in earthquake engineering in their countries. They commented on how the available knowledge is used or not used in developing earthquake disaster mitigation strategies. They requested WSSI to help raise public and government awareness of earthquake risk in the decision-making sector, in particular. Towards this objective, WSSI recognized the importance of holding High Level Meetings to be attended by government officials, business leaders, people from social and cultural institutions, as well as the mass media.

The greatest asset from the Bangkok Workshop is the feeling of partnership we cultivated among all the participants from developed and developing countries in the field of earthquake disaster mitigation science. Whenever we face hardship in managing WSSI, we remember the Bangkok Workshop and the colleagues who have the common goal to mitigate the earthquake calamity.

Two follow-up workshops were held in Bangkok approximately every 5 years to review what effects WSSI had made since the first workshop in 1993. Each of the 3-day workshops cost about 35,000 US\$ including air fares and accommodation for all the participants from developing countries.

3. HIGH LEVEL MEETINGS

WSSI has so far held more than ten High Level Meetings (HLM) in such cities as Kuala Lumpur (Malaysia), Singapore, Kathmandu (Nepal), Dhaka (Bangladesh), Colombo (Sri Lanka), Yangon (Myanmar), Hanoi (Vietnam), Kampala (Uganda), and Ulaanbaatar (Mongolia). HLM has become the most important activity of WSSI. It, however, is a long-ranged educational project in which short-term outcomes are difficult to expect.

One-day lecture meeting for a wider audience interested in disaster problems usually accompanies an HLM. In the case of the HLM held in Kampala (Uganda), in December 1997, the President of Uganda delivered a keynote speech to more than 300 professionals, and promised the government's commitment to provide increased resources.

Preparation of HLM is made by local hosts, and WSSI Directors and resource person(s) attend it with their own funds. Past experiences have clearly indicated that good partnership and strong personal ties between the local hosts and WSSI are always essential for a successful HLM.

I remember the Myanmar HLM in 1996 which turned out to be an absolute failure. A participant from Myanmar in the first (1993) Bangkok Workshop requested WSSI to hold an HLM in Yangon while both of us were in Bangkok. Myanmar was not an easy country to visit in those days.

We could not get through to a person we wanted to talk on the phone. Answers to our faxes were hard to come. It was impossible to adequately prepare the meeting at all. But we were optimistic, because we had successfully held six HLM's by then. We thought that things should go well once we were there.

When we arrived at the country, however, we found nothing had been prepared for the HLM and there was no person to talk to. We visited, one by one, a university, the national railway company, and several other disaster-related organizations. Nobody knew about WSSI nor showed any interest in earthquake disaster mitigation in Myanmar. But when we left the country, we were still optimistic. Our friend from the Bangkok Workshop came to see us on the morning of our departure to tell us that the next time should be different.

And the "next" time came soon. During our first visit, we found that there were only few seismologists and earthquake engineers in the country, and that there was almost no strong-motion seismometer in Myanmar. With the assistance of a Japanese geotechnical consulting firm, WSSI donated several strong-motion seismometers. Also through the same company, WSSI invited two scientists to Japan to teach how to handle the instruments. As the result of these and other continued grass roots efforts, we received in 1999 an official invitation from Myanmar to hold an HLM and a special lecture meeting there.

Following this invitation, in February 2003, a group of 7 WSSI-related volunteers from 5 countries traveled to Myanmar to present an introductory course on earthquake engineering and to encourage Myanmar to develop a university program for earthquake engineering as well as an earthquake resistant design code. The course was a collaborative effort between WSSI and the government of Myanmar, and attended by more than 30 engineers and scientists. Before the course started, Minister for Transport welcomed WSSI members to Yangon. He made a speech about the recent developments in Myanmar, stating how grateful he was for the WSSI visit.

The timing of the course was appropriate since Myanmar at that time was considering allowing construction of buildings considerably taller than 10 stories and there was governmental concern about the earthquake resistance of these structures. They had established the Myanmar Earthquake Society. Resolutions involving a discussion about the best way to further develop earthquake engineering in Myanmar were made and voted on. It was decided that a building design code should be written first since building design, and commercial development using buildings, are often controlled by private industry. If a design code for buildings can be developed and building regulations can be enforced, then it should be relatively easy to develop enforceable codes for other structures over which government control is likely to be stronger.

A workshop with an emphasis on geophysics and faults in Myanmar was held in Yangon in early 2007. It was found that a building code was being written. A longer course on earthquake engineering was being planned to be given by one of the WSSI Directors, but it had to be postponed because of the recent political turmoil in the country. The experiences with Myanmar have taught us many things, especially the importance of the continued grass roots efforts in the international cooperation.

4. THE POLICY OF WSSI REGARDING FUTURE HLM

When we held the 12th WSSI Board of Director's Meeting in Singapore in December 1999, IDNDR was almost coming to an end in year 2000. We, however, decided to continue the activities within WSSI beyond year 2000, and adopted an official policy of HLM based on the past experiences. It, however, was thought necessary for WSSI to define more objectively the roles of the HLM for future. This was especially important because our resources are extremely limited.

The objectives to be achieved by HLM's were summarized as follows:

- To trigger local high level efforts,
 - To build on and encourage local resources,
 - To sensitize people, professionals, administrators and politicians,
 - To help identify and prioritize local actions,
 - To assist in developing local sustainability through local efforts,
 - To assist in adding credibility to local efforts,
 - To assist in local efforts in fund raising activities, and
 - To assist in national networking.

Priority should be given to situations dominated by a combination of high seismic risk and low preparedness. More emphasis should be placed on the latter, and attention should also be given to countries with medium/low seismic risk but low preparedness. In order that precious time, energy and money will not be wasted, it may be necessary to seek dialogues between local people and WSSI before an HLM is planned.

Given the nature of a typical HLM, it should not be repeated in the same country. It should be understood that it usually takes time to achieve the goals set by WSSI, and it will not be appropriate to expect instant improvement after an HLM. It may be necessary for us to maintain a dialogue in order to encourage further local development. WSSI may help developing countries establish courses in earthquake engineering, disaster management, etc. to further increase the local awareness in earthquake disaster mitigation.

5. SAFER CITIES PROJECTS

Another successful and visible activity of WSSI is the Safer Cities Project. This is a joint initiative of WSSI and the COSMOS (Consortium of Organizations for Strong-Motion Observation Systems) of the U.S. The Safer Cities Project stands for Strong-motion Accelerographs For Earthquake Loss Reduction in Cities. The Project intends to benefit societies by redistributing unused strong-motion instrumentation to non-profit organizations for educational and nonprofit purposes in urbanized areas with few such instruments to record the next damaging earthquake.

Strong-motion seismometers in many of the COSMOS agency programs are being replaced with recent versions of instrumentation more suited to individual agency's need. The instrumentation being replaced is often in good working order, but no longer meets the requirements of the host agency. Towards extending their useful life, this project will facilitate their redistribution to developing countries. Awards have so far been given to Armenia, India, China (two areas), and Bangladesh with a total number of nearly 400 such seismometers.

The project provides instruments to acquire quantitative strong-motion measurements in buildings and on the ground in order to adequately rebuild damaged cities following major earthquake disasters and to initiate strong-motion measurement programs in urbanized areas in order that cities with high seismic risk might acquire critical recordings needed to reduce earthquake losses. It is hoped that such a project will stimulate awareness and action to mitigate earthquake hazards in densely urbanized regions throughout the world,

Transfer cost should be borne by the awarded organization, and instrumentation transferred under the signed agreement among WSSI, COSMOS, and the awarded organization shall be used for educational and non-profit purposes with no options for resale. Installation of instrument and a written report describing installations with maps of locations shall be provided within one year of receipt of instruments, and COSMOS is responsible for digitization of recorded data.

6. INTERDISCIPLINARY OBSERVATION OF THE 2001 BHUJ, GUJARAT, EARTHQUAKE

When we heard that the Bhuj earthquake had hit the northwest region of the State of Gujarat, India, on January 26, 2001, we all knew that, like many earthquakes in recent times, numerous academic, professional, and humanitarian organizations in developed countries would send teams of experts to study to publish reports which would focus individually on scientific, technical, economic and social issues. (This did take place in the case of the Indian Ocean Tsunamis.)

WSSI came up with an idea of assembling a unique reconnaissance team from developed and developing countries around the world with different interests and different professional backgrounds. A team of 21 members from 13 countries was sent to the site to conduct an eight-day trip visiting 11 cities/towns/villages in the hard-hit region.

This was the first experiment to look at the earthquake consequences as a learning process for many individuals from developing countries. Without such an experiment, many of the team members would not have been able to have the opportunity to be on the damaged site to see the technical, economic, scientific, social, and political forces that contributed to the death and destruction.

This has been a fascinating experiment and it has brought about a resounding success in terms of how we can raise awareness about earthquakes and their aftermath. The well-planned reconnaissance cost WSSI only 30,000 US\$ altogether, but it required huge efforts of voluntary work by some of the WSSI Directors and WSSI-related persons to realize it.

The reconnaissance culminated in a unique report beginning with the following sentences:

It is the dawn of the 51st Republic Day of India, January 26, 2001. Some 400 students with their teachers are marching toward the town hall of Anjar to participate in the flag hoisting ceremony in observance of the India Public Day. There is slight chill in the air on a clear and sunny morning, quite usual during the winter days. The students, future leaders of republic India, are marching through very narrow streets – perhaps less than 10-ft wide – of downtown Anjar, singing popular patriotic songs. The narrow streets are surrounded by 2-story stone/masonry buildings. Suddenly, the earth beneath them snaps, first making a loud noise as if a bomb went off, followed by violent ground shaking that lasts for over a minute. A cloud of dust arises making it difficult to see what has happened. When dust clears, the surrounding buildings are no more standing. The violent shaking of the earth has leveled them burying under its rubble the marching students and teachers, and some inhabitants of the buildings that have collapsed. Joyful singing turns into painful screams for help. Very few students and teachers escape injury or death; most of them perish, leaving their parents and loved ones behind. It is a sight that Anjar would not forget a very, very long time to come.

I have never read such moving sentences in any reconnaissance reports written by scientists from developed countries. The report of the team was well received worldwide. We believe that the make-up of the team, the purpose of the reconnaissance, and the unique and refreshing way of learning from this earthquake should become the standard under which future such efforts will be formulated. However, this has not realized in any

of the recent damaging earthquakes, and hundreds of similar reports are being published by groups of so-called experts from developed countries.

7. IMPORTANCE OF SMALL BUT WELL-FOCUSED PROJECTS

There are many local and international aid bureaucracies promoting the disaster risk reduction in developing countries. In many cases, those who benefit are the people involved in the preparation and implementation of aid projects. People in decision-making positions do not understand the importance of problems associated with natural disasters. They do not work closely with non-governmental organizations, but only with the national governments.

Disaster management projects in developing countries are often based only on imported technology and methods developed in industrialized countries. If there is not a proper adaptation of this technology to meet the local conditions and needs, the implementation of such projects results in misallocation of investments. In developing countries, regional data is not available, which is essential to make the imported methods effective. What developing countries need is not new technology but old well-tested technology that brings important benefits at low costs.

Large, expensive projects with very broad and general objectives only multiply an already growing bureaucracy and often result in a waste of time, money, and energy, rather than providing real solutions. It is better to establish small, realistic, well-focused projects that bring people from developed and developing countries to work together. Such small projects have better benefit-to-cost ratios than the expensive programs.

We are very glad that WSSI's efforts are producing some visible fruits in many places of the world. Countries such as Malaysia, Myanmar, Nepal, Pakistan, Singapore, Thailand, and Uganda have organized their national associations for earthquake engineering. They now are IAEE Member countries. A university in Sri Lanka has established a course in earthquake engineering to which WSSI donated a dynamic structural analysis computer-software. In Nepal, awareness for earthquake preparedness has been visibly raised, and a school building project has started with the corporation of a US-based non-profit organization. It was a pleasant surprise that Nepalese carpenters and bricklayers went to India to teach how to build earthquake resistant houses after the Bhuj earthquake. WSSI, with the help of a Japanese consulting firm, established a modest-sized network of strong-motion seismometers in Myanmar.

I personally believe that HLM's are the most important activity of WSSI. However, too much emphasis has so far been placed on Asian countries. Better geographical distribution should be sought in the future. Candidates may be those from island countries in the Pacific and the Caribbean Sea, and CIS (Commonwealth Independent States), those in the

Central Asia in particular. It is also important to critically review what has taken place after an HLM by holding a follow-up meeting.

As more people have come to know the name and the activities of WSSI, we need to have more systematized management. To continue HLM's on a stable basis, it is vital to decentralize the workload which has been so far concentrated to a few limited Directors. It may be necessary for WSSI to prepare a manual showing the process of preparing an HLM. At the same time, we should not ask too much to Directors because it may become a burden. After all, Directors work on their voluntary basis.

We know the problem is difficult. Every solution breeds new problems. We have always thought in the past that, when in doubt, jump! But, action should not be confused with haste. Energy and patience should be two indispensable elements in the future activities of WSSI.

FORENSIC DIAGNOSIS OF UNDERWATER SLOPE FAILURE IN JAMUNA RIVER

KENJI ISHIHARA

Professor, Research and Development Initiative
Chuo University, Japan
ke-ishi@po.ijnet.or.jp

YOSHIMICHI TSUKAMOTO

Associate Professor, Department of Civil Engineering
Tokyo University of Science, Japan
ytsoil@rs.noda.tus.ac.jp

ABSTRACT

When excavation was under progress by dredging through the sand bar deposit in Jamuna River in Bangladesh, a number of slips occurred underwater. Features of the slips are first described herein together with the results of in-situ investigations on the ground conditions. In the fluvial deposit in the Jamuna riverbed the sand is known to contain a few percent of mica mineral composed of plate-shaped grains. The inclusion of mica has been known to make the sand behave more strain-softening leading to increased vulnerability to flow type deformation. This was conceived to have been the cause of the underwater slides. To confirm this aspect, the sand was recovered from the river site and triaxial tests were performed in the laboratory extensively. The outcome of the test was compiled and arranged in a manner where the residual strength could be evaluated in a general framework of interpretation on sand behaviour. The results of the tests showed that the mica-containing sand from Jamuna River site exhibited contractive or strain-softening behaviour over a wide range of void ratio. The residual strength at the steady-state deformation obtained in the present test scheme was used to provide an explanation for the instability of the slopes in the light of what actually happened during the underwater excavation in Jamuna River.

When excavation was under progress by dredging through the sand bar deposit in Jamuna River in Bangladesh, a number of slips occurred underwater. Features of the slips are first described herein together with the results of in-situ investigations on the ground conditions. In the fluvial deposit in the Jamuna riverbed the sand is known to contain a few percent of mica mineral composed of plate-shaped grains. The inclusion of mica has been known to make the sand behave more strain-softening leading to increased vulnerability to flow type deformation. This was conceived to have been the cause of the underwater slides. To confirm this aspect, the sand was recovered from the river site and triaxial tests were performed in the laboratory extensively. The outcome of the test was compiled and arranged in a manner where the residual strength could be evaluated in a general framework of interpretation on sand behaviour. The results of the tests showed that the mica-containing sand from Jamuna River site

exhibited contractive or strain-softening behaviour over a wide range of void ratio. The residual strength at the steady-state deformation obtained in the present test scheme was used to provide an explanation for the instability of the slopes in the light of what actually happened during the underwater excavation in Jamuna River.

1. INTRODUCTION

The vast expanse of the flood plain in Jamuna River in Bangladesh has experienced volatile shifts of river course during the flood period. In a large project to construct a long bridge, it was considered necessary to protect the abutment of the bridge from scouring and erosion in which the level of the riverbed is purported to change by more than 10m overnight. In order to provide a countermeasure, excavation of underwater channels were executed by dredging from ships through the sand bar deposit. The aim was to reinforce the underwater slope with stones and geotextiles on the side of abutment. During the excavation, a number of slides took place underwater thereby inhibiting the operation of construction. In-situ investigations were carried out extensively by Dutch company and consultants and original design modified.

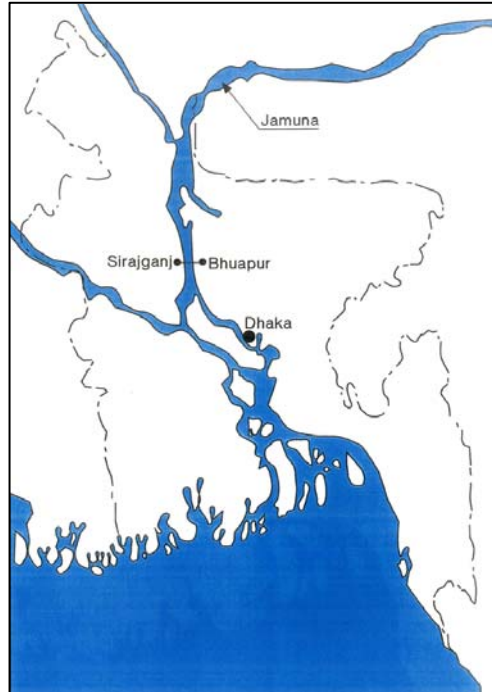
To clarify the cause of the slides, various kinds of investigations were carried out both in the field and in the laboratory. Although the causes were variously conceived, one of the points unanimously recognized was the fact that the fluvial sand deposit in Jamuna River contains a few percent of mica mineral exhibiting peculiar behaviour of deformation. In recognition of this, extensive studies were performed in the laboratory by Hight et al. (1999) and various factors such as anisotropic mode of deposition were addressed as possible causes leading to highly collapsible nature of the mica-containing sand. At the Tokyo University of Science, the scheme of laboratory studies had been underway regarding the steady-state deformation characteristics of sandy soils. Some of the results of tests were reported by Ishihara et al. (2003).

With an aim to examine behaviour of Jamuna River sand in terms of the framework established as above, a large amount of Jamuna River sand was shipped to Japan and multiple series of triaxial tests were performed to clarify the deformation characteristics of the sand. The results of the undrained triaxial compression and extension tests will be introduced in this paper within the framework of data arrangements and interpretation established thus far.

As a result of the studies, it was pointed out that the use of the major principal stress would be most appropriate to take into account effects of confinement on the residual strength of sand, and if based on this, there is no need to consider the effect of K_c -conditions at the initial stage of anisotropic consolidation. The outcome of these laboratory tests was incorporated into a simple analysis to examine the instability of the slopes observed in Jamuna River. The analysis targeted for the post-failure

conditions was performed based on the residual strength. The consequence of these studies will be described in the following pages.

2. PROJECT



In the middle reaches of the Jamuna River in Bangladesh, a 4km-long bridge called Bangabandhu Bridge connecting the towns of Sirajganj and Bhuapur was planned and constructed in 1995-1999. Its location is shown in Figure 1.

As shown in the more detailed map in Figure 2, the width of the river channel was about 11km. This area is the vast expanse of flood plain and had suffered severe destruction over the years due to intense flooding over the river channel and its surroundings. Devastation was particularly conspicuous at the time of the flooding in 1987 and 1988. In some areas, river channels are purported to have shifted their courses

Figure 1: General location map

overnight through several hundred meters. The tendency of the drift is reported to have been westwards whereby involving a huge amount of sandy soils removed by scouring in the riverbed in the west side of the Jamuna river.

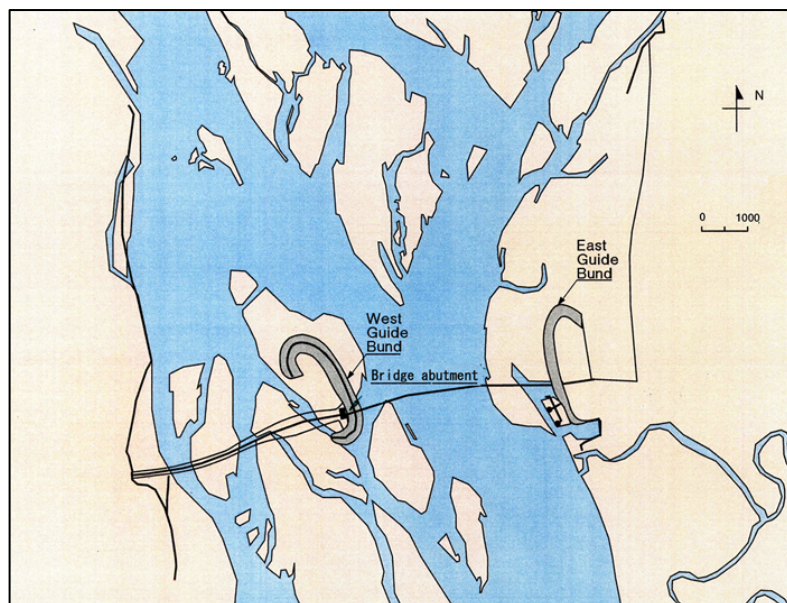


Figure 2: Locations of the Guide Bunds in Jamuna bridge site

In the design of the abutment of the Bangabandhu Bridge, it was considered mandatory to implement some countermeasures against the deleterious effects due to such scouring and to duly control the river channel. With this aim, construction of guide bunds was planned on both sides of the river as shown in Figure 2. Of particular importance was the construction of the West Guide Band, as it was intended to protect the bridge abutment behind the river from scouring or erosion of the riverbed. The construction consisted of excavating the riverbed by dredging the sand inland by ships and placing erosion-protecting armours such as geotextiles and stones over the underwater slopes on the west side. The location and horseshoe-shaped plan view of the Guide Bunds are displayed in Figure 3. The trench varying from 27 to 30m in depth was dug below water by means of cutter-suction dredgers from ships at the site of each guide bund.

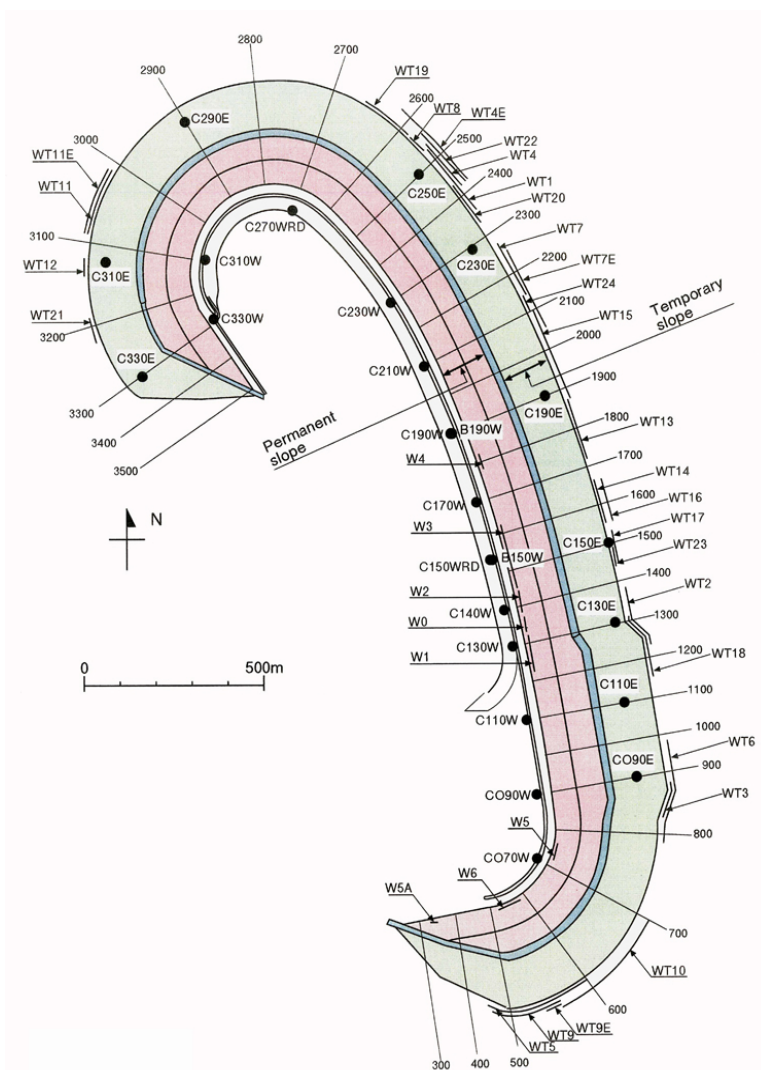


Figure 3: Locations of Slides in the West Guide Bund

3. UNDERWATER SLIPS ON EXCAVATED SLOPES

The West Guide Bund was constructed at the site of a recently formed sand island as seen in Figure 2. The materials forming the dredged slopes were composed of young, rapidly deposited sediments. The detailed plan view of the excavation is shown in Figure 3 and a typical section (E-W section) across the dredged channel is displayed in Figure 4. The slope on the west side was to be protected by the geotextiles-stone armour against the scouring, because the bridge abutment was to be installed due west of the West Guide Bund. Thus the underwater slope designated as “permanent slope” was designed so as to have a gentle slope of 1:5.0 in the middle portion. On the contrary, the slope on the east side of the dredged channel was to be left unprotected. Even though slides occur and the sand bar disappears in future due to scouring or erosion, it did not matter. Thus, the eastern slope was designed to form a steeper slope with an angle of 1:3.0 and designated as “temporary slope” in Figure 4.

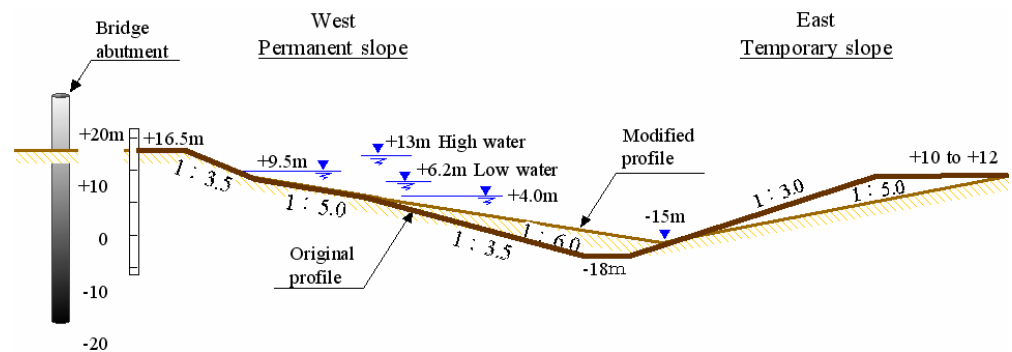


Figure 4: East-west section through West Guide Bund Channel
(from Hight et al. 1999)

The dredging work began northwards in October 1995 from the southern rim of the sand bar. As the dredging proceeded, slope failures occurred on the permanent slope on November 19th in 1995 in the cross section 1270 and another on November 22nd in the cross section 1410. They are respectively called W1 and W2 slide and shown in Figure 3. On December 3, 1995, the largest-in-scale slide denoted by W3 took place on the permanent slope at a location of Chainage 1550. This slide covered an area of about 150m wide and 150m long over the permanent slope. Afterwards many failures were found to have occurred on the temporary slope during the period of rising water level in 1996. Eleven of them were larger in scale than W3, and these are indicated by the symbol WT 6, 7, 9, 9E, 13, 15, 16, 17, 18, 22, 24 in Figure 3. Many of these slides delayed the progress of construction works, but of most serious concern were the failures on the permanent slope, because they had to be repaired to construct erosion-free slope. In recognition of the instability with an angle of 1:3.5, the design cross section on the permanent slope was changed so as to have a slope of 1:6.0 near the bottom and for the temporary slope, the angle was changed from 1:3.0 to 1:5.0 as illustrated in Figure 4. Then, the dredging work to full depth was resumed to finish excavation of the trench. As the

dredging went on, a number of slope failures began to occur again but only on the temporary slope. The failures occurred mostly during the period of March to June in 1996. Exact locations of all of these slope failures including those prior to and after the design change as well are indicated together in Figure 3.

4. CAUSES OF SLOPE FAILURES

There are two aspects to be distinguished in clarifying mechanisms of slope failures in sand deposits. These are generic cause and consequence of failure.

4.1 Causative Incidents

It was difficult to precisely identify generic causes of the slides which occurred apace in underwater environments. It was envisioned that the over cutting, overstepping or rapid cutting associated with the dredging operation had been responsible for triggering the slips. There were slow falls in the water level of the river after storms of the order of 0.1m per day over a period of five days. This might have been other causes leading to the slips. The factors such as wave actions and thunderstorms were also suspected to have triggered the slips. No matter what causes might have been, it is certain that the sand deposits had been in a precarious state narrowly keeping the stability when the excavation was made.

4.2 Consequences of Failure

After the initial failure is triggered involving a small or medium deformation, the soil may or may not develop large displacement later on. One kind of sand deposits might induce only a limited deformation which is tolerable but in another type, a fairly large amount of displacement will continue further on. In the latter case, the level of devastation incurred will be intolerably large. Thus, identification of the damage level in terms of continuation or discontinuation of deformation after the triggering of failure will pose an important aspect in recognition of the problem particularly in saturated sand deposits under water.

The identification of the consequence of failure as above can be made generally by examining the state of an existing deposit as to whether it will exhibit contractive or dilative behaviour after it has undergone triggering. In the case of the sand deposit in the Jamuna riverbed, the deposit seems to have had characteristics showing the contractive or strain-softening type of behaviour in which the residual strength at a largely deformed state is reduced significantly leading to an intolerable level of deformation after the slips were triggered. In the above context, soil characteristics were investigated in details in the field as well as in the laboratory as described below.

5. INVESTIGATION OF SOIL CONDITIONS

Following the occurrence of the slides as well as at the time the design was made, multiple series of tests were conducted both in the field and in the laboratory to elucidate nature and properties of soils which are deemed to be a cause of the slides.

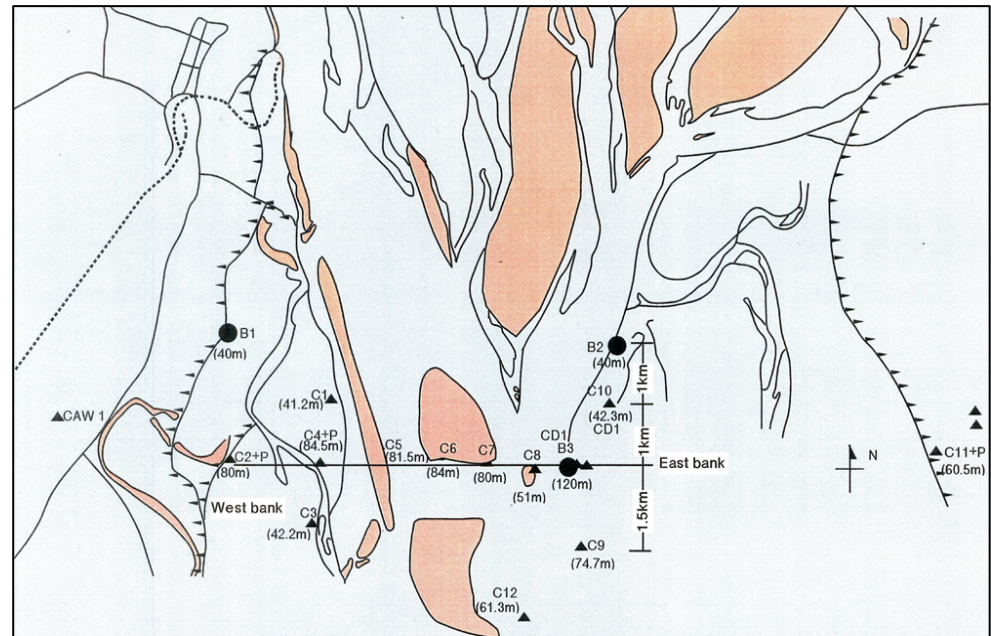


Figure 5: Location of soil investigations at the site of Jamuna Multipurpose bridge construction

5.1 In-situ tests

Deep borings were performed at three locations, viz., B1 on the west bank and B2 and B3 on the right bank, as shown in Figure 5. The standard penetration test (SPT) was also conducted at these boring sites. At the site B3, the measured N-value was, for example, 15 at a depth of 9.25m. Considering the use of a free falling hammer in the SPT practice at the Jamuna sites, the energy level is deemed as about 80% of the theoretical energy in hammer dropping. This energy level actually consumed for penetration is considered about the same as the level normally achieved in the Japanese practice. The SPT N-value at a shallow depth of 6.25m was found to be 7 at B3, 10 at B2 and 19 at the site B1. These values are relatively small indicating the presence of loose sand layer which might be responsible for triggering the slope failure.

Dutch one-penetration tests (CPT) were also performed at 15 locations as indicated by C1 to C13 shown in Figure 5. The results of CPT showed qc-value of 4-5 MPa at depths from 6-8m at the location CDI which is close to the site B3. This value indicated as well the presence of loose sand layer at this depth. By comparing the SPT N-value and the CPT qc-value obtained each in their vicinity, an empirical correlation was established by Delft Geotechnics as follows,

$$q_c = 0.31 \cdot N_{60} \quad (1)$$

where N_{60} indicates the SPT N-value corresponding to 60% of the theoretical energy. In view of the 80% of the energy achieved in the Jamuna River investigation, the above relation would be rendered to

$$q_c = 0.37 \cdot N \quad (2)$$

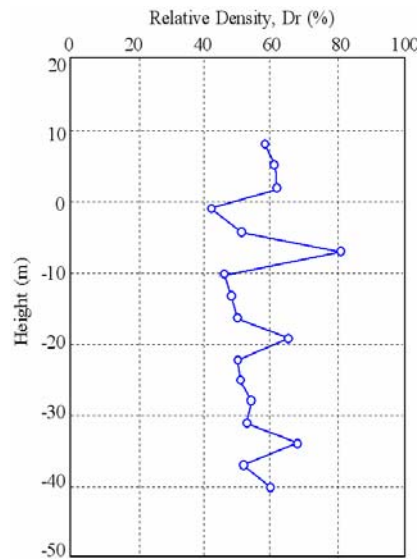


Figure 6: A typical profile of relative density at a site in Jamuna River (Hight et al. 1999)

where N indicate SPT N-value obtained by the free fall hammer which is considered to exert 80% of the theoretical energy in the SPT operation. The relative density at the site was estimated based on the data of SPT and CPT. One of the typical data by Hight et al. (1999) is shown in Figure 6 where it may be seen that the relative density takes values around $Dr = 50\%$ but the majority of data indicate values less than 65%.

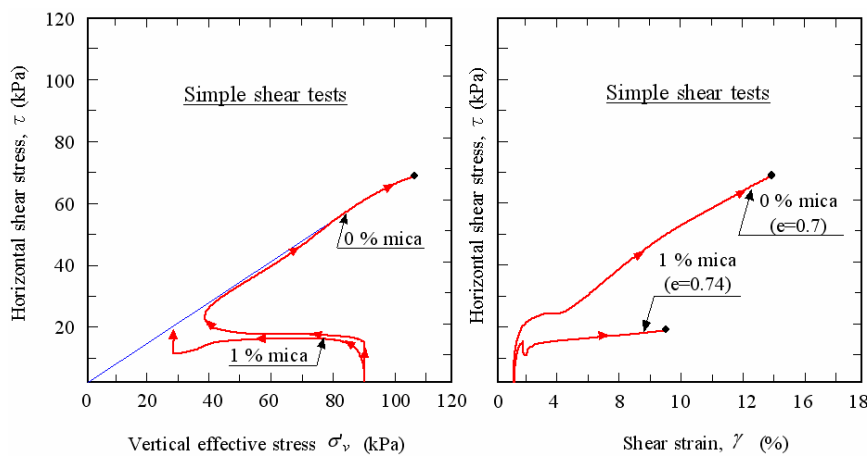


Figure 7: Effect of 1% mica on the undrained behaviour of sand in simple shear (Hight et al. 1999)

5.2 Laboratory tests

Sand samples were obtained in-situ by means of the tube sampling technique. However, the degree of disturbance appears to be somewhat high in loose deposits of sand and therefore the outcome of the laboratory triaxial tests on such samples is considered not truly representative of the conditions of sand deposits prevailing in the field.

Apart from the laboratory tests on intact sand samples, it was discovered that the sand in the Jamuna River contains a few percent of mica and its presence was suspected to have created conditions of the deposits which were highly vulnerable to triggering failure and consequent flowage of the sand. Thus, attention has been drawn to the peculiar behaviour of mica-containing sand by several investigators. One of the results of simple shear tests reported by Hight et al. (1999) is reproduced in Figure 7 in which the behaviour of clean silica sand is compared with that of the same sand but containing 1% mica.

It can be seen that the loose sand with a void ratio of $e=0.70$ exhibits ductile behaviour with a tendency to dilate at largely strained states, bringing up the effective stress path along the failure line. In stark contrast, the sand with $e=0.74$ containing 1% mica is shown to be brittle and have a potential to collapse at medium strains resulting in a small residual strength at a largely strained state. Hight et al (1999) argued that, because of the aspect ratio of the mica plate as high as approximately 50:1 compared to the rotund sand particles, the presence of even 1% mica by weights is approximately equivalent to that of 25% of mica by number of grains.

In an effort to investigate more thoroughly the behaviour of mica-containing sand, multiple series of triaxial tests has been conducted at the Tokyo University of Science on reconstituted samples of the sand recovered from the Bangabandhu Bridge site in Bangladesh. Details of the tests procedures and the manner in which data are arranged are described more in details in the paper by Tsukamoto et al. (2007). The conduct of the tests on the Bangladesh and its outcome will be described somewhat in details in the following pages.

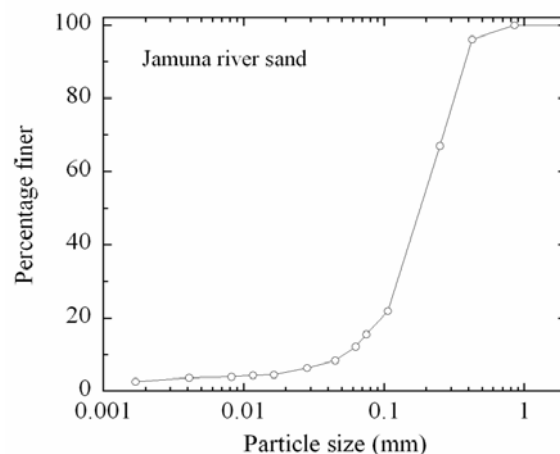


Figure 8: Grain size distribution of the Jamuna River sand tested

6. CONDUCT OF TRIAXIAL TESTS ON BANGLADESH SAND

6.1 Material properties

The sand with a few percent mica recovered from the bridge site has a typical grain size distribution curve shown in Figure 8. It is a sand with $D_{50} = 0.2$ mm and contains 10% non-plastic fines. Its specific gravity is $G_s = 2.745$ and the maximum and minimum void ratio as measured by the Standard of the Japanese Geotechnical Society was $e_{\max} = 1.202$ and $e_{\min} = 0.602$, respectively.

6.2 Test procedures

In the triaxial tests, the samples 6cm is diameter and 12cm is length were prepared by the method called wet tamping in which moist sand was placed in the mould with varying energy of compaction. By this method, it was possible to prepare reconstituted samples with widely varying range in void ratio. After preparing the samples, de-aired water was circulated to achieve a state of full saturation with a B-value greater than 0.95. Then, the samples were consolidated anisotropically under different K_C -conditions. The axial load was then increased under undrained condition when the mode of the test was triaxial compression. The triaxial extension tests were also performed by increasing the cell pressure under undrained conditions.

6.3 Results of tests

The results of the undrained compression test on samples with void ratios ranging between 0.804 and 0.871 are displayed in Figure 9 where the deviator stress $q = \sigma_1 - \sigma_3$ is plotted versus the effective mean confining stress defined as $p' = (\sigma_1 + 2\sigma_3')/3$. The saturated samples were consolidated with a vertical stress of $\sigma'_{1C} = 98kPa$ and lateral stress of $\sigma'_{3C} = 49kPa$ producing an initial state of $K_C = 0.5$. It may be seen in Figure 9 that the dilatant behaviour is exhibited when the sample is prepared with a void ratio less than about 0.83, but otherwise the sample is contractive. It is to be noticed that the sample with $e = 0.871$ has reached a steady-state with a deviator stress of $q = 15kPa$ which is smaller than the initially applied deviator stress of $q = 49kPa$. It is seen in Figure 9 (b) that large deformation began to occur at an early stage of load application and continues further on until an axial strain of 20% developed. The smallness of the deviator stress at the steady state as compared to the deviator stress at the outset would be regarded as a criterion to indicate an unstable condition where flow-type deformation could be triggered if the peak shear stress is passed over by application of a slight agitation at the beginning. Another series of tests with the same initial lateral stress of $\sigma'_{3C} = 49kPa$ but with an increased K_C -value of 0.7 is demonstrated in Figure 10 for samples with various void ratios where the general tendency is seen to be the same as those shown in Figure 9. It may be seen in Figure 10 that the sample consolidated with a

deviator stress $q_C = \sigma'_{1C} - \sigma'_{3C} = 20kPa$ with a void ratio of 0.827 has reached a steady-state with the deviator stress $q = 95kPa$ which is much greater than the initially applied deviator stress of $20kPa$. In such a condition, the flow type deformation will not be induced because of the gain in shear strength as compared to the initially applied shear stress. The last series of the tests with $K_C = 1.0$ are demonstrated in Figure 11 where it is apparently noted that the specimen with $e=0.767$ exhibited highly dilative behaviour. The characteristic feature of deformation as deduced from the above test results may be summed up as follows.

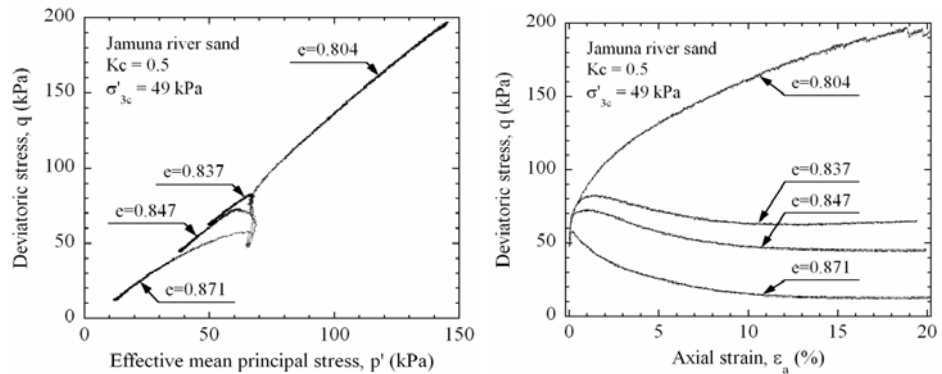


Figure 9: Results of undrained triaxial compression tests

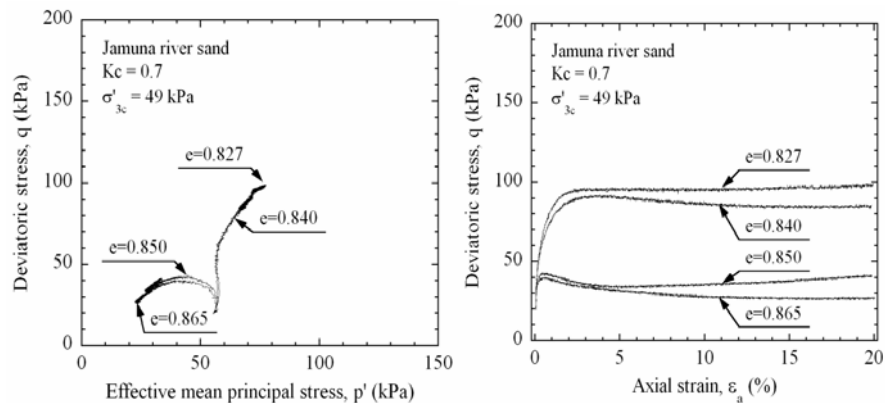


Figure 10: Results of undrained triaxial compression tests

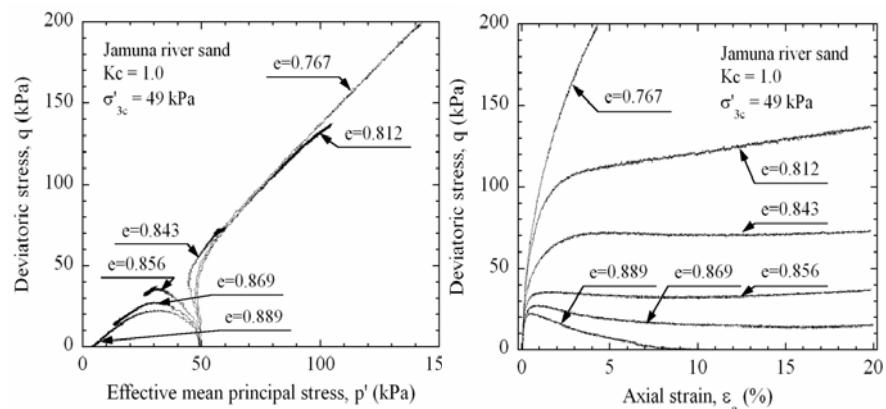


Figure 11: Results of undrained triaxial compression tests

1. It is apparent that the deformation characteristics become more dilative with decreasing void ratio and vice versa. The void ratio for the threshold can be read off as approximately $e=0.83$ from the Figs. 9 to 11.
2. Although not clearly displayed in the test results shown in Figs. 9 and 10, a number of tests on Bangladesh sand with greater confining stresses or tests on other sands have coherently shown that the deformation characteristics becomes more contractive with increased K_C -value at the stage of anisotropic consolidation. This is consistent with the main conclusion derived by Chern (1995), Vard and Chern (1985), Kato et al. (1999) and Tsukamoto et al. (2007).
3. Similar undrained triaxial tests have been performed on several other sands in Japan which do not contain mica. The outcome of the tests on such non-mica sand showed that the sand behaviour becomes more starkly dilative or strain hardening with decrease in void ratio. In contrast, the mica-containing sand from Bangladesh tends to become contractive or to remain at an intermediate state between contractive and dilative whereby developing large deformation at constant shear stress q_s and effective confining stress p'_s . This implies that the mica-containing sand would easily be put at a steady-state over a wide range of void ratio. This is consistent with results of the tests reported by Hight et al. (1999).

7. FLOW CHARACTERISTICS OF JAMUNA RIVER SAND

From a number of other tests including those shown in Figure 9 through 11, the void ratio, e , deviator stress q_s and effective mean confining stress p'_s at the steady state were read off and plotted in Figure 12 in terms of e versus p'_s . In this plot, those data from the tests with $K_C=1.0$ are displayed with white circles and those from anisotropically consolidated samples with K_C -values less than 1.0 are shown with black circles. It can be seen in Figure 12 that the steady state line is established uniquely irrespective of the K_C -conditions.

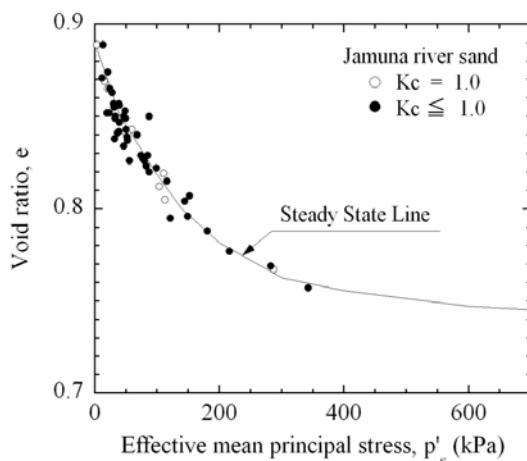


Figure 12: Steady-state line for Jamuna river sand as a plot of void ratio and effective mean principal stress

In the whole program of the tests executed at the Tokyo University of Science, it was shown that the most appropriate parameter indicative of the effects of confinement at the steady state is not necessarily the mean principal stress $p'_s = (\sigma'_{1s} + 2\sigma'_{3s})/3$, but instead the major principal stress σ'_{1s} alone. In accordance with this concept, the plot is made of the same data set alternatively in Figure 13 in terms of the void ratio versus the effective major principal stress σ'_{1s} at the steady state. It can be seen that the steady-state line is established equally well again irrespective of K_C - conditions.

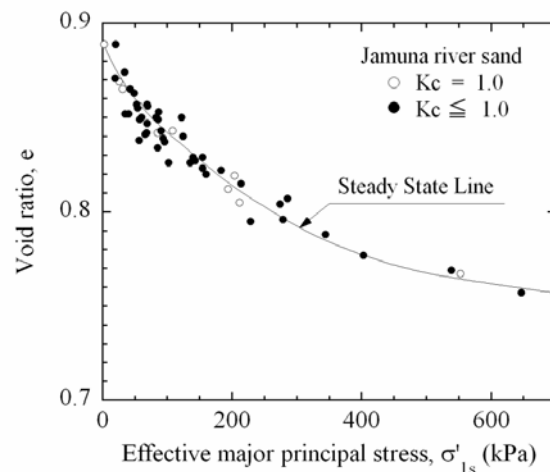


Figure 13: Steady-state line for Jamuna river sand as a plot of void ratio and effective major principal stress

It is to be recalled that the steady-state lines established in Figure 12 and 13 all do pertain, not to the initial un-deformed state of the sand, but to the state where the sample is largely deformed to a strain level greater than about 5%. One might argue that the specification of a state of soil at the time it is already deformed may not be appropriate. Thus, it is claimed to be a parameter at the initial state prior to load application that is more convenient and hence desirable in view of its practical application when soil behaviour is to be estimated for subsequent application of shear stress. Looking back over the development of soil mechanics, one can realize that, in the majority of problems, such as consolidation and undrained shear strength, it was the initial state of the confining stress that was taken up as a parameter to specify the soil behaviour in the subsequent loading. In the context as above, the initial state of void ratio and the major principal stress σ'_{1c} before the application of shear stress were picked up from the whole file of test data on Jamuna River sand and they are plotted in the diagram of Figure 14. In this diagram, a line is drawn which differentiates the sample behaviour between contractive and dilative. Such line was called the Initial Dividing Line (Ishihara, 1996). It may be seen in Figure, 14 that the Initial Dividing Line (IDL) can be obtained consistently irrespective of the K_C - state of samples at the time of anisotropic consolidation. It is to be noticed here that the steady-state line, quasi-steady state line and initial dividing line

are almost coincident particularly in the range of small confining stress less than about $\sigma'_{1C} = 100 \text{ kPa}$.

The angle of internal friction at the steady state derived from the same data file is shown in Figure 15. Although the values are slightly different between TC-tests and TE-tests, the average value would be taken as $\phi_s = 30^\circ$.

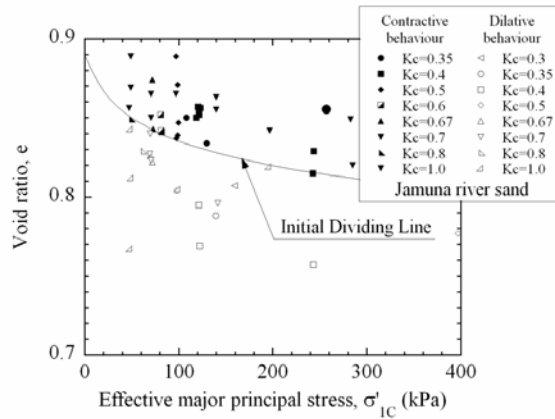


Figure 14: Initial dividing line for Jamuna river sand as a plot of void ratio and initial major principal stress

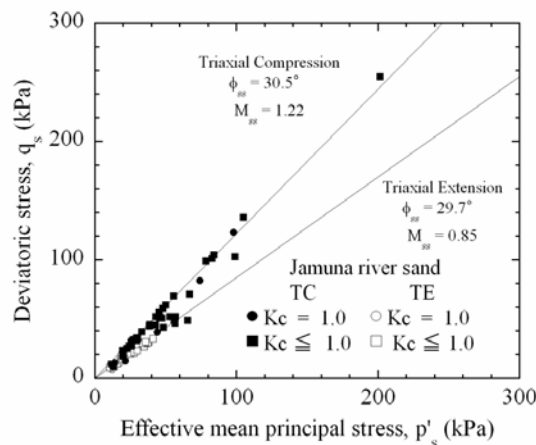


Figure 15: Angle of internal friction for the steady state

8. RESIDUAL STRENGTH OF JAMUNA RIVER SAND

It has been customary to define the residual strength, S_{us} , by referring to the minimum shear stress at the quasi-steady state (QSS) which is mobilized at the state of phase transformation for sands exhibiting contractive behaviour. In the mica-containing Bangladesh sand, the test data in Figure 9 to 11 show that the quasi-steady state (QSS) is almost coincident with the steady state (SS). Thus, these two states could be regarded practically identical for the mica-containing Jamuna River sand being considered. By denoting the deviator stress at this state by $q_s = \sigma'_{1S} - \sigma'_{3S}$, residual strength is expressed as (Ishihara, 1996, p.268)

$$S_{us} = \frac{q_s}{2} \cos \phi_s = \frac{M}{2} \cos \phi_s \cdot p'_s \quad (3)$$

$$M = \frac{6 \sin \phi_s}{3 - \sin \phi_s}$$

where p'_s is the mean effective confining stress at the QSS or SS as defined by $p'_s = (\sigma'_{1s} + 2\sigma'_{3s})/3$, M is a parameter related with the angle of phase transformation in the $p'-q$ plot, and ϕ_s is the angle of internal friction at QSS or SS. When normalizing the residual strength S_{us} to the initial mean principal stress, it is written as

$$\frac{S_{us}}{p'_c} = \frac{M}{2} \cos \phi_s \cdot \frac{1}{r_c} \quad (4)$$

Where

$$r_c = \frac{p'_c}{p'_s} = \frac{\sigma'_{1c} + 2\sigma'_{3c}}{\sigma'_{1s} + 2\sigma'_{3s}}$$

If the residual strength is normalized to the initial major principal stress σ'_{1c} , it is written as

$$\frac{S_{us}}{\sigma'_{1c}} = \frac{M}{2} \cdot \frac{3 - \sin \phi_s}{3(1 + \sin \phi_s)} \cdot \cos \phi_s \cdot \frac{1}{r'_c} \quad (5)$$

$$r'_c = \frac{\sigma'_{1c}}{\sigma'_{1s}}$$

From the majority of data on undrained triaxial compression tests “TC-test”, the residual stress at largely deformed state of the Jamuna River sand was read off and normalized to p'_c and σ'_{1c} . Similar undrained triaxial tests were also performed in the extension mode of deformation. This test is referred to as “TE-test”. The residual strength from the TE-test was also normalized to p'_c and σ'_{1c} . The outcome of such data compilation is demonstrated in Figure 16, in terms of the plot of the normalized residual strength versus the K_C -values employed in each of the tests. Among the cluster of data points, the initial state of the samples exhibiting the contractive behaviour in subsequent undrained loading is indicated by the black symbol and those showing dilative response by white symbols. It is to be noted that those data with smaller values of S_{us}/p'_c correspond to loosely prepared samples and with increasing value of S_{us}/p'_c , the samples become denser. A line dividing the two types of behaviour is drawn for each of the TC-tests and TE-tests. The two lines thus determined each from TC and TE tests are indicated in Figure 16, together with the empirical equations suggested for each of these threshold conditions. The same data sets are plotted in Figure 17 now choosing the residual strength normalized to the initial major principal stress σ'_{1c} . From the two kinds of plot shown in Figure 16 and 17, the following observation can be made.

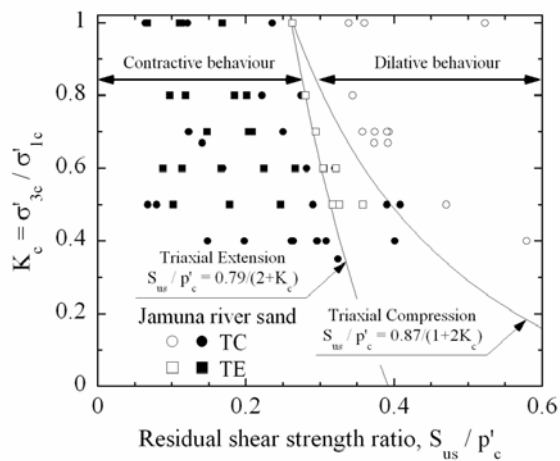


Figure 16: K_C -value versus residual strength normalized to the initial mean principal stress – comparison between triaxial compression and extension tests

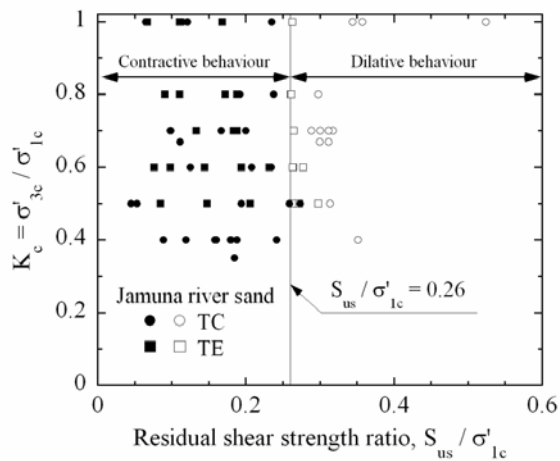


Figure 17: Factor of safety versus Koch-value or versus angle of slope for the Jamuna River sand

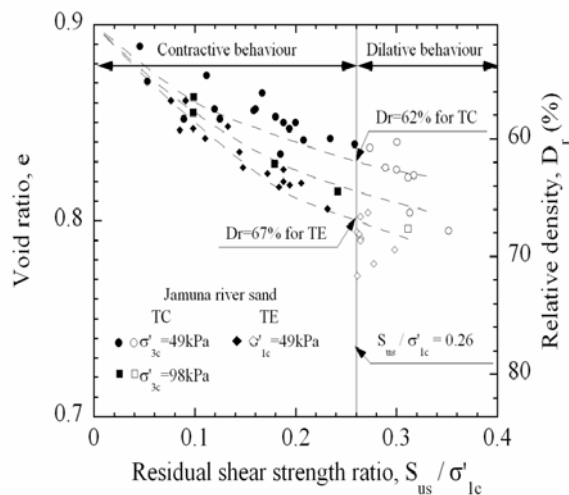


Figure 18: Residual strength ratio S_{US} / σ'_{1C} versus void ratio-comparison between triaxial compression and extension tests

1. In the case when the residual strength is normalized to the initial mean confining stress, the value of S_{us}/p'_c tends to increase with decreasing K_C -value, and also it depends upon the mode of deformation as to whether the loading is triaxial compression or triaxial extension.
2. If the residual strength is normalized to the initial major principal stress, the value of S_{us}/σ'_{1c} is determined uniquely irrespective of the K_C -value in the anisotropic consolidation, and also independently of whether the mode of deformation is triaxial compression or triaxial extension. For the mica-containing sand from the Jamuna River site, the threshold value of the normalized residual strength separating conditions of contractive and dilative behaviour is found to be $S_{us}/\sigma'_{1c} = 0.26$ as accordingly indicated in Figure 17.
3. Each data in Figure 17 belongs to the samples having different void ratios but close examination of the data has shown, although not shown explicitly, that for the state with a given void ratio, the normalized residual strength S_{us}/σ'_{1c} takes a constant value irrespective of the K_C -condition at the time of consolidation. Thus, the limiting value of $S_{us}/\sigma'_{1c} = 0.26$ can be taken as the upper bound of S_{us}/σ'_{1c} -values within the range of the void ratio in which the sand exhibits contractive behaviour.

In the type of plot shown in Figure 16 and 17, the looseness or denseness of the samples is not indicated explicitly. In order to visualize this effect, the same test data are now shown in Figure 18 in terms of the S_{us}/σ'_{1c} plotted versus the void ratio, e . It may be seen in the figure that effects of the minor principal stress, that is, σ'_{3c} -value in the TC-test and σ'_{1c} -value in the TE-test, is not so important but the influence of the mode of deformation as to whether it is TC-test or TE-test would be somewhat significant with the mode of the TE-test giving smaller normalized residual

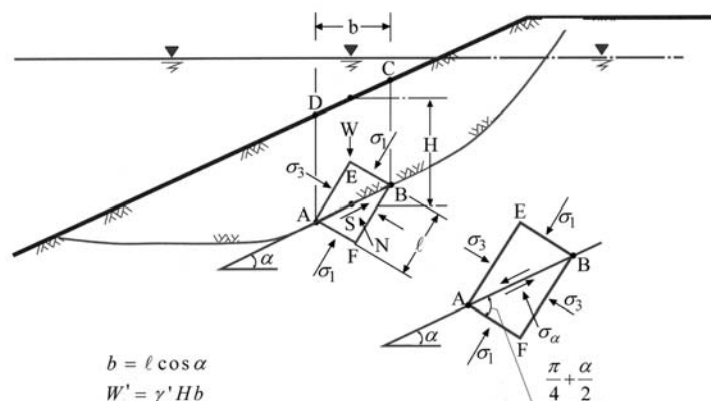


Figure 19: Forces acting on a soil element above a sliding plane in a submerged slope

strength S_{us}/σ'_{1C} as compared to that from the TC-tests. It is to be noticed that no matter whether the mode is TC-test or TE-test, the upper limit of S_{us}/σ'_{1C} takes the identical value of 0.26. The density of each samples tested is also shown by way of the relative density, Dr , with the scale indicated on the right hand side of Figure 18. If the average is taken, it can be conclusively mentioned that, for the Jamuna River sand deposited with a relative density smaller than $Dr \cong 65\%$, it will exhibit contractive behaviour. Therefore the in-situ deposits under such condition will have a potential to develop flow typedeformation irrespective of the K_C -condition if it is subjected to an external agency for triggering the slide.

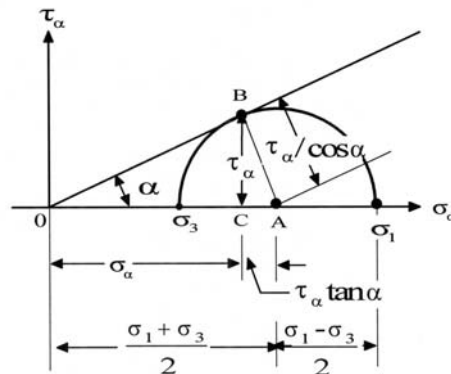


Figure 20: Mohr circle to determine σ_1 and σ_3 from σ_α and τ_α

9. SIMPLE ANALYSIS OF THE SLIDE IN JAMUNA RIVER

9.1 Basic Concept

For the sake of simplicity, let a potential sliding plane be located in parallel to the surface of the submerged slope as illustrated in Figure 19. Then, from the equilibrium of forces amongst the submerged weight of a soil mass and normal and tangential forces N and S acting on the potential sliding plane, the stresses σ_α and τ_α are obtained as

$$\sigma_\alpha = \frac{N}{\ell} = \gamma' H \cos^2 \alpha \quad (6)$$

$$\tau_\alpha = \frac{S}{\ell} = \gamma' H \sin \alpha \cdot \cos \alpha$$

where γ' is the submerged unit weight of the soil, α is the angle of the potential sliding plane, and H is the height of the soil mass being considered. Then, given the values of stress components, σ_α and τ_α , as above, it is possible to locate a point B in the Mohr diagram as illustrated in Figure 20. The direction of the line OB indicates the angle of obliquity of stress application, α , or the angle of stress mobilization. By drawing a half circle through the point B so that it is tangential to the line OB , it becomes possible to identify the points of the major and minor principal stresses σ_1 and σ_3 on the Mohr diagram. Then, from geometrical consideration, the following relations are obtained.

$$\sigma_1 = \sigma_\alpha + (\tan \alpha + \frac{1}{\cos \alpha})\tau_\alpha \quad (7)$$

$$\sigma_3 = \sigma_\alpha + (\tan \alpha - \frac{1}{\cos \alpha})\tau_\alpha$$

Introducing Eq. (6) into Eq. (7), one obtains

$$\sigma_1 = \gamma'H(1 + \sin \alpha) \quad (8)$$

$$\sigma_3 = \gamma'H(1 - \sin \alpha)$$

Thus, the ratio between the minor and major principal stresses is obtained as

$$K_C = \sigma_3 / \sigma_1 = \frac{1 - \sin \alpha}{1 + \sin \alpha} \quad (9)$$

The relation of Eq. (9) is displayed in Figure 21. It is known that the majority of natural slopes consisting of relatively soft soils have an angle ranging approximately between $\alpha = 0$ and $\alpha = 30^\circ$. Thus, the ratio, K_C , between the two principal stresses has a value between 0.3 and 1.0.

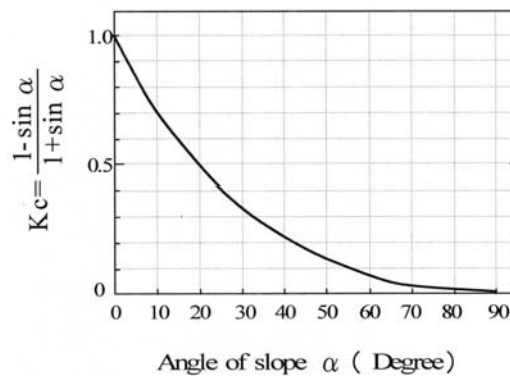


Figure 21: Relation between K_C -value and angle of slope

9.2 Typical Pattern of Deformation

The typical pattern of undrained deformation of anisotropically consolidated specimens is schematically illustrated in Figure 22 in terms of stress path and stress-strain curve. In Figure 22(a), the abscissa indicates the mean principal effective stress defined by $p' = (\sigma'_1 + 2\sigma'_3) / 3$ and the ordinate represents the shear stress defined by $q = \sigma'_1 - \sigma'_3$. In Figure 22, point A indicates an initial state of K_C -consolidation whereupon undrained shear stress application starts. When the specimen is loose, it shows an increase in deviator stress, q , to a point B at peak strength and then a decrease down to a point C corresponding to the state of phase transformation or the quasi-steady state. The bent-over in the stress path takes place at point C and the shear stress increases to a point D where large deformation starts to occur without any change in the effective mean stress p' and shear stress q . This state is called the steady state. When the specimen is loose, the minimum deviator stress is encountered, concomitant

with fairly large deformation, at point C where the phase transformation takes place from contractive to dilative behaviour.

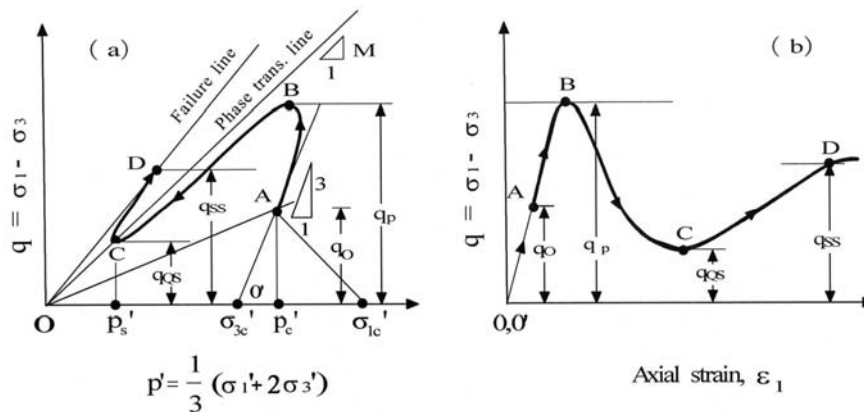


Figure 22: Typical stress-path and stress-strain relation for loose

Thus, the residual strength is defined by the shear stress q_{QS} which is mobilized at point C. The residual strength thus defined is called the strength at quasi-steady state. When the sand is very loose, the gain in the deviator stress from point C to D is not achieved. The sample continues to deform with a constant deviator stress. In other words, the quasi-steady state (QSS) becomes coincident with the steady state (SS). In the case of the Jamuna River sand, the samples are seen deforming at a constant deviator stress as apparent from the test data shown in Figs. 9 through 11. This may be due to the inclusion of mica. Thus, in the present study, the quasi-steady states will be taken as being identical to the steady state sections in the permanent and temporary slopes. Looking over the configuration of the post-failure slopes, one may envision that the failure was triggered initially at the toe of the slope and followed by flow-type movement of the soil behind it. The profiles of slopes shown in Figure 23 through 28 disclose that the soils have slid down the slope through a considerable distance resulting in thick deposits of debris at the bottom of the dredged channel. Thus, the post-failure surface in the upper part of the submerged slope can be considered to have been the plane where the soil mass had actually slid down. This surface may therefore be considered as the sliding surface on which flow of liquefied sand had taken place. It is apparent that the sliding surface thus determined is inclined with an angle smaller than the original slope angle of 1:3.0 and 1:5.0. However, to simplify calculation, it may be assumed that the moving surface of the slope during flow with large deformation was in parallel with the sliding plane, as schematically illustrated in Figure 19.

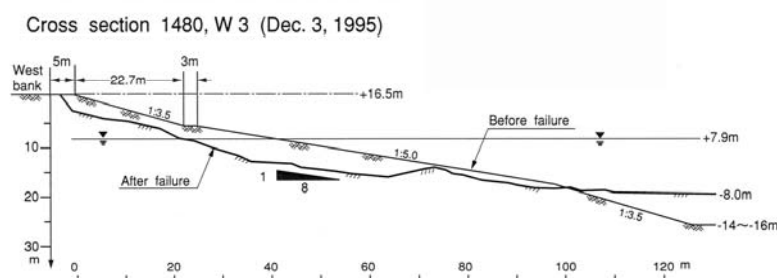


Figure 23: Slide on Dec. 3, 1995 in the permanent slope

Cross section 1500, W 3 (Dec. 3, 1995)

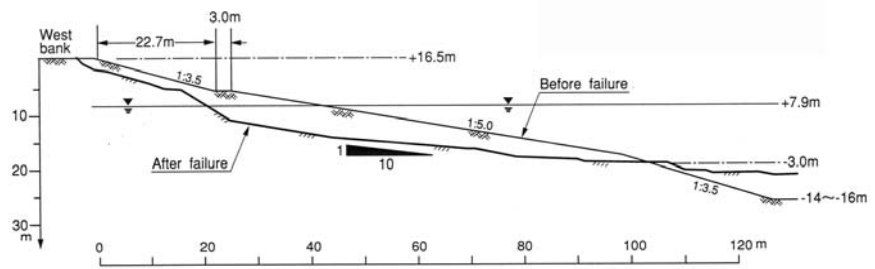


Figure 24: Slide on Dec. 3, 1995 in the permanent slope

Cross section 1550, W 3 (Dec. 3, 1995)

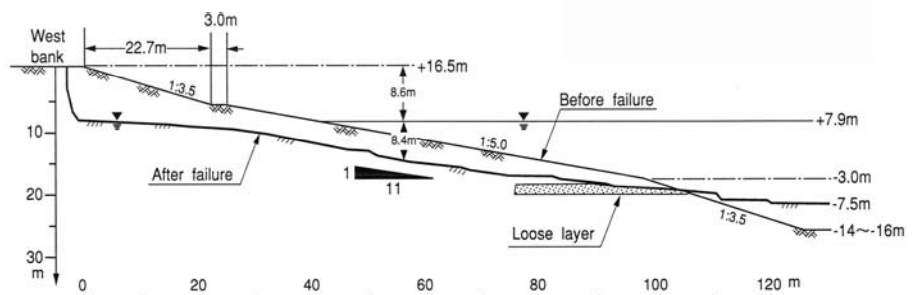


Figure 25: Slide on Dec. 3, 1995 in the permanent slope

Cross section 1800, W 4 (Dec. 15, 1995)

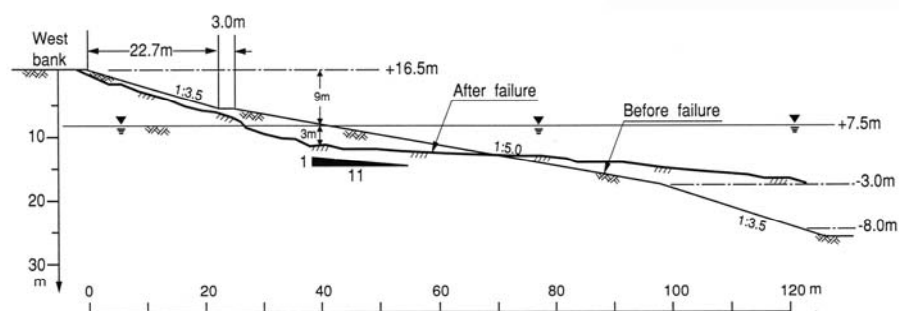


Figure 26: Slide on Dec. 3, 1995 in the permanent slope

Cross section 1800, WT 13 (May 6, 1996)

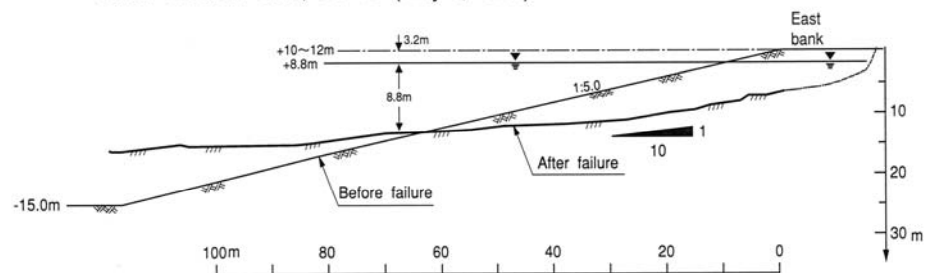


Figure 27: Factor of safety versus Koch-value or versus angle of slope for the Jamuna River sand

Cross section 2500, WT 4 (April 20, 1996)

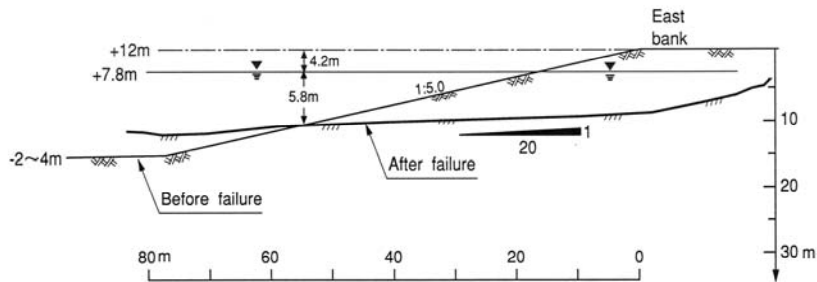


Figure 28: Slide on April 20, 1996 in the temporary slope

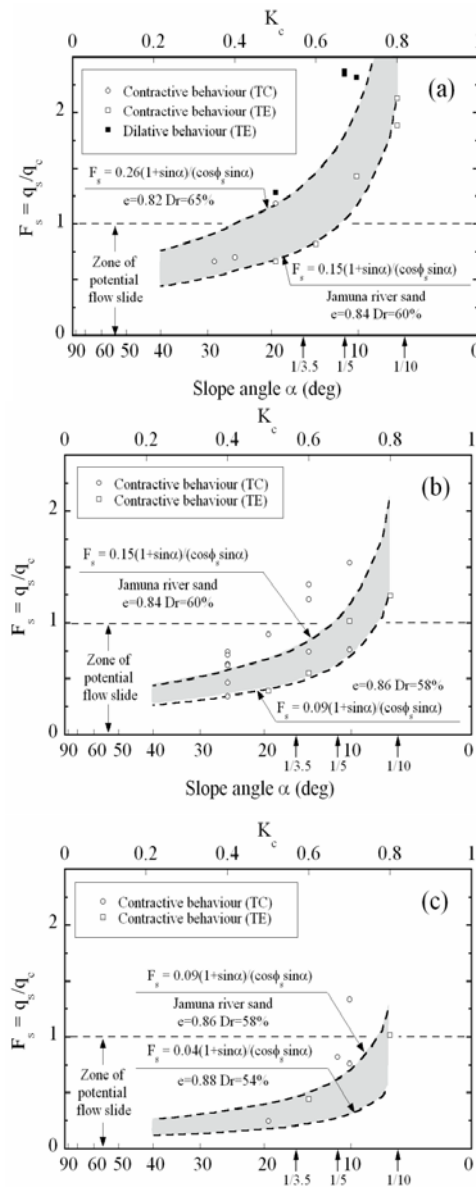
(a) Triggering mechanism

There are several cases of submarine landslides documented in literatures. One of the large submarine landslides ever reported in details would be the slide which occurred at the rim of the recent fill towards the sea at the Port of Nice in France on October 16, 1979. The fill, much of which was deposited through or in water, was constructed on a deltaic deposit of stratified clayey silt and silty sand. Features and some analysis results are reported by H.B. Seed et al. (1988). Regarding the triggering mechanism, multiple events were cited to have been possible causes for initiating the slide. These are (1) the tidal wave first inducing about 3m lowering of the sea level due presumably to a off-shore landslide and (2) the increase in an artesian pressure due to rainfalls in the preceding days at depths of about 40m in the pervious sand layer which is connected with water levels on land. Thus, it was difficult to narrow down the causes into a single event.

The clarification of the triggering cause for the slides in the Jamuna River channel is also a difficult task but the conceivable reasons variously conceived may be summarized as follows.

1. During the process of underwater excavation, the cutting by a dredger might have been carried out so fast that the rapid change in the state of stress did occur creating a highly undrained condition with the result that local failure was triggered first and retrogressed into a large slide.
2. In the course of the excavation conducted stepwise, one step of cutting might have been so large in block that the steep slope locally created did collapse enlarging the zone of slips into the entire slide.
3. There were natural phenomena frequently occurring in the region of Jamuna River. These include torrential downpour, wave actions and falling water levels. None of these phenomena could be pinpointed as a single cause of excitation, but the effects of falling water level are most likely to be one of the reasons triggering the slips.

4. Besides the externally imposed agencies as cited above, there would be an internal reason. That is the nature of the sand itself containing the mica mineral as mentioned above. The sand in the Jamuna River environment must be deposited in a precarious state narrowly keeping its stability and thus easily susceptible to triggering failure. This aspect was addressed by Kramer and Seed (1988) who asserted that the sand deposited with a large initial shear stress, that is, the one anisotropically consolidated with a smaller K_c -value, the margin of stability is narrow against additional external agency. This fact holds true for many of sand deposits, as exemplified by the test data demonstrated in Figure 9 to 11. It may be seen for example that the sand consolidated with $K_c = 0.5$ with the void ratio of 0.875 could collapse if a small deviator stress of $q = 10 \text{ kPa}$ is applied additionally.



Among several reasons as cited above, there are not strong reasons in support of the above hypotheses 1 and 2, that is, the rapid cutting and overstepping. Once these operations turned out to be undesirable, it is likely that the operators must have changed the way the cutting was performed. Therefore the sliding must have been limited to a certain area throughout the length of the channel. However, the slips did actually occur along the long-stretched zone in the channel. This fact appears to indicate that the hypotheses 1 and 2 are not likely to be the scenario triggering the slips.

It is the authors view that (1) the lowering of water levels and (2) the potentially susceptible nature of the mica-containing sand put into the K_C - conditions by excavation are most likely the two major reasons creating conditions to trigger the failure. Although the scenario is envisaged as above, it was not possible to come up with a parameter such as factor of safety to define the triggering mechanism in a quantitative manner.

(b) Factor of Safety Against Flow Slide

The flow-type failure will be induced in loose sandy deposits, if the magnitude of the residual strength is equal to or smaller than that of the shear stress induced by the gravity force. It is to be mentioned here that, among several external agencies, the gravity-induced stress would be the main force driving the soil mass to move downhill. If the soil deposit were in a loose state exhibiting the contractive behaviour with a residual strength which is smaller than the gravity-induced shear stress, then the soil mass would continue to move downwards leading to the follow-type slide. The deviator stress, q_0 , applied initially to a soil element at a depth of H under the submerged slope is evaluated, as follows, with reference to Eq. (8).

$$q_0 = \sigma'_{1C} - \sigma'_{3C} = 2\gamma'H \sin \alpha \quad (10)$$

The residual strength, S_{US} , in the soil after it has been deformed largely is known to depend on the void ratio, but if the largest normalized residual strength, $S_{US} / \sigma'_{1C} = 0.26$, within the range of contractive behaviour is taken up for consideration, residual strength would be estimated with reference to Eqs. (5) and (8) as

$$S_{US} = \frac{q_{QS}}{2} \cdot \cos \phi_S = 0.26\sigma'_{1C} = 0.26\gamma'H(1 + \sin \alpha) \quad (11)$$

The factor of safety against the flow deformation may be defined as the ratio between the deviator stress q_{QS} at the steady state and the initial deviator stress q_0 as illustrated in Figure 22. With reference to the definition given by Eq. (3), the deviator stress $q_{QS} = q_S$ is expressed as $q_S = 2S_{US} / \cos \phi_S$ and the initial deviator stress is given by $q_0 = \sigma'_{1C} - \sigma'_{3C} = 2\gamma'H \sin \alpha$ from Eq. (8). Thus, the facto of safety against flow is expressed as

$$F_s = \frac{q_{QS}}{q_o} = \frac{S_{US}}{\gamma' H \sin \alpha} \cdot \frac{1}{\cos \phi_s} \quad (12)$$

Introducing Eq. (11) into Eq. (12), one obtains

$$F_s = 0.26 \frac{1 + \sin \alpha}{\sin \alpha} \cdot \frac{1}{\cos \phi_s} \quad (13)$$

The factor of safety thus defined is shown plotted in Figure 29 (a) versus the angle of slope α and versus the K_C -value as evaluated by Eq. (9). Individual values F_s obtained from the TC-tests are indicated by circles and those from the TE-tests are indicated by rectangles.

The plot of Figure 17 showing the relation between K_C -value and S_{US} / σ'_{1C} is reproduced in Figure 30 where the value of void ratio is indicated for each value of $S_{US} / \sigma'_v = 0.04, 0.09, 0.15$ and 0.26 .

It is known from plot of Figure 30 that if the relative density in-situ is assumed to have been $D_r \cong 60\%$ corresponding to $e \cong 0.84$, the residual strength ratio would have been $S_{US} / \sigma'_{1C} \cong 0.15$. For this value, the factor of safety is obtained simply by changing the coefficient in Eq. (13) from 0.26 to 0.15. The relation between F_s and K_C for such a case is also shown in Figure 29 (a). The zone enclosed by these two curves is indicated by dark color. In the same fashion, the zone corresponding to the residual strength ratio between 0.15 ($D_r \cong 60\%$) and 0.09 ($D_r \cong 58\%$) is shown in Figure 29(b). The factor of safety corresponding to smaller value of $S_{US} / \sigma'_{1C} \cong 0.04$ to 0.09 is shown plotted against K_C -value in Figure 29 (c).

10. CONSIDERATIONS FOR INSTABILITY OF UNDERWATER SLOPES IN JAMUNA RIVER BRIDGE SITE

As mentioned in the foregoing section (see Figure 4), the angle of underwater slope in the Jamuna River excavation was 1:3.5 in the upper and lower parts on the permanent slope and 1:5.0 in the middle portion. The slide took place on Dec. 3, 1995 at the cross section 1480, 1500, 1550 within the zone of W3 (see Figure 3) and cross section 1800 in W4 on Dec. 15, 1945. These are shown in Figure 23 to 26. The slide on the temporary slope occurred in April and May in 1996. Cross section for these slides is shown in Figure 27 and 28.

There are no reliable test data available to assess the relative density of the field deposit in the Jamuna River bed, but judging from the nature of fluvial sediments and from the SPT and CPT data, it is envisaged as shown in Figure 6 that the relative density may be around $D_r=50\%$ and more likely less than $D_r=60\%$. With this assumption in mind, the residual strength of the sand in Jamuna River may be estimated roughly from the diagram of

Figure 30 in which the normalized residual strength is indicated in terms of void ratio or relative density.

It might be difficult to assess the normalized residual strength only by way of relative density but if attention is paid to the range in the normalized 0.26, this value seems to be in an appropriate range which is acceptable in the light of many data on other sands ever obtained. Under the consideration as above, it may conclusively mentioned that, (1) for the slope with 1:3.5, the factor of safety could easily be less than 1.0 for the Jamuna River bed sand with the normalized residual strength less than about $S_{US} / \sigma'_{1C} = 0.26$ which could most likely to be the case, and (2) for the slope with 1:5.0 slope, the value of S_{US} / σ'_{1C} with $F_s=1.0$ could be read off from Figure 29(a) as being about 0.15 which could be the case if there exist loose zones in in-situ deposit.

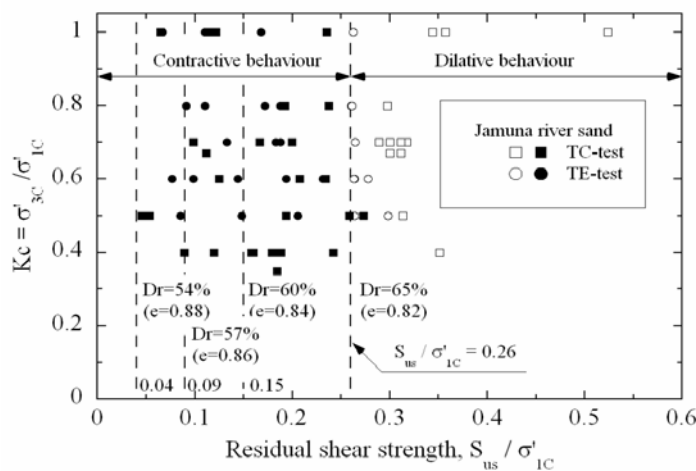


Figure 30: Void ratio versus the normalized residual strength

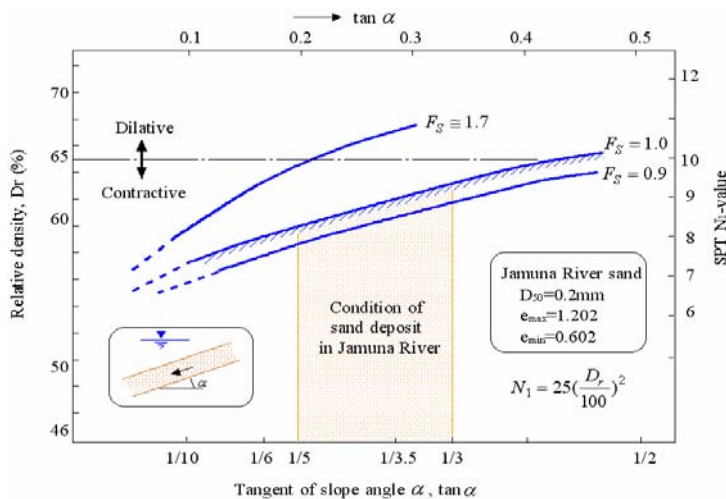


Figure 31: Relation between density, SPT N-value and slope angle for given factor of safety

The outcome of the evaluation as described above is summed up in the diagram of Figure 31 where the lines giving a factor of safety $F_S = 0.9$, 1.0 and 1.7 are indicated in terms of slope angle α and relative density. For reference sake, SPT N-value converted by the empirical relation is demonstrated in the ordinate of Figure 31 with the scale indicated on the right-hand side. Eq. (14) is quoted from the study by Cubrinovski and Ishihara (1999) by assuming that $e_{\max} - e_{\min} = 0.60$. The N_1 -value in Eq. (14) indicates the SPT N-value corresponding to an overburden pressure of 1kg/cm^2 and also about 80% of the theoretical energy in hammer hitting. Drawing attention to the line $F_S = 1.0$ in Figure 31, one may recognize that for the slope angle between 1:5.0 and 1:3.0, the factor of safety estimated lies in the zone of instability with $F_S < 1.0$ assuming the relative density smaller than about 62%.

$$N_1 = 25\left(\frac{D_r}{100}\right)^2 \quad (14)$$

In view of the actual conditions in the field at Jamuna River as described in the foregoing sections, the results of the simple analysis summarized in Figure 31 would appear to provide evidences with a reasonable level of credibility for the occurrence of the underwater slides on the excavated slopes in Jamuna River.

11. CONCLUSIVE REMARKS

The failure of the underwater slopes during the dredging excavation in the sand bar in Jamuna River in Bangladesh was introduced first and then some speculative reasons for such slips to have occurred were pointed out. To provide sound basis for interpretation of failure mechanism, results of multiple series of triaxial test in the laboratory were introduced with the framework of consistent concept in line with the test results on other sands in Japan. The main points derived from the tests are summarized as follows.

1. It is known that the sand initially consolidated with higher degree of anisotropy, that is, with a smaller K_C -value, tends to exhibit more contractive (or collapsible) behaviour when it is deformed largely into a steady-state. To take into account of this effects, it was found more appropriate to select the major initial principal stress, σ'_{1C} , not the mean initial principal stress, $p'_C = (\sigma'_{1C} + 2\sigma'_{2C})/3$, as an index parameter to express effects of confinement. Thus, when the residual strength S_{US} at the steady state is normalized to the major principle stress, σ'_{1C} , it takes a constant value irrespective of K_C -conditions.
2. Thus, the normalized residual strength S_{US}/σ'_{1C} can be expressed uniquely as a function of relative density or void ratio. Within the range of relative density where the behaviour is contractive, the upper limit of the normalized residual strength for the Jamuna

River sand is $S_{US} / \sigma'_{1C} = 0.26$ and this value is encountered when the sand is deposited at a relative density less than approximately $Dr=65\%$. On the basis of the SPT and CPT data, the in-situ relative density at the site of Jamuna River was found to be somewhere around $Dr=50\%$ which is less than 65%. This fact implies that the in-situ deposit is within the range of density where the sand exhibits contractive behaviour indicating high susceptibility to flow type deformation once the slip is triggered.

3. On the other hand, the slope angle of dredged channel in Jamuna River at the time of sliding is known to have been 1:3.5 ($\cong 16$ degree) and 1:5.0 ($\cong 11.31$ degree). By assuming the slides to have occurred on the straight-line sliding plane which is parallel to the surface of the slope, it was possible to assess the magnitude of shear stress and the major principal stress σ'_{1C} which was mobilized in the sand deposits in the slopes excavated with the angle of 1:3.5 and 1:5.0.
4. By comparing the magnitude of shear stress assessed as above with the value of residual strength evaluated from the laboratory tests, it was found that the existing shear stress must have become greater than the residual strength available at the riverbed deposit, if the in-situ sand were deposited with a relative density in the range less than about 60%.
5. It is to be noticed here that for other sands in Japan, the upper limit of density showing contractive behaviour is, by and large, smaller than $Dr=50\%$. This implies that only loosely deposited sand with a relative density less than 50% could develop flow type deformation and therefore such a sand is identified potentially more stable. In contrast, with a higher value of upper-limit density such as the mica-containing Bangladesh sand, the likelihood is high for in-situ deposits to exist with a relative density less than the upper limit. Thus, such sand is to be identified as potentially unstable. In the sense as above, the identification of the upper limit density or threshold density differentiating between conditions of contractive and dilative behaviour of a given sand will pose an important challenge in future development in this area of soil mechanics.

ACKNOWLEDGEMENTS

The study described in this paper was initiated by the first author who paid a visit of inspection to the Jamuna River site upon recommendation by Professor W. Van Impe, Past president of ISSMGE. The engineers of HAM-van Oord were kindly showed the author around the site. The triaxial tests in the laboratory were carried out by Mr. Y. Nakayama and T. Shibayama who were graduate students at the Tokyo University of Science. The authors wish to express their sincere gratitude to the persons cited above.

REFERENCES

- Chern, J.C. (1985), Undrained Response of Saturated Sands with Emphasis on Liquefaction and Cyclic Mobility, Ph. D. Theses, University of British Columbia, Vancouver.
- Cubrinovski, M. and Ishihara, K. (1999), Empirical correlation between SPT N-value and Relative Density for Sandy Soils, *Journal of the Japanese Geotechnical Society, Soils and Foundations*, Vol. 39, No. 5, pp. 61-71.
- Hight, D. W., Georgiannou, V.N., Matin, P.L. and Mundegar, A.K. (1999), Flow slides in Micaceous Sands," *Proc. International Symposium on Problematic soils, Sendai, Japan*, Vol. 2, pp. 945-958.
- Ishihara, K. (1996), *Soil Behaviour in Earthquake Geotechnics*, Oxford Clarendon Press, pp. 259-260.
- Ishihara, K., Tsukamoto, Y. and Shibayama, T. (2003), Evaluation of Slope Stability against Flow in Saturated Sand, *Reports on Geotechnical Engineering, Soil Mechanics and Rock Mechanics*, Vol. 5, Jubilee Vol. of 75th Anniversary of K. Terzaghi's *Erdbaumechanik*, pp. 41-54.
- Kato, S., Ishihara, K. and Towhata, I. (2001), Undrained Shear Characteristics of Saturated Sand under Anisotropic Consolidation, submitted to *Soils and Foundation*, Vol. 41, No. 1, pp. 1-11.
- Kramer, S.L. and Seed, H.B. (1988), Initiation of soil Liquefaction under Static Loading Conditions, *Journal of Geotechnical Engineering Division, ASCE*, Vol. 114, No. 4, pp. 412-430.
- Seed, H. B., Seed, R.B., Schlosser, F., Blondeau, F. and Juran, I. (1988), The Landslide at the Port of Nice on October 16, 1979, Report No. UCB/EERC-88/10, University of California, Berkeley.
- Tsukamoto, T., Ishihara, K. and Kamata, T. (2007), Residual Strength of Soils under Flow Deformation in Triaxial Tests, submitted to a journal.
- Vaid, Y.P. and J.C. Chern, J.C. (1985), Cyclic and Monotonic Undrained Response of Saturated Sands, *Advances in the Art of Testing Soils under Cyclic Condition, Proc. of ASCE Convention in Detroit, Michigan*, pp. 120-147.

DISTRESS IN THE TARMAC AT NEWLY OPENED SUVARNABHUMI AIRPORT

WORSAK KANOK-NUKULCHAI
Dean of the School of Engineering & Technology
Asian Institute of Technology
worsak@ait.ac.th

ABSTRACT

The investigation by Engineering Institute of Thailand (EIT) revealed that the damage was caused by the premature failure of asphalt base course due to the separation of asphalt binder from aggregate surface in the presence of moisture, commonly known as "stripping". It was quite evident from the milled damage area that water seeped from the sand blanket underneath the cement-treated base (CTB) through expansion joints. The core samples of the asphalt concrete pavement from damaged area show evidence of asphalt stripping at the base course, a typical effect of soaking water, while core samples from undamaged areas show good condition. In order to prevent further distress in the Tarmac, as the airport site is located in the floodway of Bangkok's eastern suburbs, it requires both effective flood protection and drainage systems to avoid problems caused by water seepage into the sand blanket under the airport's taxiways and runways.

1. INTRODUCTION

Last October, when the first sign of rutting was spotted in five of the six taxilanes and in one taxiway at the Suvarnabhumi International Airport, the Engineering Institute of Thailand (EIT) assigned a team of experts to join the preliminary investigation. The investigation revealed that the damage was caused by the premature failure of asphalt base course due to the separation of asphalt binder from aggregate surface in the presence of moisture, commonly known as "stripping". It was quite evident from the milled damage area (Figure 1) that water seeped from the sand blanket underneath the cement-treated base (CTB) through expansion joints.

The key question is: How, and also how long, has the water been trapped in the sand blanket?

This article intends to provide technical facts to the readers who want to understand what really happened to the airfield pavement of this brand new airport.



Figure 1: Milled asphalt at the damaged Area

2. WORRYING OBSERVATIONS

On 27 October 2006, about 2-3 weeks after the official opening of the airport, the first signs of distress were spotted at several locations in the taxiways and taxilanes, in the form of rutting, rutting with shattering and split, and rutting with hairline cracks (Figure 5). Since then, a similar pattern of failure has developed heavily in five of the six taxilanes and along the east parallel taxiway. Although both runways are still in good structural condition, plastic deformation of the asphalt wearing course was observed near the takeoff position. The extent of the damage is summarised in Figure 2.

Summary of Pavement Damage as of 25 January 2007

Airfield Pavement	Area (sq m)	Distressed Area (sq m)	Locations	Typical Damage
1 West Runway	295,500	15	Taxiway Curved	Wearing course plastic deformation
2 East Runway	318,000	78	Junction	Wearing course plastic deformation
Total Areas	613,500	93		Damage area = 0.00015%
3 West Taxiway	724,868	800	E13, E21	Rutting, cracks or shattering
4 East Taxiway	572,956	18,081	B, B2, B5	Rutting, cracks or shattering
5 Cross Taxiway	217,706	23,673	G	Rutting, cracks or shattering
6 Taxilane	303,086	54,046	T4,T5,T8, T11-T15,T17	Rutting, cracks or shattering
Total Areas	1,818,616	96,693		Damage area = 5.31%



Figure 2: Illustration of taxiways and taxilanes



Figure 3: Overview of east runway, taxiways and the drainage system

Suvarnabhumi airport covers an area of 20,000 rai (3,200 hectares). In its first phase, the airfield serves its hourly 112 flights with two runways, six taxiways and six taxilanes (Figure 3). The tarmac (Figure 4) consists of three layers of asphalt concrete, namely the base course (23 cm thick), the binder course (6 cm thick), and the wearing course (4 cm thick). Underneath are four layers of the cement-treated base (CTB), 18 cm. thick each, sitting on top of the sand blanket (approximately 80 cm thick) left over from the ground improvement process.

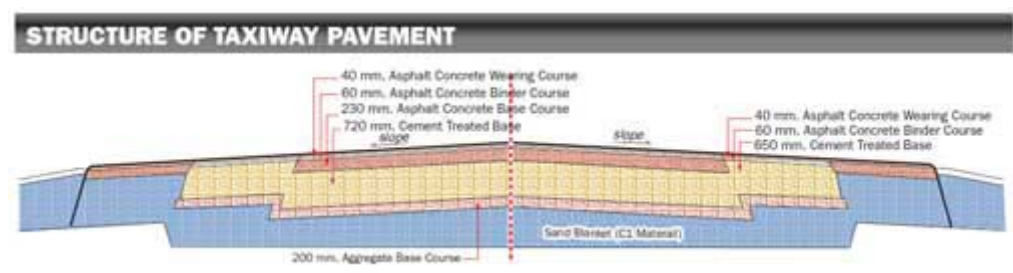


Figure 4: Structure of taxiway pavement

Plastic deformation was observed on the wearing course at the turn-around segment of the taxiway leading to the takeoff position of the runway (Figure 6). This location is normally under maximum load when the plane takes off with a full load of fuel. The high shearing stress that causes plastic deformation was imposed by braking, accelerating or turning traffic. Plastic deformation is greatest at high temperatures, especially for the AC 60/70 binder grade used in this case. The occurrence of the plastic deformation at this location is therefore a common phenomenon and only routine maintenance is required to repair this type of distress. Aside from this surface distortion, both runways are in good structural condition.



Figure 5: Typical distress in the taxiways and taxilanes.



Figure 6: Surface deformation of the runway.

Initial investigation was made by coring the asphalt concrete pavement at a diameter 100 mm throughout its 33 cm thickness from the damaged areas (Figure 3). The following observations can be made:

- All core samples from damaged area show evidence of asphalt stripping at the base course, a typical effect of soaking water, while core samples from undamaged areas show good condition.
- The water had infiltrated into and confined in the asphalt concrete base course for a long period. Thus, the base course has been immersed in and impaired by the water.
- As a result of asphalt stripping, asphalt binder was separated from aggregate surface, leading to premature loss of strength and stability of the base course.
- The load of the aircraft had then impaired the failed asphalt concrete pavement, causing rutting on the surface.

Based on the core samples, laboratory tests have indicated the correct job mix and aggregate gradation of the asphalt concrete material. This was also confirmed by a separate test at the Highway Department.

To expose the cement-treated base (CTB) for visual inspection, an area of asphalt concrete pavement was milled at the damaged area of the taxiway. It was evident that there was no sign of damage or subsidence in the CTB. However, traces of water seepage were clearly observed (Figure 7) along the rim of the expansion joints in the CTB. This evidence of seepage further hinted that a large quantity of water might still be trapped in the sand blanket.

Opening of the Distressed Pavement Structure

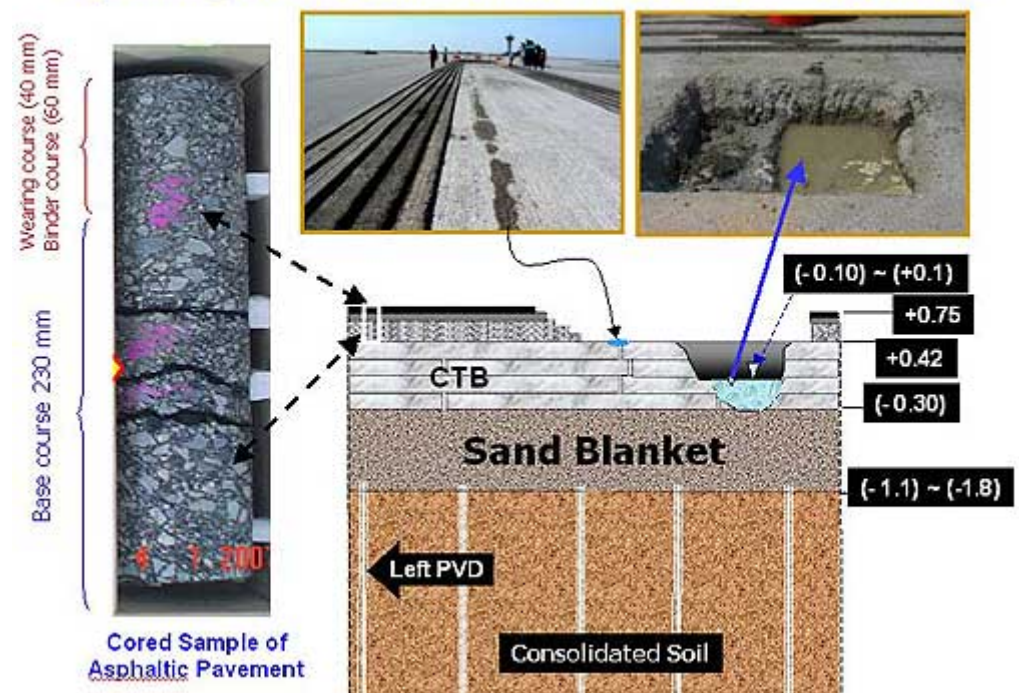


Figure 7: Illustration of milled pavement in the taxiway T11, a core sample of asphalt concrete, trace of the water seepage at CTB joint and the test pit.

On January 31, a test pit (Figure 7) was dug on Taxiway T11, where damage was found to be extensive. After the excavation went through CTB and exposed the top surface of the sand blanket, water seeped through the sand immediately until the water level reached about 20 cm above the sand blanket (or roughly at $+0.0$ MSL). The water stayed at that level even when attempts were made to clear the water.

Interestingly, to prove that water in the sand blanket is fully confined with no connection outside, a deep excavation was made nearby, but outside the pavement area (Figure 8). After the excavation, the dug hole was completely dry. No sign of water from the sand blanket had receded into this empty hole.

Meanwhile, Highway Department experts have tested the samples of sand and CTB from this test pit and reported that all materials tested have met the standards.



Figure 8: Excavation to test the connectivity of the trapped water

3. HOW WAS THE WATER TRAPPED?

Based on the official report of the investigation committee appointed by Airports of Thailand Public Company (AOT), the following reasons had been given for the trapped water:

1. Runoff of rainfall water was collected and retained within the airport compound in the pockets of sand used to fill fishponds, swamps and waterways prior to the airport construction. Water from this source might find its way into the sand blanket.
2. Surface water spilled from the drainage canals, during the flooding period, over the top soil around the unpaved neighbourhood into the sand blanket.
3. Surface water once trapped underground was not able to escape due to the lack of a subsurface drainage system. This was aggravated by the blockage of culverts and other underground structures.
4. Based on soil boring records, thin sand layers may exist originally within the soft clay layer at a level about 10 metres deep. Some of these sand layers may cross path with the leftover PVD, thus allowing running shallow ground water to seep upward into the sand blanket.

On the last point, some geotechnical experts argued against this possibility. At the end of the PVD preloading, the extra surcharge consisting of crushed rocks was removed. Thus, it is no longer possible for water to move up to the surface through the PVDs against the hydraulic gradient and against gravity at the end of consolidation process.

In addition, there is hydraulic back-pressure from the trapped water in the sand blanket making it impossible for such hydraulic upward flow to occur.

Because the airport site is located in the floodway of Bangkok's eastern suburbs, it requires both effective flood protection and drainage systems. The aim is to prevent flooding from flash floods, as well as to drain away rainwater in the catchments of the airport compound. The design of the polder system includes the perimeter polder dike, internal drainage system, two pumping stations and a perimeter road (Figure 9).

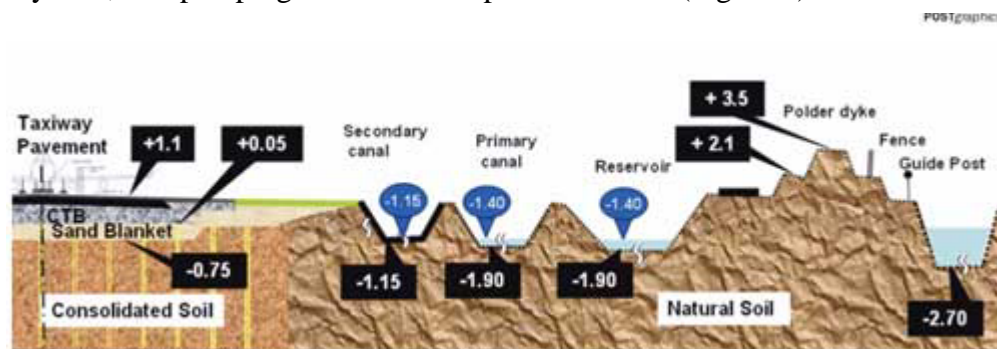


Figure 4: Profile of the flood protection and the drainage system.

Figure 9: Profile of the flood protection and the drainage system.

Basically, the internal drainage system for runoff water consists of:

1. The unlined primary canals and reservoirs both with the bed at -1.90 m MSL. Based on the design criteria, water level in the primary canals and reservoirs must be maintained not higher than -1.40 m MSL.
2. The secondary canals with concrete linings. The canal bed of the secondary canal is -1.15 m MSL. It is designed to be dry except during the raining.

The primary and secondary canals are interconnected by ditches to ensure that the runoff water from the pavement area will flow under gravity towards the two pumping stations located at the south corners of the site. In the operating manual, water in the primary canals and reservoirs must always be controlled at the pumping stations to ensure that the water level is maintained at -1.40 m MSL or lower.

With the design assumption that no rain water runoff can leak into the sand blanket, no subsurface drainage system exists to systematically drain trapped water from the sand blanket. This might be a weakness in the design criteria of the airfield pavement.

4. GROUND IMPROVEMENTS

Suvarnabhumi Airport compound is situated on formerly agricultural land, fish farms, swamps and waterways. A thick deposit of soft clay is found over 10 metres deep, with 100-120% water content, on top of medium stiff clay and stiff clay with water content of 50-90% and less than 50% respectively.

Soil is a multiphase system, comprising a solid phase (soil particles) and a fluid phase (air and water) called the pore fluid. For soft clay, the higher the volume of the fluid phase, the weaker and more compressible the soil mass. Therefore, any reduction of water in the pores of the soil, which decreases the volume of the soil mass (Figure 10) and subsequently increases the particle-to-particle contact, increases the strength of the soil and reduces its compressibility at service stage.

To be suitable for airfield pavement, pore water in the soft soil must be squeezed out to result in water content around 80%. Thus, the soft clay is transformed into medium stiff clay. This consolidation process can be accelerated by a modern technique using Prefabricated Vertical Drains (PVD).

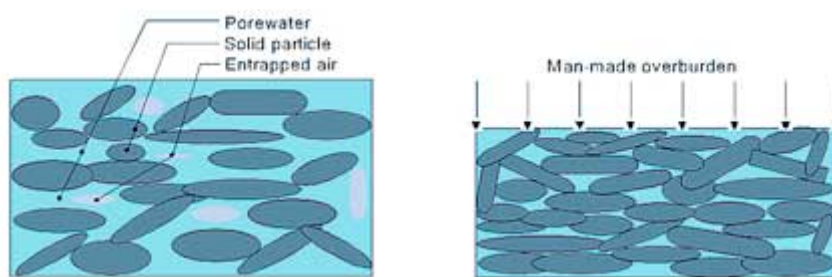


Figure 10: Natural and consolidated soft clay deposits.

PVD is a plastic tube core wrapped in a filter jacket, made of non-woven polyester or polypropylene geotextiles or synthetic paper. PVDs drain soil by squeezing out pore water, a process that can be accelerated by adjusting the spacing of PVDs. In this process, water flows a lot more quickly horizontally towards the drain and then vertically along the drains towards the permeable drainage layer at the top. The step-by-step procedure of consolidation using PVD is illustrated in Figure 11.

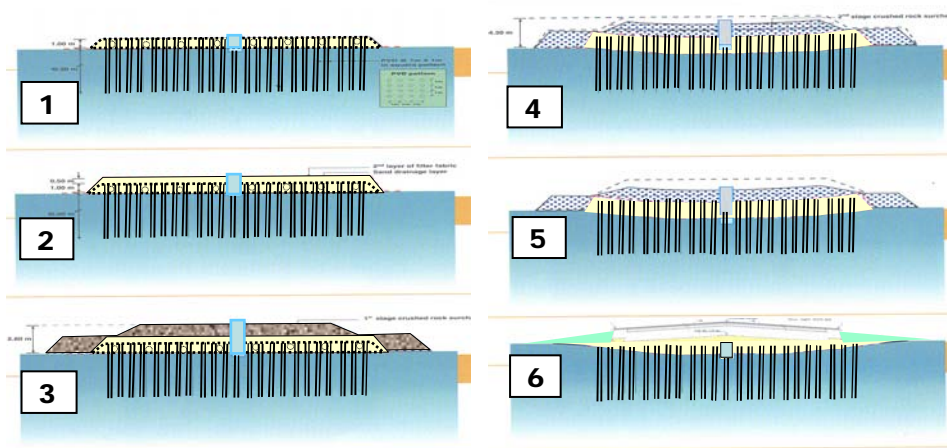


Figure 11: Consolidation process of soft clay under the airfield pavement

5. WHAT'S NEXT?

In its press release issued on 15 February 2007, the Engineering Institute of Thailand (EIT) strongly recommended that, similar to a first-aid treatment, trapped water should be drained out urgently to minimise the potential spread of cracks on taxi lanes, taxiways, and even on runway. This immediate action should be carried out with the consent and cooperation of all concerned parties including the project management consultants, the designers and the contractors.

Alternatively, the AOT should seek temporary protection from the court to implement the required first-aid treatment without damaging its rights under the contract. Meanwhile, it was reported that the AOT plans to commission a team of international experts to carry out an in-depth technical investigation in order to recommend long-term remedies.

SAFETY PROBLEMS RELATED TO DETERIORATION OF CONCRETE STRUCTURES

TAKETO UOMOTO
Professor, Civil Engineering Department,
Faculty of Engineering, Shibaura Institute of Technology, Japan
uomoto@sic.shibaura-it.ac.jp

ABSTRACT

The maintenance of concrete structures is essential and important to maintain the safety of urban area. Most of the political, economical and educational activities of a country are concentrated in urban area. If any accident or hazard occurs, the effect is tremendous. Concrete structures are durable and people easily forget about the durability aspects of concrete structures. It is very important for both the owners and engineers to recognize how important it is to maintain concrete structures to keep the people safe in urban area. Before any accident of hazards happens, we should keep eyes to the maintenance of concrete structures. This paper describes what we are doing in Japan to maintain the existing concrete structures.

1. INTRODUCTION

Up till now in Japan, the economic growth was rapid in the period of 1960 ~ 1980. More than 100million cubic meters of concrete were used to construct the structures such as buildings, bridges, tunnels, dams, etc. to support the activities of Japanese people. As a result, these infrastructures rapidly reached 50 years in service, and due to deterioration of the structures, maintenance of these structures has become a major interest among the owners and the civil engineers.

On the other hands, population of Japan will reduce from now on because of fewer babies in a family approximately 1.2 children per one family. Although high technologies have been developed in recent years, it is sure that fewer engineers have to take care of the huge amount of structures from now on, which has never experienced in the past. Due to reduction in the economical growth, the budget for both construction and maintenance will be reduced in the future. The maintenance of existing structures must be done with the following conditions: 1) rapid increasing of the amount of existing structures reaching to the age of 50 years, 2) less amount of engineers to maintain the structures, 3) less amount of budget can be used to maintain the structures. .

Although there are many hazards in each country, concrete structures are expected to be safe for long period of time. Main hazards for the structures in Japan are as follows:

1. Earthquake and volcanic action
2. Landslide and flood
3. Typhoons and strong wind
4. Fire and Thunder
5. Accidents
6. Terrorism

If the structure is deteriorated before the hazards, the structure may easily collapse and difficult to maintain the safety of the people. The Figure 1 shows an example of a collapsed pier during Hanshin Awaji Great Earthquake. As shown in the photo, the pier was deteriorated to large extent due to alkali aggregate reaction. Concrete is cracked severely and is just like a bundle of concrete blocks.



Figure 1: Collapsed reinforced concrete pier affected by alkali aggregate reaction

In order to keep the safety of urban area, it is important to study and investigate not only on hazards but also on durability aspects of existing structures. Even a small amount of concrete spalling may cause traffic accidents to large extent as we experienced in Sanyo-Shinkansen in 1999.

Considering these situations now, this paper explains what is happening now in Japan and how we are dealing with the problems through researches and engineering.

2. GENERAL MAINTENANCE METHODS BEING USED UP TILL NOW

The maintenance of concrete structures has been done mostly by the owners of the structures. In case of public structures, the ministries, etc. maintain the structure after the structures are completed. For the time being, the

methods for the maintenance differ according to the owners of the structures. Although there are some differences, the main concept of the maintenance can be summarized as follows (Uomoto and Misra, 2001):

1. Periodic inspection and evaluation of deterioration degree
2. Detailed inspection and decision making
3. Repairing and strengthening of deteriorated structures

For periodic inspections, the inspectors inspect the structures visually, sometimes with the help of binoculars and hammers, once a year or once in several years according to the importance and time after the structure is completed. The inspectors are mostly trained engineers with experiences. The detailed inspection is done when the estimated degree of deterioration exceeds certain limit, or when some new phenomenon is found during the periodic inspection. The detailed inspection is done by visual inspections with the aid of non-destructive tests or taking core samples out from the inspected structure. The purpose of the inspection is to decide the cause of the deterioration and also to evaluate whether repair and/or strengthening is needed or not.

To repair or strengthen the existing structures, it is important to design and select sufficient methods and materials. The most popular repair method for corrosion of steel bars due to carbonation is to eliminate the carbonated concrete and replace it by new concrete and apply coatings with and without FRP sheets. But in case of steel corrosion due to chlorides from the surrounding environment, the highly chloride concentrated portion of concrete are taken out, anti-corrosive treatment is applied to the surface of the bar, and polymer cement mortar is generally used to repair the concrete before coating the concrete surface.

3. NEW STANDARD SPECIFICATIONS OF JSCE

After the investigations of many deteriorated concrete structures, the importance of durability was fully recognized by the civil engineers. To deal with the problem not only JSCE, AIJ, and JCI recommending methods to deal with the problems but also the Ministries, and other authorities started to propose practical counter measures to cope with the situation. As a result, a large amount of researches has been done related to the durability of concrete structures including non-destructive inspection methods.

Among these authorities, the Concrete Committee of JSCE, the leading committee in the field of concrete in Japan, has published the translated version of “Standard Specifications for Concrete Structures-2002” in English to deal with the problems of durability (JSCE, 2005a, 2005b and 2005c). The concept written in the specifications will surely be adopted by other institutions.

The main proposals of the “Standard Specifications” are the following two items:

- 1) Propose a new method to design and construct new concrete structures that can be used for specified lifetime without large amount of maintenance cost.
- 2) Propose an effective and economical system to maintain existing concrete structures with small number of engineers and workers.

To deal with the problems for the items 1) and 2), the following two Specifications are published:

1. The Standard Specification for Concrete Structures-2002 “Structural Performance Verification” (JSCE, 2005a)
2. The Standard Specification for Concrete Structures-2001 “Maintenance” (JSCE, 2005b) and
3. The Standard Specification for Concrete Structures-2002 “Materials and Construction” (JSCE, 2005c)

The concepts of the new Standard Specifications are briefly explained in the following chapters.

3.1 Durability design of concrete structures for new structures

Performance-based durability design was introduced to “Standard Specification of Concrete Structures” by the Concrete Committee of JSCE in the year 2000 and be translated to English version in 2005 (JSCE, 2005c). Although durability of concrete structures was considered important in the previous specifications, performance-based design method was not used. The previous specifications described the importance of durability by proposing that the concrete structures are durable for a long time when specified materials, mixes, covers, etc. are used. But these specifications did not mention about the duration of service time, etc.

The proposed performance-based new durability design can be summarized as follows:

1. The concrete structure must be quantitatively checked whether the structure possesses required performance within the designed period.
2. The degree of deterioration of the structure in service on specified cause must be specified.
3. To maintain the structure above the specified degree of deterioration, the required performance must be specified.

To examine the performance on durability, a kind of limit state design scheme was introduced for the durability of concrete structures. The equation can be written as shown in Equation (1):

$$\gamma_i \cdot A_d / A_{lim} \leq 1.0 \quad (1)$$

Where, A_d is designed performance of the structure at specified time considering the specified deterioration cause, A_{lim} is limit of the performance of the structure, and γ_i is coefficient of the structure considering the importance, etc.

Generally, performance of concrete has to be verified to satisfy the required performance. Not only resistances against deterioration but also mechanism properties of concrete have to be verified as shown below (JSCE, 2005c).

1. Compressive strength
2. Carbonation rate
3. Diffusion coefficient of chloride ions in concrete
4. Dynamic modulus of elasticity
5. Resistance to chemical attack
6. Resistance to alkali aggregate reaction
7. Coefficient of water permeability of concrete
8. Fire resistance
9. Adiabatic temperature rise
10. Drying shrinkage characteristics
11. Setting characteristic

The Figure 2 shows an example of the calculated result for minimum cover thickness to prevent carbonation induced corrosion at different years of service for OPC concrete and BFSC concrete. As shown in the figure, the cover thickness required changes according to the type of cement to be used, water-cement ratio of concrete, years of service and exposed condition (wet or dry) of the structure to be constructed. When the structure is designed for long period of time, the cover thickness may become too large, and it is recommended to use other countermeasures such as Epoxy-coated bars.

3.2 Methods of maintenance newly proposed by JSCE (JSCE, 2005b)

The methods used in the new Standard Specification are basically the same as the conventional method. The differences are that the new method requires to maintain the structure within their required performances throughout their service life. Firstly, the listed below issues have to be clearly specified.

1. To maintain a structure, performances required for the structure must be clearly defined.
2. The performances required for general structures are “safety”, “serviceability”, “hazards to the public”, “aesthetics and landscape” and “durability”.

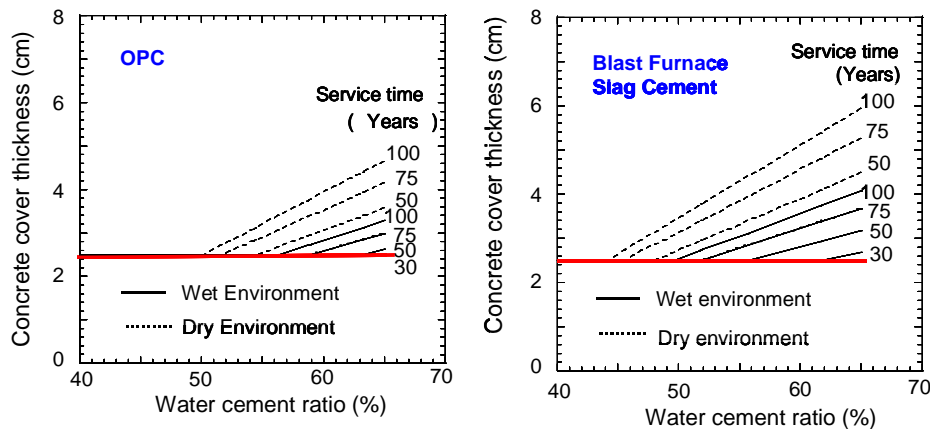


Figure 2: Calculated results of concrete cover according to JSCE Standard Specification (JSCE, 2005c)

And the basic principles of maintenance works are as follows:

1. Structures must be maintained according to a designated maintenance category by formulating a maintenance program to retain the performance within the specified tolerances throughout their service life. And maintenance system includes adequate “initial inspection”, “deterioration prediction”, “inspection”, “assessment/judgment”, “remedial action”, and “record”.
2. To maintain a structure, in addition to the assessment and evaluation at the time of inspection, assessment and evaluation must be made throughout the service life of the structure based on prediction of deterioration.
3. To predict the deterioration, required performances of the structure must be clearly defined, and also the design service life must be made clear.
4. The records on design, construction, initial inspection, deterioration prediction, periodical inspection, assessment and/or evaluation, and remedial actions must be kept throughout the service life.

Standards for maintenance of concrete structure deteriorated by different mechanisms are also discussed. The lists below are the standard maintenance method published in this standard:

1. Standard maintenance method for carbonation induced deterioration
2. Standard maintenance method for chloride induced deterioration
3. Standard maintenance method for frost attack
4. Standard maintenance method for chemical attack
5. Standard maintenance method for alkali aggregate reaction

6. Standard maintenance method for fatigue of RC slab of road bridge
7. Standard maintenance method for fatigue of RC beam of railway bridge

In detail for an example, the standard method for chloride induced deterioration recommends the model to predict chloride ion diffusion, progress of steel corrosion, and correction of the prediction. Also the methods of initial inspection, routine inspection, periodic inspection, and detailed inspection as well evaluation and judgment method are also discussed. Finally, recommendation of selection of remedial measurement both of repair or strengthening is given also the information has to be recorded.

One of the difficulties is how to predict the degree of deterioration at the end of their service life. There are several researches being done to predict the deterioration in numerical manner (JSCE, 2005b). In the published Standards, several numerical prediction methods are introduced as references for structures suffering cyclic fatigue loads, carbonation induced corrosion and chloride induced corrosion. In case of cyclic fatigue, S-N curves are used to predict the service life. In case of carbonation induced and chloride induced corrosion of steel bars, diffusion equations for carbon dioxide and chloride are used to predict the degree of corrosion. Using these prediction methods, deterioration degree can be estimated to certain degree. (See Figure 3) But for other deterioration problems, which has not been studied numerically, a quantitative model has not been proposed yet. To deal with the problem, a qualitative method “Grading method” is introduced in the Standard.

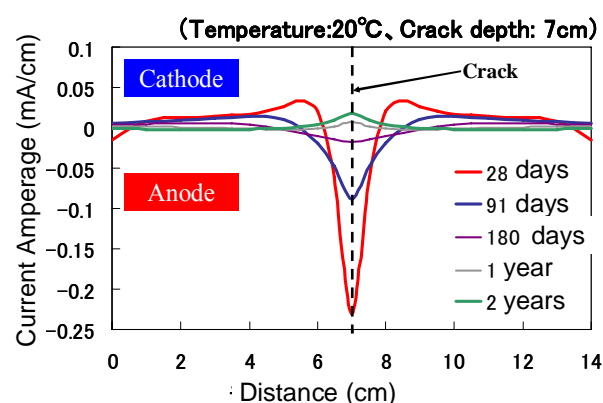


Figure 3: Quantitative prediction of corrosion in marine environment with cracks (Tsukahara et al., 2000)

4. PROBLEMS IN ACTUAL EXISTING STRUCTURES

When a civil engineer is asked by the owner to check the safety of an old existing structure, one of the largest problems is that there are neither drawings nor construction records of the structure available. No problem may occur in case of important facilities, which is maintained with great care. But in case of normal structures, the owners do not know the importance of these documents.

To deal with the problem, NDI is not enough. Fortunately, our structures are not too old, and they are mostly designed and constructed by the method specified by JSCE, AIJ or other associations. Considering these, the only way is to re-design the structure again using the methodologies used at the time of construction. Figure 4 shows an example of re-designed bridge pier constructed about 35 years ago. From the figure, it is much easier for a civil engineer to check the safety of the structure under several hazards. It will become more important for the owners and engineers to keep these documents throughout the service life of a structure.

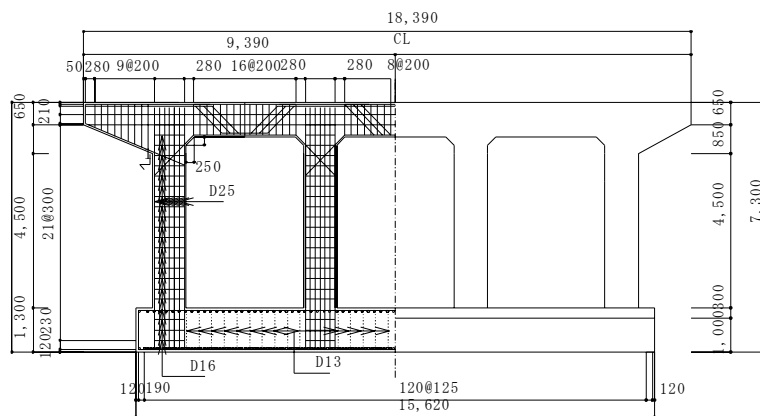


Figure 4: Re-designed reinforced concrete pier of a bridge (Okazaki, 2005)

5. CONCLUDING REMARKS

Engineering is not always complete, and further research works are needed. To sustain existing structures, durability of the structure is important. One good method is to construct durable structures, but for the existing structures maintenance is the only way to deal with the problem. Although concrete committee of JSCE has set up a good system for maintenance of existing concrete structures, there are still many things to be done: not only researches but also education to the students and engineers about durability and maintenance. I hope this paper may become a help to the concrete engineers of the world who are trying to design, construct and maintain concrete structures.

REFERENCES

- JSCE, 2005a. *Standard Specifications for Concrete Structures-2002 "Structural Performance verification"*. JSCE, Tokyo.
- JSCE, 2005b. *Standard Specifications for Concrete Structures-2001 "Maintenance"*. JSCE, Tokyo.
- JSCE, 2005c. *Standard Specifications for Concrete Structures-2002 "Materials and Construction"*. JSCE, Tokyo.
- Okazaki, S., 2005. *Development of monitoring system for RC bridge based on restoration design method*. Thesis submitted to the University of Tokyo for Master of Engineering degree.
- Tsukahara, E., Koyama, R., Hoshino, T., and Uomoto T., 2000. Estimation Method of Corroded Portion of Reinforcing Steel Bar by Natural Potential Measurement. *Non-destructive Testing in Civil Engineering 2000*, Elsevier.
- Uomoto, T., and Misra S., 2001. Role of Engineers to Improve Quality of Concrete Structures. *Proceedings of EASEC-8*, Singapore.

PROPOSAL OF A SUSTAINABLE TSUNAMI DISASTER MITIGATION SYSTEM FOR THE INDIAN OCEAN REGION

KIMIRO MEGURO¹ and MASASUKE TAKASHIMA²

¹International Center for Urban Safety Engineering
Institute of Industrial Science, The University of Tokyo, Japan

²Collage of Environment and Disaster Research
Fuji Tokoha University, Shizuoka, Japan

ABSTRACT

Triggered by a M9.0 earthquake that occurred along the Sunda Trench, Off-Sumatra, at 07:58 (local time), on December 26, 2004, a huge and devastating tsunami hit the Indian Ocean Rim countries, causing unprecedented disaster with over 300,000 dead and missing persons. The analysis of other potential tsunami scenarios in the region has revealed that 1.3 million dead and missing people may be expected, at worst. Therefore, an effective and sustainable framework against tsunami disaster is indispensable in this region.

Land use control, i.e. preventing people from residing next to the shore, is one way to mitigate tsunami disaster if people follow it. However, this is not always a proper option in the Indian Ocean Rim region where the economic activities, e.g. fishing, tourism, take place directly next to the seaside. For this case, a New Tsunami Disaster Mitigation System by combining a reliable warning system and proper evacuation facilities is proposed. Important characteristics of this system are its simplicity, economical efficiency and daily-usability.

This paper introduces the New Tsunami Disaster Mitigation System, highlighting its strengths and the works necessary for its implementation.

1. INTRODUCTION

Triggered by the M9.0 Earthquake that occurred along the Sunda Trench, Off-Sumatra, at 07:58 (local time), on December 26, 2004, a huge and devastating tsunami hit the Indian Ocean Rim countries, causing unprecedented disaster with over 300,000 dead and missing persons. The tsunami was triggered by one of the possible earthquake scenarios along the Sunda Trench. Four other potential earthquake events along the trench have been identified and the expected number of casualties in case they occur has been estimated. As a result, it was revealed that 1.3 million dead and missing people are expected, at worst, as shown in Figure 1. This number is several times larger than the observed in the December 26, 2004 event, showing that an effective and sustainable framework against tsunami disaster is indispensable in this region.

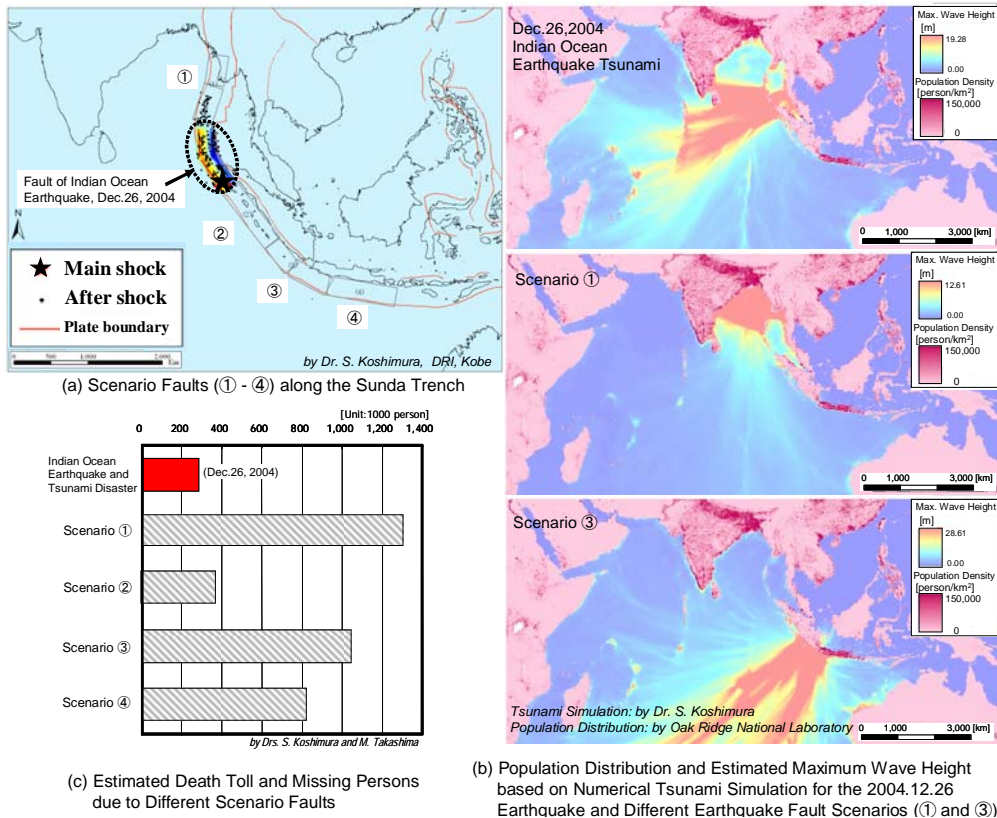


Figure 1: Estimated damage based on numerical tsunami simulation with possible fault scenarios along the Sunda Trench

Some countries along the Indian Ocean Rim have established a tsunami disaster mitigation system based on land use, i.e. prohibiting people inhabiting next to the seaside. Others are planning to adopt similar measures. Land use control is an efficient measure if people follow it. However, this is not always a proper option in case activities such as fishing and tourism, which are the pillars of the region economy, take place directly next to the shore. Under these conditions, it is inapplicable to implement land use control policies.

In the Pacific Ocean Rim region, tsunami disaster mitigation relies on a sophisticated warning system, which is used not only for disaster mitigation but also for earth science research. This system is costly in terms of both installation and maintenance. Furthermore, it requires a great deal of knowledge to operate it. Although it is very useful and appropriate for this area, where countries with financial and technological resources such as US and Japan are located, it is not applicable for the Indian Ocean region (Figure 2).

Taking the above mentioned points into consideration, a New Tsunami Disaster Mitigation System which combines a warning system suitable for the Indian Ocean region and proper evacuation facilities in terms of location, strength and sheltering capacity is proposed. With this system there is no need to relocate the people living along the seashore;

therefore, there is no impact on the local economies. The proposed system is simple, economically efficient and daily-usable.

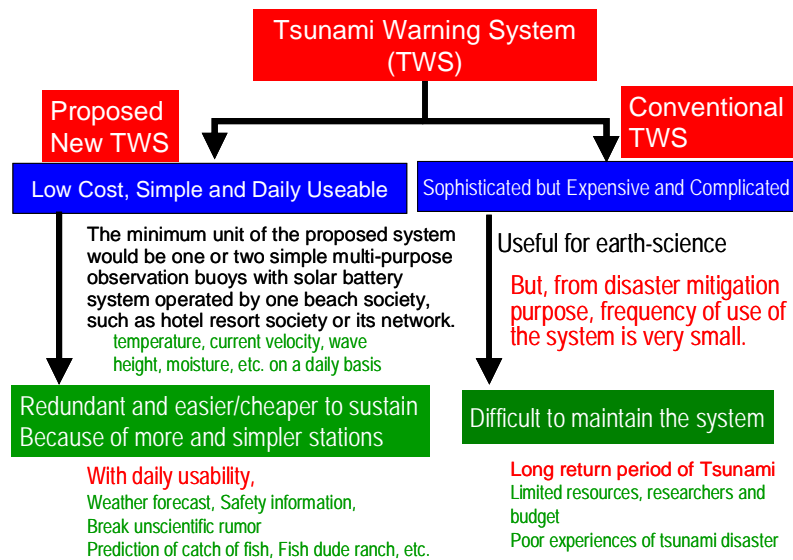


Figure 2: Comparison between conventional and newly proposed tsunami warning systems

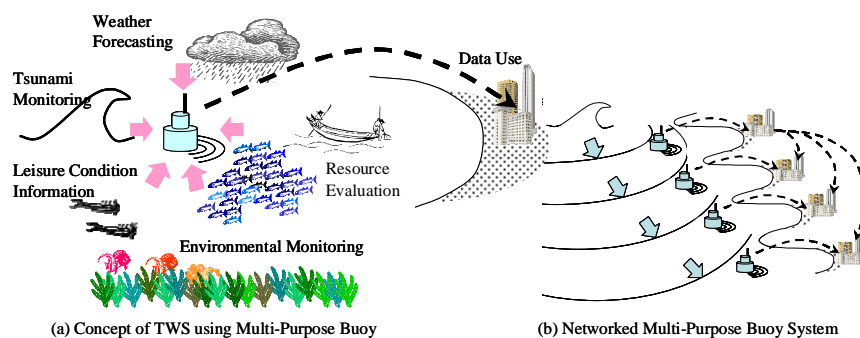


Figure 3: Concept of proposed tsunami warning system composed of networked simple multi-purposes observation buoys installed locally and internationally

2. PROPOSAL OF THE NEW TSUNAMI DISASTER MITIGATION SYSTEM

My proposed New Tsunami Disaster Mitigation System combines a reliable warning system and proper evacuation facilities. As mentioned earlier, a warning system such as the one available in the Pacific Ocean Rim region is not suitable for the Indian Ocean region which has fewer technological resources, researchers and experiences of tsunami disasters. For this reason, I am proposing to use simple multi-purpose observation buoys, which in addition to serve as a tsunami warning system, would record temperature,

current velocity, wave height, moisture, etc. on a daily basis. This information can be used for weather forecasting, safety assessment, fish catch prediction, etc. which are useful for the local businesses (Figure 3(a)). My proposal is to use numerous and simple stations so that the system is redundant and easier/cheaper to sustain. The minimum unit of the proposed system would be one or two multi-purpose observation buoys operated and maintained by hotels/resorts or beach societies in the area. These businesses will benefit from the daily collected information.

It is expected that many beach societies install the system and join the multi-purpose observation buoy network beyond the administrative or international boundaries (Figure 3(b)). In this way, it may be possible to gather daily maritime information over a wider area and eventually forecast a transoceanic tsunami. A system for transferring this information between associations, domestic and foreign, already exists.

The installation of the proposed buoy system could have additional advantages. After the December 26, 2004 tsunami, the tourism industry has suffered greatly not only due to direct impact of the tsunami in the infrastructure but also due to the unscientific rumors. Visitors that used to come to resort facilities in the region started avoiding these destinations for fear that a new disaster may occur. In order to recover the tourists' trust, the information collected by the buoy system can be very useful. It is also known that buoys may become the center of marine ecosystems which could be an attraction for scuba divers.

Proper evacuation facilities in terms of location, strength and sheltering capacity are also part of the proposed system. In the region, it is common to observe temples, churches and shrines located along the coastal line. Therefore, I am proposing to use similar community centers as evacuation facilities. This scheme has two main advantages. Because worship centers are permanently used by the people, their location is well known so that in case an evacuation notice is released, everybody can easily access them. Additionally, because the people feel strong commitment with these facilities, they take active participation in their building and maintenance.

3. ESTABLISHMENT OF THE PROPOSED TSUNAMI DISASTER MITIGATION SYSTEM

In order to establish the proposed system, several works are needed as shown in Figure 4 and the reconnaissance team, which I headed, carried out them.

- 1) Structural damage survey
- 2) Tsunami numerical simulation
- 3) Topographical survey
- 4) Questionnaire/Interview survey
- 5) Evacuation numerical simulation

The first three activities are closely interrelated and their main objective is to design the configuration and location of evacuation centers. The structural damage survey is intended to evaluate the tsunami load and corresponding damage. With this information, the relationship between tsunami wave load and wave height/velocity can be obtained. With tsunami numerical simulations using potential earthquake scenarios, it is possible to estimate the wave height and velocity and the tsunami inundation area due to future tsunami hazards. These data enable us to properly determine location and structural design criteria for evacuation facilities.

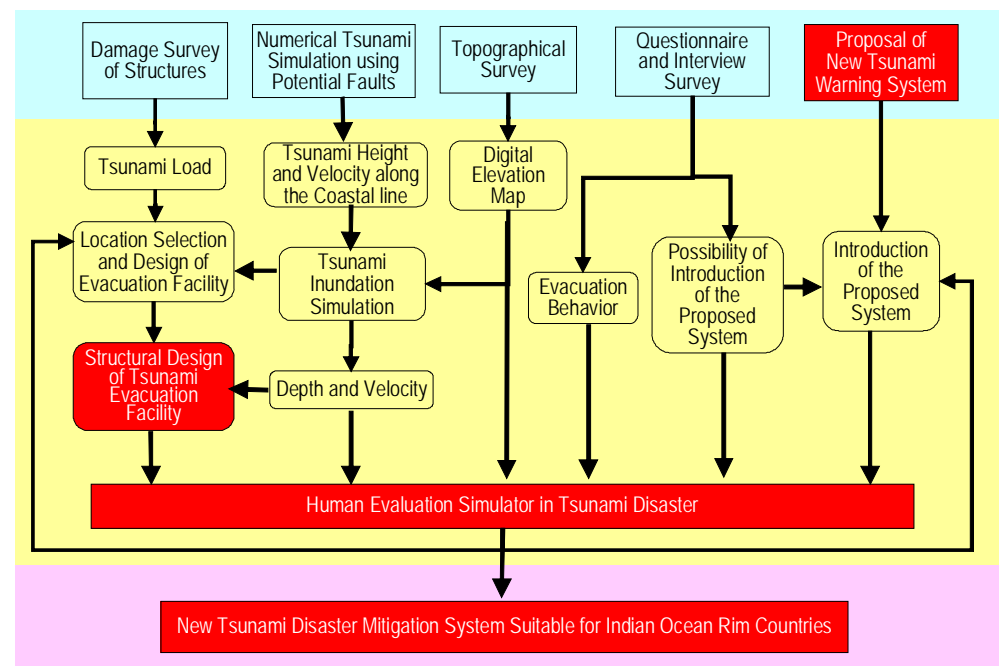


Figure 4: Establishment of the proposed tsunami disaster mitigation system

In order to guaranty that the evacuation centers are fully functional, their location should be selected so that when the expected tsunami occurs they will not be washed away. For this purpose, it is indispensable to carry out a topographical survey. Real-time kinematic GPS and laser total stations are powerful tools for this purpose.

Questionnaire and interview surveys are useful to gather data necessary for the evacuation behavior simulation. Relationships between human evacuation velocity and water depth, which are needed for this study, have already been proposed. The simulation will confirm whether the escape routes and proposed evacuation centers are suitable. Because the proposed tsunami disaster mitigation system heavily relies on the participation of regional organizations, the interviews are also helpful to assess the level of acceptance of the system among the people involved.

4. CONCLUDING REMARKS

This paper presents a New Tsunami Disaster Mitigation System for the Indian Ocean Rim region, which combines a reliable warning system and proper evacuation facilities. The warning system consists of multi-purpose observation buoys operated by local organizations such as hotels and beach associations. The system is not only used for tsunami warning but also to monitor temperature, current velocity, wave height, moisture, etc., information which can be used on a daily basis for the economic activities of the region.

The proposed evacuation facilities are designed taking into consideration: sheltering capacity, location, and structural strength. Location is especially important to prevent that the structures are washed away by the tsunami and to guaranty an easy access for the evacuees.

In order to verify the suitability of the proposed system, tsunami and evacuation simulations are recommended. Actually, the research team headed by the author has already perform this type of study with some selected areas in Japan and Sri Lanka and proved the system effectiveness. The strong points of the proposed system are its simplicity, economy and daily usability, which makes it a sustainable option for the region.

Technical Sessions

DIGITAL CHI-CHI CITY ON GOOGLE EARTH AS POST-EARTHQUAKE RECOVERY DIGITAL ARCHIVE

OSAMU MURAO
Graduate School of Systems and Information Science
University of Tsukuba, Japan
murao@risk.tsukuba.ac.jp

ATSUSHI MIYAMOTO
Tokyo Fire Department, Japan

ABSTRACT

Historical evidences reveal that disasters bring about changes in the damaged cities across the world through the recovery processes. Recent geoinformatic technologies enable us to create a virtual representation of a city on a digital model of Earth such as GoogleEarth; these representations can demonstrate the post-disaster recovery processes. The authors have tracked the post-earthquake recovery process of the Chi-Chi Township damaged during the 1999 Chi-Chi earthquake in Taiwan and constructed a virtual representation of the city based on field surveys to present its reconstruction conditions as of 2006. The objective of this study is to report how to construct a representation of a city in cyber space and to discuss the significance of recording the recovery process on a digital model of Earth.

This study first describes the background information regarding the experiment of the trial from the viewpoints of historical changes in the recording media and the significance of the disasters occurring in a city as critical points in its long-term urban development. It then outlines the six procedures adopted to create a digitalized virtual representation of the Chi-Chi Township in addition to the previous researches conducted by the authors. In the third part, the following procedures are explained in detail: (1) creating a base map using the information obtained from a previous research conducted by the authors; (2) conducting a field survey to obtain detailed photographs of building elevation and the number of stories of the objectives; (3) image processing in order to transform the captured photographs as rectangular polygons in cyber space; (4) drawing building outlines using Google Sketch Up, a three-dimensional modeling software; (5) applying the processed images as texture and painting roofs, and (6) Inserting the information related to the reconstruction process. Finally, this study discusses the usage of the abovementioned model to understand the post-disaster recovery processes and suggests the possibility of using a digitalized virtual representation of a city on a digital model of Earth as one of the methods to realize digital archives in the era of the geoinformatics.

1. INTRODUCTION

1.1 Present circumstances of spatial information science

The field of spatial information is changing dramatically with the development in remote sensing technology. In the November 2004 issue of *Nature*, Gewin (2004) stated that geotechnology and nanotechnology would be two of the biggest business fields, the third being biotechnology, in the twenty-first century. The technological innovation in the field of spatial information mentioned in this study is forecast to change urban spaces drastically. In addition, spatial information technology can prove to be an important tool to record recovery processes.

1.2 Digital archive for urban spaces

For a long time, cities have been formed as a result of the various changes in their environments. Historical evidence reveals that disasters are likely to dramatically influence the transformation of cities. For instance, Chicago has been transformed into a city bristling with skyscrapers since the conflagration in 1871. San Francisco had also attempted to achieve new urban development after the occurrence of the earthquake in 1906 by implementing the "Phoenix plan." Thus, based on historical evidence, we can conclude that disasters and reconstructions tend to be the crucial steps in influencing dramatic transformations in cities. In a previous study, the authors reported on recording disasters and reconstructions and examined a methodology to realize the same (Murao, 2006a). From the viewpoint of geotechnological and archival science, it is important to record the process of changes in a city by focusing on the most crucial moments during historical disasters and subsequent reconstructions on a virtual representation of the city on a digitalized model of the Earth. The authors have created a networked virtual representation of the Chi-Chi Township, Taiwan, which was struck by the 1999 Chi-Chi Earthquake, in order to record the reconstruction conditions on a three-dimensional representation of the city on a digitalized model of Earth accessible freely through GoogleEarth.

2. PROCEDURE

In order to create the virtual three-dimensional space, the following processes were carried out:

(1) Creating a base map

First, it was necessary to create a base map of the Chi-Chi Township in order to generate a representation of the city. The data from GIS obtained in the authors' previous research (Murao et al., 2004) was used for this purpose.

(2) Photographing the building facade

Second, a field survey was conducted at the site using the base map. The actual building conditions including their story heights and roof conditions were captured roughly. In addition, the exterior walls of the buildings were also photographed.

(3) Retouching the pictures

The pictures of the exterior walls were arranged according to the blocks and roads in front of the buildings. These were then processed in order to apply them as textures to the buildings in the three-dimensional space described later.

(4) Creating three-dimensional space using Google Sketch Up

As the fourth step, the positions were confirmed in order to appropriately lay the base map on GoogleEarth. Then, a three-dimensional digital representation of the Chi-Chi Township composed of a cluster of buildings was generated using Google Sketch Up and a framework of the scenery of the city was reproduced on a computer monitor.

(5) Applying the texture

The photographs acquired in step (3) were applied as textures to the exterior walls of the cluster of buildings created in step (4), and the roofs in the three-dimensional space were painted with colors similar to those of the actual roofs.

(6) Inserting the information related to the reconstruction process

The information regarding reconstruction obtained in the previous research was inserted into this three-dimensional representation of the Chi-Chi Township by using the placemark, one of the functions of GoogleEarth.

3. CONSTRUCTION OF DIGITAL CHI-CHI TOWNSHIP

3.1 Creating a base map

The digitalized data created by Murao et al. (2004) using GIS was applied as the base map (Figure 1) in order to construct a virtual city. Prior to this, the authors conducted a field design survey based on the IKONOS satellite images and attempted to define the actual outlines of the buildings (Murao, 2006b). The number of buildings in the target district exceeded 2,000. Then, the data of the shapes of the buildings obtained in this research was digitalized on GIS and the base map was applied to it. Further, the target district was divided into 86 town blocks for further analysis.

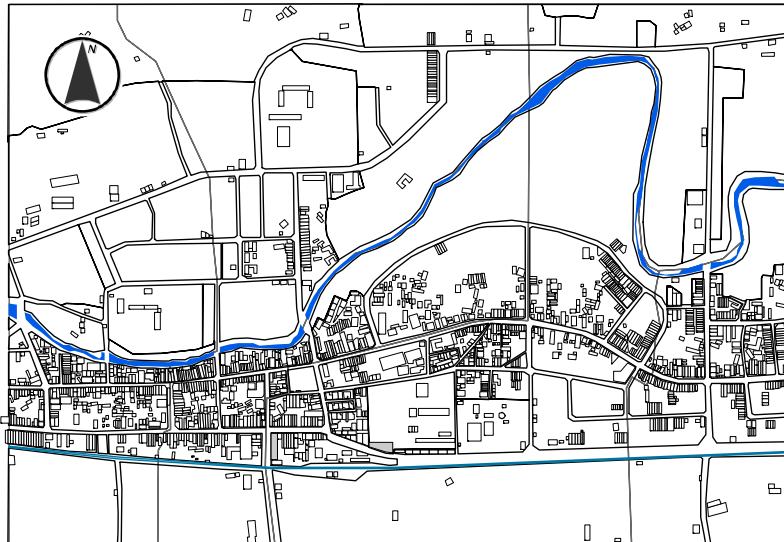


Figure 1: Base map of the Chi-Chi Township created by GIS (Murao, 2006b)

3.2 Photographing the building façade

By using the base map created in 3.1, the façades of the buildings in the Chi-Chi Township were photographed in August 2006. Four volunteers photographed the façades of approximately 1,500 buildings. The following rules were set to ensure that every photograph captured by the volunteers would be of the same quality.

Rules for photographing the building façade

- a) Set the resolution of the camera to 640×480 pixels
- b) Photograph block by block
- c) Photograph the buildings in a town block in a counterclockwise order as shown in Figure 2 (a) to enable computers to retouch the images
- d) Photograph one building per shot and, if possible, along the line of sight perpendicular to the face of the building.
- e) If the entire façade of a building cannot be captured in a single scene, photograph it by dividing the scenery into several (Figure 3)
- f) Conduct the division from the lower to the upper part and from the left to the right side in the above case

Further, the volunteers recorded the form of each roof and the story of each building while photographing it (Figure 2(b)).

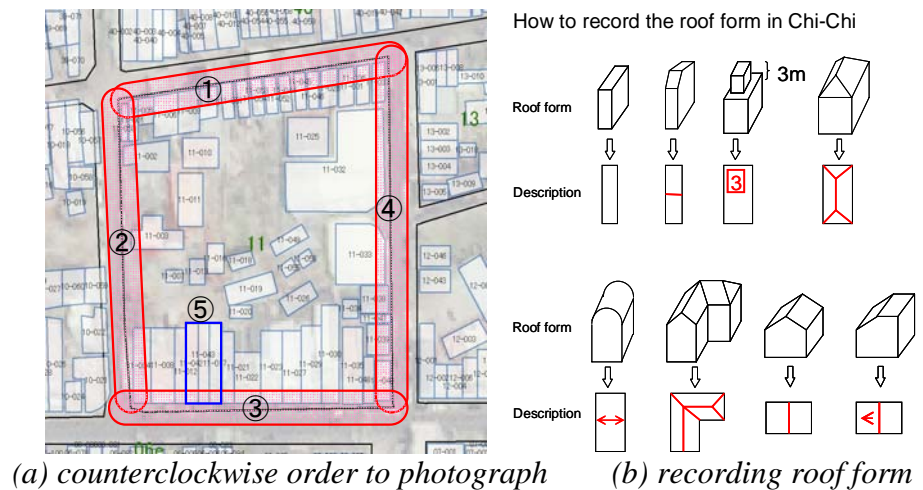


Figure 2: Precautions to be followed while photographing the building façades



Figure 3: one of the examples of the building façade

3.3 Retouching the photographs

The 1,500 digitalized images photographed in process 3.2 were classified according to their block and road. In other words, different directories were created for each block and the images photographed in each direction across the roads facing the blocks were stored in folders in these directories. Even the buildings facing the narrow roads in the blocks were photographed and classified. These images would be applied as textures on the façade of the virtual representation of the buildings in the three-dimensional model of the city. However, the images were photographed at the ground level at the site and not along the line of sight perpendicular to the face of the building. Therefore, the images were processed by using Adobe Photoshop in order to correct these differences as shown in Figure 4. After retouching each building image, an elevation image of the cluster of the buildings as seen from a road was produced in order to easily apply it to the digitalized façade. This elevation image is shown in Figure 5.



Figure 4: Correction of the building façade images photographed at the site



Figure 5: Elevation image of the cluster of the buildings as seen from a road

3.4 Creating three-dimensional space using Google Sketch Up

Next step is to create an outline of the Chi-Chi Township on a computer. However, in order to lay the created three-dimensional space on GoogleEarth (Figure 6), the following steps were necessary: First, the coordinates of the base map were positioned on GoogleEarth (Figure7). Second, the outlines of the buildings on the three-dimensional space by using Google Sketch Up, which is one of the applications of GoogleEarth. The stories of the buildings and the forms of the roofs were adjusted based on the information and photographs obtained at the site. Further, the vertical positions of the buildings were adjusted according to the elevations on GoogleEarth. With the completion of these steps, the scenery of the target district with the building outlines was finally generated.

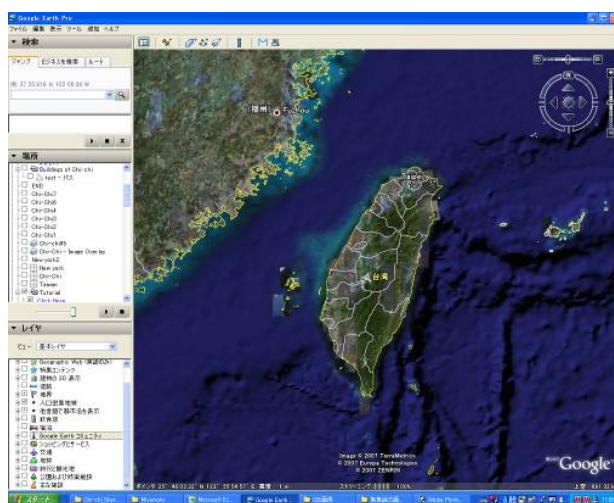


Figure 6: Landscape of Taiwan

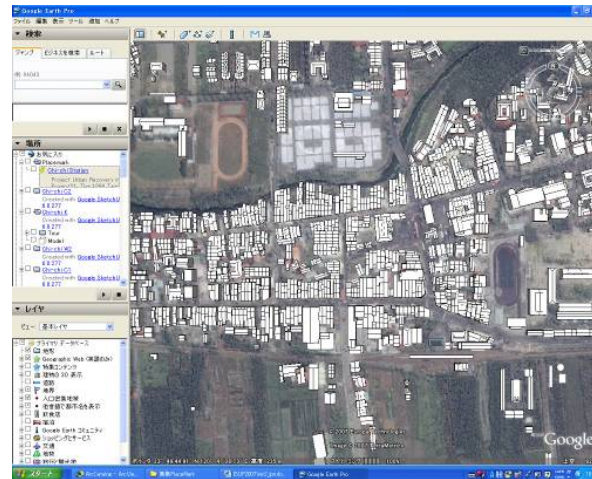


Figure7: Position of the district

3.5 Applying the texture

The last step in creating the three-dimensional space was to apply the photographs of the building elevations processed in 3.3 as textures to the frames created in process 3.4 (Fig. 8). Because it was difficult to photograph the roofs, the digitalized representations were painted in the three-dimensional space by referring to the photographs instead of applying them as textures. Fig. 9 shows the hypothetical representation of the buildings.

3.6 Inserting the information related to the reconstruction process

The information regarding the reconstruction process was inserted into the virtual representation of the city created in this study by using the placemark function of GoogleEarth. This information was obtained from the authors' previous research (e.g., Murao, 2006b) and can be displayed on GoogleEarth as described in Table 1.

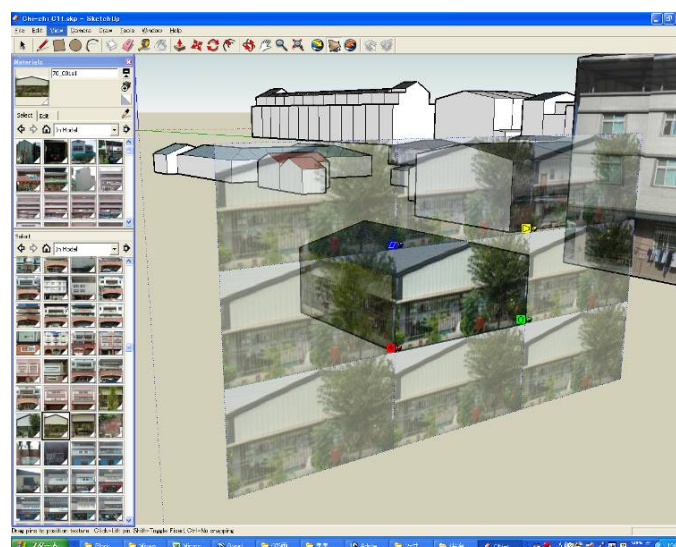


Figure 8: Application of the elevation photographs as textures to the building frames

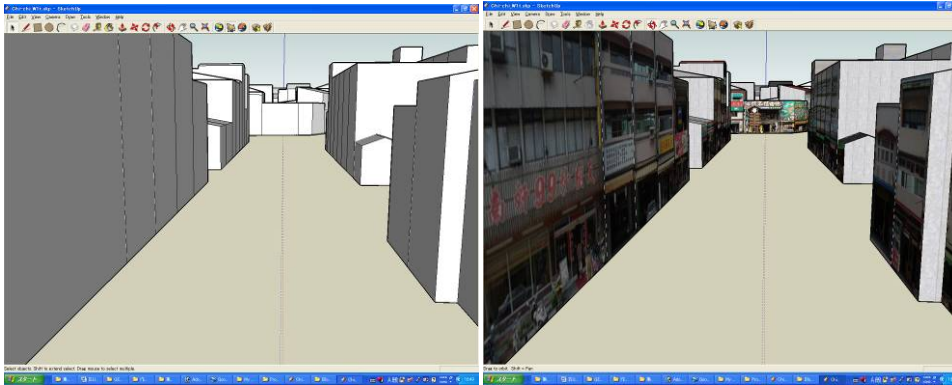


Figure 9: Example of the buildings in the virtual space with exterior walls and roofs (before and after applying the texture)

Table 1: Example of the information regarding to the reconstruction processes that can be displayed on GoogleEarth

Contents	Information Classification
Location of the facilities	description by Placemark
Explanation of the facilities	text
Image of the reconstruction process	image
Result of the analysis of the reconstruction process	graph, table, data, etc.

4. CHI-CHI CITY ON DIGITAL EARTH

This three-dimensional representation of the Chi-Chi Township was referred to as “Digital Chi-Chi City.” The virtual model of the city in cyber space represents the Chi-Chi Township as of August 2006. Fig. 10 shows the constructed digital Chi-Chi Township.

By only uploading the data constructed in this process, it enables every visitor to enter the Chi-Chi Township freely, gain an experience similar to that of an actual visit through GoogleEarth, and read the information regarding the reconstruction process obtained and processed during the authors’ previous researches. Table 2 lists the information regarding the reconstruction of the important facilities in the target district. This information is made available to the visitors by using the placemark function, as shown in Fig. 11. As research regarding the reconstruction process progresses, new information will be updated when appropriate and the range of the contents can be expanded.

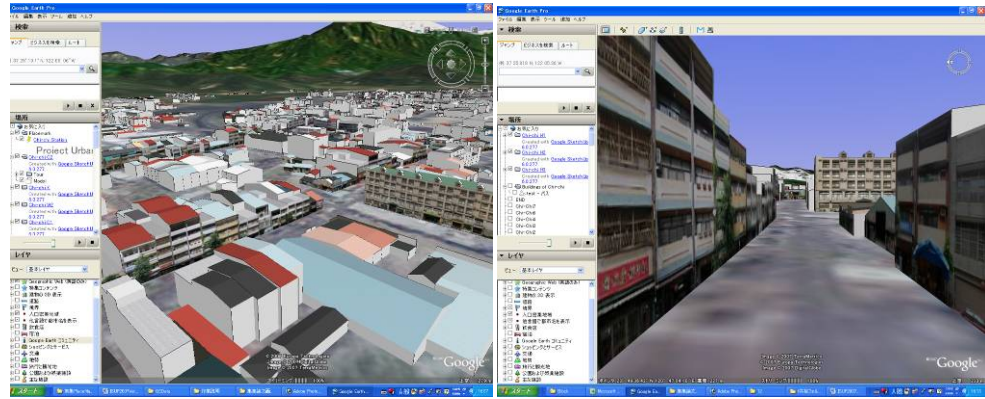


Figure 10: Overview of the Digital Chi-Chi City

Table 2: Information regarding the reconstruction of the important facilities in the target district

ID	Facilities	Structure (The Number of Stories) (Before the)	Date of Construction Start	Date of Construction Completion	GIS-ID
01	Chi-Chi Sightseeing Center	Parking Lot	2001/12/1	2006/8/31 Unfinished	S-14001
02	He-Ping National Primary School	RC (2F)	1999/9/26	2000/4/27	S-61001
03	Chi-Chi Government Office	RC (4F)	2000/4/22	2002/10/15	B-18022
04	Chi-Chi Health Center	RC (2F)	2003/4/4	2004/summer	B-41044
05	The First Market	RC (3F)	2002/10/30	2004/summer	B-09045
06	Chi-Chi Station	Wooden (1F)	2000/4/21	2000/7/24	B-07027
07	Railroad Musium	Wooden (1F)	2002/1/2	2002/3/8	B-07023
08	Chi-Chi Resort Center	RC (5F)	2000/12/27	2001/12/31	B-73001
09	Chi-Chi Public Swimming Pool	-	2000/4/9	2002/11/22	S-71001
10	Parking Lot	RC (B2F)	1997/7/9	2001/1/17	S-19001
11	Chi-Chi Police Station	RC (3F)	2002/8/10	2004/summer	B-18***
12	Chi-Chi National Junior High School	RC (2F)	2000/6/1	2000/12/1	S-80001
13	Chi-Chi National Primary School	RC (2F)	2000/6/1	2001/3/1	S-19001
14	Farmer Bank	RC (3F)	-	2001/12/19	B-06010
15	Wu-Chang Temple	RC (3F)	1999/11/1	Preserved	S-74001
16	Guang-Sheng Temple	Wooden (1F)	2000/7/1	2003/8/1	S-40001
17	Temporary Housing (I) (138+20)	—	1999/10/20	2000/1/28	S-66001
18	Temporary Housing (II) (72)	—	1999/9/26	1999/10/13	S-75001
19	Temporary Housing (III) (23)	—	1999/9/26	1999/10/13	S-86001
20	Permanent Housing constructed by Chi-Chi Governem	—	2000/8/1	2002/3/1	



Figure 11: Example of displaying the information regarding the reconstruction process using the placemark function

5. CONCLUSION

In this study, the authors report on the Digital Chi-Chi City constructed to record the reconstruction conditions of the damaged area and allow visitors to freely access a three-dimensional representation of the city on a digital model of Earth. In order to construct the Digital Chi-Chi City, the following processes were undertaken:

1. Creating a base map
2. Photographing the building façade
3. Processing the photographs
4. Creating a three-dimensional space using Google Sketch Up
5. Applying textures
6. Inserting the information regarding the reconstruction process

This Digital Chi-Chi City enables visitors from around the world to freely access the city on a digital model of Earth and gain an experience similar to that of actually visiting the Chi-Chi Township.

The characteristics and significance of the Digital Chi-Chi City are as follows;

- 1) It is a three-dimensional representation of actual city on a digital model of Earth created using the freely accessible platform of GoogleEarth.
- 2) For a city with a long history, the process of reconstruction following a disaster brings about dramatic changes in the city and becomes a crucial point in its history. The digital Chi-Chi City is a reproduction of the actual city in three-dimensional space for this geoinformatics era.
- 3) The procedure for inserting the conditions of the recovery process into the representation in the digital model of Earth exemplifies one of the possibilities wherein digital archives can be used to record reconstruction processes.

The authors will update the information regarding the reconstruction process when appropriate while continuing their research on the Chi-Chi Township.

ACKNOWLEDGEMENTS

This work was supported by the Japan Society for the Promotion of Science (JSPS) through the Grants-in-Aid for Scientific Research No. 16401022 “Architecture of Reconstruction Process of Chi-Chi Area (Taiwan) and Archives related to Urban Reconstruction in the World” and Grant-in-Aid for Exploratory Research No. 18656179 “Construction of Digital Archives for Urban Recovery using Satellite Images”. The authors would like to acknowledge Yayoi Mitsuda; the translator of the Chi-Chi research project; Yasuhisa Fujita and Kenichi Saito from Digital Earth Corporation who advised lots of things; Hideaki Nakazato and Tomomi Hayashi from

University of Tsukuba as volunteers, and the officers and residents of the Chi-Chi Township.

REFERENCES

- Gewin, V., 2004. Mapping Opportunities. *Nature*, No. 427, 376-377.
- Murao, O., Ichiko, T., and Nakabayashi, I., 2004. Evaluation of Building Reconstruction Process in Chi-Chi Area based on a GIS-Database after the 1999 Chi-Chi Earthquake, Taiwan. 13th World Conference on Earthquake Engineering (CD-ROM), No.174, Vancouver, Canada.
- Murao, O., 2006a. Memories and succession for constructing archives describing the reconstruction processes of a city as archival science in an era of town planning during the reconstruction processes after a disaster with strategies for the next generation. *Zoukei Shinsho, Kenchiku-Shiryo Kenkyusha*, 62-65 (in Japanese).
- Murao, O., 2006b. Structure of Post-earthquake Recovery Process after the 1999 Chi-Chi Earthquake -A Case Study of Chi-Chi. *Proceedings of the International Symposium on City Planning, Taipei, Taiwan*, 164-175 makes it a sustainable option for the region.

VISUAL SCREENING METHODS FOR EARTHQUAKE VULNERABILITY ASSESSMENT

A. B. AFIFA IMTIAZ

Dept. of Civil Engineering, Bangladesh University of Engineering and Technology (BUET), Bangladesh
afifaimt@gmail.com

MAHFUZA SHAMIM

Dept. of Civil Engineering, BUET, Bangladesh
mly_054@yahoo.com

ASHUTOSH SUTRA DHAR

Dept. of Civil Engineering, BUET, Bangladesh
ashutoshdhar@ce.buet.ac.bd

MEHEDI AHMED ANSARY

Dept. of Civil Engineering, BUET, Bangladesh
ansary@ce.buet.ac.bd

MOHAMMED JOBAIR, MD. ZAKARIA AHMED

Dept. of Civil Engineering, BUET, Bangladesh

ABSTRACT

Several pre-earthquake screening methods have been developed recently for rapid evaluation of vulnerability profiles of the existing building stocks. The objective of these methods is to identify, make inventory and rank all high-risk buildings in a specified region so that a strategy of priority based interventions to buildings can be formed. The Federal Emergency Management Agency (FEMA) of the United States of America has developed a method of potential seismic hazards of buildings based on rapid visual screening. The rapid visual screening method, widely known as RVS method, has generally been used for assessment of seismic vulnerability of structures. This screening methodology is encapsulated in a one page form, which combines a description of a building, its layout and occupancy, and a rapid structural evaluation related to its seismic hazard. Another approach of rapid visual screening was employed for assessment of seismic vulnerability of structure in Turkey, which was developed after the 1999 earthquake in the cities of Kocaeli and Düzce in Turkey. The method uses two level seismic assessment where at level 1, a street survey is used regarding a structural form and the ground condition while more rigorous information of the buildings are used at level 2 of the assessment. Both of the methods have been used in this research for seismic vulnerability assessment of buildings in Cox's Bazar district in Bangladesh. The study reveals that the method proposed in FEMA is much more conservative relative to method used in Turkey. The vulnerability score estimated using the FEMA method was less than the "cut off" score for almost all the buildings while the score estimated using the Turkish method was much

above the “cut off” score. This paper critically examines the two methods with reference to the seismic assessment of structures in Cox’s Bazar and identifies the key parameters contributing to the vulnerability assessment.

1. INTRODUCTION

Vulnerability Analysis of building stocks in a region is a very difficult and time-consuming process. Step by step identification of buildings at most seismic risk can make the whole procedure comparatively simpler. First step in this process can be quickly screening of buildings to determine if evaluation is required. This procedure requires only visual inspection and limited data collection. The visual screening method has been used in this research for 250 Cyclone Shelters and 52 General Buildings of Cox’s Bazar District in Bangladesh. The study included two different visual screening methods, i.e. FEMA-RVS and Turkish Simple Survey Procedure. FEMA Rapid Visual Screening (RVS) of buildings for potential seismic hazards originated in 1988, with the publication of the FEMA 154 Report. It is a “sidewalk survey” approach that enabled users to classify surveyed buildings into two categories: those acceptable as to risk to life safety or those that may be seismically hazardous and should be evaluated in more detail by a design professional experienced in seismic design. The Turkish Simple Survey procedure is a two level risk assessment procedure which has been proposed on the basis of statistical correlations obtained by employing a database of 477 damaged buildings surveyed after the 1999 Düzce earthquake (Sucuoglu and Yazgan, 2003). The first level incorporates recording of building parameters from the street side and in the second level, these are extended by structural parameters measured by entering into the ground story.

2. METHODS REVIEW

2.1 FEMA Rapid Visual Screening

The Data Collection Form of RVS includes space for documenting building identification information, including its use and size, a photograph of the building, sketches, and documentation of pertinent data related to seismic performance, including the development of a numeric seismic hazard score. Basic Structural Hazard Scores based on Lateral Force Resisting System for various building types are provided on the form, and the screener circles the appropriate one. The screener modifies the Basic Structural Hazard Score by identifying and circling Score Modifiers related to observed performance attributes, by adding (or subtracting) them a final Structural Score, ‘S’ is obtained. The scoring system of RVS is shown in Figure 1.

The score below which a structure is assumed to require further investigation is termed as “cut-off” score. The value of “cut off” score and choice of RVS form depends on the seismic zonation of the area. It is

suggested that buildings having an S score less than the “cut-off” score should be investigated by an experienced seismic design professional experienced in seismic design. If the obtained “final score” is greater than the “cut-off” score the building should perform well in a seismic event. A score of 2 is used in this study as a “cut-off” score, based on high seismic zone.

Occupancy				Soil Type								FALLING HAZARDS				
Assembly	Govt. Office	Number of Pers		A	B	C	D	E	F							
Commercial	Historic Resider	0-10	11-10	Hard Rock	Avg. Rock	Dense Soil	Stiff Soil	Soft Soil	Poor Soil	Unreinforced	Parapets	Cladding	Chimney	Other		
Emer. Service	Industrial	School	101-1000	1000+												
BASIC SCORE, MODIFIERS AND FINAL SCORE S																
Building Type	W1	W2	S1	S2	S3	S4	S5	C1	C2	C3	PC1	PC2	RM1	RM2	URM	
			(MRF)	(BR)	(LM)	RC	SW	JRM	INF	(MRF)	(SW)	JRM	INF	(TU)	(FD)	(RD)
Basic Score	4.4	3.8	2.8	3	3.2	2.8	2	2.5	2.8	1.6	2.6	2.4	2.8	2.8	1.8	
Mid Rise (4 to 7 Stories)	N/A	N/A	0.2	0.4	N/A	0.4	0.4	0.4	0.4	0.2	N/A	0.2	0.4	0.4	0	
High Rises (> 7 Stories)	N/A	N/A	0.6	0.8	N/A	0.8	0.8	0.6	0.8	0.3	N/A	0.4	N/A	0.6	N/A	
Vertical Irreg.	-2.5	-2	-1	-1.5	N/A	-1	-1	-1.5	-1	-1	N/A	-1	-1	-1	-1	
Plan Irregularity	-0.5	-0.5	-0.5	-0.5	-0.5	-0.5	-0.5	-0.5	-0.5	-0.5	-0.5	-0.5	-0.5	-0.5	-0.5	
Pre-Code	0	-1	-1	-0.8	-0.6	-0.8	-0.2	-1.2	-1	-0.2	-0.8	-0.8	-1	-0.8	-0.2	
Post Benchmark	2.4	2.4	1.4	1.4	N/A	1.6	N/A	1.4	2.4	N/A	2.4	N/A	2.8	2.6	N/A	
Soil Type C	0	-0.4	-0.4	-0.4	-0.4	-0.4	-0.4	-0.4	-0.4	-0.4	-0.4	-0.4	-0.4	-0.4	-0.4	
Soil Type D	0	-0.8	-0.6	-0.6	-0.6	-0.6	-0.4	-0.6	-0.6	-0.4	-0.6	-0.6	-0.6	-0.6	-0.8	
Soil Type E	0	-0.8	-1.2	-1.2	-1	-1.2	-0.8	-1.2	-0.8	-0.8	-0.4	-1.2	-0.4	-0.6	-0.8	
FINAL SCORE S =																

Figure 1: Sample RVS Scoring Form (FEMA-154, 2002)

2.2 Turkish Simple Survey Procedure

This is a two level seismic risk assessment procedure based on several building parameters that can be easily observed or measured during a systematic survey. The basic scoring for both the levels are based on the Height of the building (number of stories) and Local Soil Conditions where three intensity zones are specified in terms of associated PGV (Peak Ground Velocity) ranges. Once the vulnerability parameters of a building are obtained from two-level surveys and its location is determined, the seismic performance and vulnerability scores are calculated as defined in Figure 2. The final seismic Performance Score is obtained by using Equation (1). A “cut-off” performance score of 50 has been suggested for both survey levels.

$$PS = (\text{Initial Score}) - \sum (\text{Vulnerability Parameter}) \times (\text{Vulnerability Score}) \quad (1)$$

The first level is a street survey procedure and involves the observation of the parameters, the number of stories above ground, presence of a soft story, presence of heavy overhang, apparent building quality, and presence of a short column.

In the second level the parameters of first level are confirmed or modified through closer observations. Then a sketch of the framing plan at the ground story is made and the dimensions of columns, concrete and masonry walls are measured. The added parameters in this stage are pounding between adjacent buildings, topography effect, plan irregularity, redundancy, and strength index. The consistency in distribution of lateral loads to frame members is judged by redundancy and the strength index figures out the influence of size of the vertical members of the building,

material strength, frame geometry etc. on the lateral strength of the building. The results of the Level - II procedure can be used to determine the potential status of the selected buildings, and to further short-list the buildings requiring detailed vulnerability assessment.

Simple Survey Procedure (Turkish) for Risk Assessment of Concrete Buildings							
Table A: Initial & Vulnerability Scores for Level - I Survey of Concrete Buildings							
No. of Stories	Initial Score (on Soil Zoning)			Soft Story	Heavy Overhang	Apparent Quality	Short Column
	60<PGV<80	40<PGV<60	20<PGV<40				
1, 2	90	125	160	-5	-5	-5	-5
3	90	125	160	-10	-10	-10	-5
4	80	100	130	-10	-10	-10	-5
5	80	90	115	-15	-15	-15	-5
6, 7	70	80	95	-15	-15	-15	-5
Table B: Initial & Vulnerability Scores for Level - II Survey of Concrete Buildings							
No. of Stories	Initial Score (on Soil Zoning)			Soft Story	Heavy Overhang	Apparent Quality	Short Column
	60<PGV<80	40<PGV<60	20<PGV<40				
1, 2	95	130	170	0	-5	-5	-5
3	90	125	160	-10	-5	-10	-5
4	90	115	145	-15	-10	-10	-5
5	90	105	130	-15	-15	-15	-5
6, 7	80	90	105	-20	-15	-15	-5
Table B: Contd. For Level - II Survey							
No. of Stories	Pounding	Topography	Plan Irregularity	Redundancy	Strength Index		
1, 2	0	0	0	0	-5		
3	-2	0	-2	0	-5		
4	-3	-2	-2	-5	-5		
5	-3	-2	-5	-10	-10		
6, 7	-3	-2	-5	-10	-10		
Table C: Vulnerability Parameters							
Soft Story	No (0)	Yes (1)					
Heavy Overhang	No (0)	Yes (1)					
Apparent Quality	Good (0)	Moderate(1)	Poor (2)				
Short Column	No (0)	Yes (1)					
Pounding Effect	No (0)	Yes (1)					
Topography Effect	No (0)	Yes (1)					
Plan Irregularity	No (0)	Yes (1)					
Redundancy	Redundant,R (0)	Semi-R (1)	Weakly-R (2)				
Strength Index	Strong (0)	Weak (1)					
General Equation for Seismic Performance Scores (PS) for both Levels ("cut-off" PS = 50)							
$PS = (\text{Initial Score}) - \sum (\text{Vulnerability Parameter}) \times (\text{Vulnerability Score})$							

Figure2: Tables and General Equation of Turkish Procedure (Sucuoglu and Yazgan, 2003)

3. ASSESSMENT OF BUILDINGS IN COX'S BAZAR

3.1 Buildings Analyzed

From the structural consideration, only Reinforced Concrete with Unreinforced Masonry Infill Wall (URM INF) of burnt brick buildings of Cox's Bazar area have been selected for seismic vulnerability assessment. The buildings to be surveyed have been divided into two particular categories, one is the Cyclone Shelters and the other one is General Buildings used for residential or commercial purposes.

3.1.1 Cyclone Shelters

The cyclone shelters are the structures developed under the Multipurpose Cyclone Shelter Program by the Government of Bangladesh in 1993 after the great cyclone of 1991. There are 455 cyclone shelters in different places of the district (Uddin and Yasmin, 2005), which serve in

sheltering people during the cyclones and are used as schools or food storage at other times. Most of the shelters of the area were built after the 1991 cyclone with the help of Donor countries and agencies. The existing shelters are usually two to three storied keeping the Ground Floor totally open. On an average every shelter is capable of accommodating 1000 to 1200 people at disaster period.

3.1.2 General Buildings

General Buildings include the buildings used for residential or commercial purposes. They house a significant number of people and can be used as Shelters during Disaster where Cyclone Shelters are insufficient to house the inhabitants. Again analyzing these buildings enables the assessment of general construction practices of the area and thus the vulnerability due to seismic activity. It can also act as a guide for suggesting any modifications or improvements in design and construction works to make the buildings earthquake resistant.

3.2 Assessment by FEMA Method

A total number of 250 Cyclone Shelters and 52 General Buildings have been analyzed using Rapid Visual Screening (RVS) method. Considering Cox’s bazar as a high Seismic Risk zone, the cut off value was determined as 2. The results show that no score for cyclone shelter and other buildings was found to touch the cut off value according to FEMA method and all of them require further detailed analysis for vulnerability to determine the level of actual risk. Figure 3 shows summary of the RVS score for different buildings. In fact the basic score for RC building in FEMA-RVS is only 1.6 (less than the cut off), which becomes smaller after being modified by the negative parameters. This is one of the reasons for the FEMA RVS score to be less. The parameters contributing the scoring system are mainly, the height, irregularities of the buildings and type of the soil underneath. As there is no real practice of following national design code for construction works in Bangladesh, the parameters Pre Code and Post Benchmark remained inapplicable in the scoring. On a general view, the soil type of Cox’s Bazar has been considered as Stiff, so this modifier also remains constant in the whole process.

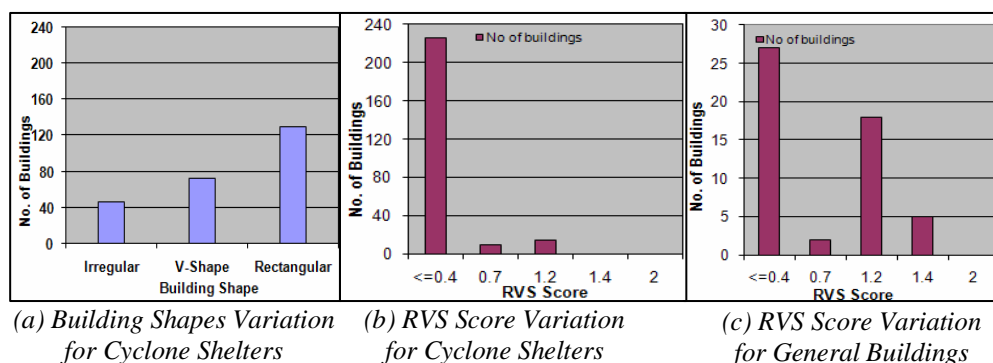


Figure 3: RVS Score Variations for the Surveyed Buildings



Figure 4: Three Distinctive Shapes of Cyclone Shelters responsible for respective Variations in Scores

In case of Cyclone Shelters, all the buildings in the area are below 4 storied. Thus the irregularities of the buildings only contribute to the score variation. The Cyclone Shelters have some common forms in shape. Most of them are of regular shapes (square, rectangular, few circular), some are “V”-shaped and the rest of the buildings have some irregularities vertically or in plan (as shown in Figure 3-a and Figure 4). Almost all the shelters have open ground floors which indicate the existence of soft/weak story effect, hence imposing vertical irregularity which is the major factor contributing in lowering the scores significantly. It has been observed that among the buildings without soft story, those having no irregularities (regular shape) score 1.2 whereas the “V”-shaped (only plan irregularity) ones score 0.7. The buildings having soft story effect with vertical irregularities or both (including plan irregularity) score ≤ 0.4 (Figure 3-b).

Almost similar picture is reflected in case of General Buildings (Figure 3-c). A new score level, 1.4, has been added here. The Mid-rise buildings which have stories greater than 3, got a positive score modification of 0.2 and thus the final score uplifted a bit. Another point to be noticed here that plan irregularity is observed less in General buildings compared to the Shelters. Thus relatively fewer buildings showed in score level 0.7 or less.

It is also possible to interpret the RVS scores, based on the presence of type of Performance Modifiers, into the probable damage due to an earthquake according to The European Macroseismic Scale (EMS). EMS is the basis for evaluation of seismic intensity in European countries. Most recently updated in 1998, the scale is referred to as EMS 98, which denotes how strongly an earthquake affects a specific place. Based on the principle that the way in which a building deforms under earthquake loading depends on the building type, EMS has categorized intensity of building damages in different categories for different structure types. The RVS scores for RC (URM INF) buildings of a High Seismic Zone obtained from the analysis have been grouped on the basis of the existence of the Performance Modifier Type. The consequent damage expected due to the presence of the particular modifiers has been implicated in terms of Probable Damage Classification and then interpreted as the Damage Description following EMS definitions. Table-1 shows this probable damage classification based on FEMA RVS Scores. However, it should also be noted that the actual

damage will depend on a number of factors that are not included in the RVS procedure. As a result, the implications should only be used as indicative to determine the necessity of carrying out simplified vulnerability assessment of the buildings. These results can also be used to determine the necessity of retrofitting buildings where more comprehensive vulnerability assessment may not be feasible.

Table 1: Probable Damage implications from RVS for RC (URM INF) buildings in High Seismic Zone

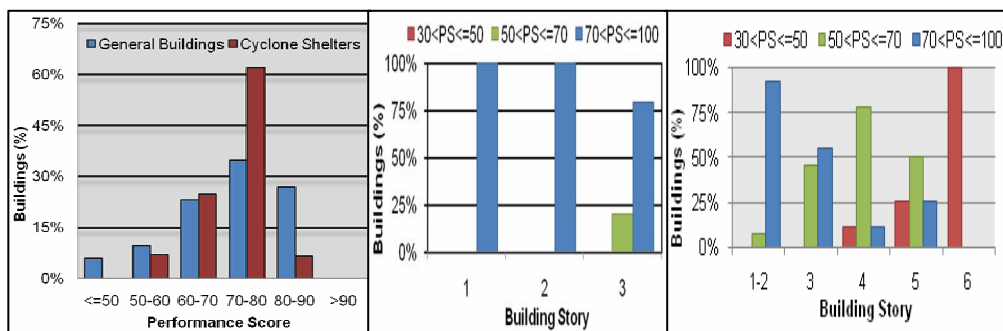
RVS Score	Probable Damage	Damage Classifications for Reinforced Concrete Buildings (Following EMS)
1.2<S<2	Very High Probability of Grade 1 Damage	Grade 1: Low Damage (No major structural damage, susceptible to more non-structural damages) Probability of fine cracks in plaster over frame members or in walls at the base or in partitions and infill
0.7<S<1.2	High Probability of Grade 2 Damage and Very High Probability of Grade 1 Damage	Grade 2: Moderate damage (Slight structural damage, moderate non-structural damage) Cracks in columns and beams of frames and in structural walls. Cracks in partition and infill walls; fall of brittle cladding and plaster. Falling mortar from the joints of wall panels.
0.4<S<0.7	High Probability of Grade 3 Damage and Very High Probability of Grade 2 Damage	Grade 3: Substantial to Heavy Damage (Moderate structural damage, heavy non-structural damage) Cracks in columns and beam-column joints of frames at the base and at joints of coupled walls. Spalling of concrete cover, buckling of reinforced bars. Large cracks in partition and infill walls, failure of individual infill panels.
S≤0.4	High Probability of Grade 4 to Grade 5 Damage and Very High Probability of Grade 3 Damage	Grade 4: Very Heavy Damage (Heavy structural damage, very heavy non-structural damage) Large cracks in structural elements with compression failure of concrete and fracture of rebars; bond failure of beam reinforcing bars; tilting of columns. Collapse of a few columns or of a single upper floor Grade 5: Destruction (Very heavy structural damage) Collapse of ground floor parts (e.g. wings) of the building.

3.3 Assessment by Turkish Method (Level – I)

All the Shelters and the General Buildings, specified previously, have been analyzed by Turkish Method (Level – I) of visual screening. Here, the assessment has been performed considering the soil zonation of Cox’s Bazar in Zone-1 (60<PGV<80). In this method much more variation in final scores

has been observed as not only the basic score but also the influences of vulnerability parameters are very much dependent on the height of the building. In fact the positive or negative score modifications due to vulnerability parameters are weighted multiplications based on their existence and number of stories of the buildings. As a result the score becomes high for low rise buildings in spite of presence of negatively influential vulnerability parameters. Due to these dependant variations, it is comparatively tougher task here to classify the damage probabilities with minute specifications, as that of RVS-FEMA method, only from final scores. Rather it is easier to indicate an overall view on safety of the building comparing the final score with the cut off value and observing their relative difference.

Figure 5-a reflects that no buildings from Cyclone Shelters and very few (5%) from General Buildings scored less than 50 (the “cut-off” score), that means according to the Level – I survey. Thus all these buildings do not need further detailing on vulnerability assessment, or they can be termed as safe. When the performance scores of the buildings have been placed against building story, it was found that other than few 3 storied ones all the Shelters scored above 70 (Figure 5-b) and all the General Buildings scoring less than 50 (Figure 5-c) were midrise (4 to 6 storied). The observed general trend is that the taller the buildings the higher the presence of negative parameters and thus the lower becomes the scores.



(a) Turkish (Level-I) Score Variation (b) PS vs. Story (Level-I) for Cyclone Shelters (c) PS vs. Story (Level-I) for General Buildings

Figure 5: Turkish (Level-I) Scoring Variations for the Surveyed Buildings

3.4 Assessment by Turkish Method (Level – II)

Though the buildings identified as unsafe or lower scored compared to the “cut-off” value in Level-I were supposed to be judged by Level-II procedure, in this investigation all the general buildings were analyzed again in the Level-II to see the difference of score variations between these two methods. No Cyclone Shelter scored less than the “cut-off” and was not considered here for this re-evaluation process. Figure 6 compares the scores of buildings according to Level-I and Level-II survey. From the results represented in Figure 6, it can be concluded that the buildings scoring more than or around 50 in Level-I behaved better in Level-II scoring higher. The

buildings failed to exceed the “cut-off” in Level-II are those which had scores much lower in the former phase.

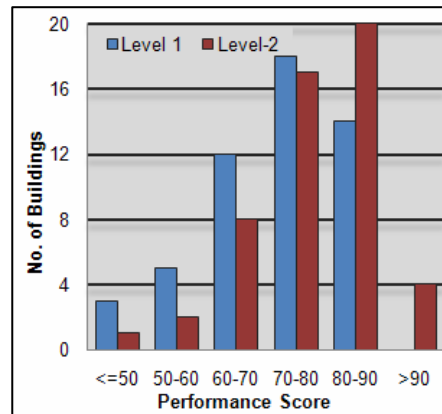


Figure 6: Turkish Scoring (Level-I & Level-II) for the General Buildings

4. COMPARATIVE REVIEW OF THE METHODS

A comparative review of the two RVS methods has been presented here with regards to the aspects considered in each of the methods. An attention was paid on applicability of the methods in Bangladesh. Figure 7 shows the comparative scoring picture of these two methods for a building.

FEMA 154 - RVS		Turkish Method (Level - I)				Turkish Method (Level - II)			
Building Type	C3 (URMINF)	Performance Criteria	Observation	Vulnerability Factor	Total Score	Performance Criteria	Observation	Vulnerability Factor	Total Score
Basic Score	1.6	Soil Zone 60<PGV<80	1	-	-	Soil Zone 60<PGV<80	1	-	-
Mid Rise (4 to 7 Stories)	0.2	No of Story	2	-	-	No of Story	2	-	-
High Rise (> 7 Stories)	0.3	Vulnerability Parameters				Vulnerability Parameters			
Vertical Irreg.	-1	Soft Story (Y/N)	N	0	0	Soft Story (Y/N)	N	0	0
Plan Irregularity	-0.5	Heavy overhang (Y/N)	Y	1	-5	Heavy overhang (Y/N)	Y	1	-5
Pre-Code	-0.2	Apparent Quality(G,M,P)	M	1	0	Apparent Quality(G,M,P)	M	1	-5
Post Benchmark	N/A	Short Column(Y/N)	N	0	0	Short Column(Y/N)	N	0	-5
Soil Type C (Dense)	-0.4	Performance Score				Performance Score			
Soil Type D (Stiff)	-0.4	85				85			
Soil Type E (Soft)	-0.8	Performance Score				Performance Score			
FINAL SCORE, S	0.7	85				80			

Figure 7: Scoring Systems of RVS and Turkish Method

The FEMA-154 RVS considers 15 structure-types (timber frame, steel frame, RC, masonry) whereas the Turkish Procedure can only be used for RC buildings which makes constraints its use for wider aspects in countries like Bangladesh where unreinforced structures occupy a major portion of the existing construction practices. Data collection form in FEMA RVS includes building information (use, size etc), photograph, sketches, pertinent data related to seismic performance – which help in developing inventories of building. On the other hand Turkish Data collection form includes few simple structural and geotechnical parameters which might not be sufficient for providing any support idea to be decisive in case of any confusion about the structure. FEMA has the provision of considering benchmark years of adopting and improving seismic codes. Turkish method evaluates the multistoried RC buildings which do not conform to the requirements of

modern seismic design and construction codes. Thus, the Turkish method may be suitable for the countries like Bangladesh where seismic design codes are of no practical use. A broad definition of Vertical Irregularity is included in FEMA method such as soft/weak story, geometric irregularities, mass irregularities, and steps in elevation /inclined walls/discontinuities in load path / hillside site. However, the Turkish method evaluates only soft story and topography effects while it is clear from past experience that structural irregularities can be significant in the performance of a building during an earthquake

Basic Scores in FEMA-RVS are based on average expected ground shaking levels for the seismicity region and the lateral force resisting system of structure where soil condition acts as a negative performance modifier and higher number of stories in a building acts as a positive modifier on the scoring system. No structural characteristics are judged and Site aspects such as potential pounding between buildings, apparent quality are noted and quantified in this method. Conversely in Turkish method Basic Scores are based on the intensity of ground motion (Zoning is represented by PGV range of the locality) and the variation of building stories. This method considers buildings up to 7 stories where the increasing number of stories reduces the performance score by influencing almost all other Vulnerability Parameters negatively. Pounding effects and apparent quality of the building as well as the structural characteristics, Redundancy and Stiffness Index, act as weighted Vulnerability Parameters in the scoring system of Turkish screening. These contradictions have been reflected prominently in the scores where no buildings found to be safe in RVS method and almost all of them were configured as satisfactory in Turkish.

The advantages of FEMA-RVS are its simplicity, relatively low cost to gather the required field data, provision of effective estimates for determining future emergency planning or mitigation, effectiveness of the process for detailed evaluations. In spite of the benefits this procedure has some shortcomings. It provides generalized results only in terms of structural score and without any explanation or specification for particular building type, only incorporates Pass/Fail results (decision of detailed evaluation required or not) rather than being explanatory on the scores, based on three pre-determined seismicity regions (lack of refinement), does not incorporate seismic event when determining the final “structural score” and over all it is a very conservative approach. It has another disadvantage that it may be too conservative and the assigned score may indicate that the building presents a greater risk than it actually does. Turkish procedure is also simple from all aspects but from the experience of survey it is noticeable that the structural measurements in Level-II, which act as very important vulnerability features, has made the method somewhat tougher as residents of the buildings do not co-operate the screeners and restrict their entry to the ground floor. Again, though this method considers more parameters than RVS, it becomes also conservative by predetermining the structural configuration to RC buildings and number of stories limiting up to 7 only.

5. CONCLUSIONS

The evaluation of two different methods in this paper has enabled the critical examination of the advantages and shortcomings of the methods. It appears that the scores obtained from the two methods indicate contradictory conclusions for the buildings investigated. Aspects considered in the RVS method provided conservative results. Both of the methods have limitations in terms of incorporating the parameters relevant for Bangladesh and many other countries. Considering these differences it might be possible to conduct a further study to configure suitable attributes for proposing a sound risk assessment technique focused particularly on the design and construction practices of the country. The study reveals that fine-tuning of the significantly contributing technical aspects of these procedures can lead to the development of an ideal Rapid Visual Screening Procedure which would provide more reliable assessment of the seismic vulnerability of the buildings, and form the basis for determining need for more complex vulnerability assessment.

ACKNOWLEDGEMENT

The authors acknowledge the funding of this research project by United Nation Office for Project Service (UNOPS) through Comprehensive Disaster Management Program (CDMP) of the Ministry of Disaster Relief and Rehabilitation of Bangladesh Government. The authors are also thankful to Mr. Mohammed Jobair and other Research Assistants of the project who helped in analyzing the data.

REFERENCES

- FEMA154, (2002). Rapid Visual Screening of Building for Potential Seismic Hazards: A Hand Book
- European Macroseismic Scale (1998). Macroseismic Intensity Scale. Classifications used in the European Macroseismic Scale (EMS). European Seismological Commission, Editor G. Grünthal, LUXEMBOURG 1998
- Sucuoglu, H. And Yazgan, U. (2003). Simple Survey Procedures for Seismic Risk Assessment In Urban Building Stocks. Seismic Assessment and Rehabilitation of Existing Buildings, 97-118, NATO Science Series, IV/29, Editors: S.T. Wasti and G. Ozcebe, Kluwer
- Uddin, A. M. K. and Yasmin, A. (2005). District Information-Cox's Bazar. Water Resource Ministry, Water Resource Planning Organization, People's Republic of Bangladesh Government.

NUMERICAL AND EXPERIMENTAL STUDY OF STRUCTURES WITH SOFT STORIES

HIMADREE ROY

Bangladesh University of Engineering and Technology, Dhaka, Bangladesh

liju_113/08@yahoo.com

IFTEKHAR ANAM

The University of Asia Pacific, Dhaka, Bangladesh

ifteanam@accessstel.net

ABSTRACT

Soft stories are one of the prime reasons of structural failure during earthquakes. However, very little attention is paid to this serious design deficiency by architects or engineers in Bangladesh. This paper presents results of numerical and experimental works performed on the seismic response of structural models with soft stories. The experimental facilities used for this purpose includes a small shake table capable of generating defined earthquake motion, using an indigenous and inexpensive approach from the combination of mechanical and electrical equipments. It is probably the first such work reported in Bangladesh and this concept can be used for developing larger shake tables, the cost of which would otherwise be prohibitive. The structural model used for the experiments is a 3-storied structure made of springs (as columns) and timber plates (as floors). Floor vibrations are recorded with time using mechanical devices. The data acquisition system is found to be very accurate as the recorded ground motion matches very well with the target ground motion data. Several experimental scenarios are created by changing the structural mass and stiffness at different floors and subjecting the structural model to scaled El Centro ground vibrations of different time durations. The experimental results match very well with the numerical predictions from computer program using dynamic analysis incorporating the nonlinear load-deflection relationship of the springs.

1. INTRODUCTION

The threat of earthquake in Bangladesh is a widely accepted reality now, particularly after devastating effects of earthquakes in almost all the neighboring countries (e.g., India, Pakistan, Sri Lanka, Afghanistan) and many others within South-east Asia. In the backdrop of such devastating earthquakes, there is growing need for serious theoretical and experimental works on seismic behavior of building structures and control of structural vibration under strong ground shaking.

The lack of testing facility on earthquake vibration is of particular concern due to the recent awareness or alarm of seismic vulnerability of the engineering structures in Bangladesh. Although some useful theoretical

works on these topics have been performed mainly at academic institutions, very few of these works have been supported by corresponding experimental verifications. In fact no work has yet been reported that had simulated real earthquake ground motion data.

Assessment of structural damage patterns has diagnosed soft stories in building frames caused by discontinuities of the story stiffness as one of the prime reasons of structural failure. However, very little attention is paid to this serious design deficiency by architects or engineers in Bangladesh. In fact due to the quick growth of high-rise buildings and lack of parking facilities in urban areas, most newly built buildings are designed with open ground floors supporting stories with masonry infills, and as a result this deficiency is even more widespread in building structures now than ever before. Due to lack of knowledge of the mechanical properties of brick masonry, the structural analysis of a frame under lateral load and vibration is often performed by taking the stiffness of RC columns and beams into consideration, but the stiffness of brick infill is almost never considered in these calculations.

In order to better understand the structural behavior of RC frames subjected to lateral loads or ground motions, it is necessary to understand the characteristics of brick masonry infills. Nonlinear dynamic analysis is often performed for the frames replacing the brickwalls by an 'Equivalent Diagonal Strut' proposed by Saneinejad & Hobbs (1995) and modified by Madan et al. (1997). Although the work on the in-plane behavior of infills is comparatively new in Bangladesh (Hossain, 1997, Azam & Amanat, 2005, Anam & Azam, 2006), it has been extensively studied over the last several decades (e.g., Omote et al., 1977, Engelkirk and Hart, 1984, Papia, 1998, Asteris, 2003) in attempts to develop a rational approach for design of such frames, many of which demonstrated the poor performance of structures with soft stories.

2. CONTEXT AND OBJECTIVES

Experimental verification of nonlinear dynamic analyses was initiated locally at The University of Asia Pacific (UAP). Results of the initial tests and numerical verification were reported by Manju (2004) and Manju et al. (2005). Since these works concentrated on sinusoidal ground motions only, the structural responses depended very strongly on the frequency of the motions (i.e., due to resonance) and could not provide a rational assessment of structural behavior during real earthquakes or assess measures of structural control or improvement.

The main objective of this work is to report development of the experimental facilities used for this purpose (Roy, 2007), including a small shake table capable of generating defined earthquake motion (scaled El Centro earthquake) using an indigenous and inexpensive approach. It is the first such work reported in Bangladesh and this concept can be used for

developing larger shake tables, the cost of which would otherwise be prohibitive. The importance of the work can be assessed in this context.

Moreover, since the effect of soft stories on the structural behavior during earthquakes is seldom considered seriously in Bangladesh, the experimental works also simulate structural models with soft stories. Their structural properties are modified easily by changing the stiffness and mass for time varying ground vibration here. Numerical results of the structural motions are compared with measured experimental results for simple building models, particularly observing the effects of soft stories.

3. NUMERICAL FORMULATION

The numerical formulation for the analysis of the model structure is based on the concepts of nonlinear structural dynamics (Chopra, 1995). The mass, damping and stiffness matrices can be generalized for a multi-degree-of-freedom (MDOF) system, so that the equations of motion of a system subjected to ground acceleration a_g can be written in the general form

$$M d^2u_r/dt^2 + C du_r/dt + K u_r = - M r a_g \tag{1}$$

where the bold capital letters (M, C, K) represent the mass, damping and stiffness matrices, the bold small letters (d^2u/dt^2 , du/dt and u) represent the acceleration, velocity and displacement vectors and $r = \{1; 1; \dots; 1\}^T$ is a displacement transformation vector. Equation (1) is solved numerically to obtain the variation of displacement vector u with time. The Constant Average Acceleration (CAA) method is used here for numerical time-step integration to solve the dynamic equations of motion.

One aspect in implementing the time-step integration method mentioned above is the dependence of the stiffness matrix K on the relative floor deformations. As the springs in the structural model are not linearly elastic, the K matrix is not a constant and needs to be updated at each time step depending on the value of the displacement vector u_{i+1} . As such, equation (1) can be rewritten as

$$(K_{eff})_{i+1} u_{i+1} = - M r a_{g\ i+1} + C (v_{eff})_i + M (a_{eff})_i \tag{2}$$

where the bold small letters a , v and u indicate acceleration, velocity and displacement vectors respectively. The nonlinear equations need to be solved by an iterative method. The direct iteration method, also known as Picard method, has been used here for the nonlinear dynamic analyses (Reddy, 1993). A computer program has been developed in order to implement the numerical method described. It is a nonlinear dynamic analysis program carried out in the time domain.

4. EXPERIMENTAL SETUP

4.1 Structural model and ground motion arrangement

The structural model used in the experimental works is a three-storied model structure in addition to the ground floor and is about 60 cm high. Each floor is composed of a (60 cm × 60 cm) timber plate (modeled as floor slabs) and nine helical springs (for columns). They are assumed to provide the entire mass and stiffness respectively of the system.

The ground floor is supported on four-legged stand by means of four rollers on the corner. The rollers are attached to the stand. On the top of the ground floor there are three other floors each supported by springs coiled to the floor below. There are provisions for attaching extra weight on each floor. Without any extra weight, each floor weighs about 2 kg.

There is a 1.5 m long plate with the scaled El Centro earthquake data (marked as shown in Figure 1). This plate data is achieved by the original El Centro earthquake data divided by a scaling factor to ensure that it is accommodated within the shake table and allows the ground floor to vibrate freely. The base floor of the model is connected to the plate by a 5 cm connector and attached by screw in the middle of the plate, which effectively simulates the ground motion for the structural model. The other floors of the structure vibrate due to this ground motion.

A rotating shaft is fixed with a motor and rotates under the plate to generate the forward motion of the plate. The motor has a capacity of 1750 rpm, and its speed can be modified by a regulator. Thus the original El Centro data (time duration of 40 seconds) was run at three time durations; i.e., 15, 20 and 25 sec. The movement of the plate along the rotating shaft is shown in Figure 2.

4.2 Measurement of displacements

The arrangement used in this work to measure the dynamic structural includes a paper moving over a movable roller, the paper being able to slide over the roller at a certain speed, controlled by an arrangement of pulley system. Once the paper starts rolling it can record the motions of any floor as it vibrates with time, using a marker set at the floor level. The main device is about 1.8 m high and the arrangement for recording the displacement can be placed anywhere along its height.

4.3 Creating soft or weak story

The structural models have some arrangements to make any story soft or weak. To do that, the number of helical springs for a floor (originally it is nine) is reduced. In several simulations used in this work, only five springs are used in the ground floor to make this storey soft compared to the other floors of the structural model. A similar procedure is used to make a soft

first floor in some experiments. These arrangements are shown in Figures 3(a) and 3(b).

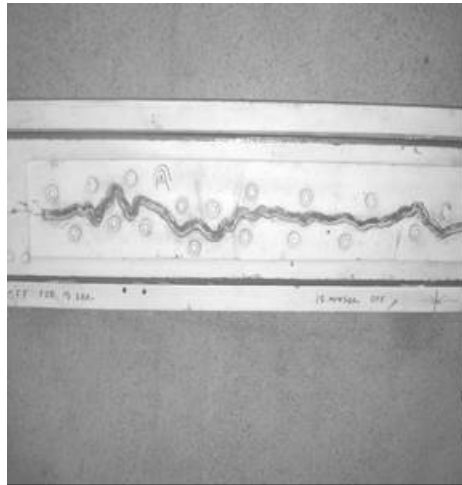


Figure 1: El Centro Earthquake plate (Marked)

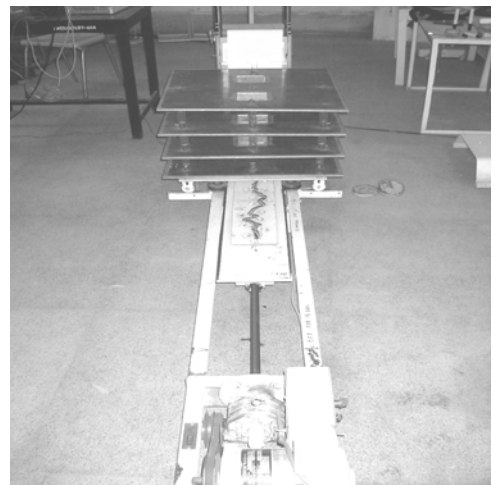


Figure 2: El Centro Earthquake plate moving along rotating shaft

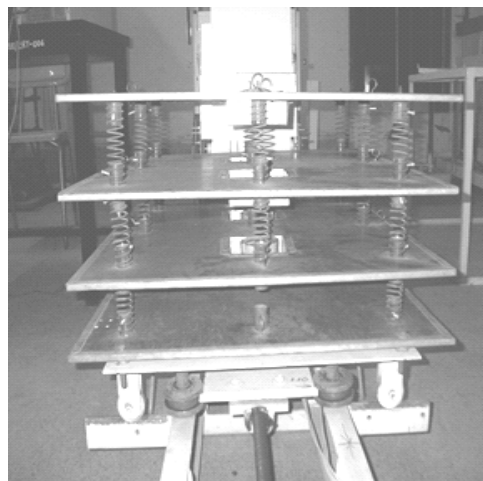


Figure 3: Arrangement with (a) Soft first story, (b) Soft second story

4.4 Properties of 3-storied structural model

The mechanical properties used for the 3-storied structural model are based on the work by Manju (2004). The load vs. deformation data shows that the floor springs have nonlinear elastic behavior with similar properties in lateral deflection on either side. The damping of each floor is determined by matching results of the free decay test of the top floor, which gave the damping ratio of each floor to be about 17%. This comparatively high damping ratio indicates significant friction within various components of the structural model.

5. RESULTS FROM NUMERICAL ANALYSIS AND EXPERIMENT

5.1 Laboratory simulation of scaled El Centro ground motion

One of the first objectives of the present work was to generate a predefined earthquake ground motion in the laboratory set up. As mentioned earlier, the El Centro ground motion scaled down (to a maximum ground motion amplitude of 3.5 cm) to allow the structural model to vibrate freely was intended to be generated here within time durations of 15, 20 and 25 seconds. Figure 4(a) shows the target ground motions while Figure 4(b) is the motion actually simulated in the laboratory in 15 seconds.

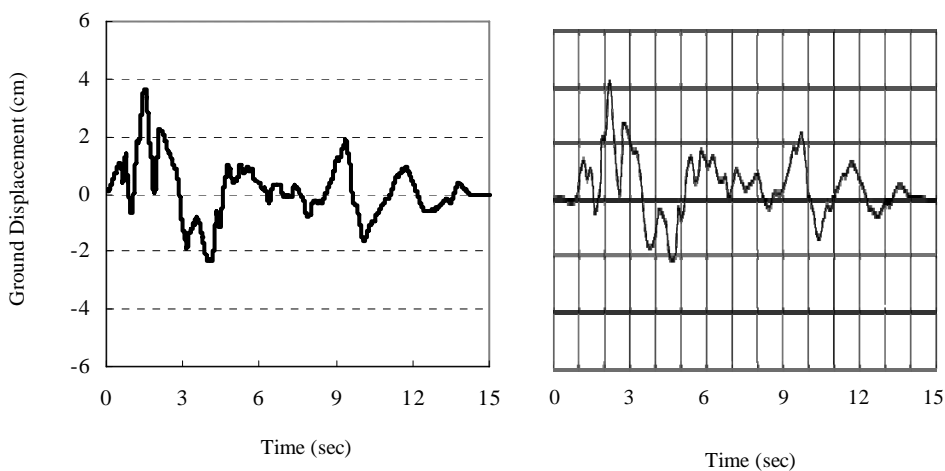


Figure 4: (a) Scaled El Cento ground motion, (b) Recorded motion in 15 seconds

The comparison between Figure 4(a) and 4(b) shows very good agreement between the intended and generated ground motions for all three time durations. There are minor discrepancies as can be observed visually, but the overall agreement is quite satisfactory. Since the process of ground motion generation requires accurate representation of the scaled motion in the 'Earthquake Plate', proper connection between the sub-structure and the structure itself, rigidity of the ground floor, effectiveness of the regulator and accuracy of the data recording device, these records show the accuracy of the arrangements.

5.2 Numerical and experimental floor deflections

A large number of experimental simulations were carried out to compare with corresponding numerical results. Deflection time series of all three floors were calculated and measured experimentally for (i) The original structure (i.e., no extra weight or soft story), (ii) Adding extra 2 kg weight at the two top floors of the original structure, (iii) Making the first story of the original structure soft, (iv) Adding extra 2 kg weight at the two top floors of the structure of (iii), (v) Making the second story of the original structure soft, (vi) Adding extra 2 kg weight at the two top floors of the structure of (v).

Table 1 and Table 2 show the numerical and experimental peaks for all the cases studied. Most of the results match quite satisfactorily, with significant discrepancies found in 3rd floor deflection for 15 sec simulation of Case (iii) (soft first story without extra weight) and particularly for 15 and 20 sec simulations of Case (v).

Table 1: Peak deflections (cm) without extra weight [Case (i), (iii), (v)].

Time	Floor	No Soft Story		Soft 1 st Story		Soft 2 nd Story	
		Exp	Num	Exp	Num	Exp	Num
15 sec	1	3.90	3.46	4.00	3.98	3.90	3.64
	2	4.90	4.52	4.40	4.29	3.00	4.38
	3	5.50	5.13	6.00	4.67	3.90	4.83
20 sec	1	5.60	4.63	3.80	4.15	3.50	4.13
	2	5.70	5.48	3.90	4.69	3.90	5.14
	3	6.20	5.96	5.50	4.96	3.00	5.50
25 sec	1	4.00	3.85	5.20	4.66	4.10	4.12
	2	4.50	4.03	5.60	5.12	4.80	4.79
	3	5.00	4.11	5.00	5.37	5.00	5.01

Table 2: Peak deflections (cm) with extra weights [Case (ii), (iv), (vi)].

Time	Floor	No Soft Story		Soft 1 st Story		Soft 2 nd Story	
		Exp	Num	Exp	Num	Exp	Num
15 sec	1	4.70	4.44	4.80	5.02	4.20	4.51
	2	5.30	5.04	6.90	6.27	5.10	6.07
	3	6.30	5.81	6.20	6.96	5.75	6.77
20 sec	1	4.20	3.69	4.00	4.29	4.00	3.91
	2	4.30	5.05	4.80	4.54	5.25	4.43
	3	5.30	5.87	5.00	4.95	5.80	4.88
25 sec	1	4.70	4.74	4.90	3.99	4.00	3.56
	2	5.50	5.90	5.10	4.79	3.90	4.49
	3	6.30	6.55	5.60	5.25	4.10	4.91

Figures 5~7 show the numerical and experimental time series variations of selected floor deflections for various time durations (15, 20, 25 sec) and experimental arrangements, with Figures (a) showing the numerical results and Figures (b) the experimental data. The agreement between the two is quite satisfactory in general, as shown by visual inspection. The figures also show the relatively rapid variations of structural motions for structures without extra weight (Figure 5) and slower variations for the others (Figures 6 and 7), due to larger time periods caused by extra weights.

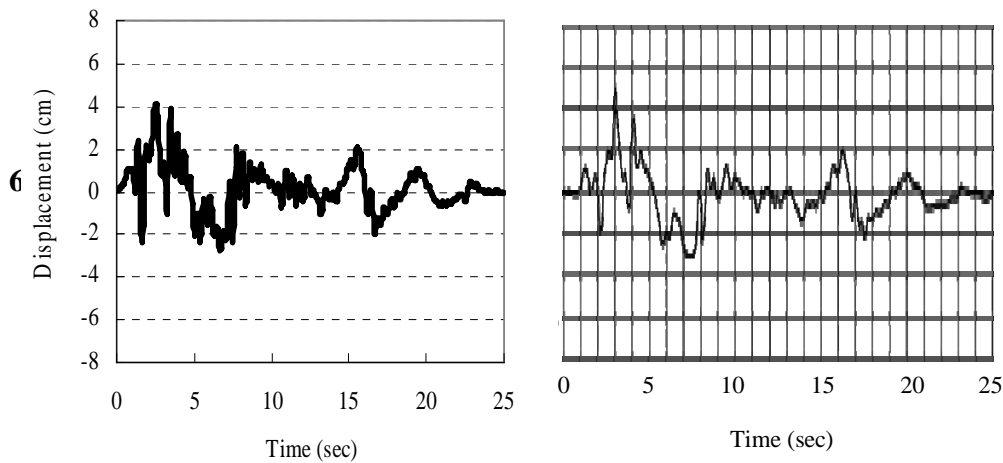


Figure 5: 3rd Floor displacement (25 sec, no wt, no soft story)
 (a) Numerical, (b) Experimental

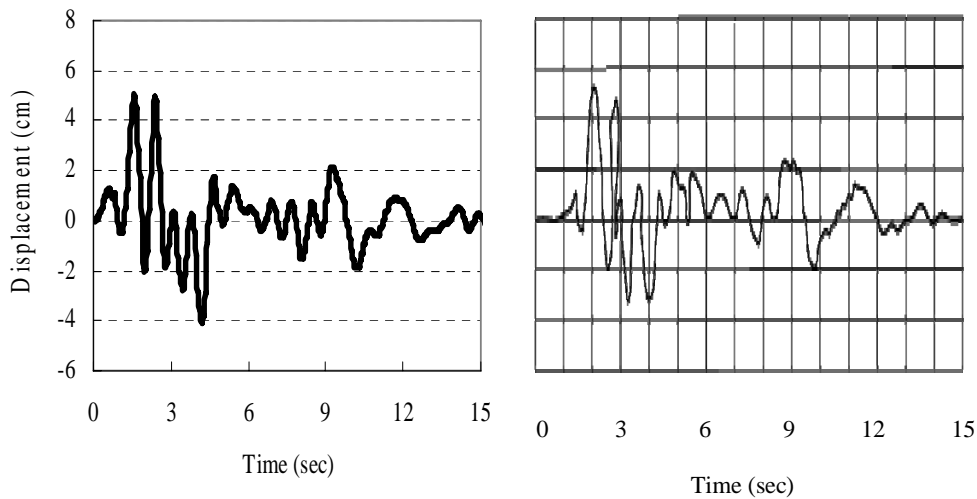


Figure 6: 1st Floor displacement (15 sec, extra wt, soft story1)
 (a) Numerical, (b) Experimental

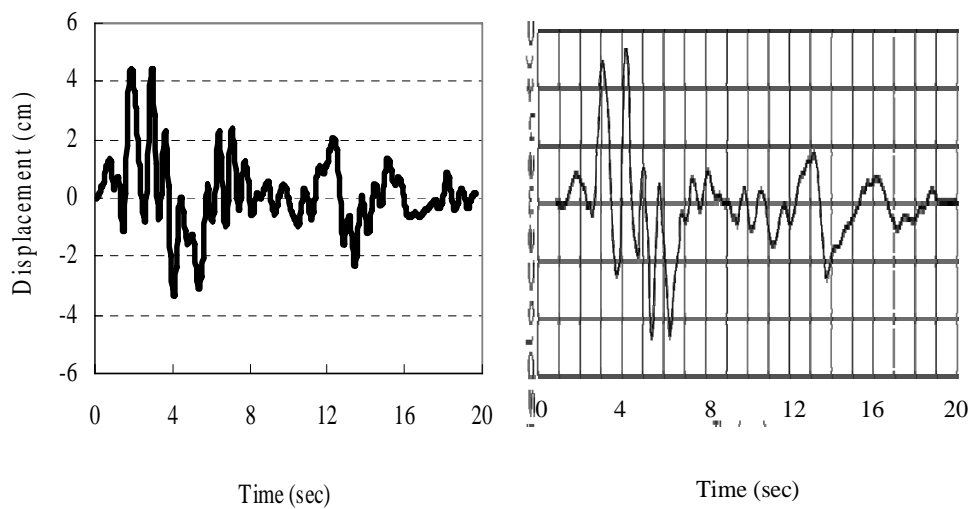


Figure 7: 2nd Floor displacement (20 sec, extra wt, soft story2)
 (a) Numerical, (b) Experimental

6. OBSERVATIONS FOR STRUCTURES WITH SOFT STORIES

The influence of soft stories is a significant aspect of the results from the analyses. The proper way to show this effect is by observing the relative floor displacements that eventually lead to column deformations and internal forces. Table 3 demonstrates selected results from numerical analysis (for 15 sec simulation) of the laboratory model.

Table 3: Peak column deformation (cm).

	Col	No Soft Story	Soft 1 st Story	Soft 2 nd Story
No	1	1.29	1.60	0.92
Wt.	2	1.08	0.69	1.41
Extra	1	1.74	3.32	1.84
Wt.	2	1.35	1.51	2.59

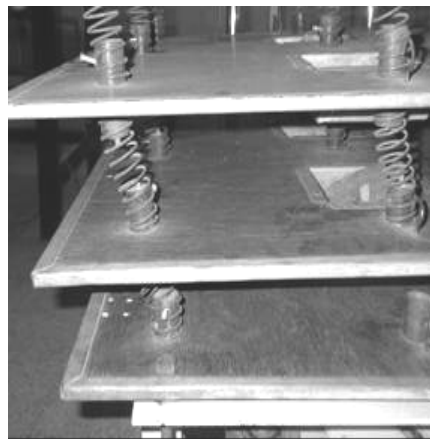


Figure 8: Large column deformation in soft first story

The influence of extra weight and soft story on the relative column displacements is quite apparent. In general, the peak deformations increase significantly (by about 25~125%) after adding extra weights. Moreover, whereas a soft first story with extra weight on the top two floors [Case (iv)] results in maximum relative column deformations of 3.32 and 1.51 cm in the 1st and 2nd story respectively, a soft second story with extra weight [Case (vi)] changes these column deformations to 1.84 and 2.59 cm respectively. All these deformations are quite large compared to the case without soft story (where the maximum column deformations are 1.74 and 1.35 cm respectively) and result in considerable distress of the soft story columns as shown in Figure 8 during the laboratory simulations.

7. CONCLUSIONS

The paper shows results of numerical and experimental works performed on the seismic response of 3-storied structural models with and without soft

stories. A (60 cm × 60 cm) shake table capable of generating defined earthquake motion was developed (the first such work reported in Bangladesh) using an indigenous and inexpensive approach. This concept can be used for developing larger shake tables, the cost of which would otherwise be prohibitive. The generated ground motions matched almost exactly with the target data, which validates the process of simulating defined ground motions.

For almost all the time series simulations performed here (varying earthquake durations, story stiffness and mass of the structural model), the numerical results of floor deflections matched very well with the experimental data, validating the numerical scheme used.

The column deformations of the laboratory model strongly depended on the presence and location of the soft story as well as extra weight, demonstrating the importance of soft stories and structural weight on the seismic response of building structures.

REFERENCES

- Anam, I., and Azam, H. M. U., 2006. Seismic behavior of nonlinear RC frames with masonry infills. *10th East Asia Pacific Conference on Structural Engineering and Construction*, Bangkok, Thailand, Vol 3, 393-398.
- Asteris, P. G., 2003. Lateral stiffness of brick masonry infilled plane frames. *ASCE Journal of Structural Engineering* 129, 1313-1323.
- Azam, H. M. U., and Amanat, K. M., 2005. Effect of infill as a structural component on the column design of multi-storied building. *UAP Journal of CEE* 1, 12-17.
- Chopra, A. K., 1995. *Dynamics of structures: Theory and applications to earthquake engineering*. Prentice-Hall, Inc., NJ, USA.
- Engelkirk, R. E., and Hart, G. C., 1984. *Earthquake design of concrete masonry buildings*. Vol. 2, Prentice-Hall Inc., NY, USA.
- Hossain, M., 1997. *Non-linear Finite Element analysis of wall-beam structures*. Ph.D. Thesis, Department. of CE, BUET.
- Madan, A., Reinhorn, A. M., Mander, J. B., and Valles, R. E., 1997. Modeling of masonry infill panels for structural analysis. *ASCE Journal of Structural Engineering* 123, 1295-1302.
- Manju, F., 2004. *Experimental verification of nonlinear dynamic analyses*. B. Sc. Engg. Thesis, Vol. II, Department. of CEE, UAP.
- Manju, F., Anwary, A. R., and Anam, I., 2005. *Nonlinear seismic analyses and experimental verification*. 3rd Annual Paper Meet and International Conference on CE, Dhaka, Bangladesh, 211-222.
- Omote, Y., Mayes, R., Chen, S. J., and Clough, R. W., 1977. *A literature survey of transverse strength of masonry walls*. Vol. 2, UCB/EERC-77/07, The University of California at Berkeley.
- Papia, M., 1998. Analysis of infilled frames using a coupled Finite Element and Boundary Element solution scheme. *International Journal of Numerical Methods in Engineering* 26, 731-742.

- Reddy, J. N., 1993. *An introduction to the Finite Element method*. McGraw-Hill Inc., NY, USA.
- Roy, H., 2007. *Numerical and experimental study of structures with soft stories*. B. Sc. Engg. Thesis, Department. of CE, UAP.
- Saneinejad, A., and Hobbs, B., 1995. Inelastic design of infilled frames. *ASCE Journal of Structural Engineering* 121, 634-643.

SEISMIC VULNERABILITY ASSESSMENT OF RC BUILDINGS OF DHAKA CITY

MOHAMMAD SAJEDUL HUQ¹, MOHAMMAD RAFAT SADAT²,
MOHAMMAD SALAHUDDIN RIZVI³ and MD. NAFIUL HAQUE⁴
Undergraduate Students, Department of Civil Engineering, BUET,
Dhaka, Bangladesh

MEHEDI AHMED ANSARY
Professor, Department of Civil Engineering, BUET, Dhaka, Bangladesh
ansary@ce.buet.ac.bd

ABSTRACT

The objective of this study is to assess the seismic vulnerability of RC buildings of selected area of Dhaka city by FEMA Rapid Visual Screening method and the Turkish Methods. The areas covered under the survey are part of Dhanmondi, Lalmatia and a part of the Mohammadpur residential area. The survey focused on earthquake issues of residential buildings such as identifying building type, plot size and shape, clear distances from surrounding structures, road width and basic information of the building: type of foundation, slab type, year of construction, number of storey, number of inhabitants etc. The detail analysis using the Turkish level-2 method covered the determination of plinth area (length x width), column size and direction, lift core size, cantilever length of the building etc.

Digital photographs of each building from at least two directions were collected. The survey process was conducted between March to May, 2007. A database consisting of 2007 buildings was compiled in MS Access. Among the buildings, 1082 are RC and rest 925 is URM buildings. Among the RC buildings, 456 have a soft storey. In case of most of the soft storied buildings, the ground floor is used as parking space. Use of Rapid Visual Screening (RVS) and Turkish (level-1) methods to survey the buildings enable to divide the screened buildings into two categories: those that are expected to have acceptable seismic performance and those that are unacceptable and need to be studied further. Those buildings which were designated as seismically vulnerable by RVS and Turkish (level-1) methods, more detailed analysis using Turkish (level-2) method and ETABS were carried out.

1. INTRODUCTION

Reinforced Cement Concrete (RC) frame buildings are becoming increasingly common in Dhaka city. Many such buildings constructed in recent times have a special feature – the ground storey is left open for the purpose of parking, i.e. the columns in the ground floor do not have any partition walls between them. Such buildings are often termed as ‘Soft Storey’ buildings. Open ground storey buildings have consistently shown

poor performances during the past earthquakes across the world (for example during the 1999 Turkey and Taiwan earthquakes, the 2003 Bam earthquake, the 2001 Bhuj earthquake and the 2005 Kashmir earthquake), a significant number of them have collapsed. For the past 10 years Bangladesh has had a boom in Real Estate sector. The prime location has been Dhanmondi area with further extension in Lalmatia and Mohammadpur. Worryingly most of the RC buildings of these areas have a soft storey. The objective of this study is to compile a database of RC buildings within a specified area of Dhaka City and to assess the earthquake vulnerability of those buildings using RVS (Rapid Visual Screening) method (FEMA, 2002) and the Turkish (level 1 and 2) methods (Sucuoglu and Yazgan, 2003).

2. THE SURVEYED AREA

The area selected for the survey started from Road 32, Dhanmondi up to the end of Ring Road, Mohammadpur. The two parallel boundaries are the Satmasjid Road and the Mirpur Road. Figure 1(a) shows the surveyed area. Figure 1(b) shows the Sobhanbag pocket with concentration of high-rises.

The reason behind selecting this area is that for the last few years' realtors were involved in building apartments in this area. These apartments tend to have a weaker ground storey as most of the structures have provisions for parking there. The selected area is basically a residential one. Recently, it has turned into a semi commercial area with a growth of Hospitals, Supermarkets, Schools, Universities and commercial structures in an unplanned way.

3. MEHODOLOGY

To assess the buildings of the surveyed area two methodologies were mainly used namely RVS (Rapid Visual Screening) suggested by FEMA and Turkish methods.

3.1 Rapid Visual Screening

Rapid visual screening (RVS) method of buildings for potential seismic hazards, originated in 1988 with the publication of the FEMA 154 Report. RVS provides a procedure to identify record and rank buildings that are potentially seismically hazardous (FEMA, 2002). This screening methodology is encapsulated in a one-page form, which combines a description of a building, its layout and occupancy, and a rapid structural evaluation related to its seismic hazard.

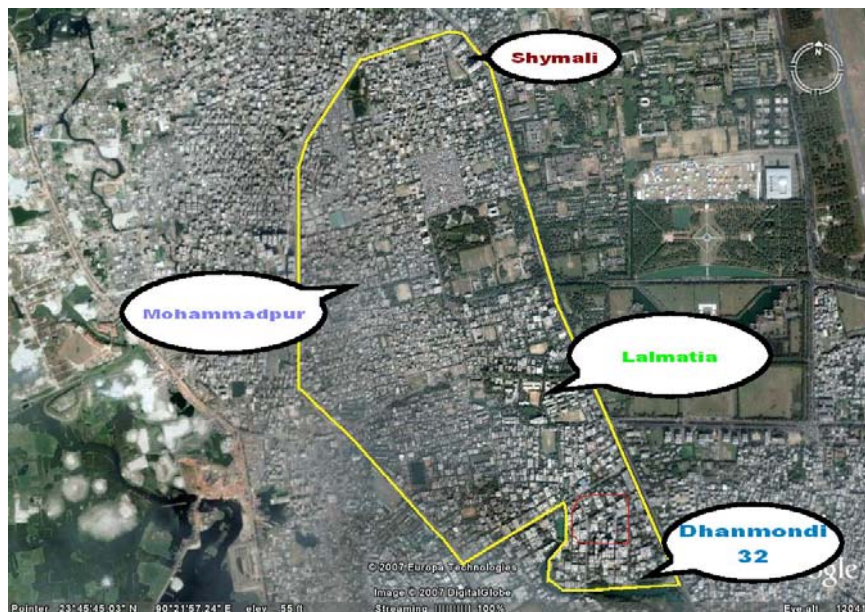


Figure 1a: Aerial View of Surveyed Area (Dhanmondi Road 32 to Shamoli)



Figure 1b: Sobhanbag Pocket with High Rise Buildings (>10 stories)

Although RVS is applicable to tall buildings, its principal purpose is to identify (1) older buildings designed and constructed before the adoption of adequate seismic design and detailing requirements (2) buildings on soft or poor soils, and (3) buildings having performance characteristics that negatively influence their seismic response. Once identified as potentially hazardous, such buildings should be further evaluated by a design professional experienced in seismic design to determine if, in fact, they are seismically hazardous.

The rapid visual screening method is designed to be implemented without performing any structural calculations. The procedure utilizes a scoring system that requires the evaluator to (1) identify the primary structural lateral load-resisting system, and (2) identify building attributes that modify the seismic performance expected for this lateral load-resisting system. The inspection, data collection and decision-making process typically occurs at the building site, and is expected to take around 30 minutes for each building. The screening is based on numerical seismic hazard and vulnerability score.

Basic Structural hazard scores for various building types are provided on the RVS form. The screener modifies the basic structural hazard score by identifying and circling score modifiers which are then added (or subtracted) to the basic structural hazard score to arrive at a final structural score, S. The basic structural hazard score, score modifiers, the final structural score S, all relate to the probability of building collapse. The result of the screening procedure is a final score that may range above 10 or below 0, with a high score indicating good expected seismic performance and a low score indicating a potentially hazardous structure. While the score is related to the estimated probability of major damage, it is not intended to be a final engineering judgment of the building, but merely to identify buildings that may be hazardous and require detailed seismic evaluation. If the score is 2 or less, a detailed evaluation is recommended. On the basis of detailed evaluation, engineering analysis and other detailed procedures, a final determination of seismic adequacy and need for rehabilitations can be made. Figure 2 shows a sample RVS scoring form.

Occupancy				Soil Type						FALLING HAZARDS									
Assembly	Govt. Office	Office	Number of Pers	A	B	C	D	E	F	Unreinforced	Parapets	Cladding	Chimney	Other					
Commercial	Historic Resider	School	0-10 11-100 101-1000 1000+	Hard Rock	Avg. Rock	Dense Soil	Stiff Soil	Soft Soil	Poor Soil										
BASIC SCORE, MODIFIERS AND FINAL SCORE, S																			
Building Type	W1	W2	S1 (MRF)	S2 (BR)	S3 (LM)	S4 RC	S5 SW	C1 JRM	C2 INF	C3 (MRF)	(SW)	JRM	INF	PC1 (TU)	PC2	RM1 (FD)	RM2 (RD)	URM	
Basic Score	4.4	3.8	2.8	3	3.2	2.8	2	2.5	2.8	1.6	2.6	2.4	2.8	2.8	1.8				
Mid Rise (4 to 7 Stories)	N/A	N/A	0.2	0.4	N/A	0.4	0.4	0.4	0.4	0.2	N/A	0.2	0.4	0.4	0				
High Rises (> 7 Stories)	N/A	N/A	0.6	0.8	N/A	0.8	0.8	0.6	0.8	0.3	N/A	0.4	N/A	0.6	N/A				
Vertical Irreg.	-2.5	-2	-1	-1.5	N/A	-1	-1	-1.5	-1	-1	N/A	-1	-1	-1	-1				
Plan Irregularity	-0.5	-0.5	-0.5	-0.5	-0.5	-0.5	-0.5	-0.5	-0.5	-0.5	-0.5	-0.5	-0.5	-0.5	-0.5				
Pre-Code	0	-1	-1	-0.8	-0.6	-0.8	-0.2	-1.2	-1	-0.2	-0.8	-0.8	-1	-0.8	-0.2				
Post Benchmark	2.4	2.4	1.4	1.4	N/A	1.6	N/A	1.4	2.4	N/A	2.4	N/A	2.8	2.6	N/A				
Soil Type C	0	-0.4	-0.4	-0.4	-0.4	-0.4	-0.4	-0.4	-0.4	-0.4	-0.4	-0.4	-0.4	-0.4	-0.4				
Soil Type D	0	-0.8	-0.6	-0.6	-0.6	-0.6	-0.4	-0.6	-0.6	-0.4	-0.6	-0.6	-0.6	-0.6	-0.6				
Soil Type E	0	-0.8	-1.2	-1.2	-1	-1.2	-0.8	-1.2	-0.8	-0.8	-0.4	-1.2	-0.4	-0.6	-0.8				
FINAL SCORE, S =																			1.2

Figure 2: Sample RVS Scoring Form for High Seismicity Zone (after FEMA, 2002)

3.2 Turkish Method

In recent times, after the 1999 earthquake in the cities of Kocaeli and Duzce, Government of Turkey and Japan International Cooperation Agency (JICA) came forward for implementing a regional seismic assessment and rehabilitation program. Researchers from various universities were involved in this program supported by the Government of Turkey and JICA. A simple Two-level Seismic Assessment Procedure for a building stock was proposed (Sucuoglu and Yazgan; 2003). In this study, most vulnerable buildings that may undergo severe damage in a future earthquake are identified. A survey of 477 damaged buildings (1-7 storey) affected by Duzce earthquake (November 1999) was carried out. This was then compiled to form a database of damaged buildings to be used for future research work. This database was employed for developing the performance score (PS) equation to determine the vulnerability of a reinforced concrete building. Figure 3 shows a sample Turkish Form.

Simple Survey Procedure (Turkish) for Risk Assessment of Concrete Buildings							
Table A: Initial & Vulnerability Scores for Level - I Survey of Concrete Buildings							
No. of Stories	Initial Score (on Soil Zoning)			Soft Story	Heavy Overhang	Apparent Quality	Short Column
	60<PGV<80	40<PGV<60	20<PGV<40				
1, 2	90	125	160	-5	-5	-5	-5
3	90	125	160	-10	-10	-10	-5
4	80	100	130	-10	-10	-10	-5
5	80	90	115	-15	-15	-15	-5
6, 7	70	80	95	-15	-15	-15	-5
Table B: Initial & Vulnerability Scores for Level - II Survey of Concrete Buildings							
No. of Stories	Initial Score (on Soil Zoning)			Soft Story	Heavy Overhang	Apparent Quality	Short Column
	60<PGV<80	40<PGV<60	20<PGV<40				
1, 2	95	130	170	0	-5	-5	-5
3	90	125	160	-10	-5	-10	-5
4	90	115	145	-15	-10	-10	-5
5	90	105	130	-15	-15	-15	-5
6, 7	80	90	105	-20	-15	-15	-5
Table B: Contd. For Level - II Survey							
No. of Stories	Pounding	Topography	Plan Irregularity	Redundancy	Strength Index		
1, 2	0	0	0	0	-5		
3	-2	0	-2	0	-5		
4	-3	-2	-2	-5	-5		
5	-3	-2	-5	-10	-10		
6, 7	-3	-2	-5	-10	-10		
Table C: Vulnerability Parameters							
Soft Story	No (0)	Yes (1)					
Heavy Overhang	No (0)	Yes (1)					
Apparent Quality	Good (0)	Moderate(1)	Poor (2)				
Short Column	No (0)	Yes (1)					
Pounding Effect	No (0)	Yes (1)					
Topography Effect	No (0)	Yes (1)					
Plan Irregularity	No (0)	Yes (1)					
Redundancy	Redundant,R (0)	Semi-R (1)	Weakly-R (2)				
Strength Index	Strong (0)	Weak (1)					
General Equation for Seismic Performance Scores (PS) for both Levels ("cut-off" PS = 50)							
PS =(Initial Score) - ∑ (Vulnerability Parameter) X (Vulnerability Score)							

Figure 3: Tables and General Equation of Turkish Procedure (after Sucuoglu and Yazgan, 2003)

3.2.1 Level-1 Survey

The trained observers collect data through walk-down visits. The parameters that are selected in Level-1 survey for representing building vulnerability are the following:

- a. The number of stories above ground
- b. Presence of a soft story (Yes or No)
- c. Presence of heavy overhangs, such as balconies with concrete parapets (yes or No)
- d. Apparent building quality (Good, Moderate or Poor)
- e. Pounding between adjacent buildings (Yes or No)
- f. Local soil conditions (Stiff or Soft)
- g. Topographic effects (Yes or No)

All of the above parameters are found to have a negative feature on the building system under earthquake excitations on a variable scale

3.2.2 Level-2 Survey

A Level 2 survey is done for the buildings when those are found to be falling into the moderate and high-risk levels using level 1 risk assessment. The trained observer teams enter into the basements and ground stories of those buildings for collecting more data for Level 2 risk assessment. Their first task is to confirm or modify the previous grading by Level-1 method on soft stories, short columns and building quality, through closer observation. The second and more elaborate task is to prepare a sketch of the ground floor plan and measure the dimensions of columns, concrete and masonry

walls. This data is then employed for calculating the Redundancy and Strength Index parameters.

Once the vulnerability parameters of a building are obtained from two-level surveys and its location is determined, the seismic performance scores for survey levels 1 and 2 are calculated by using Tables A and B respectively as shown in Fig 3. In these Tables, an initial score is given first with respect to the number of stories and intensity zone. Then the initial score is reduced for every vulnerability parameter that is observed or calculated. A general equation for calculating performance score (PS) can be formulated as follows:

$$PS = (\text{Initial Score} - \sum (\text{Vulnerability parameter}) \times (\text{Vulnerability Score}))$$

Cut-off value for seismic performance score (PS) is 50. Table C in Figure 3 presents all the vulnerability parameters used in Turkish Method.

4. COLLECTION OF BUILDING DATA

The areas covered under the survey are part of Dhanmondi, Lalmatia and part of Mohammadpur residential area. The survey was mainly focused on earthquake issues such as identifying building type, plot size and shape, clear distances from surrounding structures, road width and basic information of the building: type of foundation, slab type, year of construction, number of storey, number of inhabitants etc. The detail analysis (or the Turkish level-2 analysis) covered the determination of plinth area (length x width), column size and direction, lift core size, cantilever length of the building etc. Digital photographs of each building from at least two directions were taken. The developers' names concerned with each building are also recorded during the survey. Detailed data were collected for 10% of the buildings for Turkish Level-2 analysis, which includes column and lift core dimensions and other relevant parameters. The data was then compiled in an MS-ACCESS Database. With the help of the database, analysis of the building stocks of the area under survey was possible. Figure 4 shows a sample of the database and Figure 5 shows two sample buildings.

5. DATA ANALYSIS

The compiled database has 2007 building data stored for the surveyed area. Out of these, 1082 buildings are RC buildings and the rest 925 buildings are un-reinforced masonry (URM). Among the RC buildings 456 have soft storey.

Figure 6 shows the relation between number of buildings and number of storey. From this figure, it is evident that 6 storied buildings are predominant, as the RAJUK does not give permission to build structures more than 6 storey within the residential areas. There are some higher storey buildings outside the RAJUK area within Dhanmondi located between

Sobhanbag Mosque and Road number 25. (high rise pocket as shown in Fig. 1b). Also a few high rises are located at Lalmatia and Mohammadpur areas. Figure 7 shows the relation between numbers of buildings with presence of overhangs. The figure indicates most buildings tend to have overhang (mostly verandah). Heavy overhang makes a structure risky for earthquake according to the Turkish Method. Figure 8 shows the relation between numbers of buildings, plinth area and the number of storey. This figure also shows that 6 storey buildings are dominant. Among those most of them ranged around 2000-3000sft or >5000sft.

Entry	Building	Locatio	Soft St	Shape	Numbr	Plinth Are	Slab Ty	Year of Co	Lift	Lift cor	Total	Apparent	Numbr	Parkin	Cantile	Column n	Color	Picture Number	
1	3/1	AA	<input checked="" type="checkbox"/>	Rectangle	9	7,000.00	Beam	2002	<input checked="" type="checkbox"/>		32	Good	181	32	3.00		Acros	I-301a,b	
2	3/2	AA	<input checked="" type="checkbox"/>	Rectangle	8	2,500.00	Beam	1997	<input type="checkbox"/>		8	Good	150	4	2.00		Acros	I-302a,b	
3	3/3	AA	<input checked="" type="checkbox"/>	Rectangle	6	7,100.00	Beam	2004	<input type="checkbox"/>		1	Good	350	12	1.00		Acros	I-303a,b	
4	3/5	AA	<input checked="" type="checkbox"/>	Rectangle	6	6,900.00	Beam	2007	<input checked="" type="checkbox"/>		20	Good	115	20	5.00			I-305a,b	
5	3/9	AA	<input checked="" type="checkbox"/>	Rectangle	9	6,800.00	Beam	2000	<input checked="" type="checkbox"/>	7x9	32	Good	190	32	5.00	24x24	Acros	I-309a,b	
6	3/12	AA	<input checked="" type="checkbox"/>	Irregular	2	15,000.00	Beam	1989	<input type="checkbox"/>		1	Medium	4000	2	0.00	16x16	Acros	I-312	
7	3/19	IR	<input checked="" type="checkbox"/>	Rectangle	6	6,580.00	Beam	2003	<input checked="" type="checkbox"/>	6x8	20	Good	114	20	4.00			I-319a,b	
8	9/1	IR	<input checked="" type="checkbox"/>	Rectangle	6	2,400.00	Beam	2007	<input checked="" type="checkbox"/>		10	Good	56	7	6.00		Along	I-901	
9	9/2	IR	<input checked="" type="checkbox"/>	Rectangle	6	4,600.00	Flat	2007	<input checked="" type="checkbox"/>	5x8	10	Good	60	12	5.00	30x12		Acros	I-902a,b
10	9/6	IR	<input checked="" type="checkbox"/>	Rectangle	6	4,568.00	Beam	2007	<input checked="" type="checkbox"/>	5x7	15	Good	92	15	6.00			I-906	
11	9/8	IR	<input checked="" type="checkbox"/>	Rectangle	6	4,500.00	Beam	2007	<input checked="" type="checkbox"/>	5x7	10	Good	62	10	4.00			I-908	
12	9/14	IR	<input checked="" type="checkbox"/>	Square	4	5,800.00	Beam	2007	<input checked="" type="checkbox"/>		20	Good	117	20	6.00			I-914a,b	
13	9/20	IR	<input checked="" type="checkbox"/>	Rectangle	6	4,500.00	Beam	2001	<input checked="" type="checkbox"/>	5x7	16	Good	96	16	5.00			I-920	
14	6/4	IR	<input checked="" type="checkbox"/>	Rectangle	4	5,920.00	Beam	1998	<input type="checkbox"/>		8	Medium	42	7	0.00			I-604	
15	6/7	IR	<input checked="" type="checkbox"/>	Rectangle	6	4,500.00	Beam	2007	<input checked="" type="checkbox"/>		15	N/A	92	15	0.00			I-607	
16	6/6	IR	<input checked="" type="checkbox"/>	Rectangle	6	4,300.00	Beam	2007	<input checked="" type="checkbox"/>	5x7	15	Good	86	24	4.00			I-606	
17	6/5	IR	<input checked="" type="checkbox"/>	Rectangle	6	2,900.00	Beam	2007	<input checked="" type="checkbox"/>	5x6	5	Good	28	9	5.00			I-605a,b	
18	5/7	IR	<input checked="" type="checkbox"/>	Rectangle	9	4,580.00	Beam	2001	<input checked="" type="checkbox"/>	5x8	24	Good	143	24	4.00			I-507a,b	
19	5/8	IR	<input checked="" type="checkbox"/>	Rectangle	6	4,350.00	Beam	2006	<input checked="" type="checkbox"/>		15	Good	86	15	4.00			I-508	
20	5/3	IR	<input checked="" type="checkbox"/>	Rectangle	6	4,280.00	Beam	2002	<input checked="" type="checkbox"/>		15	Good	85	15	0.00			I-503	
21	5/4A	IR	<input checked="" type="checkbox"/>	Rectangle	6	4,200.00	Beam	2007	<input checked="" type="checkbox"/>	10.5x8	15	Good	82	15	4.00	24x24	Acros	I-504b	
22	4/9A	IR	<input checked="" type="checkbox"/>	Square	8	2,520.00	Beam	1998	<input type="checkbox"/>		14	Good	82	8	3.00			I-409a	
23	4/9B	IR	<input checked="" type="checkbox"/>	Rectangle	4	1,400.00	Beam	2000	<input type="checkbox"/>		3	Good	16	3	3.00			I-409b	
24	2/14	IR	<input checked="" type="checkbox"/>	Rectangle	6	8,100.00	Beam	2007	<input checked="" type="checkbox"/>		20	N/A	115	20	3.00			I-214	
25	2/13	IR	<input checked="" type="checkbox"/>	Rectangle	6	8,000.00	Beam	2002	<input checked="" type="checkbox"/>		20	Good	115	20	3.00			I-213	
26	2/12	IR	<input checked="" type="checkbox"/>	Rectangle	6	4,000.00	Beam	2006	<input checked="" type="checkbox"/>		11	Good	63	12	6.00			I-212	
27	2/10	IR	<input checked="" type="checkbox"/>	Rectangle	6	7,900.00	Beam	2007	<input checked="" type="checkbox"/>		20	N/A	113	24	5.00			I-210	
28	2/9	IR	<input checked="" type="checkbox"/>	Rectangle	4	4,010.00	Beam	1995	<input type="checkbox"/>		1	Medium	700	3	0.00			I-209	
29	2/6	M/R	<input checked="" type="checkbox"/>	Rectangle	9	7,850.00	Beam	2004	<input type="checkbox"/>		8	Good	300	25	4.00			I-206a,b	
30	2/1A	M/R	<input checked="" type="checkbox"/>	Rectangle	9	5,100.00	Beam	2007	<input type="checkbox"/>		1	N/A	250	23	2.00		Along	I-201a	
31	2/1	M/R	<input checked="" type="checkbox"/>	Irregular	6	5,100.00	Beam	2004	<input checked="" type="checkbox"/>		14	Good	82	14	3.00			Acros	I-201
32	11/10	IR	<input checked="" type="checkbox"/>	Rectangle	6	2,800.00	Beam	2007	<input checked="" type="checkbox"/>		10	N/A	55	7	4.00	18x12		Acros	I-1110a,b,c
33	11/4	IR	<input checked="" type="checkbox"/>	Rectangle	6	2,700.00	Flat	2007	<input checked="" type="checkbox"/>		10	N/A	57	7	4.00	21x13		Acros	I-1104
34	11/2	IR	<input checked="" type="checkbox"/>	Rectangle	6	2,550.00	Beam	1995	<input type="checkbox"/>		11	Good	48	6	3.00			Acros	I-1102a,b

Figure 4: Sample of Microsoft Access Database



Figure 5: Building with a soft story and building with a heavy overhang

Figure 9 shows the relation between numbers of buildings and corresponding RVS Score. Buildings having a score <2 are considered to be dangerous in this method. Around sixty buildings were found to be dangerous. However, it should also be noted that the actual damage would depend on a number of factors that are not included in the RVS procedure. As a result, the implications should only be used as indicative to determine

the necessity of carrying out simplified vulnerability assessment of the buildings. These results can also be used to determine the necessity of retrofitting buildings where more comprehensive vulnerability assessment may not be feasible.

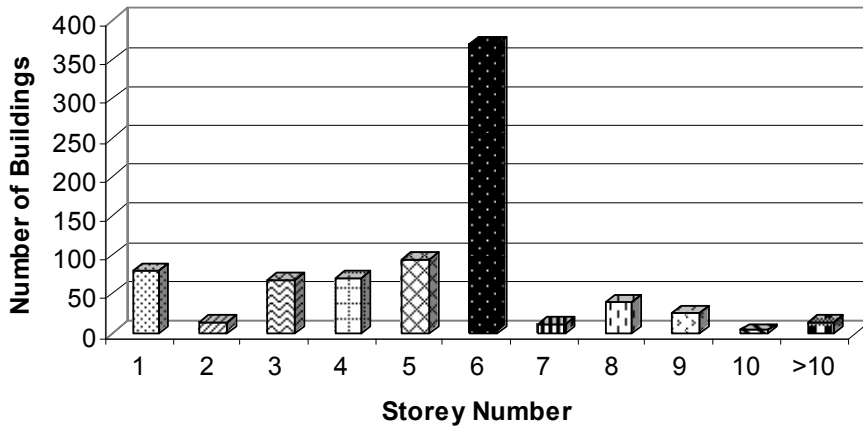


Figure 6: Relations between number of buildings and Number of Storey

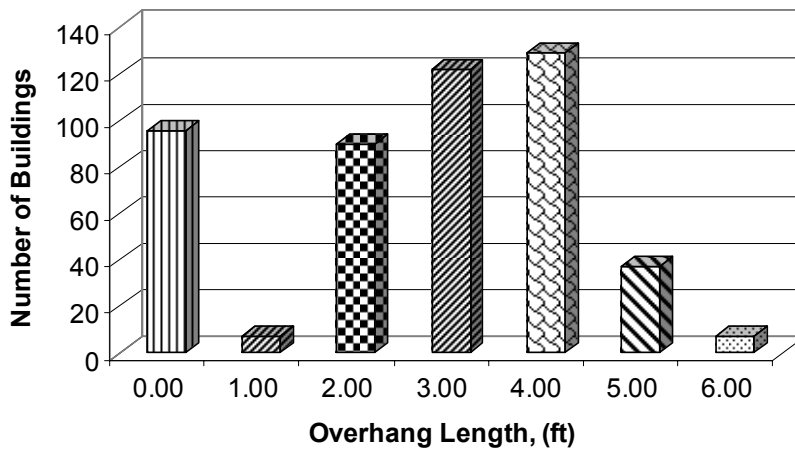


Figure 7: Relations between number of buildings and Overhang Length (ft)

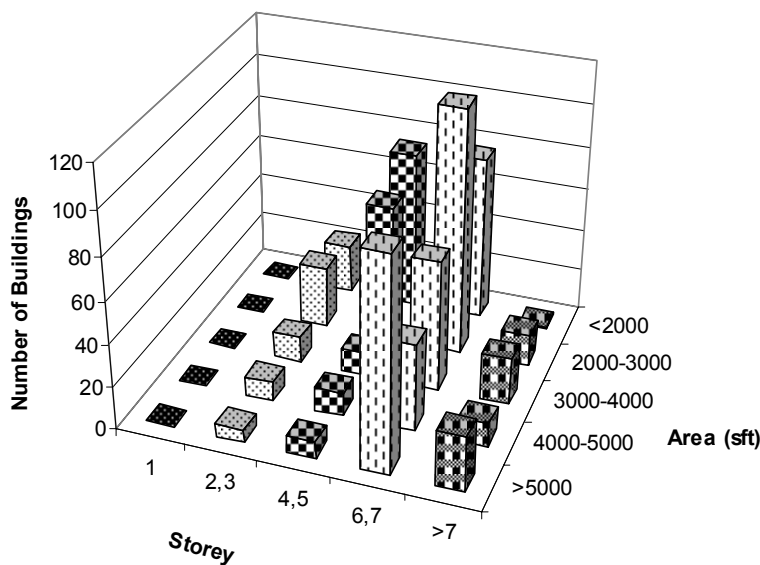


Figure 8: Relations between Number of Buildings, Number of Storey and Plinth Area (sft)

Figure 10 shows the relation between numbers of buildings and corresponding score of Turkish Level-1 method. Buildings having a score >50 are considered to be safe in this method. In this method much more variation in final scores has been observed as not only the basic score but also the influences of vulnerability parameters are very much dependent on the height of the building. In fact the positive or negative score modifications due to vulnerability parameters are weighted multiplications based on their existence and number of stories of the buildings (Imtiaz et al., 2007). As a result the score becomes high for low-rise buildings in spite of presence of negatively influential vulnerability parameters. Due to these dependant variations, it is comparatively tougher task here to classify the damage probabilities with minute specifications, as that of RVS-FEMA method, only from final scores. Rather it is easier to indicate an overall view on safety of the building comparing the final score with the cut off value and observing their relative difference. In this analysis, all buildings have higher score than the cut-off value.

Though the buildings identified as unsafe or lower scored compared to the “cut-off” value in Level-1 were supposed to be judged by Level-2 procedure, in this investigation around 10% buildings were analyzed again in the Level-1 to see the difference of score variations between these two methods. Figure 11 compare the scores of buildings according to Level-1 and Level-2 survey. From the results represented in Figure 11, it can be observed that around fifty buildings which have more than the cut-off value in Level-1 method has smaller score than the cut-off value in the Level-2 method. This reduction of score can be attributed to factors such as plan irregularity, redundancy, strength index parameters in Level-2 method.

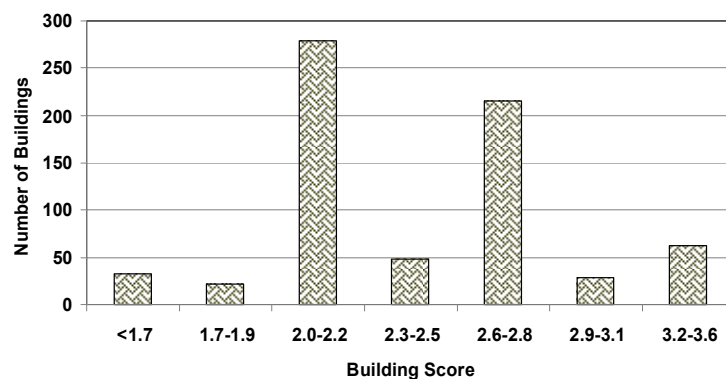


Figure 9: Relation between Number of Buildings and Building Score (RVS)

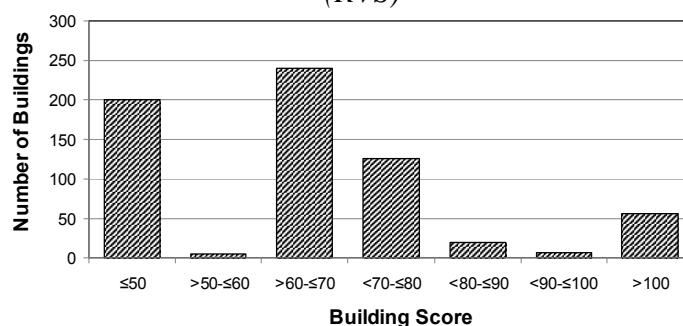


Figure 10: Relation between Number of Buildings and Building Score (Turkish Level-1)

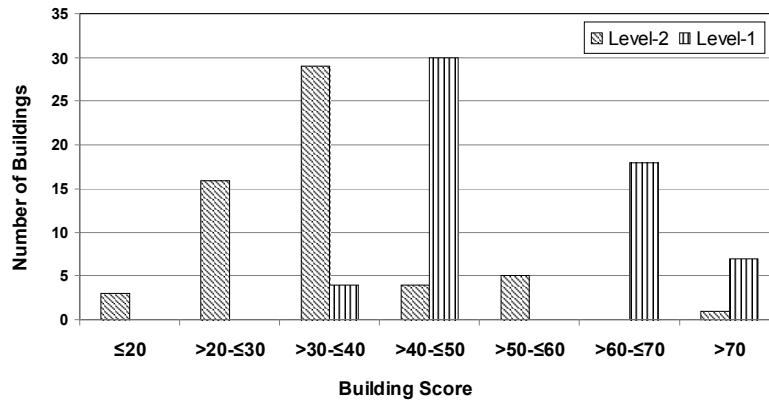


Figure 11: Relation between Number of Buildings and Building Score (Turkish methods)

6. CONCLUSIONS

In this paper, results and analysis of a building survey in some residential area of Dhaka city was presented. The analysis was basically conducted using FEMA's RVS method and Turkish Level 1 and 2 methods. The evaluation of two different methods in this paper has enabled the critical examination of the advantages and shortcomings of the methods. The Turkish method was found more significant with respect to applicability in our study region but from the experience of survey it is observed that the structural measurement in Level-2, which acts as very important vulnerability features, has made the method somewhat tougher as building owners in the survey area do not cooperate with the screeners and restrict their entry to the ground floor.

REFERENCES

- FEMA154, 2002. *Rapid Visual Screening of Building for Potential Seismic Hazards: A Hand Book*.
- Imtiaz, A. B. A., Shamim, M., Dhar, A.S., Ansary, M.A., Ahmed, Z. and Ahmed, M. Z. 2007. Visual Screening Methods for Earthquake Vulnerability Assessment. *USMCA2007*, Dhaka, Bangladesh.
- Sucuoglu, H. And Yazgan, U. (2003). Simple Survey Procedures for Seismic Risk Assessment In Urban Building Stocks. *Seismic Assessment and Rehabilitation of Existing Buildings*, 97-118, *NATO Science Series, IV/29*, Editors: S.T. Wasti and G. Ozcebe, Kluwer

ASSESSMENT OF CYCLONE SHELTERS IN COX'S BAZAR AGAINST EARTHQUAKE HAZARD

RAJAN SAHA
Research Assistant, Department of Civil Engineering, BUET, Bangladesh
rajanbuet00@yahoo.com

ASHUTOSH SUTRADHAR
Associate Professor, Department of Civil Engineering, BUET, Bangladesh
asuthoshdhar@buet.ac.bd

MEHEDI AHMED ANSARY
Professor, Department of Civil Engineering, BUET, Bangladesh
ansaryma@yahoo.com

ABSTRACT

Cyclone Shelters in Cox's Bazar district of Bangladesh has been assessed for earthquake vulnerability. Federal Emergency Management Agency (FEMA) method has been used for Rapid Visual Screening (RVS) for the evaluation. It is revealed from RVS that all of the cyclone shelters are vulnerable to earthquake loads. Detailed analysis of structures also showed similar findings. However, lack of lateral support system increased the vulnerability of the structure. Introduction of lateral supports in the form of diagonal beam appeared to improve the performance of the cyclone shelters under earthquake loads.

1. INTRODUCTION

Bangladesh is a part of the Bengal basin which is one of the most seismically active zones of the world. Lying as it does in the confluence of the India, Burma and Eurasia plate, the land is extremely prone to earthquake disasters and in the past have experienced some of the worst earthquakes in the history. Figure 1 shows world's seismic sources and location of Bangladesh. It is revealed from the figure that Bangladesh is situated at one of the densely located earthquake sources. Earthquake sources around Bangladesh are shown in Figure 2, indicating high potential of earthquake. The district of Cox's Bazar is located in south eastern part of Bangladesh (as shown in Figure 2). It is the largest sea beach in the world of 200 km length. Figure 3 shows the earthquake sources identified around the city.

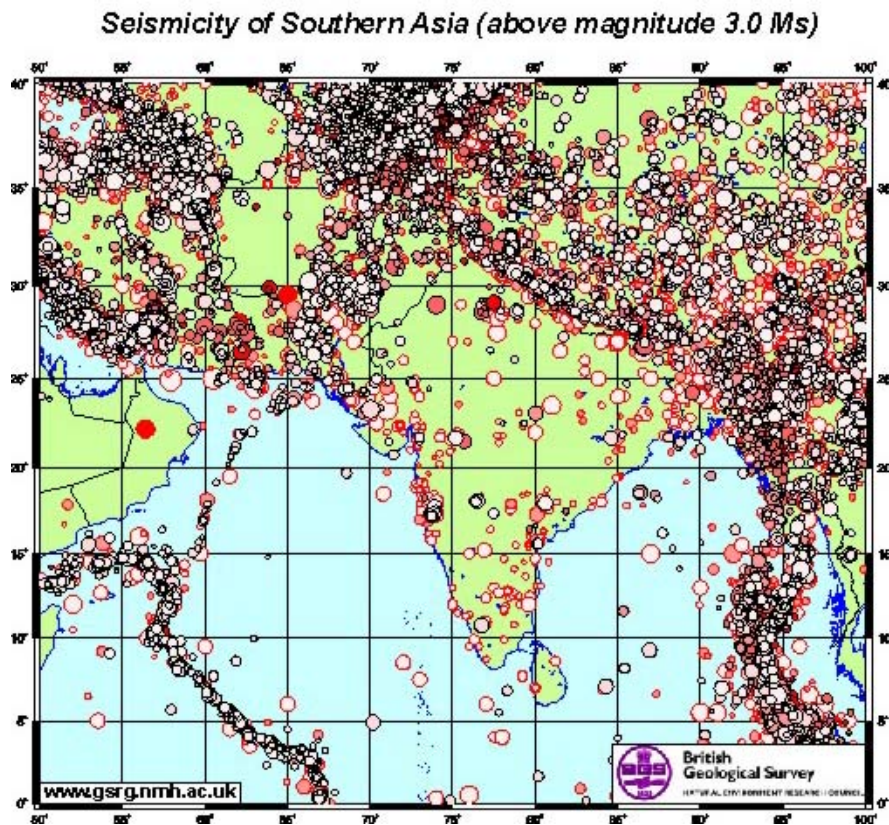


Figure 1: Earthquake sources Global view, (British Geological Survey)

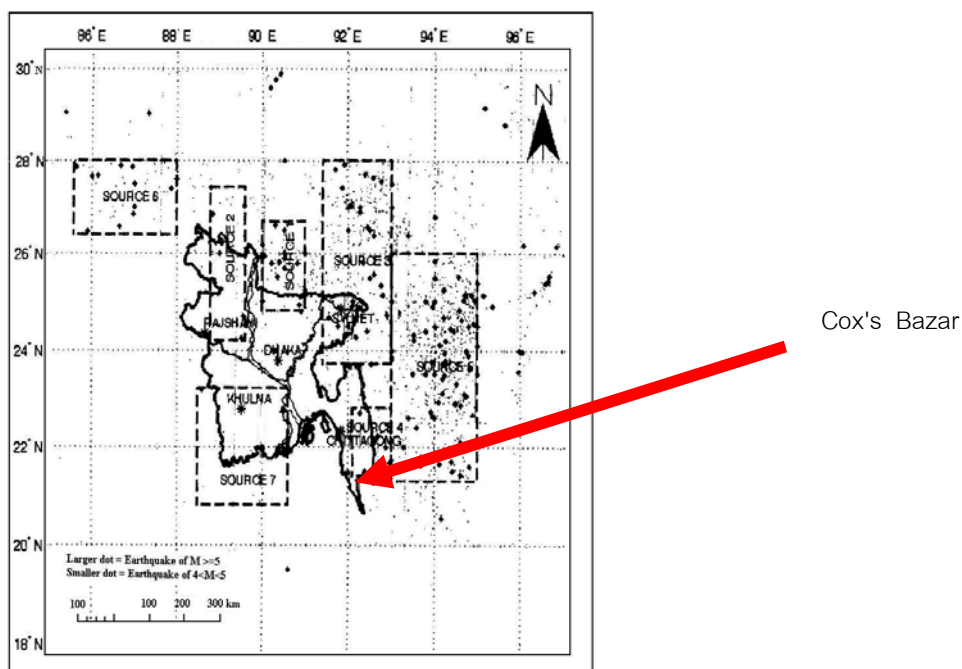


Figure 2: Location of Study area and Earthquake sources with respect to Bangladesh (after Noor et.al, 2005)

Cox's Bazar known to be as coastal district and famous for tourism. However the city is prone to various natural disasters, affecting lives and livelihood frequently. Cyclone attacked in this area in 1970, 1986, 1991 and 1997. 1970 and 1991 Cyclones were devastative. Besides, every year at least two or three times this area is threatened by cyclone. After the 1991 cyclone, the Government of Bangladesh made a policy for the protection of coastal people. For this, RCC frame structure buildings of two to three storied were constructed. These buildings are known as cyclone shelters. Almost all the shelters belong to Government of Bangladesh; some shelters are supervised by non government organizations. The buildings are of rectangular and V shape. Some buildings are of irregular shape.

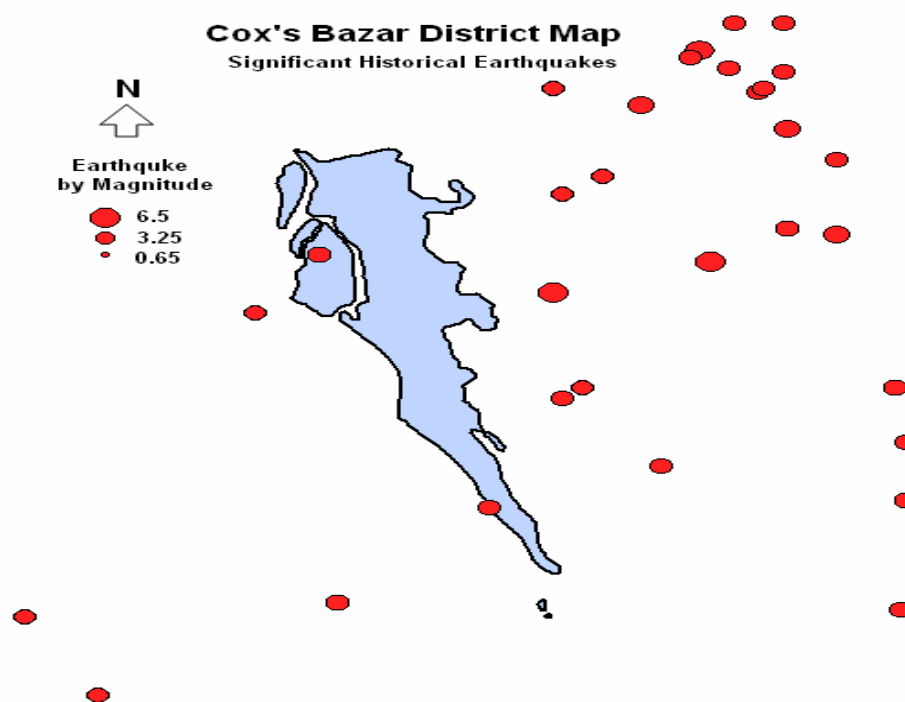


Figure 3: Historical earthquakes around Cox's Bazar.

2. SEISMIC VULNERABILITY ASSESSMENT

Assessment of the buildings is usually performed in three levels. Three levels are briefly described following:

Level 1: This procedure requiring only visual evaluation.

Level 2: Simplified vulnerability assessment procedure requiring limited engineering analysis based on information from visual observations and structural drawings or on site measurements. The method is widely known as Rapid Visual Screening (RVS) method.

Level 3: Detailed vulnerability assessment procedure requiring detailed complex analysis. This procedure is recommended for all important and lifeline buildings.

2.1 RVS Methodology

Rapid visual screening (RVS) of buildings for potential seismic hazards, originated in 1988 with the publication of the FEMA 154 Report, Rapid Visual Screening of Buildings for Potential Seismic Hazards a Handbook. RVS provides a procedure to identify record and rank buildings that are potentially seismically hazardous (FEMA, 2002). This screening methodology is encapsulated in a one-page form, which combines a description of a building, its layout and occupancy, and a rapid structural evaluation related to its seismic hazard.

Although RVS is applicable to tall buildings, its principal purpose is to identify (1) older buildings designed and constructed before the adoption of adequate seismic design and detailing requirements (2) buildings on soft or poor soils, or (3) buildings having performance characteristics that negatively influence their seismic response. Once identified as potentially hazardous, such buildings should be further evaluated by a design professional experienced in seismic design to determine if, in fact, they are seismically hazardous.

2.2 RVS Analysis of Cyclone Shelters

Cyclone Shelters are visually observed in the study area. Most cyclone shelters are of rectangular and V shaped and few of irregular shape. Figure 4 shows building shape variation of cyclone shelters under investigation. A sample RVS sheet of a rectangular shaped cyclone shelter is shown in Figure 5. This cyclone shelter shown in Figure 5 is of rectangular shape and of Reinforced Concrete Frame Structure with unreinforced masonry infill. It is categorized by URM INF in RVS sheet. URM INF (C3) has a basic score of 1.6 according to FEMA RVS method. Since there is no irregularity in the plan so there is no score for plan and vertical irregularity. There is a presence of soft storey in the building. According to FEMA 154 (2002) soft storey in a storey is identified where the lateral stiffness is less than 70% of that in the storey above or less than 80% of the average stiffness of the stories above. Soft storey is considered as vertical irregularity and score is -1 which is negative. Soil Type D is chosen because the area is in the hilly region. Thus the total score of the rectangular cyclone shelter has been found to be 0.2, which is less than the 'cut-off' score of '2' according to FEMA 154 (2002). Thus the building requires detailed analysis.

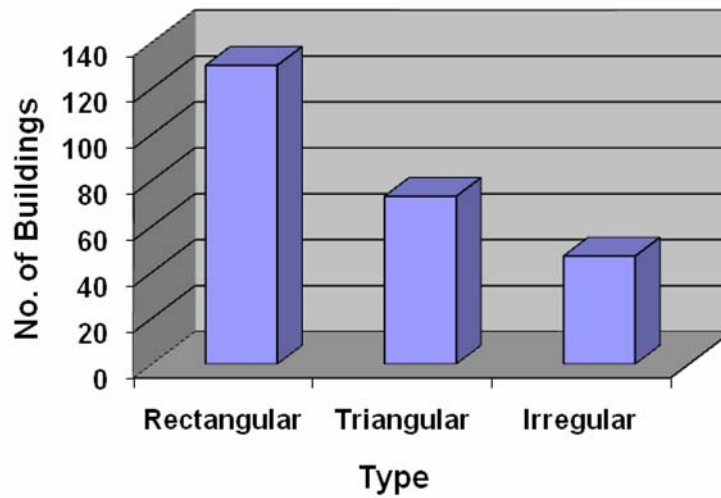


Figure 4: Building Shapes of Cyclone Shelters at Cox's Bazar

RVS Sheet for V-Shaped cyclone shelter is shown in Figure 6. Another parameter for plan irregularity is included for these types of shelter. There is a negative score and it is -0.5 for plan irregularity according to FEMA. As a result, the score for the V-Shaped cyclone shelter became -0.3. Rectangular shape cyclone shelters without soft storey showed RVS score of 1.2 and irregular shaped shelters without soft storey showed RVS score of 0.7.

Rapid Visual Screening of Buildings for Potential Seismic Hazards (High Seismicity)

Plan/Elevation

PlanElevation

Address: Chakaria, Uni: Badarkhali, Vill: Badarkhali
 Other identifiers :
 No. Stories : 3 Year Built : 1991
 Screener :
 Date :
 Total Floor Area (sq. ft.) 2958.6
 Building Name : Nidantorain gprs cum shelter
 Use : School

Photograph



Occupancy				Soil Type						FALLING HAZARDS					
Assembly	Govt.	Office	Number of Persons	A	B	C	D	E	F	Unreinfo.	Parapets	Cladding	Chimney	Other	
Commercial	Historic	Resident	0-10	Hard Rock	Avg. Rock	Dense Soil	Stiff Soil	Soft Soil	Poor Soil						
Emer. Service	Industrial	School	101-1000												
			1000+												
BASIC SCORE, MODIFIERS AND FINAL SCORE, S															
Building Type	W1	W2	S1	S2	S3	S4	S5	C1	C2	C3	PC1	PC2	RM1	RM2	URM
			(MRF)	(BR)	(LM)	(RC SW)	(URM INF)	(MRF)	(SW)	(URM INF)	(TU)		(FD)	(RD)	
Basic Score	4.4	3.8	2.8	3	3.2	2.8	2	2.5	2.8	1.6	2.6	2.4	2.8	2.8	1.8
Mid Rise (4 to 7 Stories)	N/A	N/A	0.2	0.4	N/A	0.4	0.4	0.4	0.4	0.2	N/A	0.2	0.4	0.4	0
High Rises (> 7 Stories)	N/A	N/A	0.6	0.8	N/A	0.8	0.8	0.6	0.8	0.3	N/A	0.4	N/A	0.6	N/A
Vertical Irreg.	-2.5	-2	-1	-1.5	N/A	-1	-1	-1.5	-1	-1	N/A	-1	-1	-1	-1
Plan Irregularity	-0.5	-0.5	-0.5	-0.5	-0.5	-0.5	-0.5	-0.5	-0.5	-0.5	-0.5	-0.5	-0.5	-0.5	-0.5
Pre-Code	0	-1	-1	-0.8	-0.6	-0.8	-0.2	-1.2	-1	-0.2	-0.8	-0.8	-1	-0.8	-0.2
Post Benchmark	2.4	2.4	1.4	1.4	N/A	1.6	N/A	1.4	2.4	N/A	2.4	N/A	2.8	2.6	N/A
Soil Type C	0	-0.4	-0.4	-0.4	-0.4	-0.4	-0.4	-0.4	-0.4	-0.4	-0.4	-0.4	-0.4	-0.4	-0.4
Soil Type D	0	-0.8	-0.6	-0.6	-0.6	-0.6	-0.4	-0.6	-0.6	-0.4	-0.6	-0.6	-0.6	-0.6	-0.8
Soil Type E	0	-0.8	-1.2	-1.2	-1	-1.2	-0.8	-1.2	-0.8	-0.8	-0.4	-1.2	-0.4	-0.6	-0.8
FINAL SCORE, S =										0.2					

Wall	5 inches	<input checked="" type="checkbox"/> 10 inches	<input type="checkbox"/> Tin	<input checked="" type="checkbox"/> Brick	<input type="checkbox"/> Wood	Detailed Evaluation Required <input checked="" type="checkbox"/> YES <input type="checkbox"/> NO
Foundation	<input checked="" type="checkbox"/> Foot	<input type="checkbox"/> Raft	<input type="checkbox"/> Pile			
Frame	<input type="checkbox"/> No	<input checked="" type="checkbox"/> RCC	<input type="checkbox"/> Steel	<input type="checkbox"/> Wood		
Lift	<input checked="" type="checkbox"/> Yes	<input type="checkbox"/> No				
Stair	<input checked="" type="checkbox"/> Yes	<input type="checkbox"/> No				
Gas	<input type="checkbox"/> Electricity		<input type="checkbox"/> Phone	<input type="checkbox"/> Water		
Road Width(ft)						
Cont. Lintel	<input type="checkbox"/> No	<input checked="" type="checkbox"/> Yes	<input type="checkbox"/> No	Approx. Dist From Upzila HQ Road:		
Visible Damage	<input type="checkbox"/> Crack	<input type="checkbox"/> Settle	<input type="checkbox"/> Others			
Population Vulnerability Classification						
Comments						

* = Estimated, subjective or unreliable data BR = Braced Frame MRF = Moment-resisting frame SW = Shear Wall
 DNK = Do Not Know FD = Flexible diaphragm RC = Reinforced Concrete TU = Tilt up
 URM INF = Unreinforced masonry infill LM = Light metal RD = Rigid diaphragm

Figure 5: Sample RVS Sheet for Rectangular Shaped Shelter

Rapid Visual Screening of Buildings for Potential Seismic Hazards (High Seismicity)

Plan/Elevation

Plan

Elevation

Address: Chakaria, Uni: Rajakhali
 Vill: Rajakhali
 No. Stories : 2 Year Built : 1990
 Screener :
 Date :
 Total Floor Area (sq. ft.) 1355.6
 Building Name : Sundurypara red crescent shelter
 Use : No use

Photograph

Occupancy				Soil Type								FALLING HAZARDS				
Assembly	Govt.	Office	Number of Persons	A	B	C	D	E	F							
Commercial	Historic	Resident	0-10	Hard	Avg.	Dense	Stiff	Soft	Poor	Unreinfo.	Parapets	Cladding	Chimney	Other		
Emer. Service	Industrial	School	101-1000	Rock	Rock	Soil	Soil	Soil	Soil							
			1000+													
BASIC SCORE, MODIFIERS AND FINAL SCORE, S																
Building Type	W1	W2	S1	S2	S3	S4	S5	C1	C2	C3	PC1	PC2	RM1	RM2	URM	
			(MRF)	(BR)	(LM)	(RC Sw)	(URM INF)	(MRF)	(Sw)	(URM INF)	(TU)		(FD)	(RD)		
Basic Score	4.4	3.8	2.8	3	3.2	2.8	2	2.5	2.8	1.6	2.6	2.4	2.8	2.8	1.8	
Mid Rise (4 to 7 Stories)	N/A	N/A	0.2	0.4	N/A	0.4	0.4	0.4	0.4	0.2	N/A	0.2	0.4	0.4	0	
High Rises (> 7 Stories)	N/A	N/A	0.6	0.8	N/A	0.8	0.8	0.6	0.8	0.3	N/A	0.4	N/A	0.6	N/A	
Vertical Irreg.	-2.5	-2	-1	-1.5	N/A	-1	-1	-1.5	-1	-1	N/A	-1	-1	-1	-1	
Plan Irregularity	-0.5	-0.5	-0.5	-0.5	-0.5	-0.5	-0.5	-0.5	-0.5	-0.5	-0.5	-0.5	-0.5	-0.5	-0.5	
Pre-Code	0	-1	-1	-0.8	-0.6	-0.8	-0.2	-1.2	-1	-0.2	-0.8	-0.8	-1	-0.8	-0.2	
Post Benchmark	2.4	2.4	1.4	1.4	N/A	1.6	N/A	1.4	2.4	N/A	2.4	N/A	2.8	2.6	N/A	
Soil Type C	0	-0.4	-0.4	-0.4	-0.4	-0.4	-0.4	-0.4	-0.4	-0.4	-0.4	-0.4	-0.4	-0.4	-0.4	
Soil Type D	0	-0.8	-0.6	-0.6	-0.6	-0.6	-0.4	-0.6	-0.6	-0.4	-0.6	-0.6	-0.6	-0.6	-0.8	
Soil Type E	0	-0.8	-1.2	-1.2	-1	-1.2	-0.8	-1.2	-0.8	-0.8	-0.4	-1.2	-0.4	-0.6	-0.8	
FINAL SCORE, S =											-0.3					

Wall	5 inches	10 inches	Tin	Brick	Wood	
Foundation	Foot	Raft	Pile			
Frame	No	RCC	Steel	Wood		Detailed Evaluation Required
Lift	Yes	No				YES NO
Stair	Yes	No				
Gas		Electricity	Phone	Water		
Road Width(ft)	20			Approx. Dist From Upzilla HQ Road: 20 km		
Cont. Lintel		Yes	No			
Visible Damage	Crack	Settle	Others			
Population						
Vulnerability Classification						
Comments						

* = Estimated, subjective or unreliable data BR = Braced Frame MRF = Moment-resisting frame SW = Shear Wall
 DNK = Do Not Know FD = Flexible diaphragm RC = Reinforced Concrete TU = Tilt up
 URM INF = Unreinforced masonry infill LM = Light metal RD = Rigid diaphragm

Figure 6: Sample RVS Sheet for V Shaped Cyclone Shelters

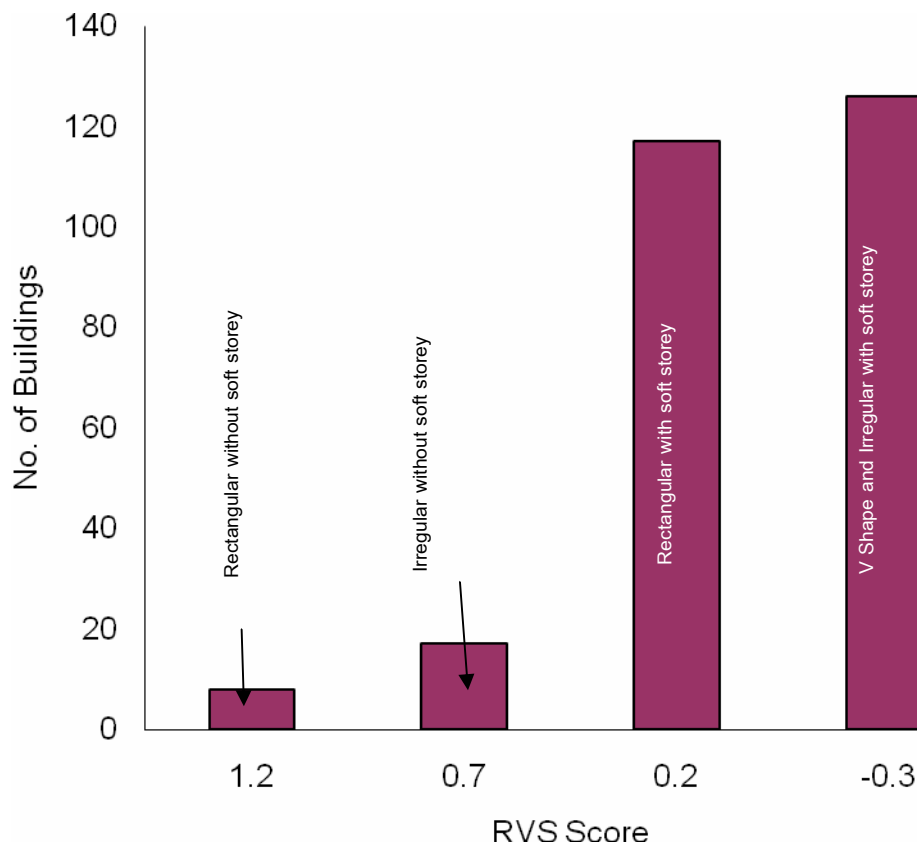


Figure 7: RVS Score variation

About 268 Cyclone shelters across Cox's Bazar has been analyzed using RVS method. RVS scores for the different types of cyclone shelter are shown in Figure 7. Almost all the building's score is less than 2. (The Cut off score) and thus detail evaluations of these are required. The low score in RVS of the system is due to the low basic score for the system with no lateral support. Detail analysis was also done on some buildings as presented in the following article. The effect of lateral support in the form of 2-diagonal beam has been explored in the detailed analysis.

2.3 Detailed Analysis of Cyclone Shelters

It is revealed that all of the cyclone shelter possesses RVS score less than the 'Cut off' score and therefore, require detailed analysis. Detailed analysis has been performed for a rectangular, a V-Shaped and an irregular shaped cyclone shelters. Analysis was performed using commercially available structural analysis software called 'ETABS' (Extended Three Dimensional Analysis of Building Structures). The first mode shape which is the lateral deflection of the ground floor level of the structure, was considered from the dynamic analysis of structures using ETABS. The mode provided the maximum natural period from the analysis and usually

govern the earthquake design. The same deformation shape in the other direction (orthogonal) is termed as 2nd mode shape in ETABS, which may have the maximum natural period and therefore investigated here.

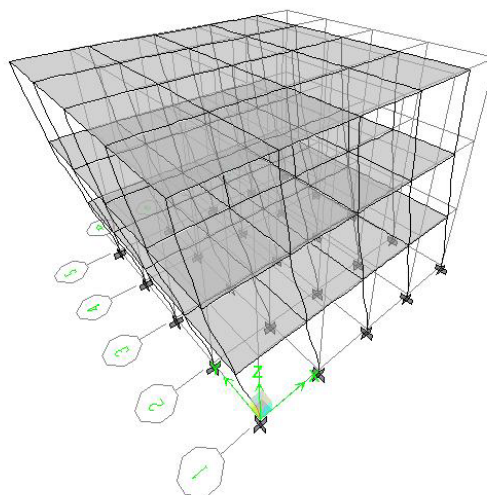


*Figure 8: Mode Shape 1 for Rectangular Shaped Cyclone Shelter
(Period 0.35 sec)*

Figure 8 shows 1st mode shape of the Rectangular shaped cyclone shelter. Natural time period for that mode was 0.35 sec. Natural period for Mode shape 2 was also 0.35 sec, since the building has similar geometry in the other (perpendicular) direction. First modal and second modal deformation of the V-shaped cyclone shelter is shown in Figure 9 and 10. Even though, the geometry is different in two perpendicular directions for the cyclone shelter, the natural period for the two modes are approximately same (0.29 sec). It is also to be noted here that natural period for the V-shaped shelter are less than the rectangular shelters, indicating better stability against earthquakes. Low time period for V-shaped shelter can be due to less number of storey for the shelter (2-storied) with reference to the rectangular shelter (3 storied). Figures 11 and 12 show the mode shapes 1 and 2 of a irregular shaped cyclone shelter. The irregular shaped shelter showed natural period of 0.51 sec and 0.5 sec respectively for the two mode shapes, which are greater than both of the V-shaped and Rectangular shaped cyclone shelters.

RVS scores and natural time periods for each type of the cyclone shelters are shown in Table 1. It is revealed that RVS score is the highest for rectangular shaped structure with no soft storey while the lowest for the V-Shaped structures. Thus the V-Shaped shelter is expected to be the worst under earthquake. However detailed analysis showed the lowest natural time period, indicating the best among the shelters. The contrary of the conclusion of the two methods indicating that further attention is required

regarding revision of the RVS methods to incorporate other necessary parameters such that both methods provide similar conclusion.

Table 1: RVS Score and Natural time period for cyclone shelter

Building Type	RVS Score with soft storey	RVS Score without soft storey	Natural Time Period form Analysis
Rectangular	0.2	1.2	0.35
V-Shape	-0.3	0.7	0.29
Irregular	-0.3	0.7	0.5

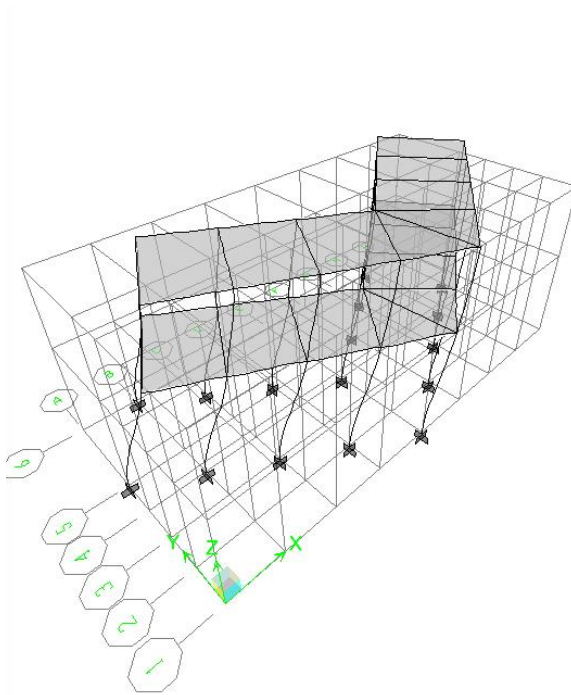


Figure 9: Mode Shape 1 for V Shaped building (Period 0.29 sec)

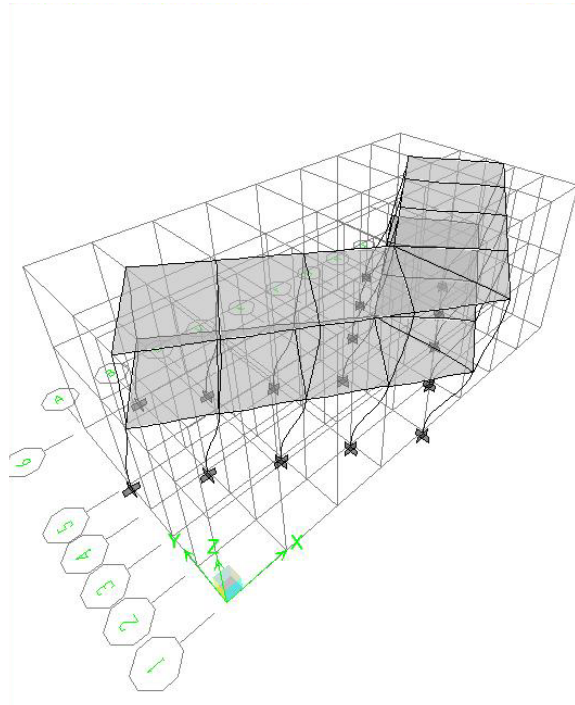


Figure 10: Mode Shape 2 for V Shaped building (Period 0.289 sec)

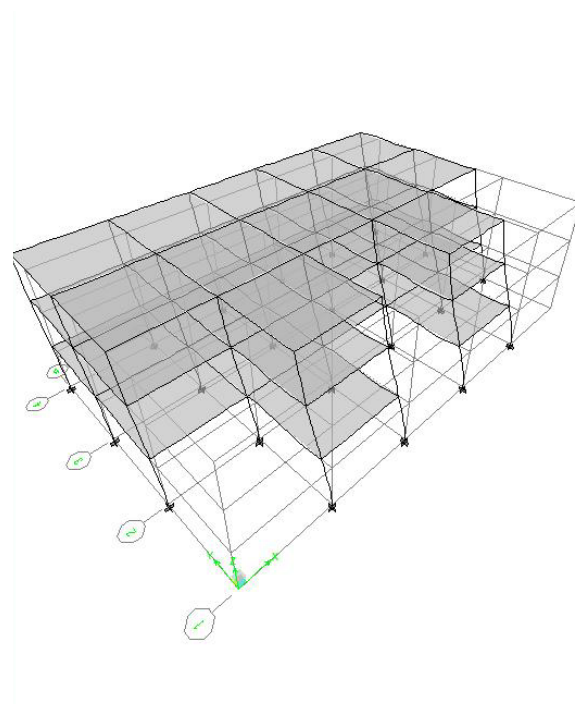


Figure 11: Mode Shape 1 for Irregular Shaped Building (Period 0.51 sec)

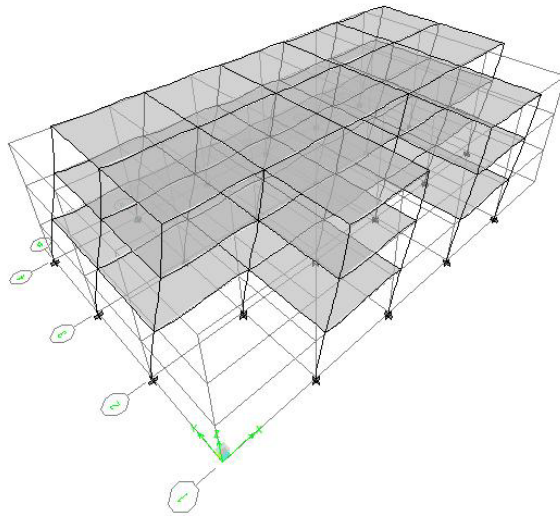


Figure 12: Mode Shape 3 for Irregular Shaped Building (Period 0.5 sec)

Empirical correlation between number of storey and natural period of building for RCC frame buildings and masonry buildings for different building in Bangladesh was obtained as (BNUS, 2006):

$$T = 0.04N + 0.133 \quad \text{[for RCC frame buildings]} \quad (1)$$

$$T = 0.06N \quad \text{[for masonry buildings]} \quad (2)$$

Where, T = Natural Period of building
 N = Number of Storey

The National Building Code (NBC) of Canada defined the natural period of a building by the following empirical equation:

$$T = 0.1N \quad (3)$$

Where N = Number of Storey.

From the equation (1) the natural period calculated for three storied building is 0.25 sec and for two storied building 0.21 sec. From equation (3) it was 0.3 sec and 0.2 sec respectively. The natural period of a building should not be larger than the equation (3) by a factor 1.2 (Amanat and Hoque, 2005). Thus the time period obtained from Eq. (1) and (3) are on the conservative side. However, the natural period obtained for the cyclone shelter from the analysis using ETABS are greater than those given by Eq. (3), indicating that the cyclone shelters are on unconservative side for earthquake loads. A study has been performed with introduction of a lateral support in the form of two diagonal beams on each side at ground floor level for the rectangular cyclone shelter.

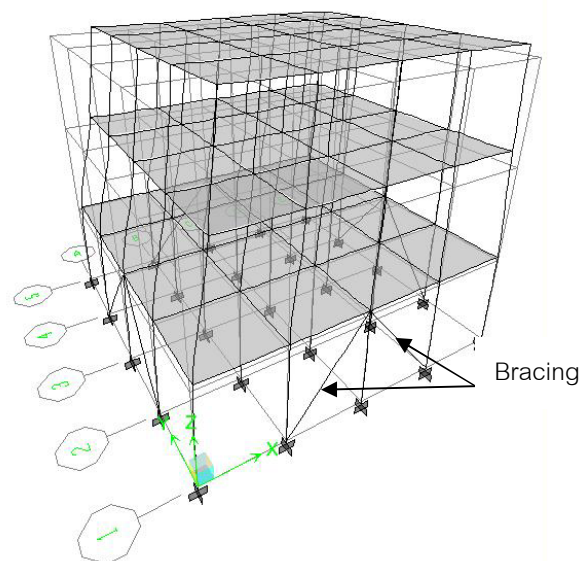


Figure 13: Mode Shape for rectangular shaped shelter with diagonal bracing (0.26 sec)

From the analysis with diagonal bracing the natural period was found 0.26 sec which is lower than the value calculated by Eq. (3) and therefore it is on conservative side. Thus introduction of lateral bracing may improve the performance of the cyclone shelters under earthquake loads.

3. CONCLUSIONS

About 268 cyclone shelters across the district of Cox's Bazar in Bangladesh have been evaluated for their vulnerability to earthquake loads. Both rapid visual screening (RVS) method and detailed analysis have been used in this investigation. In the rapid visual method the score for all of the cyclone shelter were less than the cut off score, indicating that the structures are vulnerable. Similar finding was obtained from detailed analysis. Detailed analysis performed using ETABS showed the natural time period for 1st mode of deformation to be greater than the limiting time period. Thus the structure showed less stiffness for that mode of deformation. The greater natural time periods for the structures were due to lack of lateral support system. Analysis performed introducing diagonal bracing resulted in reduction of the natural time period within the limiting value. The RVS method and the detailed analysis showed contradictory conclusion regarding performance of different types of structures. While score rate the V-Shaped structure to be the worst, detailed analysis showed it to be the best. Thus further study may be required for revision of the RVS method to include other necessary parameters that bring the both methods to have the same conclusion.

REFERENCES

- Amanat, K.M. and Hoque, E. 2005. *A rationale for determining the natural period of RC building frames having infill*, Engg. Structures Vol. 28, pp 495-502.
- Bangladesh National Building Code, 1993. Housing and Building Research Institute, 1st ed., Dhaka.
- BNUS Report, 2006. Evaluation of the seismic vulnerability of Bangladeshi buildings using non-destructive testing, ICUS Report No. 2006-2007.
- FEMA 154, 2002. *A Handbook: Rapid Visual Screening of Buildings for Potential Seismic Hazards*, 2nd Edition.
- Noor, M.A. Yasin, M and Ansary, M.A., 2005. *Seismic Hazard Analysis of Bangladesh*, Proceedings First Bangladesh Earthquake Symposium.
- Saha, R., 2006. *Earthquake Vulnerability Assessment of BUET Buildings*. Undergraduate Thesis, Department of Civil Engg., BUET, Dhaka.
- Uniform Building Code, 1994.

PARTIALLY ENCASED COMPOSITE COLUMNS: AN INNOVATIVE COMPOSITE STRUCTURAL SYSTEM

MAHBUBA BEGUM

Assistant Professor, Department of Civil Engineering, Bangladesh University of Engineering and Technology (BUET), Dhaka, Bangladesh
mahbuba@ce.buet.ac.bd

ABSTRACT

One of the recent developments in composite systems includes partially encased composite (PEC) columns consisting of a thin-walled, welded I-shaped steel section with concrete infill cast between the flanges. Transverse links are provided between the flanges at regular intervals to enhance the resistance to local instability of the thin steel plates. This innovative composite system not only reduces the cost of construction using relatively low-cost concrete by minimizing the use of higher cost steel, but also helps to overcome the complexities related to erection and design of connections of more commonly used composite columns. Several research works including both numerical and experimental works have been carried out for establishing the behaviour and the design provisions for this new type of composite column under various loading conditions. This paper presents a brief review of these research works along with the capacity prediction model for this column. The review also includes the design requirements according to CSA standard S16-01.

1. INTRODUCTION

The effective use of a combination of steel with concrete can substantially improve the behaviour and cost efficiency of columns used in the construction of medium to high-rise buildings, as compared to using steel-only columns. Two types of composite columns commonly used in North America are: concrete filled tubes (CFT) and fully encased composite (FEC) columns (Figure 1). Both of these composite systems have limitations such as limited cross-sectional dimensions of standard shapes (CFT), requirement of extensive formwork and additional reinforcing steel (FEC columns) and complex beam-to-column connections. These limitations have indirectly imposed restrictions on the use of composite columns.

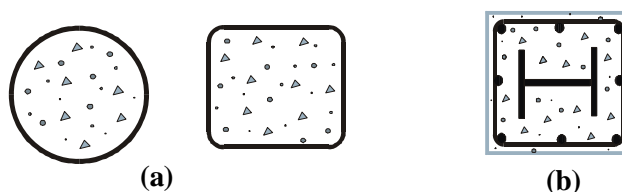


Figure 1: Common types of Composite columns, (a) Concrete Filled Tubes and (b) Fully Encased Composite Column.

In Europe, in the early 1980s, PEC columns and beams were introduced using standard-sized rolled steel sections. In 1996, the Canam Group in Canada took the initiative to propose a new type of composite column consisting of a thin-walled, welded H-shaped steel section, built-up from hot-rolled steel plate, with concrete infill cast between the flanges, as shown in Figure 2. Transverse links are provided between the flanges at regular intervals to improve the resistance to local buckling. This new system has been termed the “partially encased composite (PEC) column,” since the steel section is only partially encased by the concrete. Additional reinforcement consisting of longitudinal and transverse rebars can be provided to improve the ductility of these columns under cyclic loading.

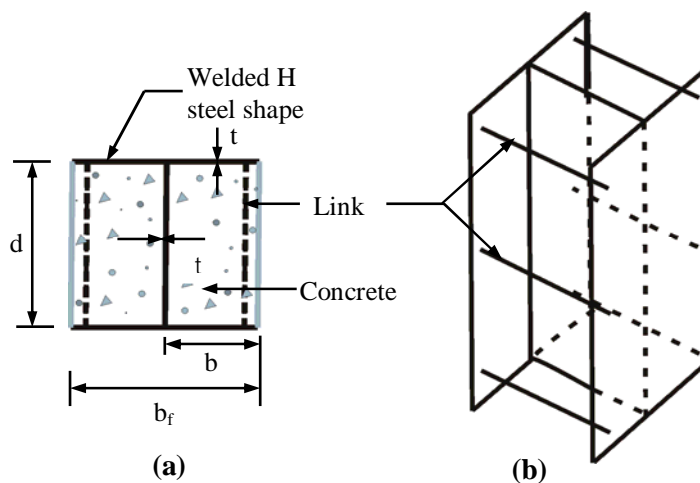


Figure 2: Partially Encased Composite Column with Thin-Walled Built-Up Steel Section, (a) Column Cross-Section and (b) 3D view of the Steel Configuration.

In PEC columns, since a built-up steel section is used instead of a standard shape, the designer has more flexibility when sizing the column cross-section. Moreover, thin steel plates are intentionally specified to obtain a more cost effective column by increasing the contribution of concrete in the load carrying capacity of the column. These factors have made PEC columns constructed with built-up shapes more attractive than those constructed with standard sections. Moreover, the high stiffness of the PEC column is expected to have beneficial effects for controlling the lateral deflection of buildings when used as a component of lateral load resisting systems and incorporating the use of high performance materials in the system. To introduce and understand the behaviour of this new composite system a brief review of the research works, including both experimental and numerical studies are presented in this paper. The capacity prediction models for PEC columns are also included along with the design guidelines as per CSA standard S16-01 (CSA, 2001).

2. EXPERIMENTAL INVESTIGATIONS

Extensive experimental research has been conducted on thin-walled PEC columns with built-up sections by several research groups (Fillion 1998; Tremblay et al. 1998; Chicoine et al. 2000; Bouchereau and Toupin 2003; Prickett and Driver 2006; Begum et al. 2007) to investigate the behaviour of PEC columns fabricated with thin-walled built-up sections. Descriptions of these experimental investigations are presented in the following sections.

2.1 Short Columns Constructed with Normal Strength Concrete

The first series of tests on short PEC columns was performed by Fillion (1998) and Tremblay et al. (1998) on specimens with $300\text{ mm} \times 300\text{ mm}$ and $450\text{ mm} \times 450\text{ mm}$ cross-sections. The specimens had a length of five times the cross-section dimension and were loaded under axial compression. The cross-section and elevation of a typical test specimen is shown in Figure 3. To study the possible size effect on the behaviour of short PEC columns, Chicoine et al. (2000) tested five $600\text{ mm} \times 600\text{ mm}$ concentrically loaded columns and compared them with the first series of tests on short PEC specimens. The test specimens were designed with variable transverse link spacing and the flange slenderness ratio to study their influences on the column behaviour. A typical test specimen is shown in Figure 3 (a).

Bouchereau and Toupin (2003) conducted tests to investigate the behaviour of short PEC columns subjected to axial compression and bending under monotonic and cyclic loading conditions. A total of 22 tests on 2250 mm long columns were performed. The column cross-section was $450\text{ mm} \times 450\text{ mm} \times 9.53\text{ mm}$ where the first two numbers indicate the depth and width of the cross-section and the third number is the thickness of the steel plates. A link spacing of 300 mm was used in all the test columns. The test program (Bouchereau and Toupin 2003) was mainly designed to simulate the conditions of a column of the bracing bents subjected to monotonic and cyclic eccentric axial loads. In each case the effect of strong and weak axis bending was investigated for two different values of load eccentricity.

The results of these tests revealed that the failure of the composite columns (Figure 3 (b)) occurred by a combination of local buckling of the steel flanges between the transverse links, yielding of the steel and crushing of the concrete. However, Bouchereau and Toupin (2003) reported that the occurrence of local buckling and concrete crushing was essentially simultaneous in all of the eccentrically loaded test specimens. The specimens with weak axis bending exhibited brittle and explosive failures as compared to other specimens. The load versus deformation response was studied for the test specimens to evaluate the influence of column size, plate slenderness ratio, link spacing and additional reinforcements. It was reported that the specimens with higher b/t and s/d ratios exhibited a faster degradation of post-peak strength than columns with lower b/t ratios and smaller link spacings (Chicoine et al. 2000). The presence of additional

reinforcement in the specimens under weak axis bending was observed to improve the behaviour of these columns significantly. The additional reinforcements also increased the ultimate capacity of the PEC columns by an average of 8%, as observed by Bouchereau and Toupin (2003). Comparing the results of the cyclic tests to corresponding monotonic tests, no significant differences in the column behaviour were observed.

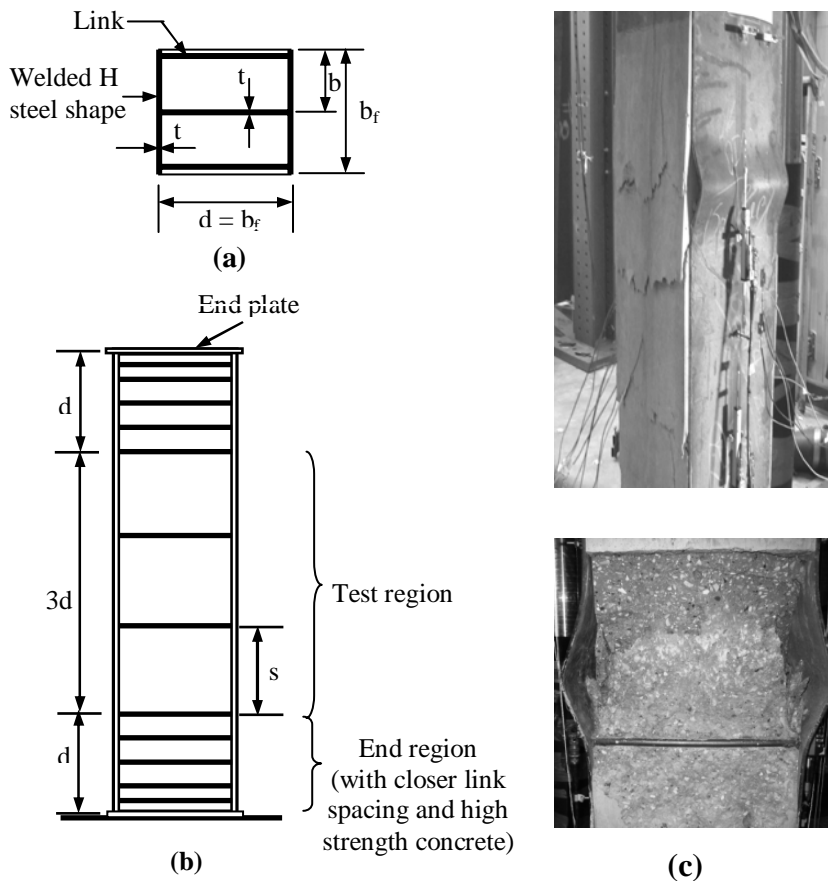


Figure 3: Typical PEC Test Column, (a) Cross-section, (b) Elevation and (c) Failure Mode (Chicoine et al. 2000).

2.2 Short Columns Constructed with High Performance Concrete

Prickett and Driver (2006) conducted a comprehensive experimental research project to study the behaviour of thin-walled PEC columns made with high performance concrete. The study included 11 short PEC columns measuring $400 \text{ mm} \times 400 \text{ mm} \times 2000 \text{ mm}$, with the primary variables being the concrete type, link spacing and load eccentricity. The plate slenderness ratio was kept constant ($b/t = 25$) for all of the test columns. Three different link spacings and three types of concrete (normal strength, high strength and high strength steel fibre reinforced concrete) were used in these specimens. Steel fibres were used to observe potential improvement in the failure mode of PEC columns with high strength concrete. Four identical PEC columns constructed with high strength concrete and subjected to axial compression and bending were also tested by Prickett and Driver (2006). Bending axis

and the amount of load eccentricity were varied to determine the effects of these parameters on the column behaviour.

As observed in the experiments, the high strength concrete PEC columns failed in a similar manner to the PEC columns with normal strength concrete: concrete crushing combined with local flange buckling. However, the failure of a high strength concrete column was found to be sudden as compared to an equivalent PEC column with normal strength concrete. Addition of steel fibres in the high strength concrete was found to improve the failure mode of the columns somewhat. Prickett and Driver (2006) also studied the moment versus curvature response and developed load versus moment interaction diagrams for the eccentrically loaded specimens. The moment versus curvature curves for specimens with strong axis bending showed a gradual decline of the peak moment as compared to the sudden decline observed in the specimens with weak axis bending.

2.3 Long Columns Constructed with Normal Strength Concrete

Four long PEC columns with a length-to-depth ratio of 20 were tested to study the overall buckling behaviour of these columns under monotonic loading (Chicoine et al 2000). All columns had a square cross-section of 450 mm × 450 mm and a flange slenderness ratio of 23. Additional reinforcements in the form of longitudinal and tie bars were provided in one of the composite specimens. The long columns were tested under concentric loading, except for one, which was tested with an eccentricity of 0.06d about the weak axis. The test results demonstrated the brittle and explosive failure modes of the long composite specimens that consisted of global flexural buckling along with local buckling and concrete crushing between two links. The ultimate capacities of the slender columns were observed to be about 80% of those of short columns with similar cross-sections and link spacings. The additional reinforcement was observed to provide no improvement in the ductility of the long composite column, as opposed to the beneficial effect observed in the short composite columns.

3. NUMERICAL SIMULATIONS

A finite element model of PEC columns with thin-walled built-up sections was first developed by Maranda (1998), using the computer program MEF, to simulate the series of tests on PEC stub columns performed by Tremblay et al. (1998). Only a quarter cross-section was modelled using shell elements for the steel plate, solid elements for the concrete and beam elements for the transverse links. Good agreement was observed between the numerical and the experimental results. However, the model developed by Maranda (1998) was not capable of predicting the post-peak responses of the test specimens.

Chicoine et al. (2002b) performed a finite element analysis using ABAQUS/Standard (HKS 2003) to reproduce numerically the behaviour of the composite column under axial compression only. Similar to the

numerical study performed by Maranda (1998), Chicoine et al (2002b) also modelled a quarter of the column cross-section with a length of one link spacing. The finite element model was developed using shell elements for the steel section, brick elements for concrete and beam elements for the transverse links. Two node spring elements were used to represent the interaction between steel and concrete at their common interface. Steel material behaviour was represented by a bilinear stress-strain curve based on the typical stress-strain curves obtained from tension coupon tests of the plates used in the column specimens (Chicoine et al 2000). The cracking model in ABAQUS/Standard was used by Chicoine et al (2002) to represent the concrete material behaviour in PEC columns. Chicoine et al. (2002) used the Riks displacement control technique to simulate the applied loading conditions in the test specimens.

The finite element model developed by Chicoine et al. (2002b) provided a very good representation of the capacity and load versus displacement response of short PEC test specimens (Tremblay et al. 1998; Chicoine et al. 2000) up to the ultimate load. The post-peak response of the columns was obtained only over a short deformation range due to convergence problems experienced by the numerical model. This can be attributed to the inadequacy of the implicit solution method for representing the highly nonlinear post-peak behaviour. The researchers identified significant challenges in simulating the local instability of the thin flanges and the triaxial behaviour of the partially confined concrete in the column.

Begum et al. (2007) were able to overcome the challenges in numerically simulating the behaviour of PEC columns. A complete finite element model including the full cross-section and entire length of the column was developed using the explicit module of ABAQUS finite element code (Begum et al. 2007). The model is applicable for concentric as well as eccentric loads. The finite element model along with the mesh configuration for a typical part between two consecutive links is shown in Figure 4. The steel plates were modelled using four node shell elements. Eight-node brick elements were used for concrete and beam elements for transverse links. A dynamic explicit solution strategy was implemented to trace a stable post-peak response in the load-deformation curve. The steel-concrete interface in the composite column was simulated using a contact pair algorithm. To represent the concrete material behaviour under partial confinement, the damage plasticity model in ABAQUS was implemented.

Begum et al. (2007) used the developed model for PEC columns to reproduce the test results of 12 normal strength, seven high strength and two steel fibre reinforced high strength concrete PEC columns. The average experimental-to-numerical ratios of the peak load obtained were: 1.01, 0.99 and 1.08, respectively, for normal strength, high strength and steel fibre reinforced high strength concrete PEC columns with standard deviations all less than 0.05. Moreover, the numerical load versus axial strain responses for the test columns were in very good agreement with the experimental responses. The failure in all the specimens observed in the numerical analyses was due to the initiation of local instability of the flange plate

between two transverse links followed by crushing of the adjacent concrete. Similar behavior was observed in the experiments. Figure 5 shows comparison between the experimental and numerical results for a typical PEC column. The full model also represented the axial capacity of the three long PEC test specimens ($L/d = 20$) with good accuracy with an average experimental-to-numerical ratio of 0.98.

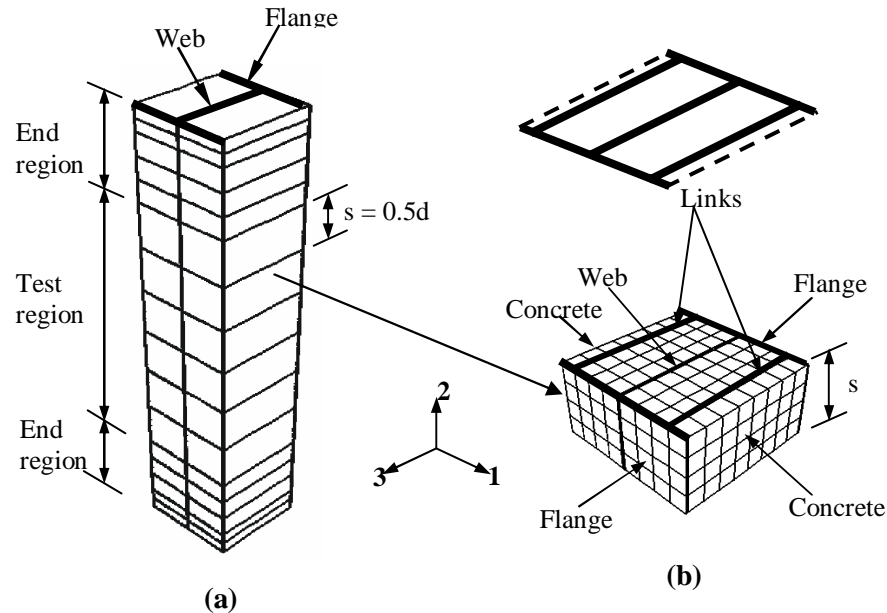


Figure 4: Finite Element Mesh Developed by Begum et al. (2007), (a) Typical Short Column Displaying the Parts between Consecutive Links, and (b) Mesh Configuration of a Typical Part in the Test Region of the Column.

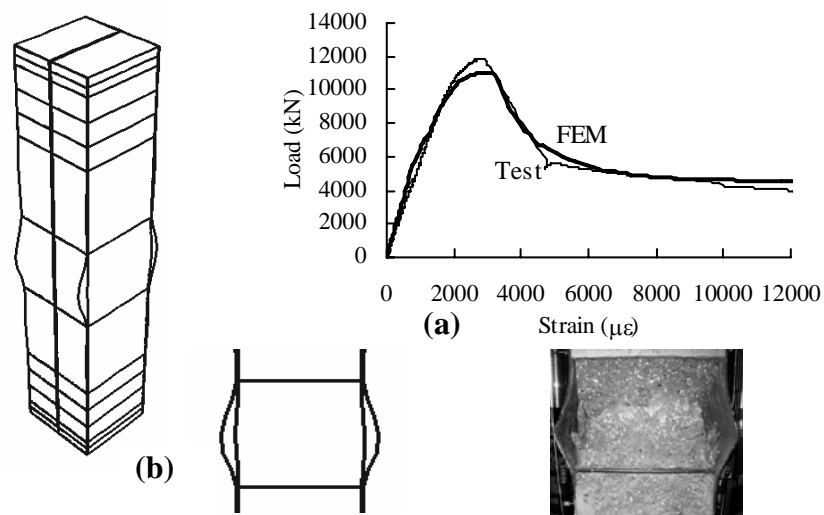


Figure 5: Comparison of Experimental and Numerical Results, (a) Load vs. Displacement Response and (b) Failure Mode.

A comprehensive parametric analysis was performed by Begum et al. (2007) to study the behaviour of PEC columns subjected to axial compression and bending about the strong axis. The parameters that were varied include the overall column slenderness ratio, load eccentricity ratio, link spacing-to-depth ratio, plate slenderness ratio and concrete

compressive strength. The results of the parametric analysis revealed that the axial capacity of a PEC column reduces as the overall slenderness ratio increases, particularly for columns with slender plates. As the plate slenderness ratio increases, the axial capacity of the column reduces, as expected, with increased brittleness in the failure behaviour. On the other hand, the brittle behaviour of long PEC columns is not affected by the b/t ratio. Thus, the advantage of using stockier flange plates diminishes as the column becomes slender. The axial capacity of the PEC column is greatly (average increase is 55%) improved by the use of high strength concrete instead of normal strength concrete. However, the load–deformation response of high strength concrete PEC columns exhibited brittle failure as compared to the normal strength concrete columns.

4. PREDICTION OF PEC COLUMN CAPACITY

4.1 Columns under Concentric Axial Loading

The experimental and numerical investigations on PEC columns with built-up sections led to the development of a capacity prediction model for these columns. In this model the compressive cross-sectional strength of the PEC column is calculated using the following expression proposed by Tremblay et al. (1998), with modifications from the work of Chicoine et al. (2002):

$$C_r = (A_{se}F_y + 0.92\psi A_c f_{cu} + A_r F_{yr}) \quad (1)$$

where A_{se} is the effective area of the steel shape as defined by Equation (2), F_y is the yield strength of the steel plate, A_c is the cross-sectional area of concrete, f_{cu} is the concrete cylinder strength and A_r and F_{yr} are the area and yield strength of the longitudinal rebars.

$$A_{se} = (d - 2t + 2b_e)t \quad (2)$$

where d is the overall depth of the cross-section, t is the thickness of the steel plates and b_e is the total effective width of the flange. To account for the effect of local buckling in the column capacity, b_e is expressed as:

$$b_e = \frac{b_f}{(1 + \lambda_p^{2n})^{1/n}} \leq b_f \quad (3)$$

$$\lambda_p = \frac{b}{t} \sqrt{\frac{12(1 - \nu_s^2)F_y}{\pi^2 E_s k}} \quad (4)$$

$$k = \frac{0.9}{(s/b_f)^2} + 0.2(s/b_f)^2 + 0.75, \quad (0.5 \leq s/b_f \leq 1) \quad (5)$$

In Equation (3), b_f is the full width of a flange plate and λ_p is a slenderness parameter calculated using Equation (4). E_s and ν_s in Equation (4) are the elastic modulus and Poisson's ratio, respectively, of

steel. The value of the factor n in Equation (3) is taken as 1.5, as proposed by Chicoine et al (2002).

Equations (1) to (4) are included in CSA S16-01 (CSA 2001) for determining the design capacity of axially loaded PEC columns with built-up thin-walled shapes, but with a slight modification in the concrete strength reduction factor. For simplicity, the strength reduction factor 0.92ψ in Equation (1) was replaced by 0.8 in CSA S16-01. However, these design equations are subjected to certain limitations imposed by the scope of the experimental and numerical research works. The yield strength of the steel plate and reinforcing bars is limited to no greater than 350 MPa and 400 MPa, respectively, and concrete strengths only up to 40 MPa are allowed (normal density). The flange width, b_f , must be within 0.9 to 1.1 times the section depth, d , and have a slenderness ratio, $b_f/2t$, not greater than 32. The thickness of the web plate must be equal to the thickness of the flanges and the connections between them must be provided by continuous fillet welds designed to develop the shear yield capacity of the web. The spacing of the transverse links is limited to the lesser of 500 mm or $0.67d$ and the area of a link must be at least the greatest of 63 mm^2 , $0.01b_f t$ and 0.5 mm^2 per mm of link spacing. Finally, the equations are applicable only to concentrically loaded columns with a clear height-to-depth ratio less than 14. As reported by Prickett and Driver (2006), the design equations for concentrically loaded columns provide conservative estimations of the axial capacity of PEC columns with high strength concrete. Therefore, it was recommended that the current upper limit for the strength of concrete be increased from 40 to 70 MPa.

4.2 Columns under Combined Axial and Flexural Loading

Bouchereau and Toupin (2002) and Prickett and Driver (2006) predicted the capacity of eccentrically loaded columns from load–moment interaction diagrams constructed using a procedure commonly adopted for reinforced concrete columns. A linear strain distribution along the cross-section, based on observations from the strain measurements taken during the test, was implemented for the construction of this diagram. The extreme compressive strain was set at $3500 \mu\epsilon$, whereas the extreme tensile strain was varied from 0 to 10 times the yield strain of the steel. For each strain gradient the ultimate load and moment capacities were calculated from the material and geometric properties of the composite cross-section. To calculate the contribution of the steel to the capacity of the composite column, the section was discretised in such a way as to have effectively uniform strain in each individual piece. For strong axis bending, the flanges were considered to be one piece, whereas the web was divided into ten pieces. On the other hand, for weak axis bending the web was considered as one piece and each flange was discretised into ten pieces (Prickett and Driver 2006).

5. CONCLUSIONS

The research on PEC columns with thin-walled sections reviewed in this paper reveals that the behaviour of this composite system with normal and high performance materials have become relatively well understood from the full scale experimental investigations for monotonic concentric and eccentric axial loads. The finite element model developed for this new composite system can adequately represent the local buckling behaviour, the ultimate load and the post-peak residual capacity for axial compression and bending. In addition, the influences of several key parameters, which could not be covered by the experimental programs, on the behaviour of these columns under axial compression and bending, were investigated using the finite element model. However, the behaviour of this composite system under cyclic loading has not been completely explored. Intensive research is therefore required to address the effects of cyclic bending moment on PEC columns with variable geometric and material properties. And therefore, the existing design guidelines for thin walled PEC columns should be extended to cover the full range of behaviour of this innovative composite system under various conditions of loading.

REFERENCES

- Begum, M., Driver, R. G. and Elwi, A. E., 2007. Numerical Simulations of the Behaviour of Partially Encased Composite Columns. *Structural Engineering Report*, University of Alberta, Edmonton, Canada.
- Bouchereau, R., and Toupin, J.-D., 2003. Étude du Comportement en Compression-Flexion des Poteaux Mixtes Partiellement Enrobés. *Report EPM/GCS-2003-03*, Ecole Polytechnique, Montreal, Canada
- Chicoine, T., Tremblay, R., Massicotte, B., Yalcin, M., Ricles, J., and Lu, L.-W., 2000. "Test Programme on Partially-Encased Built Up Three-Plate Composite Columns." *Joint Report EPM/GCS No. 00-06*, February, Dept. of Civil, Geological and Mining Engineering, Ecole Polytechnique, Montreal, Canada – ATLSS Engineering Research Centre, No. 00-04, Lehigh University, Bethlehem, Pennsylvania, USA.
- Chicoine, T., Tremblay, R. and Massicotte, B., 2002. Finite Element Modelling and Design of Partially Encased Composite Columns. *Steel and Composite Structures*, 2 (3), 171–194.
- CSA., 2001. CSA S16-01, Limit States Design of Steel Structures. Canadian Standards Association, Toronto, ON.
- Filion, I., 1998. Étude Expérimentale des Poteaux Mixtes Avec Section d'acier de classe 4, *Report n°. EPM/GCS-1998-06*, Ecole Polytechnique, Montreal, Canada.
- HKS (Hibbitt, Karlsson and Sorensen, Inc.), 2003. *ABAQUS/Explicit User's Manual*, Version 6.3.
- Maranda, R. (1998) "Analyses par Éléments Finis de Poteaux Mixtes Avec Sections d'acier En I de Classe 4" *Report n°. EPM/GCS-1998-11*, Ecole Polytechnique, Montreal, Canada.
- Prickett, B. S. and Driver, R. G., 2006. "Behaviour of Partially Encased Composite Columns Made with High Performance Concrete."

Structural Engineering Report No 262, University of Alberta, AB, Canada.

Tremblay, R., Massicotte, B., Filion, I., and Maranda, R., 1998. Experimental Study on the Behaviour of Partially Encased Composite Columns Made with Light Welded H Steel Shapes under Compressive Axial Loads. Proc., SSRC Annual Technical Session & Meeting, Atlanta.

A STUDY ON EFFECT OF LAND-USE CONTROL PLAN ALONG ACTIVE FAULTS IN JAPAN

MIHO YOSHIMURA OHARA
International Center for Urban Safety Engineering
Institute of Industrial Science, The University of Tokyo, Japan
yosimura@iis.u-tokyo.ac.jp

KIMIRO MEGURO
International Center for Urban Safety Engineering
Institute of Industrial Science, The University of Tokyo, Japan
meguro@iis.u-tokyo.ac.jp

ABSTRACT

Japan entered a longstanding depopulation process in 2006. In this situation, it is important to avoid social impact due to disasters by guiding population from vulnerable area to safer area. This research focused the risk of active faults among various kinds of natural hazards and studied on the effect of the land-use control along active faults in Japan.

First, the meaning of land-use control plan along active faults in the society whose population started to decrease was discussed. If the residences in the seismic vulnerable area along active faults are relocated to the safer area by the land-use control plan, these vacant lands could be effectively used for disaster-prevention facilities. Japan has not adopted earthquake fault zoning act due to several reasons. However, considering depopulation, the possibility of introducing fault zoning act will increase and the discussion on the land-use control plan along active faults will become more meaningful.

Then, the distribution of population and buildings in the neighborhood of the active faults was analyzed based on GIS databases of the active faults, population and building stocks. The effect of land-use control using fault zones was discussed based on the obtained results. In case of the fault zone whose width was decided to be 0.4km referring to the fault zoning act in U.S., the population inside the fault zone was 2.89 million and it corresponded to 2.3% of the total population in Japan. Half of the population living along the faults was located in Kinki area and the effect of land-use control was different according to the region. The population inside the fault zone was increased in population to the width of the zone.

1. INTRODUCTION

Japan entered a longstanding depopulation process in 2006. According to the report by the National Institute of Population and Social Security

Research (2002), the total population after 50 years is expected to decrease to about 70% of the current one as shown in Fig.1. In this situation, it is important to avoid social impact due to disasters by guiding population from vulnerable area to safer area. Recently, Japan suffered the 2004 Niigataken Chuetsu Earthquake, the 2007 Noto Hanto Earthquake and the 2007 Niigataken Chuetsu-oki Earthquake. These earthquakes reminded a danger of active faults in Japan. This research focused on the risk of active faults among various kinds of natural hazards and studied on the effect of the land-use control along active faults in Japan. First, the meaning of land-use control plan along active faults in the society whose population started to decrease was discussed. Then, the distribution of population and buildings in the neighborhood of the active faults was analyzed based on GIS databases of the active faults, population and building stocks. The effect of land-use control using fault zones was discussed based on the obtained results.

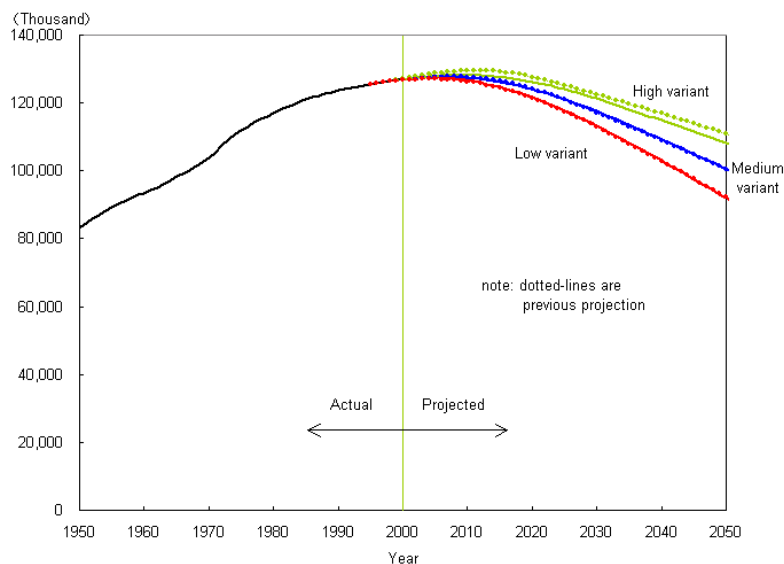


Figure 1: Population projections for Japan:2001-2050

2. MEANING OF LAND-USE CONTROL ALONG ACTIVE FAULTS

When the total population decreases, existing building stocks become unnecessary, and the numbers of vacant houses and lands increase. If the residences in the seismic vulnerable area along active faults are relocated to the safer area by the land-use control plan, these vacant lands could be effectively used for disaster-prevention facilities which have open space and warehouses for emergency supplies. These processes were illustrated in Figure 2.

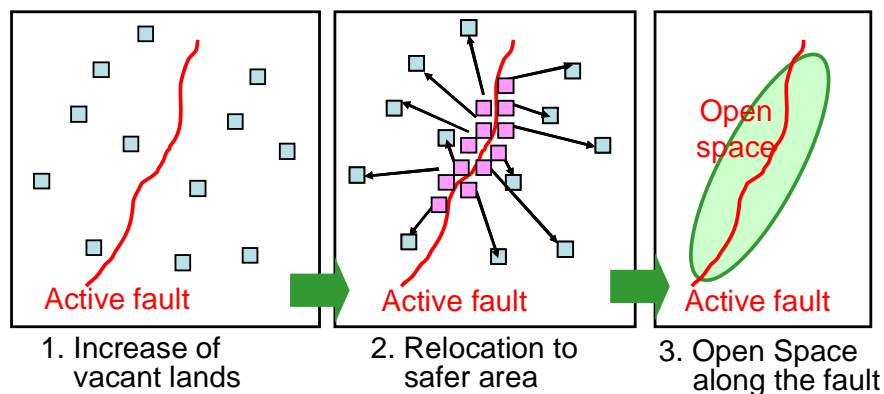


Figure 2: Process of land-use control

Table 1: Conceivable policies for controlling land use

	Direct Policy	Indirect Policy
Repression of population inflow	Regulation of new construction*	Increase in tax for new construction
	Prohibition of new construction	Increase in property tax for existing buildings
		Disclosure of seismic risk information on property sales
		Disclosure of seismic risk information on rental agreement*
Promotion of population outflow	Relocation of existing buildings	grant for relocation
	Regulation of extension or reconstruction of buildings*	Preferential tax treatment for relocation
	Prohibition of extension or reconstruction of buildings	Increase in property tax for existing buildings
	Regulation of rental agreement	Disclosure of seismic risk information on property sales
	Prohibition of rental agreement	Disclosure of seismic risk information on rental agreement*
		Publicity of seismic risk information*

Table 1 shows the conceivable policies for controlling land use. The lands along active faults could be controlled by the repression of the population inflow and the promotion of the population outflow. These could be achieved by direct method such as prohibition and regulation of land use or by indirect method such as disclosure of seismic risk information and tax control. The policies marked with * in the Table 1 are being enforced in California, U.S. by the Alquist-Priolo Earthquake Fault Zoning Act enacted in 1972

While the earthquake fault zoning act has been carried out for 30 years in U.S., Japan has not adopted it. There are several reasons why most of the Japanese specialists have opposed fault zoning. First, introduction of the fault zoning could have huge social impact because Japanese population density is high and a lot of people live on the active faults. Next, most of the active faults in Japan are dip-slip faults and there are many cases that traces of the faults don't appear on the surface. Even if the traces on the surface are estimated, uncertainty of the position should be considered. On the other hand, active faults in California, U.S. are strike-slip faults and traces on the surface are easier to be identified. However, considering that more lands will become vacant due to depopulation in the future, the possibility of introducing fault zoning act will increase and the discussion on the land-use control plan along active faults will be more meaningful.

3. DISTRIBUTION OF ACTIVE FAULTS IN JAPAN

First, GIS database of the active faults were developed by adding several data to the existing digital active fault map (2002). The total length of active faults in Japan is about 10,300 km. When the lengths of active faults were classified by the fault types, 34% of the active faults were dip-slip and 4% were strike-slip as shown in Fig. 3. “Mixed ” in Fig. 3 means the fault that has both strike-slip part and dip-slip part. In case of “Mixed I”, the rate of the length of dip-slip part is more than 70%. In case of “Mixed II”, the rate of dip-slip part is between 30% and 70%. Figure 3 shows the distribution of active faults in Japan.

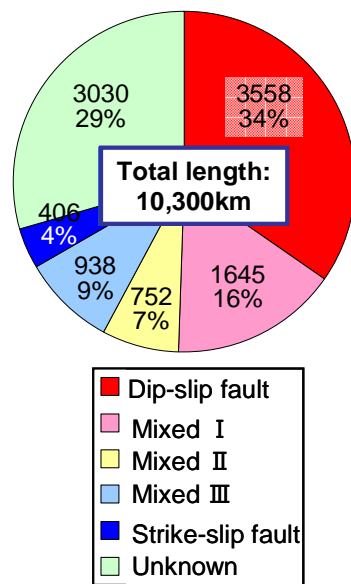


Figure 3: Composition of active fault types

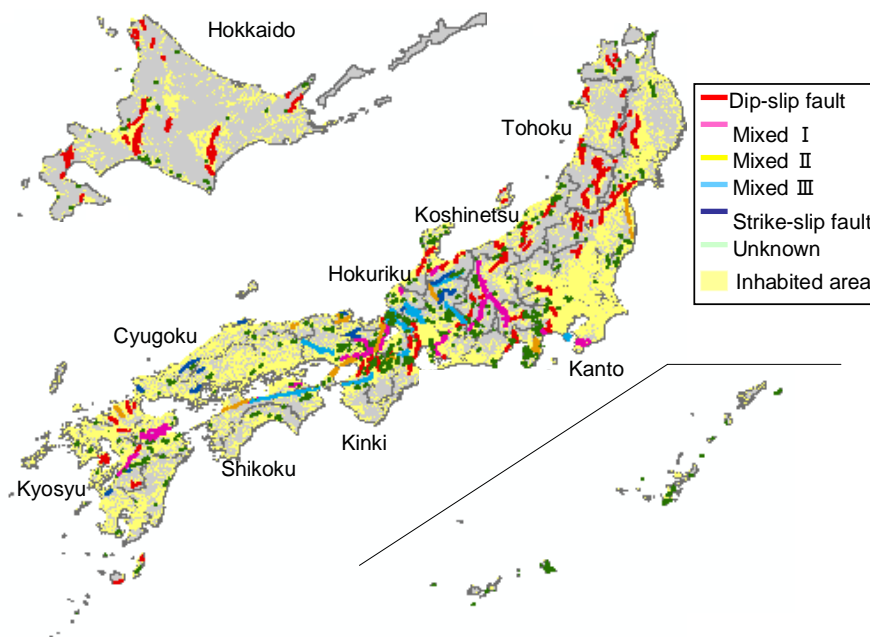


Figure 4: Distribution of active faults in Japan

4. ESTIMATION OF THE EFFECT OF LAND-USE CONTROL ALONG ACTIVE FAULTS

The distribution of population and buildings in the neighborhood of the active faults was analyzed using GIS databases of the active faults, population and building stocks. Then, the effect of land-use control using fault zones was discussed.

The GIS databases of population and building stocks were developed based on the 1km mesh data by Housing and Land Survey (1998). The fault zones were hypothetically set along the active faults as shown in Fig. 5. In California, average width of fault zones is reported to be 0.4km. Referring to it, the width of the fault zone was set to be 0.4km at first. In case of this width of zone, the population inside the fault zone was 2.89 million and it corresponded to 2.3% of the total population in Japan. 0.62 million timber residential houses were estimated to be located inside the zone. Although 4% of the active faults were strike-slip as shown in Fig. 3, the rate of the population living along the strike-slip faults were only 0.4% as shown in Fig. 6. Figure 7 describes the regional tendency of population distribution along the active faults. Half of the population living along the faults was located in Kinki area while 40% of the faults were located in Hokkaido-Tohoku or Hokuriku-Koshinetsu Area. It is said that the effect and the impact of land-use control are different according to the region.

If the width of the fault zone was increased to be 0.8km, 2km, 4km, the population inside the zones was estimated to be 4.5%, 10%, 18% of the total population, respectively. Increase in population was almost in proportion to the width of the fault zones.

Considering the uncertainty of the traces of active faults, larger fault zones are safer. However, it causes more social impact on the population living along the active faults as confirmed in Fig. 8. In order to implement land-use control along active faults in Japan, the appropriate width of fault zones should be discussed considering all the factors such as lessons learned from past earthquake damage, uncertainty of the traces of both strike-slip and dip-slip fault, social impact of the zones.

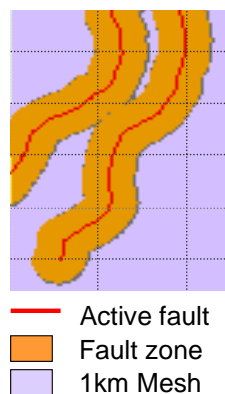


Figure 5: Example of fault zone

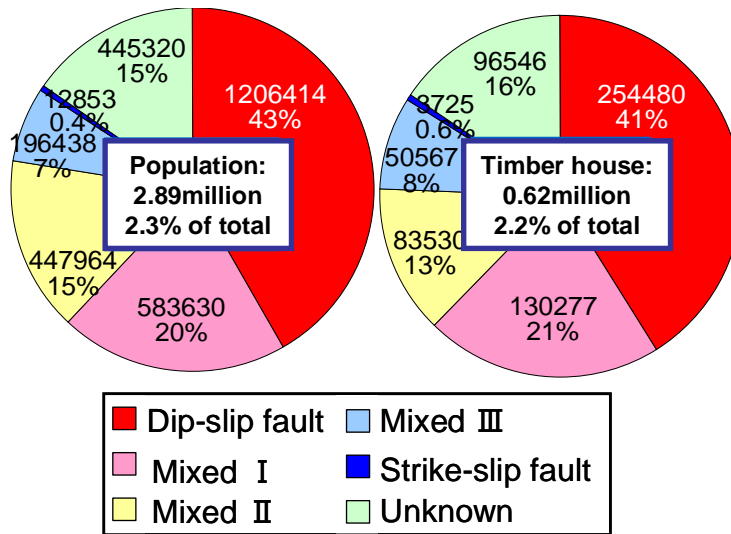


Figure 6: Population and buildings inside the fault zone

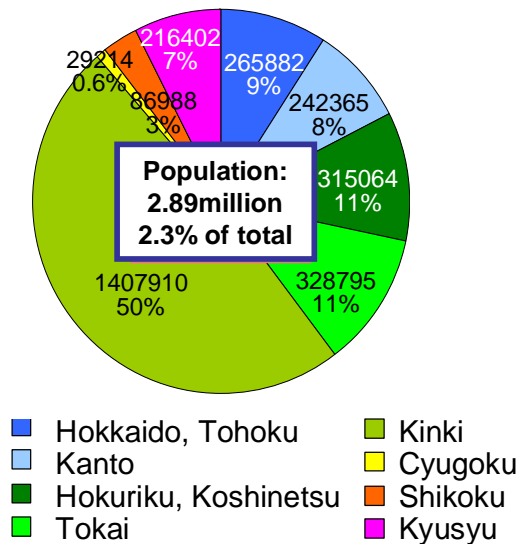


Figure 7: Regional tendency of population distribution

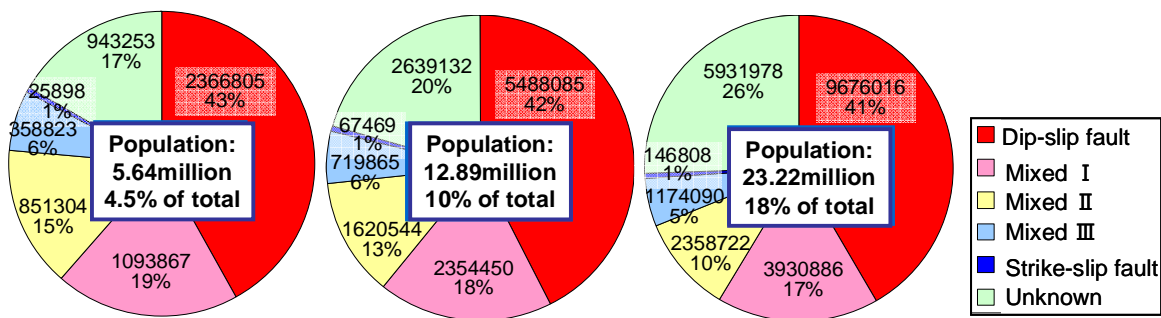


Figure 8: Population inside the fault zone when the width of zone is changed

5. CONCLUSIONS

Japan entered a longstanding depopulation process in 2006. In this situation, it is important to avoid social impact due to the disaster by guiding population from vulnerable area to safer area. This research focused the risk of active faults among various kinds of natural hazards and studied on the effect of the land-use control along active faults in Japan.

First, the meaning of land-use control plan along active faults in the society whose population started to decrease was discussed. While fault zoning act has been carried out for 30 years in U.S., Japan has not adopted it due to several reasons. However, considering that more lands will become vacant due to depopulation in the future, the possibility of introducing fault zoning act will increase and the discussion on the land-use control plan along active faults will become more meaningful.

Then, the distribution of population and buildings in the neighborhood of the active faults was analyzed based on GIS databases of the active faults, population and building stocks. In case of the fault zone whose width was assumed to be 0.4km referring to the act in U.S., the population inside the fault zone was 2.89 million and it corresponded to 2.3% of the total population in Japan. Half of the population living along the faults was located in Kinki area and the effect and the social impact of land-use control was different according to the region. The population inside the fault zone was increased in population to the width of the zone. The appropriate width of fault zones should be discussed considering all the factors such as lessons learned from past earthquake damage, uncertainty of the traces of both strike-slip and dip-slip fault, social impact of the zones.

Based on the study, the authors think that it is meaningful and possible to adopt land-use control plan along active faults in Japan for earthquake damage reduction. However, for its implementation, a study on social impact of the risk information of active faults is necessary to decide proper width of the fault zone and to get social consensus.

REFERENCES

- Schumm, S. A., Mosley, M. P., and Weaver, W. E., 1987. *Experimental geomorphology: the Study of Small Landforms*. John Wiley, New York.
- The National Institute of Population and Social Security Research, 2002. *Population Projections for Japan:2001-2050*, <http://www.ipss.go.jp/index-e.html>.
- California Geological Survey, 2007. *Alquist Priolo Earthquake Fault Zones*, <http://www.consrv.ca.gov/CGS/rghm/ap/index.htm>.
- Nakata T. and Imaizumi T., 2002. *Digital Active Fault Map of Japan*, University of Tokyo Press.
- Statistics Bureau, Ministry of Internal Affairs and Communications, 1998. *Housing and Land Survey*

APPLICATION OF GEOPHYSICAL IMAGING IN SUBSURFACE CHARACTERIZATION FOR URBAN SAFETY IN AN EARTHQUAKE - A CASE STUDY FROM DHAKA MEGA CITY, BANGLADESH

AFTAB ALAM KHAN
Professor, Department of Geology
University of Dhaka, Dhaka, Bangladesh
TUaftab@univdhaka.edu

MUHAMMAD SHAHADAT HOSSAIN
Graduate Research Assistant
Department of Geology and Geography
Auburn University, USA

ABSTRACT

Dhaka, capital of Bangladesh is one of the fastest growing megacities with its present population exceeding 14 million. It is situated in the periphery of the southern fringe of tectonically uplifted Madhupur Pleistocene Terrace bounded by both En échelon and cross faults. The recent earthquake activities and other geophysical evidences suggest that Dhaka and surroundings is geologically active. The existence of Buriganga - Dhaleshwari fault and the dominance of mud, clay and swampy deposits propelled its vulnerability to earthquake damage to the settlements and to infrastructures. The distribution pattern of both P- and S- wave suggest that the top layer is largely transverse to the distribution pattern of the layer below. The zones with high seismic velocity are characterized by low particle velocity and vice versa. Hence, the zones characterized by high particle velocity (low shear wave velocity) are considered as damage vulnerable zones. The seismic velocity has also been used to determine the resonant height of buildings at various locations. The Vertical Electrical Sounding (VES) rendered the distribution pattern of the sediments upto a depth of 240 meter. Sediments with high resistivity value / low fluid saturation cover the central and northern part of Dhaka. In the central part, clay is dominant, truncating against sand dominated zone in the southwestern part. In the northeastern part, sand increases with depth and the layers are much more continuous in nature than in the northwestern part. The 2-D imaging / Constant Separation Traversing (CST) reveal the lithological discontinuities, buried channels, regional tilting, and saturated – unsaturated fills upto a depth of 125 meter. Vertical Electrical Sounding (VES) and Electrical Tomography in combination has enabled to identify several faults such as Singair fault, Buriganga-Dhaleshwari fault, Nayarhat fault, and Tongi-Turag fault those occur in and around Dhaka. The simulated lithologic models depict the variations in lithology up to 174

meter depth. A generalized stratigraphic model exhibits three distinct stratigraphic unit e.g. Top clay, Sand, and Clay. The lithologic data exhibits the presence of a north–south trending fault in between Tejgaon and Banani in the north and in the south in the midst of BUET, DU campus and Phulbaria eventually merging with Buriganga fault.

An integrated approach has been adopted to prepare an earthquake hazard vulnerability map based on the identification of faults, subsurface lithological variations, velocity characterization, and dominant frequency response and “g” value character. Geophysical data can immensely contribute in urban risk management and effective disaster management plan and program to mitigate damage from possible earthquakes.

1. INTRODUCTION

Dhaka with an area of 815.85 sq. km. and about 14 million populations is the capital of Bangladesh. Dhaka urban area covers the spatial zone between the latitudes 23° 41' N and 23° 55' N and longitudes 90° 20' E and 90° 31' E. In a study on 20 mega cities of the world, Dhaka appeared to have one of the highest values of Earthquake Disaster Risk Index (EDRI) mainly due to its inherent vulnerability of building infrastructure, high population density, poor emergency response, and poor recovery capability. Any physical phenomenon associated with an earthquake that may produce adverse effects on human activities is termed as earthquake hazard. This includes surface faulting, ground shaking, landslides, liquefaction, tectonic deformation, tsunami, and their effects on land use, fabricated structures, and socio-economic systems. A commonly used restricted definition of earthquake hazard is the probability of occurrence of a specified level of ground shaking in a specified period. Similarly, earthquake risk is the expected (or probable) life loss, injury, or building damage that will happen, given the probability that earthquake hazard occurs. The recent earthquake activities and other geophysical evidences suggest that Dhaka and surroundings is geologically active (Khan, 2005).

Geophysical imaging pertaining to electrical resistivity and seismic velocity has been obtained for subsurface characterization of Dhaka city. Imaging by Vertical Electrical Sounding (VES) is used to decipher vertical lithological changes and character while, imaging by Constant Separation Traversing (CST) is used to decipher lateral lithological changes with fluid saturation status, buried channels, filled zones, faults and discontinuities. Cross checking on to the variations in lithology both in vertical and lateral dimensions have been performed through preparing 3D panel diagram of available drill-holes of Dhaka WASA and other agencies, and observing available geophysical well-log response. Twenty (20) borehole litho-logs of Dhaka WASA and Sixteen (16) Geophysical Well Logs were used to simulate the subsurface for cross checking. The geophysical images are in good agreement with 3D panel diagram and well-log response. The acquired seismic velocities are used to determine acceleration due to gravity (g) and resonant height of the building through dominant frequency response.

2. GEOMORPHOLOGY AND GEOLOGY

Dhaka Metropolis is surrounded by Buriganga River, a channel of Dhaleshwari River in the south; rivers Balu and Shitalakhya in the east; Tongi Khal in the north and the river Turag in the west. It occupies mostly by the southern fringe of Madhupur tract. Elevation map of Dhaka city generated by DWASA elevation data shows that the elevation of the entire eastern Dhaka ranges between 3 to 4.5m. A large part of the north-south trending central region bears the elevation between 5 and 8m with a regional gradient towards north. The southern part of the north-south trending central region covering part of Ramna, Tejgaon, Hazaribagh, Mohammadpur, and Motijheel Thanas exhibits the elevation between 9-10m. The elevation of a small segment of area at Mirpur-Pallabi reaches upto 13.5m above mean sea level. The elevation distribution of Dhaka city signifies a northward tilt of the north-south trending uplifted central region. There are distinct subsurface gradient towards east, west and south suggesting a radial and divergent gradient pattern.

Most parts of the urban areas are developed on the elevated Pleistocene highlands. However, a substantial portion of the adjoining low-lying areas has recently been brought under the accelerated rate of urban growth. Geologically, Dhaka is situated at the southern tip of Madhupur High (Pleistocene Terrace) surrounded by subsiding floodplains. The tectonics and its structural configuration largely control the sedimentation and stratigraphy of the area. Two characteristic geologic units cover the city and surroundings, viz. Madhupur clay of the Pleistocene age and Holocene - Recent alluvial deposits. The Madhupur clay is the oldest sediment exposed in and around the investigated area having characteristic topography and drainage. The differential elevation, landform and distribution of geologic units those are visualized in the landsat image terminated into a corrugated topography. A north-south trending prominent buried channel dissecting Dhaka-Savar main uplands has been identified. The surface manifestations of elevation helped to identify some prominent faults in and around Dhaka city such as Nayarhat fault, Dhaleshwari fault, Buriganga fault, and Tongi-Turag fault (Figure 1). The NE – SW trending geologic cross-section (Fig.1) exhibits a general subsurface configuration characterizing uplifted Pleistocene terrace, depressed lands, flood-plains and abandon channels (Khandoker, 1987).

3. DATA ACQUISITION AND ANALYSIS

Extensive field investigations were performed covering the entire Dhaka metropolitan area for data acquisition and generation pertaining to earthquake-hazard vulnerability assessment. Shallow subsurface data were obtained applying both Vertical Electrical Sounding (VES) and Constant Separation Traversing (CST) of geophysical technique of electrode array. Thirteen Vertical Electrical Sounding (VES) and five 2-D profiling by Constant Separation Traversing (CST) were carried out. Seismic velocity

survey was conducted with the help of hammer seismograph for determining shallow subsurface seismic velocity variations.

Seismic refraction techniques were used to obtain data on the near surface (typically to about 30 meters, although depths in excess of 200 meters can be achieved with more powerful seismic sources). The velocity measurement at Twenty-Two locations in Dhaka city has provided P-wave velocity both for top layer (V_{p0}) and for the layer below (V_{p1}). The P-wave velocity was transformed to S-wave velocity assigning suitable Poisson's ratio value derived from the material type (clay to sand) occurring at the velocity measuring site. Velocity data has also been used to determine the resonant height of the building at various locations.

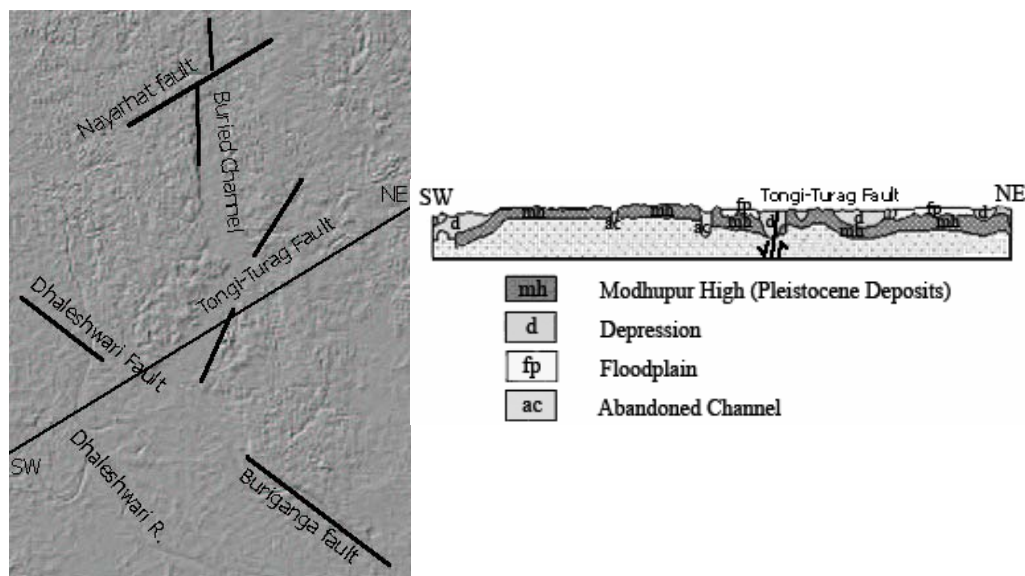


Figure 1: Geomorphic image and NE-SW cross-section of Dhaka metropolitan city showing various geomorphic features and faults.

The optimal length required for resonance has been calculated from the shear-wave velocity data. Hence, the optimal number of floors that is likely to coincide with the ground resonance has been calculated assuming 10 feet floor height. The notion of acceleration due to gravity (g) is of key importance when trying to measure any type of varying motion such as strong ground shaking. An attempt has been made to calculate the acceleration due to gravity (g) based on the shear wave velocity of the top layer, background frequency of the ground and ground displacement at all the twenty-two locations of velocity measurements.

Borehole logs are the records of vertical lithologic rock units of a particular place. Twenty (20) borehole logs were treated in 3D environment using RockWorks2004®. The selection was based on prior consideration upon the coherence and consistency of the information and even distribution of logs throughout the area. The layering information on the sand and clay horizons has been used in the lithologic model reconstruction. Geophysical logs give much more detailed picture of the subsurface and are expensive as well. Resistivity depends on the porosity and nature of the interstitial fluid.

It is seen that resistivity increases logarithmically when porosity decreases. Normally, the sand is more resistive than clay. Sand layer containing fresh water is more resistive than salt water. One test hole in the University of Dhaka campus has been logged for natural gamma and induction EM conductivity up to a depth of 270 meters. Number of geophysical resistivity logs available with DWASA was used to identify sand and clay horizons for stratigraphic reconstruction.

4. RESULTS AND INTERPRETATION

Electrical Sounding

Vertical Electrical Sounding (VES) data acquired for determination of number of layers with thickness and resistivity of each layer. In general, resistivity changes with the fluid saturation while, fluid saturation depends on pore volume and its interconnection. Normally, greater the porosity percentage and fluid saturation lesser is the resistivity and vice versa. Vertical electrical sounding data have been used to generate dominant lithological logs by using inverse modeling technique (Figure 2).

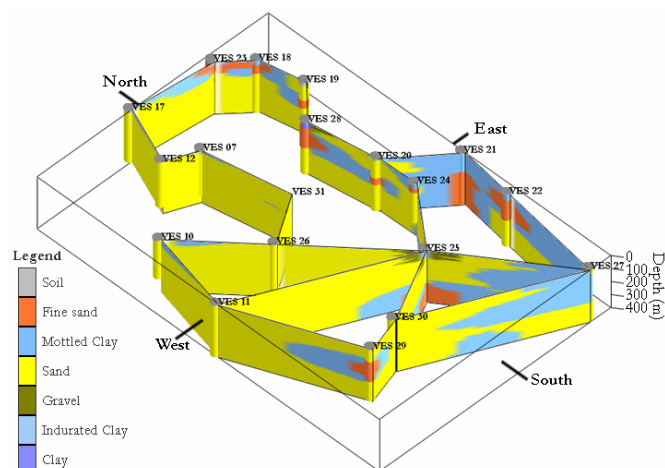


Figure 2: Vertical Electrical Soundings (VES) generating dominant lithological logs and 3D lithological perspectives.

The Dhaka metropolitan city area is characterized by dominantly clay upto 240m depth with intermittent sand. The surface is covered by both sand and clay. The northern and central part is mostly covered by sand while in the southern part and some parts in the northeast and northwest is covered by clay. The average thickness of the top clay ranges from 3 to 10m and in some places (VES 10), it reaches upto 24m. This clay unit is thicker in the middle part of Dhaka metropolitan city area. The thickness of this unit gradually decreases towards southeastern part of the studied area while in the other places it is more or less similar in thickness. Correlation between VES07 and borehole litholog at Mirpur DOHS reveal a unique matching between the vertical lithological change and VES response (Figure 3). Based on electro-stratigraphy three sub-surface zones with distinct

lithological character have been identified in the near surface viz., clay rich zone, saturated sand rich zone, and partially saturated sand rich zone (Khan and Hossain, 2005).

Correlation of vertical imaging by VES revealed distinct offsets between the layers signifying faults. The correlations have further identified faults such as Turag-Tongi fault between VES 12 & VES 07, Dhaleshwari fault between VES 30 & VES 25, and Buriganga fault between VES 25 & VES 22 with off-sets approximately 19m, 16m, and 18m respectively (Figure 4).

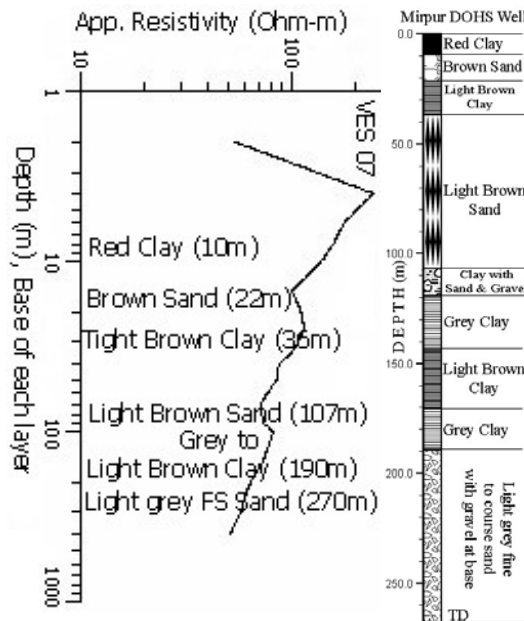


Figure 3: Correlation of VES with Borehole log at DOHS, Mirpur.

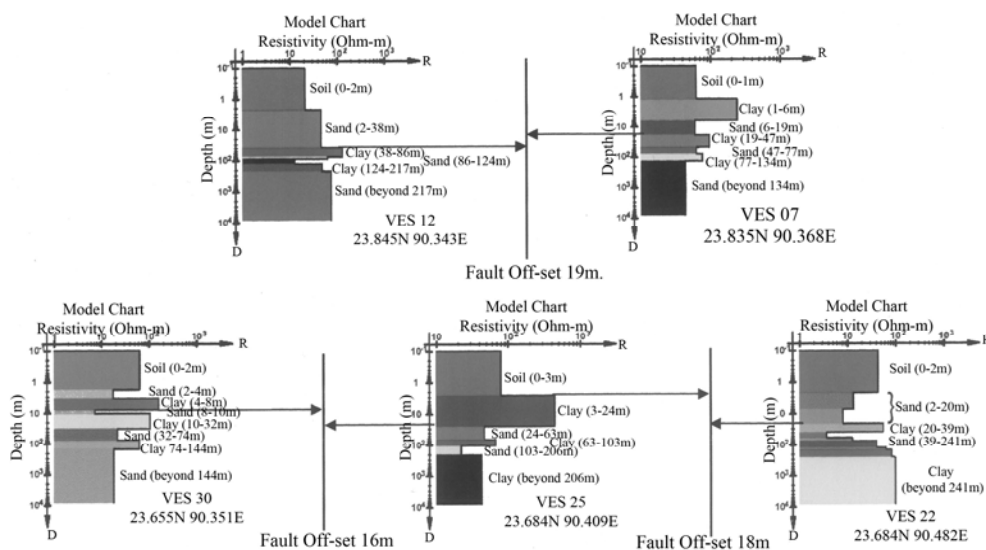


Figure 4: Correlation of Vertical Electrical Soundings (VES) showing several fault offsets.

Electrical Profiling

Subsurface correlation based on lateral imaging (Fig. 5) covering 125m depth by profiling suggests that the lateral distribution of lithology is of distinct truncating nature providing evidences of tilting, faulting, incised channeling, and fills with variable saturation status. The high resistive dry layer characterizes the zones of uplift and tilting. While, low resistive layers with greater saturation status characterize the zones of subsidence and fills. The northern block of Tongi fault is an uplifted one but tilted towards south.

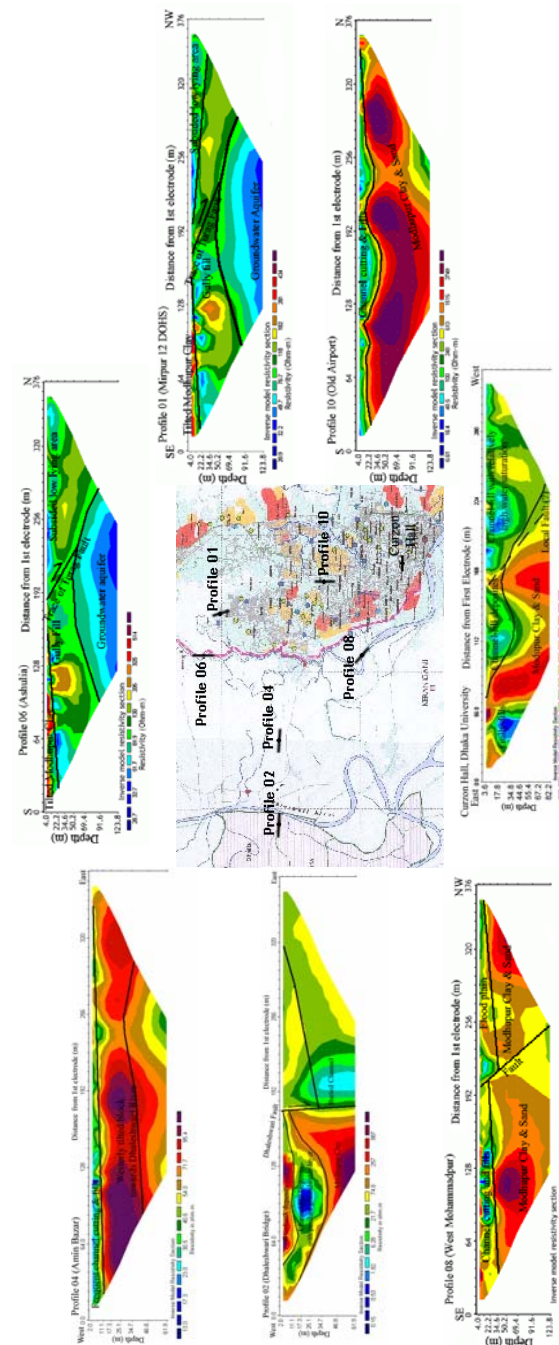


Figure 5: Subsurface correlation by lateral imaging shows lateral distribution of lithology, evidence of tilting, faulting, incised channeling, and fills with variable saturation status.

Although, Narayanganj area has been identified as an uplifted and tilted block but due to paucity of data the effects of Buriganga fault on the readjustment of subsurface status could not be identified. Nonetheless, the Buriganga fault is a basement-controlled fault that is genetically related with the uplift of Madhupur High and the subsidence of Jamuna depression (Khan, et al., 2000).

Bore-hole Geophysics

Bore-hole resistivity logs along a north-south transect across Mirpur, Banani, Rajarbagh and Jurain of Dhaka city exhibits subsidence and fills in the southern part (Jurain – Syedabad area), intense channeling and fills in the central part (Rajarbagh – Motijheel area), and uplift in the northern part (Banani – Mirpur area) (Fig. 6). It is further envisaged that an offset between uplift and subsidence occurs to the tune of about 10m exhibiting traces of Begunbari and Buriganga faults.

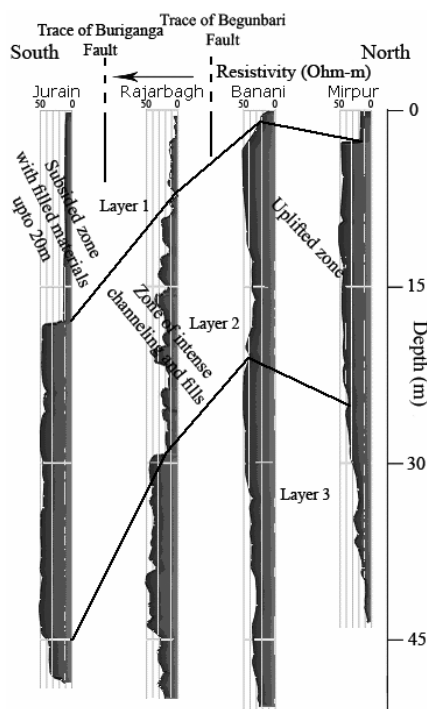


Figure 6: Bore-hole resistivity logs along a north-south transect across Mirpur, Banani, Rajarbagh and Jurain of Dhaka city exhibiting subsidence, fills, channeling and uplift.

Seismic Velocity

The shallow seismic velocity measurements at Twenty-Two locations within Dhaka city have provided P-wave velocity both for top layer (V_{p0}) and the $1P^{stP}$ layer (V_{p1}) (Fig. 7). P-wave velocity has been transformed to shear wave (S-wave) velocity using Poisson's ratio adopted on the types of materials occur at each measuring site (Fig. 8). The seismic velocity maps envisage the lateral changes in both the layers. The velocity contour maps both for

P-wave and for S-wave suggest that the distribution pattern of the top layer is largely transverse to the distribution of the bottom layer. The transverse nature of velocity distribution suggests that the sediments of the 1PstP layer have been deposited mostly in the east-west trending depositional floor while the top layer sediments have been deposited mostly in the north-south trending depositional floor.

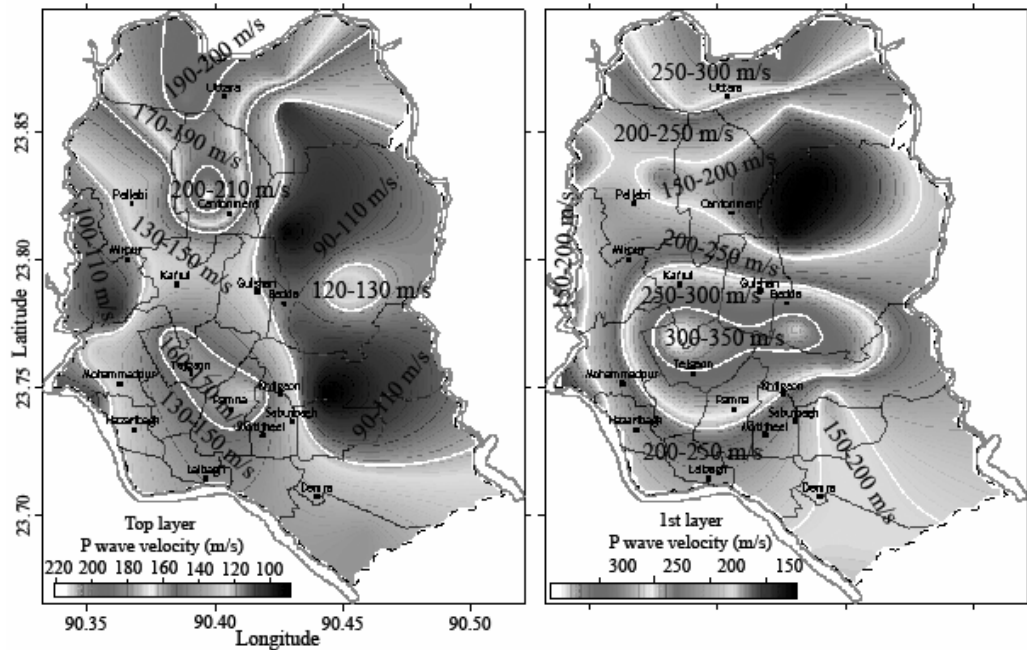


Figure 7: Shallow seismic P-wave velocity distribution of Dhaka metropolitan city both for top layer (V_{p0}) and for the 1PstP layer (V_{p1}).

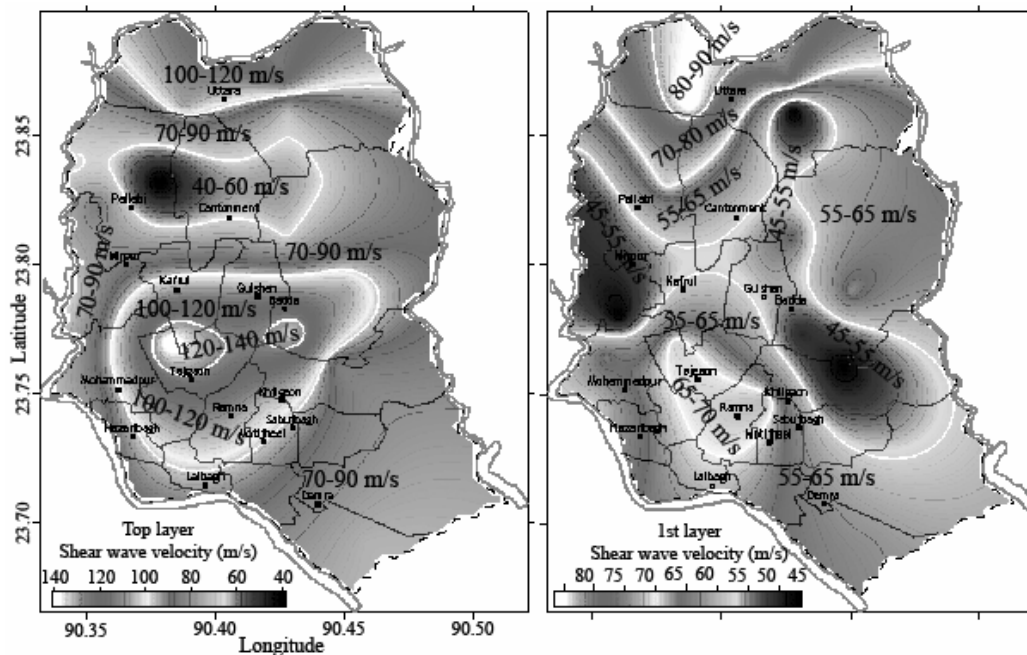


Figure 8: Shallow seismic S-wave velocity distribution of Dhaka metropolitan city both for top layer (V_{s0}) and for the 1PstP layer (V_{s1}).

The shifting nature of the depositional floor is an indication of the shifting of the transporting and depositing media. Such shifting can occur with the change in the physical configuration of the depositional floor. Hence, it is inferred that the region in and around Dhaka mega-city had been geologically active in the recent time. The high seismic velocity zones are characterized by low particle velocity and vice-versa. Hence, the zones characterized by the low shear wave velocity are inferred to be the high-risk zones of seismic hazard.

Resonance

Seismic velocity data of the study area have been used to determine the dominant frequency content (resonant length) at various locations of Dhaka city (Fig. 9). The map shows dominant frequency content ranging between 0.6 and 0.9 hertz.

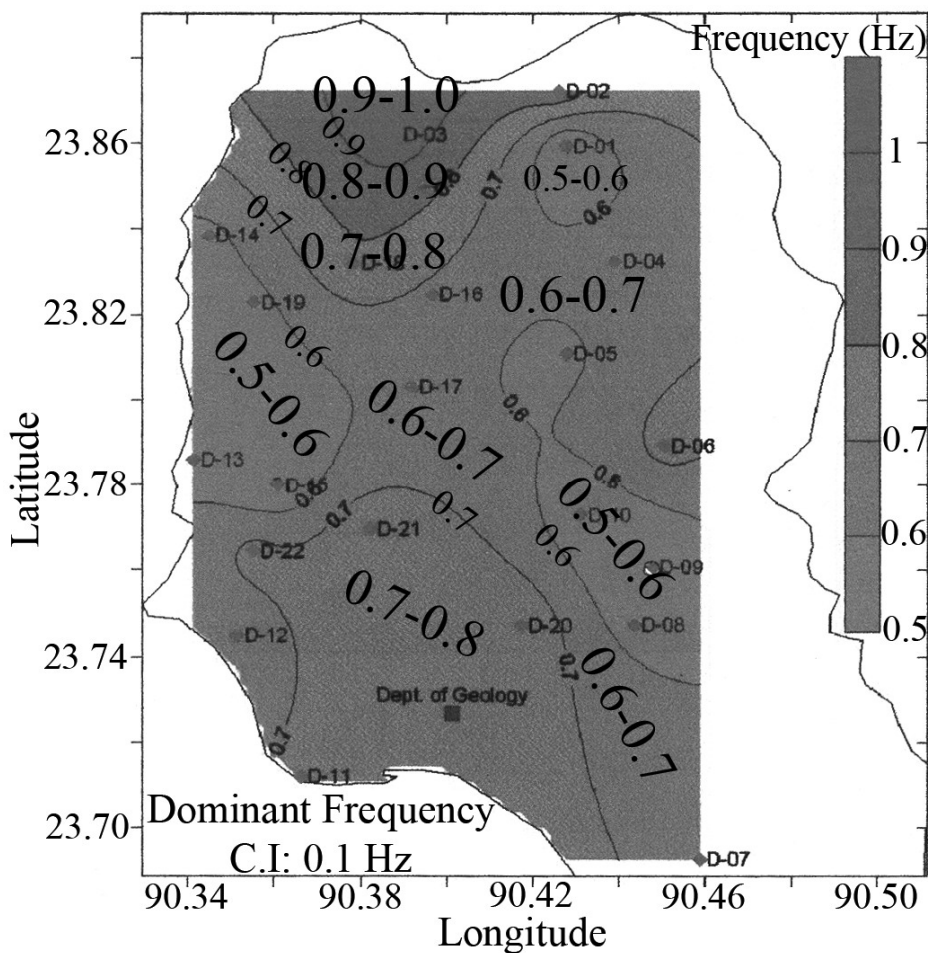


Figure 9: Dominant frequency content (resonant length) distribution of Dhaka metropolitan city.

Considering the default floor height as 10ft, the optimal height required for multi-mode resonance has been calculated from the shear-wave

velocity. The optimal number of floors that is likely to coincide with the ground resonance is shown (Figure 10).

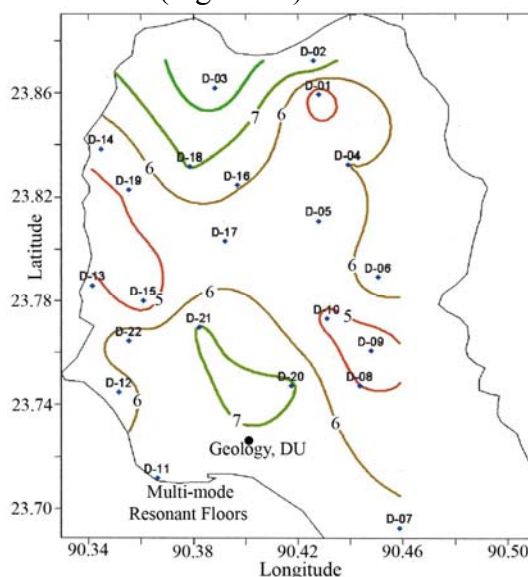


Figure 10: Optimal number of floor requirements for resonance in Dhaka metropolitan city.

Ground Acceleration (g)

The notion of acceleration due to gravity (g) is of key factor when trying to measure any type of vibrating motion such as strong ground shaking. The acceleration due to gravity ($1g = 9.8 \text{ m/sec}^2$) is a sizable rate of increase of speed, which is equivalent to a car going 100m from rest in just 4.5 seconds (Bolt, 1978).

The values of ground acceleration, velocity, and displacement vary a great deal, depending on the frequency of the seismic wave motion of an earthquake. The relations of ground displacement, ground velocity, and ground acceleration are explained in the following mathematical treatment. For a traveling simple harmonic wave, the ground displacement 'y' at a given time 't' is a function of position 'x' and time 't'.

$$y = A \sin 2\pi/\lambda (x + vt)$$

Here, A is Amplitude, λ is Wavelength, and v is Velocity.

In time T, called the period, the wave travels a distance ' λ ' is the time of a complete vibration.

The velocity of the wave is the wavelength divided by the period.

Hence, $v = \lambda/T = f\lambda$, where f is the frequency in Hz.

The angular frequency $\omega = 2\pi f$

Thus, the sideway motion can be written as

Ground displacement = $y = A \sin (2\pi/T) t = A \sin \omega t$

Ground Velocity = $\dot{y} = 2\pi A/T \cos (2\pi/T) t = \omega A \cos \omega t$

Ground Acceleration = $\ddot{y} = -4\pi^2 A/T^2 \sin (2\pi/T) t = -\omega^2 A \sin \omega t = -\omega^2 y$

An attempt has been made to calculate the acceleration due to gravity (g) based on the shear wave velocity of the top layer, background frequency of the ground and ground displacement at all the twenty-two locations of

velocity measurement. It is found that the peak ground acceleration (PGA) ranges between 0.26g to 0.49g distributed within Dhaka Metropolis (Figure 11).

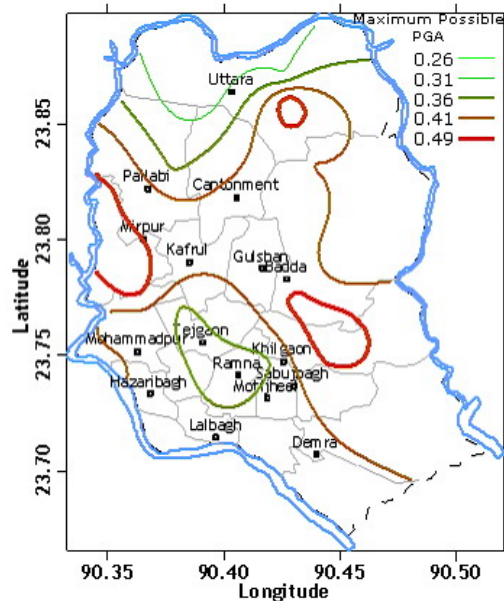


Figure 11: Peak Ground Acceleration (PGA) distribution of Dhaka metropolitan city.

Based on the lithological variations, velocity characterization, dominant frequency response, and 'g' value character, an earthquake damage vulnerability map of Dhaka city has been proposed (Fig. 12) dividing into three zones viz., High vulnerable, Intermediate vulnerable, and Low vulnerable respectively.

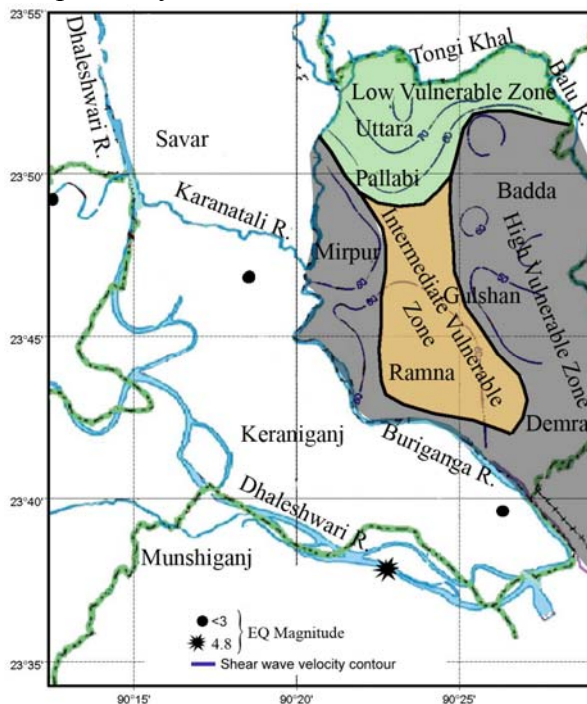


Figure 12: Earthquake damage vulnerable zones of Dhaka metropolitan city.

5. CONCLUSIONS AND RECOMMENDATIONS

Various geophysical techniques including shallow seismic velocity, resistivity CST, vertical electrical sounding (VES), borehole resistivity log, and litholog analysis are used to characterize the subsurface and to identify the earthquake hazard vulnerable zones in the Dhaka Metropolis. Electrical resistivity techniques (VES and CST) and the litholog correlation have enabled to infer near surface lithological variations. The eastern region covering Uttar Khan, Badda, Baridhara and Demra is characterized by dominantly clay and filled materials while the western region covering part of Mirpur, Mohammadpur, Shyamoli, Kallayanpur, Rayer Bazar, Pilkana, Hazaribagh is characterized by dominantly sand with considerable filled materials in the subsided near surface zones. The northern and central part is mostly covered by sand while in the southern part is covered by clay. Resistivity logs suggest that the central part of the investigated area is much more resistive than the eastern and western part of Dhaka metropolitan city. Subsurface correlation by profiling provides the evidences of lateral distribution pattern of lithology, tilting, faulting, incised channeling, and fills with variable saturation status. The high resistive layers characterize relatively dry zones of uplift and tilting. While, low resistive layers with greater saturation status characterize the zones of subsidence and both artificial and natural fills. VES, CST, and borehole resistivity in combination suggest subsidence and fills in the eastern and southern part, intense channeling and fills in the central part, and uplift in the northern and central part with several fault offsets viz., Turag-Tongi fault (19m), Dhaleshwari fault (16m), and Buriganga fault (18m).

The lithological character of the top layer both at the eastern and western part of the city is dominated by mud, clay and swamp deposits characterizing low shear-wave velocity and high particle velocity. The low ground frequency character both for eastern and western part of the city coincide well with the low shear-wave velocity zones resulting in low resonant length in these areas. Based on the subsurface lithological variations, velocity characterization, dominant frequency response, and 'g' value character, an earthquake hazard map of Dhaka city has been proposed dividing into three zones of earthquake damage vulnerability viz., High, Intermediate, and Low vulnerable zones respectively.

The study warrants more detailed investigations for active-fault identification and micro zoning.

REFERENCES

- Bolt, B. A., 1978. Earthquakes- A Primer. W. H. Freeman and Company, San Francisco. 241p.
- Caputo, R., Piscitellib, S., Olivetoc, A., Rizzob, E., and Lapennab, V., 2003. The use of electrical resistivity tomographies in active tectonics: examples from the Tyrnavos Basin, Greece. *Journal of Geodynamics*, Pergamon, v. 36, p. 19–35.

- Herrick, D.C., and Kenedy, W. D., 1994. Electrical efficiency – a pore geometry theory for interpreting the electrical properties of reservoir rocks. *Geophysics*, v. 59(6), p. 918-927.
- Khan, A. A., Akhter, S. H., and Alam, S. M. M. 2000. Evidence of Holocene transgression, dolomitization and the source of arsenic in the Bengal delta, In: A.M.O. Mohamed & K. I. Al Hosani (Edts.), *Geoengineering in Arid Lands*. Balkema Publication, Rotterdam, p. 351 – 355.
- Khan, A. A. and Hossain, M. S., 2005. Recurrence of 1885 Bengal Earthquake and hazard vulnerability status of Dhaka Metropolitan City, Bangladesh. *Oriental Geographer*, v.49 (2), p.205-216.
- Khan, A. A. 2005. Paleoseismicity, characterization of active faults and fault rupture recurrence in Bangladesh. Proc. 1Pst Bangladesh Earthq. Symp., Bangladesh Earthquake Society, p. 63-70.
- Khandoker, R. A., 1987. Orogen of Barind-Madhupur elevated areas, Bengal basin-results of neotectonic activities. *Bang. Jour. Geol.*, v.6, p.1-7.
- Telford, W. M., Geldart, L. P., Sheriff, R. E., and Keys, D. A., 1976. *Applied Geophysics*. Cambridge University Press, Cambridge. 860p.

ESTIMATION OF RISK DUE TO EARTHQUAKE HAZARD IN AP, INDIA AN IT BASED APPROACH

MD. ZIYA UR RAHMAN SIDDIQUI
Graduate Student
Computer Aided Structural Engineering
IIIT Hyderabad, India
Siddiqui@students.iit.ac.in

RANJEET JOSHI¹,
RAMANCHARLA PRADEEP KUMAR²
Earthquake Engineering Research Centre
IIIT Hyderabad

ABSTRACT

This paper describes the procedure of vulnerability assessment for building structures in AP India. The objective of this paper is to define the building classification and development of damage probability matrix using fragility curve parameters of the building structures in Andhra Pradesh (AP) by using the available information in Vulnerability Atlas of India, developed by Building Materials & Technology Promotion council Govt. of India (BMTPC). The organization of this paper is as follows. First, the types of the structures in AP are reviewed and a classification based on the available data with Vulnerability Atlas of India. Second, the description of methodologies developed under various organizations is studied, adopted and summarized. Third, the theoretical methodology of the vulnerability analysis using fragility curves parameters given by HAZUS and capacity curve generated using SAP2000 for typical building structure are presented.

Key words: HAZUS methodology, capacity curve, fragility curve, damage probability matrix.

1. INTRODUCTION

India is always vulnerable to multiple hazards. Whether they are earthquakes, floods, cyclones or droughts, every year significant losses can be observed in either of the forms. Andhra Pradesh lies in central part of the peninsular Indian shield and long considered to be a seismically passive area, But after the Jabalpur (1997), Latur (1993), and Koyna (1967) earthquakes now its seismicity is questionable and few zones with reactivated faults in the crustal layers of this region have been detected. Government of Andhra Pradesh designed the Andhra Pradesh Hazard Mitigation (APHM) and Emergency Cyclone Recovery Project (ECRP) under financial help from World Bank to mitigate hazards, preparedness and to develop good

management and technical level mechanism for effective response in Andhra Pradesh.

1.1 Earthquake risk

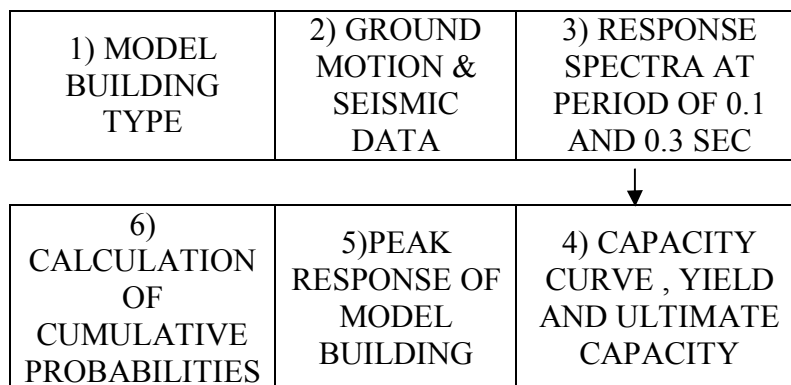
Earthquake Risk gives an estimate of damage and loss due to earthquakes. Earthquake risk can be defined in terms of three prime factors as given below:

$$\text{Earthquake Risk} = \text{Vulnerability} \times \text{Hazard} \times \text{Exposure time} \quad (1)$$

Vulnerability is one of the main factor in defining risk and it is defined as the degree to which a system is susceptible or unable to cope with adverse effect of climate change. It is more important to study and evaluate vulnerability of areas occupied by weak infrastructure system in a highly seismically active area and find out expected damage losses during earthquake. Vulnerability assessment of such seismically active area helps local authorities in proper disaster management.

2. METHODOLOGY

There are several risk assessment tools proposed by different countries and organizations like HAZUS (USA), TELES (Taiwan), RADIUS (UN) based on inventory data and inputs through GIS engine to produce result for different disaster. One of the major components of the methodology is extensive database. An inventory is made up of general building stock and groups of building with specific characteristics. The main aim of making inventory of building is for classification of building in different group with similar characteristics. The classification of building based on the construction type, material type, and structural type, buildings are classified into five categories such as wood framing, steel framing, concrete framing, reinforced concrete framing, and unreinforced concrete framing. These structure frames are further classified to different structural classes based on their material used and structural design. Figure 1 shows the methodology of earthquake loss estimation adopted by HAZUS. This methodology is divided in seven steps from input requirement to the development of Damage Probability Matrix.



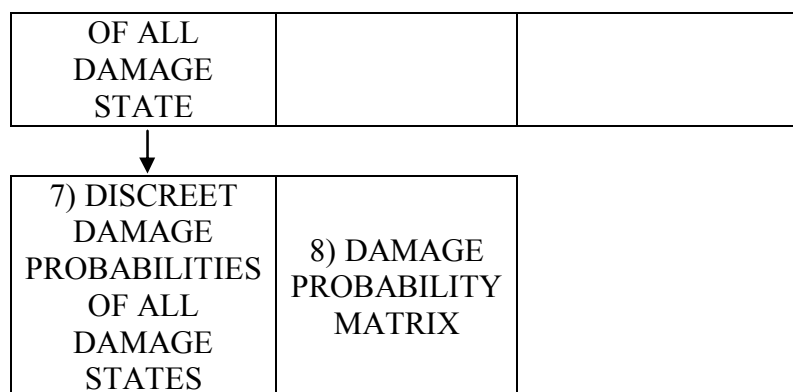


Figure 1: flow diagram of HAZUS methodology

3. BUILDING CLASSIFICATION

Based on the available data with Vulnerability Atlas of India (VAI, BMTPC Govt. of India) classification is developed and used in the development of Damage probability Matrix for a particular model type. The classification is available with VAI is as follows:

Category-A: Buildings in fieldstone, rural structures, un-burnt brick houses, clay houses

Category-B: ordinary brick buildings, building of the large block and prefabricated type, half-timbered structures, building in natural hewn stone.

Category-C: reinforced building, well built wooden structures

Category-X: other types not covered in A, B, C. these are generally light

Buildings are classified based on structural characteristics like number of stories, low-rise (1-3 stories), Mid-rise (4-7 stories) and High-rise (8+ stories) and material type: steel frame, concrete frame, brick masonry burned and unburned, stone masonry and mud wall. Figure 2 shows tow types of buildings.

A total of 10 classes of buildings are defined in Table 1 below.

Table 1: classification based on material and storey height
(Wen-I L, Chin-hsiung L 2006, HAZUS-MH 2003)

Description	Label	Low	Mid	High
Steel moment frame (Steel braced frame)	SL	1-3	4-7	8+
Steel light frame	SL2	1-3	-	-
Concrete moment frame	CM	1-3	4-7	8+
Precast concrete frame	PC	1-3	-	-
Reinforced masonry wall	RM	1-3	4-7	-
Unreinforced masonry wall	URM	1-2	-	-
Steel reinforced concrete frame	SRC	1-3	4-7	8+
Mud wall	M	1	-	-
Wood wall	W	1-2	-	-
GI and other metal sheets, bamboo etc.	X	1	-	-

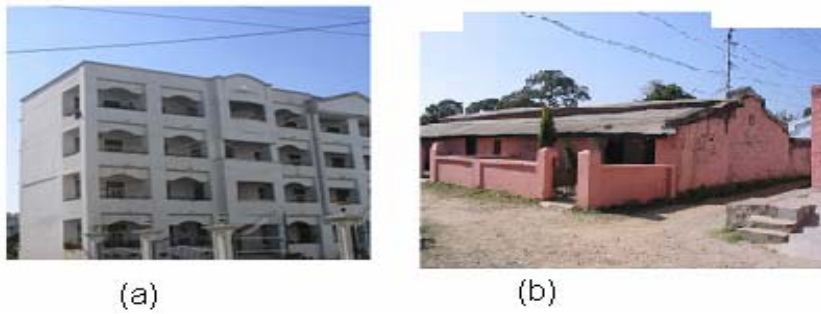


Figure 2: (a) Example of RM (Mid-Rise) and (b) is an example of URM (Low-Rise)

4. RESPONSE CURVE AND CAPACITY CURVE

The building performance (peak response) for particular ground motion is determined by intersection of capacity curve of building and seismic response spectrum, the standardized response spectrum shape as given in IBC 2006 (SELENA V2.0, 2007), which consist of four parts, peak ground acceleration, region of constant spectral acceleration at period of zero second to TAV, a region of constant spectral velocity between period TAV to TVD and region of constant spectral displacement for period of TVD and beyond. The region of constant acceleration is defined by Sa at 0.3 s (Sa@0.3). The region of constant spectral velocity is defined by Sa is proportional to 1/T and Sa at 1 s (Sa@1).

In general, the elastic design spectrum is defined by following equations:

$$Sa(T) = Sa@0.3 (0.4 + 0.6 T/T_A) \quad \text{if } 0 < T < T_A \quad (2)$$

$$Sa(T) = Sa@0.3 \quad \text{if } T_A < T < T_{AV} \quad (3)$$

$$Sa(T) = Sa@1.0/T \quad \text{if } T_{AV} < T < T_{VD} \quad (4)$$

$$Sa(T) = Sa@1.0/T * T \quad \text{if } T_{VD} < T < 10 \text{ s} \quad (5)$$

The value of TAV is based on intersection of spectral acceleration and velocity:

$$T_{AV} = Sa@1.0 / Sa@0.3 \quad (6)$$

$$T_A = 0.2 T_{AV} = 0.2 (Sa@1.0 / Sa@0.3) \quad (7)$$

The period TVD is based on the reciprocal of corner frequency (fc) this frequency is estimated by using Joyner and Boore relationship (SELENA v2.0, 2007) as a function of Moment magnitude:

$$T_{VD} = 1/f_c = 10^{[(M-5)/2]} \quad (8)$$

In order to be able to describe the elastic design spectra (for rock: site class B) in that case only PGA is give the following expression have to be used:

$$Sa@0.3 = S_{AS} = 2.5 \text{ PGA} \quad (9)$$

$$Sa@1.0 = S_{AL} = \text{PGA} \quad (10)$$

In account of amplification of ground shaking multiply amplification factor to PGA:

$$PGA_i = \text{PGA} \cdot FA_i \quad (11)$$

The construction of demand spectra including soil effect can be calculated by using following expression:

$SAS_i = SAS \cdot FA_i$ for short period amplification factor (FA_i) for site class i .

$SAL_i = SAL \cdot FV_i$ for long period amplification factor (FV_i) for site class i .

While the period T_{AV} , which defines the transition period from constant spectral acceleration to constant spectral velocity is a function of the site class. It can be determined by the following equation:

$$T_{AV_i} = \{ S_{AL} / S_{AS} \} \{ F_{V_i} / F_{A_i} \} \quad (12)$$

4.1 Capacity curve

The building capacity curve is also known as push-over curve based on engineering designed parameter and nonlinear elastic analysis method which gives accurate estimation of building displacement. The capacity curve of building construct under three control points the design capacity, the yield capacity and ultimate capacity. The design capacity represent nominal building strength, the yield capacity represent lateral strength and the ultimate capacity represent maximum strength of the building. The capacity curve represents characteristics of the structure, which is a plot of lateral resistance of building to the lateral displacement. For this study development of building capacity curve for a model of concrete structure is created by using SAP 2000 analysis program.

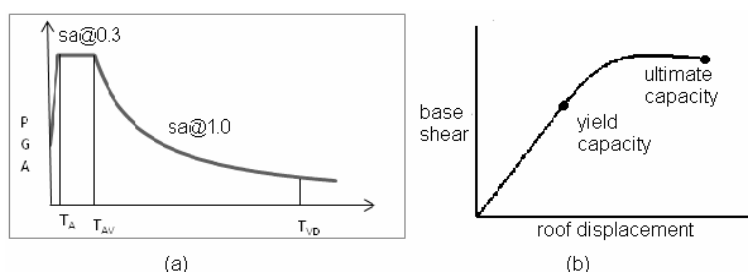


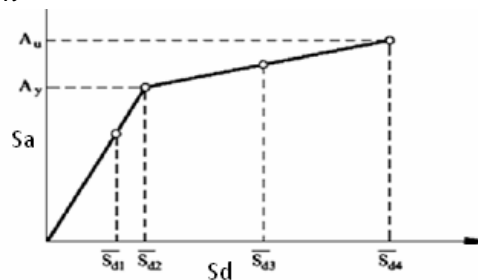
Figure 3: (a): Standard shape of response spectrum (b) example of capacity curve for concrete structure.

5. DEFINATION OF DAMAGE STATES

The peak building response is taken from the interaction of capacity curve and demand curve at the building location. The peak building response either spectral displacement or spectral acceleration at the point of interaction is used as parameter with fragility curve to estimate the damage state probabilities. The method adopted by HAZUS and in this study, damage states are divided in four classes as shown in Table 2.

Table 2: damage states thresholds defines with the agreement of capacity spectrum

Sd1 = 0.7Dy	Slight
Sd2 = Dy	Moderate
Sd3 = Dy+0.25(Du-Dy)	Extensive
Sd4 = Du	Complete



Where,

Sd is spectral displacement and suffix 1, 2, 3, 4 show slight damage, moderate damage, extensive damage, and complete collapse respectively.

Ay = yield spectral acceleration

Au = ultimate spectral acceleration.

Dy = yield spectral displacement

Du = ultimate spectral displacement.

6. CUMULATIVE DAMAGE PROBABILITIES

For a given damage state, P [S | Sd], P [M | Sd], P [E | Sd], P [C | Sd] a fragility curve is well described by the following lognormal probability density function Barbat et al, (2002), HAZUS (2003).

$$P[ds|Sd] = \Phi \left[\frac{1}{\beta_{ds}} \ln \left\{ \frac{Sd}{S_{d,ds}} \right\} \right] \tag{13}$$

Where $S_{d,ds}$ is the threshold spectral displacement, β_{ds} is the standard deviation of the natural logarithm of this spectral displacement

Table2 shows how the threshold $S_{d,ds}$ obtain from capacity spectrum, Φ is the standard normal cumulative distribution function and Sd is the spectral displacement of the structure.

Where,

P [S | Sd] = probability of being in or exceeding a slight damage state, S.

P [M | Sd] = probability of being in or exceeding a moderate damage state, M.

$P [E | S_d]$ = probability of being in or exceeding an extensive damage state, E.

$P [C | S_d]$ = probability of being in or exceeding a complete damage state, C.

Fragility curve Figure 4 which shows the probability of exceeding or being in for expected spectral displacement (obtain from performance point) for all damage states.

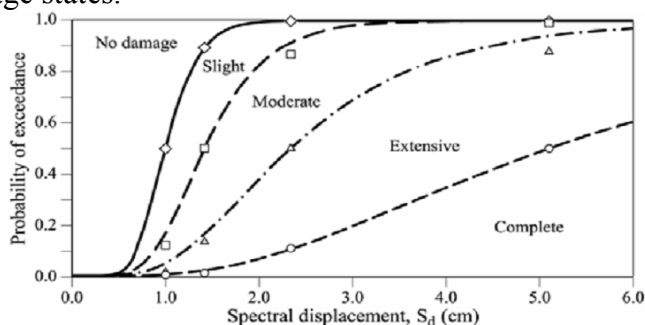


Figure 4: shows example of fragility curves

Discrete damage probabilities can be calculated as follows:

Probability of complete damage, $P [C] = P [C | S_d]$

Probability of extensive damage, $P [E] = P [E | S_d] - P [C | S_d]$

Probability of moderate damage, $P [M] = P [M | S_d] - P [E | S_d]$

Probability of slight damage, $P [S] = P [S | S_d] - P [M | S_d]$

Probability of no damage, $P [None] = 1 - P [S | S_d]$ (14)

7. EXAMPLE PROBLEM OF RM (LOW-RISE) STRUCTURE

7.1 Generation of elastic demand spectra (SELENA v2.0, 2007):

Demand spectra for NEHRP site classes B (rock site), PGA for rock site conditions $PGA_B = 0.2 g$

Step1) calculation of spectral acceleration at $T= 0.3s$ and $T= 1.0s$, According to equations (9) & (10):

$$Sa@0.3 = S_{AS} = 0.5g$$

$$Sa@1.0 = S_{AI} = 0.2g$$

Step2) site amplification factor for site given by IBC-2006 (SELENA V2.0, 2007)

Table 3: site amplification factor

Site amplification factor = $S_{AS} = 0.5g, S_{AI} = 0.2g$	Site class B
F_A	1.0
F_V	1.0

Step3) calculation of short period and long period spectral accelerations as well as Transition period

Table 4: show calculated value of short and long period acceleration

Parameter	Class B
$PGA_i = PGA \cdot F_{Ai}$	0.2
$S_{ASi} = S_{AS} \cdot F_{Ai}$	0.5
$S_{AVi} = S_{AV} \cdot F_{Vi}$	0.2
$T_{AVi} = \{ S_{AV} / S_{AS} \} \{ F_{Vi} / F_{Ai} \}$	0.4
$T_A = 0.2 T_{AV}$	0.08

Step4) Generation of elastic demand spectrum (damping $\xi = 5\%$)

For the evaluation of structural damage it is more convenient to plot the acceleration response spectrum as a function of the spectral displacement. This could be achieved due to the relation between the different spectral parameters:

$$S_d = S_a \cdot g \cdot T \cdot T / 4 \pi \cdot \pi \quad (15)$$

Figure 5 (a) shows demand spectrum and Figure (b) shows demand spectrum as a function of spectral displacement, values along abscissa of spectral displacement is calculated by using equation (14), these curve are plotted by using MS-Excel software.

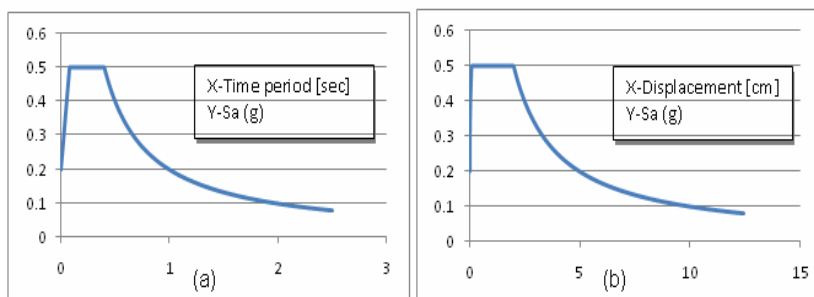


Figure 5: (a) demand spectrum (b) demand spectrum as a function of the spectral displacement

7.2 Generation of capacity curve using SAP2000:

For a low-rise reinforced concrete (RM) structure pushover analysis is carried out. Following are the details of the structure.

- Grade of Concrete is 25 Mpa
- Grade of steel is 415 Mpa
- Slab thickness 100mm
- Column 450 X 300mm, Beam 350X250mm
- Live load 4kN/m², storey height 3m

Figure 6(a) shows result of pushover analysis using SAP2000 for a structure in the form of capacity curve. The values of yield acceleration,

ultimate acceleration, yield spectral displacement and ultimate spectral displacement are given in the Table 5 which can be read directly from capacity curve. Figure 7 is a plot describes intersection of capacity curve and demand spectrum, the corresponding value of spectral displacement at the intersection point is a performance point (peak response) of the structure and peak response for taken RM (Low-Rise) structure is given in Table 6.

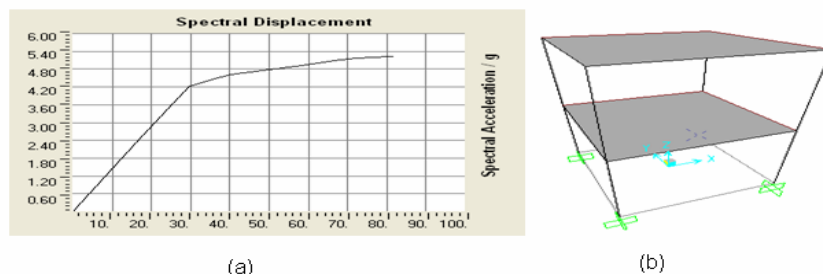


Figure 6: a) capacity curve b) Example of RM (L) structure generated in SAP2000

Table 5: yield and ultimate values from capacity curve for RM (L)

Yield capacity		Ultimate capacity	
Dy cm	Ay (g)	Du cm	Au (g)
2.9	0.42	8.18	0.53

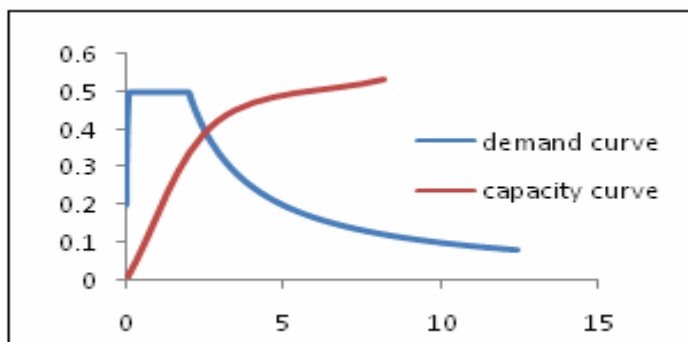


Figure 7: Intersection of capacity curve and demand curve

Table 6: peak building response from intersection of demand and capacity curve

Peak building response in cm	
Model building RM (L)	Reinforced concrete structure
Sd (cm)	3 cm

7.3 Calculation for cumulative damage probability:

According to equation 13 For a given damage state, $P [S | S_d]$, $P [M | S_d]$, $P [E | S_d]$, $P [C | S_d]$ $S_{d,d}$ is the threshold spectral displacement,

Table 2 shows how the threshold $S_{d,ds}$ obtain from capacity spectrum (Barbat et al 2002) and β_{ds} is the lognormal standard deviation parameter that describes the total variability of damage state (HAZUS 2003), Table 7 show the values of $S_{d,ds}$ and β_{ds} for each damage state, values of β_{ds} taken from HAZUS in this study.

Table7: Parameter for fragility curve defined by HAZUS for RM (L) type model building

	Slight		Moderate		Extensive		Complete	
Type	$S_{d,ds}$	β_s	$S_{d,ds}$	β_M	$S_{d,ds}$	β_E	$S_{d,ds}$	β_C
RM(low-rise)	4.872	1.05	6.96	1.07	10.128	1.09	19.63	0.91

Table 8 shows calculation of probability of being in or exceeding damage states by using equation 13, and the discreet damage probabilities is calculated by using equations (14) and it is represented in Table 9

Table 8: calculation of cumulative probabilities of RM (L)

Damage state	Sd	$S_{d,ds}$	β_{ds}	X Sd/ $S_{d,ds}$	ln(x)	y ln(x)/ β_{ds}	$\Phi[y]$
Slight	7.5	4.872	1.05	1.53	0.42	0.40	0.6554
Moderate	7.5	6.96	1.07	1.07	0.06	0.05	0.5199
Extensive	7.5	10.128	1.09	0.74	-0.30	-0.27	0.3859
Complete	7.5	19.63	0.91	0.38	-0.96	-1.06	0.1446

Table 9: damage probability matrix for RM (L)

Damage probability Matrix for RM(L)				
Model type	Slight P[S]	Moderate P[M]	Extensive P[E]	Complete P[C]
RM(L)	0.1355	0.1340	0.2413	0.1446

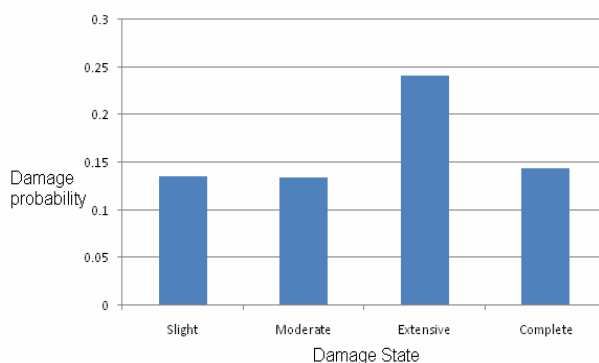


Figure 8: damage probability graph of RM (L) building type

The Figure 8 represents the discrete damage probabilities of class RM (Low-rise) for all damage states calculated by method explained above and shows Structure is more vulnerable to Extensive damage and less vulnerable

to Moderate damage for a generated response spectrum of $PGA = 0.2g$ for site class B (rock site).

8. CONCLUSIONS

The efforts applied to compute the Damage Probability Matrix for a given building type is with the objective to develop a tool or a computer based program which provides assessment of risk due to earthquake for an area like Andhra Pradesh or any other part of the country.

The next objective is generation of capacity parameters for all building types, development of more distinct classification based on seismic design level and probability matrices for collective numbers of buildings.

The last step of the project will be development of user interface by using programming language like C# or Visual Basic, and the expected time to complete the project is within the next 3 months.

REFERENCES

- Wen-I L, Chin-hsiung L 2006. *Study on the fragility of building structures in Taiwan*, Natural Hazards (2006) 37:55-69, National university of Kaohsiung.
- Ggulati. B 2006. *Earthquake assessment of buildings: applicability of HAZUS in Dehradun, India*. Unpublished report, Indian institute of remote sensing, Dehradun, India.
- Barbat A. H, Lagomarsino S, Pujades L.G. 2002. *Vulnerability assessment of dwelling buildings*. projects: REN 2001-2418-C04-01 and REN2002-03365/RIES Universitat Politècnica de Catalunya, Barcelona, Spain, University of Genoa, Genoa, Italy.
- HAZUS-MH 2003. *Advance engineering building module*. Report by: Department of Homeland Security Emergency Preparedness and Response Directorate FEMA Mitigation Division Washington, D.C.
- SELENA v2.0 2007. *seismic loss Estimation using a logic tree approach*. prepared by Sergio Molina-Palacios, Dominik H. Lang, and Conrad D. Lindholm at NORSAR Kjeller, Norway.
- Vulnerability Atlas of India (2007), Building Materials & Technology Promotion council Govt. of India.
- International Code Council (2006). *International Building Code (IBC-2006)*. United States, January 2006, 664 pp.
- Joyner, W.B. and Boore, D.M. (1988). *Measurement Characterization and Prediction of Strong Ground Motion*. Proc. of Earthquake Engineering and Soil Dynamics II, 43–102. Park City, Utah, 27 June 1988. New York: Geotechnical Division of the American Society of Civil Engineers

MODEL TESTS MEASURING EARTH PRESSURE ACTING ON BURIED STRUCTURE DUE TO DIFFERENTIAL SETTLEMENT

REIKO KUWANO

International Centre for Urban Safety Engineering,
Institute of Industrial Science, The university of Tokyo, Japan
kuwano@iis.u-tokyo.ac.jp

TOSHIYUKI HORII

Wakachiku Construction Co. Ltd., Japan
toshiyuki.horii@wakachiku.co.jp

HIDETOSHI KOHASHI

Material and Geotechnical Engineering Research Group,
Public Works Research Institute, Japan
kohashi@pwri.go.jp

ABSTRACT

A series of trap door tests was conducted to evaluate the change in earth pressures acting on a buried structure in a high embankment due to differential settlements. A model structure, box or pipe, was placed on the centre of a soil chamber having movable base platens at both sides. Differential settlements were given by moving the base platens down simultaneously.

It was found that the size, shape and burial depth of a buried structure and mechanical properties of backfill soil are governing factors for the increment of vertical earth pressure at the top of the structure, while the construction/settlement history showed only minor effects. Even a simple calculation, where the friction forces generated between the soil mass above the structure and surrounding soil are taken into account, can offer reasonable estimation for the increment of earth pressure.

1. INTRODUCTION

Earth pressures acting on underground structures are highly dependent on the interaction between ground and structure. Increase in the vertical earth pressures acting on a buried structure in high embankment should be, therefore, considered, depending on the size and depth of structure and type of foundation, since differential settlements are often expected in such conditions. However, in practice, the increment of vertical earth pressures on underground structures is estimated in the empirical manner, mainly based on the information of past earth pressure measurements in the limited number of sites (see for example General guidelines for road earthworks,

1999). In such estimation, the degree of settlement and/or mechanical properties of backfill materials are not always taken into account.

In this study, a series of trap door tests was conducted to see how differential settlements affect on earth pressures acting on a buried structure in sandy soil.

2. APPARATUS AND TEST PROCEDURE

Figure 1 schematically shows a model ground including a soil chamber, a buried model structure and the locations of earth pressure transducers. The soil chamber is 100cm wide, 60cm long and 60cm deep. The base of the chamber is separated into 3 platens. The centre base platen is fixed, on which a rigid box/pipe structure was placed, while both side platens can move down simultaneously. Earth pressure transducers were directly attached on top and sides of the model structure, and the center of moving base platens.

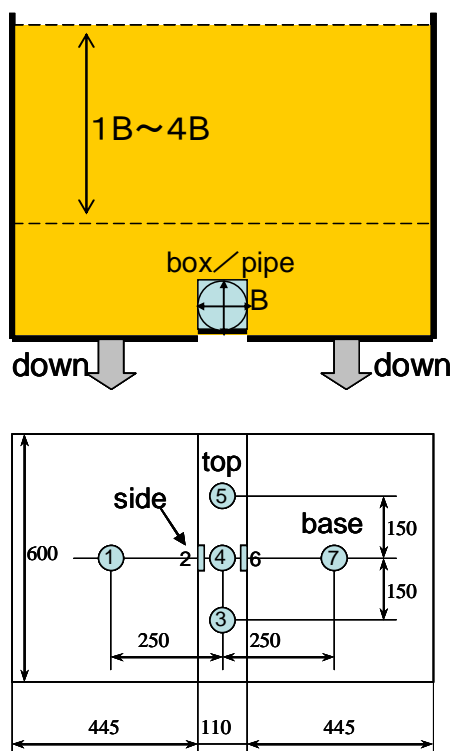


Figure 1: A soil chamber having separated moving base platens and location of earth pressure transducers.

Toyoura sand and sand with fines were used for the material of model ground. Each sand was compacted at the relative density of approximately 80% in layers of 2.5cm, up to the specified height. Soil cover was varied from 11cm to 44cm, i.e. 1B to 4B, where B is the width (and in this case also the height) of the buried structure. A downward movement of moving base platens was given at a displacement rate of 0.1mm/min up to

approximately 1mm. The measurements were continued up to at least 20 minutes after the movement of base platen was completed. Test cases and conditions are shown in Table 1.

Table 1: Test conditions.

Model Ground	Soil cover (cm)	Test Case	Type of Model Structure	Case No.
Sand $\rho_d: 1.57\text{g/cm}^3$	44	1 stage test; Downward moving of base platen by 1mm with soil cover of 44cm	Box	X1
			Pipe	P1
	11, 22, 33, 44	4 stage test; Downward moving of base platen by 1mm for each stage. Soil cover for the 1 st stage was 11cm, then backfilling to 22cm, 33cm and 44cm (displacement of 4mm in total)	Box	X2
			Pipe	P2
Sand +Fines 20% $\rho_d: 1.53\text{g/cm}^3$	44	1 stage test	Box	X3
			Pipe	P3
	11, 22, 33, 44	4 stage test	Box	X4
			Pipe	P4

3. TEST RESULTS

3.1 Change in earth pressures with settlements of surrounding ground

Relationships between displacements of moving base platen and earth pressures at three locations in test Case X1 and P1 are shown in Figure 2. Measured values from pressure transducers No.1 and 7, No.2 and 6, and No.3 to 5 are averaged and shown as pressures at “base”, “side”, and “top”, respectively. Overburden pressures calculated from depths of pressure transducers (55cm for base, 44cm for top) are also shown in broken lines.

In case X1, with settlements of surrounding ground, the earth pressure acting on the top increased, while the base pressure decreased. The value of “top” pressure doubled at a displacement of 0.3mm, then gradually increased up to 2.4 times of the initial value at a displacement of 0.9mm. The horizontal earth pressure acting on the side of the box, initially about a half of overburden pressure, showed marginally increase as the surrounding ground settled. Similar trend was observed in Case P1, except that pressure change at top was larger than those in case X1, possibly due to an effect of stress concentration caused by its convex shape.

(Box)

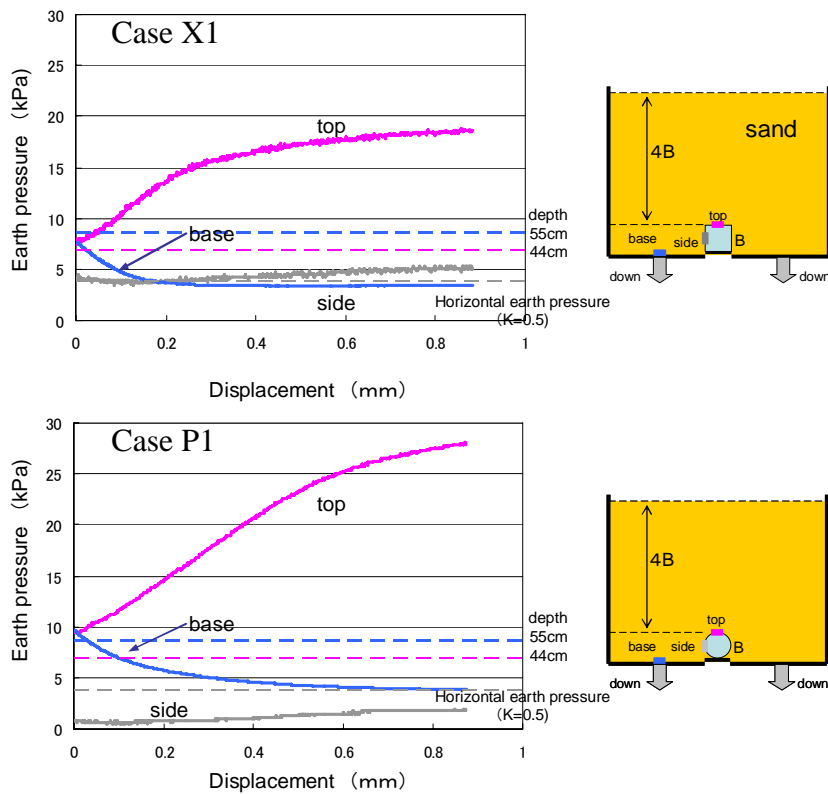


Figure 2: Change in earth pressures during a downward movement of base platens (Case X1 & P1)

3.2 Effects of construction/settlement history

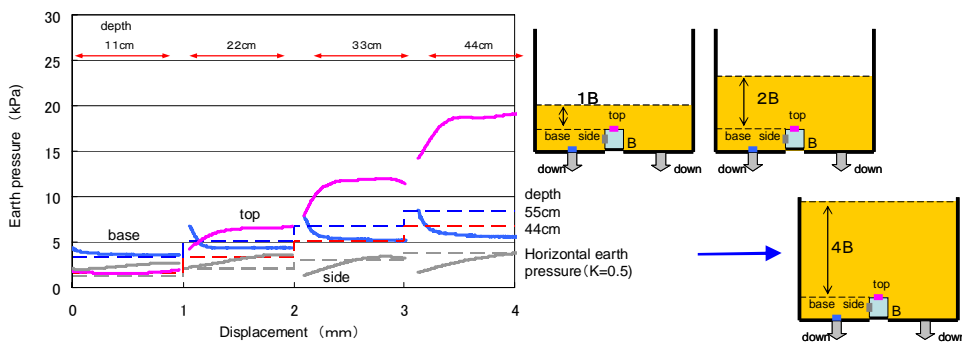


Figure 3: Changes in earth pressures during 4 stages of moving base platens descent (Case X2)

Changes in earth pressures in Case X2 are shown in Figure 3. In this case, the model ground was constructed at four stages. At the beginning, a soil cover was constructed to be 11cm, 1B (where B is the width/height of the box). A displacement of 1mm was given, then the next construction, backfilling up to a soil cover of 2B, was made. Test was conducted at soil depths of 1B, 2B, 3B and 4B in the same manner. Overall displacements were, therefore, 4mm. In this 4-stage test, as shown in Figure 3, the same

trend, increase in “top” and “side” pressures and decrease in “base” pressures are seen at all the stages.

Figure 4 shows change in ratios of “top” pressures during and the beginning of stage (before a descent of moving platens). Except for the step 1, the final increase ratios are about 1.3 to 1.5. Most of the earth pressure increase was generated within a displacement of 0.2 to 0.3mm.

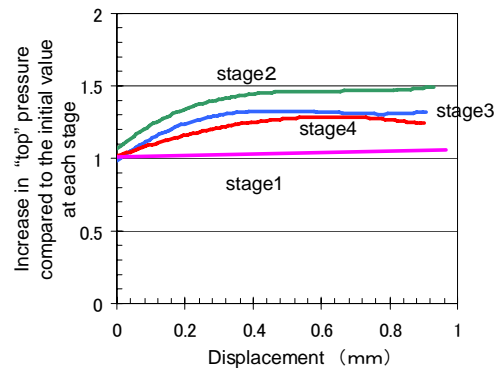


Figure 4: Changes in “top” pressures compared to the initial values at each stage (Case X2)

3.3 Effects of backfill soil

The test results of Case X3 are shown in Figure 5, in which the model ground was made of sand with 20% fines content. The change of earth pressures was far moderate and gradual compared to that in Cases with Toyoura sand. The final increase in “top” pressure was about 1.5 times of the overburden pressure.

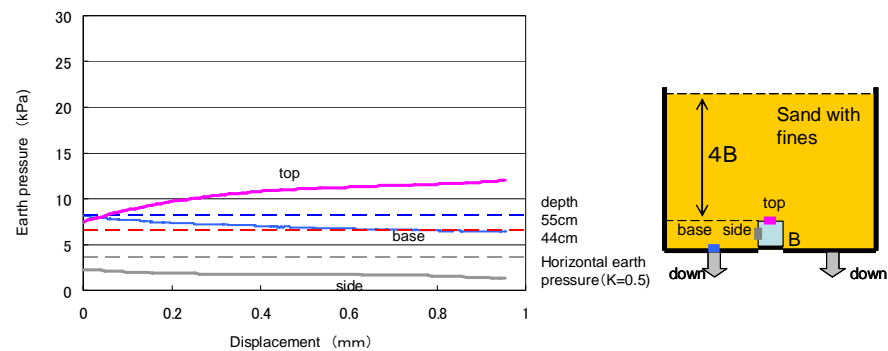


Figure 5: Changes in earth pressures during a descent of moving base platens (Case X3)

3.4 Increase in pressure acting on top of the box

Variations of ratios of “top” pressures to overburden pressures for box and pipe structures are plotted against displacements of a base platen in Figure 6.

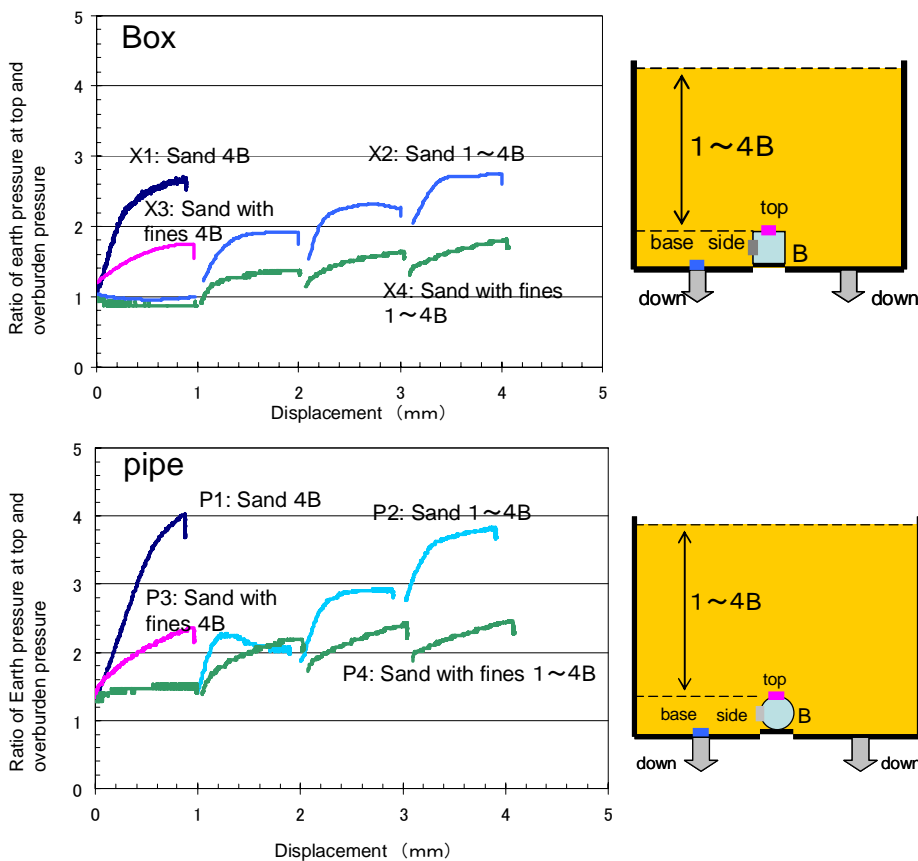


Figure 6: Ratios of "top" pressures and overburden pressures

For all the cases, there was small decrease in ratios during at least 20 minutes resting time after a displacement of 1mm was given, due to the stress relaxation. For Cases X2, X4, P2 and P4, plotted curves are discontinuous between stages. As the backfilling progressed, the ratios automatically decreased due to the increase of depth.

The figure indicates that the governing factors for the increase of earth pressure acting on a buried structure are;

- a) Depth of a buried structure
- b) Mechanical properties of backfill soil, and
- c) Relative displacement between soil and structure. On the other hand, construction and/or displacement history appeared to have an only minor effect, as the final values of ratios are similar between 1 stage test and corresponding 4 stage test. Increase in earth pressure at top for pipe structure was distinctively large compared to that for box possibly because of stress concentration.

4. ESTIMATION OF EARTH PRESSURE INCREMENT

Change in the distribution of earth pressures due to a displacement of moving platens is calculated, based on the simple assumption that the soil

mass above the buried structure is pulled down due to the downward frictions acting on the boundary by the surrounding soil, as shown in Figure 7.

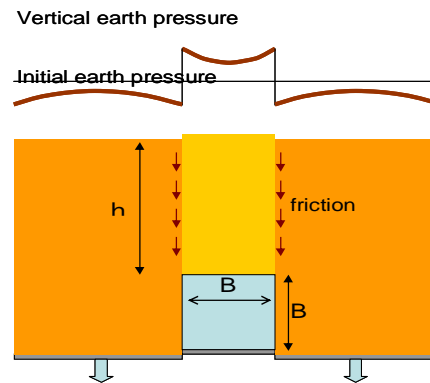


Figure 7: Earth pressure distribution during a movement of base platens for a buried box structure

When a depth of the structure is h , the friction force for both sides per unit length, F , is;

$$F = 2 \times \int_0^h K \gamma z \tan \phi \cdot dz = K \gamma h^2 \tan \phi \quad (1)$$

where K is earth pressure coefficient, γ is unit weight of soil, and ϕ is angle of shear resistance. A ratio of “top” pressure and overburden pressure, α , is;

$$\alpha = \frac{B \gamma h + F}{B \gamma h} = 1 + \frac{K h \tan \phi}{B} \quad (2)$$

where B is a width of a box.

Here, although the vertical pressure at a depth of z is simply estimated to be γz , the vertical earth pressure during a descent of moving platens varies especially around the box. Kikumoto et al. (2005) estimated the distribution of vertical earth pressures for trap door testing based on Terzaghi’s theory. The distribution of earth pressures for this test series should be analogous and schematically shown in Figure 8. Yoshimmaru et al. (2006) performed numerical simulation for the earth pressures acting on a buried box, showing that the vertical earth pressure just above and vicinity of a box increase as a result of the settlement of soil surrounding a box. In this study, the value of K was tentatively chosen to be 0.6, considering the fact that the “side” pressure increased a little during a descent. In reality, the distribution of earth pressure on a box is not necessarily uniform, yet the value of α calculated from the equation (2) is the average pressure. The factor of structure’s shape, β , is therefore introduced, as shown in equation (3), in the calculation of “top” pressure, considering the non-uniform distribution of earth pressure. The value of β would be larger for a buried pipe, and smaller for a box with the larger width.

$$\alpha = \beta \left(1 + \frac{K h \tan \phi}{B} \right) \quad (3)$$

Estimated values of α are presented in Figure 8. Parameters for the calculation are given in Table 2.

Table 2: Parameters for the estimation of earth pressure increase

	Sand	Sand with fines	Box (B×B)	Pipe
Angle of shear resistance, ϕ	35°	20°		
Earth pressure coefficient, K	0.6			
Effect of shape, β			1.0	1.3

The value of ϕ for sand with fines is an only tentative estimation.

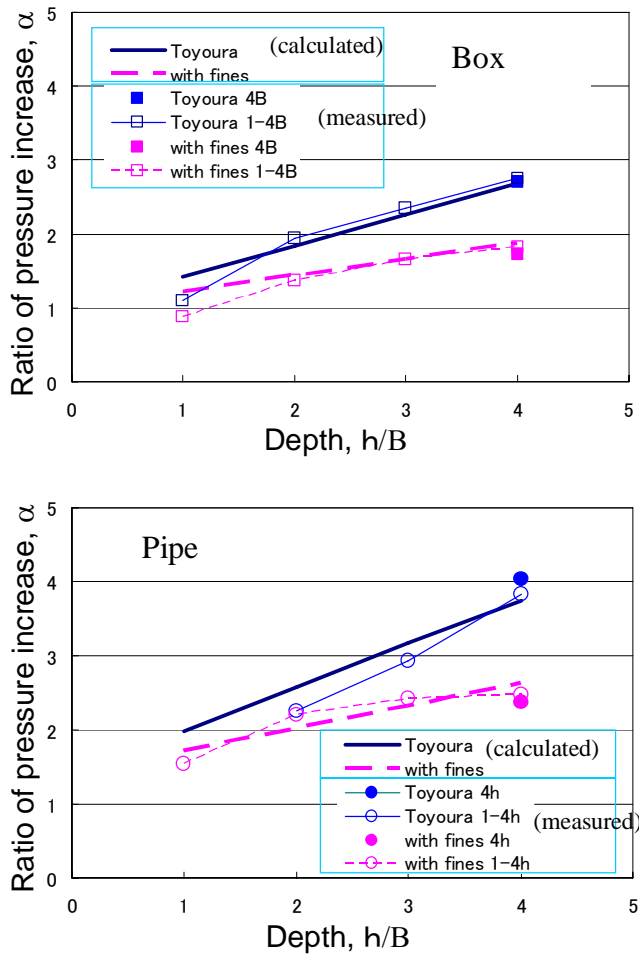


Figure 8: Ratio of “top” pressures and over burden pressures, comparison between the estimation and experiment.

The evaluation of earth pressures acting on buried structures are, when the differential settlement occurs, generally not so easy, as the structure and surrounding soil are subjected to complicated phenomena, like ground arching, soil-structure interaction, and so on. But even a simple calculation adopted in this study can give approximately reasonable values. Besides the continuous effort for accumulating field data, a theoretical approach should be also considered to improve the estimation.

5. SUMMARY

In order to evaluate the increase in vertical earth pressures acting on a buried structure due to the differential settlements, such as a box culvert or a buried pipe in high embankment, a series of trap door tests was conducted. The following tentative conclusions has been obtained so far;

- An increase in vertical earth pressures on a structure is affected by a depth of a buried structure, mechanical properties of soil, and possibly the shape of structure. Mechanical properties of backfill materials are not taken into account in the current empirical estimation in practice.
- Construction and/or settlement history has little effect.
- Increments of vertical pressures obtained in series of experiment can be roughly simulated by the simple calculation, where the friction forces generated between the soil mass above the structure and surrounding soil are taken into account.

REFERENCES

- General guidelines for road earthworks - culvert work -*, 1999. Japan road association, ISBN 978-4889504101, Maruzen Print Co. Ltd. (in Japanese).
- Kikumoto, M., Kishida, K., Kimura, M. and Tamura, T., 2005. Formula for calculating the distributions of vertical earth pressures around a tunnel, the 40th domestic conference of geotechnical engineering, *Proceedings of the 40th annual conference*, Japanese Geotechnical Society, Hakodate, July 2005, Paper No. 918. (in Japanese).
- Yoshimaru, T., Sakajo, S., and Nishioka, T., 2006. Numerical analysis of earth pressure acting to the embedded box tunnel, the 41st domestic conference of geotechnical engineering, *Proceedings of the 41st annual conference*, Japanese Geotechnical Society, Kagoshima, July 2006, Paper No. 876. (in Japanese)

LANDSLIDE HAZARD ANALYSIS FOR URBAN AREA USING RASTER DATA SET

MD. ZAHID HASAN SIDDIQUEE
Research Assistant
Dept. of Civil Engineering, BUET
zh027@yahoo.com

MOSUR AHMED
Stereo Manager, Decode Limited
Dhaka, Bangladesh

RUBEL DAS
Research Assistant
Dept. of Civil Engineering, BUET

ABSTRACT

Landslide is one of the deadliest natural calamities that can play havoc on the lives and resources. The intensity is always higher in urban areas than that of counter parts because of higher population densities and man made structures. Countries like Philippines (17th February, 2006) and Bangladesh (11th June, 2007) have experienced some of the serious landslides recently. Many other cities in Asia have also potential threat for landslides. This is an important issue for securing urban safety especially in the mega cities of Asia. A landslide is a geological phenomenon which includes a wide range of ground movement, such as rock falls, deep failure of slopes and shallow debris flows. Although gravity's action on an over-steepened slope is the primary reason for a landslide, there are other contributing factors affecting the original slope stability. In this paper an attempt is made to focus on three main factors generating landslides such as morphology of the soil, land use pattern and the steepness of the area. Here weighted maps are prepared for each of the category following statistical method based on pixel values of the Raster data (images). For instance pixels having higher values in the image for geological category pose greater threats from landslide disaster while the areas having lower pixel values indicate the less risk for landslides. Using the aforesaid methods weighted maps for each of the type (geology, soil and slope) has been made. Hereinafter all three weighted maps are overlaid to have a combined index map for landslides in the study area. The index map represents the potential threat areas for landslides with color intensities. The result of this study can be very helpful for new developments in the landslide prone cities in Asia. This can also play an important role for the built up areas in the city regarding mitigation and preventive measures from landslides.

1. INTRODUCTION

Landslides are the phenomena which represent the general heading of mass movement. The term therefore describes a movement of a mass of rocks or soil from a higher point to a lower one. Movements may include falling, sliding and flowing. The first is the movement of masses or blocks in free fall; the second is the movement along more or less well-defined surfaces, the third, is movements of masses in a fluid-plastic or viscous state. Movements should be downwards and outwards with a free face, thus excluding subsidence. Subsidence is a mass movement, in which a mass goes downwards induced by gravity and/or specific water conditions. The displaced material may include parts of the regolithe and/or bedrock. The materials involved can therefore be rocks at various levels of alteration or the product of desegregation phenomena in the past. Gravity is the principal force involved. The movement of the masses is due to the action of the force of gravity, but other forces like those due to earthquake or due to water filtration can be involved. On the basis of what is stated above, a complete definition of a landslide event could be the following: Movement of soil or rock controlled by gravity, superficial or deep, with movement from slow to rapid, but not very slow, which involves materials which make up a mass that is a portion of the slope or the slope itself.

2. TYPES OF LANDSLIDES

There are different types of landslides and they can be categorized in a number of ways. The most common ones are described bellow in short.

2.1 Debris flow

In this type of landslides slope materials which are saturated with water resulted into debris flow or mud flow. Consequently the slurry of rock and mud may uproot trees, houses, and cars. This can also block the bridges and tributaries causing flooding along its path.



Figure 1: A landslide caused by one of the 2001 El Salvador earthquakes

Muddy-debris flows in the affected areas cause severe damage to structures and infrastructure and often claim human lives. Muddy-debris flows can start as a result of slope-related factors, and shallow landslides can dam stream beds, provoking temporary water blockage.

2.2 Earth flow

This is the flow of viscous and saturated fine-grained materials that move at any speed along the downward slope. Typically, they can move at speeds from .17 to 20 km/h. Though these are a lot like mudflows, in general they are slow moving and are covered with solid material carried along by flow. Clay, fine sand and silt, and fine-grained, pyroclastic material are all susceptible to earthflows. The velocity of the earthflow is all dependent on how much water content is in the flow itself: if there is more water content in the flow, the higher the velocity will be.



Figure 2: A rock slide in Guerrero, Mexico.

This type of landslides is much likely to happen during periods of high precipitation, which saturates the ground and adds water to the slope content. Fissures develop during the movement of clay-like material creates the intrusion of water into the earthflows. Water then increases the pore-water pressure and reduces the shearing strength of the material.

2.3 Sturzstrom

Sturzstrom happens rarely and the much of this type are not yet understood. Often very large, these slides are unusually mobile, flowing very far over a low angle, flat, or even slightly uphill terrain. They are suspected of "riding" on a blanket of pressurized air, thus reducing friction with the underlying surface.

2.4 Shallow landslide

The sliding surface is located within the soil mantle or weathered bedrock in this form of landslide. They are normally to a depth from few decimetres to some meters. Shallow landslides include debris slides, debris flow, and failures of road cut-slopes. Landslides occurring as single large blocks of rock moving slowly down slope are sometimes called block glides.

2.5 Deep-seated landslide

Here in this type the sliding surface is in most of the cases deeply located below the maximum rooting depth of trees which may vary to a depths greater than ten metres. Deep-seated landslides usually involve deep regolith, weathered rock, and/or bedrock and include large slope failure associated with translational, rotational, or complex movement.

3. CAUSES OF LANDSLIDES

In broad category there are two types of causes for landslide such as natural causes and man made causes. A concise discussion is provided in the following sections over the causes of landslides.

3.1 Natural Causes

Earthquake has a very strong relation with landslides. During the earthquake it creates the huge stress that make the weak slope to fail resulting in a landslide. River erosion and heavy rains are the two other important reasons that can trigger the landslide. Volcanic eruptions can produce loose ashes and debris to flow those can also be an important contributing factor to make a landslide.

3.2 Man Made Causes

Deforestation, mining and overgrazing are the main causes made by human activities which lead to landslides. Stockpiling or from man-made structures may stress weak slopes to fail those can lead to a landslide.

4. METHODOLOGY

Based up on the following formula Weight Map for each of the category has been made. Then the three weighted maps for the type geology, slope and land use are put together to generate the combined map. This index map is a color coded one that shows the potential threat area for the landslide hazards. The landslide density per class is divided by the landslide density in the entire map. Negative weights when the landslide density is lower than normal. Positive when it is higher than normal

$$\ln W_i = \ln \left[\frac{Densclas}{Densmap} \right] \ln \left[\frac{Npix(Si)}{\frac{Npix(Ni)}{\sum Npix(Si)}} \right]$$

W_i = the weight given to a certain parameter class (e.g. a slope class)
 $Densclas$ = the landslide density within the parameter class
 $Densmap$ = the landslide density within the entire map
 $Npix(Si)$ = number of pixels which contain landslides in a certain parameter class.
 $Npix(Ni)$ = total number of pixels in certain parameter class

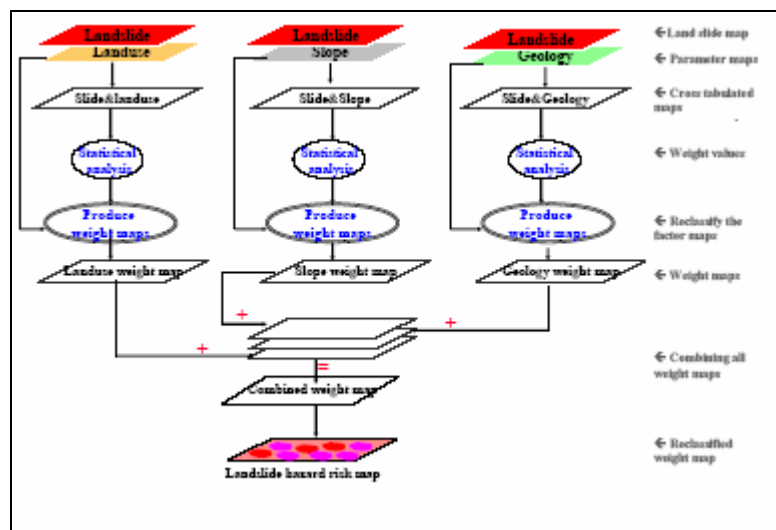


Figure 3: Diagram for work flow

5. AVAILABLE DATA

Data is most important item in spatial analysis. Once the database is ready it is only a matter of time to have the desired output. We had the vector and raster data set for land use, geology and slope of the study area. The raster data is composed of small square parts called pixel. This type of data can be monochromatic or panchromatic. The study area is located in near Bogota, the capital city of Columbia.

Input dataset:

- Geology map (vector, ArcView Shape file)
- Landslide map (vector, ArcView Shape file)
- Landuse (raster)+tfw file
- Slope map (raster)+tfw file

We have used GIS software called GeoMedia form a company Intergarph International. For analyzing the raster dataset we have used an extension of GeoMedia called “Grid”.

6. ANALYSIS

Analysis covers the working procedures in GeoMedia Professional for generating raster maps and then making weighted maps for the landslide risk analysis. A brief from each of the sections is documented in the following paragraphs.

6.1 Rasterizing the vector maps

There were two data sets with a nature of vector format. As we need them to be in raster format, we have converted them from vector to raster ones. Here we have specified the pixel size in order to avoid the conflict in the output data. Having completed rastarization the data sets are recoded followed a randomization process.

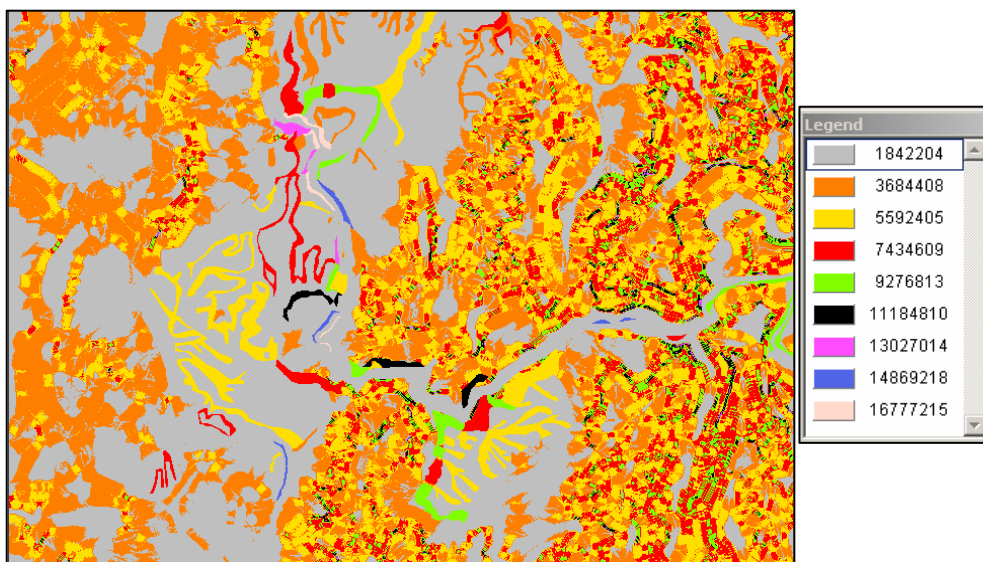


Figure 4: Number of total pixels in different classes

6.2 Preparation Weight Maps

The landslide density per class is divided by the landslide density in the entire map. Using the principle above weight maps for land use, slope and geology are prepared. In this coding 0 indicates no threats regarding landslide while positive numbers represents potential threats for landslide in the study area.

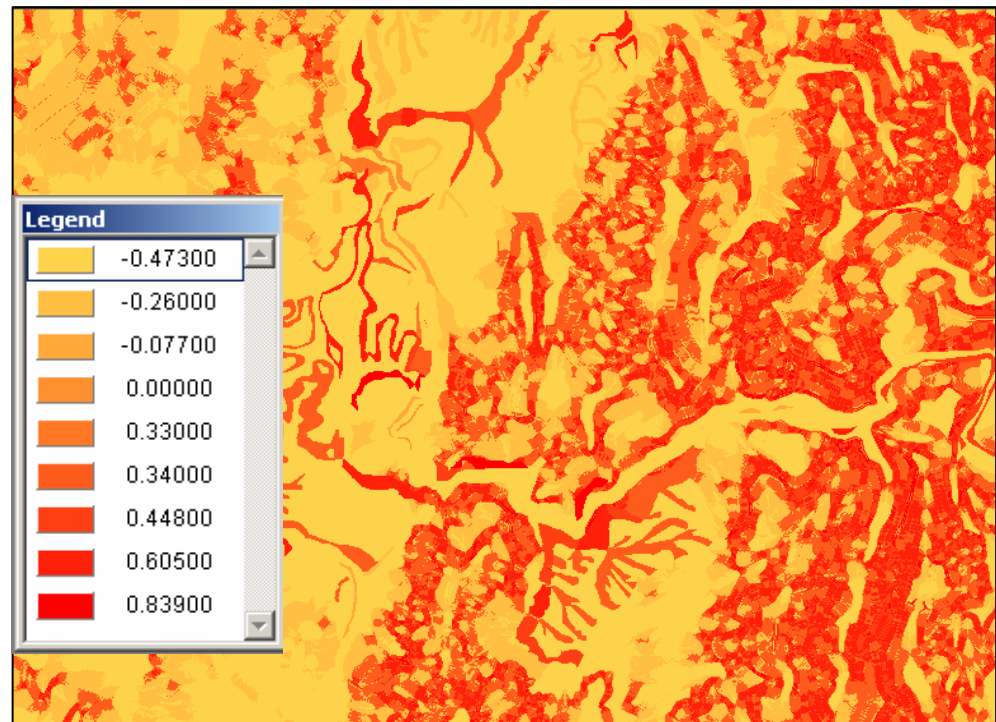


Figure 5: Weight Map for Slope Category

6.3 Combining all for Risk Maps

For making the landslide hazard maps, the weighted maps from all categories like slope, land use and geology are put together. The output map is colour coded map which indicates the potential threats of landslides with positive numbers; zero represents neutral position regarding the risk of happening landslides and the negative numbers the less the risk of occurring landslides.

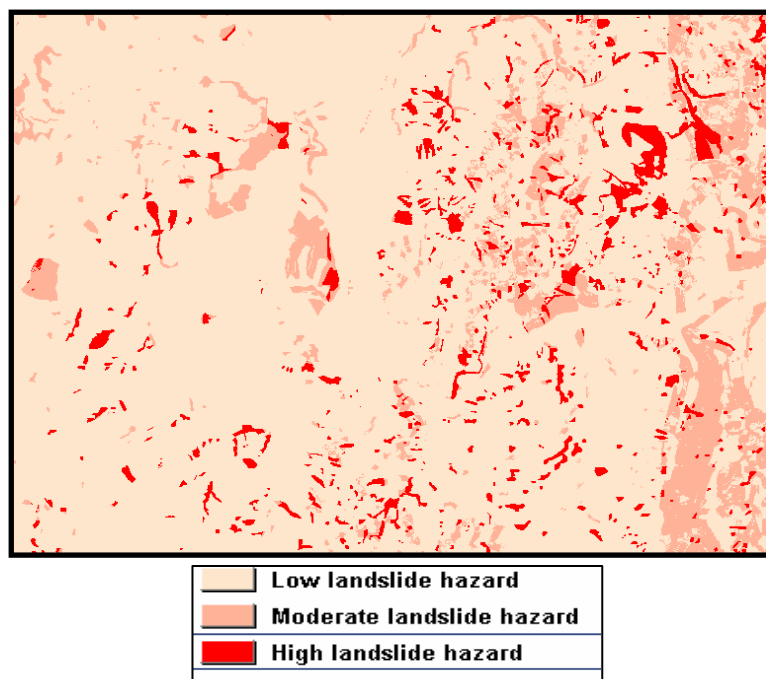


Figure 6: Final Landslide Hazard Map

7. CONCLUSION

Landslide is a devastating natural calamity and this is even more hazardous in densely populated urban areas. These can play havoc on both resources and lives. The outcome of this paper can be very helpful for the professionals from different fields like planners, engineers environmentalists. This can also help the decision makers to find out the suitable areas for new urban developments. In recent years there were some severe landslides in Asian cities like in Southern Leyte landslide in the Philippines on 17 February 2006 and Chittagong (Bangladesh) on 11th June 2007. The mega cities in Asia are not out of this risk. So preparation of Landslide Hazard Maps for these cities can make a significant contribution to mitigate losses of resources and lives.

REFERENCES

- Integrating. (2005): GeoMedia command Wizard. Online Guide of GeoMedia Professional. Integrating Corporation, USA.
- Naranjo, J.L., van Westen, C.J. and Soeters, R. (1994). Evaluating the use of training areas in bivariate statistical landslide hazard analysis- a case study of Colombia, ITC Journal 1994-3, pp 292-300.
- Van Westen, C. J. (1994). GIS in landslide hazard zonation: a review, with examples from the Andes of Colombia. In: Price, M. and Heywood, I. (eds.), *Mountain Environments and Geographic Information Systems*. Taylor & Francis, Basingstoke, U. K. pp 135-165.
- Web Links
- http://en.wikipedia.org/wiki/Landslide#Landslide_types
- <http://www.answers.com/biomass>
- <http://www.wissenschaftswirtschaft-bw.de/index.php4>

SEISMIC MICROZONATION OF COX'S BAZAR IN BANGLADESH

A. B. AFIFA IMTIAZ

Dept. of Civil Engineering, BUET, Bangladesh
afifaimt@gmail.com

MEHEDI AHMED ANSARY

Dept. of Civil Engineering, BUET, Bangladesh
ansary@ce.buet.ac.bd

ASHUTOSH SUTRA DHAR

Dept. of Civil Engineering, BUET, Bangladesh
ashutoshdhar@ce.buet.ac.bd

MOHAMMED JOBAIR

Dept. of Civil Engineering, BUET, Bangladesh
jobair98@yahoo.com

ABSTRACT

Landslide is one of the deadliest natural calamities that can play havoc on the lives and resources. The intensity is always higher in urban areas than that of counter parts because of higher population densities and man made structures. Countries like Philippines (17th February, 2006) and Bangladesh (11th June, 2007) have experienced some of the serious landslides recently. Many other cities in Asia have also potential threat for landslides. This is an important issue for securing urban safety especially in the mega cities of Asia. A landslide is a geological phenomenon which includes a wide range of ground movement, such as rock falls, deep failure of slopes and shallow debris flows. Although gravity's action on an over-steepened slope is the primary reason for a landslide, there are other contributing factors affecting the original slope stability. In this paper an attempt is made to focus on three main factors generating landslides such as morphology of the soil, land use pattern and the steepness of the area. Here weighted maps are prepared for each of the category following statistical method based on pixel values of the Raster data (images). For instance pixels having higher values in the image for geological category pose greater threats from landslide disaster while the areas having lower pixel values indicate the less risk for landslides. Using the aforesaid methods weighted maps for each of the type (geology, soil and slope) has been made. Hereinafter all three weighted maps are overlaid to have a combined index map for landslides in the study area. The index map represents the potential threat areas for landslides with color intensities. The result of this study can be very helpful for new developments in the landslide prone cities in Asia. This can also play an important role for the built up areas in the city regarding mitigation and preventive measures from landsliEarthquake hazard zonation for urban areas, mostly referred to as seismic microzonation, is the first and most important step towards a seismic risk

analysis and mitigation strategy in densely populated regions, since damage due to an earthquake may vary even within a few meters due to variation in local site conditions. The Microzonation presents peak ground acceleration, soil liquefaction and spectral amplification which are required for seismic hazard mitigation. These factors are highly dependent on the local soil conditions and on the expected earthquakes. Cox's Bazar and the nearby area fall in the High Risk Zone for earthquakes. There has been also a rapid urbanization of Cox's Bazar in the last few decades including construction of significant number of buildings and other structures. It is essential to develop seismic microzonations of the area based on site characterizations. Historical Information reveals that earthquakes of magnitude between 6 and 7 have occurred around the city in the past. In this study, borehole investigation conducted at 30 locations across the district is used for liquefaction potential analysis. Seismic Microzonation map has been developed for Liquefaction Potential based on the analysis. Influence of local soil conditions on ground shaking and subsoil stability around the district has also been discussed.

1. INTRODUCTION

Cox's Bazar, located in the southeastern part of Bangladesh, is a strategically and economically important city of the country. It is a coastal district and famous for its natural beauty and as a tourist place. The longest sand beach of the world is located at Cox's Bazaar. The district is exposed to most devastating natural disasters of the country. The earthquake has recently appeared as additional threat to this region. Therefore, it is essential to develop an earthquake preparedness program for the region in order to reduce the potential losses expected from the disaster. Soil liquefaction is a phenomenon in which a soil below the ground water table loses a substantial amount of strength due to pore pressure generation from strong earthquake ground shaking. Liquefaction can have a significant and sometimes devastating effect on buildings supported on the upper soil layers constructed without consideration of its consequences of liquefaction. Cox's bazar, situated beside the Bay of Bengal, consists of 8 Upazilas namely Cox's Bazar Sadar, Kutubdia, Maheshkhali, Ramu, Teknaf, Ukhia, and Pekua. According to the parameters of Land based zonation of Coastal Region, all these Upazilas are under Exposed Coastal Area where one fourth of the district is island (Uddin and Yasmin, 2005). It is mostly a hilly region consisting of alluvial flood plain and sandy sea shore area. The area bottom of the hill can liquefy if the intensity of shaking is high, which may cause land slide in the hilly region. On the other hand floodplains and sea shore areas consisting of fine sand and silt deposit with shallow water table in most of the places may liquefy during a strong earthquake. Most of the buildings in the region were constructed without any seismic design consideration. Presently strengthening or retrofitting efforts are essential for these buildings in order to protect lives and properties. This paper deals with the development of a liquefaction potential map for Cox's Bazar District to quantify the spatial variation of the liquefaction condition for expected typical earthquakes.

2. CAUSES OF SOIL LIQUEFACTION

The general trend on understanding about the basic causes of liquefaction of sands is a quite qualitative measure. If a loose saturated sand deposit is subjected to ground vibrations, it tends to compact and decrease in volume. The effective stress in the sand deposit is equal to the difference between the overburden pressure and the pore water pressure. If drainage is unable to occur, the tendency to decrease in volume results in an increase in pore water pressure. So, with increasing oscillation, the pore water pressure will be equal to the overburden pressure causing the effective stress to become zero. Since the shear strength of a cohesionless soil is directly proportional to the effective stress, the sand loses its strength completely and develops a liquefied state.

In more quantitative terms, it is now generally believed that the basic cause of liquefaction in saturated cohesion less soil during earthquake is the buildup of excess hydrostatic pressure due to the application of cyclic shear stress induced by the ground motions. These stresses are generally considered to be due primarily to upward propagation of shear waves in a soil deposit; although other forms of wave motions are also expected to occur.

3. ASSESSMENT OF SOIL LIQUEFACTION

3.1 Methodology

There are a number of different methods by which the potential for liquefaction of a soil can be evaluated. The types of methods can be classified into four categories (Rashid, 2000):

Category-1: Evaluation of liquefaction potential roughly based on topographical and geological information

Category-2: Evaluation of liquefaction potential from N-value and grain size distribution data, and estimates of peak surface acceleration.

Category-3: Evaluation of liquefaction potential from laboratory cyclic shear testing of undisturbed samples, in light of dynamic response analysis.

Category-4: Evaluation of liquefaction potential by conducting in-situ cyclic or blasting tests, or laboratory shaking table tests.

Because of their simplicity, methods that fall in the first and second category are generally useful for formulating microzonation maps of liquefaction potential for wide areas. Methods in the last two categories provide a more rigorous examination of liquefaction at a single site, but are too tedious and costly for survey-type applications. In this study, the second procedure was adopted to formulate microzonation map of liquefaction potential.

The second procedure involves a more direct use of geotechnical data, such as SPT-N value and mean particle diameter, and estimates of peak surface acceleration (Seed and Idriss, 1971). A liquefaction resistance factor

F_L , is calculated which is used to evaluate the liquefaction potential index, I_L . The method is briefly explained below.

3.2 Liquefaction Potential Based on N-Values

A simple method suggested by Seed and Idriss (1971) was used here to evaluate the Liquefaction Resistance Factor, F_L which can also be termed as Factor of Safety. It is the most common and traditional method that uses correlations between the liquefaction characteristics of soils and the Standard penetration Tests or N-value along with other parameters such as grain size distribution curves of soils, overburden pressure, and estimated peak surface acceleration. The assessment of the liquefaction resistance factor at any depth by this method involves comparison of the predicted cyclic stress ratio (τ/σ'_0) that would be induced by a given design earthquake with the cyclic stress ratio required to induce liquefaction. For this method, F_L is calculated for a given depth of soil layer by the following formula.

$$F_L = R/L \tag{1}$$

Liquefaction is assumed to occur at that depth if F_L is less than 1.0. Here, R is the in-situ capacity of soil to resist liquefaction expressed by Cyclic Resistance Ratio (CRR) for earthquake of magnitude 7.5 and L is the earthquake load induced by a seismic motion expressed by Cyclic Stress Ratio (CSR). Cyclic Resistance Ratio for earthquake of magnitude 7.5 is determined based on corrected SPT as shown in Figure 1 (Seed et al. 1983).

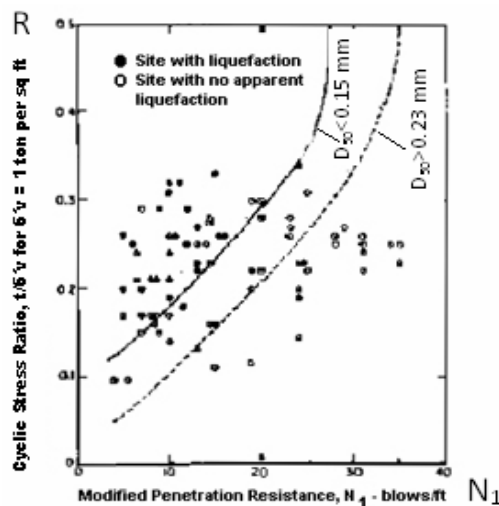


Figure 1: Curves for getting $CRR_{M=7.5}$ from corrected SPT blow count (Seed et al. 1983)

Table 1: Seed and Idriss (1983) original MSF

Earthquake Magnitude	MSF
6	1.32
6.75	1.13
7.5	1.00
8.5	0.89

Magnitude Scaling Factor (MSF), obtained from Figure 2, is used to determine the Factor of Safety against Liquefaction for earthquakes other than of magnitude 7.5 and calculated as

$$FS = F_L = CRR_{7.5}/CSR * MSF \quad (2)$$

The shear stresses developed at any point in a soil deposit during an earthquake appear to be due primarily to the vertical propagation of shear waves in the deposit. If the soil column above a soil element at depth “h” behaved as a rigid body, the maximum stresses on the soil element would be

$$(\tau_{max})_r = (\gamma h)/g \cdot \alpha_{Smax} = \bar{\sigma}_0/g \cdot \alpha_{Smax} \quad (3)$$

Where,

- $(\tau_{max})_r$ = total overburden pressure
- α_{Smax} = estimated peak surface acceleration (in percentage of g)
- γ = unit weight of the soil
- g = acceleration due to gravity

The average cyclic stress ratio $(\tau_{av}/\bar{\sigma}'_0)$ induced by an earthquake is given by the expression (Seed and Idriss 1971);

$$CSR = L = \tau_{av}/\bar{\sigma}'_0 = 0.65 (\alpha_{Smax} /g) (\bar{\sigma}_0 /\bar{\sigma}'_0) r_d \quad (4)$$

Where,

- $\bar{\sigma}'_0$ = effective overburden pressure
- r_d = a stress reduction factor with a value less than 1 given by $(1-0.015z)$ in which z (meters) is the depth of ground surface

Since the standard penetration resistance, N, measured in the field actually reflects the influence of the soil properties and the effective confining pressure, it has been found desirable to eliminate the influence of confining pressure by using a normalized penetration resistance N_1 , where N_1 is the measured penetration resistance of the soil under an effective overburden pressure of 1 ton per sq. ft. So, before using the graph in Figure 1, normalized to the field SPT-N value is needed as follows:

$$N_1 = C_N \cdot N \quad (5)$$

Where,

- N_1 = modified N values

C_N = a correction factor

The correction factor, C_N was provided by Murthy (1991) and presented here as Figure 2.

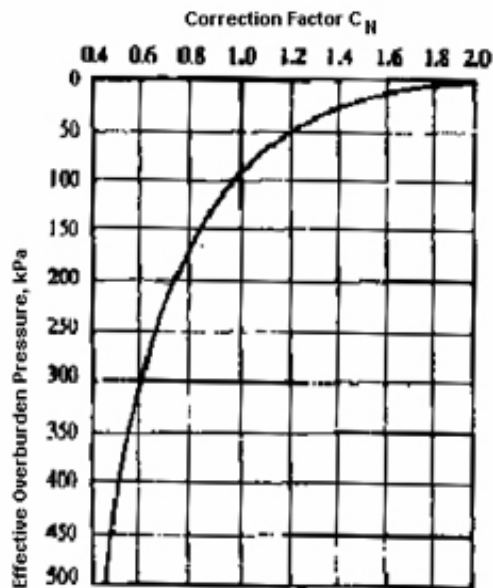


Figure 2: Curves for Correction Factor from Effective Overburden Pressure (Seed et al. 1983)

The severity of foundation damage caused by soil liquefaction depends to a great extent on the severity of liquefaction, which cannot be evaluated solely by the F_L . Generally speaking, liquefaction under the following condition tends to be severe:

1. The liquefied layer is thick
2. The liquefied layer is shallow
3. The F_L of the liquefied layer is far less than 1.00

In order to take care of the above effect, the Japanese Bridge Code (Japanese Road Association, 1991) recommended a modification to procedure then suggested by Seed et al. In this method the factor of safety values, F_L (Seed and Idriss, 1971) against resistance to liquefaction have been computed up to top 20 meters depth for all the bore holes and these values have been subsequently converted into liquefaction potential index (I_L) given by the following equation (Iwasaki et al., 1982):

$$I_L = \int_0^{20} F(z) \cdot w(z) dz \quad (6)$$

Where,

$$F(z) = (1 - F_L) \text{ for } F_L \leq 1.0; \quad F(z) = 0 \text{ for } F_L > 1.0$$

$$w(z) = (10 - 0.5z) \text{ for } z \leq 20 \text{ m}; \quad w(z) = 0 \text{ for } z > 20 \text{ m}$$

I_L	= 0,	No Liquefaction
	= 0-5,	Low Liquefaction
	= 5-15,	Medium Liquefaction
	= >15,	High Liquefaction

I_L has been used in this paper to express the measure of liquefaction potential for a particular location and for further zonation of the area based on a particular range of this index.

4. ASSESSMENT OF SOIL LIQUEFACTION IN COX'S BAZAR

4.1 Site Soil Condition and Data Collection

The procedure employed in this paper to assess the liquefaction resistance of a soil deposit and predict the liquefied thickness, is based on Standard Penetration Test (SPT) blow counts in soil bore logs. A total of 30 soil boring logs with SPT have been used for liquefaction potential study of Cox's Bazar District. Most of the soil data are collected from the depths up to 30 meters. Almost all the boring data include SPT N-value measured at 1.5 m (5ft) interval. The soil borehole locations used in this study are shown in Figure 3. Figure 4 shows sample bore log along with SPT-N values.

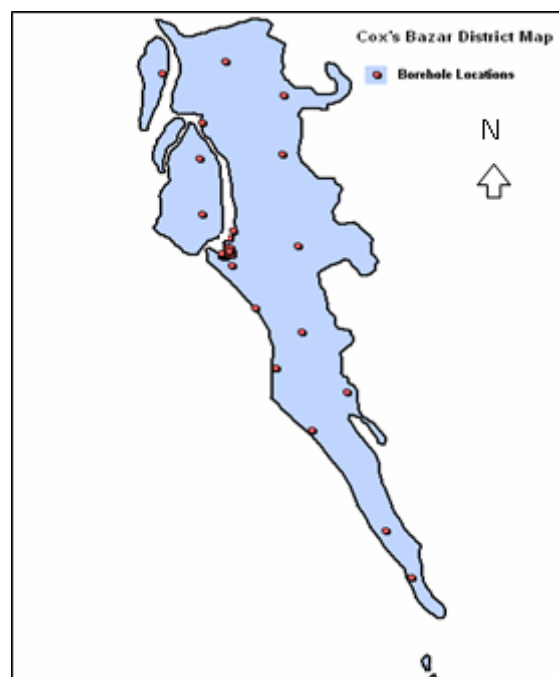


Figure 3: Cox's Bazar District Map Showing Soil Borehole Locations

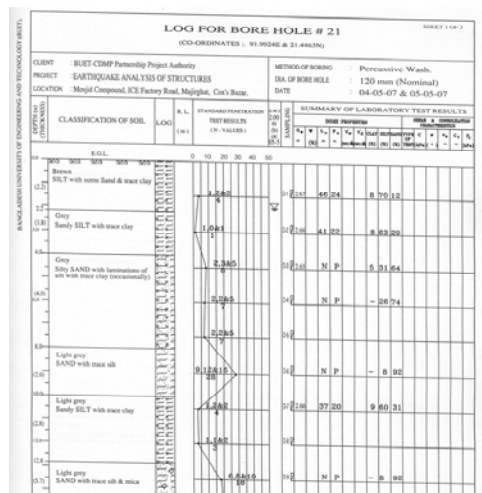


Figure 4: Sample SPT blow counts in a bore log

4.2 Estimation of Liquefaction Potential

In this simplified procedure of liquefaction estimation, SPT values (Figure 4), unit weight of soil, location of water table and estimated magnitude of earthquake or estimated peak surface acceleration at site are required. A series of historical earthquake data, from 1955 to 2006, have been analyzed to find out the relevant intensities based on Earthquake intensity-attenuation relationship for Bangladesh (Sabri, 2001) and thus to determine the PGA values.

The maximum ground surface acceleration for Cox's Bazar has been estimated, as 0.32 g, from the historical earthquake data. The magnitude has been found to be around 6.24 and the relevant Magnitude Scaling Factor (MSF), as shown in Table 1, has been used to convert $CRR_{M=7.5}$ for the selected earthquake by using equation (2). Particle diameter data for a particular depth of soil was obtained from sieve analysis report (Figure 5) which have been used in curve selection from Figure 1 to obtain $CRR_{M=7.5}$. At last the liquefaction resistance factor F_L , for the top 20 m of soil and the resulting liquefaction potential, I_L , for the 30 sites have been calculated.

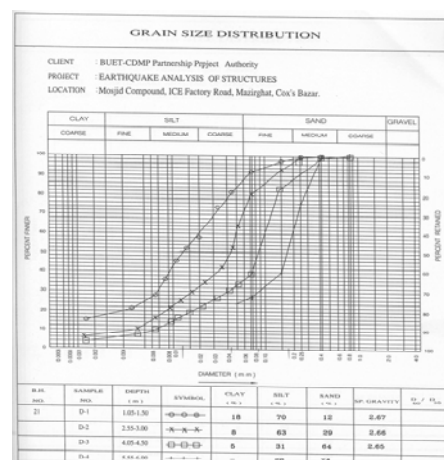


Figure 5: Sample Grain Size Distribution Curves

The computed results from the liquefaction potential analysis have been exported to a GIS environment for further processing and visualization. They have been classified into different classes according to the extent of liquefaction observed and plotted on the Cox's Bazar district map dividing the study area into 4 zones namely, high, medium and low probability of liquefaction and no liquefaction zones. From the findings, finally a zonation map (Figure 6) has been developed for liquefaction potential by using spatial interpolation and converting the vectorial point features into continuous raster map through grid generation which has been shown as Figure 7. It has been observed that the Sandy Silts with trace clay, Layer of Silt and Sand, Silty Sand having greater particle diameters and low to medium SPT N-values are responsible mostly for higher liquefaction potentials. The liquefaction potential index was very low for the borehole locations around Teknaf which has resulted in No to Low liquefiable zones in the map. Most of the locations near Chakaria and Kutubdia were found to have extremely high I_L values which have been reflected on the map. For the rest of the borehole locations, there were different variations in the computed I_L , from Moderate to High values. During grid generation to get continuous raster map in GIS, the program counted on the more contributing points on the surface. By combining the variations of effects of the points the Moderate liquefiable zonation boundary was determined. The generated microzonation map can be used as a guideline for General and Effective Land Use planning, Zoning Ordinances, Capital Invest Planning, Ground-failure Susceptibility Estimation, Post Disaster Planning, Disaster Mitigation Planning etc.

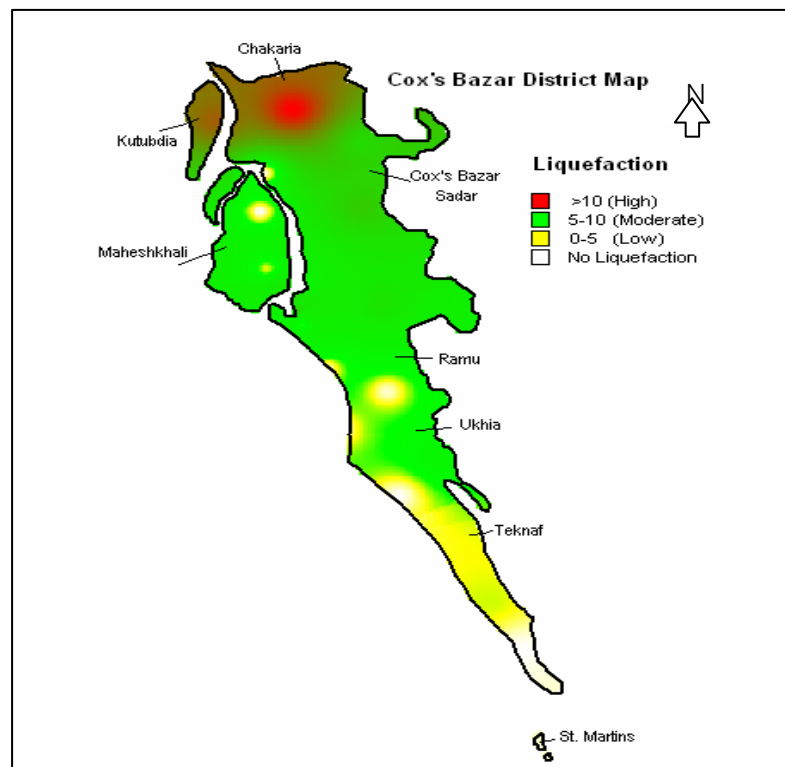


Figure 6: Seismic Microzonation Map of Cox's Bazar for Liquefaction Potential

5. CONCLUSIONS

Many countries of the world use zoning maps based on geological assessments of seismic hazards to consider dynamic effects in design codes in order to ensure the safety of structures under earthquake loading. In this paper, an attempt has been made to develop a firsthand liquefaction potential map for the District of Cox's Bazar using Seed's simplified procedure combined with modification from Japanese Road Association 1991. It can be concluded from this study that mainly Chakaria and Kutubdia Upazilas are highly susceptible to soil liquefaction. The result of this study would be helpful for policy makers and professionals to incorporate these guidelines in the seismic design process as well as strengthening of the existing structures in these zones.

ACKNOWLEDGEMENT

The authors acknowledge the funding of this research project by United Nation Office for Project Service (UNOPS) through Comprehensive Disaster Management Program (CDMP) of the Ministry of Disaster Relief and Rehabilitation of Bangladesh Government.

REFERENCES

- Iwasaki, T., Tokida, K., Tatsuoka, F. Watanabe, S., Yasuda, S. and Sato, H. 1982. *Microzonation for soil liquefaction Potential using Simplified Methods*. 3rd International Microzonation Conference, Proceedings, 1319-1329.
- Iwasaki, T. 1985. *Soil liquefaction Students in Japan: State of the Art*. Soil Dynamics and Earthquake Engineering, 5(1), 2-68.
- Japanese Road Association 1991. *Specifications for Highway Bridges, Part V. Earthquake Resistant Design*.
- Murthy, V. N. S., 1991. *Soil Mechanics and Foundation Engineering*. Volume 2, Revised and enlarged third edition, SAITECH, Bangalore, India.
- Rashid, MA (2000). *Seismic Microzonation of Dhaka City based on site amplification and liquefaction*. M.Engg. Thesis, BUET, Dhaka.
- Sabri, S. A., 2001. *Earthquake intensity-attenuation relationship for Bangladesh and its surrounding region*. M.Engg. Thesis, BUET, Dhaka, Bangladesh .
- Seed, H.b. and Idriss, I.M. (1971). *Simplified Procedure for Evaluating Soil Liquefaction Potential*. Journal of the Soil Mechanics and foundations Division, ASCE, 97(SM9), 1249-1273.
- Seed, H.B. Idriss, I.M. and Arango, I., 1983. *Evaluation of Liquefaction Potential Using Field Performance Data*. ASCE Journal of Geotechnical Engineering, 109(3), 458-482, March 1983.
- Uddin, A. M. K. and Yasmin, A. (2005). District Information-Cox's Bazar. Water Resource Ministry, Water Resource Planning Organization, People's Republic of Bangladesh Government

INFLUENCE OF RE-CURING CONDITION ON DAMAGE AND RECOVERY OF MORTAR EXPOSED TO FIRE

MICHAEL HENRY

Department of Civil Engineering, University of Tokyo, Japan
mwhenry@iis.u-tokyo.ac.jp

YOSHITAKA KATO

International Center for Urban Safety Engineering,
Institute of Industrial Science, University of Tokyo, Japan
katoyosh@iis.u-tokyo.ac.jp

ABSTRACT

Concrete structures exposed to fire suffer from strength reduction and explosive spalling, and must be repaired before returning to service. Existing repair methods typically involve the removal of unsatisfactory concrete and casting of a fresh patching material in order to meet strength, durability, and fire protection requirements. However, this method generates waste and consumes resources. A potential repair system utilizing the re-curing of fire-damaged concrete to recover mechanical properties would eliminate the generation of waste and reduce material consumption while optimizing the life cycle performance of the existing structure.

This research attempted to gauge the potential for strength recovery by re-curing fire-damaged mortar under different conditions and measuring the change in strength relative to the pre-fired strength. Observation of the pore structure was performed, and these changes were related to the changes in strength. It was found that strength recovery is possible when the damaged mortar is supplied with water, although pre-fired strengths were not achieved. Damage prevention was found to be more effective than re-curing when considering the final strength of the re-cured specimen. The formation of cracks contributed to large strength reductions in some specimens; steel fibers were found to be effective in reducing the strength loss due to their crack-bridging behavior. Pore structure recovery was also observed. Discrepancies between strength and pore recovery could be explained by cracking of specimens caused by differential thermal shrinkage or quenching.

1. INTRODUCTION

Concrete, when used in structural applications, is generally considered to have good fire performance due to its low thermal conductivity and high specific heat. One of the advantages of concrete over steel is that concrete structures do not require fireproofing to achieve an acceptable fire rating,

thus reducing construction costs. However, this does not mean that concrete is impervious to fire. Fire damage to concrete includes explosive spalling and reduced strength, durability, and fire protection.

If a structure has been exposed to fire, the severe visual appearance of fire-damaged concrete may lead to the premature decision to demolish the structure. However, it is important to evaluate the level of damage caused and determine whether repairs can be made to the structure in order to extend its usable life. Once the extent of damage is known, appropriate measures for repairing that damage can be carried out. A repair method must satisfy two major goals: restore loss of strength and maintain member/structural durability and fire protection. Typically, this involves the removal of damaged concrete and casting of a patching material. However, this method generates large amounts of waste and consumes resources. A repair method utilizing the re-curing of fire-damaged concrete would optimize the life cycle potential of the material itself, which increases the performance of the structural members and thus the structure as a whole. If re-curing could achieve the two goals mentioned before, then it could be utilized as a repair method which not only restored structural performance, but reduced waste generation and material consumption, as well as utilized the full potential of the concrete material itself. Past research has indicated that fire-damaged concrete has the potential for re-curing by the supply of water, which initiates rehydration of dehydrated cement and regrowth of the pore structure. However, the various factors which affect the strength loss and subsequent recovery have not been fully explained.

This research observed the strength recovery potential of fire-damaged mortar under different re-curing conditions. Changes in the microstructure were also observed and related to the changes in strength. Resolving the differences between changes in strength and pore structure allowed for the understanding of the effect of re-curing condition on strength loss and recovery.

2. EXPERIMENTAL PROCEDURE

2.1 Materials

Three cement mortar mixes were used in this research (Table 1): normal-strength (NS), high-strength (HS), and steel fiber-reinforced (S6). The water-cement (W/C) and sand-cement (S/C) ratios varied between the NS and HS series; the S6 series used the same mix ratios as the HS series but changed the air-entraining (AE) agent and high-range water-reducing admixture (HRWA) volumes to achieve acceptable workability properties.

Steel fibers, with a diameter of 0.6 mm and length of 30 mm, were provided by the Bridgestone Corporation (product number 30/.60CX).

The furnace capacity limited the specimen size to 500×100 mm cylinders. After casting, specimens were sealed and cured in the molds for

three days and then demolded and placed in a water curing tank until two weeks from casting, when they were moved to air curing at 60% relative humidity (RH) and 20°C. High-temperature exposure was performed 28 days from casting.

Table 1: Mix Proportions

Mix Series	Mix Ratios (by mass)		Admixtures (%C)		Steel Fiber (%vol)
	W/C	S/C	AE	HRWA	
NS	0.5	2.3	0.2	-	-
HS	0.3	1.8	0.4	1.5	-
S6	0.3	1.8	0.4	2.5	0.6

2.2 High-temperature exposure

Fire damage was simulated by exposing the mortar specimens to high temperature in an electric furnace. The exposure temperature was set at 550°C because this temperature was found to induce the highest amount of damage without explosive spalling for the W/C ratio and specimen size and shape used in this research. A two-hour exposure time was selected based on observation of the effect of time on residual strength.

2.3 Re-curing conditions

After removal from the furnace, specimens were placed into one of two cooling conditions: air (60% RH, 20°C) or water (water-saturated, 20°C). After one hour in these cooling conditions, specimens were moved to the re-curing phase in the same two conditions (air and water). However, some specimens were moved from air cooling to water re-curing, resulting in three total re-curing conditions: air, air-water, and water (Figure 1). Testing of properties was performed before heating, after cooling (one hour), and after three and 28 days re-curing.

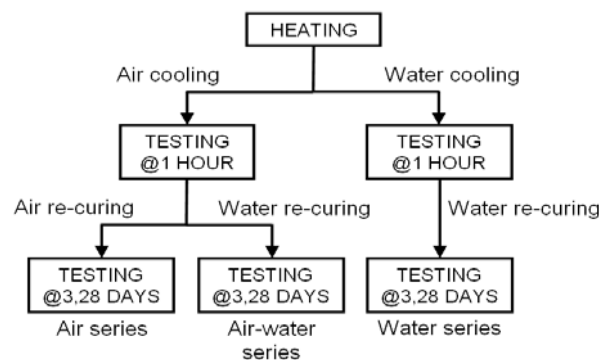


Figure 1: Flow chart for re-curing and testing

2.4 Physical tests

The damage and recovery of the mortar specimens was measured on two scales: load-carrying capacity (compressive strength) and micro structure (Mercury Intrusion Porosimetry, or MIP). Compressive strength was reported as absolute and residual compressive strength. Residual strength is the ratio of the exposed strength to the unexposed strength (equation 1), and allows comparison between mixes by normalizing the strength. The average values were taken from three specimens.

$$R = f / f_0 \times 100 (\%) \quad (1)$$

Where R: residual strength rate (%), f: average exposed strength (MPa), f_0 : average unexposed strength (MPa).

MIP was utilized to observe the changes in total porosity due to heating and re-curing. MIP specimens were taken from the mortar cylinders after compression testing.

3. RESULTS

3.1 Strength loss & recovery behavior

The residual compressive strength results, calculated per (equation 1), and the strength loss and recovery percentage are shown by re-curing condition (Figure 2). All series exhibit a general similar trend. For air re-cured specimens, most strength loss occurs by day 3, with no or little change to 28 days. Water re-cured specimens lose a large amount of strength after 1 hour of water cooling, but show consistent strength recovery up to 28 days. Air-water specimens lose strength during 1 hour of air cooling, but then recover strength during water re-curing similar to water re-cured specimens. Air-water specimens show the highest strength at 28 days for all series, followed by water re-cured specimens, then air re-cured specimens.

It can be seen that the S6 series exhibited the highest final residual strength for all re-curing conditions – 63.6% (air), 77.6% (water), 94.5% (air-water) – followed by the HS series. NS series exhibited the lowest residual strength rates. Strength loss was greatest for the water re-cured specimens at 61.5% for HS and 56.6% for S6, except in the case of the NS series. For the NS series, the formation of large surface cracks during the air re-curing period contributed to a 75.6% decrease in strength. The least amount of strength loss was observed for the air-water re-curing condition: 43.1% (NS), 29.5% (HS), and 17.6% (S6). Strength recovery was highest for water re-curing – 30.6% for NS, 33.9% for HS, and 34.2% for S6 – and lowest for air re-curing.

The highest final residual strengths were observed for the air-water re-curing condition. Air-water re-cured specimens suffered the least amount of strength loss, and only a moderate amount of strength recovery, yet the

combination of air cooling and water re-curing resulted in the highest residual strengths. This would indicate that damage prevention has a greater impact on final residual strength than strength recovery.

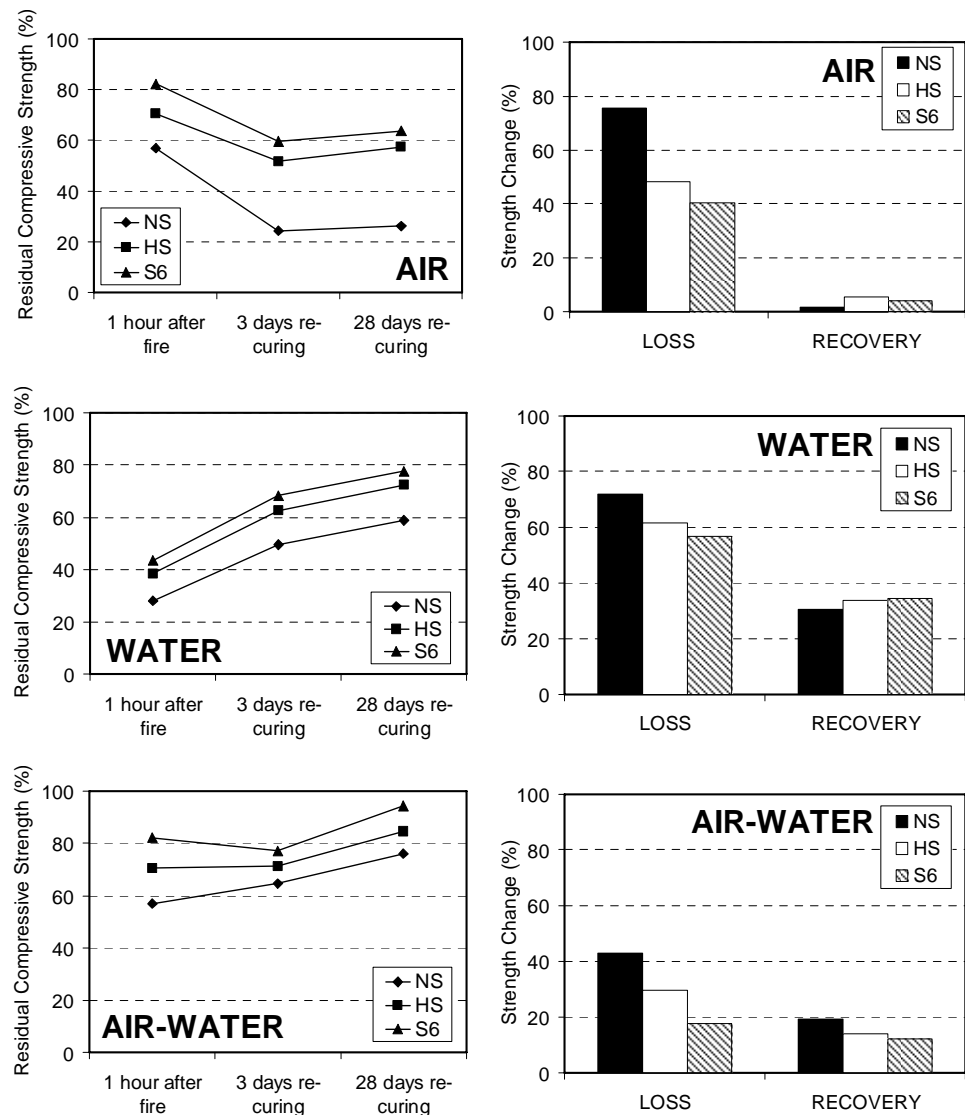


Figure 2: Air, water, and air-water residual strength results

3.2 Strength & porosity comparison

In order to determine the sources of strength loss and recovery in fire-damaged mortar, porosity was measured and the behavior was compared to the strength change behavior for the HS series (Figure 3). As an increase in strength typically corresponds to a decrease in porosity, and vice versa, any deviations in this pattern would indicate outside factors affecting the strength change behavior.

It can be seen that there are three locations where the strength and porosity behavior deviate significantly. For the air re-cured series, the strength between 1 hour and 3 days decreases significantly, but the porosity

remains constant. For the water re-cured series, the strength after 1 hour is much lower than that for the air re-cured series, but the porosity is relatively similar. Finally, for the air-water re-cured series, the strength between 1 hour and 3 days remains constant but the porosity decreases.

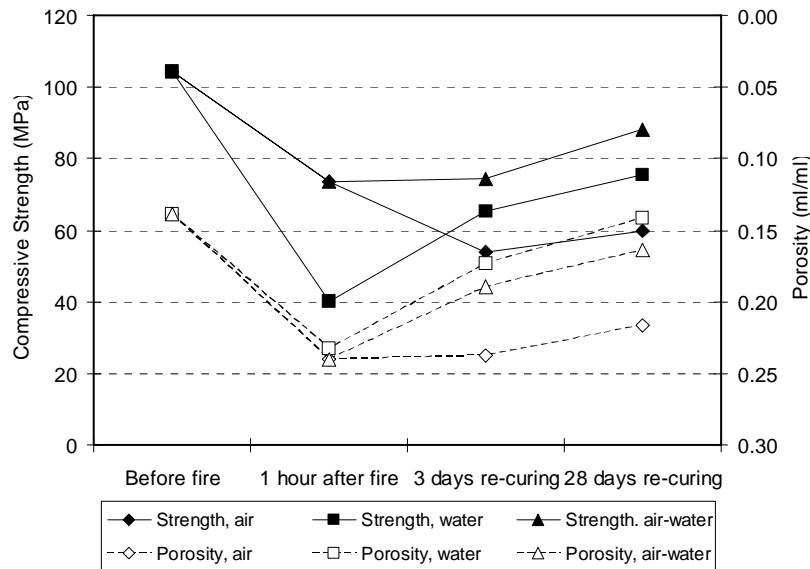


Figure 3: HS series strength and porosity comparison

4. MECHANISM

4.1 Strength loss mechanism

In order to resolve the differences between the strength and porosity behavior as shown previously (Figure 3), it is necessary to consider the differences in cooling and re-curing conditions.

Air- and water-cooled specimens shared a similar decrease in porosity after 1 hour of cooling. Furthermore, as the deterioration of the cement paste due to heating is assumed to be the same as the exposure conditions were the same, the difference in strength must be a function of the cooling condition. For specimens cooled in the air, the cooling is by convection processes, which results in a gradual decrease in temperature. Specimens which were cooled by submersion in water after removal from heating undergo a much more rapid decrease in temperature and “quenching,” which, it is believed, results in the formation of imperfections in the form of micro cracks. Therefore, the difference in strength after 1 hour of cooling is caused by the damage to the matrix from micro cracks caused by quenching.

For air re-cured specimens, strength loss was observed to occur between 1 hour and 3 days. It was found that specimens re-cured in the air suffered large surface cracks during this time period (Figure 4). NS series specimens showed the largest surface cracks. Surface cracking also occurred on HS and S6 specimens, but the crack widths were much smaller. The

severity of surface cracking corresponded to the relative level of strength loss across the three series under the air re-curing condition. Furthermore, porosity remained constant over that time period, indicating that the strength loss must be caused by a different source.

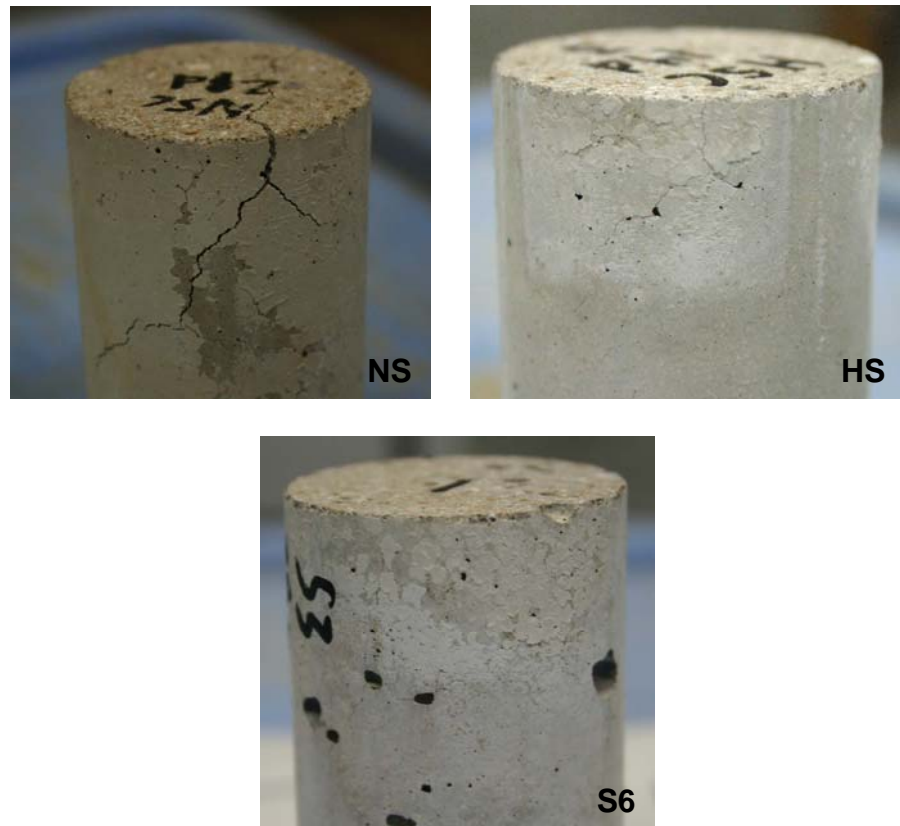


Figure 4: Surface cracking of NS, HS, and S6 air re-cured specimens

The formation of surface cracks is caused by the convection cooling process. As the specimen cools, a thermal gradient is formed due to the gradual temperature loss, which results in the outer part of the specimen losing heat more quickly than the inner part. Differential thermal shrinkage occurs as the difference in temperature across the specimen increases, resulting in the formation of surface cracks.

4.2 Strength recovery mechanism

Strength recovery is driven by the supply of water to the damaged mortar. For air re-cured specimens, the water supply is very low, as the specimen is being re-cured in a 60% RH environment. Therefore, the strength recovery behavior is very small.

For the water and air-water re-cured series, the re-curing condition – water submersion – is the same after the 1-hour cooling period. However, the amount of strength recovery is greater for water re-cured specimens. The difference in this strength recovery behavior is due to the initial cooling condition. For the water re-cured series, specimens are removed from the

furnace and immediately placed into room-temperature water. Therefore, the temperature difference between the specimen and the water is very high, so water is sucked into the pore structure as part of the cooling process. This water helps speed up the strength recovery process by shortening the time required for water to penetrate into the pore structure. Air-water specimens are cooled in the air for an hour before placement in water, so the temperature difference between the specimen and the water is much lower. This has the dual effect of reducing the amount of damage done by “quenching,” as the thermal shock is much lower due to the lower temperature difference, as well as reducing the amount of water sucked into the pore structure. Therefore, the strength recovery process is slowed by the damage due to thermal shock as well as the lower water supply.

5. CONCLUSIONS

This research attempted to gauge the potential for strength recovery of fire-damaged mortar and determine the sources of damage by placing the specimens in different cooling and re-curing conditions. Air and water conditions were used to test the effects of thermal conductivity (thermal shock) and water supply in order to view the recovery of strength. Pore structure was also measured under these conditions, as density and strength are related.

It was found that strength loss by cooling was caused by two mechanisms: micro cracking, due to immediate submersion in water after heating, and surface cracking, due to differential thermal shrinkage under gradual cooling. Specimens which were cooled in the air for 1 hour but then placed into water re-curing, before the formation of surface cracks, had the lowest strength loss as the damaging conditions of the other two re-curing conditions were avoided. Strength recovery under water supply was observed for both water and air-water re-cured specimens, but the quenching effect, which caused strength loss, also resulted in speeding up the recovery process by supplying water quickly to the pore structure. Applying the damage mechanisms by re-curing conditions could resolve the difference in strength and porosity behavior.

REFERENCES

- Tovey, A.K., 1986. Assessment and Repair of Fire-Damaged Concrete Structures – an Update. *ACI Special Publication 92: Evaluation and Repair of Fire Damage to Concrete*, 47-62.
- Taylor, H.F.W., 1990. *Cement Chemistry*, Academic Press Limited, London.
- Poon, Chi-Sun, Azhar, Salman, Anson, Mike, Wong, Yuk-Lung, 2001. Strength and Durability Recovery of Fire-Damaged Concrete after Post-Fire-Curing, *Cement and Concrete Research* 31, 1307-1318.
- Lin, Wei-Ming, Lin, T.D., Powers-Couche, L.J., 1996. Microstructure of Fire-Damaged Concrete, *ACI Materials Journal* Vol. 93, No. 3, 199-205

Georgali, B., and Tsakiridis, P.E., 2005. Microstructure of Fire-Damaged Concrete: A Case Study, *Cement and Concrete Composites*, Vol. 27, Issue 2, 255-259

STRATEGIC MAINTENANCE OF PORT AND HARBOR CONCRETE STRUCTURES BASED ON LIFE-CYCLE MANAGEMENT

HIROSHI YOKOTA
MITSUYASU IWANAMI, TORU YAMAJI, EMA KATO
Port and Airport Research Institute, Yokosuka, Japan
hiroy@pari.go.jp

ABSTRACT

Port and harbor structures have to keep structural performance over required levels in harsh marine environments. This can be achieved both with sufficient durability design and maintenance work based on the concept of life-cycle management. Focusing on a reinforced concrete superstructure of open-type wharf, this paper presents the methodologies of rational and efficient maintenance work based on maintenance strategies formulated in relation to durability design.

1. INTRODUCTION

The life of port and harbor structure is rather long. A structure designed today must be expected to meet demands during its lifetime that cannot be foreseen. At the initial design of a structure, designers must have several assumptions, in which probably worst conditions are considered, so that the structure can keep its structural performance over required levels. However, a number of existing structures unfortunately require remedial action including repair and strengthening due to loss in structural capacities as a result of chloride-induced corrosion of reinforcement embedded into concrete. This may be caused by insufficient durability design with optimistic assumptions against materials deterioration and by lack of proper maintenance work after construction of the structure. To meet these facts, strategic maintenance is the only way to be taken in relation to the result of initial durability design. To realize the strategic maintenance, the comprehensive life-cycle management is one of the key technologies.

The life-cycle management is a series of actions to evaluate the grade of deterioration and structural performance degradation by inspection, to predict the future progress of performance degradation, and to propose the alternatives of appropriate remedial action based on life-cycle cost minimization or performance maximization under budget capping. The authors have tried to establish the life-cycle management system for a reinforced concrete superstructure of open-type wharf that is one of the most vulnerable structures in ports and harbors. This paper introduces the methodologies of rational and efficient maintenance work based on maintenance strategies formulated in relation to durability design.

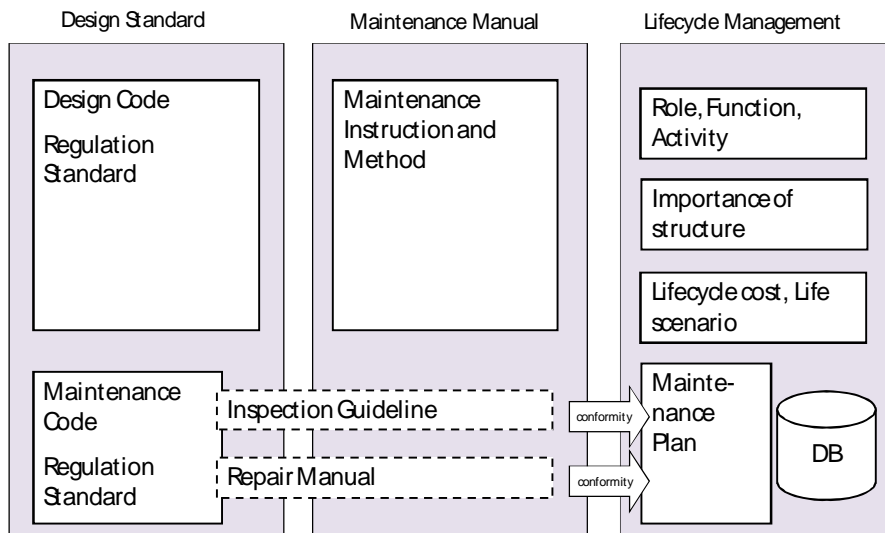


Figure 1: Collaboration between durability design and maintenance work

2. MAINTENANCE STRATEGY

It is usually very hard to keep structural performance of a port and harbor concrete structure over required levels for the whole service life because it is exposed to marine environments with rich chloride ion supply. Therefore, sufficient durability design has to be employed at the initial design stage, in which some kinds of mitigating measures are needed. One simple measure that anyone can realize is to increase concrete cover, but it seems distant because a concrete cover of about 200 mm or even larger is required. Instead of taking actions only by means of durability design, maintenance work during service period should be collaborated to ensure the structural performance. Figure 1 shows the collaboration system between durability design and maintenance work before and after construction of structure, respectively. With both durability performance verification at the design stage and performance assessment at the maintenance work, the structure can keep its structural performance over the requirements.

For realizing rational and effective maintenance work, a maintenance strategy should be properly formulated during the durability design of structure before construction or after regular inspection for already existing structure. Importance and substitutability of structure and difficulty of maintenance work should be well taken into account for the strategy-making. Figure 2 shows three maintenance strategies indicating basic concepts of how structural performance will be guaranteed beyond the performance limit or the maintenance limit. Strategy I is defined that the structural performance is always kept above the maintenance limit during the design working life. This strategy is realized by use of highly durable materials and/or preventive measures. Examples of durable materials and measures are epoxy-coated reinforcement, highly durable permanent formwork, extremely high quality concrete such as UFC, etc. Maintenance work in this strategy is not ignorable even serious deterioration is not expected to occur. Instead, the maintenance is required on the regular-basis including careful

monitoring to avoid unexpected deterioration. Strategy II is defined that even performance degradation is expected in the design stage, minor remedial actions are repeatedly applied before the maintenance limit is reached. In Strategy II, it is necessary to predict the progress of deterioration and draw up a maintenance plan based on the result of prediction. Maintenance in this category allows performance degradation due to deterioration at the design stage, but minor remedial action should be taken as early as possible when deterioration exposes. Strategy III is a kind of corrective maintenance, in which performance degradation is allowed to occur but major remedial actions may be applied once or twice for performance recovery.

Since an open-type wharf is expected to be highly safe and serviceable during performing cargo-handling work, its main performance requirements are safety and serviceability. It is, therefore, preferable to adopt Strategy I or II for the maintenance of a superstructure of open-type wharf.

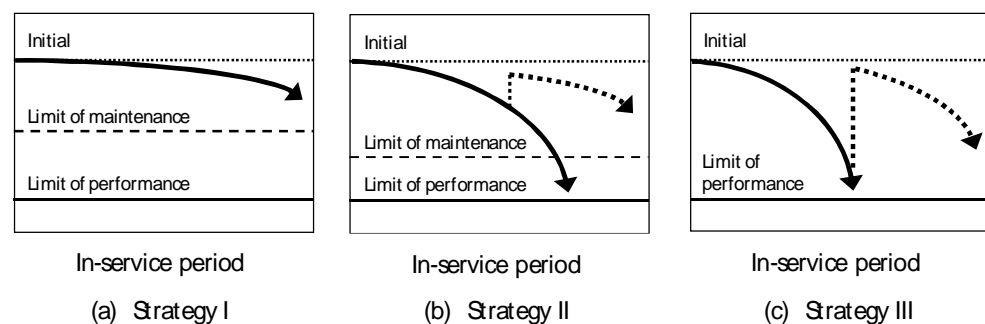


Figure 2: Definition of three maintenance strategies

3. LIFE-CYCLE MANAGEMENT

3.1 Overall concept

The maintenance work is carried out to assess the present conditions of structure and to quantify the level of structural performance. In addition, by predicting future progress of performance degradation, the most appropriate method of remedial action is chosen for minimizing the life-cycle cost or maximizing structural performance recovery under budget capping. A general procedure of maintenance work is shown in Figure 3, which is based on the life-cycle management (LCM) concept. The life-cycle management system is composed of the following five main components:

- Inspection of the present conditions of structural members
- Assessment of structural performance
- Prediction of future progress of performance degradation
- Proposal of method and timing of remedial action
- Decision of action among proposed alternatives

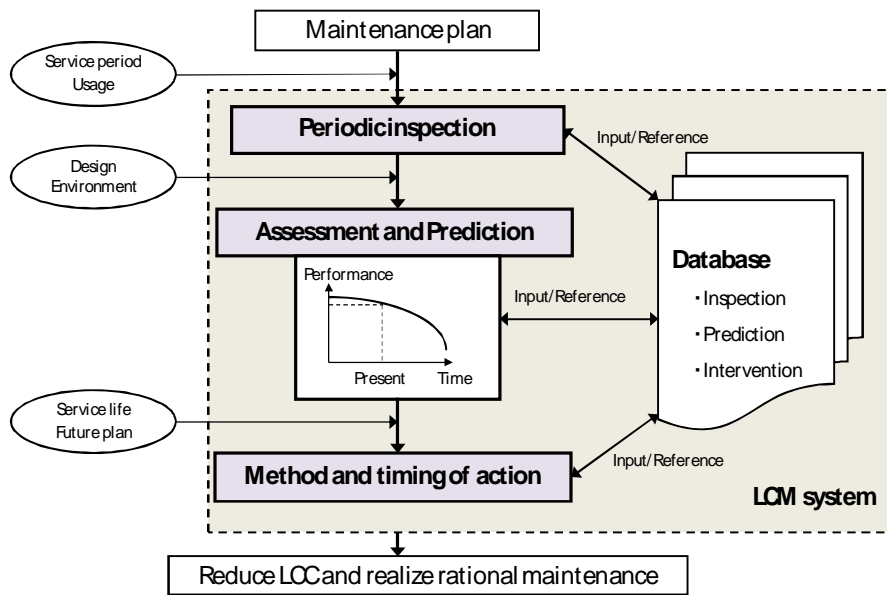


Figure 3: Procedure of life-cycle management

3.2 Judgment of deterioration

Judgment of deterioration is made by a two-step inspection system as shown in Figure 4; namely, primary inspection and detailed inspection. The state of deterioration is visually evaluated and judged using the deterioration grade: Grade *d* to *a* according to the general grading criteria in the maintenance manual for port and harbor structures (Port and Airport Research Institute, 2007). Grade *d* refers to a sound condition without any signs of deterioration, while Grade *a* is the most severe deterioration state. For example, the criteria of judgment for a reinforced concrete superstructure of open-type wharf are summarized in Table 1. For proper judgment, inspection should be carried out with regular intervals. At the moment, the standard time interval is set at 2 years.

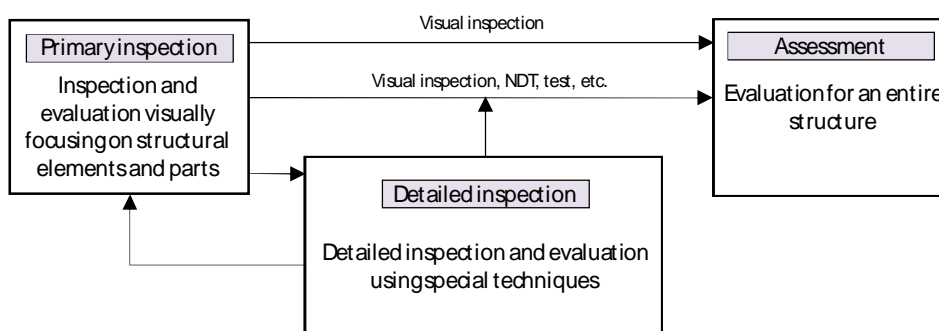


Figure 4: Process of assessment

When the primary inspection is insufficient to provide proper data for assessment, the detailed inspection is carried out. The detailed inspection includes visual inspection by well-trained divers for submerged parts, measurement with non-destructive or destructive techniques, etc. After the onset of corrosion of reinforcement, structural performance will be degraded very rapidly. Therefore, material deterioration should be captured before its

appearance on the surface of member. For this purpose, non-destructive techniques are of use. However, before their application, the effectiveness and accuracy should be well examined under real environmental conditions.

Table 1: Grade of deterioration of wharf superstructure

Item	Method	Judgment criteria	
Cracking, delamination, and spalling	Visual inspection on cracks, surface appearance etc.	a	Widely extended spalling off of concrete cover or cracks of 3 mm or wider
		b	Partially spalling off of concrete cover or many corrosion cracks
		c	Some corrosion cracks or partial delamination
		d	Nothing observed
Corrosion of reinforcement	Visual inspection on corrosion and rust stain	a	Broken reinforcement, directly exposed reinforcement, or heavy rust stain
		b	Much rust stain
		c	Partially extended rust stain
		d	Nothing observed

3.3 Assessment

It is required to quantitatively make overall assessment of a structure from the viewpoint of structural performance. The visual inspection is only able to provide the change in appearance of structural member, but structural performance has to be evaluated as precisely as possible.

The relationship between structural performance (structural capacity) and the grade of deterioration is shown in Figure 5. This figure was obtained by loading tests on reinforced concrete beams prepared for exposure tests for more than 20 years and extracted slabs from real structures which had been in service for more than 30 years (Yokota, et al., 2006a). When the deterioration grade reaches Grade *b*, structural performance tends to become lower than the design requirement level. These facts are well considered for the overall assessment from the viewpoint of structural performance.

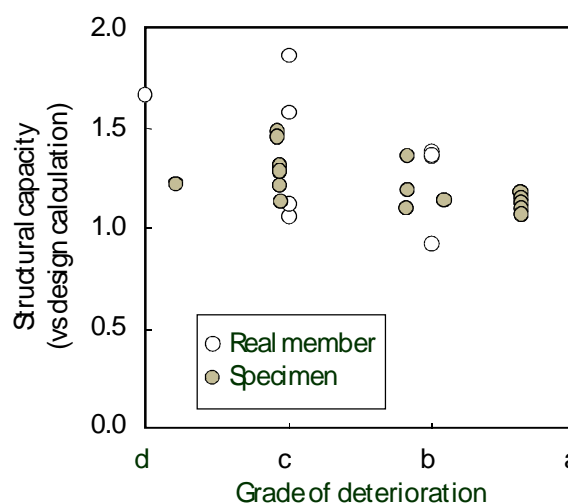


Figure 5: Structural capacity vs. grade of deterioration

3.4 Prediction

Since deterioration of a reinforced concrete member is induced and accelerated by chloride ion provided by sea water, the chloride ion profile inside concrete and the volume loss of reinforcement are predicted as main indices for durability performance. The calculation theory based on Fick's second law of diffusion of chloride ion in concrete has been widely used for the prediction of deterioration progress. For simulating the diffusion of chloride ion in concrete with this theory, it is necessary to quantify three fundamental parameters: chloride ion content on the surface of concrete, C_0 , an apparent diffusion coefficient of chloride ion in concrete, D_{ap} , and the concrete cover depth, c . C_0 represents the environmental condition around structural members and D_{ap} represents the diffusivity of chloride ion in concrete depending on the quality of concrete particularly on the type of cement and the water-to-cement ratio. When the chloride ion content reaches a threshold value at the position of reinforcement, corrosion of reinforcement will start and progress rapidly. The threshold value for onset of reinforcement corrosion is specified to be 2.0 kg/m^3 for a superstructure of open-type wharf. This is based on experimental test results as shown in Figure 6 (Yamaji, et al., 2001).

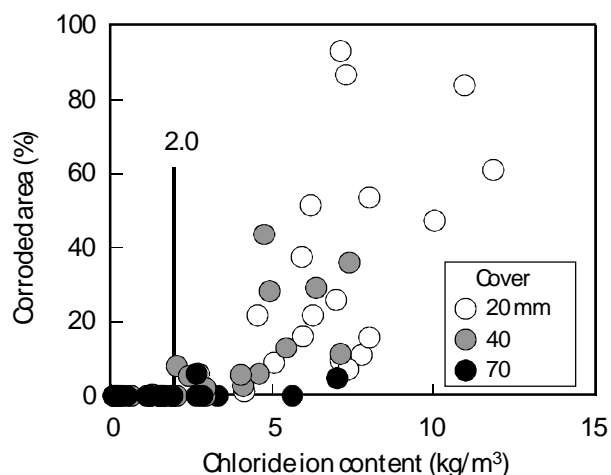


Figure 6: Threshold chloride ion content to initiate rebar corrosion

As the progress of deterioration of a structure differs widely by its location because of inhomogeneous characteristics of materials and diversity of environmental conditions, the proper determination of C_0 and D_{ap} is not so easy. An example of wide variations of values C_0 and D_{ap} in one reinforced concrete slab of open-type wharf is shown in Figure 7 (Yokota, 2006). They were obtained for concrete cores taken out from one slab of almost 1.5 m square. In the figure, the rectangular box shows the area indicating the range of $\mu \pm 1\sigma$ (μ : average value and σ : standard deviation). The figure does not show the correlation between the average value and the standard deviation. The slab shows that the proportion of measured results inside the box is only about 50%. In the practical investigation of existing structures subjected to marine environments, chloride ion profile of concrete has generally been estimated according to

one or a few sampled concrete. However, it seems that such a few numbers of concrete cores may not be representative.

The fact indicates that it is practically rather difficult to accurately predict the progress of deterioration and remaining structural capacities by using the diffusion theory. Instead of this, the authors have tried to investigate the applicability of a calculation model to predicting the progress of deterioration by analyzing the variation of visually observed deterioration grades with the Markovian chain model (Yokota, et al., 2006b). This approach is of use to understand the overall tendency of deterioration in consideration of its variation by the experienced progress of deterioration. In the model, the state and the transition are main components, and a probability of shifting from a certain state to the next state is expressed by a transition probability. A structural member (slab or beam) belongs to a certain grade of deterioration; the present grade of deterioration shifts to the next grade in a time step with a certain transition probability while the other structural members remain in the present deterioration grade with the remaining probability. When a transition probability is determined with good accuracy, the overall trend of future deterioration can be predicted. The example of application is shown in Figure 8. This figure shows collected data from all the structural members in a specific port, in which the transition probability is obtained through fitting the actual distribution and simulated distribution. Based on the prediction result after 15 years, the number of members probably judged as Grade *a* may increase up to about 3 times.

For the application of the Markovian chain model to prediction, many data should be collected and accumulated for members under almost the same environmental and material/structural conditions.

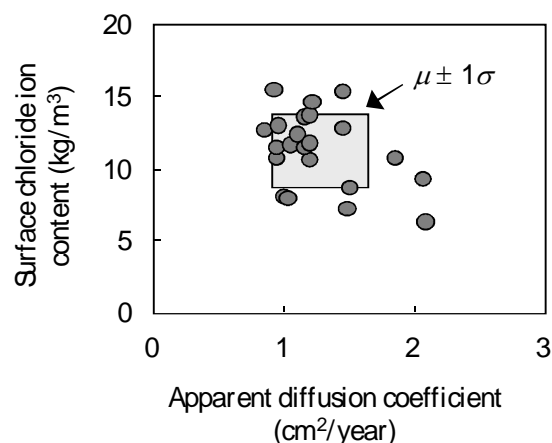


Figure 7: Variability of C_0 and D_{ap} within one slab

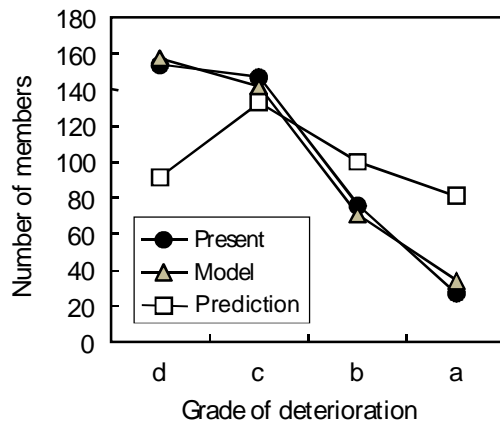


Figure 8: Prediction by Markovian chain model

4. LIFE-CYCLE COST ESTIMATION

To determine the maintenance strategy or to consider the appropriate timing and method of remedial action, estimation of life-cycle cost (LCC) is one of the best indices. LCC is calculated for several maintenance scenarios among maintenance strategies as mentioned earlier. In the calculation, the initial cost, maintenance cost including inspection cost, and the cost of planned remedial action are totaled.

An example of estimated LCC is shown in Figure 9 (Japan Society of Civil Engineers, 2007). In Strategy II, all concrete surfaces of slabs and beams are coated, and they are re-coated at the end of the life of the coating material (assumed to be 10 years in this figure). In Strategy III, the timing of repair is deferred as much as possible. When the second half of the acceleration period begins 25 years after the completion of the structure, section repair and surface coating are carried out extensively for the relatively deteriorated parts of the structure. It is assumed that the cross sections of 95% of all members are section-repaired. LCC thus calculated is expressed in terms of the ratio to the initial construction cost in the case that a general reinforced concrete superstructure within Strategy III is constructed. The social discount rate is not taken into account in the calculation.

At the end of design working life (50 years in this calculation), Strategy I has the smallest LCC even its initial cost is largest. It should be confirmed here that the more durable structure in construction, the lower LCC achieved. Since Strategy I is not likely to cause deterioration resulting in performance degradation and only primary inspection is needed, LCC at 50 years after construction is not significantly higher than the original construction cost. For the scenario considered in Strategy II, one option is to carry out coating at the beginning of construction because deterioration of structures exposed to severe environmental conditions is very fast. It should be noted that this scenario based on Strategy III shows the largest LCC and the amount of incremental increase in cost is so large that single-year costs are far larger than those for the other two scenarios.

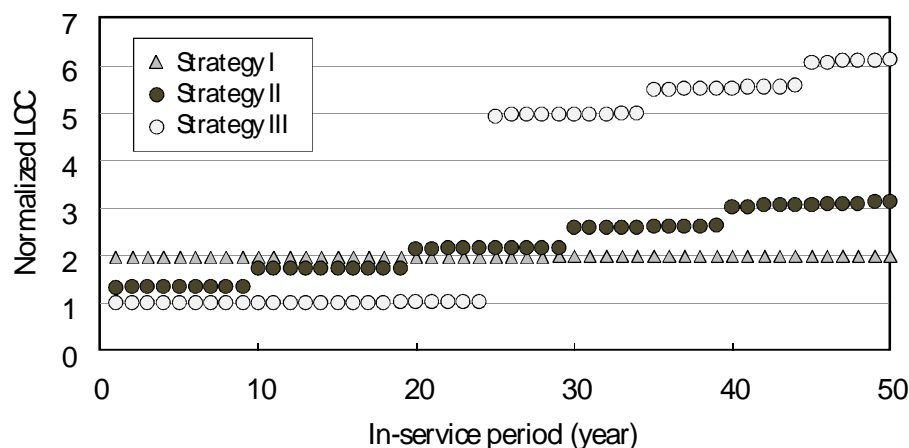


Figure 9: Example of LCC estimation for 50 years

LCC is calculated based on various assumptions, but it provides important information needed for making decisions about the future direction of maintenance. An advantage of Strategy II is that the accuracy of the initial deterioration estimation can be checked during the maintenance process so that they can be modified to more realistic predictions. Another advantage is that maintenance cost can be equalized more or less because necessary funds can be prepared in advance. Strategy III should be avoided from the viewpoint of LCC. If neither Strategy I nor Strategy II can be used for some reason, it is necessary to draw up funding and technical plans in advance. In Strategy III particularly, various problems may arise with the progress of deterioration, affecting the conditions under which the structure is to be used. It is, therefore, necessary to determine the best timing for taking measures through regular inspections.

LCC calculated here can be a useful indicator by which an appropriate scenario can be selected according to the determined maintenance strategy. Durability verification results obtainable at the design stage, however, have large safety margins because of considerable variability at the design stage. A deterioration investigation of open-type wharf, for example, showed that in many cases the corrosion of reinforcement did not occur even when chloride ions accumulate far exceeding the threshold chloride ion concentration. It is necessary, therefore, to draw up maintenance plans with full understanding of this variability and assumption of deterioration predictions. It is essential to take proper maintenance measures during the service life of the structure instead of unquestionably believing the estimates.

5. CONCLUDING REMARKS

The life-cycle management system including prediction of the progress of deterioration was developed and being implemented for maintenance of port and harbor structures in Japan. After modification of the original system, the authors expect that rational and effective maintenance is realized so that LCC reduction and performance maximization can be attained.

REFERENCES

Japan Society of Civil Engineers, 2007. *Example of Design Calculations Based on JSCE Standard Specifications for Concrete Structures*. JSCE Guidelines for Concrete, No.10.

Port and Airport Research Institute, 2007. *Manual on Maintenance and Rehabilitation of Port and Harbor Facilities*, Coastal Development Institute of Technology, in Japanese.

Yamaji, T., Mohammed, T. U., Aoyama, T., and Hamada, H., 2001. Effects of Exposure Environment and Cement Types on Durability of Marine Concrete, *Proceedings of the Japan Concrete Institute*, Vol.23, No.2, 577-582, in Japanese.

Yokota, H., 2006. Variability in Chloride-Induced Deterioration of Marine Concrete Structures, *Proceedings of International Seminar on Durability and Lifecycle Evaluation of Concrete Structures-2006*, Hiroshima, 41-50.

Yokota, H., Iwanami, M., Kato, E. and Takahashi, H., 2006a. Prediction of Performance Degradation of RC Members Due to Chloride-Induced Deterioration, *Proceedings of the 10th East Asia-Pacific Conference on Structural Engineering & Construction (EASEC-10)*, Bangkok, 493-498.

Yokota, H., Komure, K., and Takahashi, H., 2006b. Lifecycle Management of Concrete Deck by Markov Model. *Lifetime Engineering of Civil Infrastructure*, Edited by Miyamoto, A. et al., 137-149

VARIATION OF CORROSION CHARACTERIZATION OF REINFORCING BAR IN EXISTING RC STRUCTURE

EMA KATO¹, MITSUYASU IWANAMI², HIROSHI YOKOTA³
Port and Airport Research Institute, Japan
katoh-e@pari.go.jp

TAKUMI SHIMOMURA
Nagaoka University of Technology, Japan

ABSTRACT

It is important to characterize the corrosion profile of a reinforcing bar embedded in concrete when it is suffered from chloride-induced deterioration. In a real structural member, a reinforcing bar is not uniformly corroded, which results in very wide variations in its cross-sectional loss along its axial direction. The mechanical properties of corroded reinforcing bar may be affected by the wide variation. However, an actual corrosion profile has been rarely investigated in real structures and information on the variation has been insufficiently accumulated.

In this paper, corrosion profiles of reinforcing bars were investigated for real reinforced concrete slabs of open-type wharf that has been in service under marine environment for 29 years. Through the tests and analyses, the variation of corrosion characterizations and mechanical properties of corroded reinforcing bars are discussed.

1. INTRODUCTION

When reinforced concrete structures are located in coastal and offshore areas, the most important deterioration phenomenon to which attention should be paid in design and maintenance is corrosion of reinforcement embedded into concrete. Corrosion of reinforcement can initiate cracks of concrete due to the volume expansion of corrosion products. Such cracks may accelerate the further progress of corrosion, and subsequently structural performance such as load carrying capacity and ductility will be deteriorated (Kato, et al., 2006). However, the relationship between the degree of corrosion of reinforcement and structural performance of concrete members has not yet been quantitatively evaluated. During regular maintenance work of harbor structures, generally, the appearances of concrete members are visually observed and are subjectively evaluated based on the deterioration grade specified in the manual (Port and Airport Research Institute, 2007).

Many researchers and engineers are now actively studying the remaining structural capacities and producing a lot of useful results on them with testing artificially deteriorated reinforced concrete members. However,

in a real structural member, a reinforcing bar is not uniformly corroded compared with an artificially corroded one. Moreover, the mechanical properties of corroded reinforcing bar may be affected by the non-uniformity of corrosion.

In this paper, corrosion profiles of reinforcing bars were investigated for several real reinforced concrete slabs of an open-type wharf that has been in service under marine environment for 29 years. Through the tests and analyses, the variation of corrosion characterizations and mechanical properties of corroded reinforcing bars are discussed.

2. METHODS OF INVESTIGATION AND TEST

2.1 Outline of slabs extracted from RC deck of pier

Two slabs, slab A and Slab B, were extracted from an open-type wharf located in the splash zone at Japan Sea. After service for 29 years, they were replaced by new slabs because many cracks and delamination of cover concrete were observed on the bottom surfaces. The details of the materials used, such as the mix proportion of concrete and the strength of reinforcing bars, are not available because of lack of design and execution records. The two slabs were identical in their dimensions (300mm thick, 900mm wide, and 2000mm long). In each slab, two layers of round bars of 13mm in the diameter were embedded in the concrete. Average cover thicknesses of both slabs are listed in Table 1. Figure 1 shows the surface appearances of the bottoms and location of the bottom layer reinforcing bars. Some cracks along the bottom layer reinforcing bars and some random cracks were observed in slab A. In slab B, probably because of poor casting work, there was a large honeycomb area. In other areas, corrosion cracks along the steel bars and delamination of cover concrete were observed. Average compressive strength of concrete was 42N/mm^2 , which was obtained from test for concrete cylinders cored from non deterioration parts. Symptoms relating to ASR deterioration were not observed in both slabs.

Table 1: Position of reinforcing bar from the bottom surface.

Location	Axis	Slab A	Slab B
Bottom layer	X	39	38
	Y	53	54
Top layer	X	151	152
	Y	146	157

(mm)

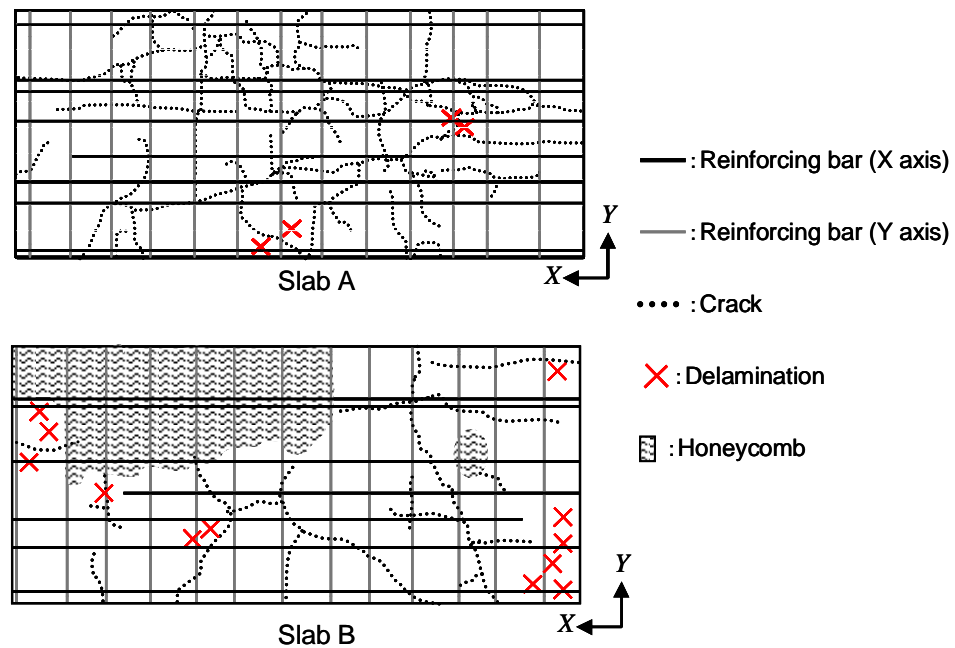


Figure 1: Bottom surface of RC slabs

2.2 Method of investigation for corrosion property

2.2.1 Weight loss of steel bar

The bottom layer reinforcing bars were taken out from the slabs and their weight losses were measured with the following procedures: at first, the bar was cut into small pieces with 100mm long and sand blasted to remove corrosion products and concrete sticking on its surface. Then, the piece was immersed in 10% diammonium hydrogen citrate solution to completely remove corrosion products. The weight loss of piece was obtained by comparing its weight with that of a non-corroded piece. If the corrosion products were not observed on the surface of a piece, the piece was considered to have no corrosion (weight loss=0.0%). The total numbers of piece were 265 in slab A, which were sampled from 8 reinforcing bars in the longitudinal (X) direction and 13 bars in the transverse (Y) direction, and 249 in slab B, which were sampled from 7 bars in X direction and 13 bars in Y direction.

2.2.2 Distribution of cross-sectional area of steel bar

For a total of 27 pieces chosen at random, surface geometries were measured using laser-scanning machine. Outline of the measurement is shown in Figure 2. The surface geometry measurement was conducted separately for the lower and upper halves of piece. The measurement length was 60mm. Measurement pitches were set at 0.5mm in the cross-sectional direction and 1.0mm in the axial direction. Distribution of cross-sectional area of each piece was obtained by integrating the laser irradiation distances in the cross-sectional direction of lower and upper halves. The measured cross-sectional area is probably not exactly the same as the real cross-

sectional area because the interference of the pit-hole corrosion. Figure 3 shows three examples of the distribution of cross-sectional area. Its nominal cross-sectional area is 132.7mm^2 if not corroded.

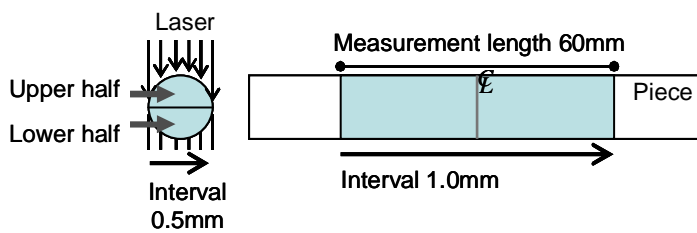


Figure 2: Outline of laser measurement

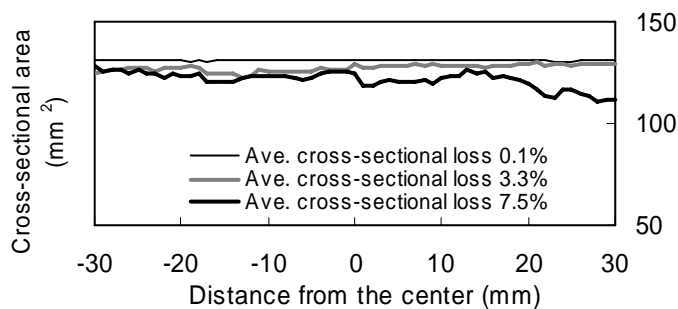
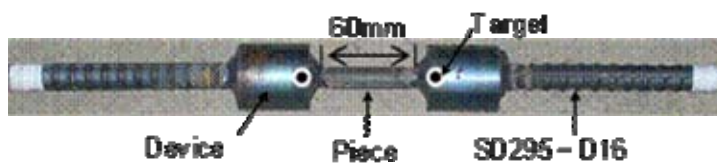


Figure 3: Distribution of cross-sectional area

2.3 Measurements of mechanical properties of steel bar

The tension test was conducted to obtain yield and tensile strengths and elongation of the piece after the cross-sectional area measurement. Picture 1 shows the testing specimen prepared for the tension test. Two deformed bars (SD295-D16) of 150mm long were welded to both ends of the piece with 20mm long lap. The total length of the piece for the tension test was about 60mm. Targets for the elongation measurement were set to near the end of the welding device as shown in Picture 1. Three pieces which were failed by slipping out from the welding device were excluded from the following discussion.



Picture 1: Testing specimen for tension test

3. CHARACTERIZATION OF REINFORCEMENT CORROSION

3.1 Variation of weight loss

Figures 4 and 5 show the distribution of the weight loss of bottom layer reinforcing bar in slabs A and B, respectively. They were drawn with the measured results of corresponding pieces. The directions of X and Y in these figures are shown in Figure 1. In slab A, the maximum weight loss is

observed in the cracked part along the longitudinal bar. Those cracks were considered to accelerate the corrosion of reinforcing bars in Y axis. In slab B, weight loss due to corrosion was remarkable in the honeycomb parts. Figure 6 shows the relationship between cover depth and weight loss. In addition, weight losses corresponding to the honeycomb parts were excluded in the figure. Though the effect of crack on the corrosion rate cannot be ignored, the weight loss due to corrosion tended to decrease as the cover depth increases. This result agrees with the basis of durability design of RC structure. In addition, the previous research by Tsutsumi, et al. also reported the same result (1996). Hence, it was reconfirmed that depth and quality of cover concrete played important roles in maintaining the durability of RC structures.

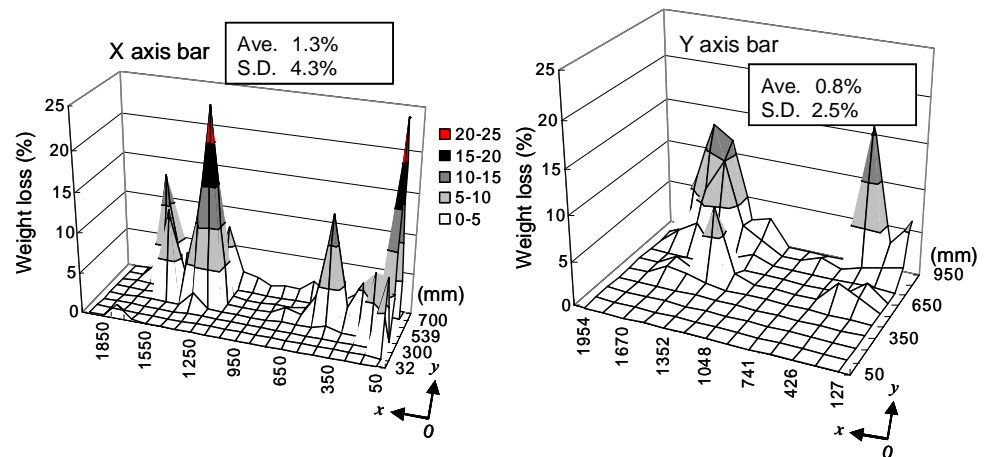


Figure 4: Weight loss distribution in slab A

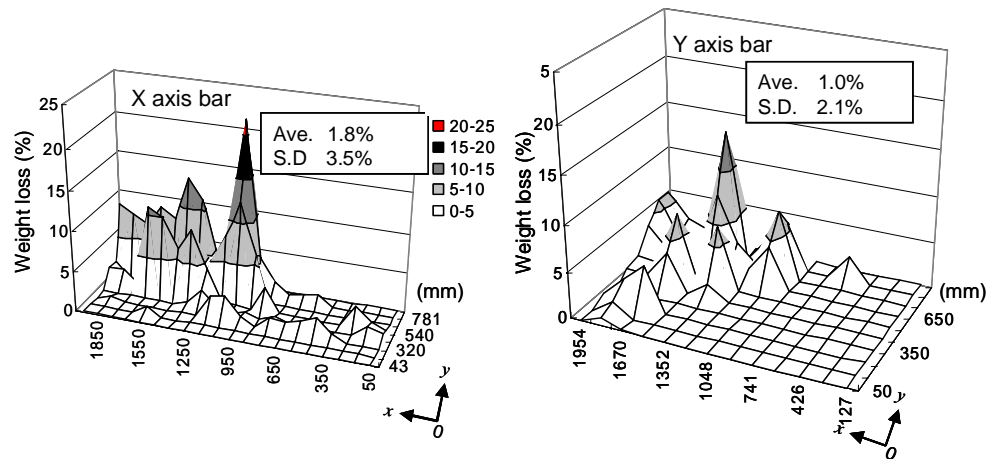


Figure 5: Weight loss distribution in slab B

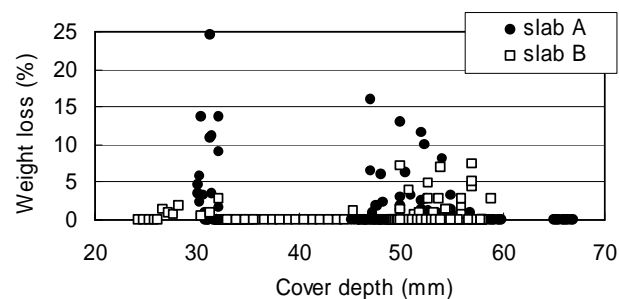


Figure 6: Cover depth vs. weight loss

3.2 Variation of cross-sectional loss

Figure 7 shows the relationship between average cross-sectional losses of piece in lower and upper halves of the bottom layer reinforcing bar. The average cross-sectional loss in the lower half was larger than that in the upper half. This was considerably caused by the influence of the interfacial transition zone formed due to bleeding.

Figure 8 shows the relationship between average and maximum cross-sectional losses. Based on the linear approximation, the maximum cross-sectional loss was 2.3 times of the average one. This value was slightly larger than that reported in the previous research by Ooyado, et. al (2005). The difference is considered to be caused by the differences in the corrosion methods and the surface geometries of reinforcing bar.

Figure 9 shows the relationship between the average cross-sectional loss and the coefficient of variation in cross-sectional area. The coefficient of variation becomes large as the average cross-sectional loss increases.

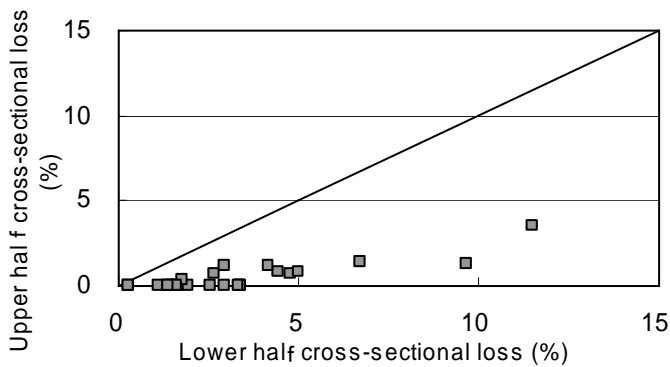


Figure 7: Cross-sectional loss in lower and upper halves of pieces

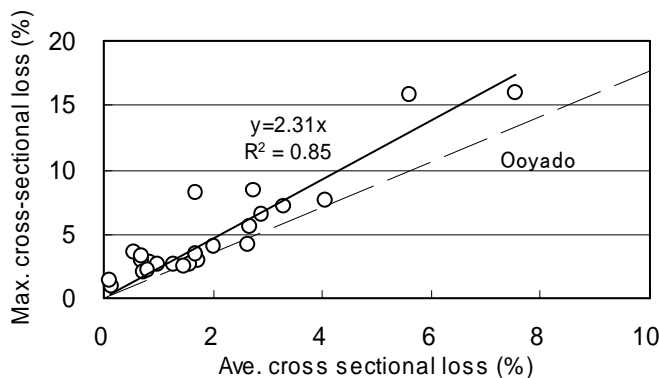


Figure 8: Average and maximum cross-sectional losses

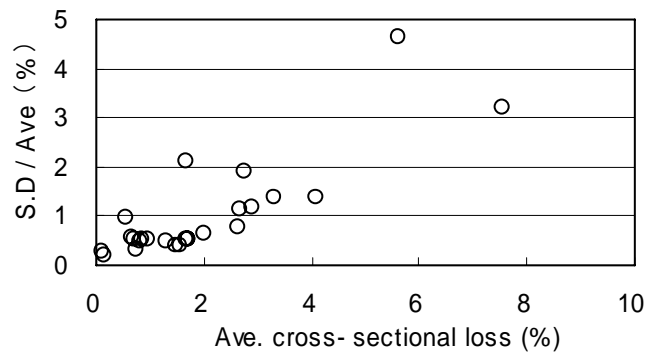


Figure 9: Variation of cross-sectional losses

4. INFLUENCE OF CORROSION ON MECHANICAL PROPERTIES

Mechanical properties of corroded reinforcing bars were usually evaluated by the weight loss because of its easiness for measurement. However, the weight loss was considered to be insufficient as a corrosion index because the surface geometry of corroded reinforcing bar was varied as shown in Figure 3. In this study, mechanical properties of corroded reinforcing bar were examined with consideration of the variation in cross-sectional loss.

Figure 10 shows the relationship between average cross-sectional loss and yield and tensile strengths of piece. Yield and tensile strengths were calculated by dividing yield and tensile loads by the minimum cross-sectional area; in other words, the maximum cross-sectional loss. Straight and broken lines show approximations obtained by the least square method and the range of $\pm 20\%$ from the approximate value respectively. Because the theoretical strength of reinforcing bar does not depend on its cross-sectional area, the inclinations of approximate lines are considered to be 0.

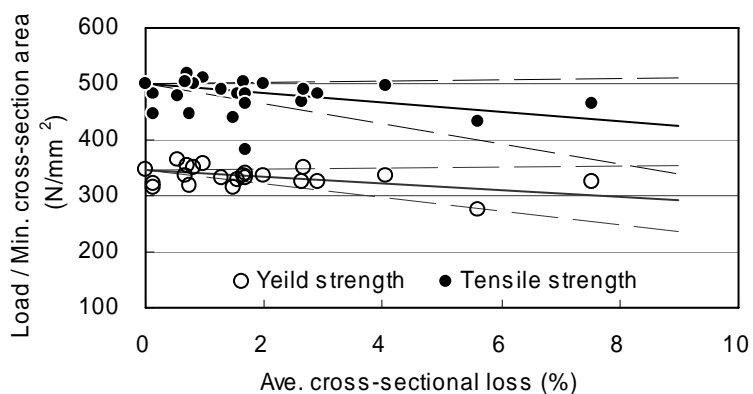


Figure 10: Average cross-sectional loss vs. strengths

Figures 11 and 12 show the relationships between average and maximum cross-sectional losses and elongation, respectively. In Figure 11, the relationship between average weight loss and elongation reported by Kobayashi (2006) was also presented. The elongation became small as the cross-sectional loss increases, and the effect of corrosion on the elongation was larger than that on the strengths. Kobayashi (2006) also reported the same conclusion. However, the relationship between cross-sectional loss and elongation was more widely distributed compared with that between cross-sectional loss and strength.

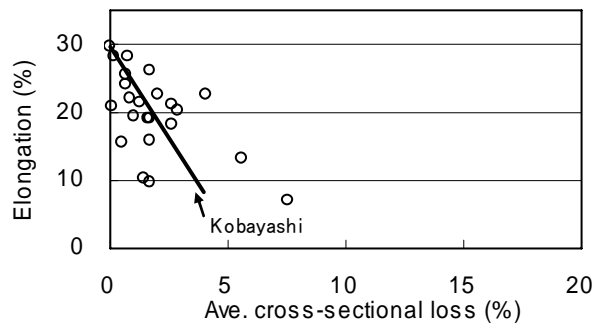


Figure11: Average cross-sectional loss vs. elongation

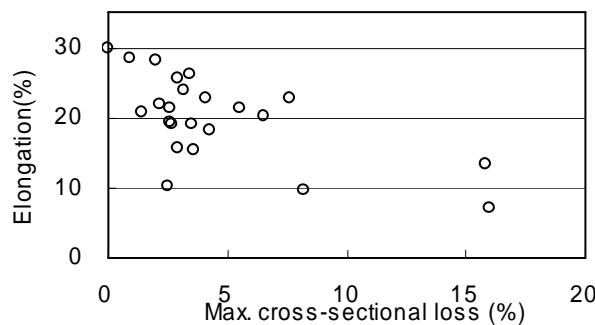
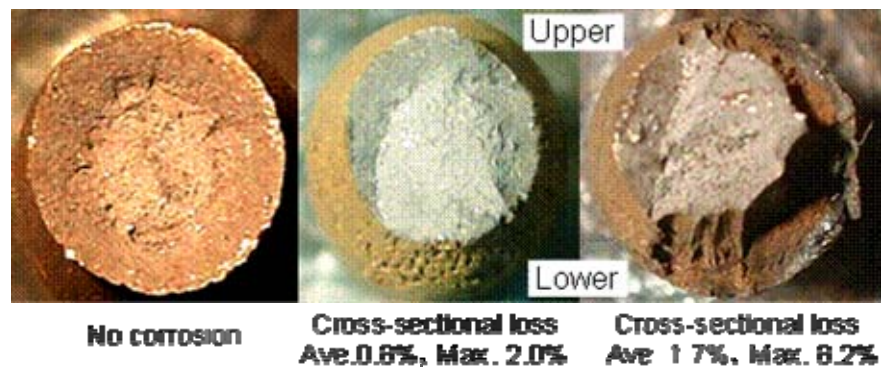


Figure12: Maximum cross-sectional loss vs. elongation

Picture 2 shows the cross-sections at breaking location. In the case of sound piece, because the cross-section was not lopsided, the tensile stress was considered to distribute uniformly on the cross-section. On the other hand, the cross-section of corroded piece was asymmetry even though the cross-sectional loss was small. According to the previous research on fatigue property of corroded reinforcing bar by Moriwake, et al. (1996), uneven cross-section due to corrosion caused a crack under fatigue stress, and consequently, the progress of that crack greatly influenced on the fatigue property. Though the way of current loading test was different from fatigue test, the lopsided stress seemed to have effects on the yield and tensile strengths and elongation. Therefore, the mechanical properties of corroded reinforcing bar are significantly affected by the unevenness of cross-sectional area. In this study, the cross-sectional loss in the lower half of piece was larger than that in upper half as mentioned in 3.2. This fact was considered to affect the yield and tensile strengths. Moreover, because this

effect considerably became large after yielding, as a result, the variation of the elongation was relatively large as shown in Figure 12.



Picture 2: Cross-section at breaking location

5. CONCLUSIONS

- 1) The weight loss of reinforcing bar in slabs of open-type wharf showed extremely large variations along the axis of bar.
- 2) The cross-sectional loss of the lower half of piece was larger than that of the upper half because of the existence of the interfacial transition zone formed due to bleeding.
- 3) Unevenness of cross-sectional loss had an influence on the mechanical properties of piece because of the lopsided action of tensile stress.

REFERENCES

- Kato, E., Iwanami, M. and Yokota, H., 2006. Deterioration in ductility of RC beams with corroded reinforcement, *Proceedings of the 2nd Fédération Internationale du Béton Congress*, Naples.
- Kobayashi, K., 2006. The seismic behaviour of RC member suffering from chloride-induced corrosion, *Proceedings of the 2nd Fédération Internationale du Béton Congress*, Naples.
- Ooyado, M., et al., 2005. Evaluation of bending strength of corroded reinforced concrete members, *RTRI report* 19(12), 4-9. (in Japanese)
- Port and Airport Research Institute, 2007. Manual on maintenance and rehabilitation of port and harbour facilities, Coastal Development Institute of Technology. (in Japanese)
- Tutsumi, T., et al., 1996. Evaluation on parameters of chloride induced damage based on actual data in situ, *Journal of Materials, Concrete Structures and Pavement*, 544(V-32), 33-41. (in Japanese)
- Moriwake, A., et al., 1996. Estimation of fatigue life of reinforced concrete members deteriorated by chloride attack, *Proceeding of the Japan Concrete Institute* 18(2), 1529-1534. (in Japanese)

EVALUATION OF THE SEISMIC VULNERABILITY OF BANGLADESHI RC BUILDING USING NON-DESTRUCTIVE TESTING

SYED ZILLUR RAHMAN¹, MEHEDI AHMED ANSARY²,
MUNAZ AHMED NOOR³, RAJAN SAHA⁴
Department of Civil Engineering, BUET, Dhaka, Bangladesh
ansary@ce.buet.ac.bd

HISASHI KANADA¹, MIHO YOSHIMURA²,
KIMIRO MEGURO³, TAKETO UOMOTO⁴
ICUS, IIS, The University of Tokyo, Japan

ABSTRACT

Bangladesh has long been believed to be a country with medium seismic hazard. But the practical design and analysis of buildings have not paid attention to seismic aspects. However, in recent years many reliable reports have revealed that Dhaka, the capital city of Bangladesh, has a potential risk from distant earthquakes to amplify the ground motion. For this reason the seismic design and analysis of buildings cannot be neglected any more. Nevertheless the dynamic properties of the buildings, which are important to seismic design and analysis, have been limitedly studied in Bangladesh. The objective of the study was to assess the vulnerability of Bangladeshi buildings using non-destructive testing, namely microtremor measurements and Ferroskan. For this purpose, 18 reinforced concrete (RC) buildings were surveyed mainly within BUET campus. This paper presents the information of surveyed buildings including findings of reinforcement detailing and microtremor analysis of buildings. Using Ferroskan, reinforcement diameter and location within the RC buildings were detected. Microtremor measurements were used to determine the predominant period of RC buildings.

Earthquake vulnerability of the surveyed buildings was assessed based on: 1) the possibility of resonance in case of an earthquake, i.e. whether the structure natural period was close to that of the soil; 2) the construction quality, based on whether reinforcement arrangement and concrete strength followed the design drawings; and 3) structural irregularities, based on visual inspection. The natural period of some buildings was found to be close to that of soil, so their seismic response may be considerably amplified during an earthquake. Results obtained from Ferroskan survey showed that the reinforcement did not match the design detailing. Cover and spacing of lateral ties in columns and stirrups in beams widely vary from design. Empirical correlation between number of story and natural period of buildings with RC frame was also proposed.

1. INTRODUCTION

The aim of this study is to detect the earthquake vulnerability of Bangladeshi RC buildings by means of determining the location of the reinforcement and their spacing and Microtremor observation. So there are mainly two parts of the study. They are

- Microtremor measurement
- Detection of reinforcement

The importance of dynamic properties of buildings become paramount when seismic design of the buildings is considered. This is because the response of structures mainly depends on the characteristics of both excitation forces and dynamic properties of buildings. In this regard, in order to design and analyze the earthquake resistant buildings, it is necessary to identify the dynamic properties of the buildings. For instance, the fundamental frequency is employed to determine the site-structure resonance factor in the base shear formula used in the static approach of many earthquake codes. In general, the approaches to the identification the dynamic properties of buildings can be categorized into three main approaches: (1) empirical, (2) numerical analysis, and (3) direct measurement approaches. The empirical approach provides simplified formulas for estimating the fundamental periods of buildings in terms of geometric dimensions of the buildings. The second approach, the numerical analysis, is normally used during the design process. A finite element model of the building, which consists of the mass and stiffness matrices of the system, is first formulated. Dynamic properties such as natural frequencies and vibration mode shapes are obtained by the Eigen analysis. The third approach is the direct measurement approach, which first measures dynamic responses of existing buildings, and then identifies their dynamic properties from the measured responses.

On the other hand, detection of reinforcement includes number of reinforcement, spacing of reinforcement, and cover over the reinforcement etc. Ferroskan is used to determine this reinforcement details. The determination of reinforcement in RC building is very important for earthquake resistant. These buildings include academic buildings, residential buildings, schools, students' dormitory and fire stations. Most buildings are within BUET campus in Dhaka, Bangladesh.

2. METHODOLOGY

To identify the dynamic properties of buildings, the empirical approach is normally considered practical and widely used in a preliminary design process. This is because it is convenient to estimate these properties by simple empirical formulas, which are provided by building codes in seismic provisions. However, empirical formulas, which are recommended in many countries, are different because the required level of design force and the characteristics of building construction in different countries are different.

As a result, the empirical formula based on the statistical data of measured dynamic properties in one country may not be valid to another country. Therefore, the numerical analysis approach, which normally uses a finite element model, may be employed to solve this problem. Design engineers have to incorporate all appropriate modeling assumptions to represent the real behaviors of buildings in order to identify accurate dynamic properties. In practice, many design engineers usually formulate the finite element model of the buildings with structural members such as beam, column, and shear wall members and they normally assume that the foundations of the buildings behave like a rigid foundation type (all degrees of freedom are constrained at ground level of first floor columns). However, above modeling, which considers only the structural members and the rigid foundations, is not appropriate to identify the dynamic properties of buildings because the dynamic properties mainly depend on the total stiffness of the buildings, which is also influenced by the stiffness of non-structural members, and the flexibility of the foundations. In order to identify correct dynamic properties, the most accurate approach is the direct measurement approach because the properties are derived from actual dynamic response of existing buildings.

In recent years, several direct measurement techniques for determining the dynamic properties of structures have been developed. These techniques can be categorized into three basic methods 1) forced vibration method, 2) free vibration method, and 3) ambient vibration method. Among these techniques the ambient vibration measurement is the most attractive option. The signal processing techniques can be categorized into time domain and frequency domain techniques. In the time domain technique, response-time history is employed directly in the identification of dynamic properties of structures. While in the frequency domain technique, response-time history has to be firstly converted into frequency domain by Fourier analysis. Dynamic properties are then extracted from the frequency spectrum, which is the plotting of Fourier magnitude response against frequencies. Although both techniques can be employed to identify the dynamic properties of buildings, the frequency domain technique gives a better physical interpretation than the time domain technique because it presents the response of buildings in the form of the frequency spectrum. This frequency spectrum can be used directly to identify natural frequencies from the frequencies corresponding to the peak values of Fourier magnitude and calculate vibration mode shapes from the spectral ratio method. In addition, an algorithm in the time domain technique is more complicated than frequency domain technique, which provides the algorithm in the form of Fast Fourier Transform (FFT).

Detection of reinforcement includes number of reinforcement, spacing of reinforcement, and cover over the reinforcement etc. Ferroskan is used to determine this reinforcement details. Ferroskan works through electromagnetic method. When electric current run through a coil of the apparatus, magnetic field is formed. Due to the magnetic field, electric current run in the steel bar. Due to induced electric current in steel bar, magnetic field is formed around the bar. The field induces electric current in

the secondary coil to be measured. When electric current runs through a coil of the electro-magnetic sensor, magnetic flux is measured. Electric current runs in steel bar due to magnetic flux produced by coil of sensor. Electromotive force of coil changes. Thickness of cover concrete or diameter of steel bar can be estimated from magnetic flux change. Induced magnetic field depends on the distance between sensor and reinforcement. When bars are too close, it becomes difficult to differentiate the numbers of bar. Principles of the method are used in Ferroskan.

3. MICROTREMOR MEASUREMENT

Soil characteristics can be assessed by microtremor measurement. Hard soil gives high frequency and soft soil gives low frequency. A structure may experience a vibration period at which it oscillates in the earthquake vibration motion and will tend to response to that. Natural frequency of structure is obtained based on the spectral ratio of horizontal component of the building to that of ground. Wave propagation mechanism of microtremor and its relation with ground vibration characteristics were studied from the beginning of microtremor studies (Aki, 1957; Kanai and Tanaka, 1961). Meanwhile practical application of microtremor in the field of engineering has advanced tremendously. One of the powerful and simplest applications of microtremor observation is in seismic micro zoning. Basically there are two types of microtremor observations to the number of observation points. These are point and array observations of microtremors (Ansary et al., 1996). From the array observation of microtremor of period greater than 1 sec, Rayleigh-wave and Love-wave originating from natural sources, such as sea wave, variation of air and wind pressure can be recognized. On the other hand short-period microtremor of period less than 1 sec is thought to be generated by artificial noises such as traffic vehicles, industrial plants, household appliances, etc. Some researchers (Sato et al., 1991; Tokimatsu and Miyadera, 1992; Tokimatsu et al., 1994) have showed that microtremors are mainly composed of fundamental mode of Rayleigh-wave and some (Nakamura, 1989; Wakamatsu and Yasui, 1995) have showed that short-period microtremor bears resemblance to shear-wave characteristics. On the other hand, micro tremors can also be dominated by Love-wave (Tamura et al., 1993). Recently, Suzuki et al. (1995) have applied microtremor measurements to the estimation of earthquake ground motions based on a hypothesis that the amplitude ratio defined by Nakamura can be regarded identical with half of the amplification factor from bedrock to the ground surface. However, the real generation and nature of microtremors have not yet been established.

4. PROCEDURE

For Microtremor observation, the team members fix the sensors first. They tried to fix one sensor at the roof top of the building, one at the free field near the building and other at any floor level of the building. In some building the team cannot place one sensor at the rooftop, and then they place

it at the top floor level of the building. Sometimes they have to take observation of two building together to save time. After taking the observation with the help of a program the time domain velocity data is converted to frequency domain data and find out the natural period of the buildings. For Ferroscon observation the team identified the column and marked them in drawing as well as in the structural part of the building. Then they scan it carefully with the scanner and store the data. The collected raw data were analysed with the help of the ferroscon software. Microtremor measurement instrument and Ferroscon instrument are shown in Figure 1.



Figure 1 (a): Microtremor equipment with Battery, 3-component velocity sensor, GEODAS-10-24S

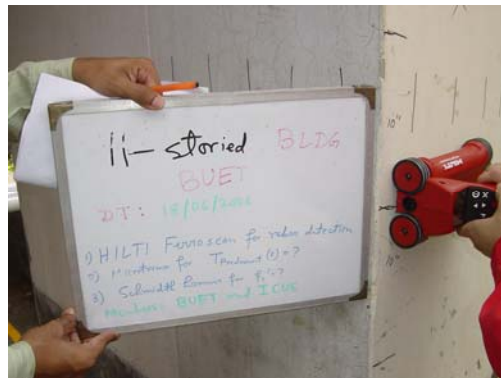


Figure 1(b): Marking of reinforcement placement at a column of 11 story Tower building

5. DETECTION OF EARTHQUAKE VULNERABILITY OF BUILDINGS

There are totally 84 buildings owned by BUET. The team studied all RC buildings which cover academic buildings, Residential buildings, and Student's Dormitories of BUET campus. Academic buildings include Civil Engineering Building, EME Building, Architecture Building, URP Building, ARC Building, Library Building, IFCDR Building, Controller Building and New Academic building (under construction). Residential buildings include

Eleven Story Tower Building, building number 62. Student's Dormitories include Sher-e Bangla Hall, Titumir Hall. School Building includes Engineering University School Building. The buildings exist outside the BUET campus includes Headquarters of the Forest Department and Fire Service Station (head office building at Fulbaria and a branch office at Lalbag). Earthquake vulnerability of the surveyed buildings are assessed from natural frequency obtained by analysis of microtremor data (resonance), reinforcement detection by ferroskan, concrete compressive strength by Schmidt hammer test and visual inspection (structural irregularities). An example of a observed building is given in details. Table 1 shows the information about the building. In Figure 2 structural element layout plan of 11 story tower building is shown. Figure 3 shows the Microtremor observed time domain and converted frequency domain data. The peak value clearly shows the fundamental period of the building. Figure 4, 5 and 6 show the designed and observed reinforcement details of the building. It clearly shows the variation of location and spacing of reinforcement from designed section. The predominant period of the building is not close to that of the soil, so there is no possibility of resonance. The building has major structural irregularities such as soft story and re-entrant corner. Concrete compressive strength from Schmidt Hammer Test is not satisfactory. Variation of clear cover from design is high. Spacing of lateral ties in column is not as per code. So, seismic vulnerability condition of the building is high.

6. EMPIRICAL FORMULA FOR FUNDAMENTAL PERIOD OF BUILDINGS

Most of the building codes define the magnitude of force, which should be sustained by buildings at specific stress level, related to the building period and provide the empirical formula to determine the lower bound fundamental period in order to establish the minimum load requirements. National Research Council (1995) defines that if the number of story is N then the fundamental period will be

$$T = 0.1 N$$

With this relation a graph is plotted in Figure 7. From analysis of Microtremor observations, natural periods are also obtained. Microtremor observations give lower results for frame structure type buildings than that in National Research Council. For frame structures buildings empirical relations is developed which is shown in Figure7.

Table 1: Information of Eleven Story Tower Building

<p>General Information Year of Construction: 2002 Type of Structure: Frame structure No of story: 11 Floor area: 673 sqm/floor Foundation: Footing, pile Lift: yes Stair: yes Shear wall: yes</p>	<p>Compressive Strength by Schmidt Hammer Beam: 20.0 MPa (2917 psi) Column: 20.5 MPa (3005 psi) Shear wall: not available</p>
<p>Structural Irregularities in Plan: Torsional irregularity: no Re-entrant corner: yes Diaphragm discontinuity: yes Out of plan vertical element offset: no Nonparallel system: no Structural Irregularities in Height: Storey stiffness irregularity: yes Storey mass irregularity: yes Storey geometry irregularity: no Discontinuity of structural element: no Discontinuity in capacity: no</p>	

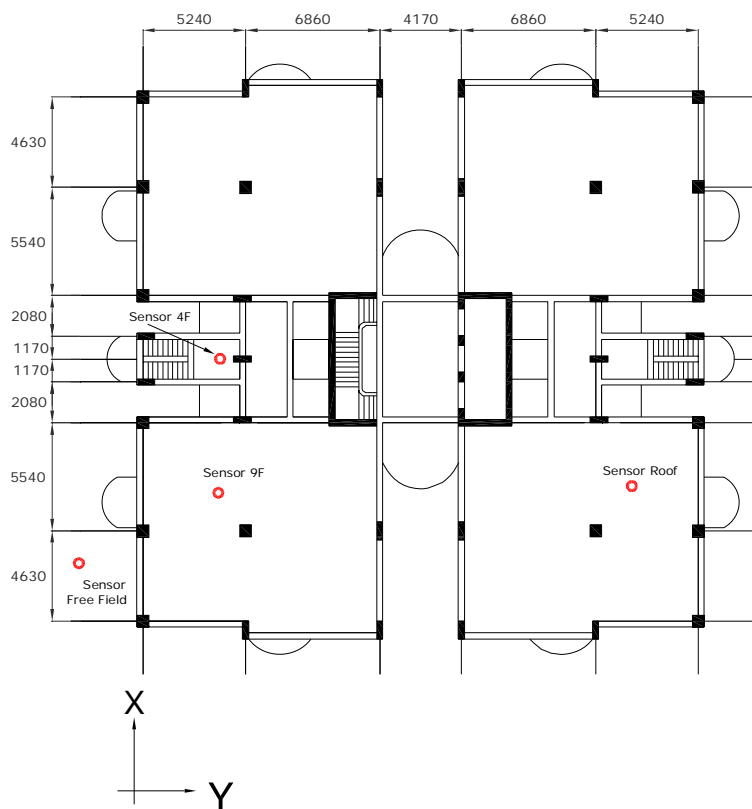


Figure 2: Structural element layout plan of Eleven Story Tower Building (linear dimensions are in millimeter)

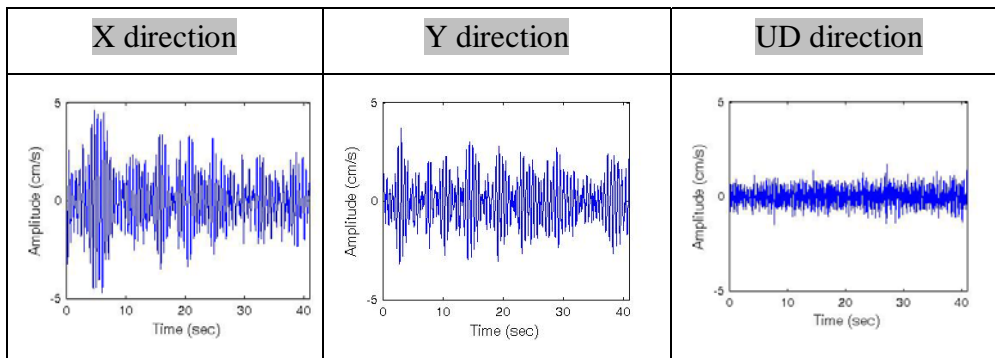


Figure 3(a) Time history of Eleven Storey Tower Building (top floor)

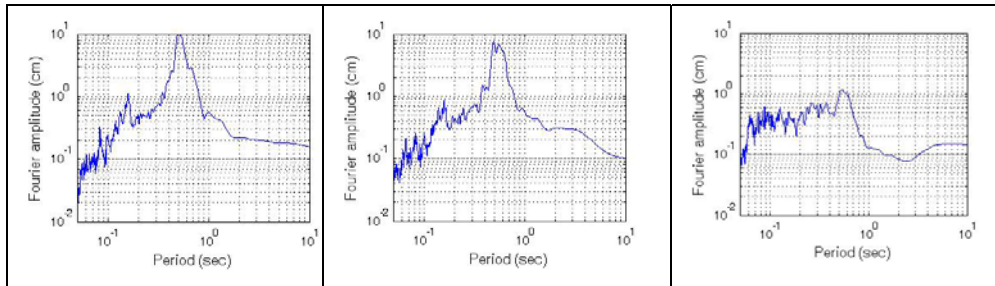


Figure 3(b) Fourier Spectrum of Eleven Storey Tower Building (top floor)

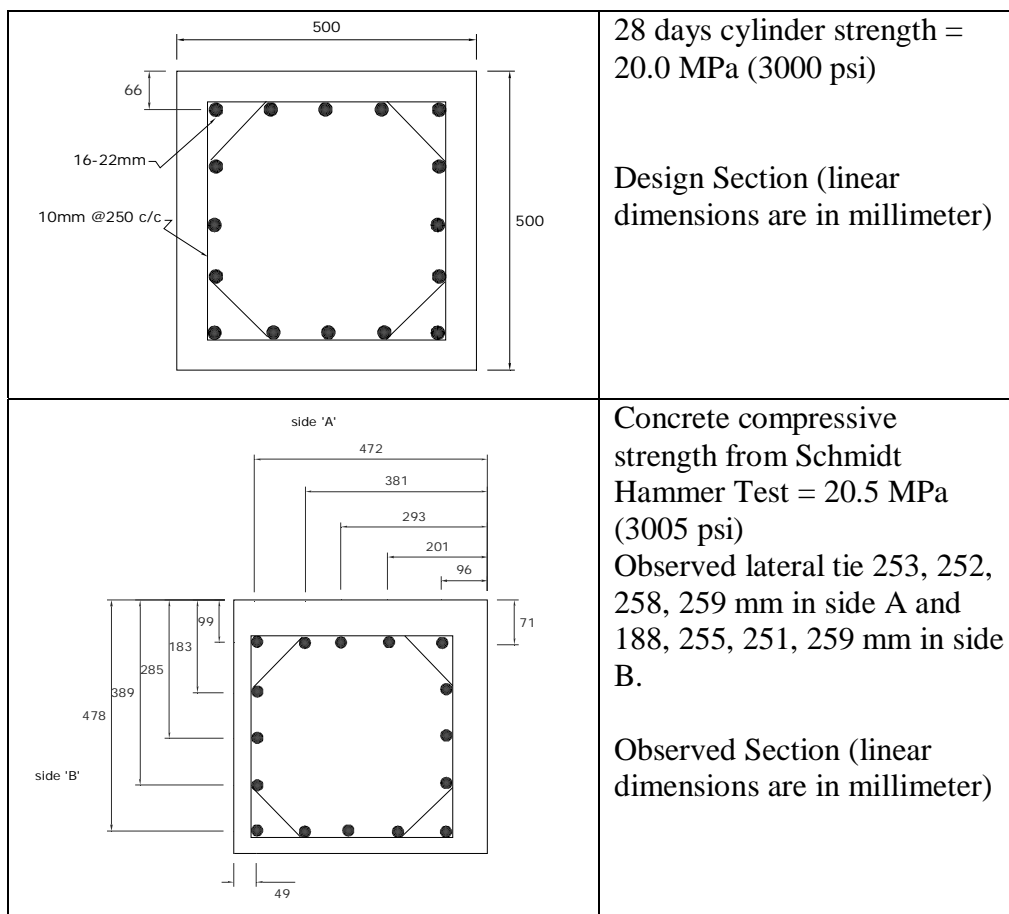


Figure 4: Designed and observed section of a typical column

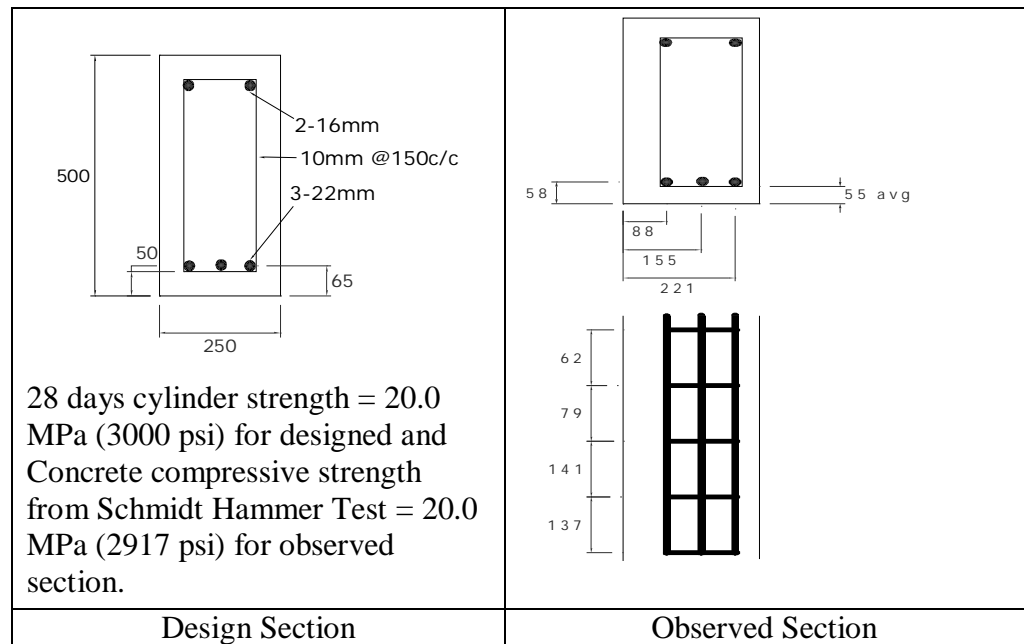


Figure 5: Designed and observed section of a typical beam

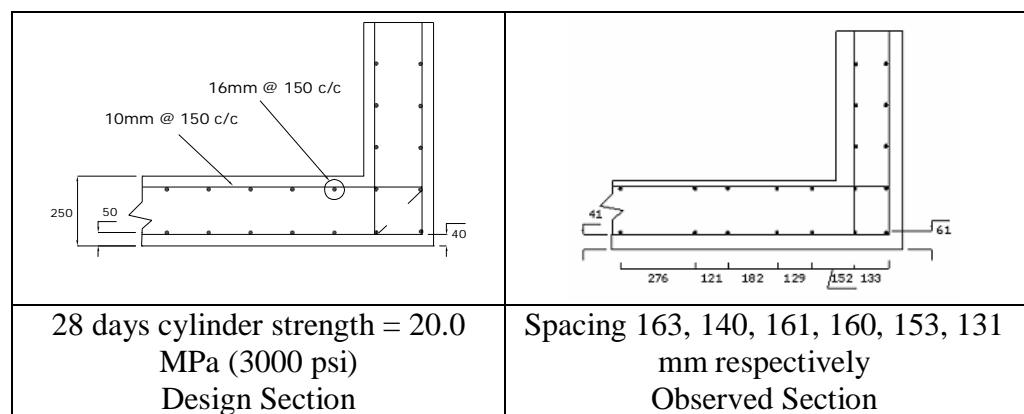


Figure 6: Designed and observed section of a shear wall (Lift Core)

Table 2: Predominant period of 11 story tower building and ground

Building name/no.	Floor level	Predominant Period of building (Sec)		Avg. Predominant Period of building (Sec)		Predominant Period of ground (Sec)	
		X	Y	X	Y	X	Y
		Direction	direction	Direction	direction	Direction	direction
Eleven-Story Tower Building	Roof	0.50	0.50	0.50	0.50	0.70	0.65
	9 th	0.50	0.50				
	4 th	0.50	0.50				

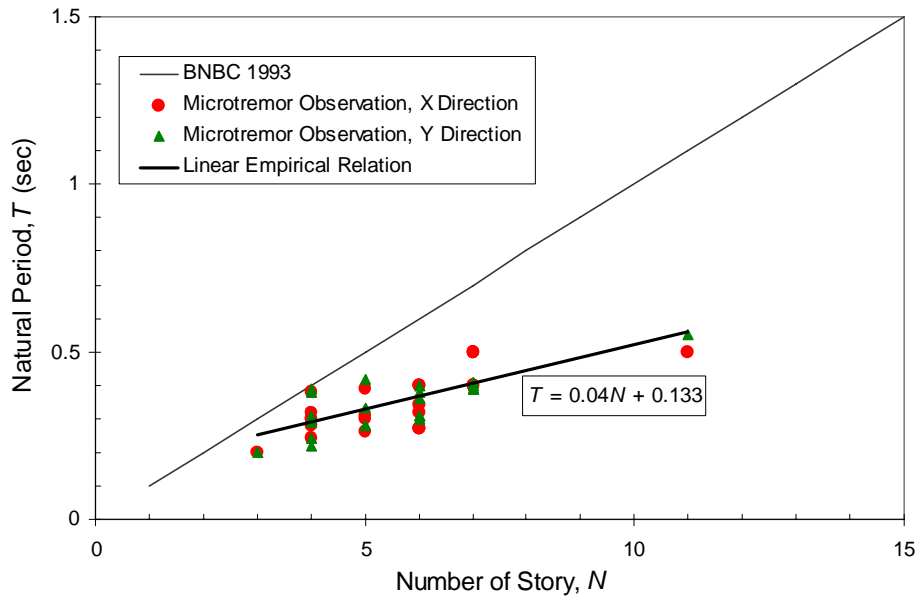


Figure 7: Empirical relation between number of story and Natural Period of surveyed RCC Buildings

7. CONCLUDING REMARKS

In this study, the dynamic properties of low and medium-rise reinforced concrete buildings with various heights within BUET campus were investigated. The controlled human excitation was applied to amplify the ambient vibration responses in order to improve the accuracy of the identification of dynamic properties. There are totally 84 buildings within BUET campus that are categorized as 15 RC building and 69 Masonry building. Also, three buildings were investigated outside BUET campus. This study covers 18 RC buildings for microtremor analysis and Ferro scan analysis. Amidst the 18 buildings, Microtremor analyses of 17 RC building were performed in details. Moreover, Ferrosan studies of 13 RC buildings were performed. Empirical correlation between number of story and natural period of RC buildings is developed.

Amidst seventeen RCC frame structure buildings natural period of four buildings are not close to that of soil, so they are out of danger of resonance and natural period of the remaining thirteen buildings are close to that of soil, so their seismic response can be considerably amplified. Among surveyed RCC frame buildings seven buildings have soft story. Results obtained from ferrosan data analysis are not satisfactory. Variation of cover and spacing of lateral ties in columns and stirrups in beam from design are above acceptable limit. Concrete compressive strength from Schmidt hammer test is found satisfactory for four buildings and unsatisfactory for nine buildings. Empirical correlation between number of story and natural period of building for RCC frame buildings is

$$T = 0.04N + 0.133 \quad \text{Where, } T = \text{Natural period of building}$$

N = Number of story

Earthquake vulnerability of the surveyed buildings are assessed from natural frequency obtained by analysis of microtremor data (resonance), reinforcement detection by Ferroskan, concrete compressive strength by Schmidt hammer test and visual inspection (structural irregularities). Amongst seventeen buildings earthquake vulnerability nine buildings is moderate and that of five buildings is high. Five buildings for which earthquake vulnerability is high, detail structural analysis is required to confirm the situation.

REFERENCES

- Aki, K. (1957). Space and time spectra of stationary stochastic waves, with special reference to microtremors, Bull. of earthquake research institute, 35, 415-456.
- Ansary, M.A., Yamazaki, F. and Katayama, T. (1996). Application of Microtremor Measurements to the estimation of site amplification characteristics, Bulletin of ERS, Vol 29, pp: 96-113.
- Nakamura, Y. (1989). A method for dynamic characteristics estimation of subsurface using microtremor on the ground surface, QR of RTRI, 30, 25-33.
- National Research Council (1995). The Building Code: Canada.
- Saha, R. (2006). Earthquake Vulnerability Assessment of BUET Buildings, Undergraduate Thesis, Department of Civil Engg., BUET, Dhaka.
- Sato, T., H. Kawase, M. Matsui, and S. Kataoka (1991). Array measurement of high frequency microtremors for underground structure estimation, proc. 4th int. conf. on seismic zonation, 11, 409-416.
- Suzuki, T., Y. Adachi, and M. Tanaka(1995). Application of microtremor measurements to the estimation of earthquake ground motions in Kushiro city during the Kushiro-oki earthquake of 15 January 1993, Earthq. Eng. Struct. Dyn., 24, 595-613.
- Tamura, T., O. Nagai, H. Kikubo, and H. Sumita (1993). Characteristics of wave group microtremors obtained by array measurement, J. Struct. Consr. Eng. AIJ 449, 83-91 (in Japanese)

DUCTILITY OF CONCRETE STRUCTURES WITH LATERAL AND COMPRESSION REINFORCEMENT

MD. SHAH AZIZ AKAND

The University of Asia Pacific, Dhaka, Bangladesh
sohoj_pl@yahoo.com

IFTEKHAR ANAM

The University of Asia Pacific, Dhaka, Bangladesh
ifteanam@accessstel.net

ABSTRACT

The paper presents results of numerical and experimental works on the effect of confining reinforcement and compression bars on the ductility of concrete cylinders and RC beams in particular. The study demonstrates the importance of lateral and longitudinal reinforcement on the ductility of RC structures, which is one of the most important parameters in their earthquake resistant design. The tests on standard concrete cylinders show that their ultimate strains are more than doubled if confined by hoop-steels at a spacing of 10 cm. Bending tests are performed on simply supported beams under third-point loading with and without compression reinforcements. The test results show that lateral reinforcements increase the crushing strains of concrete considerably while compression reinforcements ensure that there is no significant loss of member strengths even after the crushing of concrete. On the other hand, the distress and loss of strength of beams without compression reinforcements spacing is significant. The experimental load versus midspan deflection data show satisfactory agreement with numerical results in general, although the numerical simulations do not satisfactorily model the structural behavior at concrete spalling and after the crushing of concrete, particularly in the absence of compression bars.

1. INTRODUCTION

One of the primary tasks of an engineer designing an earthquake resistant building is to ensure that it possesses enough strength and ductility to withstand the size and types of earthquake the structure is likely to experience during its lifetime. Structural engineers need to understand the effect of ductility on the building response when it is subjected to earthquake force. If properly induced in the building system, ductility will improve the behavior of the building system primarily by reducing the forces in the structure. Therefore, it is an essential attribute of an earthquake resistant design of structures that serves as an energy absorber in a structure and reduces the transmitted force to one that is sustainable. At the same time, the brittle failure of several RC frame structures during earthquakes is

largely attributed to the lack of awareness or knowledge about the ductility requirement of the members among practicing engineers.

The importance of ductility and detailing of RC sections have been demonstrated for years in the works of several researchers, the more recent ones including Bertero et al. (1991), Machida et al. (1999), Engelkirk (2003). That the ductility and strength of concrete is greatly enhanced by confining the compressive zone with closely spaced lateral steel has also been demonstrated by various workers. In order to quantify the ductility of confined concrete, a number of stress-strain models for confined concrete have been derived. The importance of enhancing the ductility capacity of RC sections became well known after the 1971 San Fernando earthquake. Kent and Park (1971) developed a stress-strain model of confined concrete, followed by many others, accounting for the effect of lateral confinement.

But axial load has been found to affect unfavorably the ductility of flexural members. In fact, it has been shown that ductile failure occurs only with axial loads considerably less than the balanced load. On the other hand, compression reinforcement can increase significantly the flexural ductility of RC sections, as demonstrated by Blume et al. (1961).

2. CONTEXT AND OBJECTIVES

Ductility is perhaps the single most important factor in the earthquake resistant design and detailing of RC structures. The importance of shear and compression reinforcements in the detailing of RC structures has long been emphasized in several building codes including the Bangladesh National Building Code (BNBC, 1993). Despite the presence of a chapter (Chapter 8 of PART 6) on *Detailing of Reinforced Concrete Structures* in BNBC 1993, seismic detailing is known very little and practiced even less by the structural designers of Bangladesh. The recently published *Earthquake Resistant Design Manual* by Bangladesh Earthquake Society (Ansary & Noor, 2006) is a welcome introduction to this type of literature here. The present work is the first of its kind at The University of Asia Pacific (UAP), and perhaps in Bangladesh. Its importance can be assessed in this context.

The main objective of the current work is to study the effectiveness of lateral reinforcements/confinement as well as compressive reinforcement on the ductility of RC structures. It demonstrates results of numerical and experimental works performed at The University of Asia Pacific on the effect of shear and compression reinforcement on the ductility of concrete cylinders and RC beams (Akand, 2007).

The tests on standard (15 × 30 cm) concrete cylinders are performed by varying the spacing of confining reinforcement and studying the effect on their ultimate strains. Moreover, the stress-strain relationship of concrete and steel are modeled from the experimental data. Bending tests are performed on simply supported beams of 1.8 m span with (15 × 20 cm) sections under third-point loading with and without compression

reinforcements with stirrups at 5, 10 and 20 cm spacing. The experimental load versus midspan deflection data are compared with numerical results.

3. THEORETICAL AND NUMERICAL WORK

3.1 Material models

Among the two constituents of Reinforced Concrete, concrete is much stronger in compression than in tension (tensile strength is of the order of one-tenth of compressive strength). While its tensile stress-strain relationship is almost linear, the stress-strain relationship in compression is nonlinear. As mentioned before, several equations have been suggested to model this nonlinear relationship. Among them, the well known Hognestad model (1952) [given by Equation (1a) and (1b)] has been chosen and slightly modified in this work [Equation (2)].

$$f_c = f_c' [2(\varepsilon/\varepsilon_0) - (\varepsilon/\varepsilon_0)^2], \text{ if } \varepsilon \leq \varepsilon_0 \quad (1a)$$

$$\text{and } f_c = f_c' [1 - 0.15 (\varepsilon/\varepsilon_0 - 1)/(\varepsilon_u/\varepsilon_0 - 1)], \text{ if } \varepsilon > \varepsilon_0 \quad (1b)$$

$$f_c = f_c' [2(\varepsilon/\varepsilon_0)^{n/2} - (\varepsilon/\varepsilon_0)^n] \quad (2)$$

In this work, the maximum crushing strain (ε_u) and the strain at ultimate strength of concrete (ε_0) were found to coincide since the concrete cylinders crushed at the maximum stress f_c' and equation (1b) was not needed; i.e., the stress-strain (σ - ε) relationship was given only by a slightly modified form of equation (1a). The parameter n is calculated from best fitting the data with equation (2). The nonlinear formulation of RC beams was based on the work by Anam & Shoma (2002) incorporating geometric and material nonlinearity.

3.2 Effect of lateral confinement

Lateral confinement is one of the most important features influencing the seismic behavior of reinforced concrete. It refers to the influence that lateral reinforcement (in the form of hoops or spirals) has on concrete namely the favorable effect on ductility and strength. Mainly two types of lateral reinforcement are used to confine concrete; i.e., circular steel spirals and square or rectangular steel hoops. Tests (Aoyama & Noguchi, 1979) show that spirals are more effective than rectangular hoops regarding the favorable effect on ductility and strength.

As all the stress-strain models of confined concrete have limitations, the model by Corley (1966) has been chosen in this work for as it involves the least computational effort. This model recommends that a lower bound for the maximum strain for concrete confined with rectangular links is

$$\varepsilon_{cc} = 0.003 + 0.02 (b/L_c) + (\rho_v f_y / 138)^2 \quad (3)$$

where 0.003 represents the ultimate strain of unconfined concrete, (b/L_c) is the ratio of the beam width to the distance from the critical section

to the point of contraflexure, ρ_v is the ratio of the volume of confining steel to the volume of concrete confined and f_y is the yield strength (MPa) of the confining steel. Once the value of ϵ_{cu} is known, the ductility ratio can also be calculated for singly reinforced as well as doubly reinforced sections.

3.3 Moment-Curvature relation for RC section

The $M-\phi$ relationship of arbitrary RC sections can be derived numerically by the application of simple principles of Strength of Materials. The arbitrary area can be divided into a number of segments. For a given curvature, the position of the neutral axis is determined by trial and error; i.e., assuming a neutral axis, calculating the strain and stress at various points of the section and equating the compressive and tensile forces. Once the neutral axis is chosen, the moment M is easily calculated by summing the moments of all the forces on the section. Using the moment-curvature relationship thus specified, the load vs. deflection relationship for the third-point loading of a simply supported beam is obtained numerically.

4. EXPERIMENTAL SETUP

A significant portion of this research concentrated on the experimental work in the Structural Mechanics and Strength of Materials Lab of UAP. It primarily involved the laboratory testing of a simply supported beam under third-point loading, varying the stirrup spacing and amount of compression reinforcement. The axial stress-strain relationships of concrete cylinders and steel reinforcements were evaluated prior to the tests. Some background fieldwork was also necessary as preparation for this work, primarily involving concrete mixing, rod bending, stirrup binding as well as casting and curing of concrete cylinders and beams. Figure 1(a) and 1(b) show binding of longitudinal tensile and compressive reinforcements as well as lateral (stirrup) reinforcements.

Two sets of concrete cylinders were cast in the laboratory for the subsequent beam casting and tests. Set 1 consisted of unconfined concrete cylinders (15 cm diameter and 30 cm height) while Set 2 included unconfined as well as confined cylinders, using 4 hoops spaced uniformly over the cylinder height. Every cylinder was compacted by vibrator and cured for 60 days in Set 1 and 28 days for Set 2.

4.1 Casting of concrete beams

Set 1: There were three types of beams, each being a rectangular beam length of 1.8 m and section (15 cm \times 20 cm) but with stirrup spacings of 5, 10 and 20 cm. Two layers of rod (12 mm bars) were placed in the beam members; i.e., 2 compression rods at top and 3 tensile rods at bottom.

For Set 2: Similar to Set 1, the only difference is that it used 3 tensile rods at bottom and 2 timber bars in compression only for binding the

stirrups. As the strength and modulus of timber is of the same order as concrete's, it was used here instead of steel to better simulate the behavior of singly reinforced beams. Like the cylinders, the Set 1 beams are also cured for 60 days and Set 2 beams for 28 days.

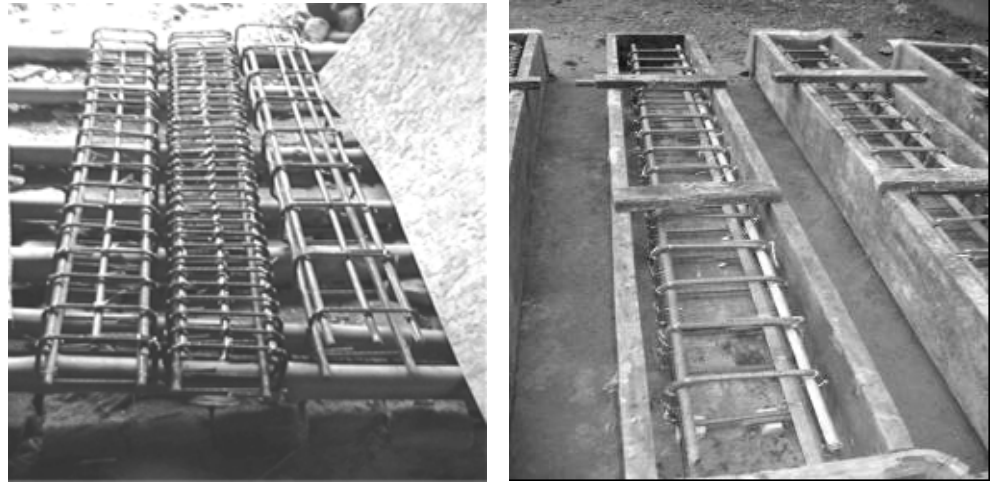


Figure 1: Rod binding with (a) Different spacing of lateral reinforcement, (b) Timber rod as compression reinforcement

4.2 Setting up beam members in the testing instrument

The 1.8 m span beam is supported by a steel I-section of similar length. However, the effective span of the beam is made 1.5 m corresponding to the distance between supports. Load is applied at the mid section and divided into two equal parts by a 50 cm simply supported bridge. Figure 2(a) and 2(b) show pictures of the experimental set up.

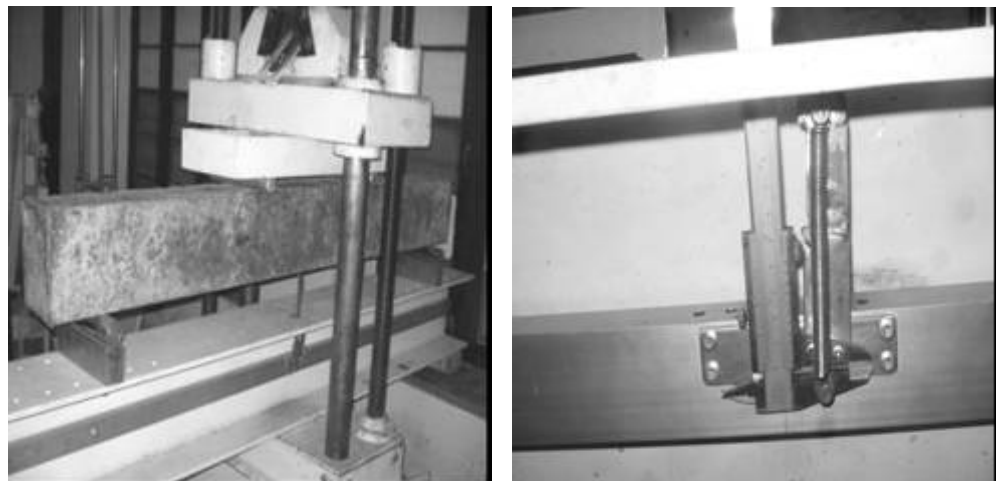


Figure 2: Experimental set up shows (a) Beam under Third-Point Loading, (b) Arrangement to measure beam deflection

5. RESULTS FROM NUMERICAL ANALYSIS AND EXPERIMENT

5.1 Effect of lateral confinement

As mentioned, the concrete cylinders of Set 2 were tested without confinement as well as after confining them with 10 mm bars (4 hoops), calculating ϵ_{c0} by modifying equation (3) slightly to incorporate the material properties and structural member used in this work. The ultimate strength of confined concrete is also calculated here analytically [Mander et. al. (1988)]. Table 1 shows that the analytical results compare reasonably well with the experimental values of concrete strength and ultimate strain.

Table 1: Effect of confinement reinforcement.

No. of Hoops	S (cm)	ρ_v (%)	ϵ_{cc} (10^{-3})		f_{cc}' (Mpa)	
			Calc	Measured	Calc	Measured
0 (Unconfined)	*	0	3.36		20.41	
4	10	2.03	6.23	7.37	23.92	23.37

5.2 Material and sectional properties for numerical modeling

Since the material properties for concrete (i.e., its strength and ductility) depend on the confining reinforcements, they need to be specified for the numerical analyses. Table 2 shows the variation of ultimate crushing strain and strength of concrete with confinement spaced at 5, 10 and 20 cm. It may be mentioned here that the unconfined strength and strain were used for the portion outside the stirrup reinforcement while the confined values were chosen for the concrete within the closed stirrups.

Table 2: Material properties for beams.

Set	Stirrup Spacing (cm)	ϵ_{cc} (10^{-3})		f_c' (MPa)	
		Unconfined	Confined	Unconfined	Confined
1	5	2.79	11.10	34.3	44.6
	10		6.12		38.4
	20		4.87		36.9
2	5	3.36	11.40	20.4	25.3
	10		6.62		22.4
	20		5.42		21.7

5.3 Experimental and numerical results for beams

As mentioned, Set 1 and Set 2 beams were tested for stirrup spacing of 5, 10 and 20 cm. Only selective load vs. deflection graphs are shown in this paper (for two extreme cases); i.e., results for three beams of Set 1 (with compression rods) with stirrup spacing of 5 cm are shown in Figure 3, while Figure 4 shows the corresponding graphs for Set 2 beams (virtually without any compression rod, i.e., with timber bars in the compression zone) with stirrup spacing of 20 cm. In both cases, Figure (a) shows the experimental graphs of the three beams and Figure (b) shows the numerical results.

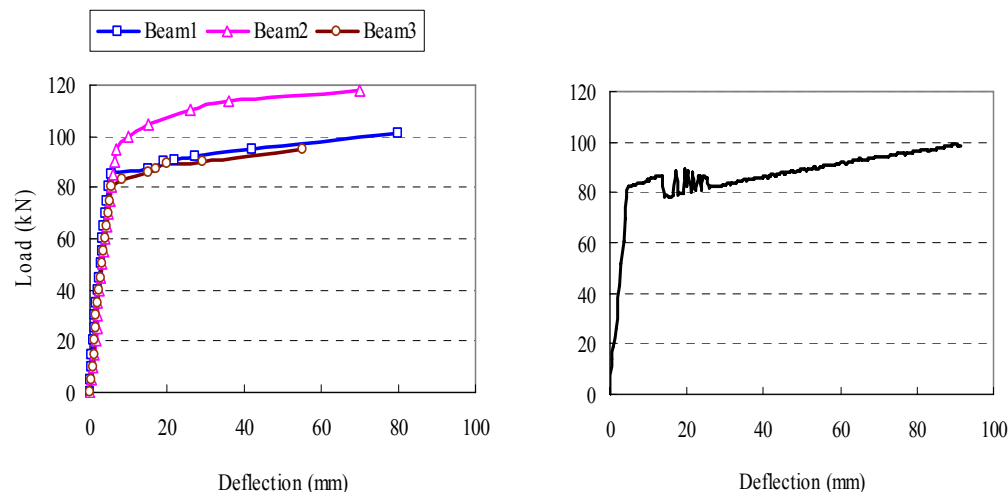


Figure 3: (a) Experimental and (b) Numerical Deflection vs. Load graphs of Set 1 beams (Stirrup @ 5 cm)

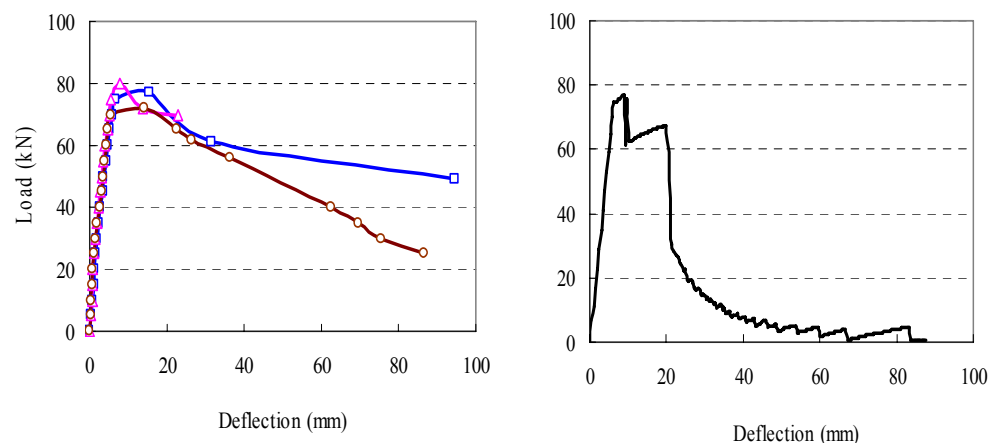


Figure 4: (a) Experimental and (b) Numerical Deflection vs. Load graphs of Set 2 beams (Stirrup @ 20 cm)

Since the results for the individual beams are somewhat different from each other, they are difficult to compare with the corresponding numerical data. More conveniently, Table 3 and 4 compare average values of the important parameters of the load-deflection graphs for Set 1 and Set 2 respectively (i.e., loads and deflections corresponding to elastic limit, spalling and crushing of concrete).

Table 3 shows reasonable agreement between theoretical and experimental loads and the corresponding deflections. This is somewhat true for Table 4 also except in case of spalling, where the numerical and experimental results differ significantly. This is perhaps due to the fact that equation (3) does not incorporate the spalling of concrete, a limitation compensated by the effect of compression reinforcement for Set 1.

The tables also demonstrate the positive effects of lateral reinforcement on the ductility of RC beam sections, particularly in the

absence of compression rods. For example, in Set 1 (Table 3) the average value of ultimate deflection corresponding to stirrup spacing of 5 cm is 68 mm (90 mm using numerical analysis) but it decreases to 52 mm (74 mm from numerical analysis) and 52 mm (59 mm from numerical analysis) for stirrup spacings of 10 and 20 cm respectively. The effect is less serious for the ultimate loads (decreasing from 105 kN to 99 kN and 92 kN), but much more significant in the absence of compression rods (Table 4).

Table 3: Experimental and numerical results for Set 1 beams.

Stirrup Spacing	Sample	Elastic Limit		Spalling		Crushing	
		Load (kN)	Def (mm)	Load (kN)	Def (mm)	Load (kN)	Def (mm)
5 cm	Avg	87	6.0	95	20	105	68
	Num	83	6.3	78	14	99	90
10 cm	Avg	83	5.8	93	23	99	52
	Num	83	6.8	82	22	95	74
20 cm	Avg	82	6.1	90	20	92	52
	Num	83	7.8	84	26	92	59

Table 4: Experimental and numerical results for Set 2 beams.

Stirrup Spacing	Sample	Elastic Limit		Spalling		Crushing	
		Load (kN)	Def (mm)	Load (kN)	Def (mm)	Load (kN)	Def (mm)
5 cm	Avg	80	5.4	75	25	91	61
	Num	71	6.8	36	7.3	74	46
10 cm	Avg	77	5.4	79	20	77	37
	Num	73	6.3	60	9.3	69	25
20 cm	Avg	70	5.3	71	17	71	17
	Num	74	6.3	61	9.3	67	20

Here the ultimate beam deflection for stirrup spacing of 5 cm decreases from 61 mm (46 mm from using numerical analysis) to 37 mm (25 mm from numerical analysis) for stirrup spacing of 10 cm and only 17 mm (20 mm from numerical analysis) for stirrup spacing of 20 cm. The corresponding decrease in ultimate loads (experimental) from 91 kN to 77 kN and 71 kN is also more significant compared to Set 1. However, Figure 4 shows that the numerical model does not simulate properly the beam behavior after crushing of concrete.

6. OBSERVATION OF FAILURE CHARACTERISTICS

Figure 5 shows the nature of compression failure of unconfined and confined cylinders along with the confinement reinforcements. The presence of confining reinforcements checks the overall rupture of the cylinders; i.e., the failure surfaces do not propagate from top to bottom of the cylinder. The condition of the longitudinal and shear reinforcements after failure of the beams are shown in Figure 6. Although the compressive steel

reinforcements are in order for Set 1 [Figure 6(a)], this is not the case for the timber reinforcements of Set 2 [Figure 6(b)]; i.e., showing the ones with stirrups spaced at 20 cm that failed due to compression and almost the entire concrete volume has crushed and detached at the failure sections.

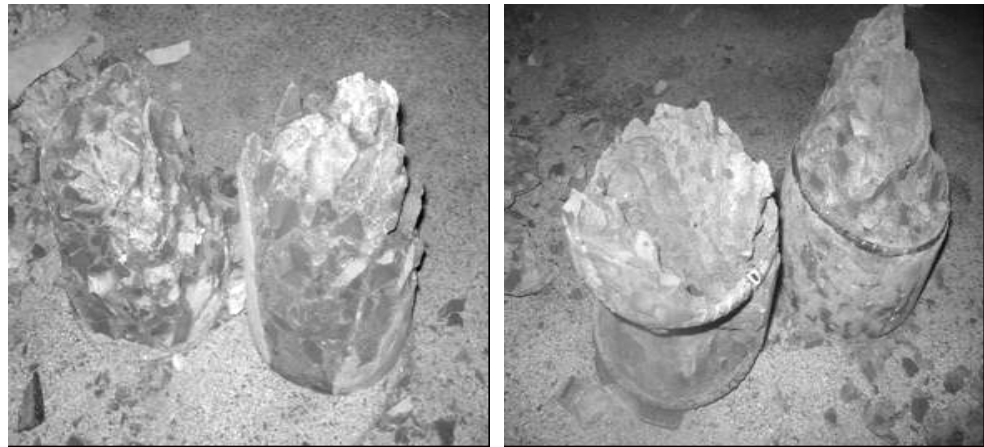


Figure 5: Crushed cylinder and failure surfaces for (a) Set 1, (b) Set 2

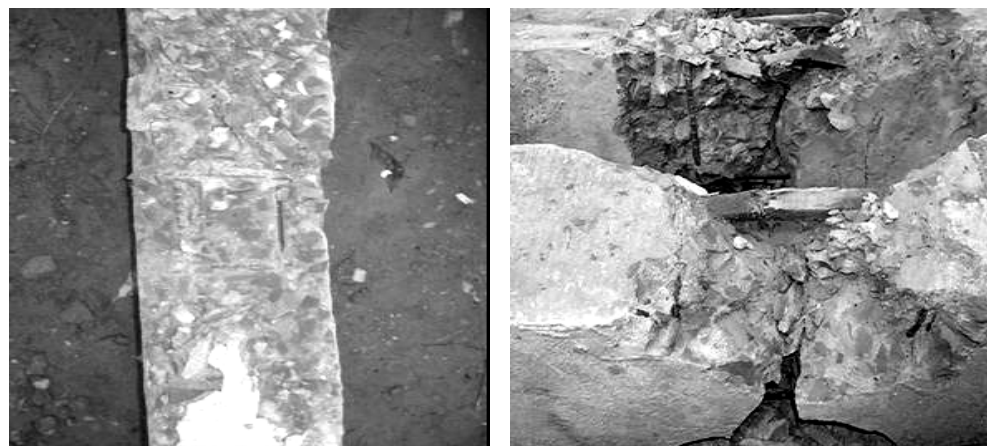


Figure 6: Reinforcements after failure of (a) Set 1 beam, (b) Set 2 beam

7. CONCLUSIONS

This work was particularly aimed at studying the effect of compressive and shear reinforcements in improving the ductility of RC sections, although their effect on concrete strength was also studied. The ductility (and the compressive strength to some extent) of concrete obtained from cylinder tests were indeed found to increase significantly due to confinement by lateral hoops. The ultimate stress and strain predicted from literature matched reasonably well with the experimental values. Also, there was significant increase in the ductility (and some increase in strength) of the beams with closely spaced stirrups (particularly beams without compressive reinforcements), compared to beams with sparse stirrups.

The agreement between the numerical and experimental results was very good at the elastic limit, unsatisfactory (sometimes poor) at concrete spalling and reasonable at the ultimate limit. The numerical analysis could not model properly the beam behavior after concrete crushing.

Experimental and numerical results from the beam tests showed marked difference between the behavior of beams with (Set 1) and without compression reinforcements (Set 2). Even at failure, though the compressive steel reinforcements for Set 1 were in order, the compressive timber reinforcements of Set 2 (particularly ones with stirrups spaced at 20 cm) failed and almost the entire concrete volume crushed at the failure section.

REFERENCES

- Anam, I., and Shoma, Z. N., 2002. *Nonlinear properties of Reinforced Concrete structures*. 2nd Canadian Conference on Nonlinear Solid Mechanics, Vancouver, Canada, Vol 2, 657-666.
- Akand, M. S. A., 2007. *Effect of shear and compression reinforcement on the ductility of RC members*. B. Sc. Engg. Thesis, Department. of CE, UAP.
- Aoyama, H., and Noguchi, H., 1979. Mechanical properties of concrete under load cycles idealizing seismic actions. *Bulletin D'information CEB* 131, 29-63.
- Bangladesh National Building Code, 1993. *BNBC-93*, Dhaka, Bangladesh.
- Ansary, M. A., and Noor, M. A. (editors), 2006. *Earthquake resistant design manual*, Academic Press & Publishers Library, Bangladesh.
- Bertero, V. V., Anderson, J. C., Krawinkler, H., Miranda, E., 1991. *Design guidelines for ductility and drift limits*. UCB/EERC-91/15, Earthquake Engineering Research Center, UC Berkeley, USA.
- Blume, J.A., Newmark, N.M., and Corning, L.H., 1961. *Design of multi-storey Reinforced Concrete buildings for earthquake motions*. Portland Cement Association, Skokie, Illinois, USA.
- Corley, W.G., 1966. Rotational capacity of Reinforced Concrete beams. *ASCE Journal of Structural Engineering* 92, 121-146.
- Engelkirk, R.E., 2003. *Seismic design of Reinforced Concrete and Precast Concrete buildings*. John Wiley & Sons, NY, USA.
- Hognestad, E., 1952. Fundamental concepts in ultimate load of Reinforced Concrete members. *ACI Structural Journal* 49, 48-53.
- Kent, C. C., and Park, R., 1971. Flexural members with confined concrete. *ASCE Journal of Structural Engineering* 97, 1969-1990.
- Machida, A., Moehle, J., Pinto, P., Park, P., and Matsumoto, N., 1999. *Ductility consideration*. Proc. of Comparative Performance of Seismic Design Codes for Conc. Str. Engg. Studies, Vol 1, Elsevier Sc., USA.
- Mander, J. B., Priestley, M. J. N., and Park, R., 1988. Theoretical stress-strain model for confined concrete. *ASCE Journal of Structural Engineering* 114, 1804-1826.

RESIDUAL SEISMIC CAPACITY ESTIMATION OF RC FRAMES WITH UNREINFORCED CONCRETE BLOCK INFILL

HO CHOI

JSPS Postdoctoral Fellow, The University of Tokyo
choiho@iis.u-tokyo.ac.jp

YOSHIAKI NAKANO

Institute of Industrial Science, The University of Tokyo, Japan
iisnak@iis.u-tokyo.ac.jp

ABSTRACT

The objective of this study is to develop a post-earthquake seismic evaluation method for RC frames with unreinforced concrete block infill. For this purpose, full-scale, one-bay, single-story specimens are tested under cyclic loadings. In this paper, the residual seismic reduction factors are discussed analytically and experimentally to estimate the residual seismic capacity based on the observed damage class, and the damage classes of Korean typical school building, which should be properly functional as refugee centers as well as structurally safe after an earthquake, are investigated analytically under Korean design acceleration level.

1. INTRODUCTION

The objective of this study is to develop a post-earthquake seismic evaluation method for reinforced concrete (referred to as RC) frames with unreinforced concrete block (referred to as CB) infill. For this purpose, full-scale, one-bay, single-story specimens having different axial loads in columns and different opening configurations of infill are tested under cyclic loadings. During the tests, residual crack widths, which can also be found in damaged buildings, are carefully measured to estimate the residual seismic capacity from the observed damage.

In this paper, the residual seismic capacity of RC frames with CB infill is discussed analytically and experimentally, and the reduction factors are proposed to estimate the residual seismic capacity based on the observed damage class. Finally, the damage classes of Korean typical school buildings, which should be properly functional as refugee centers as well as structurally safe after an earthquake, are investigated analytically under Korean design acceleration level.

2. OUTLINE OF EXPERIMENT

Figure 1 shows a standard design of Korean school buildings in the 1980s (The Ministry of Construction and Transportation, 2002). In this paper, 2 specimens representing first and fourth story of 4 story RC school buildings are investigated. They are an infilled wall type 1 (IW1) assuming the first story and an infilled wall type 2 (IW2) assuming the fourth story. The design details of specimen IW1 are shown in Figure 2. For loading history, peak drift angles of 0.1, 0.2, 0.4, 0.67, 1.0, and 2.0% are planned. A constant axial load of 1,440kN (720kN for each column) is applied to specimen IW1 while 360kN (180kN) to specimen IW2.

Specimen IW1 has vertical and horizontal cracks in mortar between CB units and flexural cracks in RC columns at +0.1%. Shear cracks are then observed in both columns at +0.4%. Since the shear cracks rapidly open at -1.5% in the column bottom of compression side, the test is terminated. Specimen IW2 has a crack pattern in both columns and wall, which is almost the same as that of specimen IW1. Although the strength deterioration is observed at +2.0%, a rapid increase in crack width is not found. Since the shear cracks rapidly open at +3.33% in the column bottom of compression side, the test is terminated. The response of the specimens including crack patterns and their mechanism is discussed by Nakano and Choi (2005).

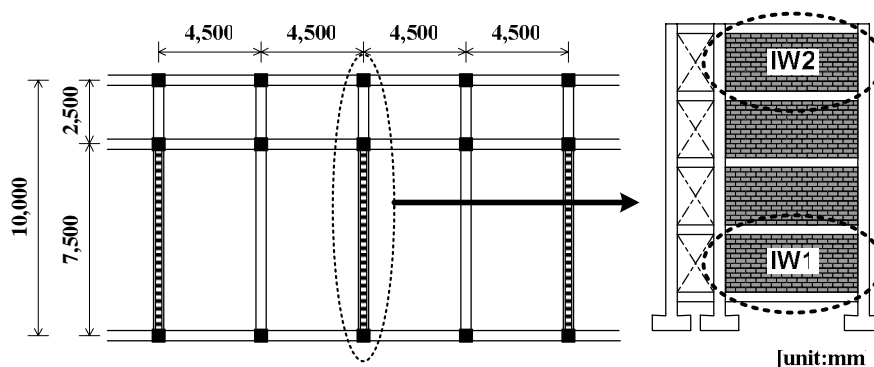


Figure 1: Standard design of Korean school buildings in the 1980s

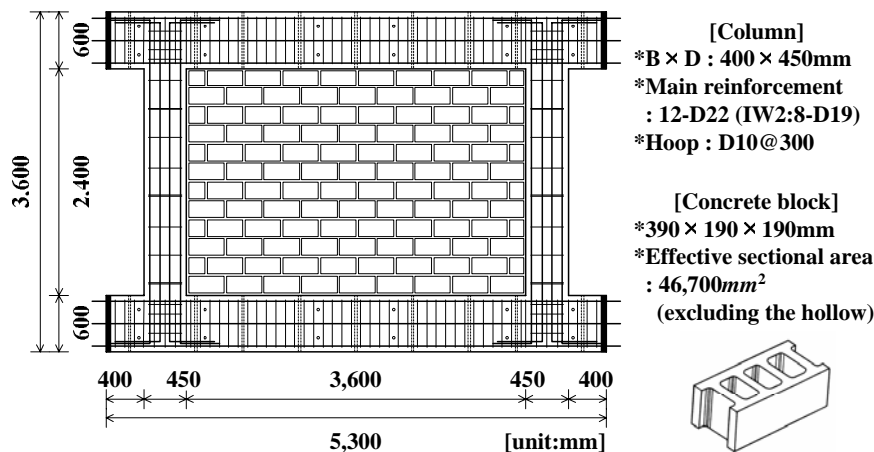


Figure 2: Details of specimen IW1

3. BASIC CONCEPT OF RESIDUAL SEISMIC CAPACITY EVALUATION

Figure 3 shows the basic concept employed in this study to evaluate the residual seismic capacity from residual crack widths observed in earthquake-damaged buildings. The seismic capacity is defined as the hysteretic energy that a structure can absorb during an earthquake, which is consistent with the basic concept found in the Japanese Standard for Seismic Evaluation of Existing RC Buildings (JBDPA, 2001 and 2005), since the procedure proposed herein to evaluate the residual seismic capacity is designed to be analogous to that of the Standard for existing (i.e., pre-earthquake damaged) buildings.

When the load-deformation relationship of a structure or members is investigated through loading tests prior to an earthquake and the response of the structure such as the peak deformation δ_p and/or the residual deformation δ_0 are given after an event, the residual seismic capacity $E_r (= E_T - E_d)$ can be calculated by the discrepancy between initial seismic capacity E_T prior to earthquake damage and dissipated seismic capacity E_d based on the load-deformation curve as shown in Figure 3(a).

Since the peak and residual deformations of buildings are, however, usually unknown after an earthquake unless they are instrumented, other information that can be surely obtained in the damaged buildings and quantitative data that can serve as a good estimator of the peak and/or residual deformation are therefore necessary to practically evaluate the residual seismic capacity. In this study, the residual crack width W_0 that can be quantitatively measured on damaged buildings is focused to estimate the residual deformation δ_0 as shown in Figure 3(b), and their W_0 - δ_0

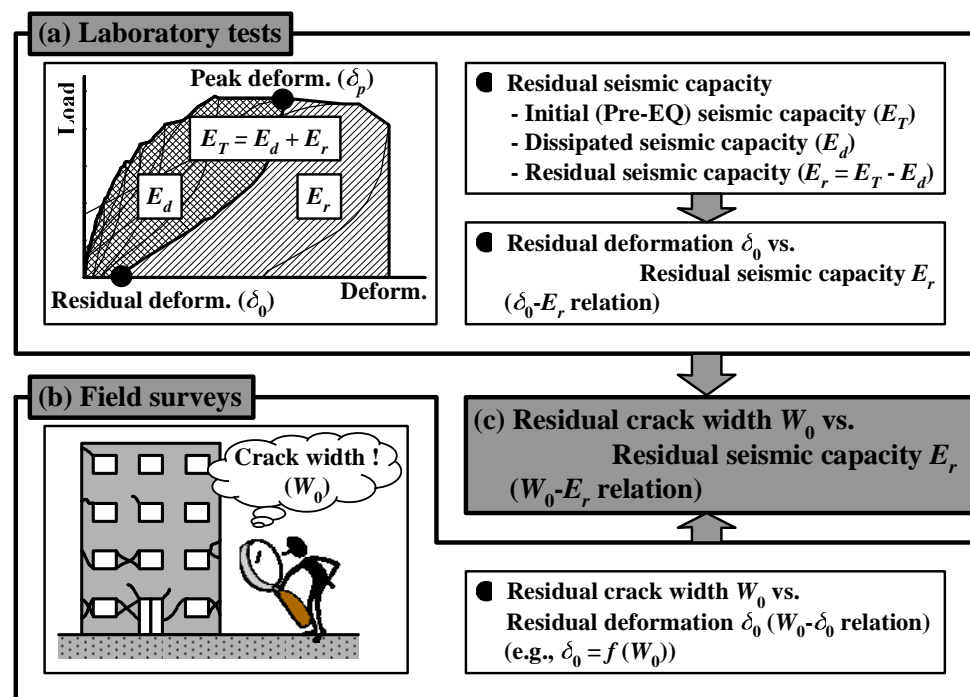


Figure 3: Basic concept of residual seismic capacity evaluation

relationships are experimentally and analytically studied. Once the W_0 - δ_0 relation and the δ_0 - E_r relation of typical buildings where damage is expected during an earthquake are clarified and the W_0 - E_r relation is then established, the residual seismic capacity E_r of a damaged building can be evaluated through the crack width W_0 that can be measured during a damage survey.

In the following sections, the δ_0 - E_r relation (see Figure 3(a)) is only investigated for RC frames with CB infill.

4. RELATIONSHIP OF RESIDUAL DEFORMATION AND RESIDUAL SEISMIC CAPACITY

4.1 Estimation of Residual Seismic Capacity by Residual Deformation

In this section, the relationship of the residual deformation (δ_0) and the residual seismic capacity (E_r) is investigated. For this purpose, the load-deformation curves obtained during the loading tests are approximated with a simplified model, and the seismic capacity reduction factor η is employed based on the model.

The load-deformation curve is first characterized by the following three basic points on the curve, the yield drift angle R_y , the maximum response drift angle R_p , and the ultimate drift angle R_u , where the drift angle is defined as the ratio of deformation to the column height ($h=2,400mm$) of specimens. In this study, R_y , R_p , and R_u are defined as shown below.

- R_y : Drift angle when column longitudinal reinforcement yields
- R_p : Drift angle when a structure reaches its maximum response deformation
- R_u : Drift angle when the lateral load carrying capacity decreases to 80% of the peak load

Figure 4 shows the characteristic points R_y and R_u of specimens IW1 and IW2 together with damage class determined considering its definition for RC members in the Guidelines for Post-Earthquake Damage Evaluation and Rehabilitation of RC Buildings in Japan (2001) shown in Table 1 and Figure 5.

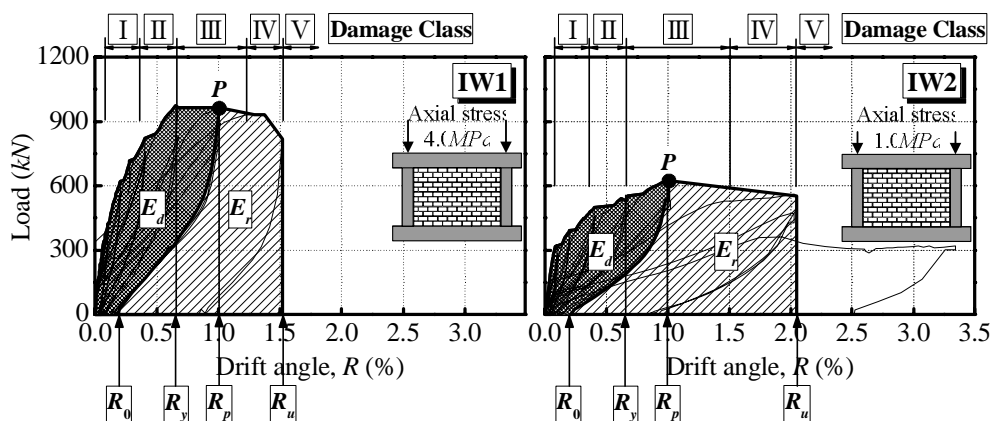


Figure 4: Load-drift angle relationship of specimens IW1 and IW2

Table 1: Damage Class Definition of RC Columns and Walls (JBDPA, 2001)

Damage class	Description of damage
I	- Visible narrow cracks on concrete surface (Crack width is less than 0.2 mm)
II	- Visible clear cracks on concrete surface (Crack width is about 0.2 -1.0 mm)
III	- Local crush of concrete cover - Remarkable wide cracks (Crack width is about 1.0 - 2.0 mm)
IV	- Remarkable crush of concrete with exposed reinforcing bars - Spalling off of concrete cover (Crack width is more than 2.0 mm)
V	- Buckling of reinforcing bars - Cracks in core concrete - Visible vertical and/or lateral deformation in columns and/or walls - Visible settlement and/or leaning of the building

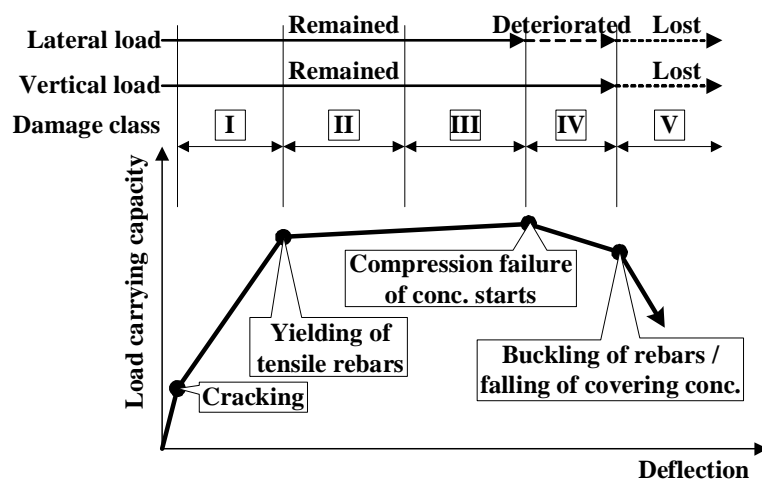


Figure 5: Schematic illustrations of damage class vs. load carrying capacity (Ductile Member, JBDPA, 2001)

The ultimate ductility factor μ of each specimen defined by R_u/R_y is approximately 2.0 and 3.0, respectively. When the structure's response has the peak drift angle R_p and the residual deformation angle R_0 , the dissipated hysteretic energy E_d normalized with respect to the column height can be calculated from the area enclosed by the curve $O-P-R_0$. The residual energy E_r , therefore, can be calculated from the remaining area shown hatched in Figure 4. Assuming that the hysteretic energy defined above corresponds to the seismic capacity, E_r represents the residual seismic capacity.

To facilitate to apply this procedure to hysteretic loops with different strength and ductility, a seismic capacity reduction factor η defined by the ratio of the residual capacity E_r to the initial capacity $E_T (=E_d+E_r)$ is then employed in this study. To find the R_0 - η relationship of a structure in a more general manner, the load-deformation curve is represented with a simplified hysteretic model with assumptions (1) through (3) described below. Figure 6 shows the simplified hysteretic model.

- (1) The Takeda model is employed for the basic hysteretic rule assuming (a) no hardening in post-yielding stiffness and (b) stiffness degradation factor α of 0.7 derived from the test results during unloading.
- (2) The load Q_{cr} and drift angle R_{cr} at cracking point are assumed $Q_y/3$ and $R_y/15$, respectively, where Q_y and R_y are the characteristic points at yielding.
- (3) The descending branch beyond the ultimate drift angle R_u linearly decreases to $(\mu+1)R_y$ onto X-axis where the ductility factor μ is defined by R_u/R_y , which is analogous with the concept found in Maeda et al. (2000).

Figure 7 shows the relationship between the seismic capacity reduction factor η and the residual drift angle R_0 for different ultimate ductilities together with the test results. As described earlier, the ductility factors of IW1 and IW2 are approximately 2.0 and 3.0, respectively, and Figure 7 shows good agreement of numerical simulations with test results.

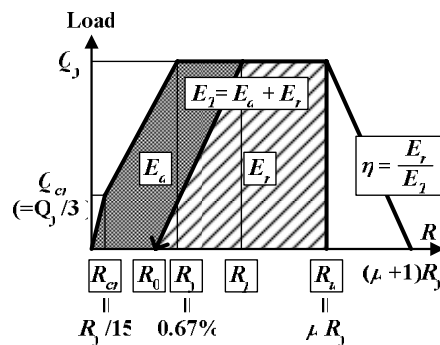


Figure 6: Simplified hysteretic model

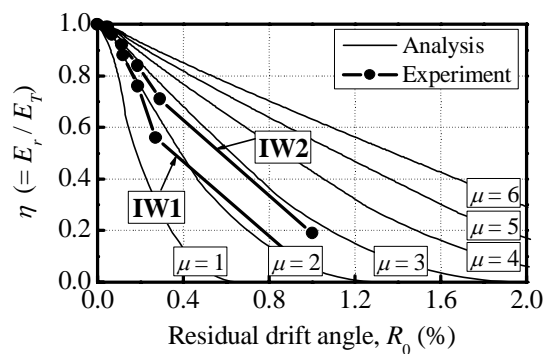


Figure 7: Relationship of R_0 and η

4.2 Estimation of Residual Seismic Capacity Corresponding to Damage Class

It should be noted that damage evaluation of buildings in the field is often made based on damage classification such as shown in Table 1 rather than direct and detailed description of measured digital data.

To facilitate to apply the relation found in Figure 7 in practice, the reduction factor η is plotted in Figure 8 with respect to the damage class I through V considering the relationship of peak drift angle and damage class

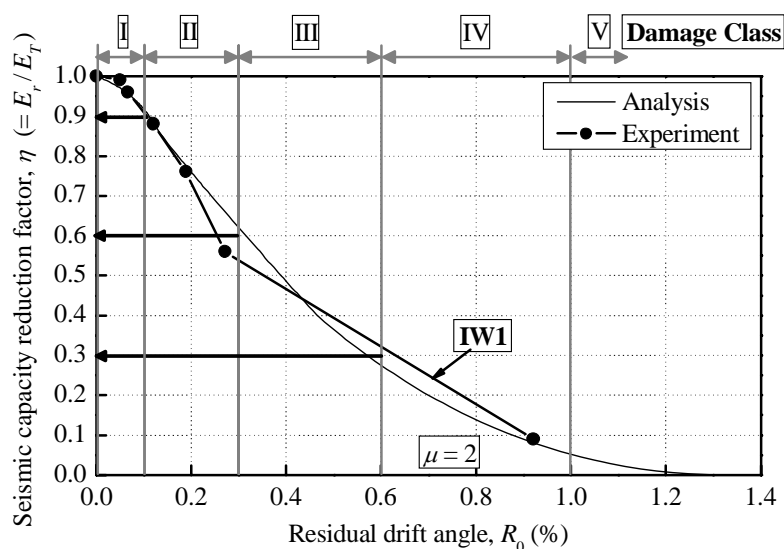


Figure 8: Seismic capacity reduction factor η vs. damage class

Table 2: Seismic capacity reduction factor η corresponding to damage class

Damage Class	Proposed in this study for RC frames with CB infill	Specified in the Guidelines (JBDPA, 2001)	
		Brittle RC column / RC wall	Ductile RC column
I	0.90	0.95	0.95
II	0.60	0.60	0.75
III	0.30	0.30	0.50
IV	0.00	0.00	0.10
V	0.00	0.00	0.00

shown in Figure 4, where data of specimen IW1 is used since serious damage is often found in the first story.

The results are summarized in Table 2 comparing factors specified in the Guidelines (JBDPA, 2001), where the proposed factors are determined as the average of experimental and estimated values at the boundary of two adjacent damage classes in Figure 8. Note that the factors for damage classes IV and V are assumed 0 to conservatively evaluate the results. As shown in the table, the values of η determined in this study are almost the same as those for brittle RC column and wall in the Japanese Guidelines, since specimen IW1 is not ductile enough to maintain the peak load far beyond yielding.

The residual seismic capacity E_r of RC frames with CB infill can be estimated from the following procedure.

- (1) Calculate the seismic capacity E_T of an original (i.e., pre-earthquake damaged) sub-assembly or frame with CB infill.
- (2) Classify its damage into one of five categories based on a damage survey.
- (3) Determine the seismic capacity reduction factor η based on the damage class made in (2) above. (see Table 2)
- (4) Calculate the residual seismic capacity E_r as ηE_T .

5. DAMAGE CLASS OF KOREAN TYPICAL SCHOOL BUILDING

5.1 Ground Motion Data

In this section, the damage classes of Korean typical school buildings, which should be properly functional as refugee centers as well as structurally safe after an earthquake, are investigated analytically against future earthquakes. Since the earthquakes of maximum acceleration level determined Korean seismic design provisions have been not occurred, six artificial ground motions are used in this study. A target elastic spectrum with 5% of critical damping $S_A(T, 0.05)$ is then determined by Equation (1).

$$S_A(T, 0.05) = \begin{cases} 0.18 + 2.64T & T < 0.1 \text{ sec} \\ 0.44 & \text{cm/sec}^2 \quad 0.1 \text{ sec} \leq T < 0.52 \text{ sec} \\ 0.23/T & T \geq 0.52 \text{ sec} \end{cases} \quad (1)$$

where T is the natural period of the SDOF model. The following 6 records are used to determine phase angles of ground motions: the NS component of El Centro 1940 record (referred to as ELC), NS component of Kobe 1995 record (KOB), EW component of Hachinohe 1968 record (HAC), NS component of Tohoku University 1978 record (TOH), NS component of Uljin 2004 record (ULJ) which has the highest maximum acceleration level of earthquake data measured Korean Meteorological office, and random excitation (RAN). Table 3 shows the maximum acceleration of artificial ground motion and Figure 9 shows the elastic acceleration response spectra of artificial ground motions with 5% of critical damping.

Table 3: Input ground motion

Ground Motion Record ID	Max. Ground Acceleration (cm/sec ²)
ELC	341.7
KOB	-821.0
HAC	183.0
TOH	258.0
ULJ	72.5
RAN	-

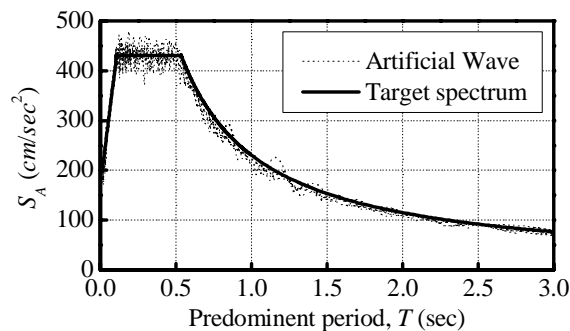


Figure 9: Elastic acceleration spectra

5.2 Damage Class Estimation of Korean Typical School Building

In this section, the damage classes of Korean typical school building based on the standard design specification in the 1980s are estimated using six artificial ground motions mentioned previous section. In this paper, 4 story frames as shown in Figure 1, where transverse direction including CB walls used as partition walls is selected since high seismic capacity is expected, are analyzed.

To simulate the inelastic behaviors of model structure and to estimate the damage classes, the Takeda hysteretic model is employed with assumptions (1) through (3) described below.

- (1) The model is assumed as no hardening in post-yielding stiffness and stiffness degradation factor α of 0.7.
- (2) The yield load Q_y is calculated as the sum of shear strengths of three columns and one CB infill (the average shear stresses of CB infills for specimens IW1 assuming the first story and IW2 assuming the fourth story are approximately $0.4N/mm^2$ and $0.3N/mm^2$, respectively, from test results, and those for the second and the third stories are roughly assumed $0.35N/mm^2$). The yield drift angle R_y is assumed 0.67% from test results. The load Q_{cr} and drift angle R_{cr} at cracking point are assumed $Q_y/3$ and $R_y/15$, respectively.
- (3) The ultimate ductility factors μ of specimens IW1 and IW2 are approximately 2.0 and 3.0, respectively, and those for the second and the third stories are roughly assumed 2.5.

Figure 10 shows the inelastic behaviors of first story of model structure, where is often found serious damage, for six artificial ground

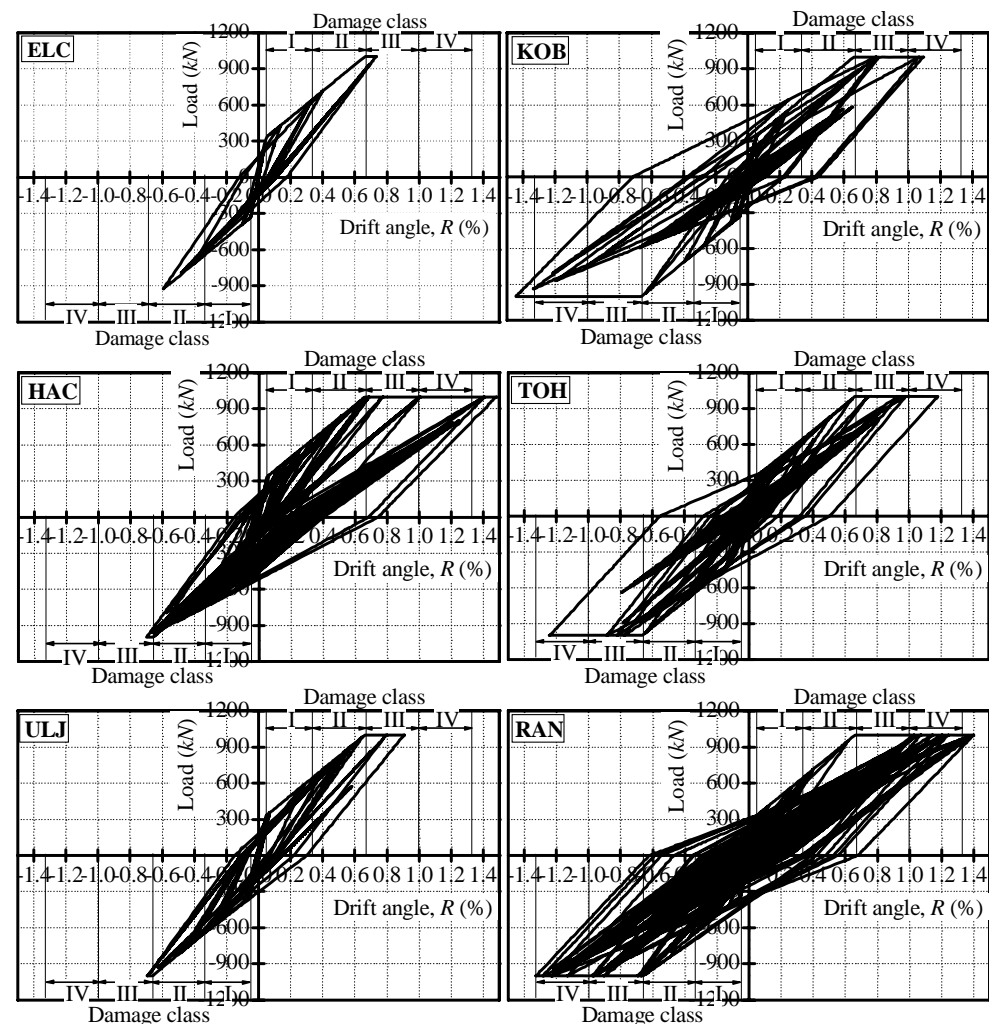


Figure 10: Inelastic behaviors and damage classes of first story

motions together with the damage classes. As shown in the figure, the behaviors and damage classes are different due to phase angles of each ground motion. However, all of results exceed the maximum strength, and the results of KOB, HAC and RAN particularly exceed the ultimate drift angle of 1.35% and reach in the state of damage class V (i.e., collapse). This result means that Korean typical school buildings cannot escape more than moderate damage and do not play a role as refugee centers after the earthquake of Korean design acceleration level.

6. CONCLUSIONS

RC frames with concrete block (CB) infill representing typical school buildings in Korea are tested under cyclic loading to estimate the residual seismic capacity from residual crack widths measured on CB walls. The results can be summarized as follows.

- (1) The load-deformation curves obtained during the tests are then approximated with a simplified hysteretic model, and the relationship of the residual drift angle R_0 and the residual seismic capacity reduction factor η is established based on the model. The results show good agreement with test results, which imply that the procedure proposed herein can be applied to estimate the residual seismic capacity of RC frames with CB infill having different strength and ductility.
- (2) The values of η proposed in this study for RC frames with CB infill corresponding to each damage class are found almost the same as those for brittle RC column and wall specified in the Japanese Guidelines for Post-Earthquake Damage Evaluation, since the proposed values are based on data of specimen IW1, which is not ductile enough to maintain the peak load far beyond yielding.
- (3) The damage classes of first story of model structure, where is often found serious damage, for six artificial ground motions exceed the maximum strength, and the results of KOB, HAC and RAN particularly exceed the ultimate drift angle of 1.35% and reach in the state of damage class V. This result means that Korean typical school buildings cannot escape more than moderate damage and do not play a role as refugee centers after the earthquake of Korean design acceleration level.

REFERENCES

The Ministry of Construction and Transportation, 2002. A Study on the Seismic Evaluation and Retrofit of Low-Rise RC Buildings in Korea. pp. 113-155 (in Korean).

Nakano, Y. and Choi, H., 2005. Experimental Study on Seismic Behavior and Crack Pattern of Concrete Block Infilled RC Frames. *New Technologies for Urban Safety of Mega Cities in Asia (USMCA)*, ICUS/INCEDE Report 2, Singapore.

JBDPA (The Japan Building Disaster Prevention Association), 1977, 1990, and 2001 (in Japanese), and 2005 (in English). Standard for Seismic

Evaluation of Existing Reinforced Concrete Buildings.

JBDPA (The Japan Building Disaster Prevention Association), 2001. Guidelines for Post-Earthquake Damage Evaluation and Rehabilitation (in Japanese).

Maeda, M., Bunno, M. and Nagata, M., 2000. A Study on the Damage Class Estimation of RC Buildings Based on Residual Seismic Capacity of Members. *Proceedings of the Japan Concrete Institute*, Vol. 22, No. 3, pp. 1447-1452 (in Japanese).

THE EFFECT OF INFILLS ON THE DYNAMIC BEHAVIOR OF RC FRAMES

SAMY MUHAMMAD REZA¹, RAQUIB AHSAN²
and MEHEDI AHMED ANSARY³

Department of Civil Engineering, BUET, Bangladesh
samyreza@gmail.com

ABSTRACT

Response of a structure to earthquakes significantly depends on its infill condition. For general design purposes, usually structural analysis is performed according to equivalent linear static method. This is not safe for structure with soft story. Structures with soft story are associated with greater deflection than normal structures. A structure does not behave linearly when subjected to large deformation. Nonlinear analysis is associated with increase of deformation and thus greater vulnerability. In this study Frames with and without infills have been analyzed considering nonlinearity and damping effects. Responses of structures, both linear and non-linear with different infill conditions, to harmonic ground motion have been examined. From this study it has been found that frames with more than 10 stories are more vulnerable due to soft-storey effect than bare frames. Vulnerability of a structure depends very much on the ground motion frequency.

1. INTRODUCTION

Frame structures are frequently used in multistoried buildings, mainly due to ease of construction and rapid progress of work. Column and girder framing of reinforced concrete, or some times steel, is infilled by panel of brickwork, block work, cast in place or pre-cast concrete. When an in-filled frame is subjected to lateral loading, the infills behave effectively as struts along its compression diagonals to brace the framed. Therefore, the infills serving as external walls or internal partitions, contribute some effect on stiffness of the framing system. This contribution totally depends on the properties of infilled materials, openings etc.

Without contribution of infill stiffness is greatly reduced. So, a bare frame is much less stiff than frame with infill. In case of soft story a sudden reduction of stiffness takes place. Response of these frames to earthquake will be different.

For large displacement, structures do not act linearly. Based on elastic behavior, structures subjected to a major earthquake would be required to undergo large displacements. However, North American practice requires that structures be designed for only a fraction of the forces associated with those displacements. The relatively low design forces are justified by the observations that buildings designed for low forces have behaved

satisfactorily and that structures dissipate significant energy as the materials yield and behave inelastically. This nonlinear behavior, however, usually translates into increased displacements, which may result in major nonstructural damage and require significant ductility. Displacements may also be of such magnitude that the strength of the structure is affected by stability considerations.

The objective of the study is to develop a program, by which response of multi-degrees of freedom system to ground motion can be determined. To determine natural frequency of building frames of different height and different infill conditions, by the proposed program. To compare response of building frames with different infill conditions to ground motion by linear and nonlinear analyses, nonlinear analysis without damping and nonlinear analysis with damping.

The 6-story, 10-story and 15-story 3-bay building frames are modeled for frame with full infill, frame without any infill and frame with soft story. Columns provide lateral stiffness and infill walls contribute lateral stiffness. A bilinear model of stiffness is established. Columns and infill enter the inelastic zone at the same time. Natural frequencies are determined by applying free vibration.

2. MODELING OF FRAME

Response of buildings to earthquake varies for their height, infill condition, and structural irregularity. To get an idea how they perform, building frames of different story levels and infill conditions have to be analyzed.

3 bay 6 story, 10 story and 15 story building frames have been studied. Each bay is of 20 feet span. Each frame has been studied for three conditions: with soft story, no soft story (with full infill) and with no infill. Figure 1 shows frames of different infill conditions.



Figure 1: Frames of different infill conditions

2.1 Mass of each story

Only dead load of structure is considered for earthquake load. Dead load is 60 psf, floor finish is 25 psf, partition wall is 20 psf. Floor dimension is 20ft * 20ft. Dead load of each bay is $186.67 * 10^3$ kg and mass of each story is $57.14 * 10^3$ kg.

2.2 Structural characteristics

2.2.1 Column property

Dimension of column is 350mm × 350mm and column height is 3000mm. Column behaves elastically till lateral deformation of 10mm and reach to failure at 100mm of lateral deformation. Stiffness of column in elastic zone is $23 * 10^6$ N/m and in inelastic zone $1.08 * 10^6$ N/m. (Saatcioglu and Ozcebe, 1989)

2.2.2 Inelastic model

The model of hysteretic loop is taken from Chopra (1995). The only modification is k_2 , which is not zero here. The model is based on force limit. If F_y is exceeded inelastic limit starts. Figure 2 presents a hysteretic loop showing different paths and force levels

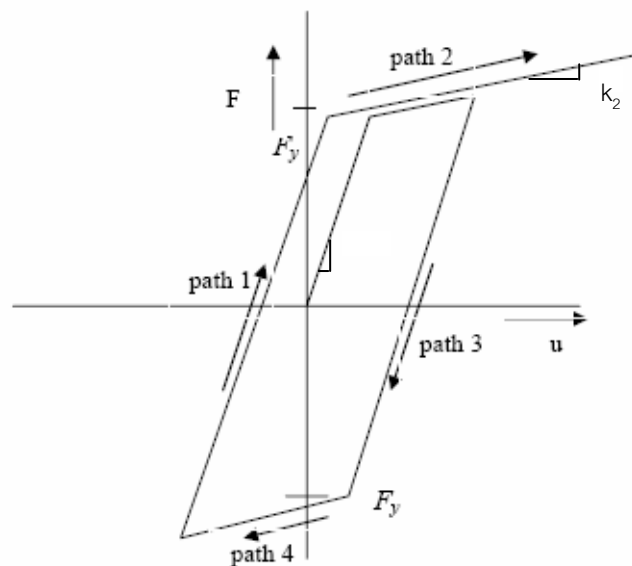


Figure 2: Hysteretic loop, showing different paths and force levels

2.2.3 Lateral stiffness of frame

Frame has 4 columns. Stiffness of column in elastic zone is $92 * 10^6$ N/m and in inelastic zone $4.32 * 10^6$ N/m. Infill adds stiffness to frame. Frames with infill are assumed four times stiffer than frames without infill. (Stafford-smith, B. and Carter, 1969, Stafford-Smith, B., 1962, Stafford-Smith, B., 1966).

2.2.4 Additional damping coefficient c

For the hysteretic loop, previously mentioned, damping is considered for column and infill. Here, damping in ground, beam and joints is not considered. For these parameters an additional damping coefficient has been considered.

$$\text{Damping ratio, } c = 4Dm\pi f_n$$

Where, D is the damping ratio and m is the mass at each storey.

Natural frequency f_n will be determined by applying free vibration to the structures. We know the mass of each story is known. Then c of each story is determined.

2.3 Dynamic loading condition

6 story, 10 story and 15 story frames of different infill conditions were analyzed for combinations of ground accelerations and frequencies.

Ground accelerations used are: 1m/s^2 , 1.5m/s^2 , 2m/s^2 .

Frequencies used: 0.5Hz, 0.75Hz, 1Hz and 1.25Hz.

2.4 Initial condition

The structure is assumed to be static at the instant of application of dynamic load, i.e. initial velocity \dot{u} and initial displacement u of the structure and base were assumed to be zero.

3. ELASTIC ANALYSIS

Response of frames with linear stiffness to harmonic ground excitations are presented in Figure 3. From Figure 3(a) it can be observed that frame with soft story acts like a two degrees of freedom system, as first story inter story drift is too large compared to others. In Figure 3(b) it can be seen that, frame with full infill meets very small inter story drift compared to frame with soft story, even it does not exceed the elastic zone. In Figure 3(c) it can be seen that, amplitude of inter story drift vs time graph increases with time.

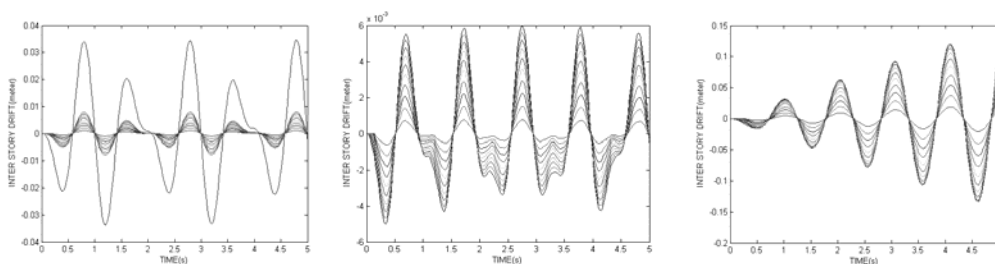


Figure 3: Maximum inter story drift vs time of 10 story frame (a) with soft story (b) with infill (c) without infill

Response of a building frame to ground motion depends upon the natural frequency of the frame itself. The natural frequency of building frame depends on various parameters. Frame height, width primarily controls natural frequency. Empirically, the natural frequency is $\frac{10}{n}$, where n is the number of story of the building. Natural frequency further depends upon infill condition of the frame. Frames, of same height, with soft story, with infill and with no infill certainly possess different natural frequencies, as infill contributes to the stiffness of the frame. Free vibration of a structure may provide with the information of its natural frequency. For that purpose, first some initial ground movement is applied to the frame. After a certain time external excitation (ground movement) stops, then the frame continued to oscillate in free vibration, this can be seen in Figure 4.

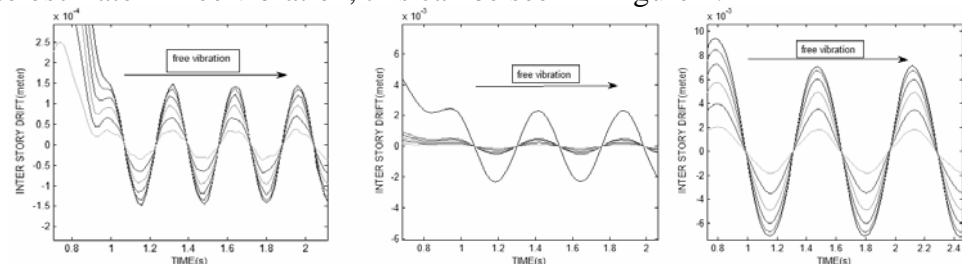


Figure 4: Free vibration of 6 story frame (a) with infill (b) with soft story (c) without infill

Figure 5 shows natural frequencies of 6, 10 and 15 storied frames with different infill conditions and natural frequency from the empirical formula, $10/n$. Natural frequency is proportional to the square root of stiffness ($f_n \propto \sqrt{k}$). In this modeling, stiffness of a story with infill is four times than that of story without infill. Therefore, it is apparent that natural frequency of frame with infill should be twice of the natural frequency of frame without infill and by analysis of 6, 10 and 15 story frame this is found to be almost true. Moreover, natural frequency of frame with soft story (ground story has no infill) is very close to the average of the previous two. Natural frequency from the empirical formula, $10/n$, is marginally higher than that of frame without infill. Therefore, it seems that, this empirical formula is applicable to the frames without infill.

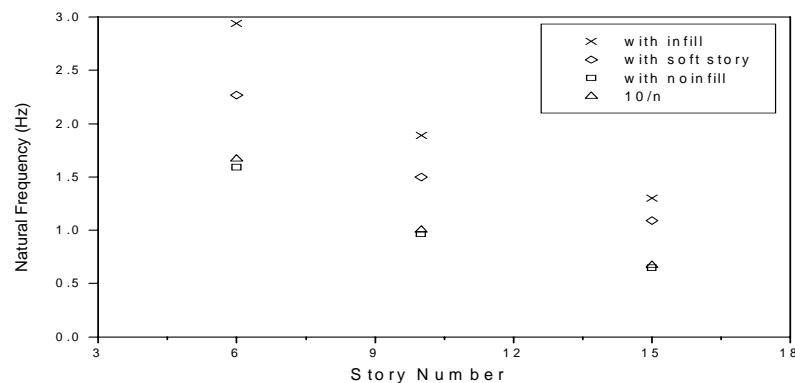


Figure 5: Comparison of natural frequencies of different story levels with different infill conditions with thumb rule calculation

Clearly, frame with infill (no soft story) performs better than frame with soft story and frame with no infill in terms of maximum inter story drift. From Figure 6 it can be seen that maximum drift of frame with no infill is marginally larger than that of frame with soft story, from frequency 0.5Hz to 0.75Hz. After that, the deviation keeps increasing.

The analyses were performed up to 1.25Hz for all the frames. However, in terms of frequency ratio, i.e., the ratio of the excitation frequency to the natural frequency of the frames, the range is different for different frames. From Figure 6(b) it can be observed that actually frames with soft-story go through larger inter-storey drift that even frames without any infill for the same range of frequency ratio.

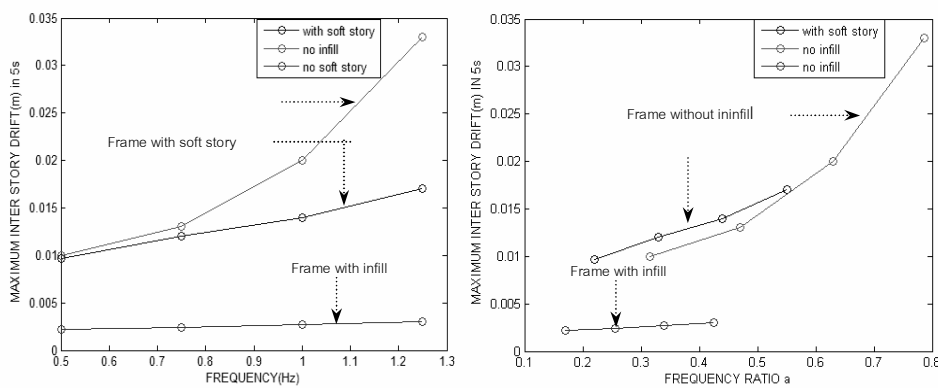


Figure 6: Comparison of different infill conditions, linear analysis for a 6-story frame

Figure 7 represents that for 10 storied frames, as frequency ratio gets nearer one, the rates of increase of maximum inter story drift increases due to resonance.

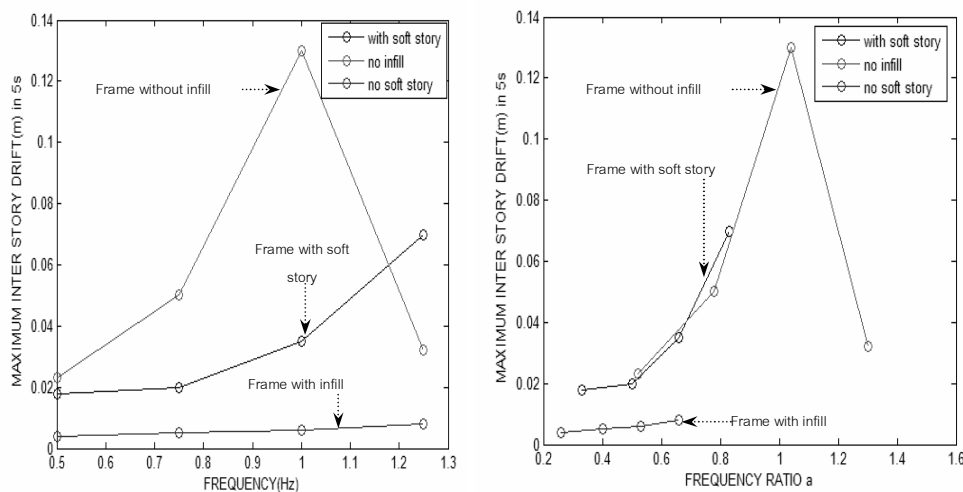


Figure 7: Comparison of different infill conditions, linear analysis for a 10-story frame

From ground frequency 0.5Hz to 1Hz (frequency ratio range 0.385 to 0.77) plot of frame with full infill is linear, then increase in rate of

maximum inter story drift occurs, because, frequency ratio gets closer to one. Frame without any infill is more vulnerable than frame with soft story from frequency .5Hz to 0.8Hz (Figure 8). Over 0.8Hz frame with soft story is vulnerable. The reason is frequency ratio of frame without infill deviates from one after ground frequency 0.645Hz. Frequency ratio of frame with soft story is 0.69 at ground motion frequency 0.75Hz. After that maximum, inter story drift increases sharply.

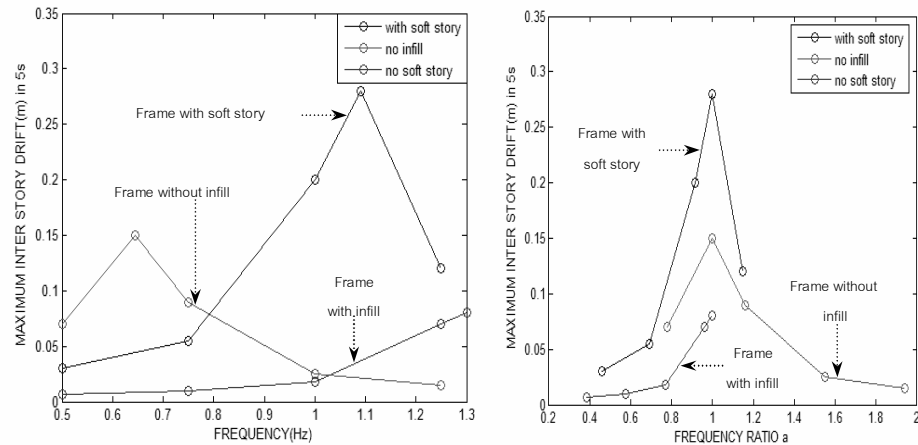


Figure 8: Comparison of different infill conditions, linear analysis for a 15-story frame

4. INELASTIC ANALYSIS

Figure 9 shows that, in nonlinear analysis, properties of structure change with time. Sometimes stiffness decreases significantly, which cause large displacement. If earthquake continues, structure ultimately reaches to destruction. Moreover, damping has also effect on response of frame.

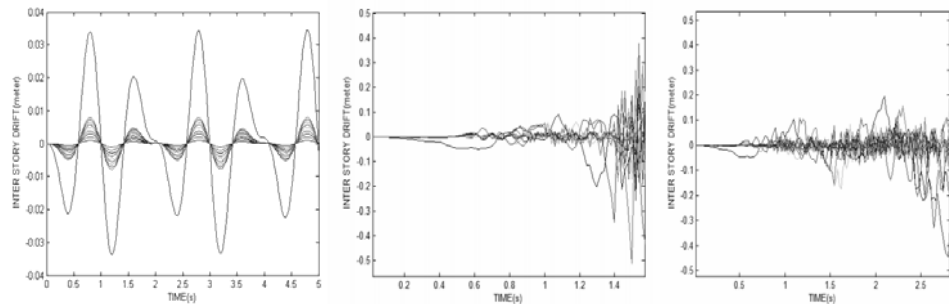


Figure 9: Response of a 10 storied frame with soft story for ground acceleration = $2m/s^2$, frequency = 1Hz (a) elastic analysis (b) inelastic analysis without any additional damping (c) with 5% additional damping

For 6- story building Figure 10 shows that, frame without infill is more vulnerable than frame with soft story from frequency range of 0.5Hz to 1.25Hz. For frame with soft story, time of failure increases up to frequency ratio 0.44, then it falls again.

For 10-storied building frame, Figure 11 shows that, soft story condition performs better than no infill condition like 6-story frame. However, obviously, difference of time of failure decreases here. For frame with soft story failure time remains same from frequency 0.5 to 1.25Hz. Then, it increases until 1Hz and then again falls. For frame without infill failure time increases although. Irregularity in natural frequency of frames in nonlinear analysis is responsible for these behaviors.

From Figure 12, it is apparent that for 15 storied frames, soft story behavior is more vulnerable within frequency range 0.65 to 1.15Hz. For frame with soft story time of failure falls in ground motion frequency 0.75Hz, then rises up to 1Hz, then again falls till 1.09Hz, which is the natural frequency, then time of failure again increases. For frame without infill time of failure rises gradually up to frequency 1Hz, and then begins to fall.

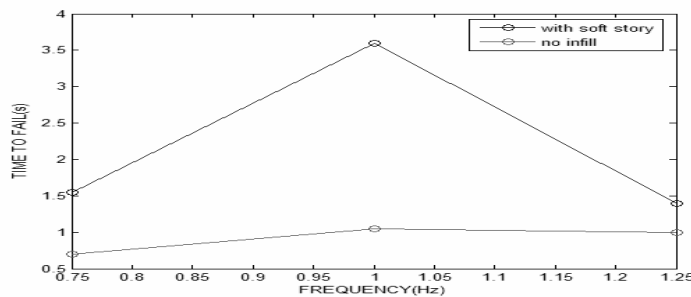


Figure 10: Comparison of different infill conditions, inelastic analysis for a 6-story frame

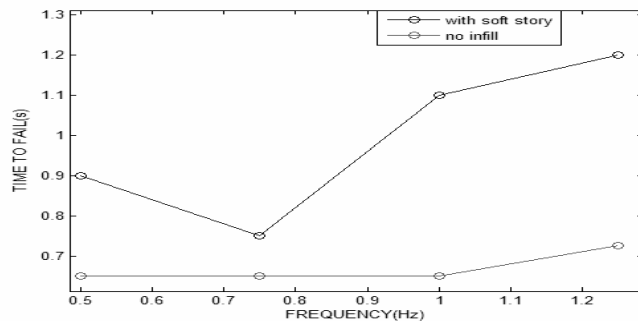


Figure 11: Comparison of different infill conditions, inelastic analysis for a 10-story frame

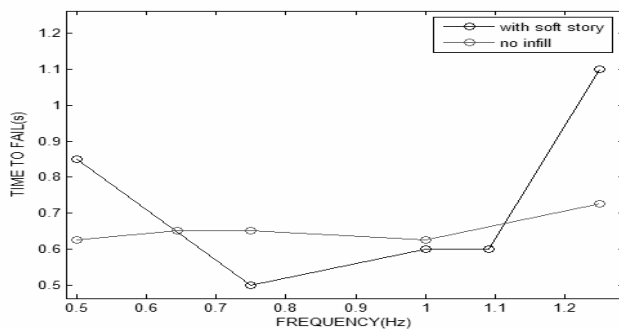


Figure 12: Comparison of different infill conditions, inelastic analysis for a 15-story frame

5. CONCLUSIONS

Six, ten and fifteen story building frames (linear, nonlinear with zero damping and nonlinear with 5% damping) were analyzed for different infill conditions. Once non-linearity is induced at some particular excitation frequency stiffness may decrease significantly causing large displacement. If earthquake continues, structures may ultimately lead to collapse. Natural frequency of frame has been derived by applying free vibration. The derivation is only possible for elastic modeling. It has been found in the present study that natural frequency of frame without infill is almost equal to the natural frequency found by the empirical formula $10/n$. Natural frequency of frame with full infill is the highest, natural frequency of soft story is in-between the former cases. Vulnerability of structure not only depends on story number but also on ground motion frequency. For some frequency ranges frame with soft story is vulnerable and for some others frame with soft story is more vulnerable. For all cases frame with full infill performs the best. For all cases, frame with soft story has been found more vulnerable for higher stories. For lower stories frame without infill has been found more vulnerable.

Guarantee

REFERENCES

- Stafford-smith, B. and Carter, (1969), "A Method of Analysis for Infilled Frames", Proceedings of the Institution of Civil Engineers, vol. 44.
- Stafford-Smith, B. (1962), "Lateral Stiffness of Infilled Frames," Journal of the Structural Division, ASCE, vol. 88.
- Stafford-Smith, B., (1966), "Behavior of Square Infilled Frames", Journal of the Structural Division, ASCE, vol. 92.
- Murat Saatcioglu, M. and Guney Ozcebe, G., (1989), "Response of Reinforced Concrete Columns to Simulated Seismic Loading", ACI Structural Journal, page 3.
- Chopra, A. K., (1995), "Dynamics of Structures", Pearson Education.

ANALYSIS OF AXIAL VIBRATION OF PILES IN LAYERED SOIL AND APPLICATION TO BATTER PILE FOUNDATIONS

RAQUIB AHSAN

Bangladesh University of Engineering and Technology, Bangladesh
raquibahsan@ce.buet.ac.bd

JORGEN JOHANSSON
Tokyo University, Japan
jorgen@iis.u-tokyo.ac.jp

KAZUO KONAGAI
Tokyo University, Japan
konagai@iis.u-tokyo.ac.jp

HIDETAKE TANAKA
Tokyo University, Japan
hidetake@iis.u-tokyo.ac.jp

ABSTRACT

A Semi-analytical approach for solving the problem of interaction of a pile with semi-infinite layered soil medium in axial vibration is discussed here. An application involving the effect of both lateral and axial stiffness of batter piles in horizontal vibration is then presented in this paper. Modal parameters of a pier supported by batter piles are studied for different batter angles. For smaller batter angles the predominant mode of vibration corresponds to the mode induced by a force at the pier-top. For larger batter angles the mode induced by ground movement becomes predominant.

1. INTRODUCTION

Many researchers have proposed different methods, both analytical and numerical, for analyzing axial vibration of pile foundations in soil [Nogami and Novak, 1976; Kausel and Peek, 1982; Mylonakis and Gazetas, 2002; and Cairo et al., 2005]. In the present paper, a semi-analytical method similar to the Thin Layered Element Method (TLEM), which was developed by Tajimi and Shimomura (1976) for lateral vibration of piles, is presented for axial vibration. Mizuhata et al. (1985) also presented solutions of axial vibration of piles based on TLEM. However, the present method has been derived independently and is validated and reported here for better understanding of the method.

There have been very few studies regarding the effect of axial stiffness of batter piles on structures in the event of horizontal vibration. Tazoh et al. (1988) discussed strain distribution along the length and other

important features of batter piles through seismic observation and analysis. Ingham et al. (1999) performed non-linear dynamic analysis of a bridge bent supported with batter piles but considered only lateral Winkler type springs acting on the batter piles ignoring the coupling effect among the different layers of soil. In the present paper, a pier of an existing old railway bridge has been analyzed with a simple model. The simple model comprises of an SDOF model of the pier, rigid pile cap and pile head stiffness as derived from the semi-analytical method. The effect of both axial and lateral stiffness of batter piles on the modal parameters of the pier is discussed here.

2. AXIAL VIBRATION OF A PILE IN LAYERED SOIL

In the present formulation soil is considered as an elastic medium horizontally layered and semi-infinite in lateral extent (Figure 1). The soil has a fixed boundary at the bottom end of the pile length.

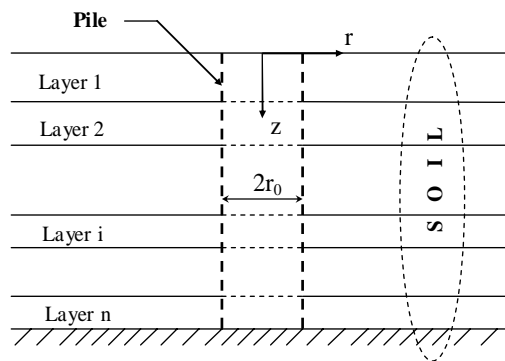


Figure 1: Schematic diagram of the layered pile-soil model

2.1 Soil stiffness

If u_r and u_z are respectively the displacements in radial and vertical directions, wave motion equations in cylindrical coordinates for an axis-symmetric problem are given by,

$$(\lambda + 2\mu) \frac{\partial \Theta}{\partial r} + 2G \frac{\partial \tilde{\omega}_\theta}{\partial z} = \rho \frac{\partial^2 u_r}{\partial t^2} \quad (1)$$

$$(\lambda + 2\mu) \frac{\partial \Theta}{\partial z} - \frac{2G}{r} \frac{\partial}{\partial r} (r \tilde{\omega}_\theta) = \rho \frac{\partial^2 u_z}{\partial t^2} \quad (2)$$

where the Lamé's constants λ and μ are complex numbers in order to take material hysteretic damping into account and ρ is the mass density.

The dilation Θ and rotation $\tilde{\omega}_\theta$ are given by,

$$\Theta = \frac{1}{r} \frac{\partial}{\partial r} (r u_r) + \frac{\partial u_z}{\partial z} \quad (3)$$

$$2\tilde{\omega}_\theta = \frac{\partial u_r}{\partial z} - \frac{\partial u_z}{\partial r} \quad (4)$$

The displacement components of soil may be described in terms of the following potential functions:

$$\begin{Bmatrix} u_r \\ u_z \end{Bmatrix} = \begin{Bmatrix} v_r \\ v_z \end{Bmatrix} e^{i\omega t} \quad (5)$$

$$\begin{Bmatrix} v_r \\ v_z \end{Bmatrix} = \begin{bmatrix} H_1^{(2)}(\alpha r) & 0 \\ 0 & H_0^{(2)}(\alpha r) \end{bmatrix} \begin{Bmatrix} \phi(z) \\ W(z) \end{Bmatrix} \quad (6)$$

where ω is the frequency of steady-state vibration and $H_j^{(2)}$ is Hankel function of the second kind of order j . $\phi(z)$ and $W(z)$ are the transformation variables of the potential function.

Substituting the potential functions in equations 1 and 2 yields,

$$\alpha^2(\lambda + 2\mu)\phi - \mu \frac{d^2\phi}{dz^2} + \alpha(\lambda + \mu) \frac{dW}{dz} - \rho\omega^2\phi = 0 \quad (7)$$

$$-\alpha(\lambda + \mu) \frac{d\phi}{dz} + \alpha^2\mu W - (\lambda + 2\mu) \frac{d^2W}{dz^2} - \rho\omega^2W = 0 \quad (8)$$

Applying Galarkin's Method and assembling the global matrices, the above equations are solved in the manner of an Eigen-value problem. There exist a total of $4n$ solutions of α , where n is the number of soil layers. When radiation condition is considered, the number of appropriate Eigen-values is $2n$.

A foundation with a circular cross-section is assumed to be embedded upright in the stratified soil. The boundary displacement components in radial and vertical directions are respectively expressed as,

$$\{\mathbf{V}_r\} = \sum_{\alpha} H_1^{(2)}(\alpha r_0) \{\phi\}_{\alpha} q_{\alpha} \quad (9)$$

$$\{\mathbf{V}_z\} = \sum_{\alpha} H_0^{(2)}(\alpha r_0) \{\mathbf{W}\}_{\alpha} q_{\alpha} \quad (10)$$

where, q_{α} is the effective contribution corresponding to α .

Modal matrices can be defined as,

$$[\mathbf{X}] = [\{\phi\}_1 \ \{\phi\}_2 \ \cdots \ \{\phi\}_{2N}] \quad (11)$$

$$[\mathbf{Z}] = [\{\mathbf{W}\}_1 \ \{\mathbf{W}\}_2 \ \cdots \ \{\mathbf{W}\}_{2N}] \quad (12)$$

Now,

$$\begin{Bmatrix} \{\mathbf{V}_r\} \\ \{\mathbf{V}_z\} \end{Bmatrix} = \begin{bmatrix} & & & [\mathbf{X}] \\ & & & \vdots \\ & & & \\ [\mathbf{Z}] & & & \\ & g_{\alpha} & & \\ & & & \vdots \end{bmatrix} \{\tilde{\mathbf{q}}_{\alpha}\} = [\mathbf{J}_z] \{\tilde{\mathbf{q}}_{\alpha}\} \quad (13)$$

where, $\tilde{q}_\alpha = q_\alpha H_1^{(2)}(\alpha r_0)$ and $g_\alpha = \frac{H_0^{(2)}(\alpha r_0)}{H_1^{(2)}(\alpha r_0)}$.

The global force vector can be expressed as,

$$\frac{1}{2\pi r_0} \{ \mathbf{P}_{z_s} \} = \left[\begin{array}{c} [\mathbf{B}_G]^T [\mathbf{X}] + [\mathbf{A}_s] [\mathbf{Z}] \\ \alpha \\ \ddots \end{array} \right] \{ \tilde{\mathbf{q}}_\alpha \} = [\mathbf{D}_z] \{ \tilde{\mathbf{q}}_\alpha \} \quad (14)$$

where,

$$[\mathbf{B}_G]^e = \frac{\mu}{2} \begin{bmatrix} 1 & 1 \\ -1 & -1 \end{bmatrix}, \quad [\mathbf{A}_s]^e = \frac{1}{6} \mu H \begin{bmatrix} 2 & 1 \\ 1 & 2 \end{bmatrix}$$

From equations 13 and 14,

$$\{ \mathbf{P}_{z_s} \} = [\mathbf{R}_z] \left\{ \begin{array}{c} \{ \mathbf{V}_r \} \\ \{ \mathbf{V}_z \} \end{array} \right\} = [\mathbf{R}_{z_1} : \mathbf{R}_{z_2}] \left\{ \begin{array}{c} \{ \mathbf{V}_r \} \\ \{ \mathbf{V}_z \} \end{array} \right\} \quad (15)$$

where, $[\mathbf{R}_z] = 2\pi r_0 [\mathbf{D}_z] [\mathbf{J}_z]^{-1}$.

Ignoring coupling with \mathbf{V}_r ,

$$\{ \mathbf{P}_{z_s} \} = [\mathbf{R}_{z_2}] \{ \mathbf{V}_z \} \quad (16)$$

Equation 16 provides information regarding soil stiffness along different depths of the pile along with the coupling among the soil layers.

2.2 Stiffness of a pile embedded in soil

The vertical force-displacement relationship of a pile can be expressed as,

$$\{ \mathbf{P}_{z_p} \} = [\mathbf{K}] \{ \mathbf{w} \} \quad (17)$$

Considering compatibility, from equations 16 and 17 one gets,

$$[\mathbf{R}_{z_2}] + ([\mathbf{K}] - \omega^2 [\mathbf{M}_z]) \{ \mathbf{V}_z \} = \{ \mathbf{P}_z \} \quad (18)$$

Equation 18 describes the pile-soil interaction. Pile head stiffness can be obtained by solving the equation. Deformation of pile due to Inertial and kinematic interaction can also be determined.

Pile head stiffness obtained using the present method is verified with the results obtained by Nogami and Novak (1976). Ratio between dynamic pile head stiffness to static stiffness k_{dyn}/k_{stat} for varying ratios of pile length to pile outer radius L/r_0 and shear wave velocity of soil to longitudinal wave velocity of pile v_s/v_{pile} are produced in Figures 2, 3 and 4. Here Poisson's ratio ν of 0.4, the ratio of soil density to pile density ρ/ρ_p of 0.6 and

damping ratio D of 2% is assumed. The curves presented in Figures 2, 3 and 4 are identical with the results obtained by Nogami and Novak.

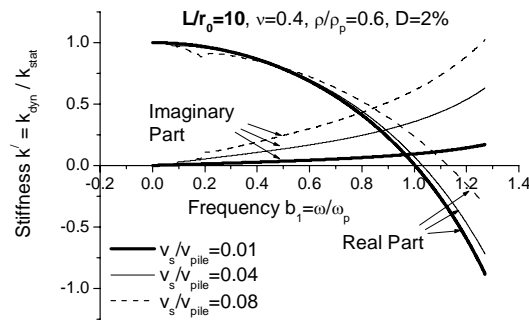


Figure 2: Variation of normalized pile stiffness with frequency and soil stiffness for very short piles

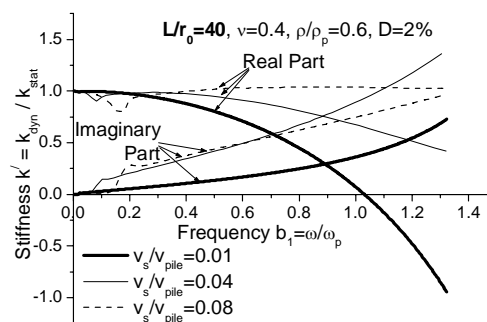


Figure 3: Variation of normalized pile stiffness with frequency and soil stiffness for moderately slender piles

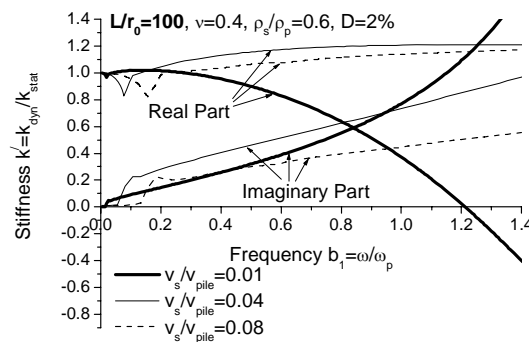


Figure 4: Variation of normalized pile stiffness with frequency and soil stiffness for slender piles

3. MODAL ANALYSIS OF A PIER WITH BATTER PILES

The orientation of the axial and lateral stiffness of a batter pile is inclined by the batter angle. Thus as shown in Figure 5 the substructure (i.e., the pile cap along with the pile-soil system) may be modeled with axial and lateral springs substituted for the piles and soil. The stiffness components for the degrees of freedom of the pile-cap can be expressed as,

$$\begin{aligned} \mathbf{K}_{cap1,1} &= \sum_i K_{x,i} \sin^2 \theta_i + K_{z,i} \cos^2 \theta_i \\ \mathbf{K}_{cap1,2} &= \mathbf{K}_{cap2,1} = \sum_i (K_{x,i} - K_{z,i}) \sin \theta_i \cos \theta_i \\ \mathbf{K}_{cap1,3} &= \mathbf{K}_{cap3,1} = \sum_i x_i (K_{x,i} \sin^2 \theta_i + K_{z,i} \cos^2 \theta_i) \\ \mathbf{K}_{cap2,2} &= \sum_i K_{x,i} \cos^2 \theta_i + K_{z,i} \sin^2 \theta_i \\ \mathbf{K}_{cap2,3} &= \mathbf{K}_{cap3,2} = \sum_i x_i (K_{x,i} - K_{z,i}) \sin \theta_i \cos \theta_i \\ \mathbf{K}_{cap3,3} &= \sum_i x_i^2 (K_{x,i} \sin^2 \theta_i + K_{z,i} \cos^2 \theta_i) \end{aligned}$$

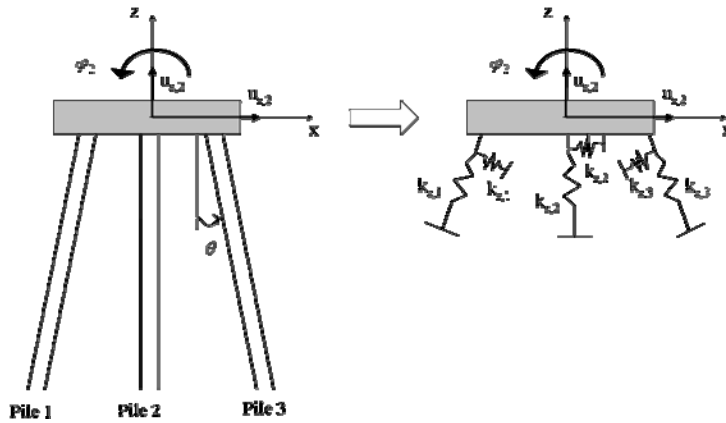


Figure 5: Pile cap supported with pile-head springs

The stiffness equation for the superstructure may be written as,

$$\begin{Bmatrix} F_{z,1} \\ F_{x,1} \\ M_1 \\ F_{z,2} \\ F_{x,2} \\ M_2 \end{Bmatrix} = \begin{bmatrix} \frac{EA}{L} & 0 & 0 & -\frac{EA}{L} & 0 & 0 \\ 0 & \frac{12EI}{L^3} & \frac{6EI}{L^2} & 0 & -\frac{12EI}{L^3} & \frac{6EI}{L^2} \\ 0 & \frac{6EI}{L^2} & \frac{4EI}{L} & 0 & -\frac{6EI}{L^2} & \frac{2EI}{L} \\ -\frac{EA}{L} & 0 & 0 & \frac{EA}{L} & 0 & 0 \\ 0 & -\frac{12EI}{L^3} & -\frac{6EI}{L^2} & 0 & \frac{12EI}{L^3} & -\frac{6EI}{L^2} \\ 0 & \frac{6EI}{L^2} & \frac{2EI}{L} & 0 & -\frac{6EI}{L^2} & \frac{4EI}{L} \end{bmatrix} \begin{Bmatrix} u_{z,1} \\ u_{x,1} \\ \phi_1 \\ u_{z,2} \\ u_{x,2} \\ \phi_2 \end{Bmatrix}$$

$$= \begin{bmatrix} \mathbf{K}_{col1,1} & \mathbf{K}_{col1,2} \\ \mathbf{K}_{col2,1} & \mathbf{K}_{col2,2} \end{bmatrix} \begin{Bmatrix} \mathbf{u}_1 \\ \mathbf{u}_2 \end{Bmatrix} \quad (19)$$

For harmonic vibration,

$$\begin{bmatrix} \mathbf{K}_{col1,1} - \mathbf{m}_1 \omega^2 & \mathbf{K}_{col1,2} \\ \mathbf{K}_{col2,1} & \mathbf{K}_{col2,2} + \mathbf{K}_{cap} - \mathbf{m}_2 \omega^2 \end{bmatrix} \begin{Bmatrix} \mathbf{u}_1 \\ \mathbf{u}_2 \end{Bmatrix} = \begin{Bmatrix} \mathbf{0} \\ \mathbf{0} \end{Bmatrix} \quad (20)$$

The solution of the Eigen-value problem of equation 20 would yield the Eigen frequencies and corresponding normal modal vectors of the system.

4. APPLICATION

The method described in Section 3 is applied to the pier-pile system of an existing railway bridge which is located in Shizuoka prefecture in Japan. The foundations of the bridge consist of both vertical and batter piles (Figure 6). The piles are steel piles with 254 mm outside diameter and 9 mm thickness. Shear wave velocities of soil at different depths at the site are given in Table 1. In order to determine the dynamic behavior of a typical pier-pile system of the bridge some micro-tremor measurements were made at a pile cap and a cross-girder of the bridge in the present study. From the micro-tremor measurement it was found that the predominant frequency for the superstructure is 2.6 Hz. for longitudinal vibration and 2.4 Hz. for transverse vibration.

At first the dynamic stiffness, both lateral and axial, of a single upright beam has been calculated for the specific site characteristics as explained in Section 2. Lateral and axial impedances of a single pile are presented in Figures 8 and 9. With the assumption that for small batter angles the pile head impedances of a batter pile may not too different than a straight pile, for the given pile arrangement as shown in Figure 7, a modal analysis was performed. With the assumption that the piles reached the bed-rock, the length of the piles was taken as 44 m. The results of the modal analysis show that the lowest modal frequency is 1.32 Hz for longitudinal vibration and 2.32 Hz. for transverse vibration.

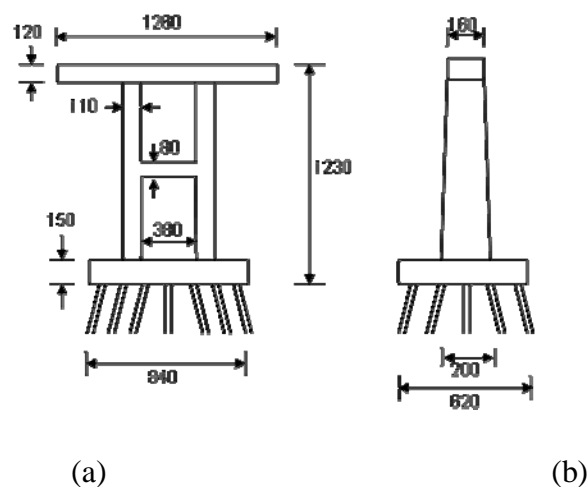


Figure 6: Schematic diagram of a typical pier of the bridge (a) front elevation (b) side elevation (dimensions are in cm)

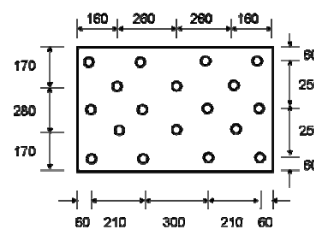


Figure 7: Pile layout of a typical foundation (dimensions are in cm)

Table 1: Soil profile at the site of the bridge.

Depth (m)	Shear wave velocity (m/s)
0 - 1.5	113
1.5 - 8.0	82
8.0 - 19.0	76
19.0 - 25.0	61
25.0 - 31.0	81
31.0 - 41.2	116
41.2 -	510

The modes of vibration at these frequencies are schematically shown in Figures 10 and 11. All the displacement and rotational degrees of freedom are nearly in-phase. The mode shows greater deformation at the pier top and clockwise rotation for rightward motion. The mode is most likely to be induced in case of load acting at the pier top e.g., wind load. For longitudinal vibration the predominant frequency determined by the modal analysis is much lower than that determined by the micro-tremor measurement. The reason is probably the present 2D model fails to consider the significant stiffness in the longitudinal direction due to its 3D configuration. Thus this 2D model is not appropriate for longitudinal vibration. On the other hand, the predominant frequency in the transverse direction as obtained by the modal analysis matches very well with the measured value. Since the torsional rigidity of the deck and longitudinal girders are insignificant compared to the flexural stiffness of the pier, the 2D model could simulate the dynamic behavior of the system in transverse direction.

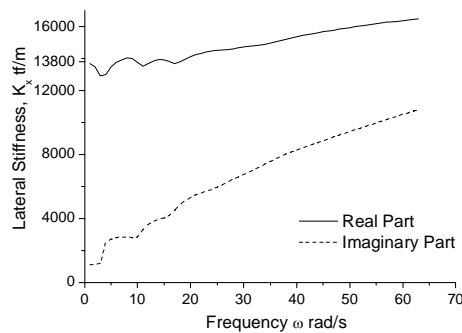


Figure 8: Lateral stiffness of a single pile of the bridge

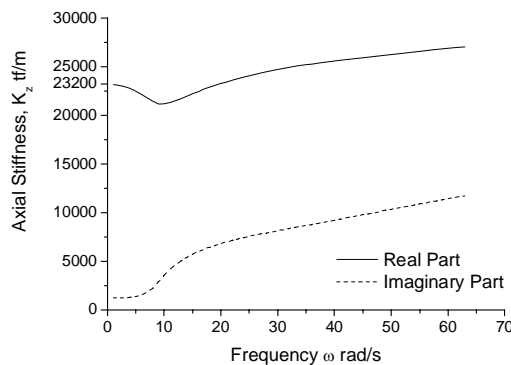


Figure 9: Axial stiffness of a single pile of the bridge



Figure 10: Fundamental mode shape of a typical pile-pier system of the bridge for longitudinal vibration (not in scale)

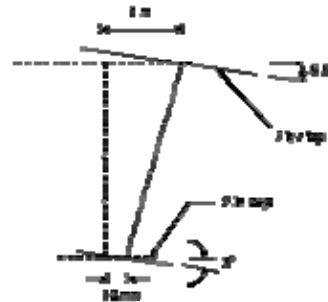


Figure 11: Fundamental mode shape of a typical pile-pier system of the bridge for transverse vibration (not in scale)

To understand the effect of the inclination of the batter piles in transverse vibration, modal analyses have been performed for the same pile-pier system with different batter angles of piles. The results are presented in Figure 12. Pile inclination has the most prominent effect on pile cap deformation. For a certain batter angle between 15° and 20° , the pile cap deformation in the first mode of vibration becomes zero. Beyond this particular batter angle the pile cap deformation again increases and actually becomes out-of-phase with the pier top deformation. For greater batter angles, the pier top deformation is out-of-phase and rotations are in phase with pile cap deformation; which means a right-ward pile cap deformation is associated with a left-ward pier top deformation and anti-clockwise rotations at both pier top and pile cap. Thus for greater batter angles the mode of vibration induced by a force at the pile cap or by ground vibration becomes predominant.

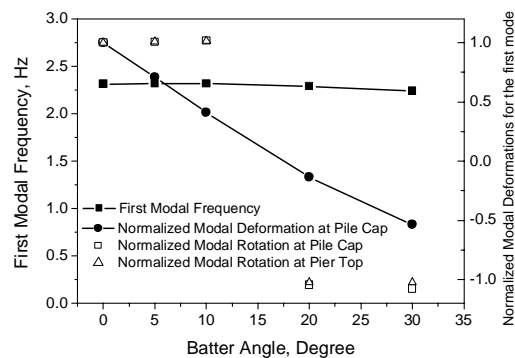


Figure 12: Variation of modal parameters of pile-pier system with batter angle

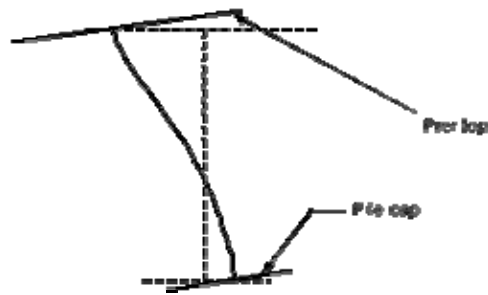


Figure 13: First mode of vibration for greater batter angles

5. CONCLUSIONS

Modal analysis of a 2D model of the pile-pier system of an existing bridge has been performed. In the present analysis both axial and lateral stiffness of batter piles have been considered. When compared with ambient vibration records, the results of the modal analysis seem to agree well in the case of transverse vibration, but not in longitudinal vibration due to significant 3D effect. The most significant effect of the inclination of batter piles is reduction of pile cap deformation up to a certain batter angle. Beyond this particular batter angle when pile cap deformation becomes zero, the mode shape changes abruptly. Mode imposed by forces at the pier top is predominant for lower batter angles. Whereas modes corresponding to the pile cap deformation is predominant for higher batter angles.

ACKNOWLEDGEMENT

The present study was conducted during a research fellowship awarded to the first author by Japan Society for Promotion of Science (JSPS).

REFERENCES

- Cairo, R., Conte, E., and Dente, G., 2005. Analysis of pile group under vertical harmonic vibration. *Computers and Geotechnics* 32, 545-554.
- Ingham, T. J., Rodriguez, S., Donikian, R., and Chan, J., 1999. Seismic analysis of bridges with pile foundations. *Computers and Structures* 72, 49-62.
- Kausel, E., and Peek, R., 1982. Dynamic Loads in the Interior of a Layered Stratum: An Explicit Solution. *Bulletin of the Seismological Society of America* 72, 1459-1481.
- Mizuhata, K., Kusakabe, K., and Katayama, K., 1985. Vertical vibration of floating pile by thin layer method: comparison with experimental results. *Summaries of technical papers of Annual Meeting, Architectural Institute of Japan* B, 393-394 (In Japanese).
- Mylonakis, G., and Gazetas, G., 2002. Kinematic pile response to vertical p-wave seismic excitation. *Journal of Geotechnical and Geoenvironmental Engineering* 128, 860-867.
- Nogami, T., and Novak, M., 1976. Soil-pile interaction in vertical

vibration. *Earthquake Engineering and Structural Dynamics* 4, 277-293.

Tajimi, H., and Shimomura, Y., 1976. Dynamic analysis of soil structure interaction by the thin layered element method. *Transactions of Architecture Institute of Japan* 243, 41-51 (In Japanese).

Tazoh, T., Shimizu, K., and Wakahara, T., 1988. Seismic observations and analyses of grouped piles. *Shimizu Technical Research Bulletin* 7, 17-32.

SEISMIC ASSESSMENT OF PILE FOUNDED KHILGAON FLYOVER

MOHAMMAD MOSLEM UDDIN

Assistant Engineer

PWD Design Division-2, Purta Bhaban, Segunbagicha

Dhaka 1000, Bangladesh

moslem_1990@yahoo.com

MEHEDI A. ANSARY

Prof., Dept. of Civil Engg.,

BUET, Dhaka 1000, Bangladesh

TAHSIN R. HOSSAIN

Assoc. Prof., Dept. of Civil Engg.,

BUET, Dhaka 1000, Bangladesh

MUNAZ A. NOOR

Assoc. Prof., Dept. of Civil Engg.,

BUET, Dhaka 1000, Bangladesh

ABSTRACT

Khilgaon Flyover comprises three main arms-Rajarbagh, Saidabad and Malibagh arms forming T-junction at Khilgaon road and rail intersection. In addition, it has a loop at Malibagh side. The sub soil stratum of the site is composed of Dhaka clay and is not susceptible to liquefaction under a moderate earthquake. However, recent earthquakes like Asia-Tsunami (2004) and Kashmir Earthquake (2005) made experts think that Bangladesh may experience a severe earthquake at any time. For this reason, a proposed structure need to be designed considering a probable earthquake and re-evaluation of existing structures is necessary. In this study, seismic response of the Khilgaon flyover was investigated. Both seismic static and dynamic analyses were performed. In both cases, a typical 26 m long simply supported span and a bored cast in situ RC pile under a typical pier were investigated. Superstructure and substructure were analyzed separately. In substructure, modeling equivalent Winkler-type pile foundation model was used. For static analysis, Single Mode Spectral Analysis Method as specified in AASHTO-LRFD (2004) was adopted. In dynamic analysis, response spectrum method was adopted. BNBC (1993) response spectrum acceleration was used as input acceleration. Finite element software SAP2000 was used as modeling tool for 3D analysis of superstructure as well as the substructure. Structural responses, i.e. mode shapes, pier top deflection, pier base forces, pile top deflection, forces at pile etc. were observed and estimated. Reinforcement was checked as per AASHTO load combination. It is observed that static analysis produces conservative values than dynamic analysis. In both cases, structures were found to be safe.

1. INTRODUCTION

From a natural hazard viewpoint, Dhaka is among the most vulnerable cities in the world. Parts of Bangladesh including Dhaka, Chittagong and Sylhet had been experiencing tremor from earthquake at almost regular interval that caused significant damage to lives and properties. A recent study conducted by Ansary (2003) revealed that an earthquake with intensity VIII could cause damage to up to 40 percent buildings in certain areas of Dhaka city. Bangladesh National building Code (1993) placed Dhaka in Seismic Zone 2 with PGA value of 0.15g. The seismic zones mentioned in the national code were not based on analytical assessment of seismic hazard and were mainly based on the location of historical data (Ansary and Choudhury, 2004). An updated seismic zoning map based on analytical study was recently developed (Sharfuddin, 2001). Based on the philosophy behind the seismic zoning and experience from recent earthquake it can reasonably be assumed that a major earthquake event in Dhaka region is capable of producing huge damage than that assumed in existing zoning map-BNBC 1993 (Ansary and Choudhury, 2004).

During the last five years, two flyovers namely Khilgaon flyover and Mohakhali flyover were constructed. Construction of Gulistan-Jatrabari flyover and Tongi flyover has already been started. More flyovers at Moghbazar and Kuril are proposed. Khilgaon flyover as shown in Figure 1 is located at Khilgaon Rail and Road intersection in Dhaka city. Main Rail track, to and from Dhaka, passes this area. Any damage to this structure will cost huge lives and property. Main objective of this study was to investigate the behavior of the Khilgaon flyover under seismic forces.



Figure 1: Aerial View of Khilgaon Flyover (From Google Earth, 2006)

2. SOIL-STRUCTURE INTERACTION

Soil-structure interaction is very important for any kind of structure. Seismic forces like gravity forces develop deformation in foundation resulting changes in stresses within soil, which ultimately dictates behavior of the structure. Two general approaches are available for rationally incorporating soil-structure interaction effects into structural analysis (Wolf, 1985). In the *direct method*, the structure and a portion of the founding soil are incorporated in finite element modeling. Some drawbacks of this model including the need for larger model, energy absorbing boundaries and detail soil properties make its use prohibitive for all but most extensive analysis demands. A simpler, more efficient approach is the “substructure method” (McGuire et al., 1998). With this method, superstructures and substructures are analyzed separately. A simplified model for substructure is constructed that can approximate the behavior of the soil at the foundation. This simplified model is then coupled with structure at the supports, and structure is analyzed. The foundation model is composed of set of structural elements, ranging in complexity from elastic springs alone to complicated non-linear spring/damper combinations arranged in series and/or parallel for each degree of freedom. They are chosen based on the assumed foundation behavior obtained either experimentally or analytically (McGuire et al., 1998).

3. METHODOLOGY

Evaluation of response of a structure in conjunction with the supporting soil presents a challenging and multi-facetious task. The complexity of the problem comes from the fact, that the interaction between soil and structure engenders various phenomena of different physical nature often with mutually opposing influence. The analytical and numerical approaches applied in the engineering practice typically employ simplifying assumptions, which preclude them from handling all these effects simultaneously. This accounts for considerable difficulty in analyzing the problem entirely.

In this study a detail seismic assessment of the flyover at Khilgaon rail and road intersection was performed. Linear dynamic response spectrum analysis was performed for a simply supported span and for a single pile foundation under pier of the flyover considering type II soil condition and zone coefficient of 0.15. Finite element software SAP2000 (CSI, 2003) was used as modeling tool.

4. DESCRIPTION OF THE FLYOVER

4.1 Site Conditions

Most of the part of the Khilgaon flyover rests mainly on original Dhaka clay. Top portion of soil up to around 8 m depth is stiff to very stiff

reddish brown sandy silt with clay followed by a 13 m thick (8 to 21 m) medium to dense fine sand with silt and trace mica underlain by a very dense light brown clayey fine sand with silt trace mica from a depth of 21-25 m downward. However, topsoil up to 3.5 m at some part of main flyover composes of fill and organic matter and soft clay. Subsurface profiles along Rajarbagh arm and Saidabad-Malibagh arm of main flyover at Khilgaon flyover site are shown in Figure 2 and Figure 3 respectively.

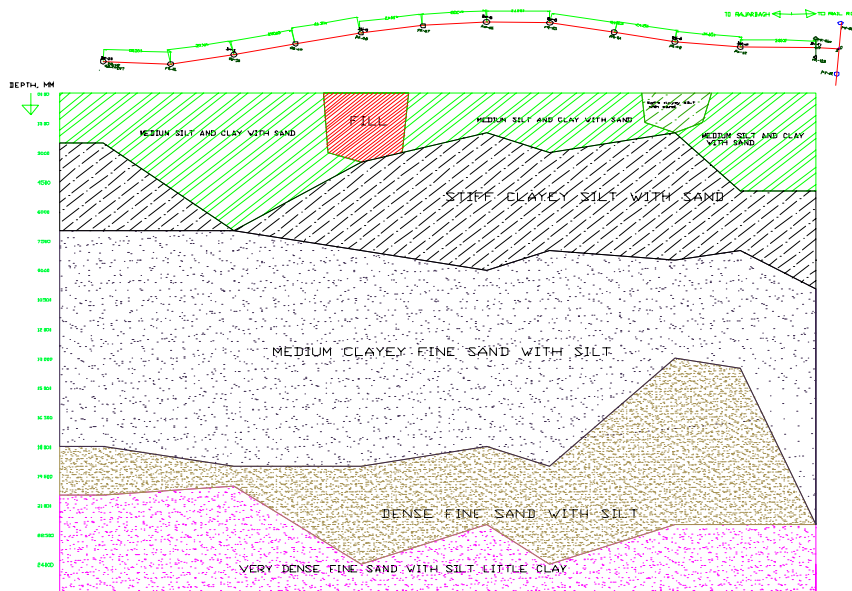


Figure 2: Subsoil Profile along Rajarbagh side of the Flyover (Uddin, 2006)

4.2 Superstructure

Fourteen-meter wide main flyover is of 4-lanes. A concrete divider separates two-lane roadways on each side of the centerline of the flyover. Length of main flyover comprising 29 simply supported 22 m to 30 m long spans is about 778 m. Most of the spans are around 26 m long. Expansion joints were provided between adjacent two spans. Lengths of main flyover at Rajarbagh, Saidabad and Malibagh arms are 285 m, 303 m and 190 m respectively. A typical span comprises of 0.21 m thick RC deck slab resting on 1.66 m deep pre-stressed concrete (PC) girder, which transmits loads through RC pier cap and 2 m diameter single pier system to cast insitu RC pile foundation. Pier caps are of 2 m constant width and varying depth ranging between 2 m at pier-pier cap joint and 1 m at free end. Each single pier rests on 4 to 6 nos. bored cast insitu RC piles of 0.9 m diameter and 30 m length connected with RC pile caps. Pier 1 at Rajarbagh arm near rail and road intersection comprises 1.5 m diameter two columns, each of which rests on 4 numbers 0.61 m diameter 30 m long bored cast in situ RC piles. This pier comprises 1.5 m deep and 1.5 m wide cap. Figure 4 shows elevation of a typical pier bent at main flyover. A typical 2.0 m diameter pier was reinforced with 58 numbers 25 mm diameter main bars.

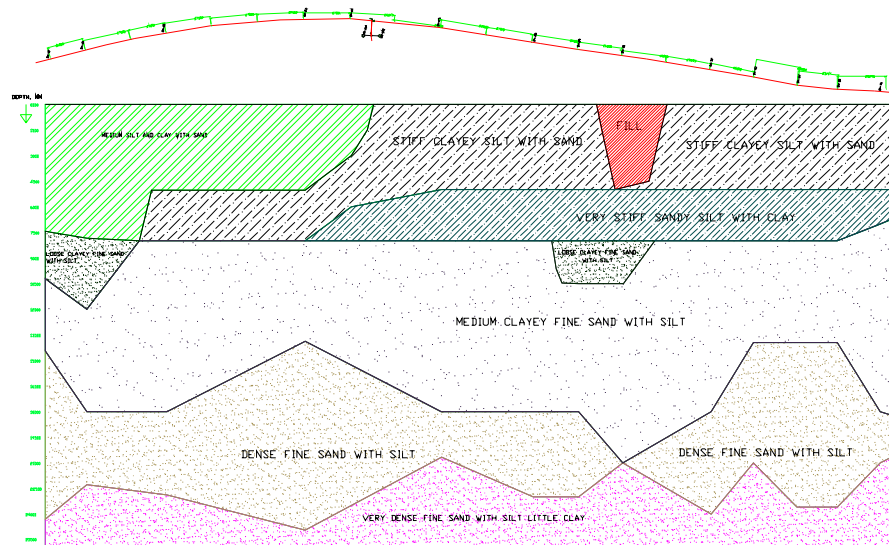


Figure 3: Subsoil Profile along Saidabad-Malibagh Arm of the Flyover (Uddin, 2006)

Pre-stressed concrete girders rest on pier cap through neoprene elastomeric bearings. Single bearing of 0.55m x 0.35m x 0.091m thick was set under each girder. A 0.05 m thick wearing coat was provided at the deck. Pier height in main flyover varies between 5 m and 8 m. There is a loop at Malibagh side of main flyover. Length of loop is about 477 m of which around 140 m is continuous RC 2.4 m deep box supported by single pier and the rest portion is RC deck resting on PC girders, which rest on pier cap – pier system founded on piles. Loop width varies between 7 m and 8.5 m. The expected material strengths are $f'_c=25$ MPa for concrete of normal RC, $f'_c=35$ MPa for pre-stressing concrete; $f_y=415$ MPa for mild steel and $f_u=1860$ MPa for high tensile wire for pre-stressing. Lengths of reinforced earth ramps at Rajarbagh, Saidabad and Malibagh are 222 m, 220 m and 202 m respectively. Abutments at junction of main flyover and ramp rest on RC pile foundation.

4.3 Foundation

All the piers rest on bored cast insitu 0.9 m diameter 30 m long RC pile. Numbers of piles under all piers are not the same. Depending on load at pier base, passage of sewerage line along or near the centerline of the flyover at some part, 4 to 6 numbers of piles were provided at each pier. Group of piles are connected to pier through RC pile cap. Abutments are also rest on RC bored cast insitu pile foundation. Figure 5 shows general pile arrangement under a typical pier at Khilgaon flyover. A 0.9 m diameter 30 m long bored cast insitu RC pile under a typical pier is reinforced with 10 numbers 25 mm diameter bars at top 7 m and the 10 numbers 20 mm lowest 23 m.

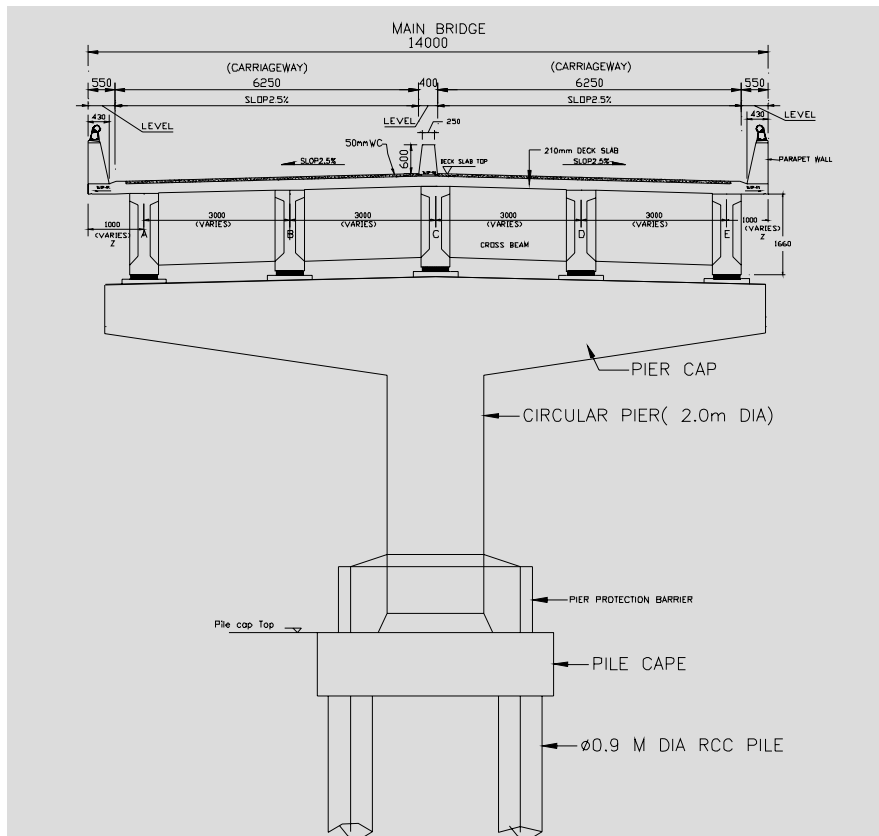


Figure 4: Elevation of a Typical Pier Bent (Source: DCL, 2005)

5. STATIC ANALYSIS

Adopting AASHTO-LRFD (2004) single mode spectral analysis method forces at pier base and piles under pier of the Khilgaon flyover were estimated. Span dead load of 6436 kN as estimated from the sectional property of elements was used for seismic static analysis. Loads were applied at pier top. Pier was considered cantilever in the both longitudinal and transverse directions. Seismic design forces at 2 m diameter 7 m high pier bases for both the directions are-base shear 868 kN and base moment 6076 kN-m. Maximum pier top drift under seismic forces for either longitudinal or transverse direction was found to be 15 mm.

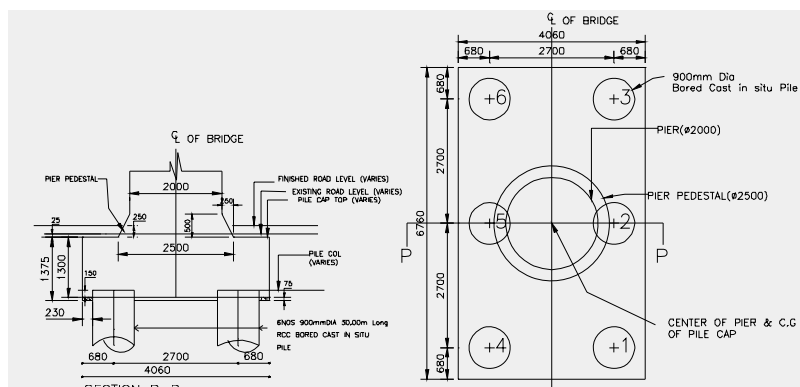


Figure 5: Pile arrangements under a typical pier at Khilgaon flyover (Source: DCL, 2005)

For determination of seismic design forces at pile, six piles under a single pier were modeled with pile cap as plate elements. Piles were modeled as beam element. To idealize soil support, spring constants determined based modulus of lateral subgrade reaction of soil were imposed at 1 m interval of the pile. SAP2000 computer software was used as modeling tool. Seismic design forces at pier base-868 kN lateral forces and 6076 kN-m moments were applied at pile cap center.

Seismic design forces in a single pile for longitudinal directions-shear 301 kN, moment 590 kN-m & axial force 715 kN and for transverse direction-shear 302 kN, moment 576 kN-m. & axial force 1785 kN. Maximum pile top deflection under seismic forces for either longitudinal direction or transverse direction was found to be nine mm

6. RESPONSE SPECTRUM ANALYSIS

6.1 Superstructure Model

A typical simply supported span of the Khilgaon Flyover was selected for 3D analyses. Model incorporates five concrete I-girders connected with rectangular RC cross beams. Girders rest on RC pier cap through neoprene elastomeric bearing. Girders are simply supported over pier caps and at this point, no moment in the longitudinal direction in the girder is produced. To idealise this condition in the model, moment release was assigned at ends of girders. A pier cap was modeled with twelve beam elements of variable depth to represent variable depth of the actual pier cap. Length of each beam element in the pier is one meter. Piers are modeled as 2 m diameter circular beam element. RC crossbeams were modeled as rectangular beam elements. Span loads were directly applied on members. Loads on pier cap from adjacent span were applied as point load. Fixed supports were assigned at pier base. A 3D model for a typical 26 m span superstructure is presented in Figure 6.

Of the twelve-number of modes at modal analysis, first four significant mode shapes of the model are presented in Figure 7. In first mode, the deflection observed of the structure was both in transverse and vertical directions in single curvature. Transverse direction movement was dominating. In second mode, movement observed of the structure was both in transverse and vertical directions with predominating vertical direction movement. In third mode, the movement observed was both in transverse and vertical directions. Rotational movement about vertical axis was observed in third mode. In fourth mode, movement observed of the structure was in vertical direction forming bow in the deck.

Seismic design forces at pier base are- longitudinal shear 835 kN and moment 5583 kN-m, transverse shear 446 kN and moment 3554 kN. Pier top deflections for longitudinal and transverse RS forces were found to be 15 mm and 10 mm respectively. Period of the model at first mode was found to be 0.7 sec.

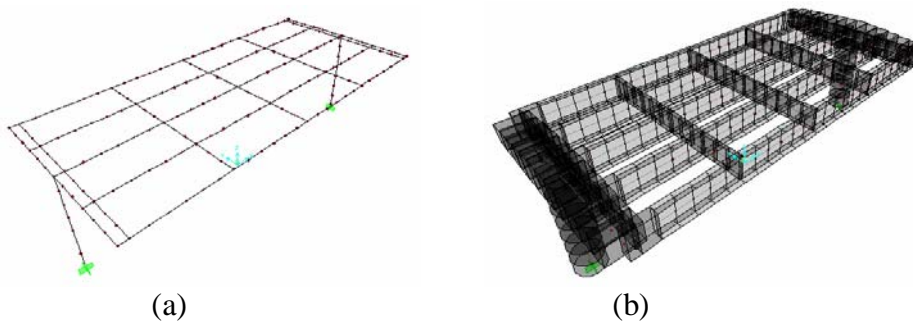


Figure 6: 3D FE model of a typical span of flyover; (a) Line diagram (b) In filled diagram

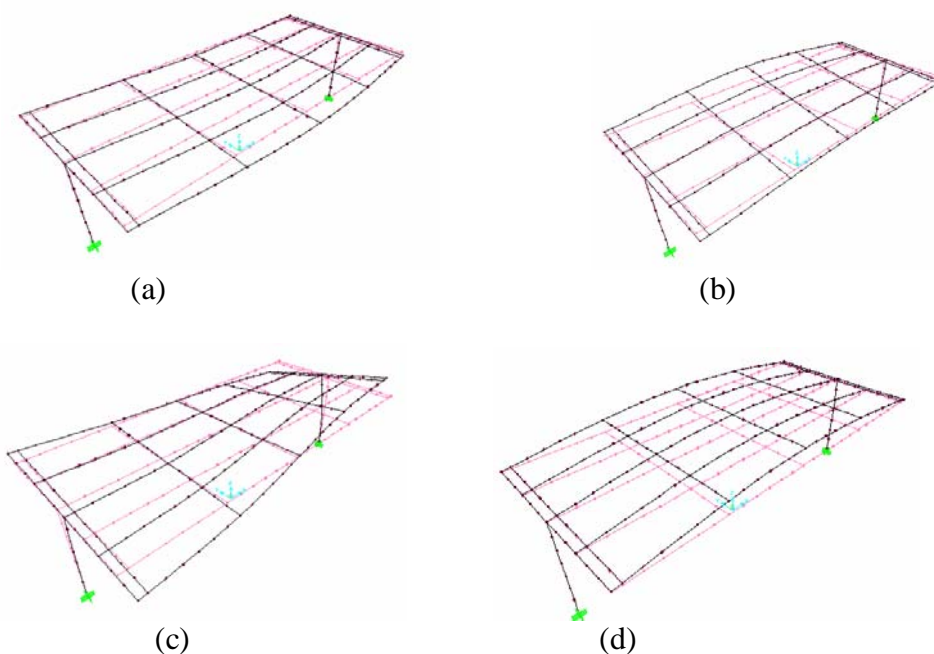


Figure 7: First four mode shapes of a typical span; (a) 1st mode, (b) 2nd mode, (c) 3rd mode and (d) 4th mode shapes

6.2 Pile Model

A typical 0.9 m diameter and 30 m long 6-pile group was modeled as circular beam element. Pile cap was modeled as 1.3 m thick plate elements. Lateral supports at 1 m interval along pile length were provided as spring constants. Total dead load reaction at pier obtained from superstructure model was applied at center of the cap. Of the twelve-number of modes at modal analysis, first four significant mode shapes of the model are presented in Figure 8. In first mode, deflection observed of the structure was both in longitudinal and vertical directions with predominating longitudinal direction movement. In second mode, deflection observed was in transverse direction in single curvature. In third mode, deflection observed was in vertical direction. In fourth mode, rotational movement about vertical axis, creating torsion in the piles, was observed.

Forces in a single pile from RS dynamic analysis are- for longitudinal directions-shear 212 kN, moment 442 kN-m & axial force 798 kN and for transverse direction-shear 308 kN, moment 410 kN-m & axial force 1586 kN. Maximum pile top deflection for either longitudinal or transverse direction was found to be 6 mm. Period of the model was found to be 0.3 sec.

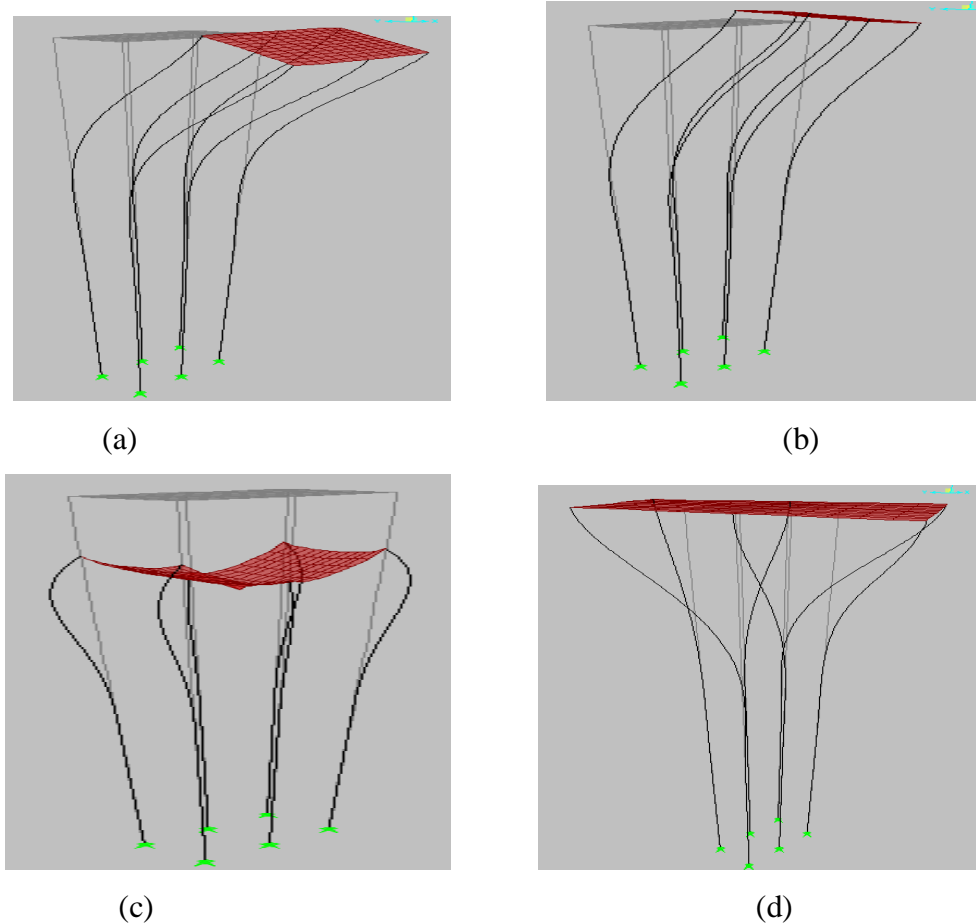


Figure 8: Mode shapes of typical a 6-pile group under pier of the flyover
(a) 1st mode, (b) 2nd mode, (c) 3rd mode and (d) 4th mode shape

7. CONCLUSIONS

In this study, seismic responses of a typical span and a typical bored cast insitu RC pile under a pier of Khilgaon flyover were assessed. SAP2000 (CSI, 2003) FEM software was used as a modeling tool. BNBC (1993) response spectra with soil type II was used as input acceleration. Later these results from dynamic analysis were compared with the results from AASHTO's static single mode spectral analysis method. It is observed that static method produces higher forces at both pier and pile. The flyover structure was found to be safe under seismic forces.

REFERENCES

- AASHTO, 2004 *LRFD Flyover Design Specification*, SI Units, 3rd Edition, American Association of State Highway and Transportation Officials, Inc., Washington, D.C.
- Ansary, M.A. 2003. *Economic Loss of Dhaka due to an Earthquake of Intensity VIII*, Insurance Journal of Bangladesh, Vol. 54, pp. 107-133.
- Ansary, M.A. and Choudhury, J. R., (2004), *Risk due to natural disasters in Dhaka city and measures for mitigation*, Fourth International Workshop on Seismic Analysis in the South Asia Region, 12-15 September 2004, Dhaka, Bangladesh. Pp. 23-35.
- Choudhury, J.R. and Ali, H. 1992. *Assessment of Seismic Hazard in Bangladesh*.
- Computers and Structures, Inc., SAP2000, Version 8.1, *Integrated Structural Analysis and Design Software*. Berkeley, CA, 2000.
- Development Constructions Ltd. 2005. *As Built Drawings, Construction of Flyover at Khilgaon Rail and Road Intersection in Dhaka City*, House No. 11, Road No. 19A, Sector No. 4, Uttara, Dhaka, Bangladesh.
- HBRI and BSTI 1993. *Bangladesh National Building Code, BNBC 1993* Dhaka, Bangladesh
- McGuire, J.W., Cannon, I.B.S., Cofer, W.F. and McLean, D.I. 1998. *Seismic evaluation of pile-founded highway flyover on saturated Peat* Journal of structural engineering, ASCE, 124 (1), pp. 71-79.
- Sharfuddin, M. 2001. *Earthquake Hazard Analysis for Bangladesh*, M.Sc. Engg. Thesis, Department of Civil Engineering, Bangladesh University of Engineering and Technology, Dhaka, Bangladesh.
- Uddin, M. M 2006. *Assessment of Khilgaon Flyover under Seismic Load*, M. Engg. Thesis, Department of Civil Engineering, Bangladesh University of Engineering and Technology, Dhaka, Bangladesh

PROPOSAL OF A METHODOLOGY TO DESIGN PP-BAND MESHES TO RETROFIT LOW EARTHQUAKE RESISTANT HOUSES

PAOLA MAYORCA and KIMIRO MEGURO
International Center for Urban Safety Engineering
Institute of Industrial Science, the University of Tokyo
paola@iis.u-tokyo.ac.jp

ABSTRACT

Past earthquakes have shown that the collapse of seismically weak adobe/masonry structures is responsible for most of the fatalities in developing countries. It is, thus, urgent to improve their seismic performance in order to reduce future fatalities and to protect the existing housing stock. To encourage seismic retrofitting, inexpensive and easy to implement technical solutions are desirable. Retrofitting by polypropylene band (PP-band) meshes satisfies these requirements. These bands commonly used for packing are resistant, inexpensive, durable and worldwide available.

Experiments and advanced numerical simulations have shown that PP-band meshes can dramatically increase the seismic capacity of adobe/masonry houses. Nevertheless, a simple yet accurate design method is still needed to optimize the mesh arrangement and assess its performance. PP-band meshes increase the structure ductility and energy dissipation capacity through controlled structure cracking. Therefore, it is very important to calculate transient and permanent displacements so that damage level and eventual repaired cost can be estimated.

In order to develop a simple methodology to design PP-band mesh retrofitting, time history responses of several PP-band retrofitted adobe/masonry structures subjected to different strong ground motions were calculated and analyzed to identify the most relevant factors influencing the behavior. The analyses showed that the most important factor controlling maximum transient and permanent displacements was the residual strength immediately after cracking. It is impossible to avoid cracks with PP-band meshes and when they occur, a strength drop is expected. It was found that if the relation between the residual and maximum strength is above a certain value, there are no remarkable variations in the structure maximum and transient displacements. The results obtained in this study will be used to propose a simple methodology to design PP-band mesh retrofitting for adobe/masonry houses.

1. INTRODUCTION

Past earthquakes have shown that the collapse of seismically weak adobe/masonry structures is responsible for most of the fatalities in developing countries. It is, thus, urgent to improve their seismic performance in order to reduce future fatalities and to protect the existing housing stock. To encourage seismic retrofitting, inexpensive and easy to implement technical solutions are desirable. Retrofitting by polypropylene band (PP-band) meshes satisfies these requirements. These bands commonly used for packing are resistant, inexpensive, durable and worldwide available.

A simple methodology to design PP-band mesh retrofitting is yet to be developed. This is absolutely necessary to estimate the expected structural response, in terms of transient and permanent deformations, for a particular demand. As a first step to develop such a design method, time history responses for several PP-band retrofitted adobe/masonry structures subjected to different strong ground motions are calculated and analyzed to identify the most relevant factors influencing the structural performance.

2. MODEL USED

2.1 Model formulation

Static tests [Sathiparan et al., 2004] have shown that the shear force – lateral deformation curve of a PP-band retrofitted wall can be roughly idealized as shown in the left curve of Figure 1. V_c and Δ_c correspond to the shear strength and cracking deformation of the masonry wall whereas V_r and K_r correspond to the residual strength and stiffness after the wall cracking. The first two parameters are mainly dependent on the masonry itself, V_r depends on both masonry and PP-band mesh and K_r depends mostly on PP-band.

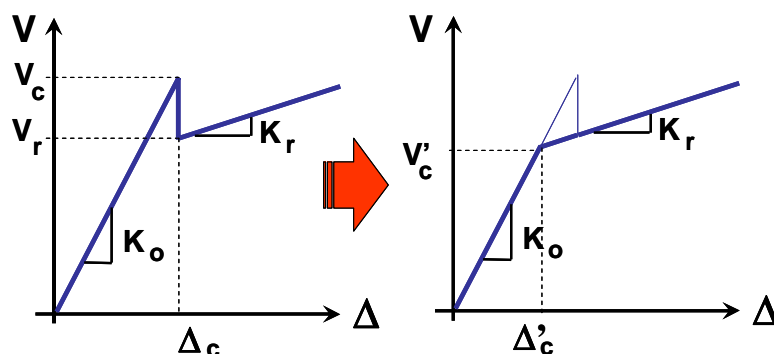


Figure 1: Idealization of shear force versus lateral deformation for a masonry wall retrofitted with PP-band mesh

To perform the non-linear time-history analysis, the force-deformation curve is further idealized as shown on the right side graph. This

simplification is assumed to be conservative as a fraction of the wall strength is not considered. In the graph:

$$\Delta'_c = \frac{V_r - K_r \Delta_o}{K_o - K_r} \tag{1}$$

$$V'_c = \frac{K_o}{K_o - K_r} (V_r - K_r \Delta_o) \tag{2}$$

To perform the cyclic analysis a hysteresis rule is necessary. For this purpose, a Modified Clough model, i.e. with degrading stiffness, was chosen for this study.

2.2 Model verification

The model was verified with available experimental data. The parameters considered are shown in the table below.

Table 1: Material properties

Parameter	Value
K_o [kN/mm]	5.00
K_r [kN/mm]	-0.20
Δ'_c [mm]	6.40

Figure 2 shows the comparison between the model and the experimental results. The envelope of both curves and the reloading branches coincide very well. Although the unloading branch is stiffer in the model, the overall response corresponds well to the experimental observation. It has been suggested that the hysteresis rule may not be critical for the estimation of the structural response [Miranda, 2006]. Therefore, the model was considered appropriate for the study.

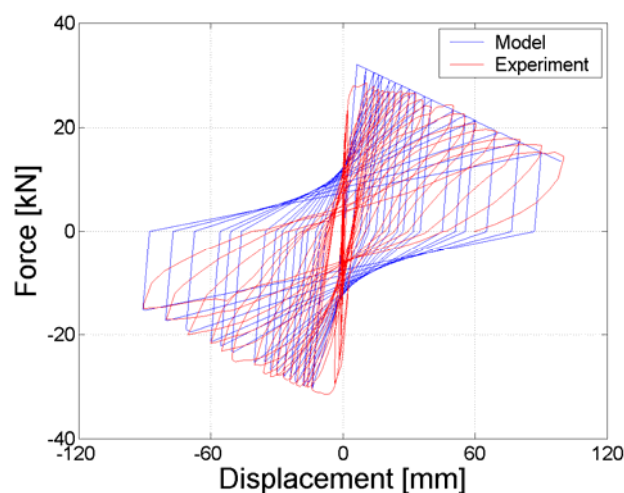


Figure 2: Comparison of the experimental response of a wall subjected to cyclic loads with the model prediction

3. PARAMETRIC STUDY

PP-band meshes improve the seismic performance of adobe/masonry houses by increasing its ductility through controlled cracking. Strength is not drastically improved with this retrofitting methodology although some additional strength is provided by the mortar covering.

In order to assess the seismic capacity of the retrofitted structures, it is necessary to estimate the amount of transient and permanent displacements. The former are important because beyond a certain limit they may lead to unstable behavior, buckling and eventual roof collapse. The latter define whether the structure can be reused and how much it may be necessary for repairing it.

To estimate the expected transient and permanent displacements as well as which parameters of the retrofitted walls (V_c , V_r , Δ_c , K_r) affect these the most, a parametric study using the model presented above was carried out. Eighteen structures with different force deformation characteristics subjected to three strong ground motion records were analyzed using 1-DOF systems. Tables 2 and 3 summarize the structure and ground record characteristics respectively.

The structural parameters were chosen so as to represent one of the two main walls of a 3-m high, 3-m long 1-story adobe/brick house. Three ratios of V_r/V_o were considered. These values are directly related to the volume of PP-band mesh and how tightly it is installed on the wall. It was experimentally determined that after applying a mortar cover on the retrofitted wall, this ratio was close to 0.8. The ratio K_r/K_o is higher for denser PP-mesh and was chosen null or negative based on the results of cyclic static tests and numerical simulations.

Table 2: Material properties considered for the parametric study

Parameter	V_o [kN]	K_o [kN/mm]	V_r/V_o	K_r/K_o
Adobe	35	10	0.50, 0.75, 1.00	0.00, -0.01, -0.02
Brick	100	50	0.50, 0.75, 1.00	0.00, -0.01, -0.02

Table 3: Strong ground motion records considered for the parametric study

Earthquake	Station	PGA ¹⁾ [g]	PGV ²⁾ [kine]	PGD ³⁾ [mm]
Imperial Valley (1940)	El Centro USGS St. 117	0.313	29.8	133.2
Loma Prieta (1989)	Capitola CDMG St. 47125	0.529	36.5	91.1
Cape Mendocino (1992)	Cape Mendocino CDMG St. 89005	1.497	127.4	410.1

¹⁾ Peak Ground Acceleration, ²⁾ Peak Ground Velocity, ³⁾ Peak Ground Displacement

Figure 3 shows the absolute acceleration response spectra of all the strong ground motion records used in the parametric study. The predominant period of a 1-story adobe/masonry structure is around 0.1 and 0.2s. The selected input motions are increasingly demanding in this range with the Cape Mendocino Earthquake being the severest of them all.

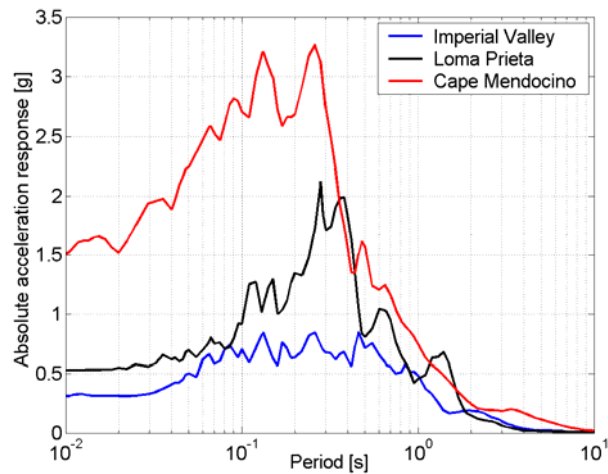


Figure 3: Strong ground motion response spectra (Damping = 5%)

Figures 4 and 5 show the time-history response of the adobe and masonry structures in blue line. The red line corresponds to the envelope of the monotonic curve. Note that the columns correspond to cases in which V_r/V_o is constant whereas the rows correspond to cases with the same K_r/K_o .

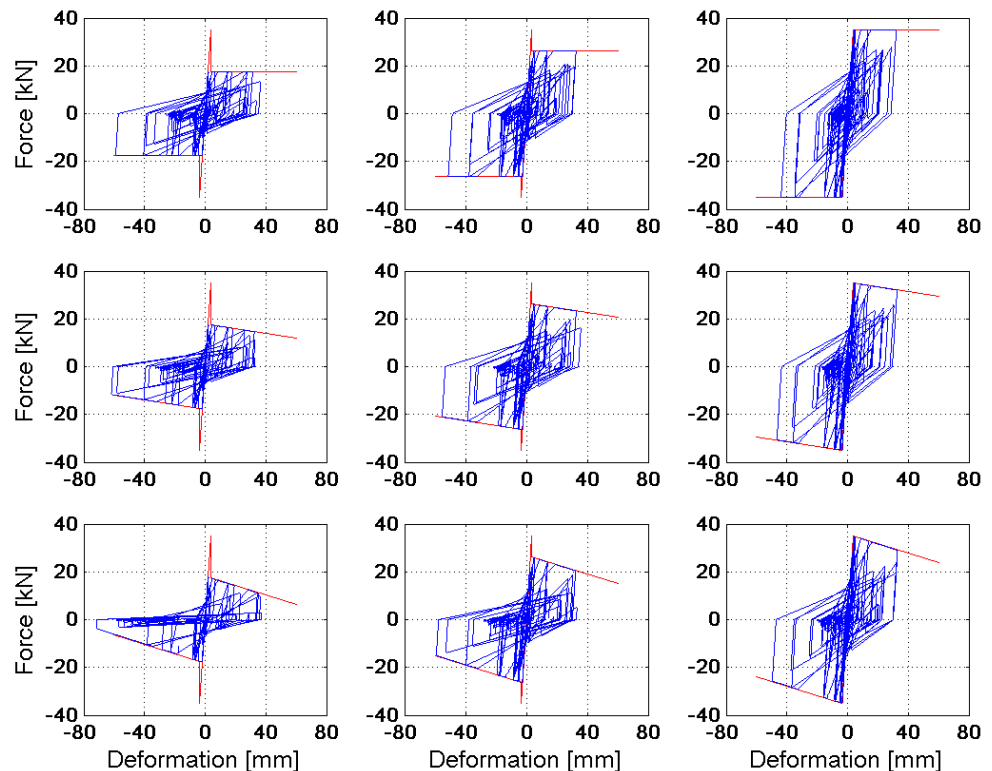


Figure 4: Time-history response of adobe structure (Loma Prieta Earthquake)

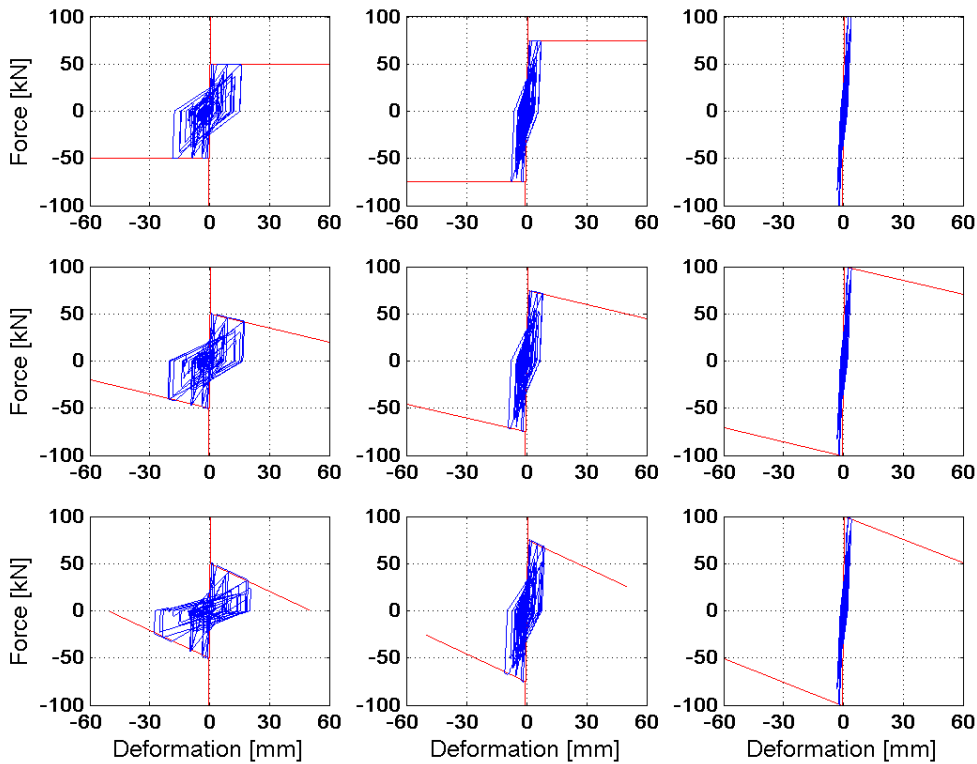
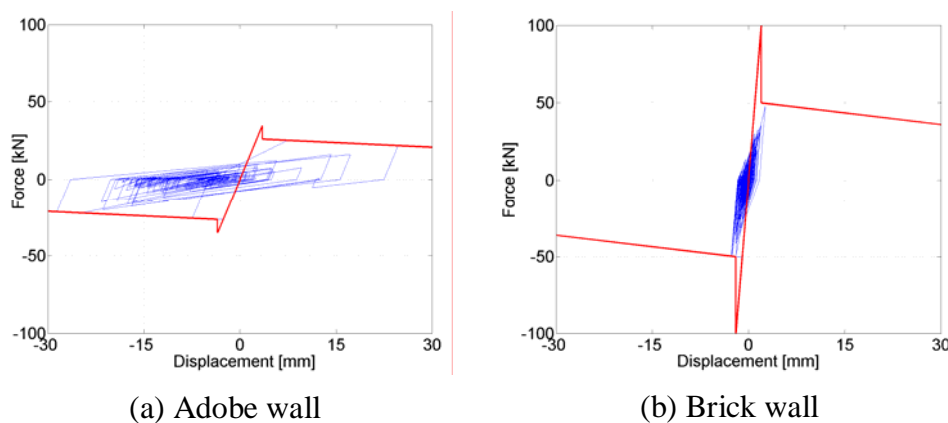


Figure 5: Time-history response of brick structure (Loma Prieta Earthquake)

3.1 Discussion

Figure 6 shows the comparison of the structural response of adobe and masonry walls subjected to the El Centro strong ground motion record. It can be seen that the adobe structure had larger maximum and permanent displacements. This is because the adobe weaker structure experiences a larger ductility demand. This ductility is provided by the PP-band mesh.



(a) Adobe wall

(b) Brick wall

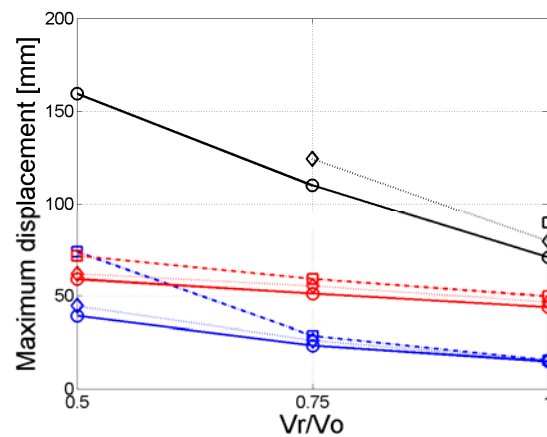
Figure 6: Response of adobe and brick walls subjected to El Centro strong ground motion record

The maximum and permanent displacements for each structure and strong ground motion record are plotted in Figures 7 and 8 for adobe and

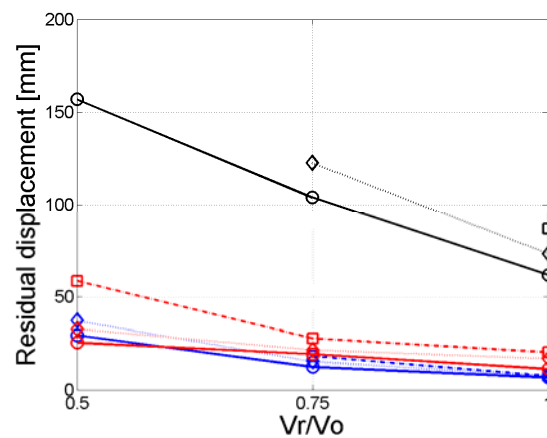
masonry, respectively. In the case of the Cape Mendocino strong ground motion, some structures became unstable during the analysis and hence the results are not plotted. As mentioned before, adobe structures have longer maximum and permanent displacements.

It can be observed that for all the cases, the ratio V_r/V_o has more influence on the seismic performance than K_r/K_o . If V_r/V_o is controlled, i.e. kept over 0.75, the structural performance does not change dramatically even for decreasing K_r/K_o ratios.

The maximum and permanent drifts for the adobe walls are less than 2.5% for the El Centro and Loma Prieta records. This can be considered an acceptable performance. Although in some cases the adobe wall becomes unstable under the Cape Mendocino strong ground motion, as long as V_r/V_o is 1, which is possible to accomplish with a good construction quality control, the maximum and permanent deformations are well within adequate levels.



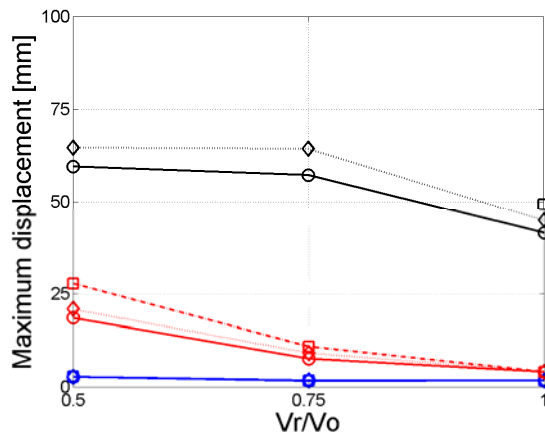
(a) Maximum displacements



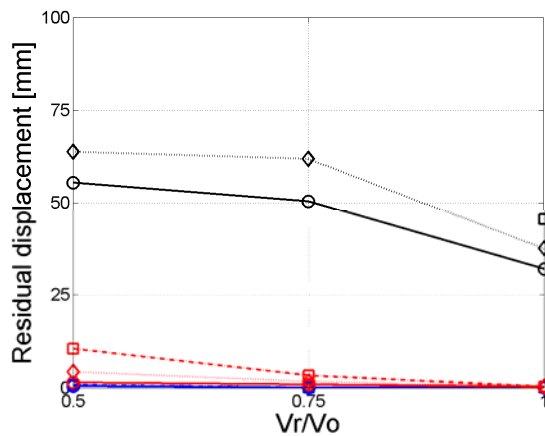
(b) Residual displacements

Figure 7: Maximum and residual displacements of adobe walls (Blue: El Centro record, Red: Loma Prieta record, Black: Cape Mendocino record; circle: $K_r/K_o=0$, diamond: $K_r/K_o=-0.10$, square: $K_r/K_o=-0.20$)

The performance of the masonry retrofitted walls is also good with residual displacements below 10mm for El Centro and Loma Prieta records.



(a) Maximum displacements



(b) Residual displacements

Figure 8: Maximum and residual displacements of masonry walls (Blue: El Centro record, Red: Loma Prieta record, Black: Cape Mendocino record; circle: $K_r/K_o=0$, diamond: $K_r/K_o=-0.10$, square: $K_r/K_o=-0.20$)

4. CONCLUSIONS

An approach to estimate PP-band mesh retrofitted houses seismic performance is proposed. Because PP-band mesh cannot avoid cracking, the key issue for design is to control damage by limiting maximum and residual displacements. Eighteen structures subjected to three strong ground motions were analyzed. The results suggest that the most important parameter for a good seismic performance is the structure strength immediately after cracking, V_r . Experiments have shown that it is possible to control this parameter by providing enough density of PP-band mesh and covering the retrofitted structure with mortar.

The material model used for the analysis follows the cyclic behavior of the structure well. However, the unloading stiffness is higher than that obtained through experiments. Although it is not expected that this fact will

significantly affect the results of the analysis carried out, it should be investigated by further refining the model.

The analysis presented in this article will be used to develop a simple design methodology for PP-band mesh retrofitting. For this purpose, it is still necessary to evaluate the seismic performance of walls under out-of-plane conditions to verify that the meshes prevent this type of failure.

REFERENCES

Guragain, R., Mayorca P., Kawin W., and Meguro K. 2006. *Simulation of brick masonry wall behavior under in-plane cyclic loading using applied element method*, Proc. of the 8th International Summer Symposium of JSCE, pp. 55-58.

Mayorca, P., Sathiparan, N., Guragain, R., Nesheli, N., and Meguro, K. 2006. *Seismic Behavior of Masonry Houses Retrofitted with PP-Band Meshes Evaluated through Shaking Table Tests*, Proc. of the 1st European Conference on Earthquake Engineering and Seismology, Geneva, Switzerland, CD-ROM.

Miranda, E., *Reflections on the Use of Elastic or Secant Stiffness for Seismic Evaluation and Design of Structure*, Proc. of the 1st European Conference on Earthquake Engineering and Seismology, Geneva, Switzerland, CD-ROM.

Sathiparan, N., Mayorca, P., Nesheli, N., Guragain, R., and Meguro, K. 2005. *In-plane and Out-of-plane behavior of PP-band retrofitted masonry wallttes*. Proc. of the 4th International Symposium on New Technologies for Urban Safety of Megacities in Asia, Singapore.

Pacific Earthquake Engineering Research (PEER) Center Strong Ground Motion Database, peer.berkeley.edu/smcat/ as retrieved on Oct. 15, 2007

MODELING NONLINEAR STRESS-STRAIN RELATIONS OF MATERIALS

MD. RAQUIBUL HOSSAIN¹, MOHAMMED SAIFUL ALAM²
SIDDIQUEE³ and SYED ISHTIAQ AHMAD⁴

Department of Civil Engineering, Bangladesh University of Engineering
and Technology, Dhaka 1000, Bangladesh

ABSTRACT

Mathematical modeling of nonlinear stress-strain relations of material is a major concern for simulation of nonlinear response of structure. Such a good stress-strain relationship is highly required for both the monotonic as well as cyclic elasto-plastic constitutive models. In this paper, a simple nonlinear stress-strain equation is proposed which can reasonably simulate a wide range of nonlinear stress-strain behavior. The generated stress-strain relation has a gradient, which is continuous and differentiable all through the curve having a zero slope at the peak strength state.

1. INTRODUCTION

For the finite element analysis of materials under both monotonic as well as cyclic loading, a good nonlinear stress-strain relationship is indispensable. Often a simple hyperbolic equation (Konder (1963)) is used to model the stress-strain relation. Also, many models have been introduced to simulate the nonlinear stress-strain relations such as Griffith and Prevost (1990), Tatsuoka et al (1993), Tanak (2002), Al-Karni et al (2006) etc. Some of these models cannot model the initial gradient of the stress-strain relations whereas some does not show a zero tangent at the peak strength state. Also, some model are only limited to the hardening part of the stress-strain relationship.

A mathematical model of nonlinear stress-strain relationship must satisfy several conditions like (i) the curve should have an initial gradient, (ii) it must go through the peak strength state, (iii) the corresponding gradient of the peak state must be zero, (iv) the curve should be all through continuous and differentiable, (v) a single function must be able to simulate both the pre-peak hardening part as well as post-peak softening part.

The simple hyperbolic function like Konder (1963) cannot predict the failure realistically though it can be forced to go through the particular point of peak strength. Beyond the peak strength, the stress continues to increase with increasing strain as the curve approaches to the failure condition asymptotically. A modified hyperbolic function is proposed by Griffith and Prevost (1990) that satisfies all the four criteria cited before. But it cannot predict the post-peak behavior and the parameters required for the function are complicated to calculate.

Tatsuoka et al (1993) proposed a nonlinear stress-strain relation called General Hyperbolic Equation (GHE), which can simulate the pre-peak stress strain behavior as well as post-peak strain softening relation with a smooth transition at the peak state. But the GHE has a complicated formulation, which requires a large number of parameters.

Takaka's model can simulate a series of stress strain curves with the limitation that it has a very stiff initially and it is not differentiable at zero strain. The model proposed by Al-Karni et al (2006) has the ability to model both the hardening and softening part of the complete stress strain curve with an initial gradient. But the model also requires several material and calibrating parameters.

In this paper a simple nonlinear stress-strain model is proposed which can reasonably simulate a wide range of stress-strain relations for both hardening as well as softening parts.

2. MODEL OF NONLINEAR STRESS-STRAIN RELATIONS

The proposed model is an equation that relates the stress σ with the strain ε as follows,

$$\sigma = \sigma_p \frac{\varepsilon_p + a}{\varepsilon_p^2} \varepsilon \left(\frac{\varepsilon_p + a}{\varepsilon + a} - \frac{a}{\varepsilon_p + a} \right) \quad (1)$$

Where σ_p is the peak strength and the corresponding strain is ε_p and a is the material parameter which controls the shape of the curve. To find the value of a for the hardening part of the stress strain curve, equating the derivative of the curve at $\varepsilon = 0$ with the initial gradient E_0 , we get,

$$\left(\frac{d\sigma}{d\varepsilon} \right)_0 = E_0 = \sigma_p \frac{\varepsilon_p + a}{\varepsilon_p^2} a \left(\frac{\varepsilon_p + a}{a^2} - \frac{1}{\varepsilon_p + a} \right) \quad (2)$$

Also from the model and its derivative we can see that it satisfies the first four criteria cited before.

To model the post-peak behavior, we can find the value of a by equating the equation of the curve at $\varepsilon = \varepsilon_r$ and $\sigma = \sigma_r$ we get,

$$\sigma_r = \sigma_p \frac{\varepsilon_p + a}{\varepsilon_p^2} \varepsilon_r \left(\frac{\varepsilon_p + a}{\varepsilon_r + a} - \frac{a}{\varepsilon_p + a} \right) \quad (3)$$

Where, σ_r is the residual strength and ε_r is the corresponding strain.

Thus, the proposed model finally satisfies the last criterion and it is a complete model to simulate the nonlinear stress-strain relations of materials.

3. SIMULATION OF NONLINEAR STRESS-STRAIN BEHAVIOR

From the proposed model we can see that a range of stress strain curves can be found depending on the initial gradient, which gives various a for the hardening part of the model. As a result various hardening stress strain curve can be simulated by varying the material parameter a . Figure 1 presents a range of simulated normalized stress strain hardening curves for various the material parameter a .

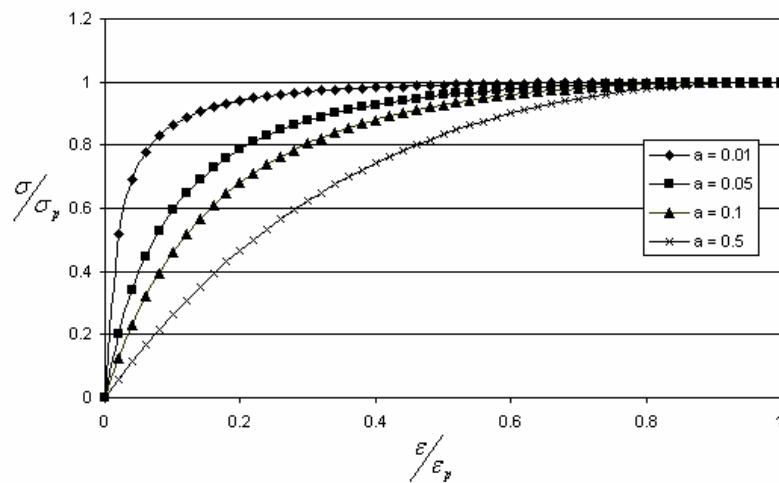


Figure 1: Normalized stress vs. normalized strain hardening curves for various a .

Similarly, we can get a range of softening curves with various material parameter a by equating the equation of the curve at $\epsilon = \epsilon_r$ and $\sigma = \sigma_r$. Figure 2 shows a range of simulated normalized stress strain softening curves by varying the material parameter a .

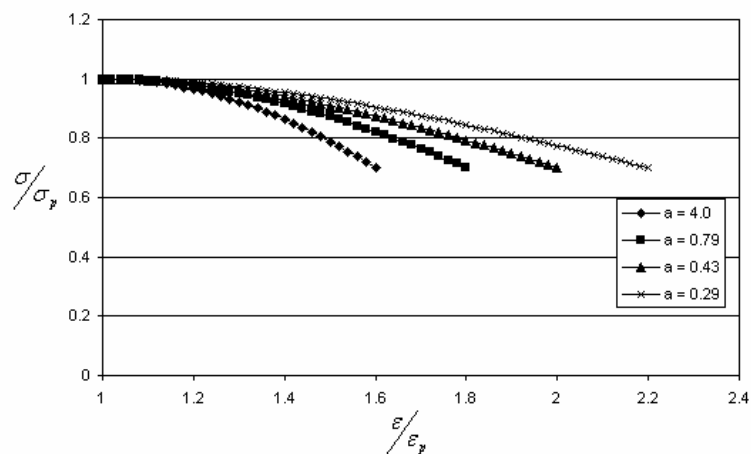


Figure 2: Normalized stress vs. normalized strain softening curves for various a .

Thus, the proposed model can simulate a wide range of nonlinear stress-strain relations satisfying all the five criteria. The model parameter a can be easily estimated from the initial modulus of elasticity, E_0 for the hardening part and from the residual strength, σ_r for the softening part of material response.

4. CONCLUSIONS

Most widely used hyperbolic function to simulate nonlinear stress-strain relations has some limitations of not predicting the failure condition realistically. A mathematical model is proposed in this paper to simulate the nonlinear stress-strain relations for both the hardening part and softening part of material response. This model has the ability to fulfill all the five criteria required to model a stress-strain curve. So, a wide variety of nonlinear stress-strain relations of material can be simulated using the proposed model.

REFERENCES

- Al-Karni, A. and Alshenawy, A., (2006), Modeling of stress-strain curves of drained triaxial test on sand, *American Journal of Applied Sciences* 3 (11), 2108-2113.
- Griffith, D.V. and Prevost, J.H., (1990), Stress strain curve generation from simple triaxial parameters, *International Journal for Numerical and Analytical Methods in Geomechanics*, Vol. 14, 587-594.
- Konder, R.L., (1963), Hyperbolic stress-strain response: cohesive soils, *Journal of Soil Mechanics and Foundation Division*, ASCE, 89(SM1), 115-143.
- Tatsuoka, F., Siddiquee, M. S. A., Park, C. S., Sakamoto, M. and Abe, F., (1993), Modeling stress-strain relations of sand, *Soils and Foundations*, Vol. 33, No. 2, 60-81.
- Tanak, T.(2002), Elasto-plastic strain hardening-softening soil model with shear banding, em2002.

ENHANCEMENT ON DISASTER PREVENTION AND MITIGATION IN KAOHSIUNG CITY

TAI-PING CHANG

Department of Construction Engineering, National Kaohsiung First
University of Science and Technology, Kaohsiung, Taiwan, ROC
tpchang@ccms.nkfust.edu.tw

ABSTRACT

In this project, we deal with the enhancement of disaster prevention and mitigation in Kaohsiung city, Taiwan. To achieve this goal, the project organization contains several groups such as natural disaster, human error disaster, information communication and emergent medical cure team. First of all, we organize teamwork and plan mechanism of assistance operation, then we perform the analysis and review in Today's Kaohsiung City as the preliminary work. Secondly, we adopt our professional techniques to do the disaster potential analysis and perform the analysis of possible disaster characteristics. In due course, we assist local government on revising and enhancing Standard Operation Procedure (SOP) and assist local government on disaster reflection. Finally, we construct the Website of cooperation agency and do educational training and technology transfer at the same time. Furthermore, we also enhance related works for Kaohsiung city government.

1. INTRODUCTION

Recently, National Science and Technology Center for Disaster Reduction (NCDR) in Taiwan selects some associated research institutions or laboratories as collaborative institutions based on its regulations to coordinate local governments on advancing disaster prevention and enhance efficiency on disaster reflection. Therefore, both NCDR and collaborative institutions can co-develop affairs related to disaster prevention through cooperation and technology transfer, and strengthen capacity on local governments' disaster rescuers. In 2006, National Kaohsiung First University of Science and Technology (NKFUST) was chosen as the collaborative institution to support Kaohsiung city to enhance the disaster prevention and mitigation in Ksohsiung city. This project is executed or cooperated by nine groups: the collaborative institution, landslide disaster team, flood team, seismic bridge damage team, seismic soil liquefaction team, toxic disaster team, fire disaster team, technology and communication team, and emergent medical cure team. Not only we do the disaster prevention and mitigation, but also we do educational training and technology transfer at the same time. Furthermore, we also enhance related works for Kaohsiung city government.

2. OPERATION TASKS AND PROSECUTION METHODS

We accomplish the following tasks in this project for developing the ability on diverse disasters prevention, reaching the goal on research transfer and mitigating the damages in Kaohsiung city.

1. Organize Teamwork and Plan Mechanism of Assistance Operation
2. Analysis and Review in Today's Kaohsiung City
3. Perform Disaster Potential Analysis
4. Perform Analysis of Possible Disaster Characteristics
5. Assist Local Government on Revising and Enhancing Standard Operation Procedure (SOP)
6. Assist Local Government on Disaster Reflection
7. Construct the Website of Cooperation Agency
8. Establish Emergency Medical Cure Team

In this paper, only Mechanism for Assistance Operation (MAO), Disaster Potential Analysis and Analysis of Possible Disaster Characteristics are discussed in somewhat details in the following three sections. All the other operation tasks are mentioned briefly above due to the complexity and sophistication of their natures.

3. MECHANISM FOR ASSISTANCE OPERATION (MAO)

The role of National Kaohsiung First University of Science and Technology (NKFUST) is to provide some technical assistances on disaster prevention and/or mitigation to Kaohsiung city, the complete teamwork of NKFUST on MAO can be illustrated in Figure 1.

4. DISASTER POTENTIAL ANALYSIS

There are many kinds of disaster involved in this project, we perform the disaster potential analysis for all of them. It is quite obvious that each type of disaster has its own importance in some particular areas, but we can't present the potential analysis for all the types of the disaster in this paper.

Therefore, here we merely select a few significant disasters in Kaohsiung city for demonstration, the complete disaster potential analysis of all the types of disaster can be found in our project report. To accomplish all the tasks, not only we adopt the most updated professional techniques and concepts, but also we follow all the rules and restrictions in accordance with the regulations established by Kaohsiung city.

Teamwork of NKFUST on MAO

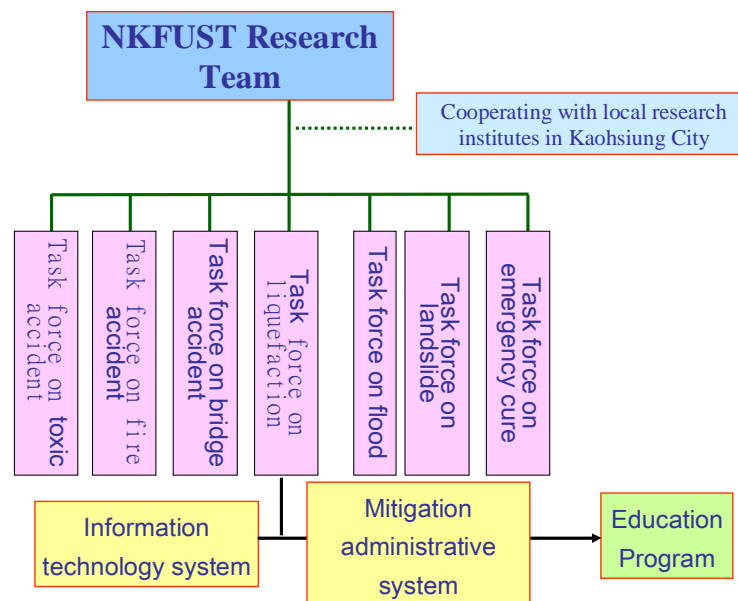


Figure 1: Teamwork of NKFUST on MAO

4.1 Typhoon-Flood disaster potential evaluation

This project uses four different kinds of precipitations (150mm, 300mm, 450mm, 600 mm) to do the simulation for the flood area and flood depth along the Love River in Kaohsiung city. According to our analysis, the above precipitations are daily deluge about 1.1 years, 5 years, 20 years and 100 years return period respectively in Kaohsiung city. In addition, we investigate the influence due to tide, precipitation, drainage and pumping stations along Love River. According to the collected GIS information, when the precipitation is under 150mm per day, the area near Love-river has high flood potential as it can be seen from Figure 2; when the precipitations are under precipitation 300mm, 450mm, 600mm per day, the district of Chen-gin, Shin-shi, Yenchen, Gushan and Nanjhe have high flood potential as shown in Figure 3. The total length of rainfall drainage system in Kaohsiung is planned to be 392 kilometers by the end of 2005. In 2006, the completed length is 378 kilometers, which is approximately 96.4% of the scheduled target. The annual precipitation in Kaohsiung is expected to be 1800 mm (record for 2005 is 2821.4mm). First-level design for flood for downtown area is 5-year return period (70.9mm/hr) while river area is 20-year return period.

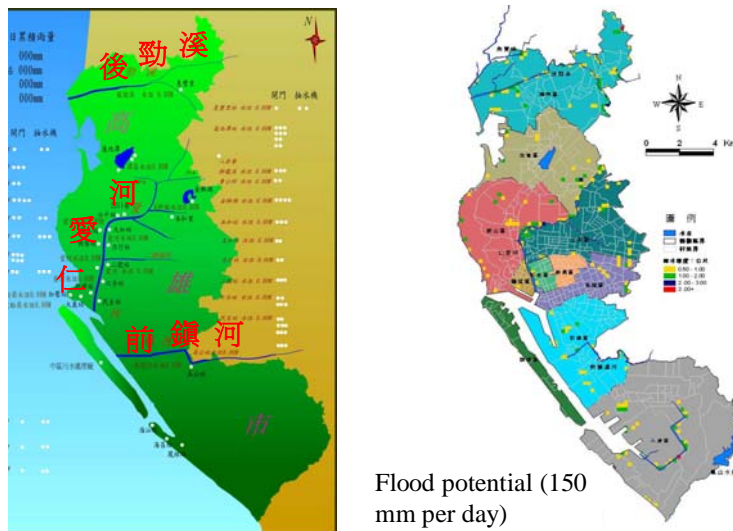


Figure 2: Flood potential analysis under precipitation 150mm per day

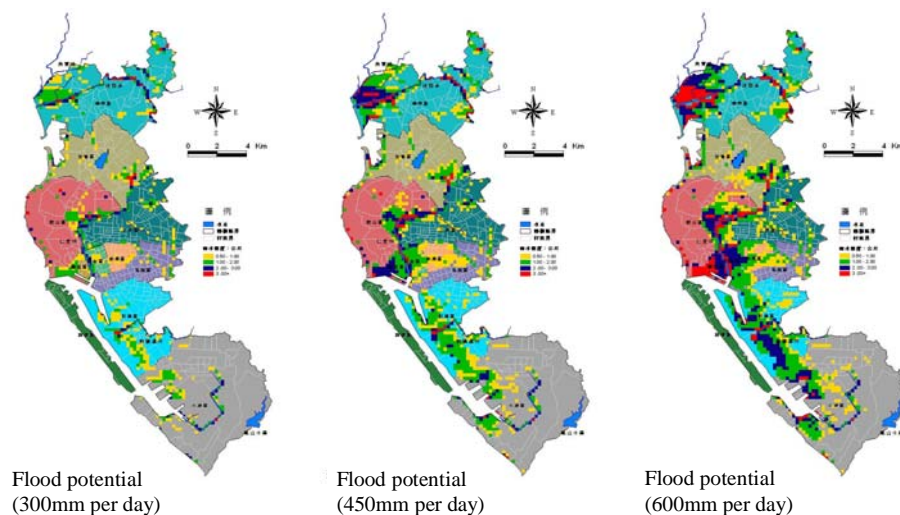


Figure 3: Flood potential analysis under precipitation 300mm, 450mm, 600mm per day respectively

4.2 Toxic disaster potential evaluation

The Hazardous Risk (HR) is defined as the probability of hazard occurring per year within one Kilometer radius, which is equivalent to hazardous radius (Km) multiplied by occurring probability (1s/yr). The hazardous risk is divided into four levels: (A) Heavy Polluted Zone : Red Zone (HR>600) (B) Seriously Polluted Zone : Green Zone (HR>300) (C) Moderately Polluted : Blue-Green Zone (HR>200) (D) Low Polluted

Zone : Blue Zone (HR<20). In Figure 4, the toxic disaster potential analysis in Kaohsiung city is performed and presented.

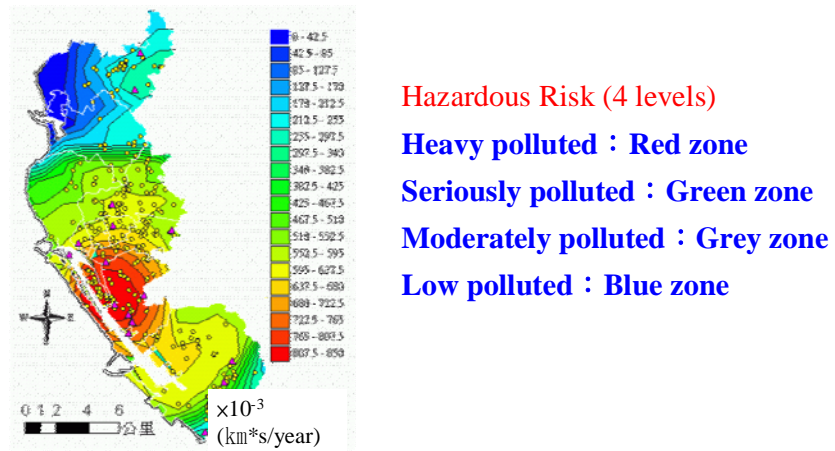
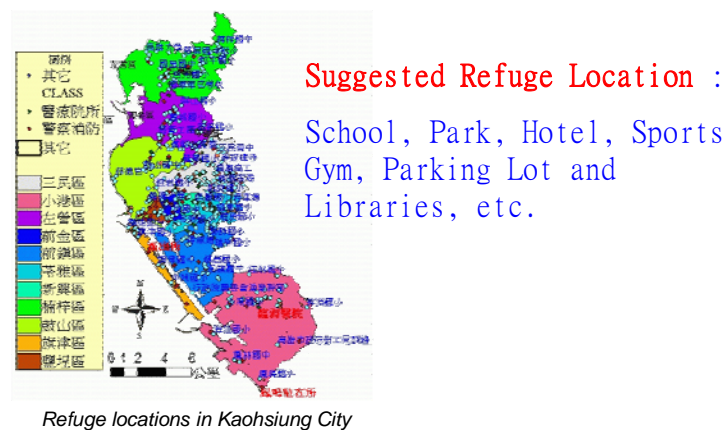


Figure 4: Toxic accident potential analysis

Once the toxic disaster happened, the most important task is to evacuate the people and put them in the safe places. Our team select some emergent refuge locations and establish the data base for these locations. The suggested refuge locations are school, park, hotel, sports gym, parking lot and libraries, etc. The selected refuge locations are depicted in details as shown in Figure 5.



Refuge locations in Kaohsiung City

Figure 5: Refuge locations in Kaohsiung City

4.3 Fire disaster potential evaluation

As it can be seen from Figure 6, Zuo-Ying district in Kaohsiung City reflects high potential of fire accidents since it has become a complex area containing houses and stores. In addition, we notice that Shan-Ming village in Siao-Gang district ranks the second place on fire accident potential analysis. However, the density of the population in this village is pretty low,

the reason is that village and the nearby areas are the main operation area of petrochemical industry.

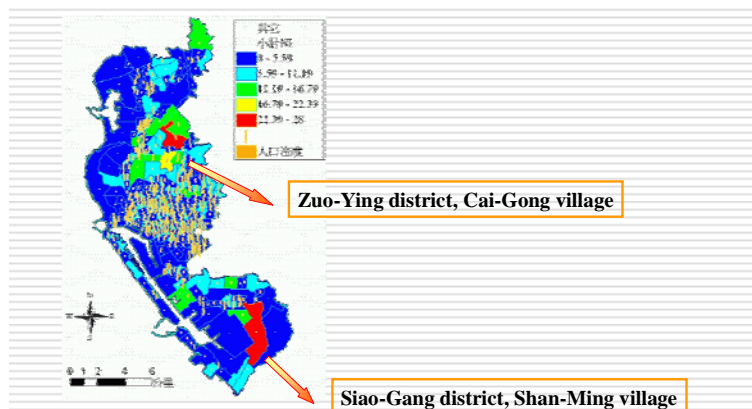


Figure 6: Fire accident potential analysis

5. ANALYSIS OF POSSIBLE DISASTER CHARACTERISTICS

For simplicity, here we only consider the features of toxic accidents and fire accidents.

5.1 Feature of toxic accident

From 2003 to 2006, the toxic damage types in Kaohsiung are focused on toxic leakage (47%) and fire accident (33%) as shown in Figure 7. While analyzing the accident places, we find that non-chemical plants (35%) and transportation accidents (35%) happen most frequently, which is presented in Figure 8. Based on the human accident records in Kaohsiung city, the toxic leakage (47%) and transportation accident (35%) are the top two factors, we discover that the most possible reasons for this kind of disaster are leakage of chemical plants and leakage of chemical tank cars. Therefore, from the disaster prevention and mitigation point of view, we should take the most serious accident into first consideration as well as the economic influence, etc.

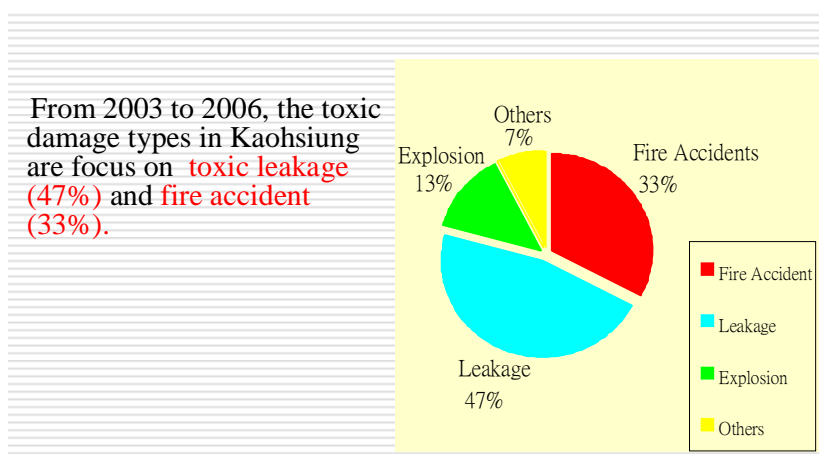


Figure 7: Toxic accident types

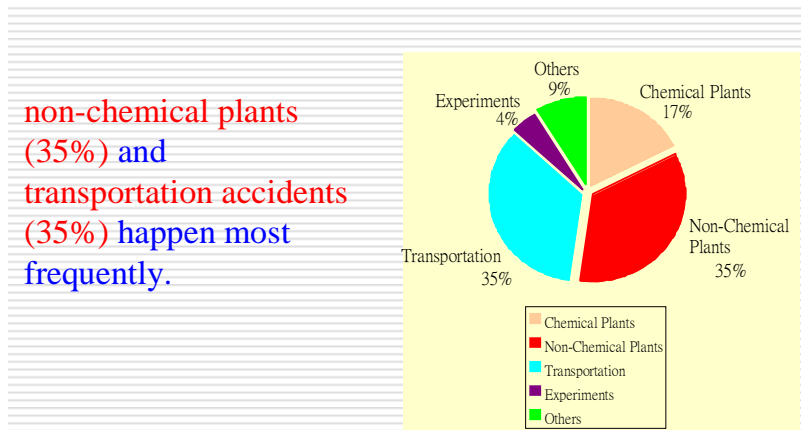


Figure 8: Distributions of toxic accident places

5.2 Feature of fire accident

While analyzing the causes of fire accidents, we can see that the distributions are as follows: electric equipments (41%), human errors (21%), arson (15%), and unknown reasons and others (23%), which is presented in Figure 9. In addition, we find that the 1~5th floors got on fire most frequently (81%), and the second would be the 6~12th floors (15%) as shown in Figure 10. General fire accidents have characteristics like growing feature, uncertain feature and sporadic feature. Even though the percentage of floors above 12th floors is only 4%, it still has possibility to have fire accidents. There are many kinds of causes on fire accidents, therefore, we should evaluate the influence on losses and investigate the past heavy cases in Kaohsiung city. We classify the following types as setting direction:

- (A) Fire accidents on dangerous plants and explosion.
- (B) Fire accidents on business (stores, movie theater, KTV, etc.).
- (C) Fire accidents on military ammunition depots.
- (D) Fire accidents on special locations (old communities, markets, temples, etc.).
- (E) Fire accident on high-rise buildings.

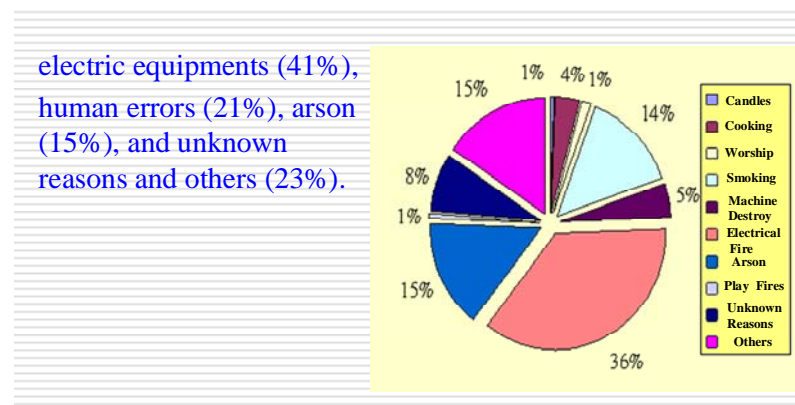


Figure 9: Causes of fire accident in Kaohsiung City during 1993-2004

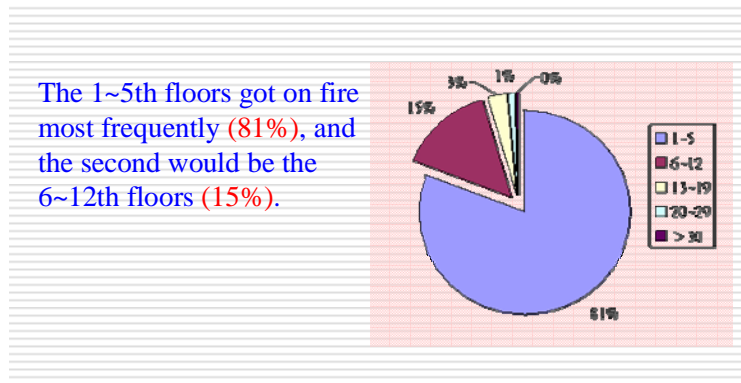


Figure 10: Floors on fire in Kaohsiung City during 1997-2004

6. CONCLUSIONS

The conclusions are summarized in the following:

1. This project is executed or cooperated by nine groups: the collaborative institution, slope disaster team, flood team, seismic bridge damage team, seismic soil liquefaction team, toxic disaster team, fire disaster team, technology and communication team, and emergent medical cure team. The tasks we do are stated in the above, besides, we do the educational training and technology transfer at the same time. Furthermore, we also enhance related works for Kaohsiung city government.
2. Concerning disaster prevention project in Kaohsiung area, the revised tasks which contains finished chapters, team works and schedule will be tracked, arranged and designed as a form and also be delivered to different bureaus and agencies. Therefore, our team can make sure whether or not the project's organization and content meet Kaohsiung government's need.
3. The setting of disaster prevention organization in Kaohsiung city is not only collecting the latest information from foreign countries, but also making an on-the-spot investigation in Japan (University of Tokyo, Tokyo and Kobe Earthquake Memorial Hall, and disaster prevention center in Kyoto University) in order to arrange a well-organizing disaster prevention department.
4. This project uses four different kinds of precipitations (150mm, 300mm, 450mm, 600 mm) to do the simulation for the flood area and depth along the Love River in Kaohsiung city. According to our analysis, the above precipitations are daily deluge about 1.1 years, 5 years, 20 years and 100years return period respectively in Kaohsiung city. In addition, we investigate the influence due to tide, precipitation, drainage and pumping stations along Love River.
5. The task of integrating disaster prevention information reaches the goal of collecting disaster prevention information in Kaohsiung city, and inquiring related affairs for disaster prevention bureaus and agencies. The website which is provided by our collaborative institutions can support different disaster prevention staffs to apply for and becomes an information integrating platform.

There are still some important tasks for future study, they are listed as follows:

1. Organizing Teamwork and Operation Mechanism
2. Current Situation Review and Enhancing Disaster Prevention Project
3. Information Collecting and Disaster Potential Analysis
4. Support Local Government on Natural Disaster Reflection and Post-Disaster Investigation
5. Information Review and Organizing Suggestions
6. Education Training and Technology Transfer
7. Effect Evaluation

ACKNOWLEDGEMENT

This work was partially supported by the National Science and Technology Center for Disaster Reduction (NCDR) in Taiwan, Republic of China under Grant NCDR 95-A5000-CO-N004. The author is grateful for this support.

REFERENCES

- Bengt Mattsson, 1997. The importance of the time factor in fire and rescue service operations in Sweden, *Fire Safety journal*, vo1.29.
- Daniel A. Crowl, and Joseph F. Louvar, 2003. *Chemical Process Safety*, Second Edition, New Jersey, 109-162.
- F. P. Lees, 1996. *Loss Prevention in the Process Industries*, 2nd Edition, ISBN 0-7506-1547-8, Butterworth-Heinemann, Oxford, UK, Vol. 1: 3/12-16 .
- AIChE, 1989. *Guidelines for Process Equipment Reliability Data*, with Data Tables, American Institute of Chemical Engineers, 203-205.

MODELS OF A TECHNICAL PLATFORM FOR EMERGENCY MANAGEMENT

WENGUO WENG

Center for Public Safety Research,
Tsinghua University, Beijing, 100084, P.R. China
wgweng@tsinghua.edu.cn

ABSTRACT

China government attaches much importance to public safety, and the National Emergency Response Plan was issued by the China State Council present a blueprint on how to prevent and deal with a variety of emergency events including natural disasters, accidents, public health and social safety. Technical platform is a powerful tool for dealing with emergency events according to the Plan. One of the functions of technical platform is to predict incidents' trend and consequence under different situations. Center for Public Safety Research is developing a technical platform, whose models are presented in this paper. Also we present some supports for developing further this platform in order to continuously perfect its functions for future use.

1. INTRODUCTION

In the recent years, the Chinese economy has maintained a good growth, which results from the national policy of deepen reform and opening-up. When China government pushes forward the country's socialist modernization drive, strengthens and improves macro-controls, and accelerates economic restructuring, some unstable and uncertain factors are on rise. One of the most important problems is public safety (Wen, 2006). China government is convinced that public safety is a lion in the way during the process of creating a well-off society in an all around way. And so it attaches much importance to public safety. The clout of public safety is that all of the related work is human-oriented, which means the human lives are most important in dealing emergency management.

On Jan. 8, 2006, The China State Council issued the national plan on emergency response (China State Council, 2006), through a series of response plans for public emergency events have been studied and developed since 2003. The National Emergency Response Plan aims to increase the government's capability to protect public, deal with unexpected incidents, minimize the losses of the incidents, maintain social stability, and promote the harmonious and sustainable development of the country. The Plan stipulates that the State Council is the highest organ in the management of emergency response. An office in charge of emergency response management will be set up by the State Council to collect information of various incidents and coordinate the emergence response work.

The National Emergency Response Plan is an all-hazards plan that provides the structure and mechanisms for national level policy and operational coordination for emergency management. It can be partially or fully implemented in the context of a threat, anticipation of a significant event, or the response to a significant event. Selective implementation through the activation of one or more of the system's components allows maximum flexibility in meeting the unique operational and information-sharing requirements of the situation at hand and enabling effective interaction between various ministries and commissions, local, and other entities (Fan and Su, 2005).

According to the Plan, technical platform is a powerful tool for dealing with emergency events. There are many functions of technical platform, e.g. detection, monitoring, prediction, alert, decision-supporting, etc. One of the most important functions is to predict incidents' trend and consequence under different situations. In this paper, models of technical platform, developed by Center for Public Safety Research, Tsinghua University, are presented. And in the next section, the basic functions of a technical platform for emergency management are introduced. Section 3 gives some models of this platform in details, followed by concluding remarks.

2. BASIC FUNCTIONS OF A TECHNICAL PLATFORM

Technical platform for emergency management is built upon for dealing with emergency accident. We also call it as emergency response platform (ERP). With it, we not only response to emergency, but also manage daily emergency-related things, e.g. on duty, receiving alarm, etc.

According to the National Emergency Response Plan, the emergency response platform will provide a powerful tool to activate and implement the emergency response plan. And so ERP is designed to make the response operations more scientific, effective, and efficient. It is a centralized solution for incident correlation, information sharing, resources aggregation, disaster analysis, response and investigation of emergency incidents.

When dealing with emergency incidents, what is needed from emergency response platform is a key problem in developing ERP. In face of disastrous incidents, eg. flood, typhoon, earthquake, fire, hazardous gas leak, traffic accident, SARS, terrorist attack, etc. how to effectively find and analyze the information that we care about is one of the most important problems that ERP must solve. And the second is how to scientifically predict incidents' trend and consequence, and alert as quick as possible, under different situations such as incident location, wind speed, wind direction, weather, rainfall, leaking materials, storing pressure, total amount, material toxicity, surrounding environment, crowd, building structure, refuge area, etc. The third that EPR should solve is how to scientifically make decision, conduct integrated coordination and effectively do operation considering many factors, e.g. spot situation, crowd evacuation, rescue

organization, resource aggregation, equipment assemblage, supply, shortest route, scheme optimization, fire fighting, and water, fuel and power supply, etc.

Based on the National Emergency Response Plan, we think the basic functions of emergency response platform are listed below:

- Risk analysis and safety evaluation;
- Information gathering and analysis for emergency (data, voice, video, display, reading, identification and selection);
- Development prediction and analysis of disaster;
- Early-warning scheme and broadcast;
- Evaluation of human evacuation and sites;
- Optimization and starting of emergency response plan;
- Real-time information gathering for location and emergence sites;
- Dynamics emergence commander and logistic of emergency aids;
- Evaluation of functionality and capability of emergence response.

It is obvious that one of the most important functions is to predict incidents' trend and consequence under different situations. Models would be developed for prediction, based on which the emergency measures are carried into execution. The prediction models, presented in the next section, are developed according to the different disasters' attribute and mechanism.

3. MODELS FOR EMERGENCY RESPONSE PLATFORM

It is obvious that models for predicting incidents' trend and consequence is the base of emergency response platform, and also an important component of ERP. With models, ERP can provide the most important and valuable spot to measure and monitor considering that it is impossible to monitor all spots may trigger disaster. And it also quickly predicts the incident's trend and provides the accurate early-warning information, based on which government can make accurate decision and conduct successful commanding. According to the function of models in ERP, models can be divided into three types. One type is for pre-disaster, which predicts the possible occurrence of spot spreading disaster and provides the base for risk evaluation. The second type is for during disaster, which quickly predicts the trend of disaster and provides the guide for decision and commanding. The third type is for post-disaster, which recurs the disaster progress and provides the chance for checking the emergency response. Next some models are provided.

3.1 A Systematic Risk Analysis Model

Appropriate risk analysis approach in case of accidents is one rational way to conduct efficient emergency response. The risk assessment procedure is based on representing the study area in the form of a grid of 'cells'. The consequence assessment is performed by evaluating the

individual risk of each cell and aggregate weighted risk of a cluster of cells. Individual risk (${}^{t+1}IR_{ij}$) and aggregate weighted risk (${}^{t+1}AWR_{ij}$) have been deemed to be a function of accident intensity (${}^{t+1}AI_{ij}$), population density (PD_{ij}), and population sensitivity (PS_{ij}) (Ji and Weng, 2007):

$${}^{t+1}IR_{ij} = f({}^{t+1}AI_{ij}, PS_{ij}) \quad (1)$$

$${}^{t+1}AWR_{ij} = f({}^{t+1}IR_{ij}, PD_{ij}, PS_{ij}) \quad (2)$$

During accidents, the accident intensity propagates via diffusive effect, transporting effect and dissipative effect. Accident intensity spreading is controlled by both 'inner factor' and 'outer factor'. The dynamics of propagation of the intensity is first controlled by the diffusive effect which is the inner factor. This implies that intensity flux liberated from the accident epicenter travels outwards to the adjoining cells and once each of these incident cells become saturated with the intensity, they in turn begin to act as new intensity sources and the intensity flux begins to diffuse from these cells into their respective neighborhoods. The intensity gradient is the driving force governing this outward propagation of the intensity flux. The intensity gradient expresses different meaning in different accidents. It means concentration gradient in toxic gas dispersion and temperature gradient in heat radiation and so on. According to common sense, some accident spreading is also controlled by some outer factors. For example, wind and terrain slope will affect the distribution of the toxic gas concentration and temperature difference between the ambience and the accident hazards will result in convection. Therefore, we say that the intensity propagation is also governed by the transporting effect. The dissipation effect is also an important outer factor which perhaps changes the style of the intensity spreading. While spreading, barriers such as building, river and trees and sedimentation will weaken the accident intensity.

According to the above analysis, the algorithm of the systematic approach is developed, shown in Figure 1. To illustrate the application of the systematic approach, we make simulations on a fictitious city based on THU-CPSR city model, which is designed to simulate a real city with the scale of 5250m \times 4410m. There are two commercial buildings, ten residential buildings, one school, two workshops, three LNG gas containers and a petrochemical industry in the city. There are river and virescence area to separate the industry area and residential area. Therefore, the model can represent a complex city with a cluster of potential hazardous sources and heavy population density. The city model is shown in Figure 2. The fictitious city is divided into uniform grids of 35m \times 35m. L, M and N (see Figure2) are potential hazardous sources which may cause pool fires. The vulnerable areas are A, B, C, D, E, F, G, H, I and J (see Figure2) which represent residential areas with heavy population. A hypothetical scenario is used to illustrate the application of the approach. A gasoline leak in one of the gasholders formed a liquid pool at M and flashing of the liquid gasoline results a pool fire. If the radiation heat at L and N exceeds the threshold value (10kW/m² is used here), derivative pool fires may happen.

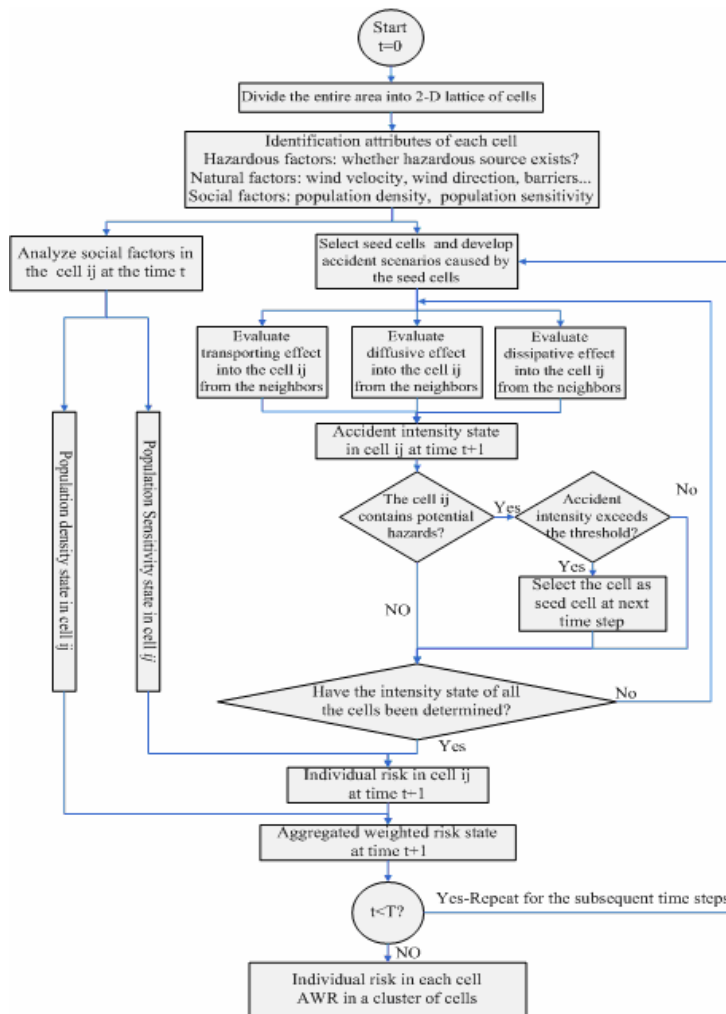
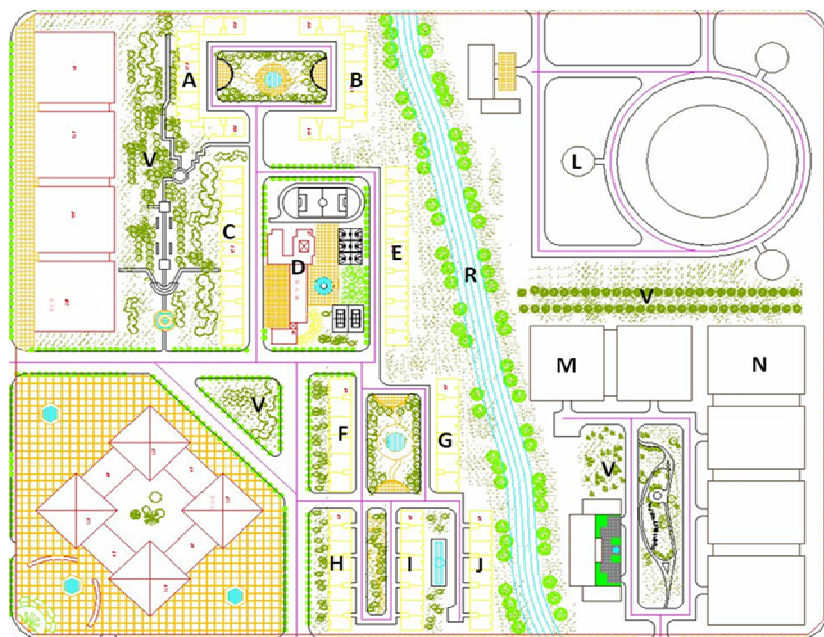


Figure 1: Algorithm for the modeling of systematic risk incorporating multiple factors for emergency response based on cellular automata method



A-J: residential area, R: river, L- N: hazardous source, V: virescent area

Figure 2: THU-CPSR city model

Individual risk is analyzed and the simulation results of individual risk contours are discussed (Figure 3). From contours of individual risk, one can obtain the real-time individual risk and the information about the distribution of individual risk. As expected, for emergency manager, individual risk is much more practical than accident intensity during emergency response. For example, at $t=600s$ and $t=800s$ (Figure 3(b)), although the thermal intensity in most of the residential area is more than 1 kW/m^2 , but the individual is much less than 1×10^{-6} . Therefore, the manager can easily judge that at this time most of residential areas are safe (we think that the individual risk less than 1×10^{-6} is safe). At $t=1200s$ (Figure 3(c)), the individual risk around building G is more than 1×10^{-6} , and the area is not safe anymore. With time going by, the unsafe area expands gradually. At $t=2600s$ (Figure 3(d)), almost all of the residential buildings are in dangerous state except building A. Besides, according to the contours of individual risk, emergency managers can issue pre-warning information to guide the people to evacuate. If one neglects tertiary accident, it is a good strategy to guide people to evacuate to the northwest area. However, a high risk source L exists in the north and it will cause accident at $t=1425s$. Comprehensively considering these factors, a West side evacuation is strongly recommended (Figure 3(e) and Figure 3(f)). Aggregated weighted risks in the ten residential areas were also computed at different time. The results are given in table 1. Some significant conclusions can be obtained to help emergency managers allocate emergency rescue resources. Social factors such as population sensitivity are important for emergency response. For example, the AWR is very low in all the ten areas at $t=600s$ and $t=800s$. At $t=1200s$ and $t=1600s$, the AWR at area E, G and J is much higher than that at other areas, especially area G where the AWR is the highest. At $t=2000s$, the area E become the most dangerous area. After $t=2000s$, nearly almost areas have high AWR.

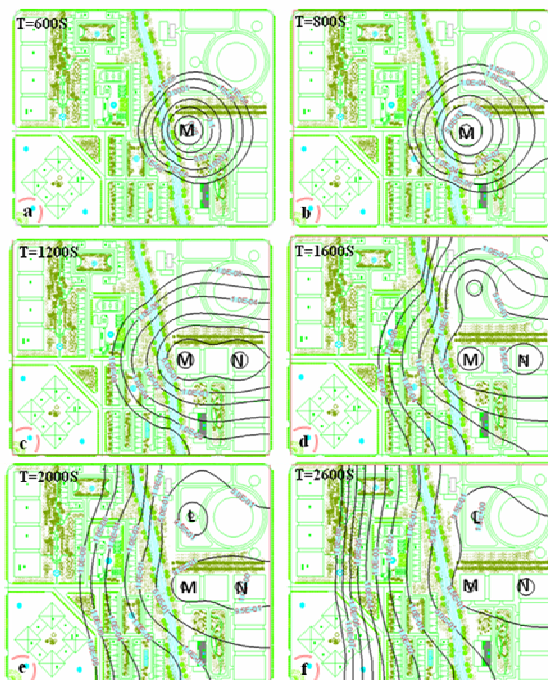


Figure 3: Contours of individual risk under heterogeneous conditions at different time. At $t=0$, accident happened at M

Table 2: Aggregated weighted risk in ten residential areas at different time

Time(S) Residential Area NO.	600s	800s	1200s	1600s	2000s	2600s
A	0.00000	0.00000	0.00000	0.00000	0.00000	0.05801
B	0.00000	0.00000	0.00000	0.00000	0.032977	70.69564
C	0.00000	0.00000	0.00000	0.00000	0.00007	0.45264
D	0.00000	0.00000	0.00000	0.00111	0.20018	34.11988
E	0.00000	0.00072	0.18784	4.60475	98.56041	1126.08296
F	0.00000	0.00000	0.00008	0.01596	0.70950	27.93128
G	0.00463	0.07861	1.46759	9.16649	35.34787	115.56289
H	0.00000	0.00000	0.00000	0.00007	0.01881	3.57464
I	0.00000	0.00000	0.00006	0.02229	1.22451	46.84007
J	0.00000	0.00001	0.01515	1.31135	24.86859	316.95609

Based on above analysis, the following resources allocation strategy is advised: (1) at the first half an hour of emergency response, more rescue resources should be sent to E, G and J. (2) after that, D, F, H and I gradually need more resources.

3.2 A Fire Spread Model for Old Towns

Old towns like Lijiang City have enormous historic, artistic and architectural values. The buildings in such old towns are usually made of highly combustible materials, such as wood and grass. If a fire breaks out, it will spread to multiple buildings. In this fire spread model based on cellular automata (Gao and Weng, 2007), the analysis area is divided into equal size grids called cells. Older areas usually have narrow streets and densely-built houses. In Lijiang City, houses are generally 4 to 7 m long and 2 to 4 m wide. The streets are generally 3 m wide. The streams running through town are about 3 m wide. The numerical accuracy and computational efficiency were balanced with 3 m by 3 m cells in this study.

The city fire spread model advanced in Ref. (Murosaki et al., 1984) showed that the building materials, the weather conditions and the regional characteristics most strongly affect the fire spread. These three factors were defined on based on the special characteristics of Lijiang City. The buildings in Lijiang City are classed as: (1) wooden buildings having 1, 2, 3 or 5 floors, (2) earthen buildings having 1, 2 or 3 floors, (3) brick buildings having 1, 2 or 3 floors, (4) brick and steel buildings having 1 to 7 floors, (5) steel buildings having 2 to 8 floors, and (6) other buildings like canchas, toilets and unoccupied buildings. The different buildings have different building structure parameters S and ratios of wood P . Besides the structural factors, the different buildings tend to catch fire in different ways. The equation given in Ref. (Wakamatsu, 1878) was used to calculate $p(t_{ckl})$:

$$p(t_{ckl}) = \begin{cases} \frac{4.0}{t_2 - t_1} t_{ckl} + \frac{0.2t_2 - 4.2t_1}{t_2 - t_1} & t_1 \leq t_{ckl} \leq \frac{t_2 - t_1}{5} + t_1 \\ \frac{5.0}{4(t_2 - t_1)} (-t_{ckl} + t_2) & \frac{t_2 - t_1}{5} + t_1 \leq t_{ckl} \leq t_2 \end{cases} \quad (3)$$

$$t_1 = (3 + 3a/8 + 8d/D)/(1 + 0.1v) \quad (4)$$

$$t_2 = (w_f / 5.5)/(A_w \sqrt{H} / A_f) \quad (5)$$

Where $p(t_{ckl})$ is the ability of cell $[kl]$ to cause the fire to spread. The time t_1 is defined as the cell $[kl]$ starts burning to when it can cause the fire to spread. a is 3 m which means length of one cell. d is a unfixed variable, which changes according to the time and conditions (Wakamatsu, 1978; Yasuno and Nanba, 1999). D is the farthest distance that the fire can spread for a given certain wind speed, calculated as (Jirou and Kobayashi, 1997):

$$D = 1.15(5 + 0.5V) \quad (6)$$

Where V is the wind velocity. The time t_2 is defined as the time from when cell $[kl]$ catches fire to what it burns out. w_f is the fire load. Based on investigations, w_f for wooden structures is 60.0, for earthen structures is 45.0, for brick structures is 20.0 and for others structures what do not be burned is 0.0. A_w is the average opening area for doors and windows in each floor. A_f and H are the area height of each floor in one building.

The equation to the farthest fire spreading distance presented in Ref. (Jirou and Kobayashi, 1997) is a function of only the wind velocity and direction. The effect of west wind is shown in Figure 4. The wind effects have 4 levels and 8 directions for 32 different wind effects (Frederic, et al. 2006). The model considers the effects of each wind effect.

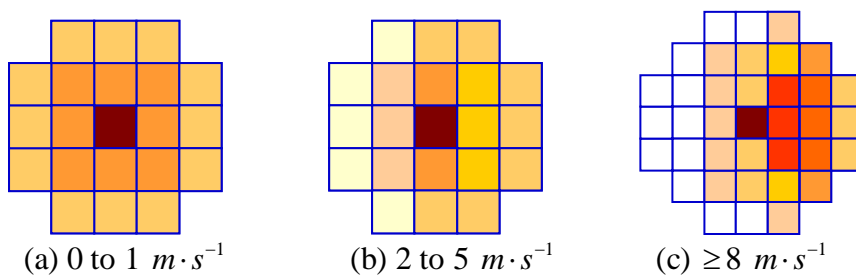


Figure 4: Effect of western wind

Lijiang City is in a mountainous area, so the topography is certainly not smooth. Some buildings were built near or in the mountains, so the model must consider the fire spreading from buildings to trees in the mountains and from trees to the buildings. The fire spread among trees differs from that among buildings, so the model must consider the tree characteristics, ground slopes, etc. The relative topography of two nearby cells are used to describe the slopes. The topography has eight directions, including 4 horizontal and 4 vertical directions (Geoffrey, et al. 2006). The

parameter po_{ij} shows the effects of the slope between adjoining cells on the fire spreading. The value of po_{ij} for each cell is depended based on topography angle with $po_{ij}= 0.1$ for 0-20, 0.3 for 20-40, 0.5 for 40-60, 0.7 for 60-80, 0.9 for 80-90. Higher values of po_{ij} will result in larger, stronger fires.

The fire states in each cell are: (1) cells are unable to burn, (2) cells are able to burn, but are not burning, (3) cells have just begun burning, but are not yet able to spread, (4) cells are burning strongly and are able to spread, and (5) cells are burned out. The transitions between cell states have a fixed order. When the cell catches fire, the cell state transitions to state (3). Some time after the cell catches fire, the cell state changes from (3) to (5). If the cell is in state (1) or (5), the cell state never changes. The fire spreading model must determine whether cell [ij] changes state from (2) to (3). The changes probability is determined by the fire spreading judgment index F_{ij} . Cells with different characteristics have different F_{ij} (Frederic, et al. 2006). The index for buildings and trees are based on the weather and cell characteristics:

$$\text{building rule: } F_{ij} = S_{ij} * P_{ij} * W_{ij} * p(t_{kl}) * \alpha * w^\beta \quad (7)$$

$$\text{tree rule: } F_{ij} = S_{ij} * P_{ij} * W_{ij} * p(t_{kl}) * po_{ij}^{fx_{ij}} * w^\beta \quad (8)$$

Here S_{ij} is a building or tree parameter set to 1.0 for wooden buildings, 0.0 for steel buildings, and between 0.0 and 1.0 for other structures. P_{ij} is the ratio of wood in the structures. w is wind effect in each cell which varies from 0.0 to 0.5 according to the distance from the burning cell. α ($0 < \alpha \leq 1$) is an adjustable parameter, whose value is changed to wind effects such as slowing of the spreading velocity. β is an adjustable wind parameter, which determined the range and direction of the fire spreading. po_{ij} ($0 < po_{ij} < 1$) is the coefficient of ground slope coefficient. fx_{ij} is the exponent of slope effect. W_{ij} is the combustibles loading in each cell. When F_{ij} is larger than a random value ($0 \leq \text{RAN} \leq 1$, whose value is chosen stochastically), the state of the cell is changed from (2) to (3), and the cell is defined to have caught fire. When the time after catching fire is more than t_1 , the cell state is changed to state (4). When the time is more than t_2 , the cell state is changed to state (5). The results will show how the fire spreads in the old town areas.

The model was used to simulate a fire spreading in Lijiang City as an example of an old town. The values parameters were $\alpha = 0.4$, $\beta = 1.0$, $D = 12.0$, and $d = 2.0$. For wooden structure $P = 1.0$, $w_f = 60.0$, for half combustible materials $P = 0.8$ and $w_f = 45.0$, for almost no combustible materials $P = 0.5$ and $w_f = 20.0$, and for no combustible materials $P = 0.0$,

$w_f=0.0$. Figure 5 shows the process of fire spreading in the Lijiang old town area. The wind was assumed to be from the east at the 4-5 level. The light gray is burning, but has no ability to spread, the dark gray is strongly burning and spreading, and the black represent the burned out cells. Figure 5(a) means fire broken out. In Figure 5(b) the fire has spread about 110 minutes and 1170 m² burned to ash. Here, the fire spread direction is mainly affected by the wind direction. In Figure 5(c) at t =122 min, the fire has spread from buildings to trees on the mountain with 1278 m² burned out. Once the trees catch fire, the fire spreads quickly, as shown in Figure 5(d) at t=230 min. Thus, the fire velocity and scope depends on the cell characteristics and some extra conditions.

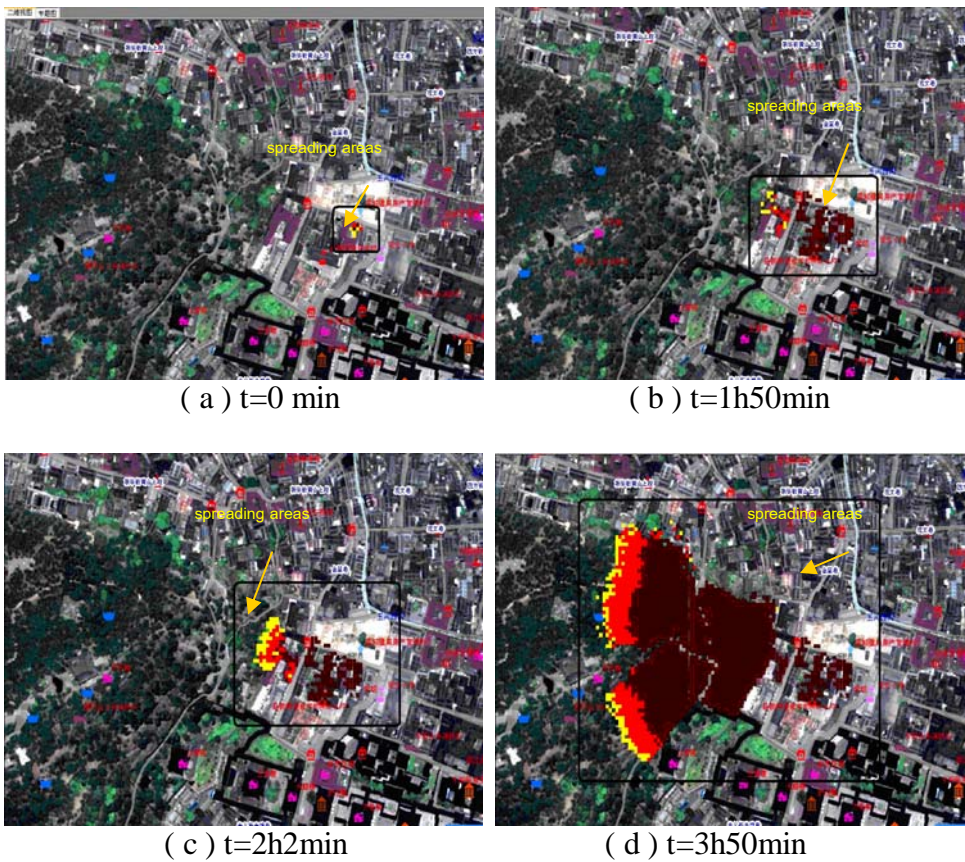


Figure 4 Process of fire spreading in Lijiang old town

There are many models in the technical platform for emergency management developed by CPSR, e.g. hazardous gas leakage model, water pollution prediction model, evaluation model for crowd evacuation, analysis model for Avian Influenza, estimation model for explosion effect, etc. Due to the limit of this paper, the details of these models are not presented here. Also we can develop more and more models in the technical platform.

4. CONCLUDING REMARKS

This paper firstly introduces the National Emergency Response Plan issued by the China State Council. Secondly the basic functions of emergency

response platform (i.e. technical platform for emergency management) are provided. According to the Plan, Center for Public Safety Research is developing a technical platform. And thirdly the details of prediction models of this technical platform are introduced.

This presented technical platform for emergency management is just elementary form, and its models should be extended and validated. The platform is an integration of existing technologies, and so it needs to develop some supports for key technologies for the future technical platform to manage more effectively emergency:

- Full-scale typical disaster and multi-disaster coupling experimental systems;
- Full-scale crowd evacuation experimental systems;
- Individual protective equipment experimental systems;
- Mobile emergency response platform; and
- Simulation computational system, etc.

Natural disasters and man-activity related incidents are common enemy of human being, and public safety is a general problem all over the world. International cooperation and exchange among the countries should be enhanced, so as to jointly cope with calamity with more efficiency. Center for Public Safety Center, as a member of the community, will make further efforts in public safety research and education, and hopefully contributes to a better and safer environment for human life.

ACKNOWLEDGEMENTS

This work was sponsored by the Program for New Century Excellent Talents in University (NCET-06-0061), Ministry of Education, the Basic Research Foundation (110041706) of Department of Engineering Physics, Tsinghua University, and the Scientific Foundation for Returned Overseas Chinese Scholars, Ministry of Education.

REFERENCES

China State Council, 2006. *National Emergency Response Plan*. (In Chinese)

Fan, W.C. and Su, G.F., 2005. Progress in emergency management research for a Mega-city in China. *4th International Symposium on New Technologies for Urban Safety of Mega Cities in Asia*, October 18-19, Singapore.

Frederic M., Xavier S. and Lucile R., 2006, Fire spread experiment in Mediterranean shrub: Influence of wind on flame front properties. *Fire Safety Journal*, 229-235.

Gao, N. and Weng, W.G., et al., 2007, Fire Spread Model for Old Towns Based on Cellular Automaton, *Tsinghua Science and Technology*. (In Press)

Geoffrey C., Robert K. and Robert G., 2006, Comparison of the sensitivity of landscape-fire-succession models to variation in terrain, fuel pattern, climate and weather. *Landscape Ecology*, 21: 121-137.

Ji, X.W. and Weng, W.G., et al., 2007, A cellular automata-based systematic risk analysis approach for emergency response. Submitted to *Risk Analysis*.

Jirou K and Kobayashi, K., 1997, Large area fire. In: Fire Institute of Japan (eds.) *Fire Handbook third edition*, Tokyo, Kyoritsu Publication Co., Ltd. (In Japanese)

Murosaki Y, Ohnishi K and Matsumoto K., 1984. Research on spreading factor of an urban expansion fire. *Journal of the City Planning Institute of Japan*, 373-378. (In Japanese)

Wakamatsu T., 1978. The risk of fire. In: Editorial committee of architectural outline (eds.) *Architecture outline No. 21 theory of architectural fire prevention*, Tokyo, Syokokusya, 279-298. (In Japanese)

Wen, J.B., 2006. *Government work report*. (In Chinese)

Yasuno K and Nanba, Y., 1999, City fire prevention design. In: Horiuchi (eds.) *New edition architectural fire prevention*, Tokyo, Asakurasyoten, 182-187. (In Japanese)

THE STATE-OF-THE-ART OF DISASTER MITIGATION AND PREVENTION MANAGEMENT IN TAIWAN URBAN AREA

KAI-LIN HSU

Assistant Professor

Department of Construction Engineering,

National Kaohsiung First University of Science and Technology, R.O.C.

vichsu@ccms.nkfust.edu.tw

ABSTRACT

Owing to natural factors (such as global weather changes, plate movements) and man-made factors (such as population increase and concentration, expanding urban limits caused by economic development, massive land development, increasing urban function) in last decades, like most regions on the world, Taiwan's natural and man-made disasters are happening more frequently. The causes and contents of disasters become more complex, and losses from disasters also increase. Due to the frequent occurrences of natural and man-made disasters, as well as a rise in losses, government and public sector have made efforts in technology development, legislation and application in order to strengthen disaster prevention and response capability. The central and local governments of Taiwan have invested vast resources in recent years to improve the entire system of warning and operational response both in the technical and organizational aspects.

For example, Chi-Chi earthquake (M 7.6) hit Taiwan on September 21, 1999, resulted in more than 2470 life losses, and more than 10billions U.S.D. in economic losses. In addition, Typhoon Shiang-Sen swept Taiwan with strong wind and hard rain on October 31, 2000, causing severe flooding in Taipei and Keelung, and making a Boeing 747 explode, claiming 81 lives and causing a natural and man-made multiple disaster while departing from the airport. With higher frequency and larger scale disasters, preventing the happening of disasters and establishing an emergency response system in order to achieve an efficient hazard management have become a very important issue nowadays.

This paper will review Taiwan's recent development in disaster management programs. An overview of the major programs which were initiated after several catastrophic disasters will be given. Next, characteristics of the programs will be presented in terms of use of existing networks, the role of initiator, and program subjects. Finally, discussion and suggestions for future development of the disaster management program will be proposed.

1. INTRODUCTION

Recently, in order to promote hazard mitigation practices more systematically, the Executive Yuan (i.e. the Cabinet) of the central Taiwan government promulgated “Hazards Mitigation Program” in 1994 as the basis for national and local disaster prevention tasks in Taiwan. According to this program, Taiwan has established 4 levels of hazard mitigation organizations at the central and local governments (including Province/Municipality, County/City, and Township/Shiang levels) (see Figure 1). Based on its essence, governments at all levels have their own Hazard Mitigation Councils (HMC), and at the Central, Province/City, and County/City levels, Hazard Mitigation Committee and Technical Advisory Committee have to be established under the supervision of HMC. The Hazard Mitigation Committee is the administrative organization; while the Technical Advisory Committee provides consulting services for different levels of government hazards mitigation councils. Also, as the basis and references to hazard mitigation tasks of different levels, this program stipulates that the Central Hazards Mitigation Council have to elaborate “Primary Hazards Mitigation Plan”, ministries under the Executive Yuan have to put in place “Specific Hazards Mitigation Plans”, and local governments have to put in place “Local Hazards Mitigation Plans”. When a large scale disaster strikes, the Emergency Operation Center (EOC) will be set up immediately in order to carry out emergency response. National Science Council initiated a national program entitled as “National Science and Technology Program for Hazards Mitigation (NAPHM)” in Nov 1997

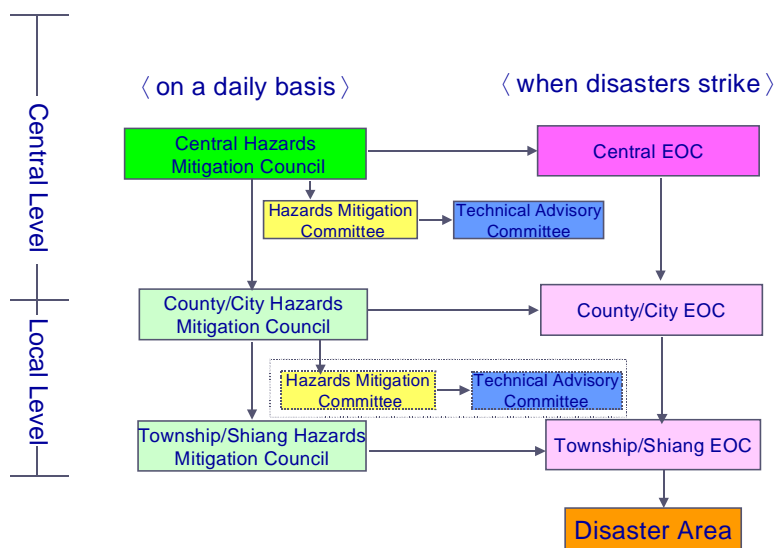


Figure 1: Hazard Mitigation System

to consolidate the efforts of various government agencies for systematically promoting the up-, mid-, and down-stream research coordination, and

integrating the research results and transfer on the practical implementation. The related agencies would follow the guidelines of NAPHM in planning and executing programs about technology innovation and administrative improvement. The appropriate, long-standing and constant strategies based on the solid research outcomes could generate the profound effects on disaster reduction. However, it is necessary to have a regular organization to coordinate related agencies, set up long-term research goals, and develop the application and implementation. In May 2003, the Executive Yuan announced “Establishment Guidelines for National Science & Technology Center for Disasters Reduction”. This center has been founded in July 2003, with major tasks of research and development, technical supports, and application and implementation, making the significant impacts on hazards mitigation in Taiwan.

Nevertheless, this program NAPHM, as well as hazard mitigation systems and hazard mitigation plans, had faced the challenges of various forms of disasters including natural hazards such as the loss about USD \$589 million/year due to the annual average of 3.6 typhoon (e.g. Figure 2), the serious impacts on society due to large-scale earthquake, the gradual shortage and distribution of water, etc. and man-made such as labor death rate about 0.077/ (1,000 workers), SARS, avian influenza, etc. In particular, the Chi-Chi earthquake on September 21, 1999, which resulted in severe casualties and economic losses, has great impact on and exposes the weakness of this hazard mitigation system. Therefore, to improve and enhance this system, as well as to raise the capabilities of hazard mitigation and emergency responses, have become crucial issues. Based on devastating experiences of Chi-Chi earthquake and other severe disasters, there are many problems drastically needed to be improved after reviewing current disaster prevention and emergency management practices. This article will discuss the administration’s disaster prevention and rescue system from an extensive perspective, in order to obtain the best operation process. We wish that Taiwan will become a country that can prevent and endure disasters, providing the citizens a carefree life, safe environment and the protection towards their lives and property.



Figure 2: Taipei MRT damage during typhoon period due to the flood caused by the continuous heavy rainfall.

2. TAIWAN'S DISASTER RESCUE SYSTEM AND OPERATING MECHANISM

In recent years, major problems related to hazard mitigation and emergency response that were aggressively improved and enhanced can be divided into three broad categories: laws and regulations, researches and practices of science and technology, enhancement of civilian organizations and communities.

2.1 Disaster prevention and rescue system

Taiwan's disaster prevention and rescue system, as defined by the Disaster Prevention and Rescue Act, has the system divided into three tiers – the central government level, the central-ruled municipality and county municipality level, and the local government level of townships, villages and municipalities. Though the Disaster Prevention and Rescue Act has not enlisted administrative districts on a separate level, the Taiwan urban-area governments have their municipal disaster prevention and rescue systems which are divided into a two-tier scheme, comprising of the municipal and district levels. At normal times, the organization of Taiwan urban-area's disaster prevention and rescue system is comprised of the Taiwan urban-area disaster prevention joint mission, the Taiwan urban-area disaster prevention and rescue commission, the Taiwan urban-area government disaster prevention and rescue expert consulting committee and so forth. In the event that Taiwan urban areas are at risk of major disasters, the emergency response body would be turned into corresponding organizations, which primarily comprised of the municipal and district disaster response centers, with an emergency response task force set up within various administration bureaus and divisions, in addition to field command center installed at the disaster sites, and the Taiwan urban-area rescue squad. In post-disaster rebuilding, there is the post-disaster rebuilding promotional committee; a logistical diagram depicting how the units work together is shown as follows:

2.1.1 Disaster mitigation consultation

The disaster mitigation consultation is hosted regularly per year or if necessary. The members who joined the consultation consist of the commissioners of departments, the chief of districts, civil organizations, military personnel, public utility. The district disaster mitigation consultation is held while the municipal disaster mitigation consultation was in operation. The members who joined the district disaster mitigation consultation are staff of the districts and the district chief is certainly convener of the district disaster mitigation consultation.

2.1.2 Disaster prevention and rescue committee

City disaster prevention and rescue committee is the staff members unit of disaster mitigation consultation. The chairperson is the deputy mayor of the city; vice-chairpersons are general secretary and commissioner of fire

department. Executive officer is one of the city counselors, all committee members are composed of the city departments representatives, to execute disaster preventive strategy and policy, including planning, assessment, integration. The executive secretary is responsible to assist all affairs. The committee set up the sections, such as unified planning section, disaster advertising section, disaster response section, restoration section, resource management section, etc.

2.1.3 Experts consulting committee

The Taiwan urban-area cities have set up the experts consulting committee by law to propose consultation about the future direction. The city mayor is the chairperson of experts consulting committee, and the deputy-mayor is the vice chairperson. The committee members, divided into flooding, earthquake, security, system, information sections, etc. are to review all the execution, scientific research of disaster mitigation works.

2.1.4 Emergency operation center (EOC)

The municipal EOC is formed in the beginning or in anxiety of disasters happened, depending on scale and range of disasters. The mayor of the city is the commander of EOC, and the deputy-mayor is the vice commander. The members joining EOC are senior officials of departments, military institutions, public utilities, etc.

2.2 Disaster prevention and rescue operating mechanism

In a move to quickly mobilize rescue units and personnel coming from relevant administration bureaus and divisions in the event that the city should be at risk or under major disasters to excel an integrated disaster rescue yield, an “Emergency disaster reporting system” has been installed at the Bureau of Fire Administration’s disaster rescue care duty dispatch/command center, which encompasses a rapid command reporting system, fax transmission system, handset short-messaging reporting system, handset priority voice communication system, wire telephone system, exclusive disaster alert telephone and so forth that can be used to activate the emergency reporting system in the event of a disaster and notify relevant disaster rescue personnel to report to the disaster response center or dispatch rescuers to disaster-hit areas to provide emergency rescue work. To facilitate conducting emergency field rescue work in major incident and disaster sites, a forward command center is set up depending on the state of a disaster site that would facilitate dispatch and command in close vicinity, where a district magistrate would head the mission as field disaster commander, in charge of commanding field crews to carry out rescue related undertakings in life rescuing, traffic control, peripheral security surveillance, emergency care response and so forth.

3. DISASTER REVIEWS- TAIPEI EXPERIENCE

3.1 921 earthquake

As major earthquakes, measuring 7.3 on the Richter scale, broke out in Chi Chi of central Taiwan at 1:47am, September 21, 1999, which though quite a distance away from Taipei City, it nevertheless dealt a major blow to the city as Dong Hsing Building, had collapsed as a result of the tremors, leaving 73 dead, 14 missing, 138 injured in a catastrophic incident, marking it the worst natural disaster in Taipei history since 1884.

Following the quakes, Taipei city suffered major power outage as the city was besieged in complete darkness, at which point a large volume of incident phone calls began to reach Taipei city Government bureau of fire administration's 119 duty dispatch center, and response centers at various government levels had been set up immediately after, where all disaster rescue personnel had voluntarily reported to duty without notice. To ensure a smooth execution of various crucial rescue efforts, a three-tier zone control had been set up at the site that helped to segregate disaster rescuers, logistical staff, disaster-hit family members, the press and such, with an effective integration of rescue efforts from private rescue organizations. On day three following the quake disaster, orders were given to begin excavating the site, coordinated with large shake and manual digging, that aimed to screen for any life sign, layer by layer, which had led to the rescue of the Sung brothers on day still, a factual proof that the city administration's rescue efforts were on track.

Table 1: Statistics on Taipei City's 921 quake damages

Type	Incident count
Human casualty	74 persons (including one suffering from cardiac arrest prior to arriving at the hospital)
Declared missing	14 persons
Number injured and sent for medical treatment	138 persons
Toppled buildings	3 cases
Hazardous buildings	23 buildings assessed as hazardous
Building found with crack lines	199 buildings
Gas leak	213 cases

3.2 Typhoon Nari's gale disaster

With typhoon Nari declared to invade the city on Sept. 16, 2001, to effectively response to relevant disasters, the Taipei City Disaster Response Center was formally set up at 8:30 am, Sept. 15 in a move to aggressively set up disaster prevention mobilization work. Yet little than expected that as typhoon Nari stalled and hovered over Taiwan extendedly, notwithstanding

packing ample of precipitations, it not only broke the city's 105 years of meteorological records but the unrelenting torrential rains, which far exceeded the flood prevention criteria devised for the city, had led to devastating results, as floodwaters gushed through the embankment and inundated and disabled the pumping stations, causing mudslides, landslides, landfalls and severe damages to the mass rapid transit system (as shown in *Figure2*), and threatening the lifeline of the entire city. The disaster had caused devastating damages, leaving 27 casualties, 3 declared missing, 16 severely injured, besides unaccountable loss of property damages among others; relevant disasters are recapped as follows,

Following the passing of typhoon Nari, to review future strategy and to ensure a rightful execution of the rebuilding work, the Taipei city government had instilled a "Taipei city government typhoon Nari post-disaster rebuilding committee", to assist the administration examine the cause of the disaster, review relevant disaster prevention, rescue and aids work, an the city's post-disaster recovery system, as well as drafting tangible improvement recommendation and providing consultation for input in moving forward rebuilding related undertakings. In conjunction to which, committee recommendations were forwarded to relevant administration bureaus and division that would poise to improve and strengthen the city's disaster prevention system; with ongoing review efforts and infrastructure improvements, substantial progresses had been made to Taipei City's relevant disaster prevention system, bracing toward the objective of recreating the city into a disaster resistant one.

Table 2: Statistics on Typhoon Nari's gale damages

Type	Disaster recap
Slope disasters	Devastations following typhoon Nari find the city suffered over 100 landfalls of varied magnitudes, 40 disaster spots along some 26 roadways, 25 preservation zones, and around 30 endangered dwellings, with varied landfalls along hazardous side slopes.
Collapsed roadways	232 disaster spots
Embankment damages	230 meters, including those along the Shertze Dao and Shia Bashien areas.
Damaged pumping station equipment	35 equipment units located in eight stations
Shelters for disaster-hit residents	Number of disaster-hit sought shelter totaled to 2,053 persons.
MRT damages	Severe damages are reported at some of the stations along the Nankang line, Tamsui line and Pannan line.

4. FUTURE VISIONS

4.1 To launch a comprehensive round-the-clock response center

To fully grasp and utilize a host of disaster rescue information, communication, and to integrate the disaster prevention mechanism of various administrative units, which would help to discern and grapple the state of various disaster, notify relevant units and convey disaster intelligence, and to excel the center's command, monitoring, coordination and response functions that are crucial for completing the disaster rescue work and minimize disaster damages, the city administration of Taiwan urban area should have plans to launch each city disaster response center to support multipurpose and round-the-clock operating modes.

4.2 To induct a disaster response backup center

In lieu of an effective system as some of the fire brigades in the central region had collapsed at the onset of 921 earthquake in some Taiwan cities, to curtail the city's existing disaster command system from being disabled in the event of a major disaster and kept from carrying out its intended purposes, a second disaster response center and disaster rescue command center within some Taiwan cities need to be re-allocated as soon as possible based on the past experience.

4.3 To strengthen a district-based disaster prevention and rescue organization and efficiency

After 921 earthquake, many of Taiwan city mayors are more keenly reminded of the fact that a singular rescue body from the city government may fall short of supporting the emergency aid for the city residents in the event of a major disaster, for the comprehensiveness and broad-based coverage. Taken into account the fact that the district office is more familiar with the local geology and a close-knit community tie, making it most suitable to assume the frontline role in disaster prevention and rescue efforts, active efforts have been made to enlist the district offices as part of the city's disaster prevention and rescue system by pushing the program to brace toward a "regional-oriented command system". It proved to be affective for the system after Nari typhoon, 921 earthquake, SARS according to Taipei experience.

4.4 To draft a disaster command system's standard ICS operating procedure

By referring the concept and principles of the U.S. incident command system (ICS), and taking into account the state of the existing command and emergency rescue work, a set of standard disaster incident command system operating procedures are to be set up in anticipation of effectively integrate various disaster rescue manpower and resources, which is expected to instill

the Taiwan urban-area city administration teams with maximum combat readiness, and enhance the rescue efficiency at disaster scenes.

4.5 To instill a multipurpose disaster prevention park

As densely populated cities within Taiwan are, the interim placement of disaster-hit residents in the event of a major disastrous incident would emerge as a significant problem. In light of which, some Taiwan urban-area city governments have plans allocating park reserves for appointing disaster parks for every administrative district, taken into account the characteristics of regional environment and population structure, where it could serve as a recreational venue to the residents at normal times and for storing essential survival rations and equipment, and be turned into an emergency shelter for disaster-hit residents at the time of the disaster.

4.6 To instill an intelligent rescue dispatch system

As the administration's 119 duty dispatch center remains manually dispatched following its upgrade from a fire brigade in 1995, some Taiwan urban-area city administrations have plans to integrate the currently leased ANI/ALI (an incoming call and address prompting system) 119 case reporting system to its existing information management system, anticipating to provide real-time computerized command and dispatch that would help to dispatch adequate manpower, equipment and devices to the disaster site for emergency rescue within the shortest time possible.

5. CONCLUDING REMARKS

In pursuit of a sustainable yield in disaster prevention and rescue efforts, the Taiwan urban-area administrations are committed to integrating the ISO quality control concept and in promoting various standardized fire service tasks by mirroring the past disasters and vying to excel, under its existing disaster prevention and rescue framework, its administration with globalized efficiency, scientific approach, standardized implementation and rational enforcement. In conjunction to which, the city administration is committed to instill an ICS emergency incident command system, rated by various types of disasters and various stages in disaster rescue, in anticipation of developing Taiwan urban areas into metropolitan areas that are disaster-proof and disaster-resistant.

REFERENCES

- Chen, Liang-Chun, Wang, Jieh-Jiuh & Wei, Ya-Lan, 2001. Human Concern and Hazard Mitigation – The Brief discussion of Community-based Hazard Mitigation, *NAPHM Newsletter*, Vol. 4, 1-10.
- Chen, Liang-Chun, Li, Wen-Wen & Lai, Mei-Ju, 2000. The Brief Description of the Planning Process and Contents of Hazard Mitigation Act, *NAPHM Newsletter*, Vol. 2, 3-12.

The office of NAPHM, 2000. The Brief Description of the National Science and Technology Program for Hazards Mitigation, *NAPHM Newsletter*, Vol. 1, 1-8.

Ho, Hsin-Ya & Li, Wen-Cheng, 2001. The Planning of the Second Phase of the National Science and Technology Program for Hazards Mitigation, *NAPHM Newsletter*, Vol. 4, 18-20.

Ministry of the Interior, 2000. *Hazard Mitigation Act*.

Ministry of the Interior, 2000. *Disaster Prevention and Rescue Act*.

the National Disaster Prevention and Response Council, Taiwan,
<http://www.ndppc.nat.gov.tw>

EXPERIMENTAL STUDY OF FIRE PROPAGATION IN A COMPARTMENT WITH DIFFERENT APPROACHING WIND CONDITIONS

HONG HUANG

Institute of Industrial Science, The University of Tokyo, Japan
hhong@iis.u-tokyo.ac.jp

RYOZO OOKA

Institute of Industrial Science, The University of Tokyo, Japan
ooka@iis.u-tokyo.ac.jp

NAIAN LIU

University of Science and Technology of China, China
liunai@ustc.edu.cn

LINHE ZHANG

University of Science and Technology of China, China
fcrane@ustc.edu.cn

ZHIHUA DENG

University of Science and Technology of China, China

SHINSUKE KATO

Institute of Industrial Science, The University of Tokyo, Japan
kato@iis.u-tokyo.ac.jp

ABSTRACT

In order to clarify the fire propagation process in and between compartments under windy conditions, fire tunnel experiments in a reduced-scale compartment were conducted. The approaching wind velocity was set to 0.0, 1.5, and 3.0m/s, and the location of the fire source was changed between the downwind corner, upwind corner and center. The temperatures in the compartment and flame ejected from the opening were measured. The radiation flux from the opening and the wall temperature in the compartment were also recorded. It is found that the extinguishment time is reduced under windy conditions. When the approaching wind velocity is high, the external plume is greatly inclined to the downwind side, and the area of flame becomes wider. The non-dimensional temperature of the external flame was a little lower than indicated by the results of Yokoi's experiments without wind.

1. INTRODUCTION

A fire initialized in a compartment will spread to the neighboring compartment and adjacent buildings by igniting the other combustible materials and the exposed combustible surfaces. Compartment fires can generally be divided into the following stages: ignition and early growth; pre-flashover period; flashover; the fully developed or post-flashover period; and finally the decay period. Numerous studies have been done to investigate the fire's characteristics in these stages (e.g. Drysdale, 1998; Rasbash, 1991; Walton and Thomas, 1995). The pyrolysis gases generated from the combustible materials will not all burn in the compartment. Under the ventilation dominant condition, usually in the fully developed stage, the necessary air quantity for all pyrolysis gases to burn is not supplied, such that part of the pyrolysis gases are projected from the window as external flames. This provides a mechanism for fire to spread to the upper floors and adjacent buildings (Yokoi, 1960; Thomas and Law, 1972; Tanaka, 1993). The spread of fire damage increases notably under strong windy conditions. Many studies on external flames in the absence of wind have been done. Yokoi investigated the trajectory and the temperature distribution of the external flame from the window in several full-scale experimental fires (Yokoi, 1960). The proposed estimation method of the external flame using the non-dimensional temperature is still in common use now. Bullen and Thomas (1979) studied the effect of the fuel area on the external flame temperature profiles. Omiya and Hori (2001) investigated the properties of external flames taking into consideration the combustion of excess fuel gas ejected from the fire compartment by conducting a small-scale fire test. Yamaguchi and Tanaka (2005) found that the non-dimensional temperature is independent of size and fire temperature, but is determined by geometrical conditions.

However, the effect of external wind has hardly been considered in these studies, including compartment fire growth in the room and external flames. There is some research regarding the external flame characteristics in windy conditions (Takahashi, 2006), however, a detailed fire growth process from the initial fire to the fully developed fire in the compartment in the presence of external wind was not examined. In this study, a reduced-scale compartment fire experiment that considers the external wind has been conducted in a fire wind tunnel. The fire growth process from the initial fire to the fully developed fire in the compartment and the external flames from the opening were measured, and the effect of the external wind was analyzed in detail.

2. EXPERIMENTS

2.1 Fire tunnel and reduced-scale compartment model

The fire tunnel used has dimensions of 1.8 m (width) \times 1.8 m (height) \times 14 m (length). Figure 1 shows the fire wind tunnel and reduced-scale compartment model. The compartment model size is 600 \times 600 \times 600 mm³. The materials of the side walls of the model are wooden cedar boards (25-mm), fire-resistant boards (32-mm) and stainless steel sheets (2-mm) from inside to outside. The ceiling and the floor are made of the same fire-resistant boards and stainless steel sheets. 200 mm \times 200 mm windows are opened at the center of the upwind and downwind sides of the model. 250 ml of n-heptane was used as the fuel, which was placed in a stainless container (100 \times 100 mm²) and ignited.

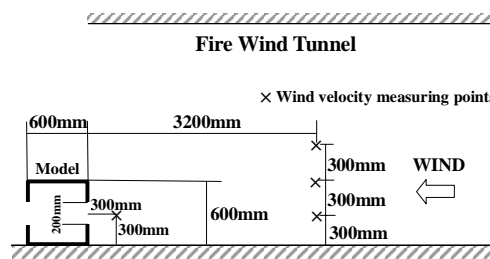


Figure 1: Fire wind tunnel and reduced-scale compartment model

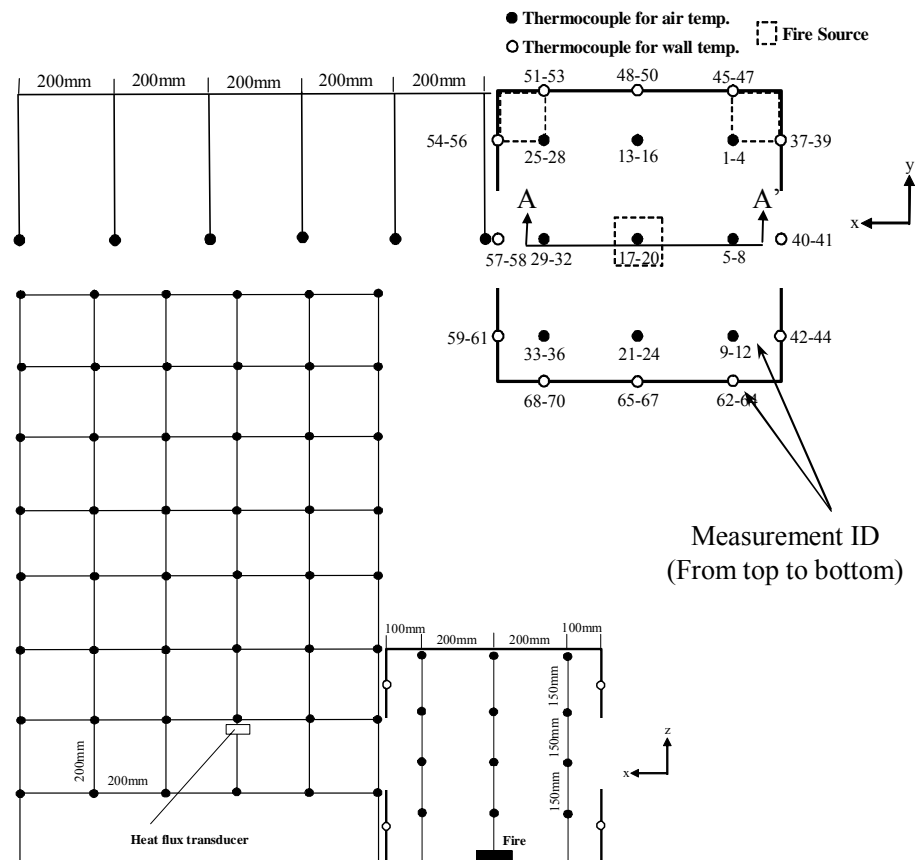


Figure 2: Measurement configuration

2.2 Measurement

As shown in Figure 1, the approaching wind was measured at three points vertically on the upwind side. The uniformity of the wind speed was confirmed in the vertical direction. A wind velocity measurement point was also positioned on the upwind side of the model to monitor the wind velocity before entering the window. Hot-wire anemometers (Kanomax, KA12) were used to measure the wind velocity. Figure 2 shows a schematic diagram of the experimental measurement configuration. The temperatures were measured in the compartment, on the wall and outside the opening. K-type thermocouples ($\phi=1$ mm) were used for the temperature measurement. The air temperatures in the compartment were measured at nine points in the horizontal direction and at four points in the vertical direction, thus a total of 36 points were measured. The wall temperatures were measured uniformly on each wall at nine points (for those walls with openings, eight points were measured). The thermocouples measuring the external flame temperature were fixed in place using a steel lattice. A total of 48 points were placed at 200-mm intervals. A heat flux meter (PMMT, HYJ-10) was positioned at one point outside the model to measure the radiant heat flux from the window. The mass loss rate of the fuel was measured by an electronic balance (Sardorius, LA64001S) set underneath the fuel container.

2.3 Experimental cases

The experimental cases are shown in Table 1. Three approaching wind velocity conditions, 0.0 m/s, 1.5 m/s and 3.0m/s were assessed. The fire source was changed between the upwind corner, downwind corner and center of the compartment. In order to facilitate verification of the flame characteristics, the experiments were also conducted under the same conditions, except that the side wall was made of fire-resistant glass.

Table 1 Experimental cases

Cases	Approaching wind velocity (m/s)	Fire source location
Case 1	0.0	Corner
Case 2	1.5	Upwind corner
Case 3	1.5	Downwind corner
Case 4	3.0	Upwind corner
Case 5	3.0	Downwind corner
Case 6	0.0	Center
Case 7	1.5	Center
Case 8	3.0	Center

3. RESULTS AND DISCUSSION

3.1 Flame characteristics and temporal temperature variation in the compartment

The pictures of the flames of the early fire in the case of wind velocities of 1.5 m/s and 3.0 m/s are shown in Figure 3. When the fire source is in the center, the flame inclined to the downwind direction. When the fire source is in the upwind corner, the flame inclined to the upwind a little towards the wall surface, whereas when the fire source is in the downwind corner, the flame significantly inclined to the upwind direction. This flow characteristic can be explained in Figure 3. If there is a main stream through the opening, vortices are formed in the corners, which leads to the inclination towards the upwind.

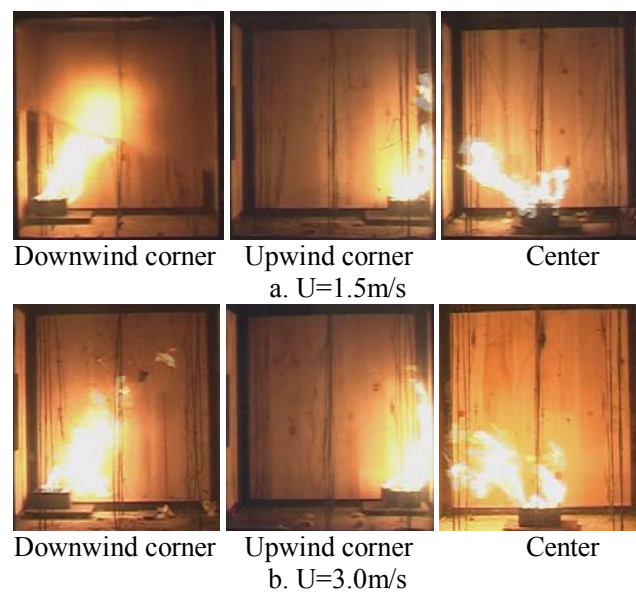


Figure 3: Flame characteristics in early fire

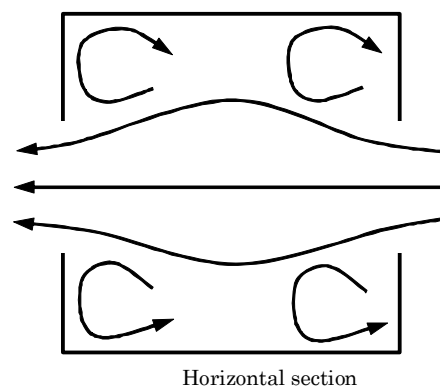


Figure 4: Image of the flow in the model

Furthermore, when the fire source is in the downwind corner, the flame inclined to the upwind direction more in the case of 3.0 m/s than that in the case of 1.5 m/s, implying that a greater vortex is formed in the downwind corner in the case of 3.0 m/s.

Figure 5 shows the mass loss rate of the fuel for all cases compared with the case where the fuel is burned in free air. It is found that the mass loss rate in the compartment is much larger than in the case of free air (no wind). This can account for the heat flux from the increasing air and wall temperature in the compartment. Faster mass loss is shown in the case of the faster approaching wind due to the additional oxygen provided. The peak of the lines shows the flashover of the compartment fire.

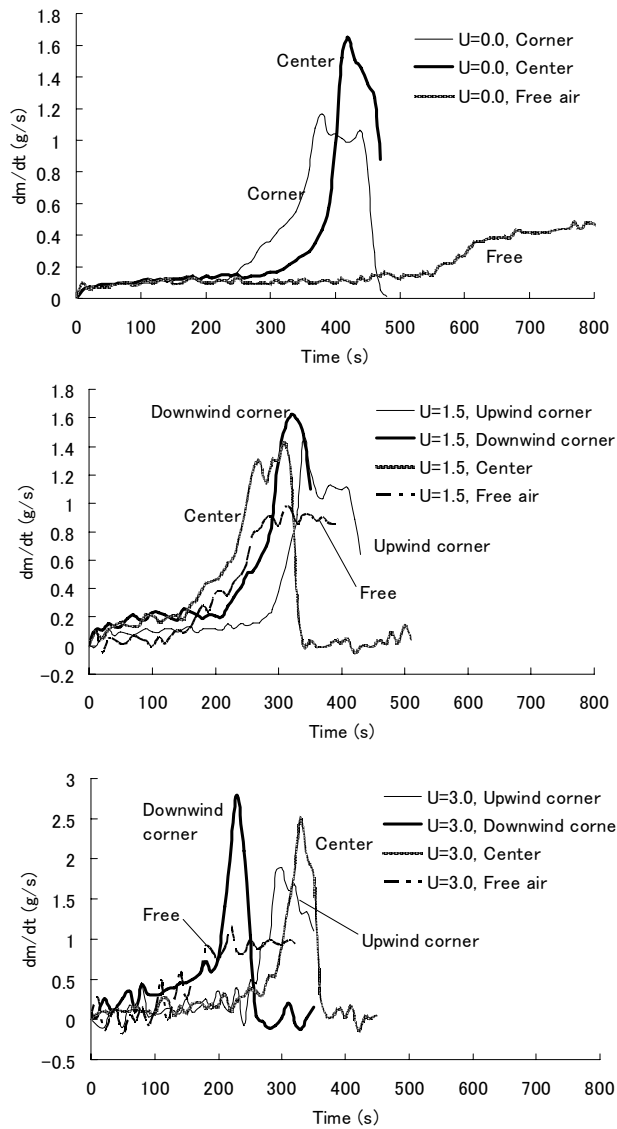


Figure 5: Mass loss rate of the fuel

As examples of the temperature measurement in the reduced-scale compartment, Figure 6 shows the temporal variations in the air temperature at the measurement points 29, 5, 13 and 21 (see Figure 2), which are close to the ceiling. Figure 7 shows the temporal variations in the wall temperature at the measurement points 38, 46, 49 and 52 (see Figure 2). It is found that compartment fire growth exhibited different behavior between cases with windy and still conditions. The temperature rises, the cedar board comprising the wall surface is gradually warmed by the fire source and reaches its ignition point, but the fire is extinguished within 15 minutes in

all cases in windy conditions. On the other hand, in the absence of wind, it is not extinguished and the cedar board on the wall burns for over 20 minutes. In the case of a wind velocity of 3.0 m/s, the temperature rises quickly, and the fire is also extinguished quickly in comparison to the 1.5-m/s wind. It may be thought that the combustible gases are blown out of the compartment and away from the wall surfaces, which are cooled by the wind. In terms of the wall surface temperature, the temperature hike at the downwind position (point 55) is fastest in Case 1 (no wind, fire source: downwind corner). This coincides with the fact that the flame is inclined towards the upwind in the presence of external wind as mentioned above.

Figure 6 shows the vertical temperature distribution at measurement points in section A-A' in different fire source locations (see Figure 2). The temperature at the ceiling is highest in the case where the fire source is at the center in still conditions.

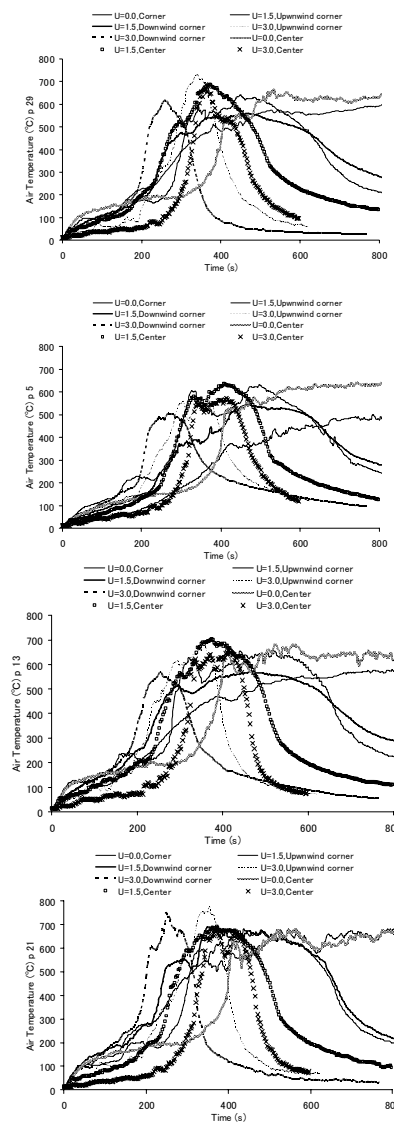


Figure 6: Temporal variations of the air temperature in the model

Higher temperatures appear in the middle in the vertical direction. This implies that the hot gas is blown out the compartment before it rises to the ceiling. The highest temperature near the outlet and lowest temperature near the inlet occur in the case of an approaching wind velocity of 3.0 m/s. From the above analysis, it can be assumed that the external wind has two contradictory effects. One is to promote combustion within the compartment and thus raise the temperature, the other is to blow away and dilute the combustible gases in the compartment and decrease the temperature, or hasten its extinguishment. Which effect predominates depends on the approaching wind velocity, amount of fuel, and the geometry of the opening and compartment.

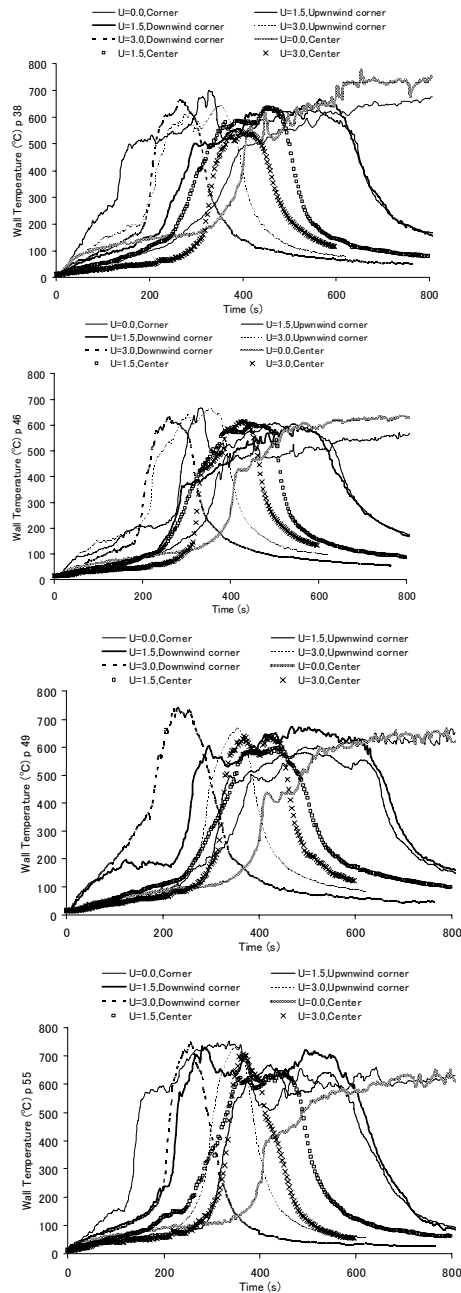


Figure 7: Temporal variations of the wall temperature in the model

3.2 External flame temperature

3.2.1 Non-dimensional flame temperature

Yokoi's research (Yokoi, 1960) is well known concerning the temperature measurement of the external flame from the window in the absence of wind. Non-dimensional temperature along the axis of the external flame is expressed by the equation below.

$$\Theta = \Delta T_0 r_0^{5/3} / (T_\infty Q^2 / c_p^2 \rho^2 g)^{1/3} \quad (1)$$

$$Q = c_p m_{out} \Delta T \quad (2)$$

Where ΔT_0 is the temperature rise at arbitrary position along the plume axis (K), r_0 is the equivalent radius of the opening ($\sqrt{BH/2\pi}$, m), B and H are the width and height of the opening respectively, Q is the enthalpy of the ejected gas (kW), ΔT is the temperature difference between the inside and outside of the compartment (K), C_p is the specific heat (kJ/kg/K), ρ is the density (kg/m³), and m_{out} is the outflow rate from the opening (m³).

The calculation of the outflow rate (m_{out}) is as follows. When the density of the ambient air is larger than the density of the indoor air, that is, when $\rho_\infty > \rho_{in}$, the outflow rate and the inflow rate which pass by each opening can be calculated by the neutral plane height Z_n using Equation (3). Where, H_u and H_l are the height of the top and the bottom of the opening

$$\begin{aligned} Z_n \leq H_l & \begin{cases} m_{out} = \frac{2}{3} \alpha B \sqrt{2g \rho_{in} (\rho_\infty - \rho_{in})} \{ (H_u - Z_n)^{3/2} - (H_l - Z_n)^{3/2} \} \\ m_{in} = 0 \end{cases} \\ H_l < Z_n < H_u & \begin{cases} m_{out} = \frac{2}{3} \alpha B \sqrt{2g \rho_{in} (\rho_\infty - \rho_{in})} (H_u - Z_n)^{3/2} \\ m_{in} = \frac{2}{3} \alpha B \sqrt{2g \rho_\infty (\rho_\infty - \rho_{in})} (Z_n - H_l)^{3/2} \end{cases} \quad (3) \\ H_u \leq Z_n & \begin{cases} m_{out} = 0 \\ m_{in} = \frac{2}{3} \alpha B \sqrt{2g \rho_\infty (\rho_\infty - \rho_{in})} \{ (Z_n - H_l)^{3/2} - (Z_n - H_u)^{3/2} \} \end{cases} \end{aligned}$$

respectively (m), α is the opening flow coefficient (set to be 0.7 here).

Furthermore, the calculation of neutral plane height is as follows. Figure 9 shows the pressure distribution inside and outside the compartment when the external wind is considered. It calculates neutral plane height from Equation (4).

$$Z_n = \frac{\Delta p + p_w}{(\rho_\infty - \rho_{in})g}, p_w = C \frac{1}{2} \rho_\infty V_\infty^2 \quad (4)$$

where, p_w is the wind pressure on the wall surface, C is the wind pressure coefficient (generally 0.75 and -0.3 are used for the upwind and downwind respectively). V_∞ is the approaching wind velocity. By substituting Equation (4) in Equation (3) and coupling the mass continuity equation of the outflow

and the inflow rate through the opening, the pressure difference ΔP between the inside and outside can be calculated. Then, the outflow rate which passes by the opening can be calculated. Finally, substituting Equation (2) in Equation (1), the non-dimensional temperature can be obtained.

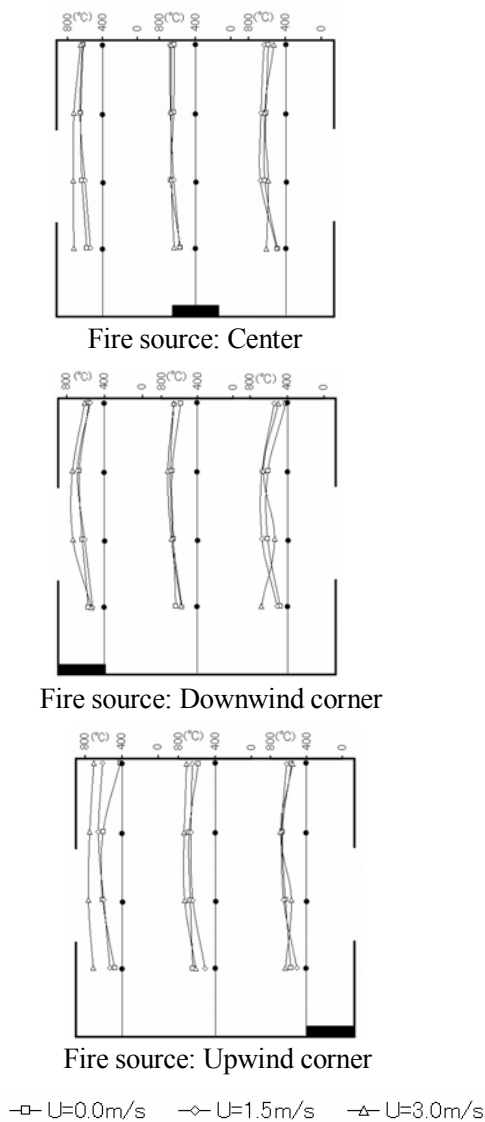


Figure 8: Vertical distribution of air temperature in the model

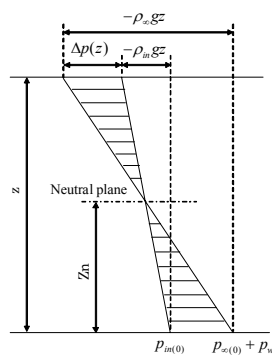


Figure 9: Pressure difference between the outside and inside of the compartment considering the external wind

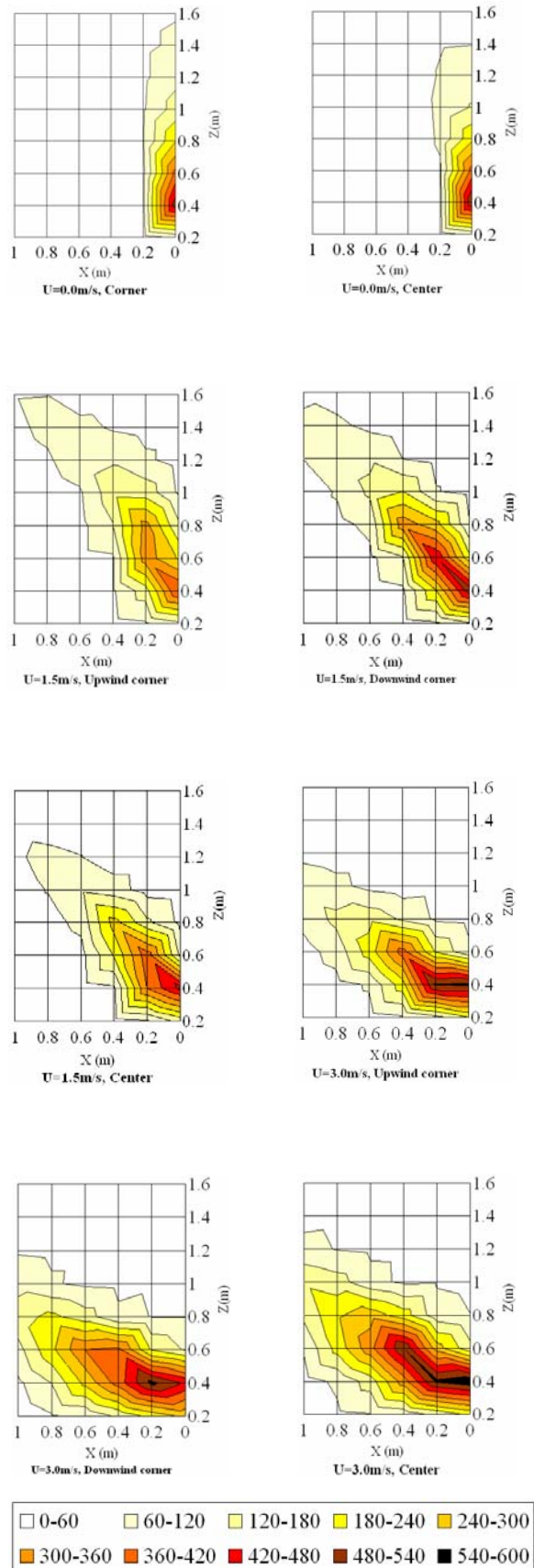


Figure 10: Temperature rises in the external flame

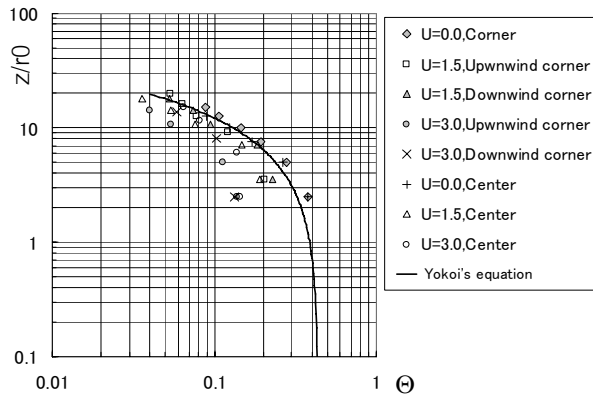


Figure 11: Non-dimensional temperature on the axis of the external flame

3.2.2 Temperature distribution and comparison with Yokoi's results

According to the measurement of the radiant heat flux outside the compartment, after the radiant heat flux reached its maximum, it maintained an almost constant value for a certain period. This period is thought to be the steady-state fully developed fire period. The average temperature rises of the external flames during this period are shown in Figure 10. Accompanying any increase in the approaching wind velocity, the inclination of the external flame increases and the flame area becomes wider. Concerning the temperature rise, it is found to be higher in the case where the wind velocity is 3.0 m/s than 1.5 m/s. It is also higher when the fire source is placed in the downwind corner rather than in the upwind corner.

The non-dimensional temperature of the external flame on the flame axis is shown in Figure 11. (z : Length on the flame axis). It agrees with the results of Yokoi's study (Yokoi, 1960) in the case of still conditions. The non-dimensional temperature of the ejected flame was a little lower than the results of Yokoi's experiments without wind.

5. CONCLUSIONS

In this study, fire tunnel experiments in a reduced-scale compartment were conducted in the presence of external wind in order to clarify the fire propagation process in and between compartments under windy conditions. The approaching wind velocity was set to 0.0, 1.5, and 3.0 m/s, and the location of the fire source was changed between upwind corner, downwind corner and center. The temperatures in the compartment and of the flame ejected from the opening were measured. The radiation flux from the opening and the wall temperature in the compartment were also recorded. It is found that the extinguishment time is reduced under windy conditions. When the approaching wind velocity is high, the ejected plume greatly inclines to the downwind side, and the flame area becomes wider. The non-dimensional temperature of the ejected flame was a little lower than the results of Yokoi's experiments without wind.

ACKNOWLEDGEMENTS

This work was supported by Grant-in-Aid for Scientific Research from the Japan Society for the Promotion of Science (No. 30376636). The authors also would like to thank Yuanfu Diao, Changshan Ding, Jian Ye, Qiong Liu and Zhengang Zhai (University of Science and Technology of China) for their hard work in the experiments.

REFERENCES

- Bullen, M. L. and Thomas, P. H., 1979, Compartment fires with non-cellulosic fuels, *17th Symposium (International) on Combustion*, 1139-1148, The Combustion Institute, Pittsburgh.
- Drysdale, D. D., 1998, *An Introduction to fire dynamics*, 2nd Edition, John Wiley and Sons.
- Omiya, Y. and Hori, Y., 2001, Properties of external flame taking into consideration excess fuel gas ejected from fire compartment, *Journal of Architectural Planning and Environmental Engineering*, 1-8, 545. (in Japanese)
- Rasbash, D. J., 1991, Major fire disasters involving flashover, *Fire Safety Journal*, 17, 85-93.
- Takahashi, Y., Hayashi, Y., Kodama, N., Omiya, Y., 2006, An experimental study on compartment fire affected by external wind, *Summaries of Technical Papers of Annual Meeting of Architectural Institute of Japan*, 241-244. (in Japanese)
- Tanaka, Y., 1993, *Introduction to building fire safety engineering*, Japan Building Center.
- Thomas, P. H. and Law, M., 1972, The projection of flames from buildings on fire, *Fire Research Note*, No. 921.
- Walton, W. D. and Thomas, P. H., 1995, Estimating temperatures in compartment fires, in *SFPE Handbook of Fire Protection Engineering*, 2nd Edition, 3.134-3.147, Society of Fire Protection Engineers, Boston.
- Yamaguchi, J. and Tanaka, T., 2005, Temperature profiles of window jet plume, *Fire Science and Technology*, 24, 1, 17-38.
- Yokoi, S., 1960, Study on the prevention of fire-spread caused by hot upward current, *Report of the Building Research Institute*, No. 34.

PROTECTIVE MEASURES OF FLOOD EMBANKMENT ALONG THE JAMUNA RIVER IN BANGLADESH

MD. MUNSUR RAHMAN¹, MOHAMMAD ASAD HUSSAIN²,
MD. MOTAHER HOSSAIN³, MAMINUL HAQUE SARKER³ and
MOHAMMAD NAZIM UDDIN*¹

¹Bangladesh University of Engineering and Technology (* PhD Student),
²Bangladesh Water Development Board and ³Center for Environmental and
Geographic Information Services, Bangladesh
mmrahman@iwfm.buet.ac.bd

ABSTRACT

During the late 1950s and mid 1960s, an earthen embankment was constructed, known as the Brahmaputra Right Embankment (BRE) extending for some 220km along the right bank of the Brahmaputra-Jamuna River primarily for agricultural crop protection against flooding. Since its construction, BRE experiences failures or damages at some vulnerable locations resulting flooding in the adjacent land during the monsoon. To protect the failures or damages of BRE, massive river training works are undertaken.

This paper reviews the history of river training works adopted along BRE and their evolution towards the development of cost effective eco-friendly structures. The failures and success stories of some of the protective measures are discussed in general. Finally, future approaches for the protection of BRE keeping the good ecological health of the river itself are discussed.

1. INTRODUCTION

The Jamuna River drains the rainfall and snowmelt from China, Bhutan, India and Bangladesh. The length of the Jamuna River in Bangladesh is about 240 km measured from its international border to the confluence with the Ganges at Aricha. The river starts rising in March/April due to snowmelt in the Himalayas and usually attains its peak between mid July and end of August. The maximum discharge at Bahadurabad, the only discharge gauging station at the Jamuna river, is estimated as 100,000m³/s. The recorded minimum flow is 2860 m³/s. The difference in water levels between flood and dry season is about 6.5m at Bahadurabad, which gradually reduces in the downstream direction. The surface water slope of the Jamuna river reduces from 7.6 cm/km at the upstream to 6.5 cm/km at the downstream (FAP 24, 1996). The rise of water levels resulting from monsoon discharge and mild longitudinal slopes, creates flooding on the floodplain that often enters inside rural agricultural land, urban and industrialized areas close to the river. During the late 1950s and mid 1960s,

an earthen embankment was constructed, known as the Brahmaputra Right Embankment (BRE) extending for some 220 km for agricultural crop protection against flooding. Since its construction, BRE experiences failures or damages at some vulnerable locations resulting flooding in the adjacent land during the monsoon. In consultation with the local people as well as BWDB Engineers, it was understood that BRE had been retired several times and shifted away from the main river resulting from failure or breaches of embankment.

To protect the failures or damages of BRE, massive river training/bank protection works are undertaken not only to reduce crop loss due to flooding but also to ensure guard against the destruction of near by rural, urban and industrial infrastructures developed so far. Several types of protective works have been constructed and in some cases combination of structures have been installed which ranges from passive measures like revetments and hard points to partly active and passive measures like groins/spurs. Bangladesh Water Development Board (BWDB) has mixed experiences of both failures and successes of such projects for the protection of BRE (Uddin, 2007).

This paper reviews the history of river training works adopted along BRE and their evolution towards the development of cost effective eco-friendly structures. The failures and success stories of some of the protective measures are discussed. Finally, a conceptual model for the protection of BRE in the future is discussed in relation to the safety of rural agricultural land as well as densely populated urban and industrial area keeping the good aquatic health of the river itself.

2. HISTORY AND EVOLUTION OF PROTECTIVE MEASURES

2.1 History of BRE River Training/ Bank Protection Works

The historical perspectives of the river training/ bank protection works have been summarized in some recent reports under Flood Action Plan (FAP 1, 1994). Before FAP studies, a considerable amount of investment has been made in bank protection work along BRE but the success story of such protective measures are very few. Relatively successful river training works could be found in Sirajgonj Town protection by means of a groin in combination of earthen spurs at the downstream where randomly dumped concrete blocks were used. The protection of Sariakandi by means of Kalitala groin is another example of partial success against river erosion.

The unplanned local disturbances created by the interventions may extend towards the longer reaches where river need to have different set of morphological equilibrium (Rahman, 1998). For example, the Kalitola groin diverts flow away from BRE and creates significant changes at the local scale as well morphological scale. It re-distributes the approach flow as well as erosion and deposition processes. Therefore, such a single structure is not desirable at the morphological scale of the river although it has some benefit

at the local scale. Usually, river training creates sudden impact on river morphology and river need longer time scale to adjust with the changed situation towards morphologically equilibrium (Wu et al., 2005).

2.2 Evolution Processes of BRE River Training Works

Bank erosion along the Jamuna basically means the erosion of floodplain. Usually, such floodplain erosion is severe during the post monsoon period. When main channel travels close to the flood embankment through erosion, damages to the BRE or failure to some part of it happens easily. Therefore, river training works along the BRE have the primary objective to keep the main channel away from the BRE by stopping or minimizing erosion.

After FAP studies, specially in FAP 1 (1994), some systematic pilot test structures were planned to execute in the form of hard point at different sites along the BRE as shown in Figure 1. The planned location for the construction of Hard points are marked as rectangular and circular symbols, while, location of the circular symbols were implemented only. These test structures were selected at priority sites as short term works that would constitute principal elements of long term master plan for the stabilization of BRE. The basis of hard point concept is not to create disturbance to the natural flow of the river like spurs or groins, rather to stabilize the present pattern of the river by limiting the boundaries of the local width of braid belt. Important places on the bank line need to be protected by creating 'Hard points' which are isolated bank revetment works with upstream and downstream terminations. The function of the hard point is to limit the extent of erosion. The length and spacing of the hard point determines the extent of area protected from the erosion and thus the maximum allowable embayment that is permitted in the locations between the structures.

Repair and maintenance works are very important in the river training works even around very expensive structures such as hard point (BWDB, 1999). The local effect of the training works triggered with natural morphological variation such as development of meander bends associated sand bars (Blondeaux and Seminara, 1985) generate very complex situation. Revetments and hard points are passive river training structures while hard points (\$21,000/m) are more than 5 times expensive as compared with the conventional revetments (\$4,000/m). Therefore, hard point-like structures are very difficult to construct under the economy of a developing nation like Bangladesh. Impermeable groins are also very expensive, for example, re-constructed Kalitala Groin (\$12700/m) having a length of 130 meter that protects around 500 meter. Specially, when foreign funding was not available to construct all the planned hard point structures shown in Figure 1, the BWDB had developed some alternative low cost approaches in order to complete protection of BRE. Using the field experiences of BWDB engineers devised RCC spurs (\$950/m) that is less expensive than any other available approaches. The RCC spurs are normally constructed in series and protect a distance of 2-4 times of its length. Single RCC spur is risky because of the long protruded length of the RCC spur into the river. The site

and length of the RCC spur has to select on the basis of morphological condition. The main considerations of construction of the RCC spur are: (i) there must be a sand bar (char land) within 1000m from the river bank; without this char land construction of RCC spur is impossible (ii) the near bank chute channel is closed by construction of earthen shank (iii) the RCC part is constructed in the char land (Uddin, 2007).

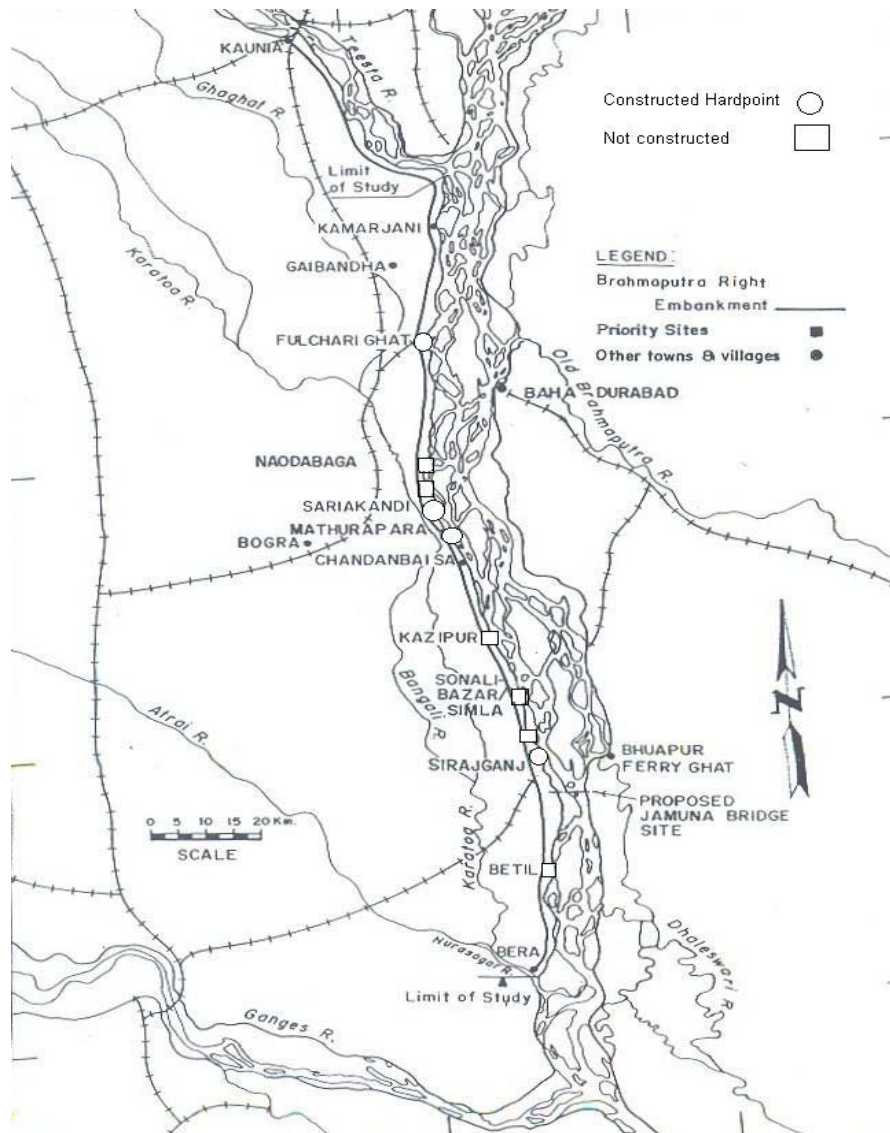


Figure 1: Proposed and implemented hard points in FAP 1 (1994).

It is already proved in some developed countries that the above conventional methods can never provide environmentally suitable solutions (Klaassen, 2002) even though these are proved to be effective against bank erosion and to some extent stream restoration (narrowing and deepening the base-flow-channels) in smaller rivers (Shields et al., 1995). Therefore, FAP also, dealt with the development cost-effective eco-friendly structures along the BRE in the form of permeable groins (FAP 21, 2001).

3. PERFORMANCE OF TRAINING WORKS

The overall performance of the training works has been evaluated on the basis of available literature (BWDB, 1999), field investigation and discussions with BWDB engineers, water experts and stakeholders. BRE provides protection against flooding to the adjacent region of the Brahmaputra right bank. Around 30 training structures (Figure 2) have been constructed along BRE mostly during the last one-decade. Due to these structures, erosion rate has been reduced significantly (CEGIS, 2005) that indicates the positive role of training works for the protection of BRE. In the following sub-sections, the performance of each type of structures has been outlined briefly.

3.1 Performance of Hard Points

Sirajgonj, Sariakandi and Mathurapara hard points were constructed in 1998. These structures experienced the biggest flood in the history of the Jamuna in 1998. The performance of Sarikandi and Mathurapara hard points were more or less good, but damages and failures had been encountered at the Sirajgong hard point. Due to unfavorable bathymetric development at the upstream of the Sirajgonj hard point, the scouring rate at the upstream part of the structure was very quick. Although the maximum scour depth did not exceed the design scour depth, some flow slides occurred during the fast scouring processes. It was clarified that such flow slides occurred due to excessive mica content in the soil on which aprons were set. The apron material could not get sufficient time for its settlement on the quickly developed scour hole. After flood 1998, the structure was repaired and rehabilitated and in recent time it is performing well.

3.2 Performance of Groins

As an example, Kalitala groin is cited here. Kalitala Groin was re-constructed in the year 2001 in one of the main channels. The length of the groin is 130 meter and it protects a relatively short length (500 meter) at the downstream. Huge scour depth is developed at the nose of the structure and during the flood season water depth becomes 55-60 meter at the nose. BWDB local office explained that the structure is in good condition and it requires significant amount of management and maintenance works.

3.3 Performance of RCC Spurs

During the period of 1999-2002, fifteen numbers of RCC spurs have been constructed at different location of BRE with variable lengths and spacing. Out of these fifteen spurs, five were damaged due to poor construction and lack of repair and maintenance works (Uddin, 2007). After critically examined the design and performance of spurs, the reason of such

failures and some modification of the shape of the spurs have been suggested by Uddin (2007). During field investigation in March, 2007 and September 2007, various modes of failures and their maintenance activities are observed. These structures are constructed on the floodplain allowing maximum scour depth of 8 meters below the construction level. CC blocks were damped as launching apron in order to protect the scour depth in excess of 8 meter. As, RCC spurs are constructed on the floodplain during the dry season, it is expected that these will divert the main channel away from the BRE. It was observed during the field investigation that the structures that are in good condition is either remaining on the floodplain or it is experiencing the hydraulic load of some branch channels (minor). Therefore, it cannot be confirmed yet, whether such structures can sustain against some major channels in the Jamuna or whether it requires some structural modifications. Some of the RCC spurs are shown in Figure 2.



Figure 2: Success (left) and failure (right) of some of the RCC spurs.

3.4 Performance of Revetments

As an example, Titporal revetment adjacent to the upstream of the Kalitala groin was investigated. The 2 km long revetment was constructed with a side slope in the main channel. The structure is functioning well except some minor damages due to some local problem. Huge CC blocks were stacked at the upstream of the revetment for emergency use.

3.5 Performance of Permeable Groins

A series of permeable groins were constructed in the pilot project FAP 21/22 during 1994-1995 at Gaibandha. Permeable groins are less costly as compared with the impermeable groins and have advantages from the river ecological view-point in many cases. Permeable groins created significant positive impact accelerating siltation in between the groin fields. But at the end of the last groin, flow hit the char land almost perpendicularly resulting severe bank erosion over there. Usually, return current at the end of the permeable groins should not be so strong and erosion downstream of the structure might not happen so severely. But it is happening in reality. May be such severe erosion downstream of the permeable groins are resulting from the changes in river morphology, specially, development of

sand bars. This need detail investigation to clarify the reason and its mitigation approaches. The shape of a permeable groin and typical embankment failure along BRE are shown in Figure 3.



Figure 3: Permeable groin (left) and embankment failure (right) along BRE.

4. SUSTAINABLE APPROACHES AGAINST RIVER EROSION

4.1 Effect of Training Works on River Morphology

River training works have significant effect on fluvial processes of a river due to the changes in sediment balance. Therefore, the morphological behavior of an alluvial river goes under sudden modification due to the installation of training works. The history of the river training works for about 300 years along the lower reaches of the Yellow River and change in its fluvial processes have been explained by Wu et al. (2005). The river looks like a suspended one above the ground level after it is fully trained. The connections between river and floodplain are cut while floodplains are considered as primary source of nutrients and habitats for the riverine ecology associated with all the plants and animals living in the river-floodplain system.

4.2 Use of Bandalling for River Training

The conceptual approach (Rahman et al., 2003) for the use of bandalling against river bank erosion was tested in the laboratory (Rahman et al, 2005) and later on some recommendations are made for the necessity of pilot test in the real river (Rahman et al., 2007). Following the guidelines from the above researches on bandal structures, River Research Institute (RRI) in its own research program has tested the applicability of bandalling along the BRE near Sirajganj during the monsoon of 2007. Total ten numbers of bandal structures with 12 meter length for each were constructed in series (approx. covers 700 meter) at the cost of 3000 US Dollars. The height of the bamboo frame bandals was around 4.5 meter. During the flood season the bandal were submerged and after monsoon flood, it was found that the most upstream two bandals were damaged whereas, the remaining eight structures are working well. Huge sedimentation near the bank side was observed. From the above field experiments and previous pilot study

under FAP 21 (2001), some of the related issues on the bandal structures for its usage as river training work are clarified. Series of bandals can make sedimentation near the bank line, but a single bandal is not effective. For a river like the Jamuna, the choice of material for bandal structures should be made carefully. Bamboo based material may not be effective, especially for the most upstream structures. Moreover, bandals may not be effective as an element of primary protection works. Rather, it may be useful as supplementary structures in between the existing river training works. From the recent field investigation during September 2007 (during recession stage), it was found that severe erosion had been taken place at the downstream of river training works along BRE including permeable groins at Kamarjani. Sometimes, between two RCC spurs are also attacked by erosion. Such erosion at the downstream of any solid or permeable structures is encountered due the return current developed at the nose of each structure as well as because of the oblique flow to the bank generated by large scale sand bars. Return current was found to be absent in the case of bandals (Rahman et al, 2005; 2006) as the straight flow passing below the bandal structures opposes the return current develops at the upper portion of the bandal plate. Therefore, return currents around bandals are mutually counter balanced. In addition to this, due to strong lateral flow acceleration (Rahman et al., 2005), bandal creates excess flow towards the main channel away from the bank line.

4.3 Proposed Approaches for Sustainable Erosion Management

Since the construction of BRE, several kilometers of embankment have been retired and some of the retired sections are located about 2 km inland from the original alignment (FAP 1, 1994). Even then, some of the reaches of BRE are very close to the main flow of the Jamuna due to erosion. As a result of the construction of massive river training works, in general, the amount of erosion has been reduced but frequent embankment breaching is happening each year at least one or two locations in between the training structures or at the downstream of the structures like groins, spurs or even hard points. Sometimes, the earthen shank of training works like RCC spurs are also attacked by oblique flow. Construction of additional massive training structures like revetments, groins or spurs can solve the erosion problem to some extent, but things will be very expensive and rivers will lose its harmony with nature that is very important for riverine environment and ecology. Moreover, oblique flow towards the bank generated by large-scale sand bars can hit BRE and in that cases conventional river training works will not be effective. Bars move both laterally and longitudinally and direction, magnitude and location of flow impingement to the bank will be changed each year. Recently, CEGIS (2005) introduced a bank erosion prediction tool for the Jamuna river. Such tool is developed on the basis of dry season sedimentary features and erosion can be predicted during the next flood season. If series of bandals are constructed in between or downstream of the existing training works where erosion is predicted by CEGIS, then recurrent erosion problem and embankment breaching resulting can be minimized. Erosion and siltation processes would be limited within the bandal fields and BRE will be safe at

nearly natural water and sediment flow regime. The conceptual model of the proposed approach where major training working will be supplemented by bandals is shown in Figure 4. The flow towards bank line will be counter balanced by the flow generated in the bandal field. Such a concept needs to be thoroughly investigated. One of the big challenges for the bandal structures is the choice of proper material during its construction in reality. The nature friendly material such a bamboo, wood etc are preferable, but considering the stability of bandals even as secondary structure in a large scale river like the Jamuna, the construction material should be strong enough. There is some urgent necessity of research work on the choice of material for the construction of bandal structures.

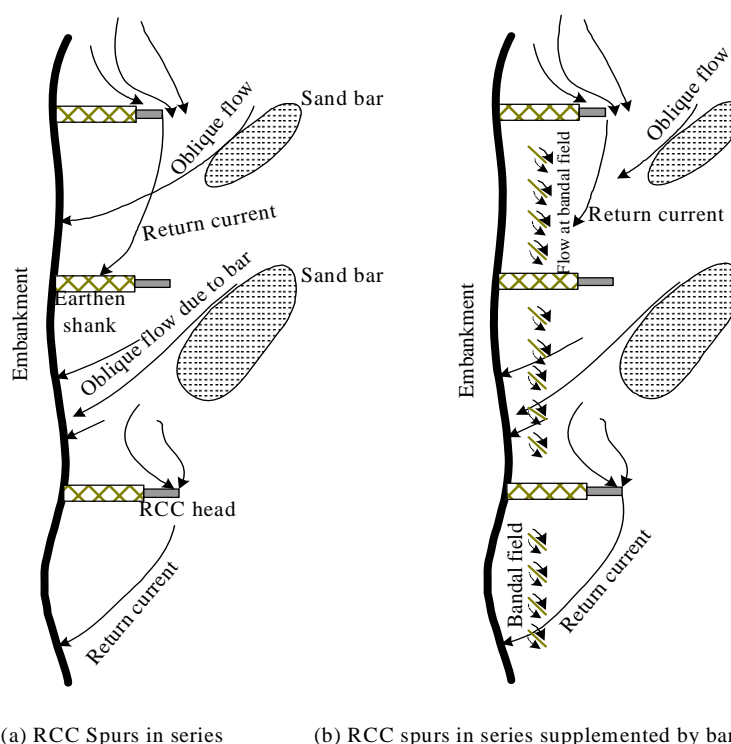


Figure 4: Conceptual model for bandals along BRE with RCC spurs.

5. CONCLUSIONS

The existing training works along the BRE are found to be inadequate for the protection of Jamuna right bank. Severe erosion at the downstream of the existing structures as well as in between the training structures are observed. Construction of additional conventional training structures seems to be very expensive and is not friendly to the riverine environment. Therefore, alternative low cost nature friendly flexible structures may conserve the river ecology to its natural shape. The effect of a series of bandals is recommended to investigate in between the existing structures. Using bandals, erosion and siltation processes would be managed to a desired limit and BRE will be safe at nearly natural condition.

REFERENCES

- FAP 24, 1996. *River Survey Project*. Final Report- Annex 5, Morphological Characteristics, Water Resources Planning Organization, Ministry of Water Resources, Bangladesh.
- Uddin, M. J., 2007. *RCC Spur in Bangladesh: Review of Design, Construction and Performance*, Unpublished Msc Thesis, UNESCO-IHE, The Netherlands.
- FAP 1, 1994. *River Training Studies of the Brahmaputra River*, Annex 3: Initial Environmental Evaluation and Annex 4: Design and Construction, Water Resources Planning Organization, Ministry of Water Resources, Bangladesh.
- Rahman, 1998. *Studies on Deformation Processes Meandering channels and Local Scouring around Spur-dike-like Structures*, Unpublished PhD Thesis, Kyoto University, Japan.
- Wu, B., Wang, G., Ma, J. and Zhang, R., 2005. Case Study: Training and Its Effect on Fluvial Processes in the Lower Yellow River, China, *Journal of Hydraulic Division, ASCE*, Vol. 131, No. 2, 85-96.
- BWDB, 1999. *River bank Protection Project*. Evaluation of the Performance of Hard Points, Review of Damage during 1999 Flood Season and Recommended Remedial Works.
- Blondeaux, P. and Seminara, G., 1985. A Unified Bar-bend Theory of River Meanders, *Journal of Fluid Mechanics*, Vol. 157, 449-470.
- Rahman, M.M., Nakagawa, H., Khaleduzzaman, A.T.M. and Ishigaki, T., 2003. Flow and scour-deposition around bandals, *Proc. Fifth International Summer Symposium, JSCE*, 177-180.
- Klaassen, G.J., Douben, K. and van der Waal, M., 2002. Novel Approaches in River Engineering, *River Flow 2002*, 27-43.
- Shields F.D. Jr., Copeland, R.R., Klingeman, P.C., Doyle, M.W. and Simon, A., 2003. Design for stream restoration, *Journal of Hydraulic Division, ASCE*, Vol.129, No. 8, 575-584.
- FAP 21, 2001. *Guidelines and Design Manual for Standardized Bank Protection Structures*, Bank Protection Pilot Project, WARPO, Ministry of Water Resources, Bangladesh.
- CEGIS, 2005. *Prediction of Bank Erosion and Morphological Changes of the Jamuna River 2006*, WARPO, Ministry of Water Resources, Bangladesh.
- Rahman, M.M., Nakagawa, H., Khaleduzzaman, ATM. and Ishigaki T., 2005. Formation of navigational channel using bandal-like structures, *Annual J. of Hydraulic Engineering, JSCE*, Vol. 49, 997-1002.
- Rahman, M.M., Nakagawa, H., Ito, N., Haque, M. A., Islam, G. M. T., Rahman, M. R. and Hoque, M. M., 2006. Prediction of Local Scour Depth around Bandal-like Structures, *Annual J. of Hydraulic Engineering, JSCE*, Vol. 50, 163-168.
- Rahman, M. M., Haque, M. A., Islam, G. M. T., Rahman, M. R. and Hoque, M. M., 2007. *Use of Bandals for Sediment Management*, Unpublished Report, IWFMM, BUET.

DEVELOPING A UNIVERSAL WATER RESOURCE ASSESSMENT MODEL FOR SUSTAINABLE WATER SECURITY

AKIYUKI KAWASAKI¹⁾²⁾, SRIKANTHA HERATH¹⁾
and KIMIRO MEGURO²⁾

¹⁾ United Nations University, Japan

²⁾ IIS, The University of Tokyo, Japan
kawasaki@hq.unu.edu

ABSTRACT

Water is proving to be at the heart of serious environmental, political and economic issues around the globe. Resolving these problems requires solutions that span across national, regional, and global scales. Recently, the concept of "water security" has gained traction as a means for conflict resolution, yet developing models and tools that support water security solutions still remain to be an urgent issue.

The ultimate goal of this study is to develop Universal Water Assessment Indicators and tools that support water-security related problem-solving using a Spatial Information Platform for Watershed Environmental Assessments based on ideas, concepts, and prototypes developed in-house at laboratory. The objectives of the study are as follows:

- *To represent a wide range of water resource indicators in an integrated format.*
- *To quantify and reveal typically concealed relationships such as total water supply and demand, and complicated links between upstream water resources and downstream users.*
- *To identify problem hot spots and effective solutions.*
- *To dynamically analyze the influences of natural and anthropogenic activity on water systems.*
- *To investigate optimal combinations of water management and water rights at each location for all involved in terms of sustainability and cost effectiveness.*

The models and tools shall include not only factors directly related to water itself like water supply and demand, water quality and flow, access, and safety; but also indirect factors change like economic and social systems, education for water use, ethnic issues, disaster response, and ecosystem services. Currently, no integrated indicators exist that properly capture the spatial distribution and temporal variability due to current regulatory and spatial limitations. Developing such Universal Water Assessment Indicators shall aid in developing concrete solutions to water security issues on a human-scale based on a GIS database. Mekong River basin was selected as a study area.

1. INTRODUCTION

During the next 50 years, population and economic growth is projected to drive up the demand for water by 30 – 85% according to the MA scenario (Millennium Ecosystem Assessment, 2005). Scenarios developed by the Intergovernmental Panel on Climate Change project an increase in global mean surface temperature of 2.0-6.4 ° Celsius above preindustrial levels by 2100, which will entail rising incidences of floods and droughts. Even now in the 21st century however, water crises are proving to be a very serious issue at the global level. Addressing and resolving these problems requires developing strategies and agreements in national, regional, and global levels. In recent years, the concept of "Water security" which seeks to resolve and avoid disputes rooted in securing water rights and water shortages, is becoming more common, and developing models and tools that contribute to water access problem solving is an urgent issue.

A broad range of models are available for assessing a single dimension of water related issues, but the focus is often limited to a particular domain of the total environment. Examples include dynamic models such as climate models, lake models, river basin models, and meteorological models; as well as static models like economic models, scenario assessment models, and risk assessment models. As each of these models is limited in scope, it is possible that some critical detail is overlooked. Another major challenge for assessment models is the incorporation of social aspects such as individual and group behavior as well as institutional arrangements and performance. The last few decades have seen a dramatic improvement in various modeling aspects. On one hand, new, advanced modeling techniques like agent-based systems and cellular automata are gaining popularity, and on the other, model input data of ever higher temporal and spatial resolutions have become available due to technological advancements in remote sensing and GIS applications. Such developments in modeling and data observation have made integrated assessments more feasible goals.

2. OBJECTIVE

The ultimate goal of this study is to develop Integrated Water Assessment Indicators and tools that support water-security related problem solving using a *Spatial Information Platform for Watershed Environmental Assessments* (Kawasaki *et al.*, 2005)(Figure 1; Figure 2). The study aims to achieve:

- Represent a wide range of water resource indicators in an integrated manner.
- Quantitatively represent hitherto concealed relationships such as the total balance of water supply and demand, and complicated links between upstream water resources and downstream water beneficiaries.
- Answer questions like "What is the problem?", "Where does it happen?", and "What kind of response is effective?" using a

panoramic view of the entire picture and making assessments of the comprehensive situation using integrated models and tools.

- Dynamically analyze the influences of nature, human activity and social systems.
- Propose various scenarios in order to investigate how to deliver the optimal (i.e. sustainable, fair and equal) combination of water management and water rights at each location for all involved.

In essence, this study will deliver detailed models and tools for in-depth spatial-temporal data via a *Spatial Information Platform for Watershed Environmental Assessments*. Final results like models and tools shall be made available on the Web to the general public in order to promote international versatility, and support collaboration among stakeholders on water security policy.

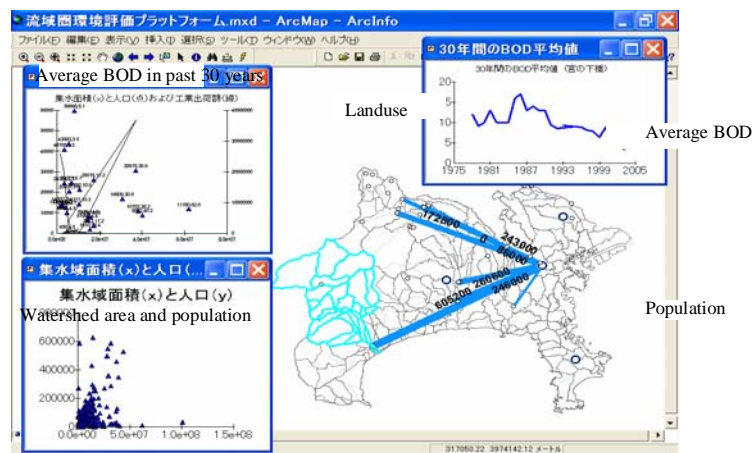


Figure 1: Analysis of water quality and socioeconomic statistics (Prototype of a Spatial Information Platform for Watershed Environmental Assessments)

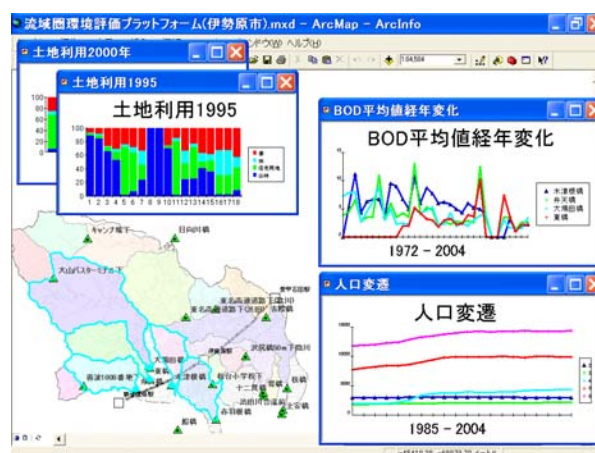


Figure 2: Time-series analysis among water quality, land use and population (Prototype of a Spatial Information Platform for Watershed Environmental Assessments)

3. OUTLINE

This study presents several Integrated Water Assessment Indicators to indicate sustainable water security for a variety of users (individuals, groups and organizations). Developing water resource indicators calls for a multidirectional and comprehensive approach, including not only factors directly related to water itself like water supply and demand, water quality and flow, access, and safety; but also indirect factors change like economic and social systems, education for water use, ethnic issues (e.g. awareness of water saving and knowledge about water discharge), disaster vulnerability, and ecosystem services (Figure 3).

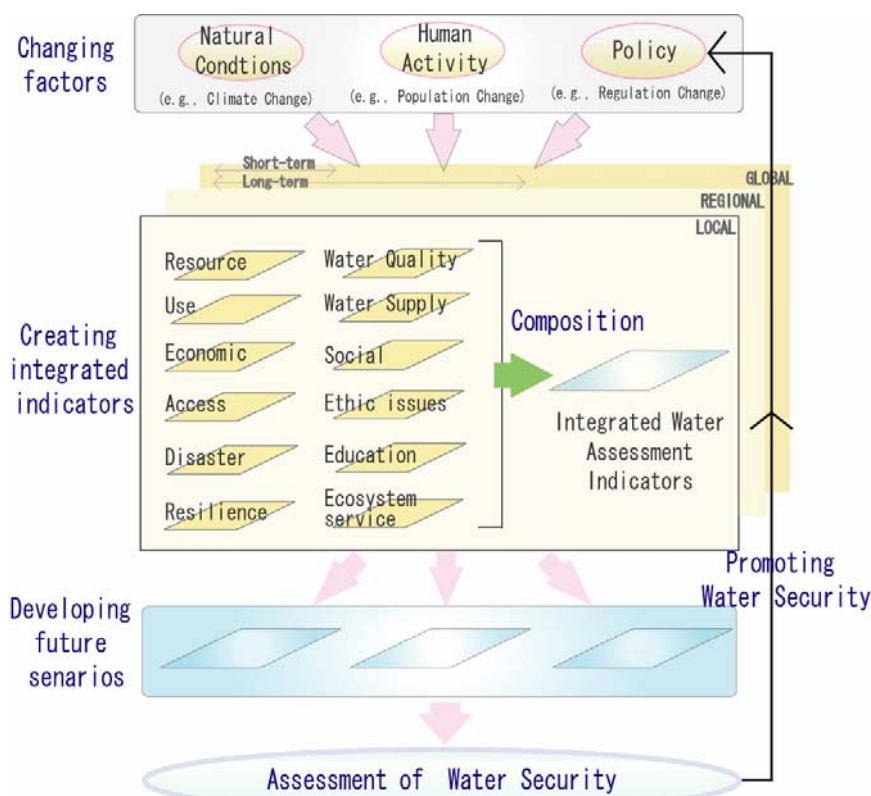


Figure 3: Flowchart for creating integrated model

4. SIGNIFICANCE

- Currently, no integrated indicators exist that properly capture the spatial distribution and temporal variability, because current assessments are implemented in terms of governmental boundaries and regional-limitations. Developing these Integrated Water Assessment Indicators allows answering the questions, "What is the problem?", "Where does it happen?", "What kind of response is effective?" in concrete locations at a human-scaled resolution (20m mesh) based on a detailed GIS database.
- Many institutes in member countries in the Forum for Globally-Integrated Environmental Assessment Modeling (GLEAM) hosted

by the United Nations University and RIVM (National Institute for Public Health and the Environment in the Netherlands) are developing Globally-Integrated Environmental Assessment Models for economic, ecological, and social sustainability. This research is significant because water resource management is still not implemented in the forum.

- Developing Integrated Water Assessment Indicators would facilitate quantitative analysis for decision making, and provide an environment for that allows stakeholders to use the models and tools on the web to support development of sustainable water security policy.

5. STUDY AREA

Mekong River basin was selected as the study area in this study. Mekong River rises in the Tibetan Plateau and empties into the South China Sea after travelling 4,000km and flows through six countries, China, Myanmar, Thailand, Lao PDR, Cambodia and Vietnam draining 800,000km². This is the largest international river in Asia. The building collaborative research and management system for “water security” are required in urgent.

Three basins in the middle lower Mekong River, Sekong, Seasan and Sre Pok river basins were selected as pilot area for intensive field survey, data collection, and conducting questionnaire (Figure 4).



Figure 4: Mekong River basin and pilot study area

6. METHODOLOGIES

6.1 Choosing and weighting indicators by literature review and interviews with authorities

Factors contributing to disputes caused by water resource security shall be clarified in the Mekong River, Nile River, rivers in southern Africa and domestic rivers in Japan. Secondly, data sources available for indicator evaluation shall be identified. Data from GIS sources, remote sensing, and social statistics would be used for assessing the status of natural environments and human activity. As for items that are difficult to quantify such as education, local awareness, regulations, and social systems, assessment methodologies and weighting shall be determined by questionnaires and interviews with authorities. Indicators that are common among all areas or unique to an area shall be determined by comparative review, since natural conditions, social systems, available databases, assessment indicators, and weighting schemes vary according to region.

6.2 Framework design and data collection through investigative surveys at foreign institutes

Theoretical frameworks, models and tools related to individual indicators shall be surveyed in order to examine various components of the integrated models and tools. A significant portion of this survey shall be conducted at a leading institute for water resource management in Australia.

6.3 Developing integrated water assessment indicators

Based on information gathered during data collection and through discussion with authorities, new models and tools shall be developed and then implemented as a series of system. The following points shall drive the development process:

- Variability of spatial resolution (functions shall adjust to differences in spatial resolution, so that 1 km resolution would be enough in mountain areas, but 5 m resolution is required in urbanized areas).
- Storing and analyzing functionality for time series data (e.g., Utilizing the time series functions of the Arc Hydro data model (Maidment, 2005; Kawasaki *et al.*, 2007))

6.4 Incorporate feedback into model and tool adjustment and revision

Models and tools shall be fine-tuned and grown based on feedback from discussions with policy makers, citizen groups, and authorities in water resources management. Finally, Integrated Water Assessment Indicators and tools that can be of practical use by various stakeholders shall be developed that single out the best forms of required data, indicators, assessment methods, and utility system.

7. DEVELOPING SPATIAL INFORMATION SHARING SYSTEM ON THE MEKONG BASIN RESEARCH NETWORK

As a first step of this research, prototype system of spatial information sharing system including GIS data, tools and models is developed on the portal web site of MekongBasinResearchNetwork (MekongNet) operated by United Nations University (Figure 5). The purpose of this site is not only enhancing research database in Mekong River basin, but also human research network in the area by providing models and tools which users can use easily such as flood simulation on the web, in addition to GIS database. Only partial database is opened to public at this moment since the GIS database created by other than United Nations University has limitation or copy right for web publishing (Figure 6). ESRI ArcIMS was used to serve GIS data on the Web. Basic data was integrated into Geodatabase format (Zeiler, 1999) and Arc Hydro will be embedded for further hydrological analysis in near future.

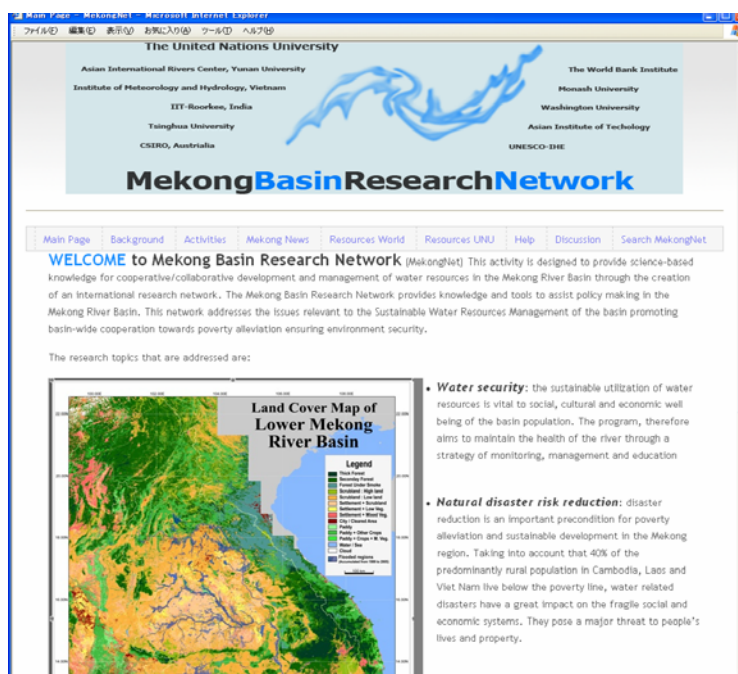


Figure 5: MekongBasinResearchNetwork (MekongNet)

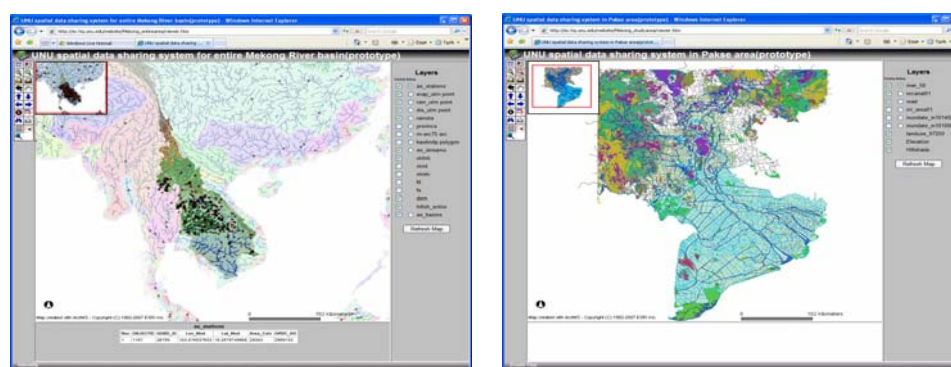


Figure 6: UNU spatial data sharing system for Mekong River basin (Prototype)

8. CONCLUSIONS

Concept, framework and methodologies of entire research were described in this paper, as well as the introduction of collaborative portal site of MekongNet and prototyped Web-based GIS data serving system. Promoting this research and improving water security in Mekong River basin require not only corporation among people among various entities across national, regional and local inside Mekong River basin, but also it's supporting system by researchers, policymakers and general public from countries of outside the region. In this research, developing a platform for improving water security in Mekong River basin was the first big target. To realize this big challenge, we are trying to prepare many places and opportunities to conduct discussion among stakeholders by overlaying various data as GIS layers and obtaining comments, advice, and corporations from various stakeholders.

ACKNOWLEDGEMENT

This study was supported financially by Research Fellowships of the Japan Society for the Promotion of Science for Young Scientists.

REFERENCES

- Maidment, D.R. (2002) *Arc Hydro: GIS for Water Resources*. Redlands, USA: ESRI Press.
- Millennium Ecosystem Assessment (2005) *Ecosystems and Human Well-being: Synthesis*. Washington DC: Island Press.
- Kawasaki, A., Sato, Y., Sadohara, S., 2005. *Creating an Integrated Water Geodatabase for Environmental Risk Management*, Proceedings of the Fourth Inter-national Symposium on New Technologies for Urban Safety of Mega Cities in Asia, Singapore, 489-498.
- Kawasaki, A., Yoshida, S. and Sadohara, S., 2007. *Outline of water resources GIS application, Arc hydro, and case studies in the United States*, Theory and Applications of GIS, determined for publication, Vol.15, no.1, 29-37.
- Zeiler, M (1999) *Modeling Our World: The ESRI Guide to Geodatabase Design*. California: ESRI Press.

APPLICATION OF REMOTE SENSING AND GIS TECHNIQUES IN WATER INDUCED DISASTER MANAGEMENT: A CASE STUDY OF BANGLADESH

MD. SHAHABUL ISLAM
(Local Government Engineering Department, Bangladesh)
shahabul1@yahoo.com

MD. MAFIZUR RAHMAN
(Bangladesh University Of Engineering & Technology, Bangladesh)
mafiz@agni.com

MD. AYNUL KABIR
(Flood Forecasting & Warning Centre, Bangladesh Water Development
Board, Bangladesh)
aynulce@yahoo.com

ABSTRACT

Flooded area, flood hazard as well as flood vulnerability in the district of Munshiganj in Bangladesh were assessed by using Remote sensing (RS) and Geographic Information System (GIS) techniques. Image data of the peak flood date from RADARSAT for the year 2004 and ASTER the image of October 2004 was analyzed for the extent of the flood area as well as the land cover of the locality. Combining them with population data a population distribution map was produced according to land use types. Conventional method of flood map by MIKE11 was also compared. Subsequently, the outcome was compared with flooded area mapped using satellite data in creating population that is at risk during a normal flood even Last of all potential flood shelters in case of severe and medium floods for mitigation measures for future planning were identified based on information such as existing schools, administrative headquarters location, topography and accessibility. For Digital Elevation Model (DEM), SRTM 2000 image was used. A landuse planning was also suggested in the study area depending on the field verification by community participation as well as GIS Techniques.

Key Words: Disaster, Flood Hazard, GIS, RS, RADARSAT, ASTER, SRTM, DEM, MIKE11.

1. INTRODUCTION

Bangladesh is known as the 'land of rivers' and the major rivers are the Ganges, the Brahmaputra and the Meghna with a complex network of 230 rivers including 57 internationally trans-boundary (cross boundary) rivers. The Ganges (Padma), the Brahmaputra (Jamuna) and the Meghna are the

large rivers systems in the world covering a combined total catchments area of about 1.6 million sq km extending over Bhutan, China, India and Nepal of which only 7% falls in Bangladesh (FFWC, 2001). Munshiganj district is situated on the mixed floodplains of rivers the Ganges, the Brahmaputra, and the Meghna. Every year even during normal rainy season floodwater drains through bordering rivers of the area to the Bay of Bengal. Most of the severe floods affect the area and cause maximum damages to the lives and properties in comparison to other areas. On the other hand, the area is densely populated and the population is rapidly increasing raising the number of people at risk. The geographical position and topographic composition have made Bangladesh vulnerable to natural disasters. Bangladesh is frequently hit by natural disasters, most of them related to water, like flood, drought, riverbank erosion and cyclone associated storm surge etc. Each of these has impact on the livelihood of those affected with different severity. Especially floods cause immense loss to lives and properties almost every year. In flood management, Bangladesh has adopted many structural and non-structural measures. One of the main non-structural measures is the flood forecasting and warning system, which is in the process of continuous advancement. Planning for flood/erosion management and mitigation is very important for disaster prone Bangladesh. Remote Sensing and Geographical Information System can play a vital role to timely and low-cost information on floods and land use status and become a good tool for disaster monitoring and sustainable management of resources.

Flood is the most devastating natural phenomenon that affects and disrupts the well being of a society, especially poor people who are vulnerable to disaster due to limitation of their resources. Most of the natural disasters in Asia are related to flood and causing maximum damage to lives and properties in comparison to other disasters. Bangladesh probably is the most affected country by natural catastrophes, especially the flood.

Bangladesh experienced an unprecedented flood during July-August 2004. About one third of the country was flooded and about 30 million of rural and urban people were directly affected. Millions were displaced from their homes and lost their earning opportunities. Official number of death was about 500 but this rose to very high level due to post flood calamities. Road, railway and other infrastructures were destroyed.

2. OBJECTIVE

- (i) To develop methodology for detecting flood hazard and flood vulnerability of Bangladesh.
- (ii) To identify appropriate locations for flood shelters.
- (iii) Land use planning specially for agriculture and fish culture.
- (iv) Prepare community based flood mitigation measures and evacuation plan.

3. DATA & SOFTWARE USED

- (i) RADARSAT 23 July'04; ASTER 20 Oct'04.
- (ii) JERS SAR (Lband) Jun.'96.
- (iii) Landsat TM 17Feb.'02, SRTM 2000.
- (iv) Mike11(1- D model) flood Map for the year 2004.
- (v) Different GIS data layers.
- (vi) Road database, Population, Hydro-meteorological data.
- (vii) ENVI 4.2; Arc View GIS 3.2, Arc GIS 9.0, Mike 11

4. STUDY AREA

Munshiganj district is south to the capital city Dhaka and lies approximately between 23°22' to 23°40' N latitudes and 90°10' to 90°43' E longitudes. The area of the district is approximately 955 sq km and is bounded by the Padma in the south, the Meghna in the east and Buriganga and Dhaleswari in the north. The population of the study area is 1,289,100 according to the population census of 2001 (BBS, 2003). The main physiographic units of the area include the floodplains of the Padma, the Jamuna, the Meghna and the Old Brahmaputra rivers. The agro-ecological regions include Brahmaputra flood plain, Meghna floodplain, active Ganges floodplain, Arial beel, old and new Brahmaputra floodplain, active Brahmaputra floodplain, and Jamuna floodplain. Ground elevation ranges approximately from 8m above the sea level in the north to 2m in the south.

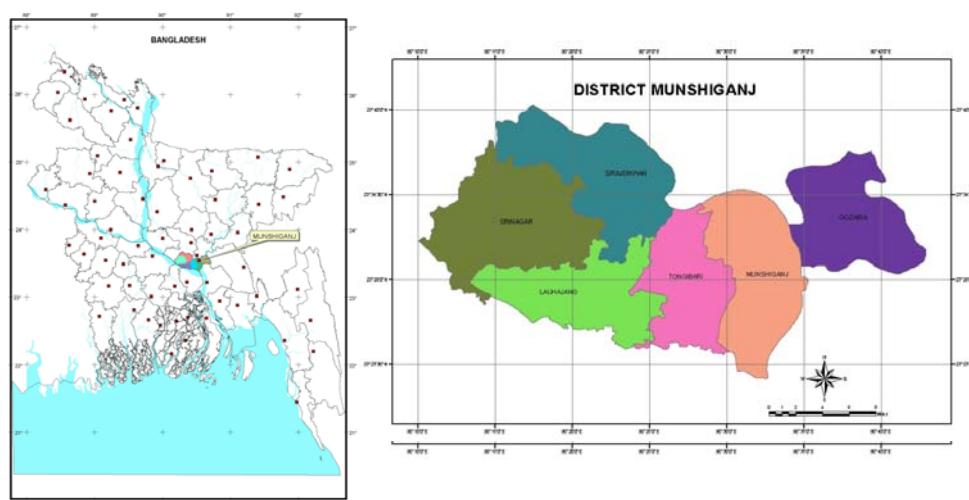
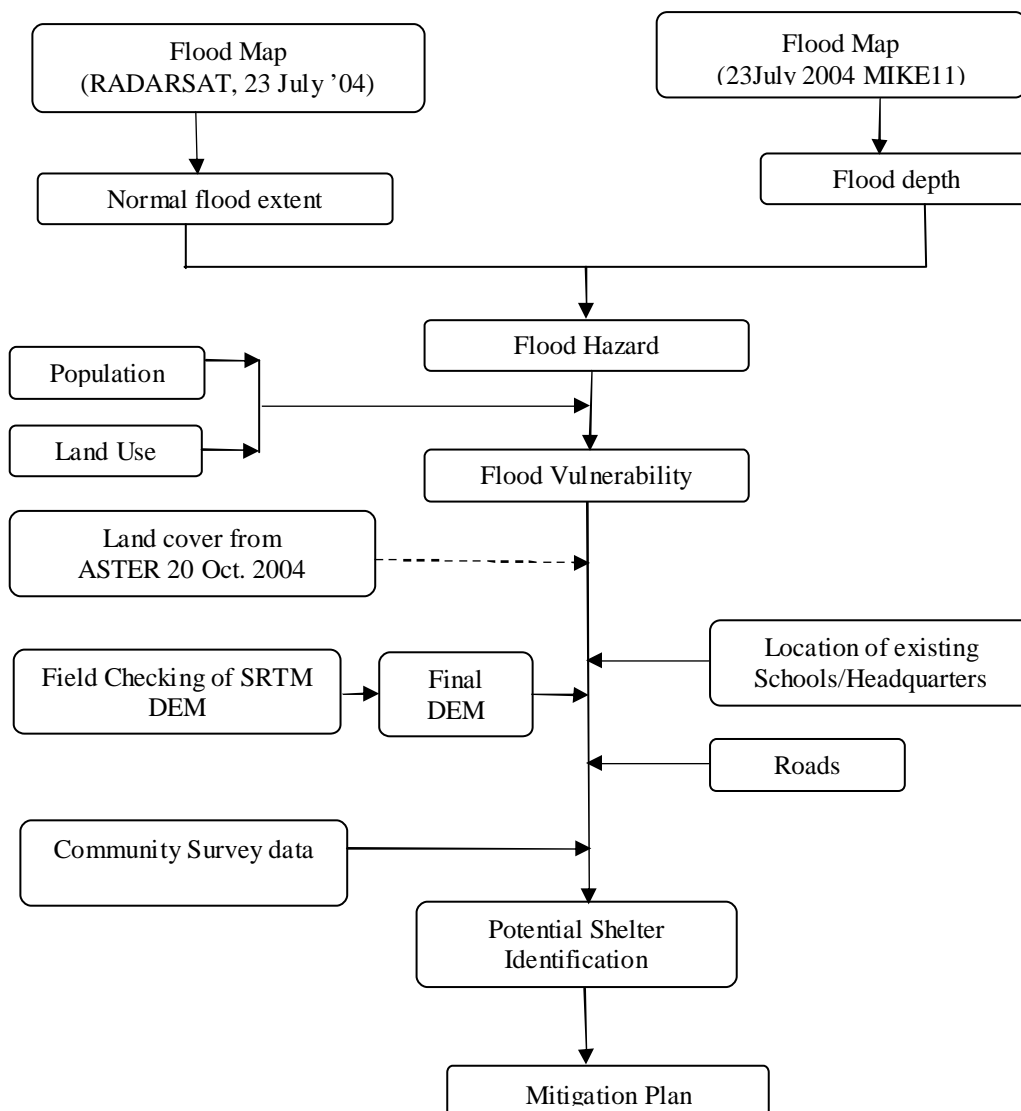


Figure 1: Location of the study Area

5. METHODOLOGY

The detail methodology is shown in flow chart below:



5.1 Flood Hazard Map

Flood extent was generated from RADARSAT 23 July 2004 along with ADEOS AVNIR and JERS SAR. Simple threshold classification technique and visual interpretation were used in interpreting both optical and SAR images. SAR images flooded interpretation was found the difficult in some locations, scattering from flooded areas was comparatively low when compared to other areas. These areas were found to have summer rice with floodwater and the brighter area was hyacinth on the floodwater therefore optical images and field verification had been used clarify flooded and non-flooded areas where there was ambiguity in interpreting satellite data. Also, the optical images helped in identifying water features that are not affected due to rainfall. The flood extent map was converted to grid then combined with flood depth data generated from Mike 11 model for the same date of RADASAT. This map was classified into 5 classes, non-flood area, low flood,

moderate flood, high flood and very high flood. The detail of classification and scoring are shown in Table 1.

5.2 Land use map

The vector data layers of landuse and landcover of the study area were generated from aerial photographs taken during 1999-2000. The land cover and the land use of the study area were found to be very heterogeneous. Therefore, visual interpretation was done using a screen digitization

5.3 Population by Landuse Map

Upazila and union based population census data of Bangladesh Bureau of Statistics (BBS) for the year 2001 was used for the study. Ratio of the population for urban and rural areas for each upazila as calculated (1:6.72 for weightage). Approximated population by each land use group by each union of that Upazila was finally calculated, then classified into 4 classes; Low population, Moderate population, High population and Very high population. The details of classification and scoring are shown in Table#1.

Table 1: Scoring Rules for flood hazard classes

Maps	Classes	Interpretation	Score
1. Flood dept (m)	• Non flood	No flood	0
	• Flood dept ≤ 1m	Low hazard	1
	• Flood dept >1-2m	Moderate hazard	2
	• Flood depth >2-3m	High hazard	3
	• Flood depth > 3m	Very high hazard	4
2. Population (Number)	• Population ≤10,000 persons	Low population	1
	• Population >10,000-16,000	Moderate population	2
	• Population >16,000-20,000	High population	3
	• Population >20,000	Very high population	4

DEM: The elevation used in Mike11 was in 300 m grid cells. This data was regrouped into 3 levels; Low elevation (<3 m), Moderate (3-5 m) and High (> 5 m). Further, this map was used to identify suitable shelter locations.

5.4 Flood Vulnerability:

Flood vulnerability map was generated from population affected in flood hazard area by combining flood hazard map and population by landuse map. The detail of classification and scoring are shown in Table#2 and the reclassified flood vulnerability levels are given in Table#3.

Table2: Score matrix of Flood Hazard

Flood Hazard (Depth) \ Population	Low (1)	Moderate (2)	High (3)	Very high (4)
Low (1)	2	3	4	5
Moderate (2)	3	4	5	6
High (3)	4	5	6	7
Very high (4)	5	6	7	8

Table3: Ranking Score of Flood Vulnerability

Ranking Score	Flood Vulnerability
2-3	Low Vulnerability
4-5	Moderate Vulnerability
6-8	High Vulnerability

5.5 Identification of Potential Shelter Locations

One of the main objectives of the study to locate school or other existing structures to be used as potential shelter during severe floods. It was assumed that a shelter should be an existing school or a hospital or a government office. Then, they should be located in non-flood area, in high land area and within road accessibility. In order to execute these criteria, DEM, Roads with 500 meters buffer were used. Based on above data, schools, hospitals, upazila and union head quarters were identified. These identified facilities area not in flood zone and with reasonable distance to roads are considered as suitable location as shelters.

5.6 Mitigation Planning

Proposed suitable shelters and landuse planning were one of the objectives of the study. Flood vulnerability map was overlaid with landuse map to examine the present landuse activities and possibility of identifying landuse practices.

6. FIELD VERIFICATION AND COMMUNITY SURVEYING

The objectives of the field visit/survey were to: i)verify classified land use in the study area, ii) verification of historical flood conditions through direct dialog with the people of the locality.

6.1 Investigation of Historical Flood Conditions

Knowledge on historical flood scenarios, social-economical status, sufferings due to the floods etc. was collected through discussions with local communities. Information related to dissemination of flood forecasts, the needs and benefits of the forecasts and the format of warning message required by the local communities.

6.2 Interpretation of ASTER Image

ASTER image was analyzed to identify the landuse patterns. Landuse was classified as four different types such as agriculture, built-up

area, settlement and water. The river was found to be nearer to the Lauhajang Upazila headquarters than it was delineated during the analysis, because of the recent river erosion at the study. The agricultural area was found mainly covered by potato crops. Water hyacinths were found spread over the floodwater, making it difficult to interpret ASTER image for generation of flood data layer. Thus, digital classification only does not give accurate flood extent. Flood depth is an essential part of flood hazard analysis and Mike 11 software was used to prepare flood depth map for the study area.

7. RESULTS AND DISCUSSIONS

(i) Flood Vulnerability in Landuse:

From the study it shows that about 2.61% of the total area of the district falls under high vulnerability, 45.31% under medium vulnerability, 13.96 % under low vulnerability & the rest 38.12% under no vulnerability.

(ii) Landuse in Different Flood Vulnerability:

- From the study it shows that about 2.45% of the total study area covers a landuse of agriculture, 0.12% of the total area covers a landuse of settlement, 0.04% covers a landuse of water and almost no area of urban landuse is in the high vulnerable area.
- From the study it shows that about 35.57% of the total area covers a landuse of agriculture, 1.59% of the total area covers a landuse of settlement, 7.96% area covers a landuse of water and 0.05% area of urban landuse is in the medium vulnerable area.
- From the study it also shows that about 6.69% of the total area covers a landuse of agriculture, 0.50% of the total area covers a landuse of settlement, 6.64% covers a landuse of water and 0.01% area of urban landuse is in the low vulnerable area.

From the study it also shows that about 26.04% of the total area covers a landuse of agriculture, 7.53% of the total area covers a landuse of settlement, 3.83% covers a landuse of water and 0.65% area of urban landuse is in the low vulnerable area.

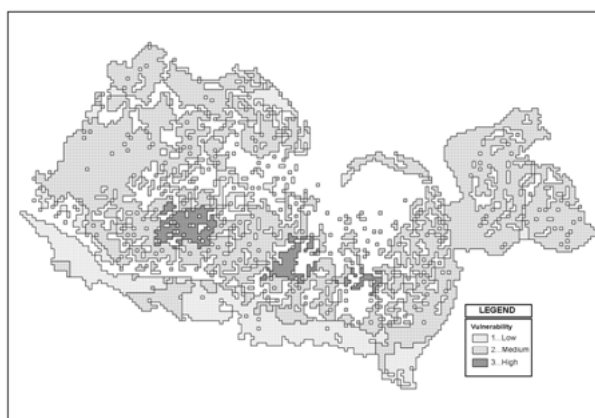


Figure 4: Flood Vulnerability at Different Scale

(iii) Shelters in the Study Area:

From the analysis it shows that 42 number of schools out of a total 1090, 2 administrative headquarters out of a total 77, 4 Growth centers out of a total of 23 of the study area can be used as shelters in case of high flood vulnerable within the district.

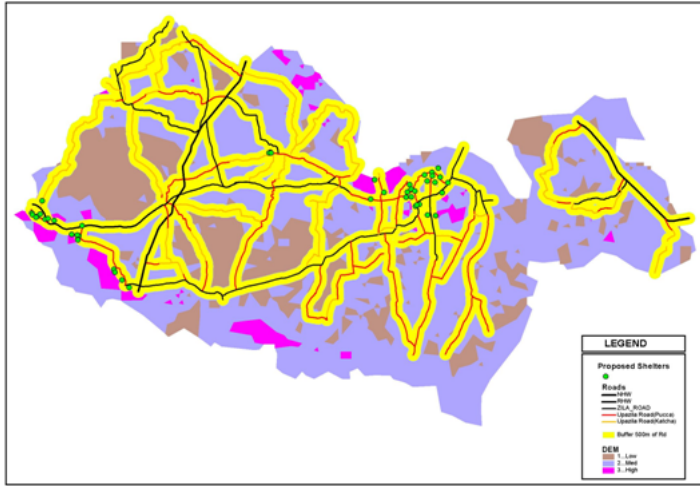


Figure 5: Location of Shelters within the study area

Table4: Number of Potential Shelters within the District

Upazila_Name	No. of Schools	Non-Flooded	Flooded	No. of Schools as Shelter	No. of Head Quarters	Non-Flooded	Flooded	No. of HQs as Shelter
Laluhajang	134	67	67	4	13	8	5	0
Munshiganj Sadar	196	142	54	18	12	8	4	1
Gazaria	143	45	98	0	9	5	4	0
Tongibari	152	92	60	2	13	10	3	0
Srinagar	264	178	86	16	15	12	3	0
Sirajdikhan	201	111	90	2	15	14	1	1
Total:	1090	635	455	42	77	57	20	2

8. CONCLUSIONS AND RECOMMENDATIONS

The study clearly narrates that remote sensing and GIS can effectively be used for flood area monitoring and identification of suitable potential shelters during the high vulnerable floods. It is also found that RADARSAT data in combination of Mike11 flood map can be used for flood area mapping with mitigative measures identification. This study is therefore suggested that an operational flood mapping system based on remote sensing and GIS techniques is very much needed in the country. This system can be used for flood mapping, shelter location as mitigative measures as well as for the damage assessment at the time of emergency.

Therefore the study will be useful to:

- (i) Develop flood area mapping in respect of different vulnerability and land use.

- (ii) Develop better capabilities to detect and monitor the environmental changes caused by flood like streamline changes, riverbank erosion, etc.
- (iii) Identify suitable flood shelters in case of severe as well as medium floods for mitigation measures for future planning.
- (iv) Develop land use planning for agriculture as well as fish farming in the locality.
- (v) If a very high resolution image is available it will be very useful for flood analysis in Bangladesh flood plain area

ACKNOWLEDGEMENT

The authors are grateful to Japan Aerospace Exploration Agency (JAXA) for sponsoring the satellite data used in the study, Local Government Engineering Department (LGED) of Bangladesh for the spatial local GIS data and Water Development Board of Bangladesh for the Flood Model data.

REFERENCES

- Bangladesh Population Census 2001, National Report (Provisional, 2003) —Bangladesh Bureau of Statistics, Planning Division, Ministry of Planning-p17, 30.
- Flood Forecasting and Warning Centre (FFWC), 2003, Annual Flood Report-2001, Bangladesh Water Development Board (BWDB), WAPDA Building (8th Floor), Dhaka, Bangladesh, 46pp.
- Flood Forecasting and Warning Centre (FFWC), 2006, Annual Flood Report- 2006, Bangladesh Water Development Board (BWDB).
- Howlader A. H. and Islam, A.Z.M.Z, 2004, Application of Remote sensing and GIS in Flood Mapping in Bangladesh, paper presented in the National Workshop on Options for Flood Risk and Damage Reduction in Bangladesh, held on 30th August 2004, Bangladesh-china Friendship Conference Center, Dhaka, Bangladesh, 9pp.
- Lal Samarakoon, Kulapamote Pathumchai and Ryuzo Yokoyama, 2004, Land Use Planning for Flood Mitigation in Dhaka City Using Remote Sensing and GIS, Earth Observation Research Center/Japan Aerospace Exploration Agency (JAXA) and Asian Center for Research on Remote Sensing, Asian Institute of Technology(AIT), ISTS-2004-n-22, p1-5.
- Local Government Engineering Department (LGED), 2005, Road Inventory, Rural Infrastructure Maintenance Management Unit, LGED.
- Local Government Engineering Department (LGED), Upazila Base Map, Geographic Information System (GIS) Unit, LGED
- Nishat A., 1998, Flood Management in Bangladesh, paper presented in the 7th Regional Seminar on Earth Observation for Tropical Ecosystem Management, held in Dhaka from 7-11 December 1998, 6p.
- N. H. Akhter Hossain, 2004, An Overview on Impacts of Flood in Bangladesh and Options for Mitigation, in Proc. of National

Workshop on "Options for Flood Risk and Damage Reduction in Bangladesh", 7-9 September 2004, Bangladesh-China Friendship Conference Center, Sher-e-Bangla Nagar, Dhaka, Bangladesh, p1-22.

RADARSAT International Inc., 1996, Focus on RADARSAT, a 3-days workshop introducing concept, operation for natural resources analysis and environmental monitoring, held at Local Government and Engineering Department (LGED) Head Quarters, Dhaka, from 10-12 December, 1996, organized by LGED/GETCO, and sponsored by RADARSAT International Inc

CLIMATIC PERTURBATION AND FLOOD RISK IN COASTAL CITIES: A COMPARATIVE STUDY IN SOUTH AND SOUTH EAST ASIA

DUSHMANTA DUTTA
School of Applied Sciences and Engineering
Monash University, Australia
Dushmanta.dutta@sci.monash.edu.au

ABSTRACT

Approximately 20% of the global population lives within 30 km of coastal areas and the number is expected to become double by 2025. The Intergovernmental Panel on Climate Change (IPCC) has predicted that the global mean sea level (msl) may rise as much as 88 cm by the end of the 21st century. The sea level rise will have wide ranging effects on coastal population and ecosystem, such as saline water intrusion, erosion of shorelines, amplified intensity and frequency of coastal flood inundation, etc.

This study was an attempt to assess socio-economic impacts of flooding under climate change conditions in low-lying large coastal cities in South and South-east Asia, intending to raise awareness on the vulnerability of developing coastal cities under climate variability and socio-economic changes towards betterment of future flood management measures. Several large coastal cities were selected for analysis based on the socio-economic vulnerability, frequency and duration of flooding, tidal effects on flooding, and also on the availability of data. A comprehensive methodology was developed and implemented to conduct pilot case studies in six selected regions of six countries in South and South-east Asia. The paper presents briefly introduces the methodology developed and the outcomes of case studies and compares the magnitudes of socio-economic vulnerability of the selected coastal cities to extreme floods under rising sea levels.

1. INTRODUCTION

The increased concentrations of greenhouse gases in the atmosphere threaten to dramatically change the earth's climate in the 21st Century. The Intergovernmental Panel on Climate Change (IPCC) projects that warming in this century could range from 1.4 to 5.8°C (IPCC, 2001). Accompanying the warming will be substantial increases in sea level and average precipitation and also changes in climate. Global sea level is currently rising as a result of ocean thermal expansion and glacier melt, both caused by recent increases in global mean temperature (Nicholls, 2002; Burroughs, 2003). With the climate already changing and further change in climate highly likely to happen, adaptation is a necessary component of any response to climate change. Many countries and specific sectors within these countries

are vulnerable to the effects of climate change (van Dam, 2003). The IPCC concluded that developing countries are much more vulnerable to climate change.

Some of this vulnerability has to do with greater exposure to climate change, e.g., having large populations in low lying coastal areas exposed to sea level rise. The coastal zone of Asia is densely populated and expected to be home to nearly 75% of the population of the region by 2025. Many of the large coastal cities in Asia have already been facing severe problems due to lower elevation and their location in floodplain of major rivers. Potentially, sea level rise will have the greatest impacts in these large coastal cities. Yet, very few countries have planned the ways to deal with these problems.

This study was conducted under a collaborative research project aimed to model the changes in flooding characteristics in several coastal cities in South and Southeast Asia under climate change and to assess its socio-economic impacts including vulnerability for offering a basis for formulating policies for sustainable development. The main objective of the study was to assess the socio-economic impacts of floods under climate change conditions. The study scope was limited to selected low-lying large cities of six countries of South and South-east Asia namely; Bangladesh, India, Pakistan, Sri Lanka, Thailand and Vietnam.

2. STUDY AREAS

The selection of the coastal cities for case studies was based on the socio-economic vulnerability, frequency and duration of flooding, tidal effects on flooding, and also on the availability of data. Based on these criteria, the cities identified in the six countries were: Barisal and Patukhali (B-P) in Maghna Delta (Bangladesh), Bhubaneswar, Cuttack and Puri (B-C-P) in Lower basin (India), Karachi (Pakistan), Matara (Sri Lanka), Bangkok (Thailand), Hai Phong city (Vietnam) (Figure 1). The main factors considered in the case studies of the coastal cities due to sea level rising in different periods of scenario analyses for comparative analysis were: magnitude of flood hazards, social vulnerability and risk in different sectors, economic vulnerability and risk in different sectors and stakeholder awareness and existing policy status. The details of these study areas including hydrometeorological and socio-economic characteristics have been presented in elsewhere ((Habib-ur-Rehman *et al.*, 2006 ; Dutta *et al.*, 2005a; Dutta *et al.*, 2005b ; Dutta *et al.*, 2005c ; Bhuiyan *et al.*, 2005 ; Swamy *et al.*, 2005 ; Ratnayake *et al.*, 2005).

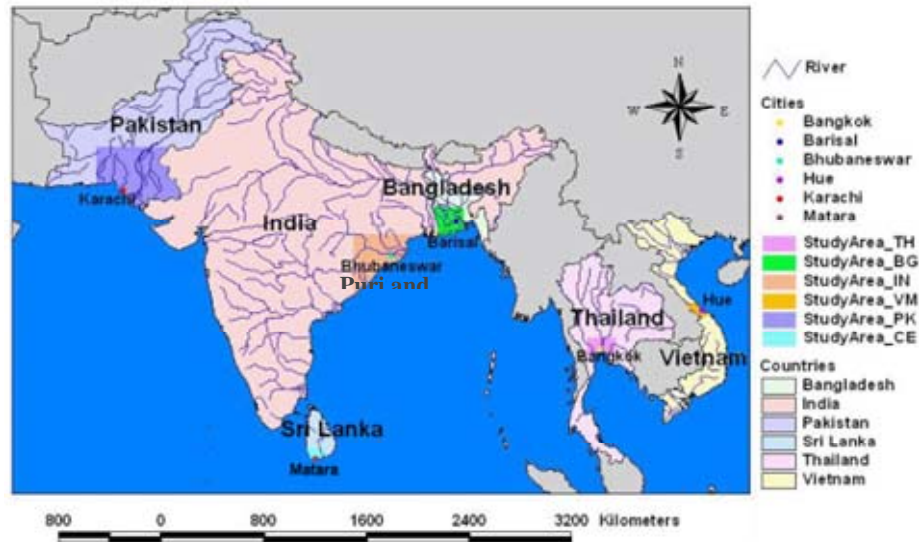


Figure 1: Location map of the study areas in six countries

3. METHODOLOGY

A comprehensive framework was developed to analyze the socio-economic impacts of floods in several large coastal cities of Asia under projected climatic and socio-economic scenarios as shown in Figure 2. The framework includes a more realistic and complex system of modeling that allows incorporating anthropogenic changes together with projected climatic changes while modeling flooding. The modeling system comprises of three components: a distributed flood model, a land use change model and an impact analysis tool.

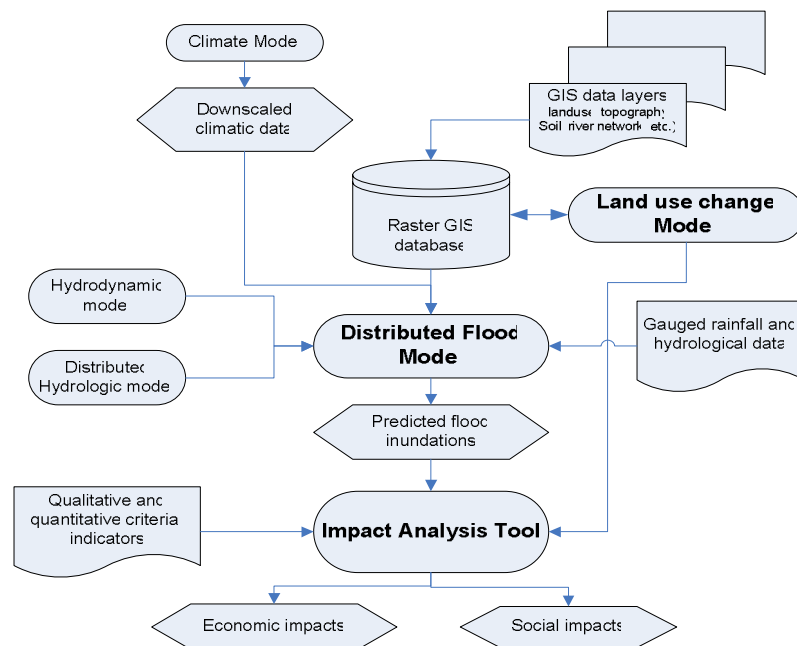


Figure 2: Comprehensive research framework

Distributed Flood Model

The distributed flood model includes two sets of models: i) a distributed hydrological model for simulating flood inundation in areas with a converging river network and ii) a hydrodynamic modeling scheme for simulating floods in areas with complex river networks with loops and diverging branches. Both the models are raster based with coupled two dimensional surface and one dimensional river network modules. The models included the provisions of incorporating various landuse and landcover and flood control infrastructure information at grid-scale. The detailed descriptions of these two models have been presented in Dutta *et al.* (2000) and Dutta *et al.* (2007), respectively.

Land use change Model

Socio-economic projections under land use change conditions are computed using the Anthropogenically Engineered Transformations of Land Use and Land Cover (AGENT-LUC) Model, developed by Rajan and Shibasaki (2000). This is a national scale, integrated, dynamic time-series simulation model for assessing the land use and land cover changes as result of the human activities. It consists of four modules: the biophysical crop yield module, the rural income module, the urban land use module and the agent decision module; and a sub-model for migration. All these modules and the sub-model interact and have feedback loops, to determine the new course of action by the agent at the next time step. The model structure is sequential. The biophysical crop yield model calculates the potential productivity of the land unit for the given conditions of soil, topography, water availability and climatic parameters. The distribution of water availability takes into account the soil conditions, amount of rain-received, and the existence of irrigation facilities. The main assumption of this model is that there is a strong linkage between the climate and crop distributions (Leemans and Solomon, 1993). The crop yield estimates are derived by modifying the approach as described in the EPIC model (Sharpley and Williams, 1990). The central concept of this approach is the growing period and the photosynthetic efficiency of the crops. The agent also acts as an interface in helping to assimilate the broader macro-information into the decision-making process at the grid level, thereby creating an action in response to the natural and economic stimuli.'

Impact Analysis Tool

An assessment of socio-economic impact is defined here as the measurement of the potential loss from a flood event by assessing the vulnerability of population, buildings and infrastructure to the flood hazard. It identifies the characteristics and potential consequences of flood, how much of the community could be affected by it, and the impact on community assets. The lack of an accepted method for carrying out assessments that could determine the socio-economic impact of floods has greatly limited the capacity to present a comprehensive picture in this study. Only the highly vulnerable socio-economic categories are considered in this study, which are population, buildings and transportation. Analysis is focused on present (year 2005) and future (2050 and 2100) scenarios. A questionnaire survey was conducted to develop a set of qualitative impact

indices for flood impact analysis for the selected categories. Secondary data relevant for socio-economic analysis were collected from respective departments and then colligated with model output for present scenario analysis. For future scenario analysis, an appropriate projection technique of socio-economic data was followed and then interpretation was derived in relation with model output. Population projection techniques followed were country specific and were detailed under country sub-sections. Due to unavailability of data, the analysis on building category was concentrated only on residential buildings in most of the case studies. In the case of study areas where data pertaining to residential buildings was not available, the count of residential buildings was extracted from population data with an approximation of four persons dwelling per residential building. Transportation category incorporated major road network laid within the study area boundary.

Current assessment relies on the total number of people and buildings, and the length of roads affected by floods due to sea level rise. The impact indices for different categories have been computed by conducting a questionnaire survey in six participating countries, Bangladesh, India, Pakistan, Sri Lanka, Thailand and Vietnam. The categories considered are: residential buildings, non-residential buildings, roads, persons less than 6 years, persons between 6 to 65 years, persons above 65 years, income less than 100 US\$, income level from US\$ 100 to 400 and income level above US\$ 400. Classification criteria are also based on different impact indices. Impact indices were prepared based on the percentage of damage. The details of the impact indices for different depth categories are given in Table 1.

Table 1: Impact indices for different damage category of floods

Percentage of damage	Impact index
0%	No impact
0-25%	Less impact
25-50%	Moderate impact
50-75%	High impact
75-100%	Highest impact

For the computation of impact on people, less than 25% damage indicates that there will be a minor health problem, if it is more than 25% but less than 50% then there will be major problem in health, less than 75% damage cause irretrievable illness. There will be a loss of life when the damage exceeds 75%. To compute the flood impact on buildings, less than 25% damage means less damage to contents, structure and outside property, then if it exceeds the range but below 50% which indicates medium damage, less than 75% damage means high damage. There will be a severe damage if the percentage of damage is more than 75%. For roads, less than 25% damage indicates that there will be a transportation interruption for few hours, if it is more than 25% but less than 50% then there will be a minor road damage, less than 75% damage cause minor road damage and transportation interruption for few days. Severe to complete collapse of

transportation system and need for rehabilitation of major road networks are needed when the damage exceeds 75%. Based on the depth and duration of floods and depending on the percentage of damage impact indices are prepared. A sample based on questionnaire survey results is presented in Table 2.

Table 2: Flood impact assessment for a particular category

Depth of flood (m)	Duration of flood				
	< 1 day	1-2 days	3-4 days	5-7 days	> 1 week
0.00-0.10	No Impact	No Impact	No Impact	No Impact	No Impact
0.10-0.60	Less	Less	Less	Less	Moderate
0.60-1.00	Less	Less	Moderate	Moderate	Moderate
1.00-3.50	Moderate	Moderate	High	High	High
> 3.50	High	High	High	High	High

4. ANALYSIS OF THE RESULTS

In this section, the results of the case studies are compared. Figure 3 shows the comparison of the population of the six areas in the study. Population trends show that the population increase rate will slow down with time. Population projections reveal that the population of the Bangkok will be doubled in 100 years time while the population in Mahanadi delta containing Bhuwaneswar, Cuttack and Puri (B-C-P) cities will be tripled by year 2100. Similarly, the population of Hue city will be increased by four folds in this century. The rate of population increase in Karachi and Matara is lower compared to other four study areas.

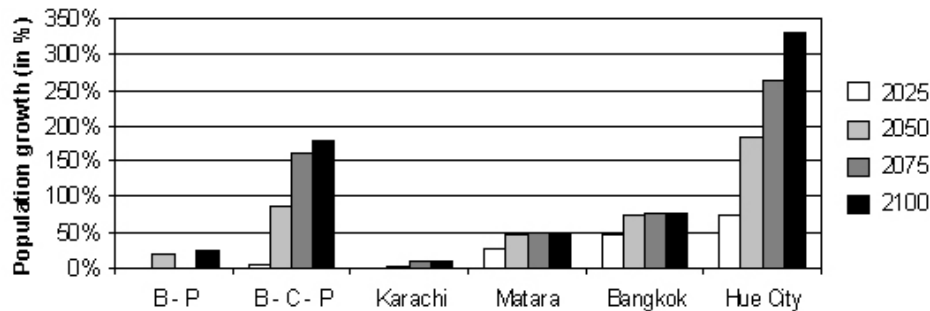


Figure 3: Projected population growth in the study areas compared to

Figure 4 shows the comparison of the projected number of buildings in six areas in the study. As no of buildings is directly related to population, the increase in the number of buildings also follow same trend as population. Prediction of the number of projected buildings reveals that the number of buildings in Bangkok city will be doubled in 100 years time while the in Mahanadi delta containing Bhuwaneswar, Cuttack and Puri cities, the number of buildings will be tripled by year 2100. Similarly, number of buildings in Hue city will be increase by four folds in this century. And, the rate of increase in number of buildings in Karachi and Matara city is lower compared to other four study areas.

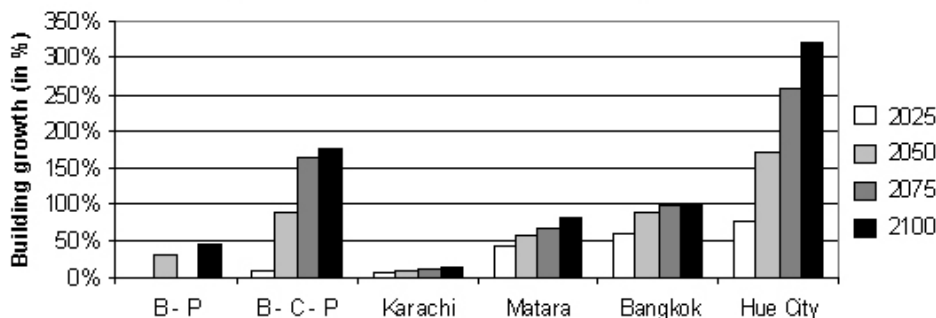


Figure 4: Projected building growth within the study areas compared to 2005

Figure 5 presents the projected impacts of the extreme flooding on population along with the future cases considering climate change impacts. In present condition, there is not much impact of flooding in Mahanadi delta area in India which includes Bhubaneswar -Cuttack - Puri cities. Similarly, people in Karachi (Pakistan) and Matara (Sri Lanka) are also not much affected by present flooding condition as more than 85% population is unaffected by flooding. Almost half population of Hue city is unaffected by present flooding scenario where as in Barisal - Patuakhali cities in Bangladesh, only 17% population is unaffected by flooding in the current scenario.

Figures 6 and 7 present the present effect of the flooding on number of buildings and on roads (highways) along with the future cases considering climate change impacts. In present condition, there is not much impact of flooding in Mahanadi delta area in India which includes Bhubaneswar-Cuttack-Puri cities on buildings. Similarly, buildings in Karachi (Pakistan) and Matara (Sri Lanka) are also not much affected by present flooding condition as more than 80% buildings are unaffected by flooding. Almost half of total houses in Hue city is unaffected by present flooding scenario where as in Barisal-Patuakhali cities in Bangladesh, only 17% houses are unaffected by flooding in the current scenario. In present extreme flood scenario, roads are not affected at all.

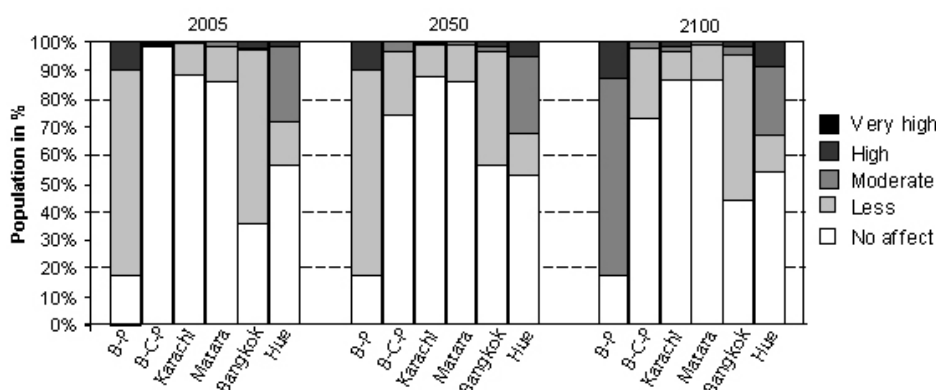


Figure 5: Impacts of floods on population within the study areas

In case of 2050 projected scenario, there is little impact of flooding on population in Karachi and Matara cities as almost 85% population will

remain unaffected due to projected flooding scenario of sea level rise. In case of Mahanadi delta area in India which includes Bhubaneswar-Cuttack-Puri cities, three fourth of projected population will remain unaffected. Almost half population will be affected in Bangkok and Hue city. Barisal - Patuakhali cities in Bangladesh will be highly affected by projected flooding scenario due to sea level rise but majority of impact falls in less affected index category. In case of buildings, the impact of projected flooding is less significant for the buildings in Karachi and Matara cities as almost 85% buildings will remain unaffected due to due to sea level rise. There is not big impact of flooding in Mahanadi delta area in India which includes Bhubaneswar-Cuttack-Puri cities as 75% buildings will remain unaffected. Almost half of total projected buildings will be affected in Hue city. In case of Barisal - Patuakhali cities in Bangladesh and Bangkok, the buildings in the cities will be highly affected by projected flooding scenario due to sea level rise but majority (75%) of impact falls in less affected index category. There will be significant impact on road in Mahanadi delta area in India which includes Bhubaneswar-Cuttack-Puri cities as almost 50% of the road will be affected by projected flooding scenario. In other cities, roads will remain almost unaffected.

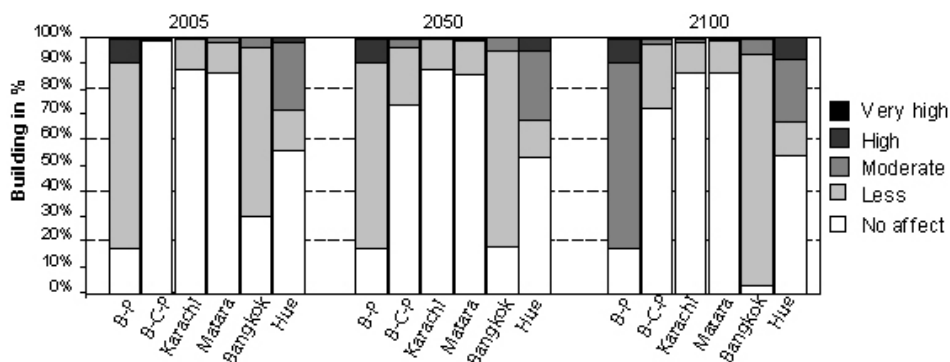


Figure 6: Impacts of floods on buildings in the study areas

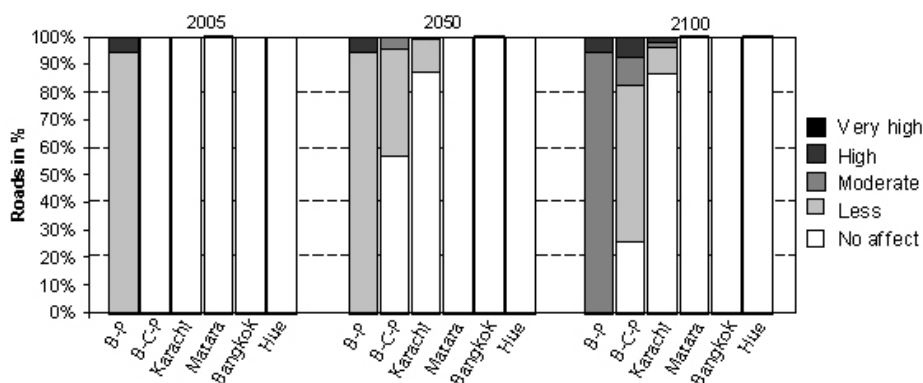


Figure 7: Impacts of floods on roads in the study areas

In case of 2100 projected scenario, there is little impact of flooding on population in Karachi and Matara cities as almost 87% population will remain unaffected due to projected flooding scenario of sea level rise. In case of Mahanadi delta area in India which includes Bhubaneswar-Cuttack - Puri cities, one fourth of projected population (about 27%) will be affected

due to sea level rise scenario. Almost half of total projected population will be affected in Bangkok and Hue city. Barisal-Patuakhali cities in Bangladesh will be highly affected by projected flooding scenario due to sea level rise and majority of impact (70%) falls in moderately affected index category. In case of buildings, the impact of projected flooding is less significant for the buildings in Karachi and Matara as almost 80% buildings will remain unaffected due to sea level rise. There is not big impact of flooding in Mahanadi delta area in India which includes Bhubaneswar - Cuttack-Puri cities as 72% buildings will remain unaffected. Almost half of total projected buildings will be affected due to flooding in Hue city. In case of Bangkok, the buildings in the cities will be highly affected by projected flooding scenario due to sea level rise but majority (90%) of impact falls in less affected index category. There will be significant impact on road in Mahanadi delta area in India which includes Bhubaneswar-Cuttack-Puri cities as almost 75% of the road will be affected by projected flooding scenario. In other cities, roads will remain almost unaffected except Karachi where there will be some impact of flooding as 25% of the roads will be affected by projected flooding scenario due to sea level rise.

Reviewing the existing policies of different countries, it has been observed that most of the countries have flood and disaster management policies but they don't touch the issue of climate change impact. For example, in case of Thailand, the existing basin management plan, flood management plan do not touch upon the issue of climate change impacts (Tawatchai, 2005). Similarly in case of India, the existing National Water Policy, National Disaster Management bill, disaster risk management program don't mention specifically mention about climate change impact issue (Sanyal, 2005). In Pakistan, policies like Water Policy, The Pakistan Water Sector Strategy, Sindh Katchi Abadis (unauthorized dwelling) Act exist but they incorporate the issue of climate change impacts. Similarly, in the National Disaster Management Plan, Flood Protection Ordinance, Coastal management policy, watershed management policy of Sri Lanka, the issue of climate change impact remains untouched in these policies (Kamaladasa, 2005). The story is not different in case of Vietnam. They have many policies related to flood management and disaster mitigation, but the issue of climate change impacts remains unmentioned in those policies. In case of Bangladesh, the issue of climate change impact has been touched upon in National Water Policy, which recognizes climate change induced flood as one of the factors determining future water supply and demand. Similarly, National Water Management Plan (NWMP) addresses the issues of coastal flooding due to sea level rise (Ali and Rahman, 2005; Islam, 2005).

5. CONCLUSIONS

From the comparative analysis it can be concluded that the coastal cities in Bangladesh is highly vulnerable to floods under climate change conditions as far as the high priority category, viz. population, is concerned. For the cities Bangkok and Hue, the extent of damage imposed by climate change is

considerable, albeit lower in comparison to cities of Bangladesh. Cities located in the Mahanadi delta of India are found to be more sensitive as far as the damage on road network is concerned. It has to be seen whether the existing policies in the respective countries are considering the climate change issue to the desired level of seriousness. The study found Bangladesh to be at the safer side as far as policy is concerned. However, the policy setup of other countries is lacking any vivid section pertaining to climate change issues, which may aggravate the future vulnerability situation, and need to be looked upon substantially.

The major recommendation developed out of this study is the need for a single organization or agency dealing with flood mitigation and which can simultaneously address climate change issues. The necessity for delineating flood mitigation and management policies from disaster management policy and the significance of incorporating climate change issues in the Coastal Development Authority Act is also recommended.

Further research should consider development of a holistic approach in assessing impact of extreme climate events (including sea level rise) to coastal systems including social, economic and environment aspects for adaptation strategies for integrated coastal zone management.

ACKNOWLEDGEMENT

The research was financially sponsored by the Asia Pacific Network for Global Change Research under its CAPaBLE Programme (Grant no. 2004-CB01NSY-Dutta).

REFERENCE

- Ali L. and M Rahman (2005). Flood protection measures and impacts of climate change in the coastal zone of Bangladesh, *Proceedings of the International Symposium on Floods in Coastal Cities under Climate Change Conditions*, AIT, Thailand, pp. 97-106.
- Bhuiyan, J.A.N, D. Dutta, A. Das Gupta and M.S. Babel (2005). Flood simulation and its socio-economic impact analysis in Meghna Delta, Bangladesh under climate change conditions, *Proceedings of the International Symposium on Floods in Coastal Cities under Climate Change Conditions*, AIT, Thailand, June, pp. 1-10.
- Burroughs (2003)(ed). *Climate into the 21st Century*, World Meteorological Organization, Cambridge University Press, 240p.
- Dutta, D., J. Alam, K. Umeda, M. Hayashi and S. Hironaka (2007). A two dimensional hydrodynamic model for flood inundation simulation: a case study in the Lower Mekong River basin, *Hydrological Processes*, 21:1223-1237
- Dutta, D., M.S. Babel and A. Das Gupta (2005a). *An Assessment of the Socio-Economic Impacts of Floods in Large Coastal Areas*, Final Report for APN CAPaBLE Project: 2004-CB01NSY-Dutta, Asian Institute of Technology, 205 pages.

- Dutta, D., S. Niu and K.S. Rajan (2005b). Modeling and socio-economic impact analysis of floods under sea level rising scenarios in Bangkok, Thailand, *Proceedings of the International Symposium on Floods in Coastal Cities under Climate Change Conditions*, AIT, Thailand, June, pp. 51-64.
- Dutta, D., J. Alam and H.M. Hien (2005c). Flood simulation and its socio-economic impact analysis under climate change condition in Hue City, Vietnam, *Proceedings of the International Symposium on Floods in Coastal Cities under Climate Change Conditions*, AIT, Thailand, June, pp. 85-96.
- Dutta, D., Herath, S. and Musiaka, K. (2000). Flood inundation simulation in a river basin using a physically based distributed hydrologic model. *Hydrological Processes* 14: 497-519.
- Habib-ur-Rehman, N.M. Khan, D. Dutta (2006). Assessment of extent of flooding under climate change condition in Coastal city of Pakistan. In: *Coastal Hydrology and Processes* (ed. by V. J. Singh & Y. J. Xu), 89-102. Water Resources Publications, LLC, CO, USA, ISBN #978-1-887201-46-9.
- IPCC. 2001. *Climate Change 2001: Impacts, Adaptation and Vulnerability*. Contribution of Working Group II to the Third Assessment Report of the Intergovernmental Panel on Climate Change (IPCC). Cambridge University Press, Cambridge, UK
- Islam RM (2005). ICZM program in Bangladesh: An overview of policy & strategy initiatives, *Proceedings of the International Symposium on Floods in Coastal Cities under Climate Change Conditions, AIT, Thailand*, pp. 107-114.
- Kamaladasa N. (2005). Flood risk management policies of Sri Lanka, *Proceedings of the International Symposium on Floods in Coastal Cities under Climate Change Conditions, AIT, Thailand*, pp. 131-136.
- Leemans R., and Solomon, A.M. (1993). Modeling the Potential Change in Yield and Distribution of the Earth's Crops under a Warmed Climate, *Climate Research*, Vol. 3.
- Nicholls, R.J. (2002). Analysis of global impacts of sea-level rise: a case study of flooding, *Physics and Chemistry of Earth*, 27: 1455-1466.
- Sharpley, A.N. and Williams, J.R. (1990). EPIC – Erosion/Productivity Impact Calculator: 1. Model Documentation, USDA Technical Bulletin No. 1768.
- Swamy, A.N., D. Dutta and S.M. Asokan (2005). Flood inundation modeling during severe cyclonic storms and socio-economic analyses for various climate change scenarios over Mahanadi Delta, India, *Proceedings of the International Symposium on Floods in Coastal Cities under Climate Change Conditions*, AIT, Thailand, June, pp. 11-18.
- Rajan, K.S. and Shibazaki, R. (2000). Land Use/Cover Change and Water Resources – Experiences from AGENT-LUC Model, *Proceedings of the APFRIEND Workshop on Mekong Basin Studies, INCEDE Report 19*, University of Tokyo, Japan, pp. 1-16.
- Ratnayake, U., D. Dutta and S. Niu (2005). Impacts of floods under sea level rising scenarios in Matara, Sri Lanka, *Proceedings of the*

International Symposium on Floods in Coastal Cities under Climate Change Conditions, AIT, Thailand, June, pp. 37-46.

Sanyal N. (2005). Flood risk management measures: Policies with special focus on coastal zone in India, *Proceedings of the International Symposium on Floods in Coastal Cities under Climate Change Conditions*, AIT, Thailand, pp. 115-120.

Tingsanchali T. (2005). Review and proposed improvement of flood disaster preparedness in Thailand, *Proceedings of the International Symposium on Floods in Coastal Cities under Climate Change Conditions*, AIT, Thailand, pp. 147-152.

Van Dam J.C. (2003) (ed). *Impacts of Climate Change and Climate Variability on Hydrological Regimes*, 1st edition, Cambridge University Press, 140p.

SPONTANEOUS URBANIZATION OF DHAKA CITY AND WATER LOGGING AS A CONSEQUENCE

UMMA TAMIMA

Lecturer, Department of Urban and Regional Planning,
BUET, Dhaka, Bangladesh.
umma_tamima@urp.buet.ac.bd

MD. SHOHEL REZA AMIN

Lecturer, Department of Urban and Regional Planning,
Jahangirnagar University, Savar, Dhaka, Bangladesh
shohelamin@gmail.com

ABSTRACT

The urban environment has distinctive biophysical features in relation to surrounding natural and rural areas. These include an altered energy exchange creating an urban heat island, and changes to hydrology such as increased surface runoff of rainwater. Such changes are, in part, a result of the altered surface cover of the urban area. For example an increase in surface sealing results in increased surface runoff. The peripheral growth, particularly to the east of the main built-up area of Dhaka City, involves a risk which many have come to accept, if not willingly, because of destruction of wetlands and natural canals. The unplanned change of land use and the encroachment of khals and lakes in the city cause a serious affect on the storm water drainage and wetlands in the Dhaka City. This paper focuses on the urbanization and drainage system of Dhaka City, finds out the impact of urbanization on the existing drainage channels and wetlands and proposes some recommendations for sustainable management of drainage system and wetlands of Dhaka City.

1. BACKGROUND OF THE STUDY

Dhaka City with its staggering population of about 12 million is recorded as one of the most populous cities in the world. The last decadal growth rate was about 45 percent, though the population growth rate was more than 100 percent in the previous decade (1981 to 1991). Population statistics of Dhaka City show that the annual growth rate was 2.9 percent from 1951 to 1961, 10.2 percent from 1961 to 1974, and 8.1 percent from 1974 to 1981 (Hasnat, 2006). Dealing with the huge population, the city seems to be disintegrated and incompetent. Even though the basic services are deteriorating to their lowest ebb, yet a substantial number of people are still out of service (Alam, 2006). The city is not only incapable of providing services but also expanding spontaneously by filling the adjacent low lands or wetlands due to the growth of the city population. Consequently the channels, wetlands and depressions, previously acted as drainage basin holding rainwater and drain it to the river system, is obstructed resulting in a

water congestion problem. A few hours of rain inundate many of the city streets and during floods the entire low-lying areas and even the major portion of Dhaka go under water for days. Though the Water Body Conservation Act 2000 is for the protection of wetlands, the application is negligible and this may lead to lose of hydrographic features of Dhaka City with progressive urbanization.

The objectives of the study are to discuss the existing status of urbanization and drainage system of Dhaka City, to find out the impact of urbanization on the existing drainage channels and wetlands and to propose some recommendations for sustainable management of drainage system and wetlands of Dhaka City.

2. URBANIZATION IN DHAKA CITY

The rate of expansion of Dhaka City in terms of area and population is the highest among all the urban centers in Bangladesh. The population of Dhaka City has increased about 10 fold and the area has expanded about 4 times because the city is the hub of all economic, administrative and other activities (Table 1 and 2). It is projected that in the next 25 years the urban population will increase to 60 percent and the rural population will decrease to 40 percent. In order to accommodate the increasing population of the city, low-lying areas, canals and lakes around and within the city are being filled to develop new settlements. Furthermore, as the western part of the city has been embanked to make it flood-free, many new settlements are already developed and under construction in the low lying areas. Therefore, long term and short term inundation in Dhaka City is a common phenomena now-a-days (Hossain *et al.*, 2006).

Table 1: Recent and projected expansion of Dhaka City

Area	1990			2010		2000 (interpolated)	
	Population	Build-up area km ²	Total area km ²	Population	Build-up area km ²	Population	Build-up area km ²
Greater Dhaka	4473000	122.1	275	8598000	215.3	6531000	168.7
Narayanganj	1111000	45.6	100	2558000	75.5	1834500	60.55
Tongi	143000	10.5	37	658000	21.3	400500	15.9
Savar	366000	41.8	243	812000	75.1	589000	58.45
Keraniganj	442000	22.3	170	813000	38.1	627500	30.2
Total	6535000	243.3	826	13430000	425.3	9982500	333.8

Source: JICA study, 1991

Table 2: Recent and projected expansion of Dhaka City

Area	1991			2006	2000 (interpolated)
	Population	Build-up area km ²	Total area km ²	Population	Population
Greater Dhaka	4228000	125.55	271.758	7350000	6106000
Narayanganj	1184000	54.374	224.366	2085000	1724600
Tongi	162000	14.967	32.255	400000	304800
Savar	329000	17.283	240.061	545000	458600
Keraniganj	569000	14.255	181.534	840000	731600
Total	6472000	226.429	949.974	11228000	9325600

Source: Dhaka Metropolitan Development Plan, 1995 - 2015

3. DRAINAGE SYSTEM OF DHAKA CITY

Greater Dhaka City area is divided into 12 drainage zones and has more than 40 khals in Greater Dhaka City under three major khal systems: Degun-Ibrahimpur-Kallyanpur khal system drains to Turag river; Dhanmondi-Paribag-Gulshan-Banani-Mahakhali-Begunbari khal system drains to Balu river; and Segunbagicha-Gerani-Dholai khal system drains to Balu and Buriganga rivers. The Dhaka West has 13 khals having a total length of more than 31 km while the Dhaka East has 27 khals of total length of about 60 km. Approximately 80% of rainwater of the city drained through these channels (JICA, 1991).

With rapid expansion of the city, the natural drainage system was interfered with and in some places destroyed. In the late sixties, a Master Plan on City Drainage and Flood Control was drawn up. Again in the early nineties, a Master Plan was formulated under the Flood Action Plan (FAP 8A). Since a long time elapsed between the preparation of the Plan and its implementation, the drainage scenario had changed quite significantly, given the various changes in the topography and land use and interventions. The natural channels and wetlands are being continuously filled up by new settlements. During the period 1990-2000, about 268 sq. km of wetlands in and around Dhaka City were filled up.

4. FUNCTIONS OF WETLANDS AND NATURAL CHANNELS IN DHAKA CITY

The wetlands are distributed in the Western (between Dhaka proper to Savar, Tongi and Gazipur) and the Eastern (urban fringe to the Shitalakha basin in the east) part of the city. However the proposed eastern embankment of the Dhaka City cut up eastern part into relatively shallow part (between it and the Dhaka proper), and a relatively deeper part (Balu-Sitalakhya basin on its east). These wetlands have important functions on the flood control, ground water recharge and have social and ecological values.

- Wetlands play a crucial role in mitigating floods via their natural 'sponge' function (Potter, 1994; Zedler, 2003, IUCN, 2006). In case

of excessive rainfall related flood discharges, wetlands function as natural sponges playing an important role in the detention and retention of water. They store (as a basin or depression) or delay floodwaters, e.g. by increasing resistance to water flow (hydraulic resistance) as a result of vegetation density and morphology or by absorbing water in soil (Baker and Eijk, 2006).

- Inhabitants of the city are using at least 1.3 billion liters of groundwater everyday supplied by Dhaka WASA. Only about 220 million liters of surface water supply has been added recently to the city's daily water supply (Khan *et al.*, 1998). Nevertheless, ever increasing coverage of ground by concrete due to urbanization, rivers, canals, ponds and low-lying areas are lessening. Motijheel, Paltan, Arambagh, Khilgaon are some of the worst affected areas of the city due to permanent fall of ground water table.
- Connection of low-lying areas with the Balu River allows inland water transport of goods and passengers. In addition, the remaining wetlands (e.g. Turag river floodplain along Tongi-Ashulia road) around Dhaka City can provide breathing spaces for the city dwellers.
- JICA (1991) in its feasibility study carried out an inventory of the ecological resources of Dhaka East, DND and Narayanganj West. The total number of identified floral species and fauna species is 112 and 177 respectively. The representative productive ecological elements are agricultural crops and aquaculture species. The open water bodies of potential aquaculture during the flood season become agricultural lands during dry season. Balu river floodplain of Dhaka east is the predominant spawning grounds of open water capture fishery. A total of 86 aquaculture species comprising 74 fish species, 10 fresh water prawn species and 2 crab species are identified along with exotic species.

5. CAUSES OF WATER LOGGING IN DHAKA CITY

Large run-off produced by monsoon shower and effect of urbanization, tidal nature of rivers and streams around the city, land depressions at certain urban neighborhoods and some drainage factors related to presence, upkeep and maintenance of system, altogether lead severe drainage congestion resulting inundation in various parts of basin areas (Bose, 2005).

The reliable experience in many countries has now led to some main principles in urban drainage management, which are (Tucci, n.d.):

- Flood control evaluation should be done in the whole basin and not only in specific flow sections;
- Urban drainage control scenarios should take into account future city developments;
- Flood control measures should not transfer the flood impact to downstream reaches, giving priority to source control measures;
- The impact caused by urban surface wash-off and others related to urban drainage water quality should be reduced;

- More emphasis should be given to non-structural measures for flood plain control such as flood zoning, insurance and real time flood forecasting.
- Management of the control starts with the implementation of Urban Drainage Master Plan in the municipality;
- Public participation in the urban drainage management should be increased;
- The development of the urban drainage should be based on the cost recovery investments.

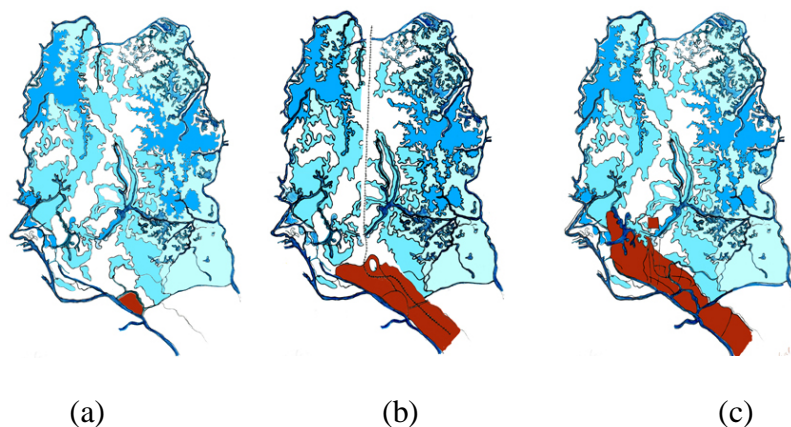
The urban drainage practices in Dhaka City do not fulfill these principles due to the following reasons:

5.1 Unplanned urbanization

The wetlands are filled up to meet up this excessive demand of land. The environment of Dhaka City is being continuously endangered and threatened by various unplanned and illegal activities of private and public bodies. Amongst the primary causes and sources of environmental degradation is the unplanned and unauthorized construction of building in and around the Dhaka city that often fails to consider and respect minimum environmental standard for the dwellers and the city itself.

Landsat TM/ETM satellite images of different time periods (1989, 1999, 2003) have been used to study the trend of loss of wetland in Dhaka. Fig. 1a, 1b, 1c, 1d, 1e and 1f show the spatial coverage of the wetland in the Dhaka City in different period of time. It can be easily understood the gradual shrinkage of wetland over the periods.

By applying graphical extension method, it can be forecasted that by the year 2037 all temporary wetlands of Dhaka will be disappeared if the current rate of loss of wetland continues. It is alarming to find that yearly rate of loss of wetland during 1999-2003 periods is 5.67 percent where as during 1989-1999 period; yearly rate of loss was 1.23 percent. Despite the enactment of the Water Body Conservation Act 2000, wetlands are disappearing everyday due to the ever-increasing housing projects (Map 2.a and 2.b).



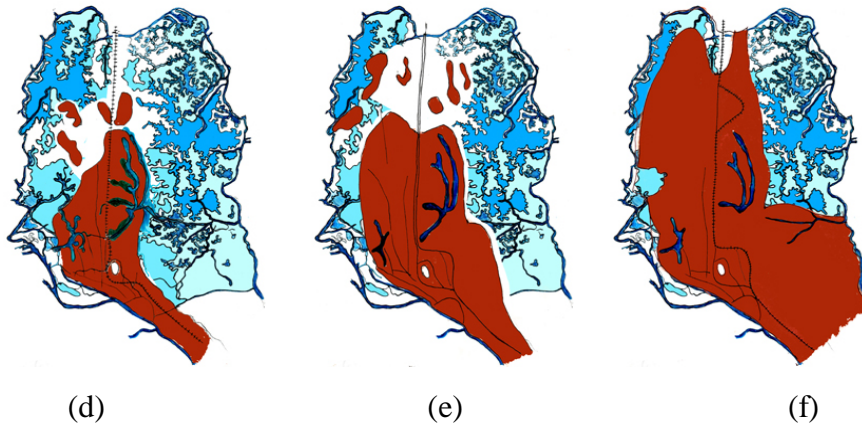


Figure 1: Dhaka in (a. Pre-Mughal period, b. British Colonial period, c. Mughal period, d. Pakistan period, e. 1980 and f. 2000 Dhaka)

Source: Hossain et al., 2006

Increase in impervious area reduces infiltration, which in turn causes increase in surface runoff generated by rainfall. As a result, capacity of existing storm drainage system becomes inadequate and overflow of drains occurs during rainy season. The link between impervious surface coverage and floods has been established since the late 1960s (Leopold, 1968; Seaburn, 1969). As the area of impervious surface coverage increases, there is a corresponding decrease in infiltration and an increase in surface runoff (Dunne and Leopold, 1978; Paul and Meyer, 2001). According to Arnold and Gibbons (1996), as the percent catchment (i.e. drainage basin) impervious surface cover increases to 10-20%, runoff increases twofold.

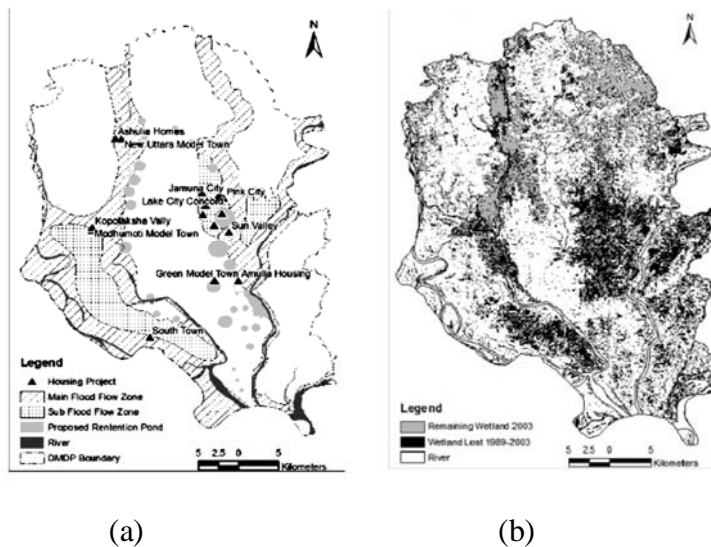


Figure 2: Loss of wetlands in DMDP area in 1968-2003 for housing development

Source: The Daily Star, 19th May 2006

5.2 Impact of Dhaka Metropolitan Development Plan (DMDP)

Vast tracts of wetlands at close proximity to the central city have been attracting private developers since the 1980s. Dhaka Metropolitan Development Plan (DMDP) has demarcated main and sub flood flow zones of Dhaka City and prohibited any kind of land filling activity on those areas. DMDP has also identified possible location for retention pond areas. After construction of the western half of the Dhaka Flood Protection Embankment, unplanned development stretched rapidly toward the low-lying areas violating all laws and regulations. Designated flood zones on the south and west of Dhaka are also experiencing a similar fate. As the government has planned to complete the construction of the eastern half of the flood protection embankment, private individuals and developers have purchased most of the low-lying lands that are expected to become flood protected. It should, however, be kept in mind that even after the completion of the Eastern Embankment, 12 percent of land should be kept as retention area for storm water storage (according to a study carried out by the JICA). It was evident from the catastrophic floods of 1988, 1998 and 2004, that the poor discharge capacities of the existing natural drainage channels are responsible for long duration of floods. City dwellers have already experienced the severity of rain-induced flood even during the late monsoon month of September in 2004. Sanitation in almost the entire city had collapsed at that time for poor drainage system. Low-lying lands around Dhaka in the past worked as natural retainers of storm water, and as natural drainage network and certainly helped to maintain balance of the ecosystem.

5.3 Causes of infrastructure development

Infrastructure development and overall change in the discharge regime of the fluvial systems along with land filling have created stress on these wetlands. The Uttara-Ashulia road aligned right across a wetland bound to affect the hydrodynamic conditions of water flow in that area. This is likely to result in higher flood level and longer stay (whatever small the period may be) of the floodwater in the wetland upstream of the road. The section of the Dhaka-Aricha road between Aminbazar and Boliarpur is probably making similar effects on the floodwater regime. The western embankment of the Dhaka City have already shell, the total area that used to be taken up by the floodwater. The major flood of 1988 inundated huge areas of western and central Dhaka including, Mirpur, Shyamoli, Kajipara, Sheorapara, Mohammadpur, etc. which is now inside the flood-protection embankment. This embankment has already reduced the space available for water of major floods by several tens of square kilometers. This must be having an increased pressure on the floodwater flow and thus on the length of the flood period. The proposed eastern embankment of the Dhaka City is also likely to have similar effect on the flood regime.

5.4 Encroachment of khals and lakes

Along with the rapid urbanization in the city in past years, many khals and lakes have been subject to encroachment. A number of khals already

have disappeared. A study by JICA (1987) observed that many portions of major drainage khals were occupied by encroachment without proper sanction, earth filling, deposition of city garbage, and buildings and roads (JICA, 1991). The city is experiencing severe problem of rainfall flooding for the last few years. This internal rainfall flood situation worsens when runoff generated from high intensity rainfall combines with high water level in the surrounding rivers. Moderate rainfall causes serious problems for some areas of the city such as Malibag, Mauchak, Shantinagar, Rajarbagh, Fakirapool, Purana Paltan, Motijheel, Green Road, and Mohammadpur etc.

5.5 Blockage of storm drains

Due to mismanagement of collection and disposal of solid waste in Dhaka City, substantial portion of waste finds its way into the storm drainage system. Sediment samples collected from storm sewers showed presence of polythene bag, plastic, cloth, rubber, metal strips, glass, paper sticks, leaves, bones and brick and stone chips in addition to soil (Chowdhury *et al.*, 1998).

6. PLANNING APPROACHES

Until the 1960s, the scale of city growth was determined by technical resources, development policies and budgeting either within the capacities of municipalities and/or government departments. The planning was very much focused on landscape design or determination of land use or physical elements. Later on, the planners attempted to carry out new planning approaches Master Plan (1959), Strategic Planning (1979) and Dhaka Metropolitan Development Plan (1995-2015) in order to control the spontaneous urbanization (Alam, 2006).

On the other hand, National Environment Policy, National Land Use Regulation also stated policies on wetlands. Water Body Conservation Act 2000 states that natural water bodies mean the places which are demarcated in the Master Plan as river, canal (khaal), depression areas (beel), lake, stream or wetland or places which are declared as 'flood flow zones' by the local government notification and such places should also include the land which retains storm water. This law prohibits any kind of development on these areas.

Despite all these rules, regulations and policies, conversion of wetland is continuing in a devastating manner. No attempt has yet been taken to demarcate the boundary of the retention ponds areas and other wetlands. The delay of completion of 'Detail Area Plan' for Dhaka is another major issue. There are few instances where the land-filling activities were prohibited through legal action such as Modhumoti Model Town, Uttara Model Town in Ashulia by Jamuna Group. Bangladesh Environmental Lawyers Association (BELA) played an important role in this respect. But these actions are very limited in number and powerful real estate companies

are converting hundreds of acres of wetland every year (The Daily Star, 2006).

7. RECOMMENDATIONS

The urban growth and sprawl in the fringe areas of Dhaka City has been partly spontaneous and partly initiated by the government and civic authorities, thus resulting in spoiling natural course of wetlands and creating flood at depressed-land areas. Given that there are overwhelming national requirement for new housing development, the effort should be concentrated on ensuring the development of sustainable communities and minimize the impact of the development on flood risk among other issues (Ogunyoye *et al.*, 2005).

- Integration between water management, land management and spatial planning is extremely important in sustainable drainage system. In order to strengthen the resilience capacity, it is essential to reserve more room for the river in spatial plans, not only in order to mitigate the present floods, but also in order to deal with the consequences of climate change. A possible expansion of the present wetlands by nature development and floodplain restoration (transforming former farmland into natural reserves) may enlarge the flood retention capacity and may help to reduce the effects of floods in urbanized downstream areas.
- Sustainable drainage systems can offer opportunities to restore wetlands and this option should be considered whenever possible. Sustainable drainage systems (SuDS) and improved resilience of buildings are of particular relevance to future housing development. SuDS is a new approach to managing rainfall that seeks to overcome the damaging effects of conventional drainage by mimicking the natural behavior of water. SuDS meets the three integrated objectives of dealing with runoff by controlling flow (quantity), preventing pollution (quality) and offering environmental benefits (amenity) in equal measure. This is called the 'drainage triangle' and defines the philosophy of SuDS rather than simply describing a collection of drainage techniques (Ogunyoye *et al.*, 2005).
- It is demonstrated that local wetlands can be very effective in urban drainage management. At least 5% of every drainage sub-catchment should be preserved as wetlands such that total area of wetlands including detention reservoir at pump/slucice gate site does not exceed 12% of the catchment area. This will not be difficult since most of the eastern part of Dhaka City are low lying and are in fact wetlands. This is also in line with the govt. policy to preserve wetlands.
- Renovation of the sewage and drainage system including providing sewer lines at un-sewered zones, increasing size of sewer conduits wherever necessary, providing exclusive storm water drainage lines, removing silts and trapped garbage from the conduits, increase of pumping capacity, reclamation and desilting of the outfall channels

and canals along with preservation and increment of wetland area can improve the drainage situation (Bose, 2005).

- A regional ecology-oriented environmental plan with legal measures for control and prevention, resource conservation areas, disaster management programme, outlines of the system of governance with participatory process are to be prepared and implemented. Various administrative authorities, agencies and private developers should work in cooperation and integrity following the community's common goal. Proper emphasis is to be given on education, research, capacity building and participatory programmes of stakeholders and public for broadened awareness and practical pro-sustainable activity in this regard (Bose, 2005).
- Develop a national standards for the valuation of floodplain wetland ecosystems that enable routine cost / benefit analyses of floodplain development / flood defense measures to routinely take account of wetland value.
- Develop a database of wetlands that describes their distribution and potential importance to drainage system and their vulnerability to change.
- New building to be built at such areas should have a plinth height of not less than 1.2 m from ground level. Old buildings should have perforation in the rooms at the ground floor so that water can be passed off during and after inundation (Bose, 2005).
- Herringbone brick laying on the earthen roads in the remote fringe areas is natural option for absorption of some runoff, than building road with cement-concrete, which is impermeable (Bose, 2005).

8. CONCLUSION

The overall growth of population along with rapid urbanization caused a high pressure on the limited land of the Dhaka City along with creation of a number of problems in the areas of environment, housing, water supply, drainage and sanitation. Various planning approaches were initiated in different time phases to overcome the problems. Unfortunately all planning initiatives have been frustrated by a number of factors due to loomed political instability and influence; lack of public accountability; lack of public awareness; desperate land and housing development taking little bit consent of the existing rules and regulations; and corruption in the enforcing agencies. Furthermore, it is a public belief that once a land is developed by any chance, there will be no possibility to evict the developed land e.g. Modhumoti Model Town. Thus a comprehensive and integrated approach is necessary along with the above-prescribed recommendation in order to preserve local wetlands and natural channels of Dhaka City for its survival.

REFERENCES

- Alam, M. S., 2006. The implications of floods for Dhaka city planning. *Options for Flood Risk and Damage Reduction in Bangladesh*, a symposium organized in 2004.
- Arnold, L.A. and Gibbons, C.J. (1996) Impervious Surface Coverage-the emergence of a key environmental indicator *Journal of the American Planning Association* 62: 243-258.
- Baker, C. and Eijk, P. V., 2006. *Sustainable Flood Management: Obstacles, challenges and solutions*. Flood Awareness and Prevention Policy in border areas (INTERREG IIIC Network 'FLAPP', Netherlands).
- Bose, S., 2005. Architectural and city planning measures for flood defense. *Floods, from Defence to Management*. Van Beek and Taal (eds.). Taylor and Francis Group. London.
- Chowdhury, J.U., Rahman, R., Bala, S.K. and Islam, A.K.M.S., 1998. *Impact of 1998 Flood on Dhaka City and Performance of Flood Control Works*. IFCDR, BUET, Dhaka
- Dunne, T. and Leopold, L. B., 1978. *Water in Environmental Planning*. New York: Freeman. 818 pp.
- Dhaka Metropolitan Development Plan, 1995. Volume-I, *Dhaka Structure Plan, Dhaka Metropolitan Development Plan (1995-2015)*, Rajdhani Unnayan Kartipakka Dhaka.
- DMDP, 1997. FAP-8A and 8B, *Master Plan for Greater Dhaka Protection Project (Study in Dhaka Metropolitan Area) of Bangladesh*, Flood Action Plan.
- Hasnat, M. A., 2006. Flood Disaster Management in Dhaka City. *Options for Flood Risk and Damage Reduction in Bangladesh*, a symposium organized in 2004.
- Hossain, A. N. H., A., Azam, K. A., and Serajuddin, M., 2006. The impact of floods on Dhaka City's water supply, sanitation and drainage and mitigation options. *Options for Flood Risk and Damage Reduction in Bangladesh*, a symposium organized in 2004.
- IUCN, 2006. www.iucn.org/en/news/archive/2006/02/02
- Japan International Cooperation Agency, 1990. *Updating Study on Storm Water Drainage System Improvement Project in Dhaka City*, Supporting Report, Dhaka WASA, Dhaka.
- Japan International Cooperation Agency, 1991. *Master Plan for Greater Dhaka Flood Protection Project, FAP 8A*, Report I and II, Flood Plan Coordination Organization (presently WARPO), Dhaka.
- Khan, M. U., Chowdhury, J. U. and Hossain, M. S. A., 1998. *Measurement and Analysis of Rainfall-Runoff in Selected Catchments of Dhaka City*. Vol. 1: Main Report, IFCDR, BUET, Dhaka.
- Leopold, L.B., 1968. *Hydrology for Urban Planning- a guidebook on the hydrologic effects of urban land use* USGS Circular 554, 18 pp.
- Ogunyoye, F. O., Breay, R., Gunasekara, R. T., and Vigor, M., 2005. Managing flood risk at source – showcasing best practice. *Floods, from Defence to Management*. Van Beek and Taal (eds.). Taylor and Francis Group. London.
- Paul and Meyer, 2001. Streams in the Urban Landscape. *Annual Review of Ecological Systems* 32:333-365.

- Potter, K.W., 1994. *Estimating potential reduction flood benefits of restored wetlands*. Water Resources Update 97: 34-38.
- Seaburn, G.E., 1969. *Effects of Urban Development on Direct Runoff to East Meadow Brook*, Nassau County, Long Island, New York. USGS Professional Paper 627-B, 14 pp.
- The Daily Star. 19th May 2006.
- Tucci, C. E. M., n.d. *Flood Control and Urban Drainage Management*. Institute of Hydraulic Research, Federal University of Rio Grande do Sul, Porto Alegre, RS Brazil
- Zedler, J., 2003. Wetlands at your service: reducing impacts of agriculture at the watershed scale. *Frontiers in Ecology*, vol. I (2): 65-72.

STUDY ON THE POTENTIAL OF TREE SHAPE CLASSIFICATION BY USING THE SIMULATED LIDAR DATA AND A TREE CROWN MODEL

TAKAHIRO ENDO and YOSHIFUMI YASUOKA
International Center for Urban Safety, Institute of Industrial Science,
The University of Tokyo, JAPAN
tendo@iis.u-tokyo.ac.jp

ABSTRACT

Light Detecting and Range (LiDAR) is one of aerial remote sensing techniques, which can acquire three-dimensional information above the ground. LiDAR measurement is not only applied to investigation of 3D city information and disaster, but also is widely applied to forestry management. In latest forest management application of LiDAR, individual tree position and height can be estimated by LiDAR data. However, in case of heterogeneous forest site, in addition to the LiDAR data, visible or hyperspectral data is needed for classification of species. There has been no study to classify species only with LiDAR data. LiDAR data with high pulse density which is able to reconstruct tree form by point clouds have potential to classify difference species. As an initial study, we examined possibility of classifying trees by simulated LiDAR data. Firstly, LiDAR data with specific pulse density was simulated by simulated 3-D tree polygons and ray tracing technique. Secondly, the developed 3-D crown surface model, which can reconstruct canopy form, was applied to the simulated LiDAR data and parameters of the model for fitting were estimated. As the result of analyzing parameters, Ginkgo biloba, Zelkova serrata and Cryptomeria jaoanica, which are main species of urban trees in Tokyo could be classified based on properties of crown form. This result indicates that LiDAR data with high pulse density has potential for classifying species without using other optical sensors, which can significantly reduce measurement cost.

1. INTRODUCTION

Recently, LiDAR which is one of advanced remote sensing technologies is becoming useful instrument for measuring 3-D information in urban area or forest area (HYYPPÄ *et al.*; 2001; PERSSON *et al.*; 2002, YU *et al.*; 2004, HIRATA; 2007). The data is the LiDAR pulse returned from the target above the ground after being emitted from an airborne devise. The data can not only measure the ground level (digital elevation model, DEM), but also can reconstruct the form of target.

In conventional forest management, it is difficult to measure tree height, breast height (DBH) and position in thick forest like jungle, since previous methods are carried out by using only manpower. Moreover, these

methods have low efficiency, costly and time-consuming. LiDAR has the potential in solving these problems, and many researchers have been using to estimate growth parameters, such as height, DBH and position. The parameters which are related to plant growth can be estimated using LiDAR data, in case of a individual tree. However, it is difficult to estimate growth parameters in mixed forest using LiDAR, because of complex crown structure. Hence, classification method or identification method of a tree is the most important point before estimation of parameters using LiDAR data. One of approaches is to use visible or hyperspectral data for classification. But, in case of using other data with LiDAR data, the cost becomes high. Moreover, it is difficult to measure same area on same day and time by difference sensors. Since LiDAR data contains 3-D information of tree crown, it is possible to reconstruct a tree crown. If classifying species from the crown alone would reduce cost of measurement and it would also provide variable information on whole leaf area and current growth activity. However, there hardly exist studies concerning tree classification methods by LiDAR point clouds alone, as the relationship between LiDAR point clouds and a form of tree crown is not clear. There are two reasons for this situation. One reason is that, there are many forms of crown shapes. Crown form depends on species, age of stand, and growing environment. (The other reason is specification of measurement which is platform type, pulse rate, emitting direction and so on, which is changed by each measurement.)

This initial study aims, firstly to develop a LiDAR data simulation system and, secondly to develop an algorithm for classification of species based on LiDAR point clouds.

2. MATERIALS AND METHODS

2.1 LiDAR data simulation system

A LiDAR simulation system using 3-D tree polygon was developed in order to simulate LiDAR data of tree crown. The tree polygon is simulated by 3dsmax (Autodesk, USA) and the natFX (Bionatics, USA) which are kind of growth simulation software. The advantage of using these softwares is that they can create an object with absolute coordinate system value which can be handled in 3DCG software, and so the 3-D model can be simulated for various situations. With regard to the simulated form of polygon, its crown form and foliages are similar with an actual tree. In addition, the system can modify the tree with a standard form to a tree with a smaller crown size and higher height which normally exists in high density forest.

LiDAR data of crown is simulated by the tree polygon and the developed original program that can control spatial resolution of pulse and direction of emitting. LiDAR data is defined as an intersection of point between the tree surface and ray by the ray-tracing calculation technique.

In this study, we selected three species; *Ginkgo biloba*, *Zelkova serrata*, and *Cryotomeria jaoanica*. There were two criteria for selection. One is crown form, the other is branch and leaf form. Forms of both the Ginkgo and the Cryotomeria are conical. On the other hand, form of *Zelkova* is bowl-shaped. Leaf types of the Ginkgo and the Zelkova are broad. Leaf type of the Cryotomeria is needle. With regard to configuration of measurement, the pulse density and the emitting direction were 10 points/m² and vertical, respectively. Five tree polygons for each species were simulated in order to average individual variations.

2.2 Concept of the developed classification method

Classification method in this study consisted of two steps. The first step was using properties of macroscopic form that were crown height (ch), crown radius (cr), ch/cr ratio and crown cover. The second step was using properties of microscopic form that was the standard deviation value (S.D.). Even if trees were similar ch/cr value, their S.D. value might be different. In this case, S.D. value would be able to classify them, and became indicator for classification. Actually, property of LiDAR's point clouds between needle leaf and broad leaf is quite different.

2.3 Approximate model of 3-D crown form

One of approximate model for tree form is an ellipsoid model reported by Sheng *et al.*[2001]. This model is suitable for coniferous form, but approximate accuracy is low around edge of bowl-shaped crown form like the Zelkova. Crown curvature is controlled by *cc* parameter in the original model. We introduced *cc* of the cosine type and the gaussian type in order to improve accuracy of model fitting. The Sheng's model with the original *cc* type, the cosine type and the gaussian type are shown in equation 1, 2 and 3. Parameter *a*, *b* are correction coefficient and flat rate of the cosine and gaussian faction, respectively.

The Sheng's original model:

$$\frac{(Z + ch - Zt)^{cc}}{ch^{cc}} + \frac{((X - Xt)^2 + (Y - Yt)^2)^{\frac{cc}{2}}}{cr^{cc}} = 1 \quad (1)$$

The original type:

$$cc_{original} = Constant$$

The cosine type:

$$d = ((Xt - X)^2 + (Yt - Y)^2)^{\frac{1}{2}} \quad (2)$$

$$cc_{cos} = b \cos\left(\frac{d\pi}{2cr}\right)^2 + a$$

The gaussian type

\:

$$d = ((X_t - X)^2 + (Y_t - Y)^2)^{\frac{1}{2}}$$

$$cc_{\text{gaussian}} = b \exp\left[-\left(\frac{d}{cr}\right)^2\right] + a$$
(3)

Where crown height is ch , crown radius is cr , crown curvature is cc , treetop coordinates is X_t , Y_t , and Z_t , d is distance on X-Y plane between the tree tip and the specific X, Y position, a is correction coefficient and b is flat rate.

Accuracy of model fitting was verified by the S.D. value between the simulated LiDAR data and the model. The properties of macroscopic form and the microscopic form were calculated from the result of the model fitting.

3. RESULTS AND DISCUSSIONS

3.1 Overview of LiDAR data simulation system

The developed system can change various pulse densities and the angles of emitting laser from anywhere, and can simulate various LiDAR data of crown form. Figure 1 shows the simulated tree polygon (*Ginkgo biloba*) as one of results. The left-hand side figure is macroscopic overview of the form. The right-hand side figure is microscopic overview of branches and leaves. Figure 2 stands for the simulated LiDAR data of *Ginkgo biloba* as one of results. Left-hand side scatter plot is the result that carried out the simulation with 90 degree of emitting angle. Right-hand side scatter plot is the result with 30 degrees of emitting angle.

The result indicates that our system could simulate the LiDAR data of the crown which was similar to that of actual tree. In order to estimate crown cover, the best emitting angle was perpendicular. In addition, right-hand side scatter plot indicates that position of stem and top may be measured since a stem of tree is hit by laser. In order to estimate a stem position, the best emitting angle may be the other angles than perpendicular.

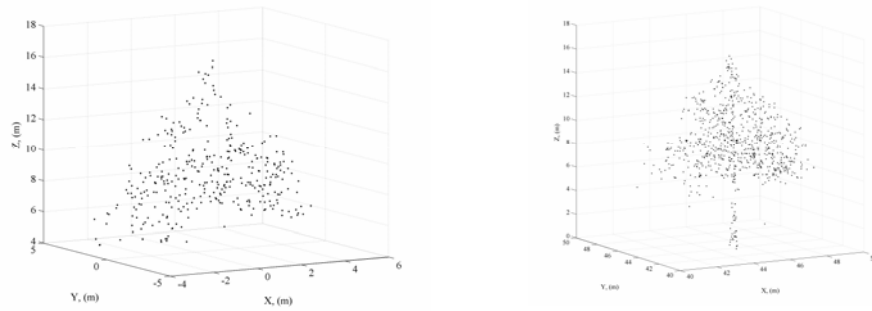


a) The macroscopic overview



b) The microscopic overview

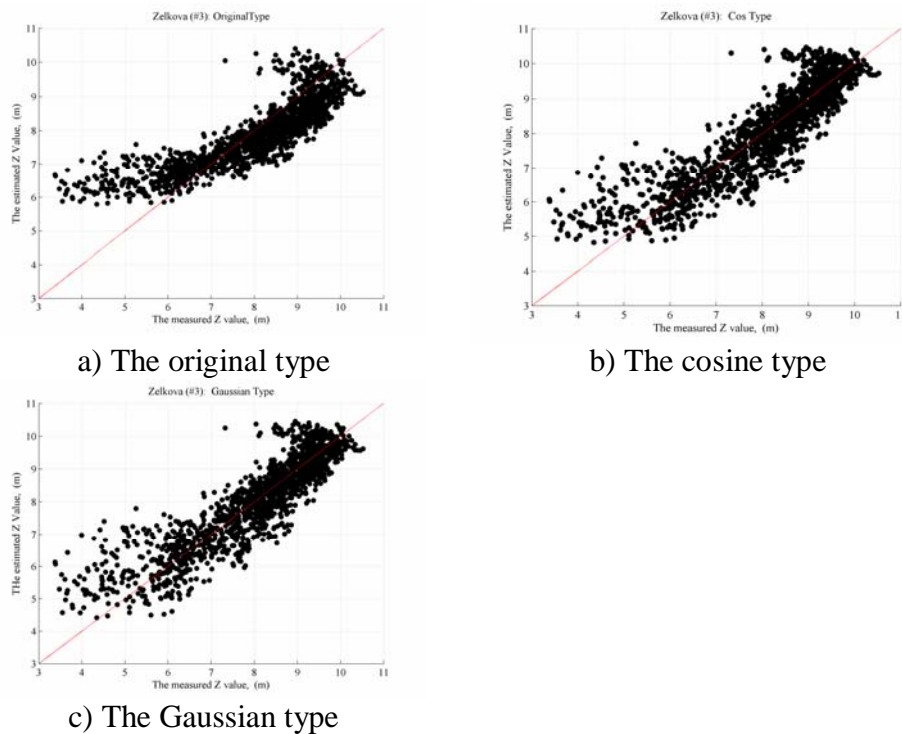
Figure 1: The simulated tree polygon of *Ginkgo biloba*; a) the macroscopic overview of the tree form (left), b) the microscopic overview of branches and leaves (right)



a) The emitting angle is 90 degree b) The emitting angle is 30 degree
 Figure 2: The simulated LiDAR data of *Ginkgo biloba*; the emitting angle is 90 degree (left) and 30 degree (right)

3.2 Approximation accuracy of the 3-D crown form model

The simulated LiDAR data was approximated by three models which are 1) the Sheng’s original type, 2) the cosine type and 3) the gaussian type. One of correlation diagrams between the Z value estimated by the 3-D approximation model and the Z value simulated by the system is shown as figure 3. Approximation accuracies by the cosine and gaussian type were improved in comparison with the original type. The modified models could not only apply to a conical form like the Ginkgo, but also apply to bowl-shaped form like the Zelkova. One of results of the Zelkova is shown as the approximated 3-D crown surfaces in figure 4. Table 1 shows the result of approximation accuracy. These values were calculated from average of 5 samples.



a) The original type b) The cosine type
 c) The Gaussian type
 Figure 3: The correlation diagram between the Z value estimated by the 3-D approximate model and the Z value simulated by the system; a) the original type, b) the cosine type and c) the Gaussian type

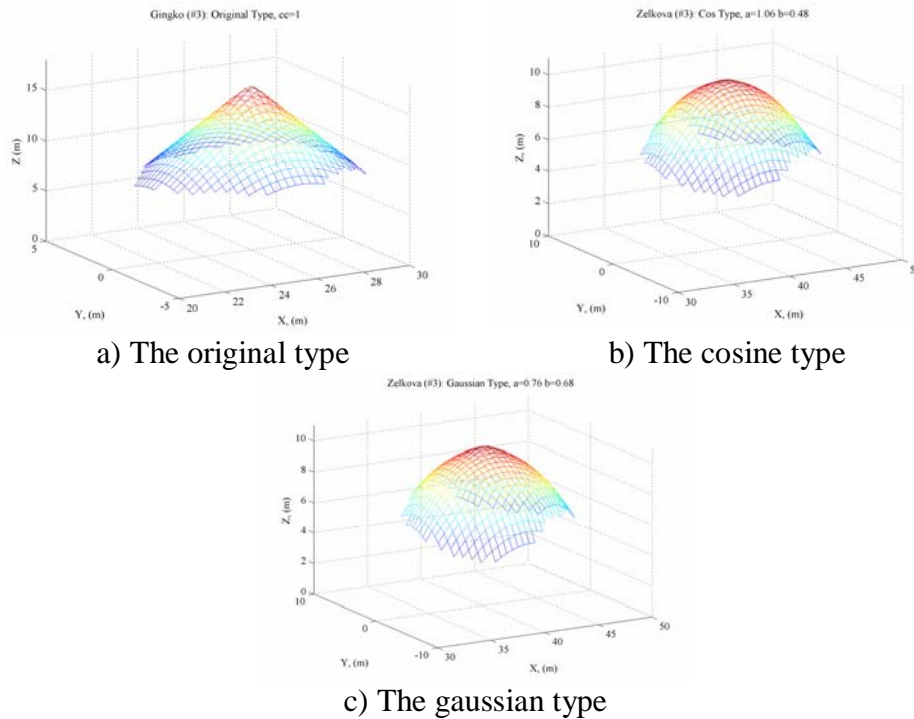


Figure 4: The approximated 3-D crown surfaces using the best S.D. value of the Zelkoba

Table 1: The approximate accuracy of the macroscopic and the microscopic properties.

	ch/cr	S.D. (m)		
		R		
		Original type	Cosine type	Gaussian type
Zelkova (ave.)	0.697	0.788	0.755	0.751
		0.782	0.796	0.798
Ginkgo (ave.)	1.959	1.876	1.309	1.313
		0.823	0.812	0.812
Cryptomeria (ave.)	2.433	2.424	2.093	2.099
		0.900	0.898	0.895

3.3 The probability of tree classification based on tree form

As the results of the first screening of the macroscopic property, the ch/cr value of the Zelkoba, the Ginkgo, and the Cryotomeria were 0.697, 1.959, and 2.433 in Table 1, respectively. Hence, the result indicates that species could be classified by only ch/cr value. Moreover, as the results of the second screening as the microscopic property, the S.D. value by the cosine type of the Zelkoba, the Ginkgo, and the Cryotomeria were 0.755, 1.309, and 2.093 (m), respectively. Also, the S.D. values by the gaussian type of the Zelkoba, the Ginkgo, and the Cryotomeria were 0.751, 1.313, and 2.099 (m), respectively. The S.D. values between the Ginkgo and the Cryotomeria were different by about 70cm in spite of similar conical form.

Therefore, this result indicates that species with the similar crown form could be classified.

4. CONCLUSIONS

The LiDAR data simulation system was developed, and the probability of classification of trees based on the crown properties was investigated in this study. An advantage of the simulation system is that, it can simulate point clouds of a tree crown under different conditions such as species, various crown forms, specific pulses density and the direction of emitting laser. Moreover, the simulated LiDAR data was almost same as actual measurement data. The system can help to analyze optimal measurement condition and to develop new algorithm for extraction of unknown growth parameters before an actual LiDAR measurement.

In addition, the approximate surface model of 3-D crown form was investigated in order to classify tree species based on the crown property. Two models with the cosine type and the gaussian type function as crown curvatures have improved approximate accuracy of both conical and bowl-shaped crown forms when compared with the Sheng's model. Therefore, these models can be used for approximate definition of crown form.

The result of having analyzed the possibility of the classification of trees of a characteristic crown form, the macroscopic property such as the ch/cr value can not only classify species, but also the microscopic property such as the S.D. value can classify species with similar crown form.

The result of this study indicates that the approximated surface model derived from point clouds have the macroscopic and the microscopic properties that has the potential to classify species with LiDAR data alone without using optical imaging or other data. This will reduce cost and increase efficiency of measurement.

REFERENCES

- HIRATA, Y., 2007. Forest measurement with airborne laser scanner and its trend, *Jpn. J. For. Plann.* 41, 1, 1-12.
- HYYPPÄ, J., KELLE, O., LEHIKONEN, M. and INKINEN, M., 2001. A Segmentation-based method to retrieve stem volume estimation from 3-d tree height models produced by laser scanners, *IEEE Trans. Geosci. & Remote Sens.* 39, 969-975.
- SHENG, Y., GONG, p. and BLGING, G.S., 2001. Model-based conifer-crown surface reconstruction from high-resolution aerial images. *Photogrammetric Engineering & Remote Sensing.* 67,8, 957-965.
- YU, X., HYYPPÄ, J., KAARTINEN, H. And MALTAMO, M, 2004. Automatic detection of harvested trees and determination of forest growth using airborne laser scanning. *Remote Sens. Environ.* 90, 451-462.72.

LIDAR: A TECHNOLOGY OF NEW ERA

MOHAMMAD ABDUL QUADER

Senior GIS analyst,
Golden Harvest Scankort GIS Ltd., Dhaka, Bangladesh
quader_000@yahoo.com

MD. ZAHID HASAN SIDDIQUEE

Research Assistant, Dept. of Civil Engineering, BUET

RUBEL DAS

Research Assistant, Dept. of Civil Engineering, BUET

ABSTRACT

The developed world is moving into a new era of using technology to manage infrastructure using accurate land information displayed in three dimensions: x and y represent horizontal coordinates and z represents elevation. Improvements in gathering and displaying elevation data make it economically feasible to gather vast quantity of data in a short period of time and have it readily available for distribution to multiple users. Light detection and ranging (LIDAR) has proven a mature technology to acquire three-dimensional point clouds for describing earth surface. So this is high time for third world countries like Bangladesh to use this technology which has application in geography, geology, geomorphology, seismology, remote sensing, atmospheric physics, and hydrology. Flood visits Bangladesh almost every year. Most data collection on flood is done by traditional methods which is extremely expensive and comparatively slow. LIDAR data, with high resolution and accuracy are suitable for improving the performance of flood models by providing more reliable initial boundary condition. Accurate and comprehensive high-resolution terrain data helps greatly in planning, design, construction and maintenance of transportation infrastructure. Improvement of drainage system, land division, utilities and the availability of soils mapping also depends on the availability of DEM (Digital Elevation Model) which is obtained from LIDAR technology. LIDAR may also be used to measure the speed of atmospheric winds, densities of certain constituents of urban atmosphere. LIDAR has a notable application in hydrology to quantify stream channel cross sections and roughness, to estimate bank erosion. LIDAR data are essential to analyze and assess the vulnerabilities of critical infrastructure for security and natural disaster mitigation.

1. INTRODUCTION

LIDAR (Light Detection and Ranging) is an optical remote sensing technology that measures properties of scattered light to find range and/or other information of a distant target.

The prevalent method to determine distance to an object or surface is to use laser pulses. Like the similar radar technology, which uses radio waves instead of light, the range to an object is determined by measuring the time delay between transmission of a pulse and detection of the reflected signal. LIDAR technology has application in geography, geology, geomorphology, seismology, remote sensing and atmospheric physics.

The primary difference between LIDAR and radar is that with LIDAR, much shorter wavelengths of the electromagnetic spectrum are used, typically in the ultraviolet, visible, or near infrared. In general it is possible to image a feature or object only about the same size as the wavelength, or larger. Thus LIDAR is highly sensitive to aerosols and cloud particles and has many applications in atmospheric research and meteorology.

2. COMPONENT OF LIDAR SYSTEM

In general there are two types of LIDAR systems: micropulse LIDAR systems and high energy systems. Micropulse systems have developed as a result of the ever increasing amount of computer power available combined with advances in laser technology. They use considerably less energy in the laser, typically on the order of one microjoules, and are often "eye-safe" meaning they can be used without safety precautions. High-power systems are common in atmospheric research, where they are widely used for measuring many atmospheric parameters: the height, layering and densities of clouds, cloud particle properties (extinction coefficient, backscatter coefficient, depolarization), temperature, pressure, wind, humidity, trace gas concentration (ozone, methane, nitrous oxide, etc.).

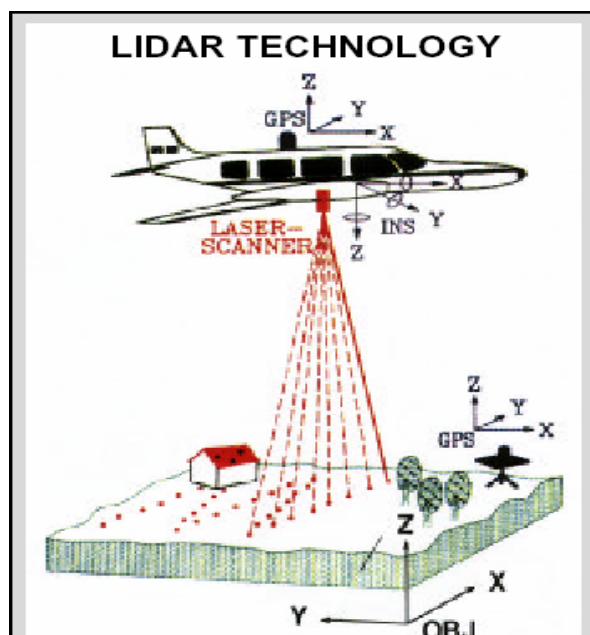


Figure 1: LIDAR uses lasers to emit light pulses that strike the ground and reflect back to the airborne sensor.

There are several major components to a LIDAR system:

2.1 Laser

600-1000 nm lasers are most common for non-scientific applications. They are inexpensive but since they can be focused and easily absorbed by the eye the maximum power is limited by the need to make them eye-safe. Eye-safety is often a requirement for most applications. A common alternative 1550 nm lasers are eye-safe at much higher power levels since this wavelength is not focused by the eye, but the detector technology is less advanced and so these wavelengths are generally used at longer ranges and lower accuracies. They are also used for military applications as 1550nm is not visible in night vision goggles unlike the shorter 1000nm infrared laser. Airborne topographic mapping LIDARs generally use 1064 nm diode pumped YAG lasers, while bathymetric systems generally use 532 nm frequency doubled diode pumped YAG lasers because 532 nm penetrates water with much less attenuation than does 1064 nm. Laser settings include the laser repetition rate (which controls the data collection speed). Pulse length is generally an attribute of the laser cavity length, the number of passes required through the gain material (YAG, YLF, etc.), and Q-switch speed. Better target resolution is achieved with shorter pulses, provided the LIDAR receiver detectors and electronics have sufficient bandwidth.

2.2 Scanner and optics

How fast images can be developed is also affected by the speed at which it can be scanned into the system. There are several options to scan the azimuth and elevation, including dual oscillating plane mirrors, a combination with a polygon mirror, a dual axis scanner. Optic choices affect the angular resolution and range that can be detected. A hole mirror or a beam splitter are options to collect a return signal.

2.3 Receiver and receiver electronics

Receivers are made out of several materials. Two common types are Si and InGaAs. They are made in either PIN diode or Avalanche photodiode configurations. The sensitivity of the receiver is another parameter that has to be balanced in a LIDAR design.

2.4 Position and navigation systems

LIDAR sensors that are mounted on mobile platforms such as airplanes or satellites require instrumentation to determine the absolute position and orientation of the sensor. Such devices generally include a Global Positioning System receiver and an Inertial Measurement Unit (IMU).

3. ADVANTAGES OF LIDAR

3.1 Accuracy

An accuracy of order of 10 - 15 cm in the vertical and 50 - 100 cm in the horizontal is claimed by manufactures and has been demonstrated by many field studies.

3.2 Time of data acquisition and processing:

The data capture and processing time is significantly less for LIDAR compared to other techniques. LIDAR can allow surveying rates of up to 90 km² per hour (Environment Agency, 1997) with post-processing times of two to three hours for every hour of recorded flight data.

3.3 Minimum user interference

User interference is minimum, as most of the data capture and processing steps are automatic except the maintenance of the ground GPS station.

3.4 Weather independence

LIDAR is an active sensor and can collect data at night and can be operated in slightly bad weather and low sun angle conditions, which prohibit the aerial photography.

3.5 Additional data

Besides relief information, laser reflectance may be used to generate intensity images to help in classifying the terrain features. Further, the systems can have fluorosensors allowing pollutant identification and chlorophyll mapping (Environment Agency, 1997)

3.6 Canopy penetration

Unlike photogrammetry, LIDAR can see below canopy in forested areas and provide topographic measurements of the surface underneath. Additionally, LIDAR generates multiple returns from single pulse travel, thus providing information about understory.

3.7 Data density

LIDAR has the ability of measuring subtle changes in terrain as it generates a very high data density (due to firing of 2000 - 80000 pulses per second).

3.8 Ground control point independence

Each LIDAR pulse is individually georeferenced using the onboard GPS, INS, and laser measurements. Only one or two GPS ground stations are required for improving the GPS accuracy by the differential method. Independence from GCPs makes it an ideal method for inaccessible or featureless areas like wastelands, ice sheets, deserts, forests, and tidal flats.

3.9 Digital compatibility

Data produced from LIDAR flights are in digital format with Easting, Northing, and Altitude values of each laser target. This makes importing of data to GIS and other image processing packages straightforward.

3.10 Cost

One of the major hindrances in the use of LIDAR had been the cost of the equipment. However, in recent years the purchase price of these instruments has been reduced so that cost is no longer a barrier to companies capable of investing in standard aerial photogrammetry equipment. Furthermore, with more and more users opting for LIDAR the cost of the system and operation is likely to go further down. Mason et al. (1999), on the basis of overall performance evaluation of available topographic techniques for coastal terrain, found that LIDAR could achieve good performance at a lower cost.

4. LIDAR APPLICATIONS

4.1 Floods

High-resolution and accurate LIDAR data are suitable for improving the performance of flood models by providing a more reliable initial boundary condition. LIDAR data having multiple returns help in generating and understanding the 3D structure of obstructions (i.e. surface roughness, vegetation, buildings, and other structures). This information can yield the friction coefficient over the various parts of a floodplain. LIDAR data are also being employed for flood hazard zoning. Flood visits Bangladesh almost every year. Bangladesh was affected by severe floods in 1988, in 1998 and also this year. According to Care, one of the world's largest private humanitarian organizations, 35 million people in South Asia have been affected by flood this year. The following table shows the loss due to floods in Bangladesh.

Table 1: Loss due to flood in Bangladesh

Type	Year			
	1987	1988	1998	2004
Human loss	1657	1517	<1000	500
Livestock		350000	26564	15143
Roads		3000 km	16000 km	45528 km
Embankments		35 km	4500 km	2500 km
Crops damages	1.21 m.h 36727 m. Tk	2.14 m. ha 35462 m.Tk	1.74 m. ha 37661 m. Tk	.85 m. ha 31839 m. Tk
Monetary loss (USD)	1000 m.	1200 m.	2800 m.	3.10 m.

Source: Hossain A.,N.,H.,A., 2006

So Using LIDAR technology to prepare flood plain maps will help the government and international community immensely in decision making and assess the loss.

4.2 Coastal applications

LIDAR has generated considerable interest among coastal researchers as a topographic tool. Highly accurate, dense, and rapidly obtained data sets are most suitable for coastal applications like sediment transport, coastal erosion, and coastal flood models.

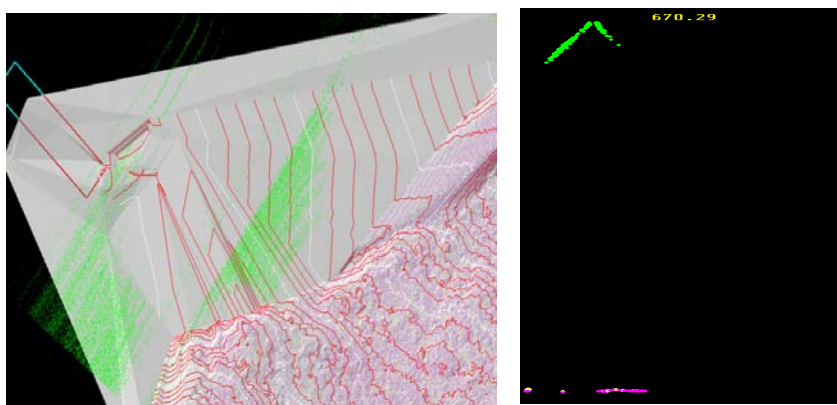


Figure 2: LIDAR data of a coastal area (showing TIN and elevation)

4.3 Bathymetry

LIDAR in its bathymetric form can map the bed topography up to a depth of 70 m. This information is useful for determining the siltation on navigation canals and ports and planning the construction details.

4.4 Hydrology

LIDAR data can be used to quantify gully and stream channel cross sections and roughness, gully and stream bank erosion and channel degradation, to estimate soil loss from gully or channel banks and to measure channel and flood plain roughness and cross sections for estimating flow rates. Further, coastal channels which are difficult to map otherwise can be automatically quantified using LIDAR data.

4.5 Landslides

LIDAR has made it possible to monitor and predict slope failure by rapidly obtaining highly accurate and dense elevation data. In post-slide conditions rapid damage assessment and mapping can be realized using LIDAR.

4.6 Forest Mapping

The unique feature of LIDAR of producing multiple returns from the canopy top, under story, and the ground has attracted many to use it for estimating forest biomass, timber volume, and other parameters.

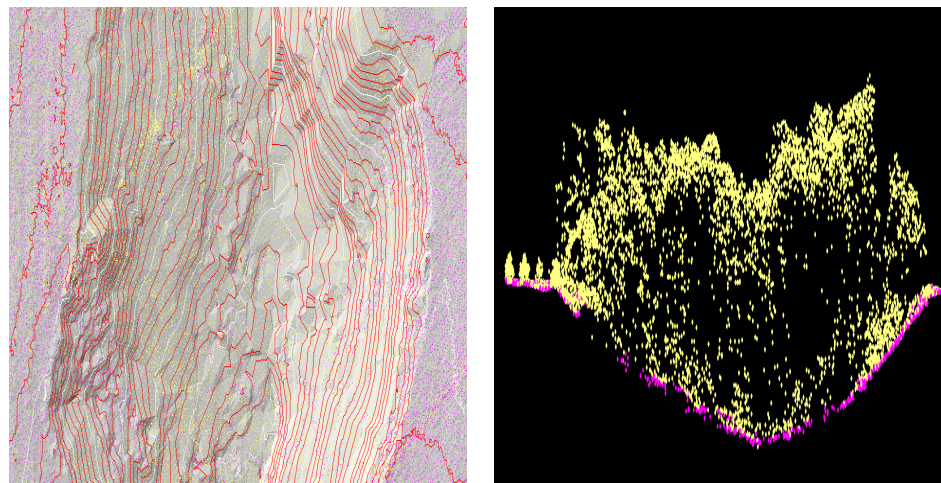


Figure 3: LIDAR data of a forest area in Norway (showing TIN view and cross section of the area)

5. CONCLUSION

LIDAR data helps to reduce data collection costs which are the main obstacle in planning and development especially in third world country.

Some disaster occurs almost every year in the country which is densely populated as well as poor. Determining the losses due to flood, identifying the earthquake prone area, landslide prone area, tsunami exposed area can be easily done if the LIDAR data are available. So disaster prone countries can save the human resource as well as the natural resources by using LIDAR technology in their national planning.

REFERANCES

- Franz, R., Trinder, J., Clode, S. and Kubik, K. 2003. *Building detection using LIDAR data and multi-spectral images*, *Proceedings of VIIIth digital image computing: techniques and applications*. Sun, C., Talbot, H., Ourselin, S. and Adriaansen, T. (editors), Sydney, 10-12 December 2003.
- Hossain, A., N., H., A and Siddique, K., U. 2006. *Options for Flood Risk and Damage Reduction in Bangladesh*. The University Press Ltd., Bangladesh.
- Haala, N. and Brenner, C. 1999. *Extraction of buildings and trees in urban Environment*. *ISPRS Journal of Photogrammetry and Remote sensing*, Vol. 54, pp. 130-137.
- Pohl, C. and Genderen, J.L. 1998. *Multisensor image fusion in remote sensing: concepts, methods and application*. *International Journal of Remote sensing*, Vol. 19, No. 5, pp. 823-854.
- Sandia National Laboratories 2004. *Synthetic Aperture Radar* .[Online], Available: <http://www.sandia.gov/RADAR/whatis.html>.
- Thuy, T. and Tokunaga, M. 2001. *Wavelet and scale-space theory in segmentation of airborne laser scanner data*. *Proceedings of 22nd Asian Conference on remote sensing*, Singapore, 5-9 November 2001.
- TopScan 2004. <http://www.topscan.de/en/literatur/index.html> [Online]

MANAGEMENT OF BUILDING ENERGY CONSUMPTION AND RENEWABLE ENERGY SUPPLY IN THE ECOLOGICAL COMMUNITIES USING GIS

MD. ZAHID HASAN SIDDIQUEE
Research Assistant, Dept. of Civil Engineering, BUET
zh027@yahoo.com

DR. URSULA EICKER
Professor, Stuttgart University of Applied Sciences,
Stuttgart, Germany

DR. DIETRICH SCHRÖDER
Professor, Stuttgart University of Applied Sciences,
Stuttgart, Germany

ABSTRACT

Building is the hub of almost all human activities in urban areas. These activities are mostly supported by energies such as electricity which makes energy management very important especially in urban areas. This paper has made an approach for enhancing energy management in the buildings using Geoinformation Systems (GIS). Energy and water consumption in the buildings can be visualized in different ways. Web GIS can address this issue well over the Internet. Buildings in the project (Shranhauserpark, Stuttgart, Germany) area have consumption data regarding heat, electricity, water and gas. GIS can perform the task of visualization in a number of ways; thematic map is one of the best where colour intensity indicates the degree of energy consumption. Moreover bar charts associated with thematic maps depict the changes of consumption values over the period of time (years, months, days etc) for each building in the unit of Kilo Watt Hours per square meter (unit of measurement). A web portal is developed for displaying maps and attributes where users or people of the study area can have the access through Universal Resources Locator (URL). Thus, they can evaluate the status of their energy consumption regarding heat, electricity, gas and water. Dissemination of these information will lead to an increasing awareness among the residents of the project area with respect to energy consumption and supply. More than half of the world's population lives in the urban areas in Asia. The number of people living in urban areas would be 2 billion by the year 2030. This huge influx of people would make a significant impact on the energy management system of the mega cities in Asia. The result of this study would support the energy management system to monitor and evaluate building energy consumption in a much more efficient way that can play a vital role to mitigate the energy crisis in the world.

1. INTRODUCTION

Internet GIS is comparatively a new term in Geographic Information System. It is getting special significance for spatial data handling over the web. In simple words this is for distributing and processing Geoinformation by the way of Internet and World Wide Web. It is getting increasing importance and acceptability for different level of bodies like geospatial data users and producers as well as governmental and non-governmental agencies. It can provide GIS functionalities both on Intranet and Internet at the same time. As Internet GIS is platform independent it reduces the necessity of purchasing costly desktop GIS software.

Internet plays a vital role in our everyday life. Necessary information is available online regarding almost every sphere of life. Energy is another widely used term. Very few things are possible without energy. On the other hand buildings accommodate greater portion of human activities. Thus how to manage energy in buildings is worth stating. Particularly in urban areas, it is very significant. Geoinformation can be the right choice for this type of energy management. This task deals with structuring a system where building energy consumptions such as electricity, water, gas and heating energy and renewable energy supply are to be managed in real time with the help of Geoinformation Systems. The users can have access to the building energy consumption data over the Internet and thereby they can evaluate the status of their respective energy consumption and supply. This will increase the awareness about energy consumption along with the efficiency of energy use among the users.

2. BACKGROUND

PolyCity is an urban conversion project. It is focused on large-scale urban development. Here the working places and living areas are integrated to result in sustainable city quarters within short distance and low energy consumption. The sustainable city quarters mean that these would be the best for the people and environment both for now and the indefinite future. The project handles a number of aspects related to urban conversion such as new construction at the city edges of Barcelona in Spain; the conversion of old city quarters with poly-generation energy and grid based energy supply at Tornio in Italy; new building construction and renovating old ones on a large former military ground near Stuttgart with biomass heat and electricity supply.

The part of the project in Stuttgart is the area of Scharnhäuserpark. This is an urban conversion and development on an area of 150 hectares in the community of Ostfildern on the southern border of Stuttgart. Working places, residential areas and green park sections are integrated here to result in a harmonious living and transportation concept with high comfort and low energy consumption.

This is also designed as an exemplary ecological community development where wood fired co-generation plants will deliver electricity and heat energy. This is in the frame of a European research project called PolyCity for urban development or urban conversion. There are some other related key components of the project like ecological communities, Geoinformation and so on. These will be discussed in brief in the following sections

3. METHODOLOGY

Each of the buildings in the project area will have an electronic device called SmartBox. At present there are few buildings with the device such as Stadthaus. The SmartBox will transmit the consumption and supply data at a certain time interval. The data from this SmartBox will be stored in server. Some programming tools will be used for establishing connection between the electronic device and the server. Necessary data is to be retrieved from the server and to be put into the MS Access database in tabular form.

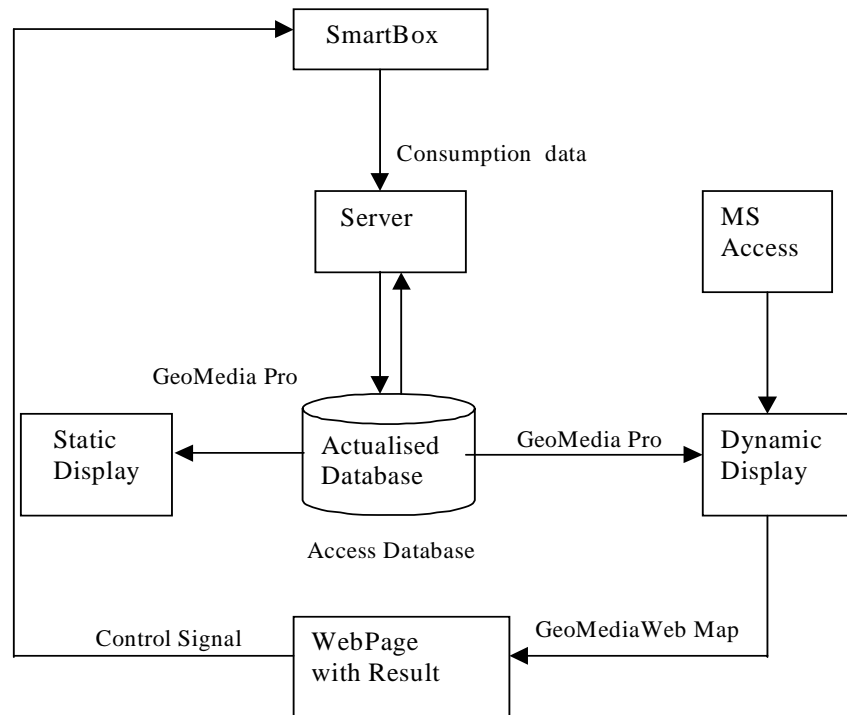


Figure 1: Flow diagram of methodology

Once the data about consumption from each building is stored in the MS Access database, it will be used in the Geoinformation System for visualization. In this case GeoMedia Professional is used to visualize the consumption data on the server computer. GeoMedia WebMap Professional is used for visualization over the web for the residents in the project area. Database stored in MS Access would be actualized at a certain time interval. These real time data are to be used for creating graphic displays.

A number of thematic maps are prepared to view the numeric values in varying color intensities. This will give the visual impression about the whole area; for example buildings with darker colour indicate more energy consumption. Bar charts associated with thematic maps will demonstrate the consumption values to facilitate the comparison among different time intervals (years). As the database will be updated at an interval of time, the thematic maps along with bar charts will also be updated at the same time. The maps and bar charts are based on the real time consumption values. So this display is dynamic. A set of static maps will also be created using the data from the Access database for a longer time span such as for a year or six months. GeoMedia Professional will be deployed to generate above stated outputs.

4. DATA AND SOFTWARE

Data is very important for any GIS project. For the current project necessary data is available in the form of MS Access and GeoMedia workspace. There is building information in access database like house number, number of stories, and name of the homeowner and so on. The consumption of energy for each building is also available in Kilowatt Per Hour (Kwh). The above stated data has to be in real time. Once all the connections are set up among the system components the target will be achieved. GeoMedia Professional 5.2 is very powerful software for analysing and managing spatial data. The GeoMediaWebMap Professional will be used for handling web related aspects of this project. For creating graphical display MS Excel or Access can be attached with GeoMedia Professional.

5. AVAILABLE DATA

Data is most important item in spatial analysis. Once the database is ready it is only a matter of time to have the desired output. The database for the area of Scharnhauser Park is in Microsoft Access. The data set for carrying out this study is with a working group from the University of Applied Sciences, Stuttgart, Germany. They have obtained it from the city office of Osfildern and a utility company called Esslingen am Neckar GmbH. The database contains information about buildings as well as energy and water consumptions. There is another data set in DXF file format containing building block. This CAD data is later transformed into GeoMedia files with area features for buildings. The MS Access data and GeoMedia files are used together to visualize the amount of energy consumption with a series of thematic maps and bar charts. The following sections give an idea about what the available resources are

6. IMPLEMENTATION

Implementation covers the working procedures in GeoMedia Professional for generating thematic maps and bar charts. A brief is provided discussion on the consumption pattern on the energy along with thematic maps.

6.1 Working with GeoMedia Professional

The features with location data are in the GeoMedia warehouse and the most of the attribute data are in the MS Access database (Scharnhäuserpark.mdb). The attribute data includes building information like building name, owner's name number of stories and so on. The database also has information about energy and water consumption for each building. For visualization of these attributes data we need to establish a relationship between the database and the warehouse.

6.2 Performing Analysis

Once the connection is set up we can start processing data inside GeoMedia Professional. We are interested about consumption values per building in a unit of KiloWatt Hour (kWh/m²) per square meter for heating. As we have already the data about heating per building we only need the total heating area to have the consumption in desired unit. We can obtain the ground plan area using Analyze Geometry function in GeoMedia. This is saved in a query named Area of Ground Plan. Still the number of floors is necessary to calculate the approximate heating area for each building.

After a number of field visits to the project area in Ostfildern the database table Gebäude is updated with height information manually. In this table the field Stockwerke contains the height information in number of stories. Inside GeoMedia Professional the query containing ground area and the table (Gebäude) with building height are joined. Now the ground area and the building heights are available in a single query.

Using Functional Attribute query we can calculate the consumption values for each building in kWh/m². The arithmetic operation includes the division of annual consumption values by the product of ground area and number of floors. The output of this calculation is saved in a query under the name of Heatperunitarea.

6.3 Thematic Maps

A thematic map symbolizes geographic features according to non-graphic attribute data through the use of colour and other user-defined display properties (Intergraph 2005).

It can give the visual impression of non-spatial attribute data over the maps. For making thematic maps customized ranges are used from 0 to 250 where the difference between two successive classes is 50. The number actually refers to the unit of kWh/m². Consumption values for a particular

building can also be read from the legend entry in the thematic maps (Figure 2).

Logical zooming is applied for the layers with street names and house numbers. So the user can have more detailed information when he/she does more zooming. The query Heatingperunitarea is used as a data source for making thematic maps. But after finishing the thematic map preparation, when it was attempted to publish on the Internet using GeoMedia WebMap Publisher, it gave error message the processing pipe can not process the Geometry information. Transforming the query into Feature Class solved the problem.



Figure 2: Thematic map for heat consumption (2003)

Following the same procedure the thematic maps for the year 2002 and 2004 were created. Each of them was put under different map windows along with a set of rational legend entries.

6.4 Creating Bar Charts

There is one module developed by Prof. Dr. D. Schröder (Stuttgart University of applied Sciences, Stuttgart, Germany) that can be used along with GeoMedia Professional to create Bar Chart or Pie Chart for making comparison with different attributes of the feature classes.

Following the dialog box (**Error! Reference source not found.**3) bellow the bars for the year 2002, 2003 & 2004 have been created and put on thematic map from the year 2003 as this year is having maximum number of buildings with consumption data for heating. The bar charts facilitate users to visualize the fluctuation in consumption values for different years in a better way.



Figure 3: Thematic maps with bar charts

In the figure above each of the building has three bars indicating the corresponding heat consumption (kWh/m^2) for 2002,2003 and the third is for 2004(

Figure 3). The right most one is for 2002; the middle one is for 2003 and the rest is for 2004. The intensity of colour indicates the degree of consumption in base map.

7. MAP ON THE WEB

The web page is ready with maps and related attributes. It is not allowed to publish the energy and water consumption data for each building on the Internet due to the privacy policy. The page is released inside the university (Stuttgart University of Applied Sciences) Intranet as a test case and it is proven successful (Figure4). The page provides all the functionalities so far assigned to the thematic maps. It is possible to get access to the web page from any of the computers inside the university network. As per the request with the URL (http://193.196.137.99/Test_aneta), the page will appear on the client's machine. The type of the output map is SVG (Scalable Vector Graphics). This is why if the client machine does not have a viewer for SVG graphics, the page prompts for downloading the viewer (Adobe SVG Viewer 3). The page has title on the left upper corner. Just beneath the title, there is a tool bar holding a number of commands for online functions. The right frame holds the legend entries while the different map windows are in the left frame. The thematic map (heat consumption) for the year 2003 along with bar charts are set to default map window so it is activated at this point.

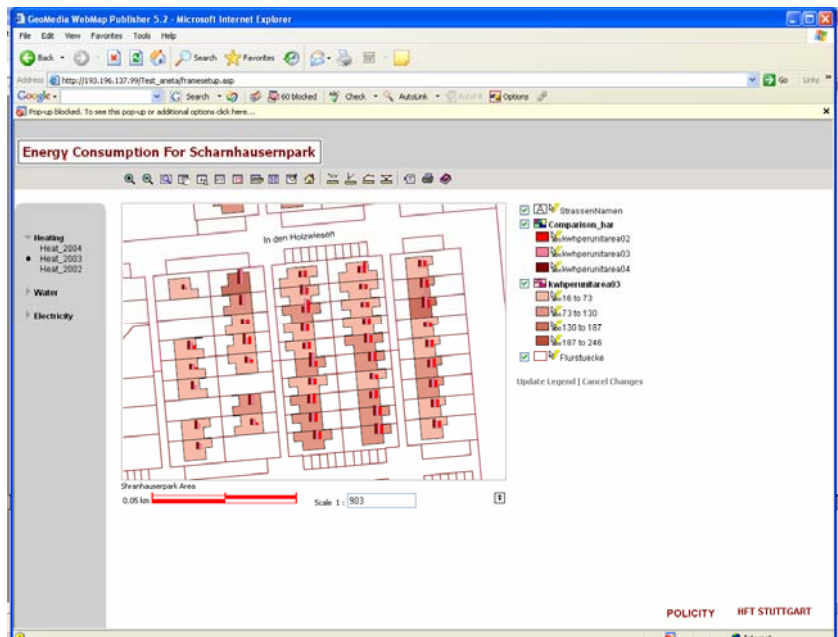


Figure 4: Overview of the page on the web

7.1 Tooltips

As the Tooltip for some features are already set, when the mouse is on the object it shows the attribute specified. For example once the mouse is over a building it will give a rectangular box with Building ID, Building Name, Use and the heating area of that building. In the figure below when the mouse is on the highlighted building it shows that the building ID is 8, name of the building is Sporthalle im Park and the approximate heating area (Figure5).

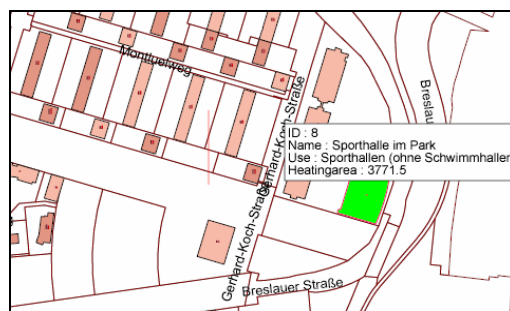


Figure 5: Map with Tooltip action

These functionalities are available for buildings having heat consumption values for different years. Bar charts are added to the thematic maps to visualize the comparison of heat consumption values for the years 2002, 2003 and 2004. When the user zooms into a single building three bars appear corresponding to heat consumptions for 2002, 2003 and 2004. Tooltips are also attached with these bars that show the values in kWh/m² for that particular building.

7.2 HotSpots

The Attribute of an object can also be viewed in a pop up dialog box by clicking on it. It is possible because of defined HotSpot actions associated with the feature class (buildings). For example the user can see heat energy consumption per m² in numbers for different years. The blank space beside Heatperunitarea indicates that this year does not have any consumption values for this particular building (Figure6).

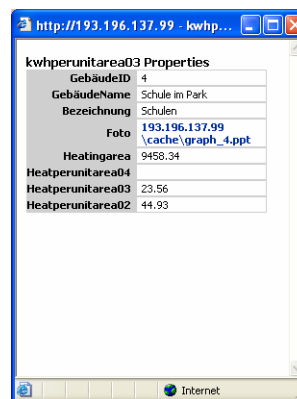


Figure 6: Property Popup box for feature

The client has the option to turn off any layer that is not desired. It can be performed by just checking out the check boxes against the layer.

8. CONCLUSIONS

A Web Portal was designed furnished with the maps and non-spatial attribute data for building energy and water consumption. The Portal provides a certain level of interactivity for the users like pan, zoom or viewing attributes. The Thematic Maps with Bar Charts show the amount of heat consumption for different years. Tooltips are assigned for mouse over action with attributes such as building ID, name and so on.

Analysis shows that the administrative & Health facility buildings consume much more heat energy than others. Electricity consumption is analyzed as per month for different years. In the year 2002 and 2003, the maximum electricity consumption occurred in May while in the next year (2004) buildings consumed most energy in April. The average electricity consumption value is 68.84 kWh/m² for these years. The data set for water and electricity consumption is not complete.

Only few buildings have data regarding water (8) and electricity (14) consumption. The consumption pattern found here in this project can change when the data set is completed.

In the PolyCity project working places, residential areas and green parks are designed in such a way that it will result in an integrated living environment with high comfort and energy efficiency. Low energy building standards are prescribed for all plots in the project area. 80 % of the total

energy demand will be supplied from renewable sources here in this project such as solar cells and biomass plant for generating electricity. Thus 30-38% of energy saving is expected in comparison to national standards.

The outcome of this paper will be integrated to the PolyCity project to make the city of Ostfildern energy efficient and comfortable for urban dwellers. Later this idea can be replicated in other cities in European countries. The result can also be interesting for urban planners, managers from utility supply companies, architects and engineers.

REFERENCES

- Intergraph. (2005): *GeoMedia Command Wizard*. Online Guide of GeoMedia Professional. Intergraph Corporation, USA.
- Murray, J. (2000). *Developing Internetbased GIS Applications*
http://www01.giscafe.com/technical_papers/Papers/papers058
- Patil, R., and Loony C. (2003). *Developing Dynamic GIS Web application*, Department of Computer Sciences, University of Nevada,
<http://www.scs.unr.edu>
- Plewe, B. (1997). *GIS Online: Information Retrieval Mapping and the Internet*. Santa Fe, New Mexico: On Word Press
- Web Links
<http://www.answers.com/biomass>
<http://www.wissenschaftwirtschaft-bw.de/index.php4>

COMPARATIVE ANALYSIS AND MONITORING OF URBAN HEAT ISLAND INTENSITY IN ASIAN MEGA CITIES BY MODIS

WATARU TAKEUCHI^{1,2}, KAWIN WORAKANCHANA^{1,2},
YOSHIFUMI YASUOKA² and VIVARAD PHONEKEO³
¹RNUS, Asian Institute of Technology, Thailand
²Institute of Industrial Science, University of Tokyo, Japan
³GIC, Asian Institute of Technology, Thailand
wataru@iis.u-tokyo.ac.jp

ABSTRACT

This study focuses on comparing the heat island intensity for cities in East and Southeast Asian mega cities and set up an operational monitoring system for them to quantify the relationship between surface temperature and biophysical land cover types. Aqua/Terra MODIS data received at Tokyo and Bangkok were used to monitor thermal conditions in 37 selected Asian mega cities. An operational monitoring system is set up in a near-real time fashion and is available at <http://webmodis.iis.u-tokyo.ac.jp/UHI>.

1. INTRODUCTION

The urban heat island (UHI) refers to the phenomenon of higher atmospheric and surface temperatures occurring in urban areas than in the surrounding rural areas due to urbanization. It is characterized by a large expanse of non-evaporating impervious materials covering a majority of urban areas with a consequent increase in sensible heat flux (Voogt and Oke, 2003). While atmospheric heat islands are normally measured by in situ sensors of air temperature via weather station networks, the surface UHI is typically characterized as land surface temperature (LST) through the use of airborne or satellite thermal infrared remote sensing, which provides a synoptic and uniform means of studying SUHI effects at regional scales (Yuan *et al.*, 2007). Satellite-measured LST has been utilized in various heat-balance, climate modeling, and global-change studies since it is determined by the effective radiating temperature of the Earth's surface, which controls surface heat and water exchange with the atmosphere.

The Institute of Industrial Science (IIS), University of Tokyo has been receiving NASA's satellites' Aqua/Terra Moderate resolution Imaging Spectro radiometer (MODIS) data starting from 2001 May in order to monitor the environment and disaster parameters around the East Asia. A MODIS can monitor the same location twice a day from visible to thermal infrared wavelength in discrete 36 channels. A MODIS-based monitoring project has been launched to analyze and assess the environment and disasters such as forest fire, flooding, agricultural activities, heat island

issues, sea surface temperature, vegetation phenology and so on (Ochi *et al.*, 2002). In order to acquire MODIS data for expanded continental-scale into Southeast Asian sub-region, IIS has provided MODIS receiving station at Geoinformatics Center (GIC), Asian Institute of Technology (AIT) and data to Geo Information, Space and Technology Development Agency of Thailand (GISTDA) through AIT.

The objective of this study is to compare the heat island intensity for cities in East and Southeast Asian mega cities and set up an operational monitoring system for them to quantify the relationship between surface temperature and biophysical land cover types.

2. METHODOLOGY

2.1 Study area

Figure 1 shows a map covering Asian mega cities selected in this study including Bangkok, Beijing, Busan, Chengdu, Chongqing, Colombo, Dhaka, Khabarovsk, Hanoi, Harbin, HoChiMinh, HongKong, Hyderabad, Jakarta, Kathmandu, Kolkata, KualaLumpur, Manila, Mumbai, NewDelhi, Osaka, PhnomPenh, PyongYang, Sapporo, Seoul, Shanghai, Shijiazhuang, Singapore, Taipei, Thimphu, Tokyo, Ulanbatar, Vientiane, Vladivostok, Wuhan, Xian, Yangon.

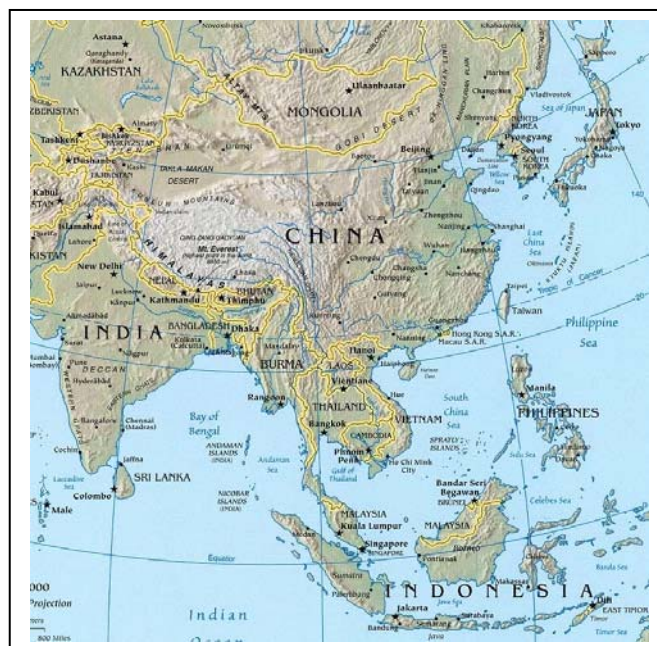


Figure 1: An area of interest in this study which is covered by MODIS receiving station installed at Tokyo and Bangkok.

2.2 MODIS Land surface temperature (LST)

Figure 2 shows a flow chart of land surface temperature mapping. Firstly, MODIS level1b data were processed into geo-coded level1b product and one-day mosaic image were generated covering 60N-S10 and 60E-150E on daytime and nighttime observations respectively. Secondly emissivity map were generated by a response function averaging supplemented by land cover map product and ASTER spectral library (Salisbury *et al.*, 1992). Then, land surface temperature map was generated by a generalized split window method and was applied in this study (Wan *et al.*, 1996). Finally, monthly land surface temperature of daytime, nighttime and difference between daytime and nighttime were generated by selecting maximum temperature on pixel basis to remove cloud contamination.

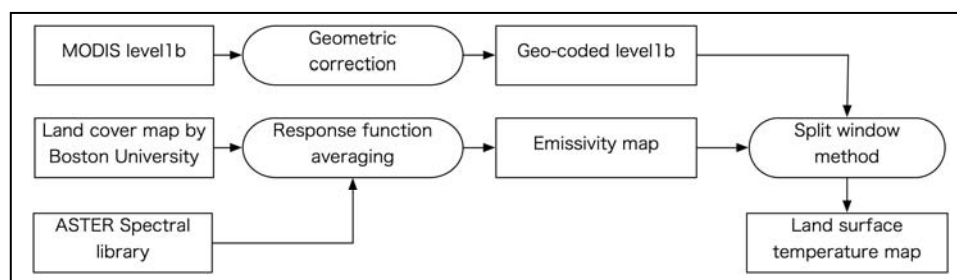


Figure 2: A flowchart of land surface temperature mapping by a generalized split window method using MODIS level1b, land cover map and spectral library over varieties of land cover types.

3. OPERATIONAL MONITORING SYSTEM

Figure 3 shows an operational monitoring system of urban heat island along with direct broadcasting of MODIS data at <http://webmodis.iis.u-tokyo.ac.jp/UHI/>. In our system, regional to continental scale disasters and environmental information can be achieved such as forest fire, heat island, land surface water, vegetation phenology and land cover or land use map.

Figure 4 shows a land surface temperature difference between day and night (left image), and land cover map (right) respectively for Bangkok, Tokyo and Shanghai. Color scale ranges from cooler to warmer colors with increasing temperature. Figure 4-(a) shows a thermal condition of Bangkok in Thailand on 2006 February in rainy season. A light blue area around 8-10 degrees in a left image of Figure 4-(a) corresponds to an urban area in a left image of Figure 4-(b) enhanced as a red color.

Figure 4-(b) shows an example of Tokyo in Japan on 2006 February in winter season. It is found that less temperature difference is found along coastal zones shown in bluish color whereas comparatively higher difference is clearly identified in inner area shown in green color. Much clear difference is visually interpreted in urban and sub-urban area as a heat island phenomenon.

Figure 4-(c) shows an example of Shanghai in China on 2006 August in summer season. This city is also affected by a wind coming from sea located in the east of the city and relatively higher temperature difference around 10 degrees in light blue correspond to an urban area which is represented as a red area by land cover map.

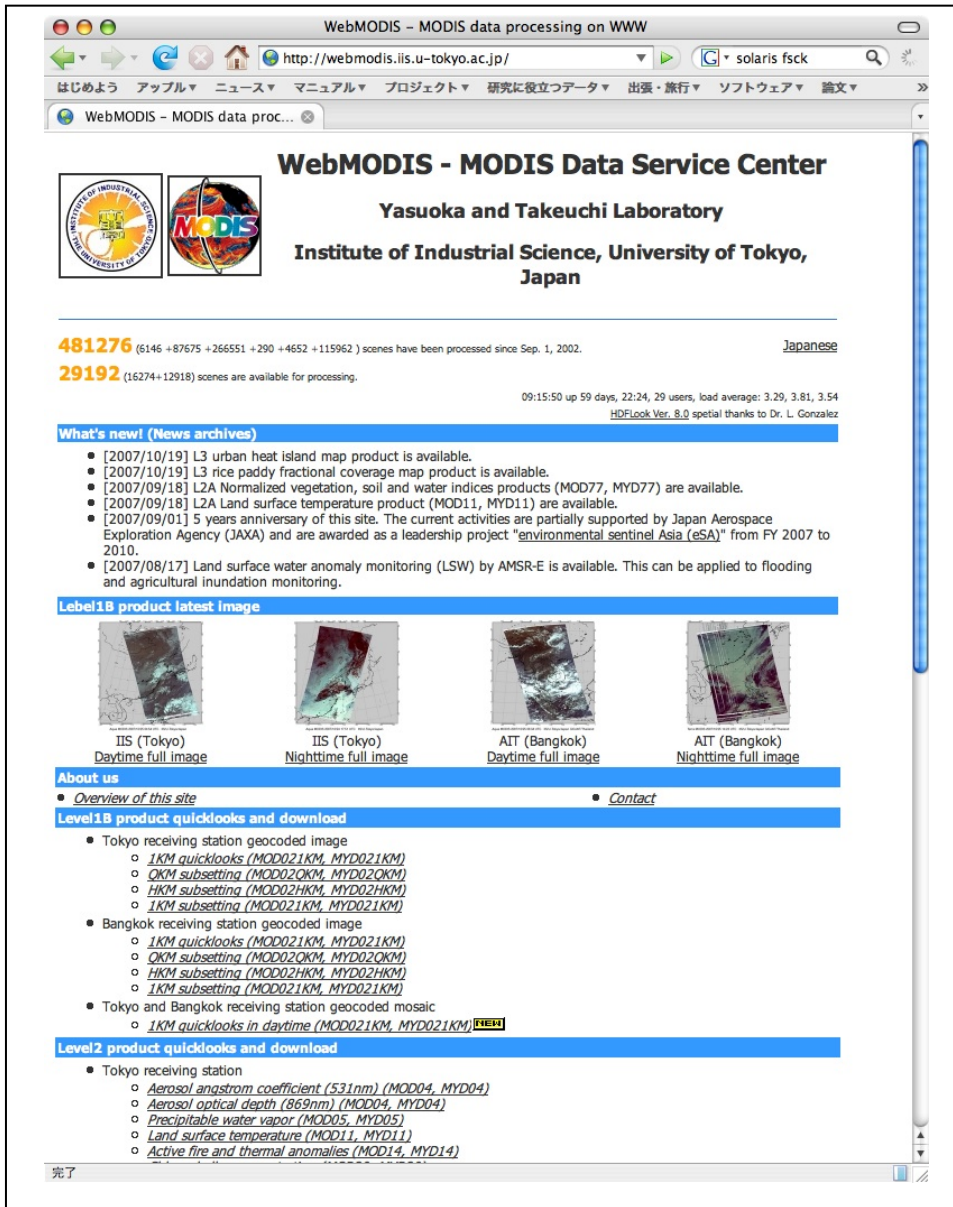


Figure 3: Web-based environment and disaster monitoring system such as forest fire, heat island, land surface water, vegetation phenology and land cover or land use map at <http://webmodis.iis.u-tokyo.ac.jp/UHI/>

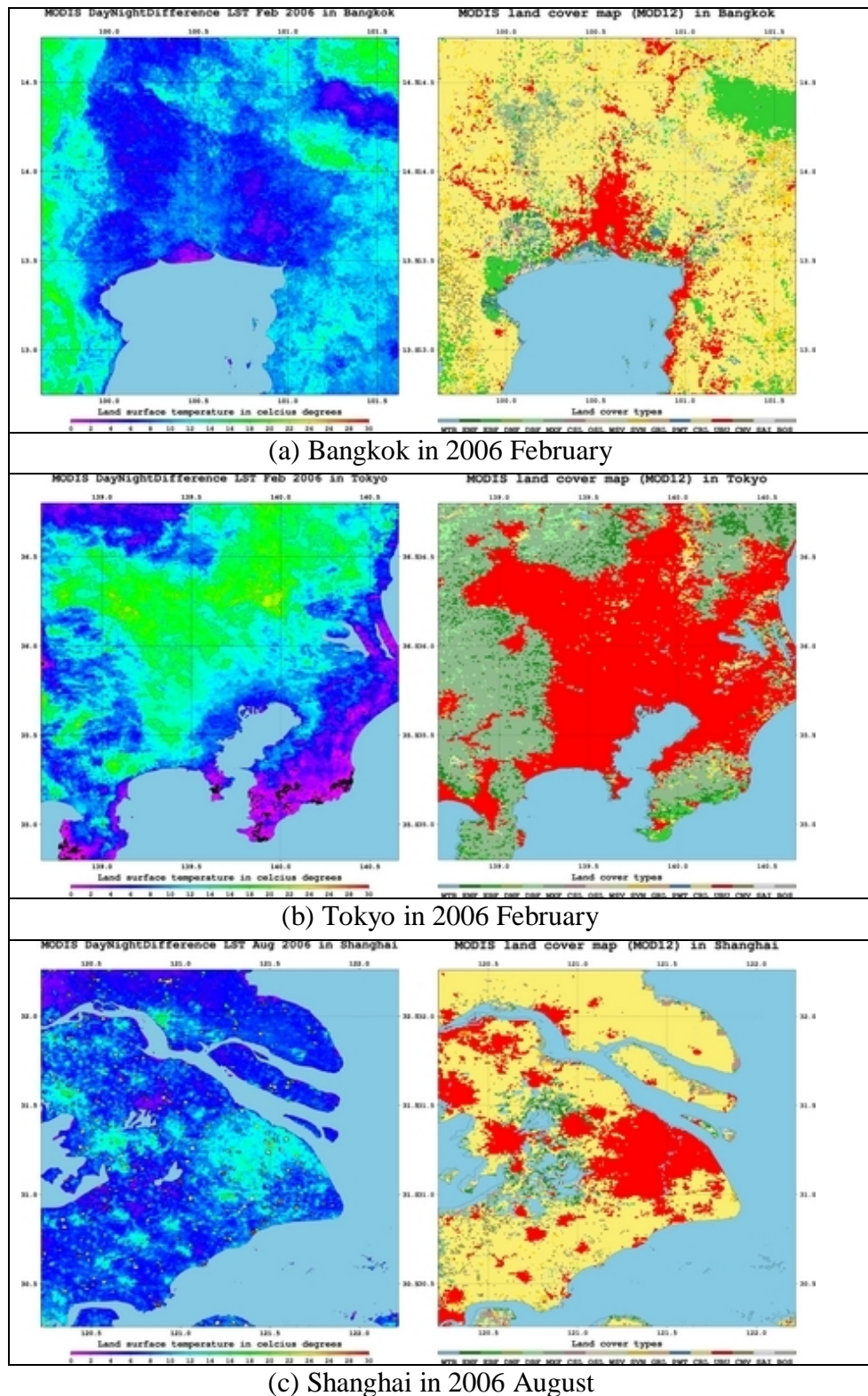


Figure 4: Land surface temperature difference between day and night (left image), and land cover map (right) respectively for Bangkok, Tokyo and Shanghai. Color scale ranges from black and cooler to warmer colors with increasing temperature.

4. CONCLUDING REMARKS

This study focuses on comparing the heat island intensity for cities in East and Southeast Asian mega cities and set up an operational monitoring system for them to quantify the relationship between surface temperature and biophysical land cover types. Aqua/Terra MODIS data received at Tokyo and Bangkok were used to monitor thermal conditions in 37 selected Asian mega cities. An operational monitoring system is set up in a near-real time fashion and is available at <http://webmodis.iis.u-tokyo.ac.jp/UHI/>

ACKNOWLEDGEMENT

This study is financially supported by the Japan Society for the Promotion of Science (JSPS) under the research project (Grant number: 19569002). The authors would like to thank JSPS for their support.

REFERENCES

- Dousset, B. and Gourmelon, F., 2003. Satellite multi-sensor data analysis of urban surface temperatures and landcover. *ISPRS Journal of Photogrammetry and Remote Sensing*, 58, 43-54.
- Yuan, F. and Bauer, M. E., 2007. Comparison of impervious surface area and normalized difference vegetation index as indicators of surface urban heat island effects in Landsat imagery, *Remote Sensing of Environment*, 106, 375-386.
- Nichol, J., 2005. Remote Sensing of Urban Heat Islands by Day and Night, *Photogrammetric Engineering and Remote Sensing*, 71(5), 613-621.
- Ochi, S., Uchihama, D., Takeuchi, W. and Yasuoka Y., 2002. Monitoring urban heat environment in East Asia. *GIS development*, 6(10), 18-20.
- Salisbury, J. W. and D'Aria, D. M., 1992. Emissivity of terrestrial materials in the 8-14 μ m atmospheric window, *Remote Sensing of Environment*, 42, 83-106.
- Small, C., 2006. Comparative analysis of urban reflectance and surface temperature. *Remote Sensing of Environment*, 104, 168-189.
- Voogt, J. A. and Oke, T. R., 2003. Thermal remote sensing of urban areas. *Remote Sensing of Environment*, 86, 370-384.
- Wan, Z. and Dozier, J., 1996. A Generalized Split-Window Algorithm for Retrieving Land-Surface Temperature from Space. *IEEE Trans. Geoscience and Remote Sensing*, 34, 892-905.
- Yuan, F. and Bauer, M. E., 2007. Comparison of impervious surface area and normalized difference vegetation index as indicators of surface urban heat island effects in Landsat imagery. *Remote Sensing of Environment*, 106, 375-386.

NUMERICAL SIMULATION OF ATMOSPHERIC POLLUTION OVER KANTO AREA USING THE MM5/CMAQ MODEL “SIMULATION OF OZONE CONCENTRATION BETWEEN TWO DIFFERENT WEATHER DAYS”

M.V.KHIEM

Institute of Industrial Science, University of Tokyo,
khiem@iis.u-tokyo.ac.jp

R.OOKA

Institute of Industrial Science, University of Tokyo,
ooka@iis.u-tokyo.ac.jp

H. HUANG

Institute of Industrial Science, University of Tokyo,
hhong@iis.u-tokyo.ac.jp

H. HAYAMI

Central Research Institute of Electric Power Industry,
1646 Abiko, Abiko-shi, Chiba-ken 270-1194, Japan.
haya@criepi.denken.or.jp

ABSTRACT

It is known that in summer, Ozone (O_3) concentration in urban areas can be strongly affected by local climatic condition in which some meteorological factors play an important role such as precipitation, cloud, fog especially urban heat island (UHI). In this study, we use the MM5/CMAQ model to investigate influence of climatic change on the atmospheric pollution over Kanto area with two case studies; (1) simulation period with mild weather, and (2) the period that it's hot and clear weather pattern associated with climatic change. The 3 domains, which cover a region of Kanto with grid resolutions of 9 km, 3 km, and 1 km respectively, have been employed for this study. Numerical simulation results showed that: (1) Atmospheric pollution was strongly effected by urban heat island event; (2) the high temperature and weak wind speed lead to significantly increase O_3 concentration; (3) simulated O_3 temporal trends showed good agreement with observation. However, the simulated O_3 in the night tends to overestimate and in case of July maximum O_3 is also higher than observation about 10 – 30 ppbV, this may relate to calculating on the vertical diffusion coefficient in the MM5 model and initial and boundary conditions of CMAQ model. This will be investigated in the next work.

1. INTRODUCTION

In recent years, the air pollution has become an important problem in parallel with the increasing energy use. The sources of the pollutants are the emissions from the industrial facilities, motor vehicles and heating systems. The meteorological factors such as precipitation, cloud, fog especially urban heat island (UHI) play an important role in the concentration of the atmospheric pollutants. (Chao, 1990; Cuhadaroglu, et al, 1977; Escourrou, et al, 1990; Miyazaki, et al, 1991; Lacour, et al, 2006;). Conversely, atmospheric pollution also has important effects in modifying urban climate in various ways such as by increasing long-wave radiation from the sky in the canopy layer, and increasing absorption of short-wave radiation in the boundary layer. It is found that UHI can raise the rate of chemical reaction between nitrogen oxides (NO_x) and Volatile Organic Compounds (VOCs), this lead to significantly increase surface ozone concentrations in city areas(Dewent, et al, 2003). In this paper, we would like to investigate influence of climatic change on the atmospheric pollution over Kanto area using two case studies; (1) simulation period with mild weather, and (2) the period that it is the hot and clear weather pattern associated with climatic change.

2. MODEL DESCRIPTION

2.1 Meteorology model

The Fifth-Generation NCAR / Penn State Mesoscale Model (MM5) version 3.7, a limited-area, nonhydrostatic, terrain-following sigma-coordinate model(Dudhia, et al, 2005), is used in this research to provide spatial and temporal distribution of meteorological fields to the air quality model. It has some characteristic such as: (i) a multiple-nest capability, (ii) nonhydrostatic dynamics, which allows the model to be used at a few-kilometer scale, (iii) multitasking capability on shared- and distributed-memory machines, (iv) a four-dimensional data-assimilation capability (FDDA), and (v) more physics options.

2.2 Air Quality modeling

The Community Multi-scale Air Quality (CMAQ) modeling system version 4.6 developed by Environmental Protection Agency (USA), which was released in 2006, was used in this study. It is a multiple scale and multiple pollutant chemistry-transport model that includes all the critical science processes such as atmospheric transport, deposition, cloud mixing, emissions, gas- and aqueous-phase chemical transformation processes, and aerosol dynamics and chemistry. The CMAQ system can simulate concentrations of troposphere ozone, acid deposition, visibility, fine particulate and other air pollutants in the context of “one atmospheric” perspective involving complex atmospheric pollutant interactions on regional and urban scales.

3. ANALYSIS OUTLINE

3.1 Analysis domain

In this study, the MM5 simulation was performed with 3 nested domains (Figure 1).

Detail configuration of model is summarized in Table 1. The 3 domains cover a region of Kanto with grid resolutions of 9 km, 3 km, and 1 km, respectively. The second domain size is 73x88 grid points and the third domain is 100x121 grid point. All of the domains have 23 vertical sigma levels from the surface to the 100-hPa level.

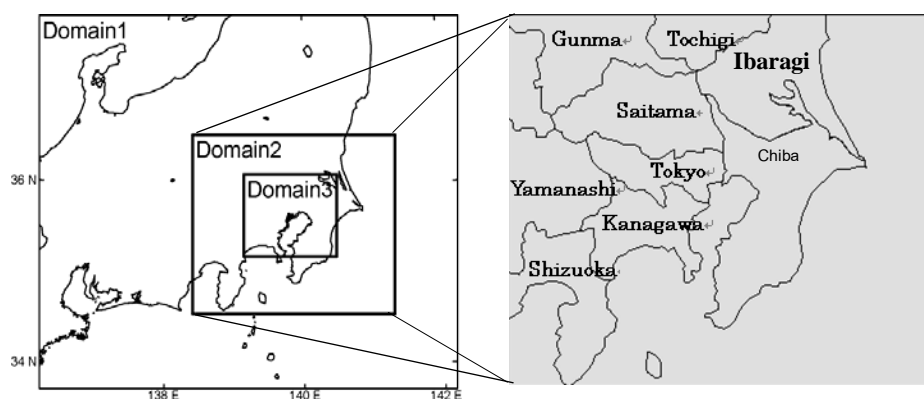


Figure1: Analysis domain

Table 1: Analysis size domains and grid resolution

	Computation domain (X[km] x Y[km])	Grid number	Horizontal resolution (km)
D1	450x540	51x61x23	9
D2	216x261	73x88x23	3
D3	99x120	100x121x23	1

3.2 Model configuration

In this study, the physics options in the MM5 simulation are following: Grell cumulus parameterization scheme (Grell, et al, 1994); MRF planetary boundary layer scheme (Hong, et al, 1996); explicit simple ice microphysics (Hsie, et al, 1984); cloud-radiation scheme (Dudhia, 1989) and FDDA. The cumulus parameterization scheme is not used for the 3 and 1-km domains. The CMAQ was configured with the following options: (1) CB-IV speciation with aerosol and aqueous chemistry; (2) the Piecewise Parabolic Method for both horizontal and vertical advection; (3) eddy vertical diffusion; (4) photolysis; (5) no Plume-in-Grid; (6) the EBI chemistry solver configured for CB05; (7) use of the 3rd-generation aerosol model; (8) use of the 2nd-generation aerosol deposition model; (9) use of RADM cloud model; (10) 14 vertical layers. More detailed description of the scientific mechanisms and implementations of CMAQ can be found in Byun and Ching (Byun and Ching, 1999).

3.3 Study period and simulation condition

In this study, the MM5 simulation is done 96 hours with two periods: (1) with the mild weather, starting from 09 JST July 19 to 09 JST July 23, 2005; and (2) with the hot weather pattern associated with UHI event over Tokyo area, starting from 09 JST August 03 to 09 JST August 07, 2005. A meteorological condition with weak surface wind and high temperature in August case is favorable for photochemical production of ozone. Global meteorological data (FNL) from NCAR with horizontal resolution of $1^0 \times 1^0$ was used to provide initial and boundary conditions for MM5 model and FDDA process. Hourly emission data used here are the horizontal 3km x 3km emission estimated by Hayami et al. (Hayami, et al, 2004) (Figure 2). After completing MM5 simulation, two periods from 00JST on 20 to 00JST on 23 July and from 00JST on 04 to 00JST on 07 August have been run for CMAQ model in domain 2 with the initial and boundary condition were derived from the observation report of Japan Clean Air Program (Table 2). Finally, the result of CMAQ model in domain 2 aimed to produce initial and boundary conditions for CMAQ runs in domain 3 with two periods from 00 JST on 21 to 00 JST on 23 July and from 00 JST on 05 to 00 JST on 07 August.

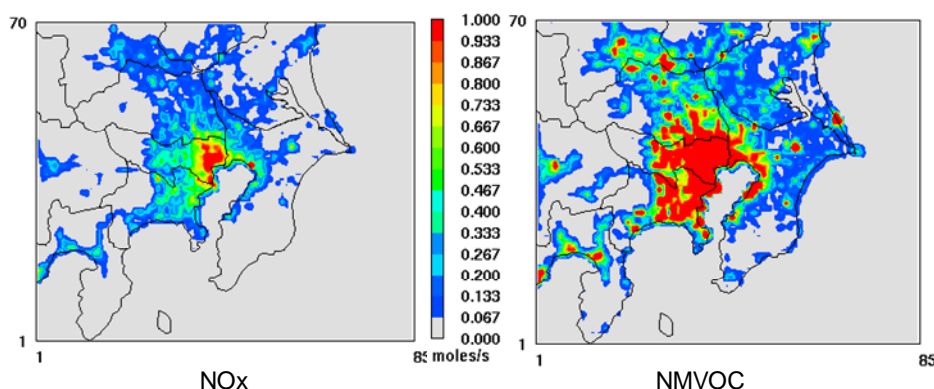


Figure 2: Hour emission data for CMAQ at 14 JST August 6 (mole/s/grid)

Table 2 : Initial and boundary condition for CMAQ model (JCAP, 1999)

Species	O ₃	NO _x	ALD	FORM	ETH	OLE	TOL	XYL	ISO	PAR
ICs	28	6.0	1.8	2.2	1.4	1.6	14.4	0.6	0.5	74.3
BCs	N	28	6.0	1.8	2.2	1.4	1.6	14.4	0.6	74.3
	E	25	6.0	1.8	2.2	1.4	1.6	14.4	0.6	74.3
	S	30	6.0	0.9	1.1	1.3	0.4	6.0	0.7	37.8
	W	28	6.0	2.0	2.4	3.2	4.2	11.4	0.7	82.7

4. RESULT AND DISCUSSION

Figure 3 shows the spatial distribution of the 2m temperature and 10m wind from MM5 simulation in domain 2 at 14 JST. In the case of July, the temperature is low and the northeasterly wind is strong, most of Kanto area was dominated by easterly and northeasterly winds. For the case of August, the weather pattern associated with UHI event, we can see the region of

temperature higher than 34°C cover Tokyo metropolitan at 14 JST on August 6 and the horizontal wind speed is a little weak. This meteorological situation supports the development of a sea breeze circulation, therefore the atmospheric pollution in the northern cities of Kanto area will be strongly influenced by UHI event. This difference in meteorological condition between two above mentioned periods can influence on atmospheric pollution over Kanto area.

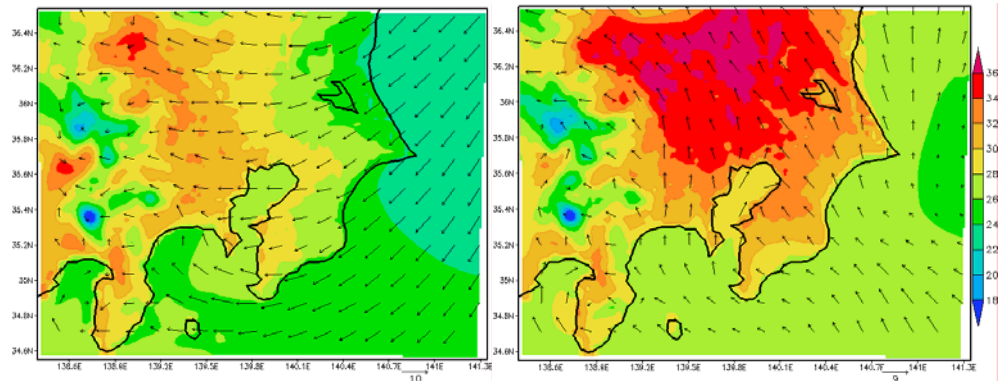


Figure 3: The MM5 simulated Temp (oC) & wind in D2 at 14 JST

Figure 4 is the spatial distribution of hourly O₃ concentration predicted by CMAQ model in domain 2 at 14 JST on July 22 and at 14 JST on August 6. The result showed that atmospheric pollution concentration under hot and clear weather condition is higher than that under mild condition (July 22) and the area with high O₃ concentration in August is also larger. In the case of July, because of the northeasterly wind, O₃ concentration is diffused to the southwestern part of Kanto. It was found the area higher 90 ppbV in Shizuoka. In the August, however, it was found that a high O₃ concentration area covers almost the northwestern part of Kanto due to transition of the south and southeastern flow predicted by MM5. Because of this direction wind some cities in the northern such as Saitama, Gunma, and Tochigi have O₃ concentration very high (more than 90 ppbV). Comparison of averaged O₃ concentration simulation of some cities between the case of July and the case of August is illustrated on Figure 5. From this Figure we can see O₃ concentration remarkably increases on the hot day (August 6) in comparison with that on the mild day (July 22). The difference of O₃ concentration can reach 10 - 30 ppbV.

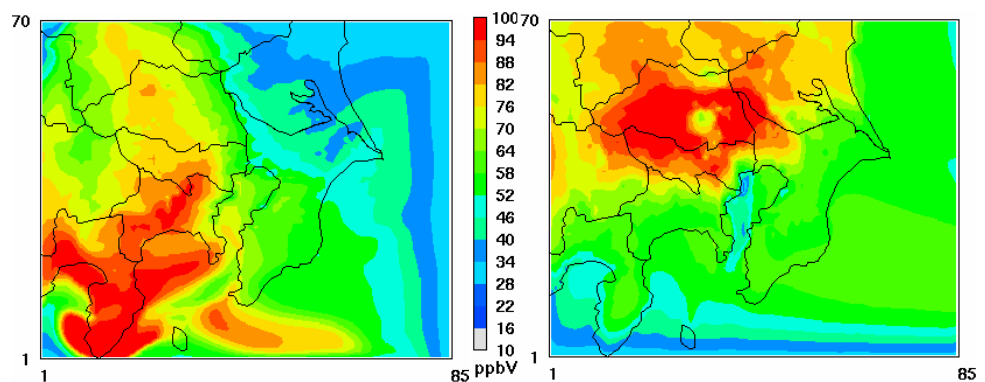


Figure 4: The CMAQ simulated Ozone concentration (ppbV) in D2 at 14 JST

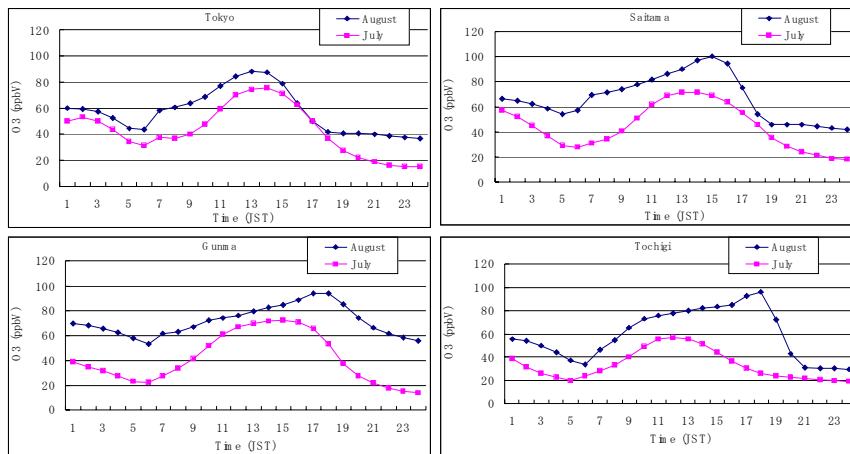


Figure 5: Comparison of averaged O_3 simulation between mild and hot day

5. VALIDATION OF MM5 SIMULATION

In order to validate the simulation of MM5 model, we compared the 2m temperature and 10m wind velocity with measured data at some stations in Kanto area; Ebina(Kanagawa), Kumatani(Saitama), Kofu(Yamanashi), Nerima(Tokyo), Hachiouji(Tokyo), and Fuchu (Tokyo) (Figure 6). For temperature on Figure 9 and Figure 10, MM5 simulate well its diurnal variation in all prediction periods (0-72h) at all stations. However, the minimum temperature intends to overestimate on the hot day (August). For wind velocity, on Figure 11 and Figure 12 we can see the MM5 model simulations agree well with measured data in term of diurnal variation, but the MM5 does not simulate small variation of observed wind velocity. This may relate to parameterization of boundary layer in model.



Figure 6: Monitor stations used for MM5

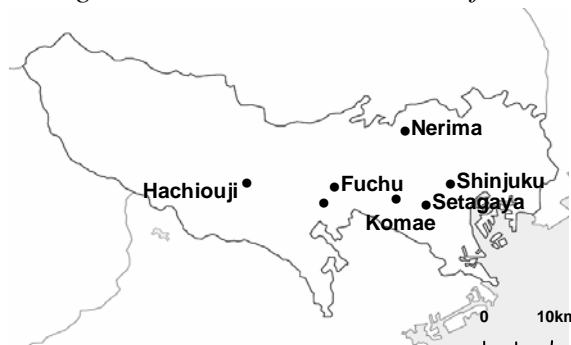


Figure 7: Monitor stations used for CMAQ

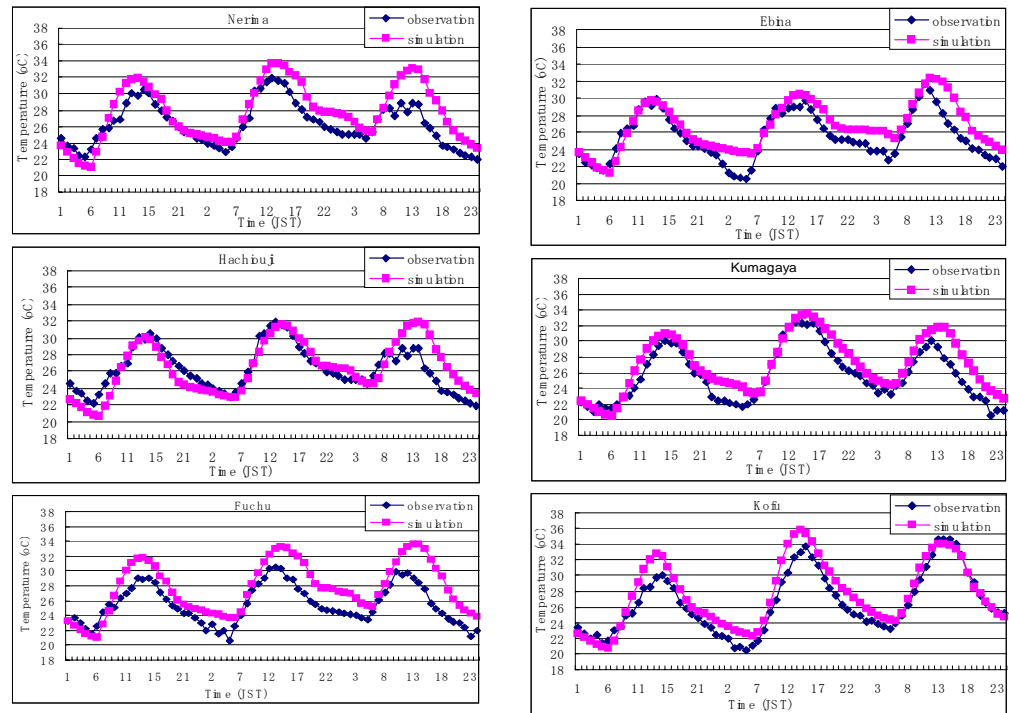


Figure 9: Temperature (2 m height) variation of observation and simulation during 20-22 July 2005 at some stations

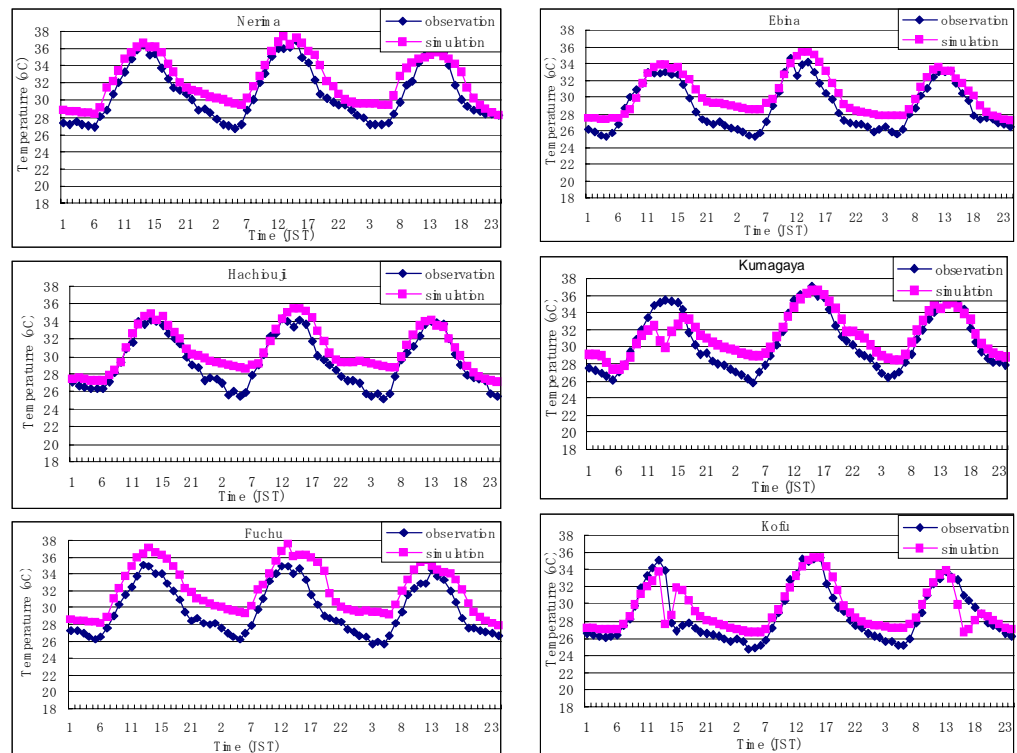


Figure 10: Temperature (2 m height) variation of observation and simulation during 4-6 August 2005 at some stations

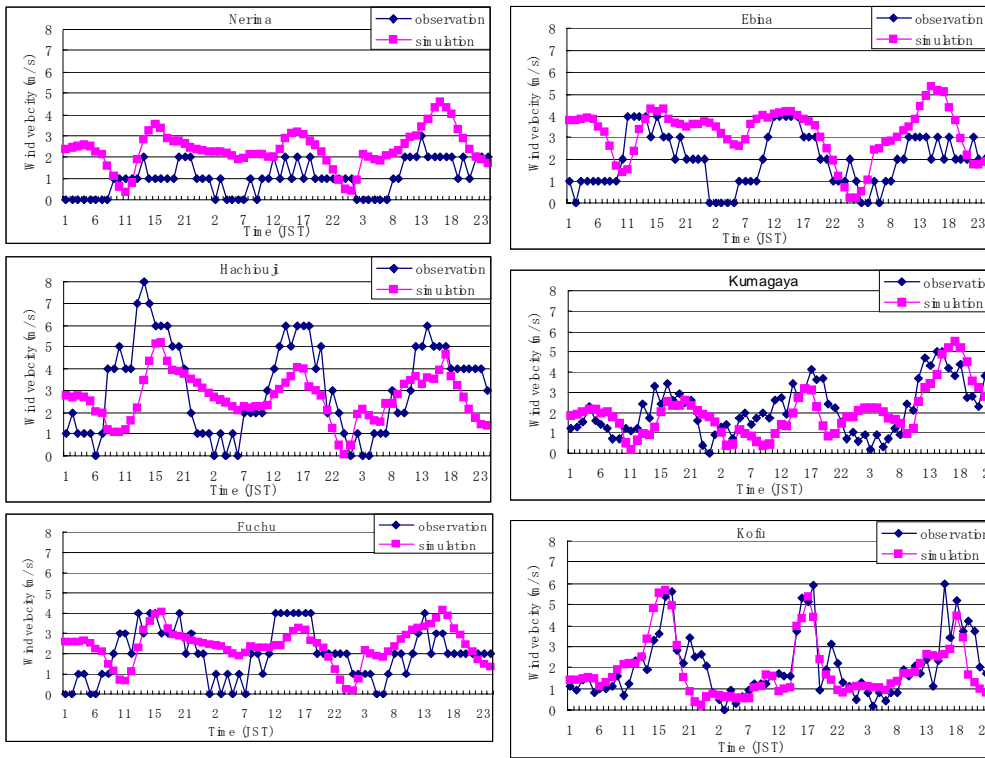


Figure 11: Wind velocity (10 m height) variation of observation and simulation

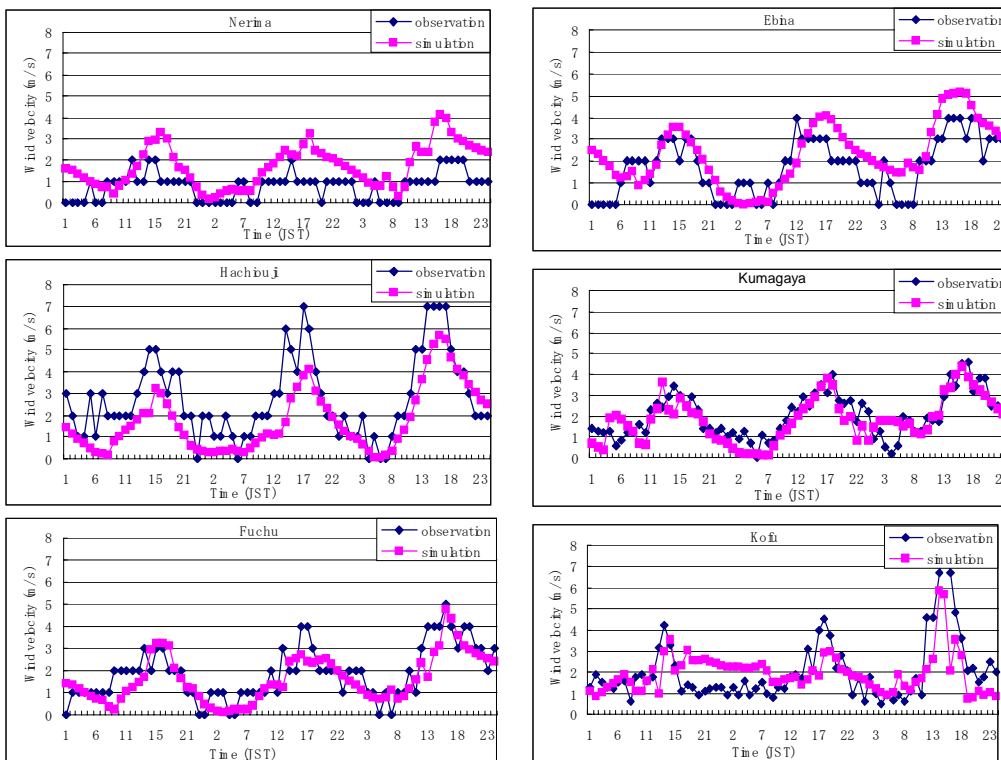


Figure 12: Wind velocity (10 m height) variation of observation and simulation during 4-6 August 2005 at some stations

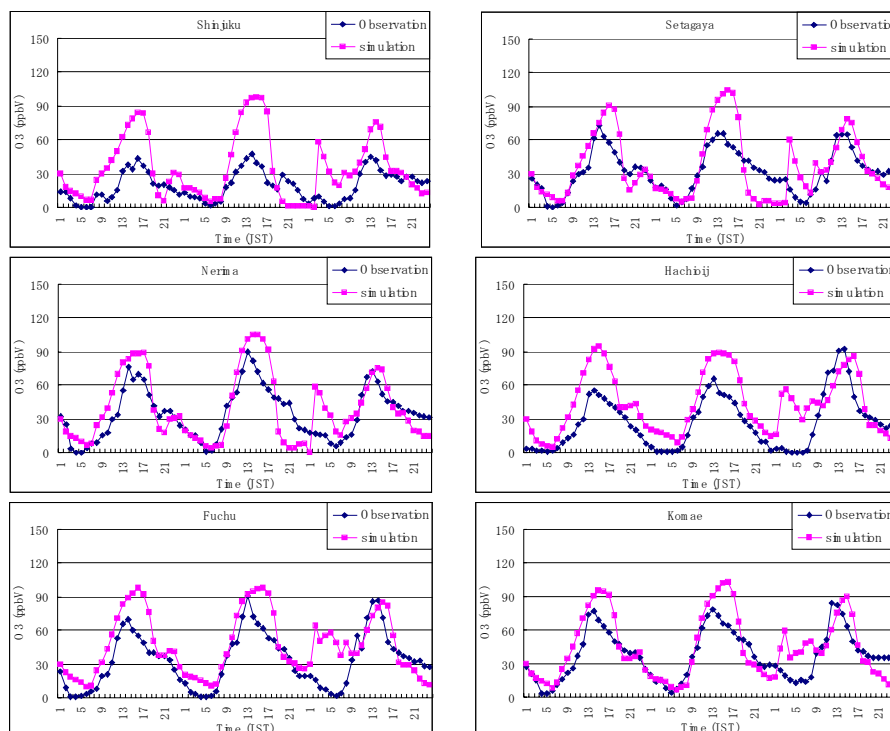


Figure 13: Ozone time series variation of observation and simulation during 20-22 July 2005 at some stations

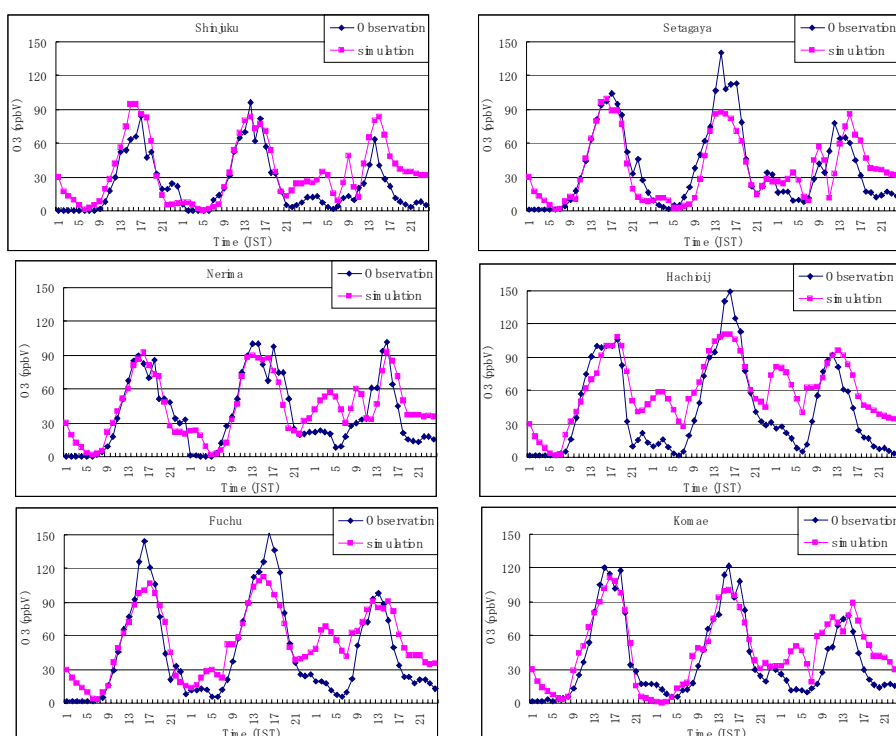


Figure 14: Ozone time series variation of observation and simulation during 4-6 August 2005 at some stations

6. VALIDATION OF OZONE CONCENTRATION

In this study, the results from the CMAQ model in domain 2 were compared with measured data from 10 air quality monitoring stations located within the Tokyo city; Shinjuku, Setagaya, Nerima, Hachioji, Fuchu, and Komae, which are shown in Figure 7. Figure 13 and Figure 14 show the ozone time series comparison between the CMAQ simulation and observations at the 6 Tokyo monitoring stations for the case of July and the case of August. Generally, simulated O₃ concentration tendency showed good agreement with observations. However, the simulated O₃ concentration in the night tends to overestimate and in case of July maximum O₃ is also higher than observation about 10 – 30 ppbV, this may relate to calculating on of the vertical diffusion coefficient in the MM5 model and initial and boundary conditions of CMAQ model.

7. CONCLUSIONS

The MM5/CMAQ model applied to simulate influence of urban climatic change on atmospheric pollution. In general, CMAQ simulated O₃ concentration showed a good agreement with the observation for both two periods. The results indicate that the high temperature and weak wind speed under UHI event lead to significantly increase averaged O₃ concentration of Tokyo city. Compare with mild day, the O₃ concentration in hot and clear day can increase 10 - 30 (ppbV) at some cities. From this research, it is said that effect of UHI event on atmospheric environment is very significant. However, the maximum O₃ is higher than observation and for the July 22 case, and simulated O₃ concentration overestimates in the night. Some reasons which could cause these discrepancies such as meteorological condition predicted by MM5, initial and boundary conditions for O₃, NO_x and VOC, emission data and so on, these factors also need to be considered in generation and distribution of O₃ concentration.

REFERENCES

- Byun, D and Ching, J., 1999, *Science algorithms of the EPA Models-3 Community Multiscale Air Quality (CMAQ) modeling system*, US Environmental Protection Agency, EPA-600/R-99/030.
- Chao, Z., 1990, Urban climate and air pollution in Shanghai, *Energy Buildings*, 15, 647–656.
- Cuhadaroglu, B. et al., 1977, Influence of some meteorological factors on air pollution in Trobzan city, *Energy Buildings*, 25, 179–184.
- Derwent, et al., 2003, Photochemical ozone formation in north west Europe and its control, *Atmos. Env.*, 37, 14, 1983–1991.
- Dudhia, J., 1989, Numerical study of convection observed during the Winter Monsoon Experiment using a mesoscale two-dimensional model, *J. Atmos. Sci.*, 46, 3077–3107.
- Dudhia, J. et al., 2005, *PSU/NCAR Mesoscale Modeling System. Tutorial Class Notes and User's Guide: MM5 Modeling System Version 3*.
- Grell, G. et al., 1994, A description of the Fifth-Generation Penn

- State/NCAR Mesoscale Model (MM5), NCAR Technical Note, NCAR/TN-398+STR.
- Hayami, H., Kobayashi, S., 2004, *Modeling of Concentration of Atmospheric Secondary Aerosol*, CRIEPI Report T03037, 17.(in Japanese).
- Hong, S.-Y. et al., 1996, Nonlocal boundary layer vertical diffusion in a medium-range forecast model, *Mon. Wea. Rev.*, 124, 2322-2339.
- Hsie, E.-Y. et al., 1994, Numerical simulation of frontogenesis in a moist atmosphere, *J. Atmos. Sci.*, 41, 2581-2594.
- JCAP, 1999, *Air Modeling (4), Observation results of Kanto area in summer*, Technical Report of Japan Clean Air Program. (in Japanese)
- Miyazaki.T et al., 1991, Meteorological factors causing high dust concentration, *Energy Buildings*, 15, 691-698.

AUTOMATIC AND REAL-TIME BRIDGE HEALTH MONITORING FOR HEAVY TRAFFIC ROUTES

SANAE MIYAZAKI
ICUS, IIS, The University of Tokyo, Japan
NTT DATA Corporation, Japan
miyazaks@iis.u-tokyo.ac.jp

YUJI ISHIKAWA
NTT DATA Corporation, Japan
ishikawayuj@nttdata.co.jp

TAKAHIDE OKUBO
Metropolitan Expressway Company Limited, Japan
okubo85@shutoko.jp

KIMIHIKO IZUMI
Technology Center of Metropolitan Expressway, Japan
izumi@tecmex.or.jp

EIICHI SASAKI
Yokohama National University
esasaki@cvg.ynu.ac.jp

CHITOSHI MIKI
Tokyo Institute of Technology, Japan
miki@cv.titech.ac.jp

ABSTRACT

A real-time bridge remote monitoring system for a quick detection of the damage caused by earthquakes and for a reliable measurement of the damage caused by its aging was developed. The system is consisted of various sensors, high-speed data transmission networks, and an information center that produces high-level information associated with the bridges-health. A demonstration system was developed on a Metropolitan expressway in Tokyo, Japan, where many heavy vehicles over regulation weight passes on. By this system, the reliability and the durability of our system was confirmed.

1. INTRODUCTION

Around 40% of Japanese bridges were constructed about 40 years ago, and they have various kinds of damage known or unknown, serious or non-serious in recent years. Even these old bridges have to be remained in service with effective maintenance because of a recent review of public

investments. Both strong earthquakes and the daily use can trigger serious disasters similar to a Minneapolis bridge collapse on Japanese bridges in a few years, and also its damage might be very huge especially in mega city areas. A quick and time-serial reporting of quantitative diagnoses to road administrators associated with bridges-health measured using scientific systems would be extremely important to establish a sustainable city. In this paper, a concept of our real-time bridge remote monitoring system using various sensors, such as video cameras and various kinds of fiber-optic sensors for a quick detection of the damage caused by earthquakes and for a reliable measurement of the damage caused by its aging was described. A demonstration system developed on Metropolitan expressway in Tokyo, Japan was also introduced.

2. SYSTEM ARCHITECTURE

The advantage of our system is on its ability to monitor the time-serial condition of bridges automatically from remote locations in real-time without electric power supply at the field. Ensuring this, as shown in Figure 1, our bridge monitoring system is consisted of five subsystems; sensor subsystem, data transmission subsystem, data analyzing subsystem, diagnosing subsystem and administration support subsystem. The detail is as follows.

2.1 Sensor Subsystem

In our monitoring system, various sensors, namely video camera and fiber-optic sensors such as strain gauges, displacement meters, inclinometers and accelerometers are attached to each bridge as a sensor subsystem. Figure 2 shows the example of these sensors.

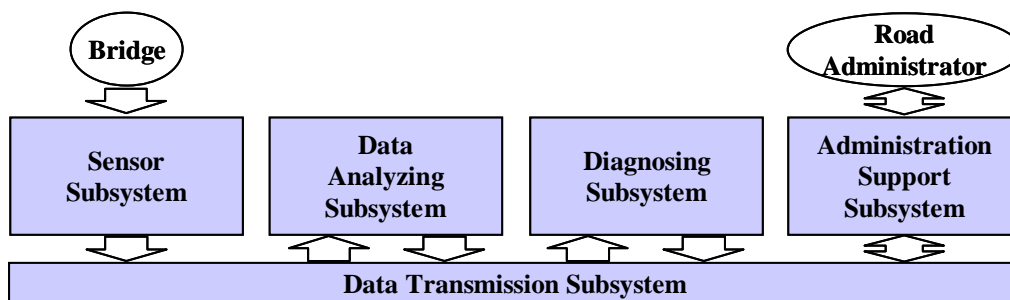


Figure 1: System architecture

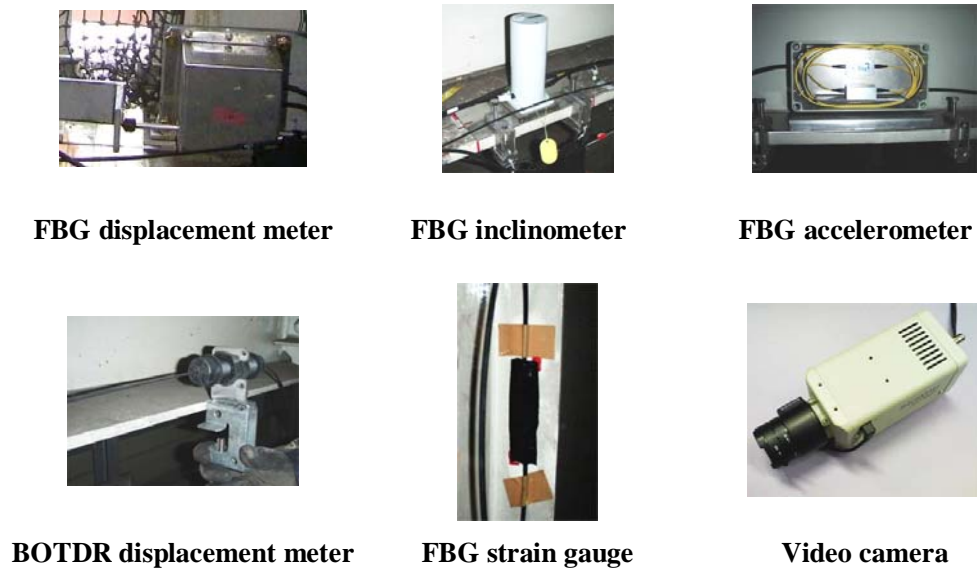


Figure 2: Example of sensors

2.2 Data Transmission Subsystem

The data measured by the sensor subsystem is automatically transmitted to the data analyzing subsystem using the data transmission subsystem. We can choose the data transmission technology, e.g. the Internet, fiber-optic communication, wireless communication, etc., appropriately to the needs of a road administrator according to its reliability, capacity, cost, etc.

2.3 Data Analyzing Subsystem

The data transmitted from the sensor subsystem using the data transmission subsystem is stored in the database, and then various calculations and analyses are automatically done using the data analyzing subsystem.

2.4 Diagnosing Subsystem

As a next step, the diagnosing subsystem generates the gap information between the measurement data and the pre-known normal data using the output of the data analyzing subsystem. The gap information is represented in three ranks, namely “large”, “small” and “non”.

2.5 Administration Support Subsystem

The administration support subsystem visually provides the information generated by the data analyzing subsystem and the diagnosing subsystem to support road administrators for the decision of their next actions, etc.

3. FEASIBILITY STUDY ON HEAVY TRAFIC ROUTES

As a feasibility study, a demonstration system was developed on Metropolitan expressway, which consists mostly of bridges, in Tokyo, Japan. The reliability and the durability of the system was also examined.

3.1 Overview of our demonstration system

Figure 3 shows a geographical location of our demonstration system. The detail of our test site and our system are as follows.

3.1.1 Test site characteristics

Our test site is Komazawa and Sangen-jaya on the route No.3 of Metropolitan expressway that is one of the heaviest traffic routes in Tokyo Metropolitan City, where many heavy vehicles over regulation weight passes on. The route No.3 of Metropolitan expressway, which wholly consists of bridges, was constructed in the middle of 1960's, and about 110,000 vehicles, including 30% heavy vehicles, pass through this route per day; namely 50,000 vehicles go toward the metropolitan core, and 60,000 vehicles go away from the metropolitan core. Therefore, both aging damage and daily damage caused by the traffic are extremely serious in our test site, and practically various maintenance is enforced on the route perpetually.

3.1.2 System configuration

Our demonstration system is consisted by five parts in accordance with our system architecture described in Section 2. As shown in Figure 3 and 4, the sensor subsystem is set between Komazawa and Ikejiri on the route No.3 of Metropolitan expressway. We use twenty-four FBG displacement meters, eight BOTDR displacement meters, eight FBG inclinometers, twelve FBG strain gauges, four FBG accelerometers and two FBG heat gauges for our measurement. The data measured using these sensors is collected at Ikejiri local station located 1.8 km away from Komazawa (and 5 km dummy fiber is added for our experiment), and is transmitted to the data analyzing subsystem in our information center located at Otemachi IDC by using the data transmission subsystem; here we use a fiber optic communication network provided by NTT, and then the data is calculated and analyzed for generating measurement data and diagnosis information using the data analyzing subsystem and the diagnosing subsystem, respectively. After that, measurement data and diagnosis information are transmitted to the administration support subsystem located at the road administrator's office, Toranomom by using a similar data transmission subsystem, and then they are visually provided to the road administrators for supporting their decision making.

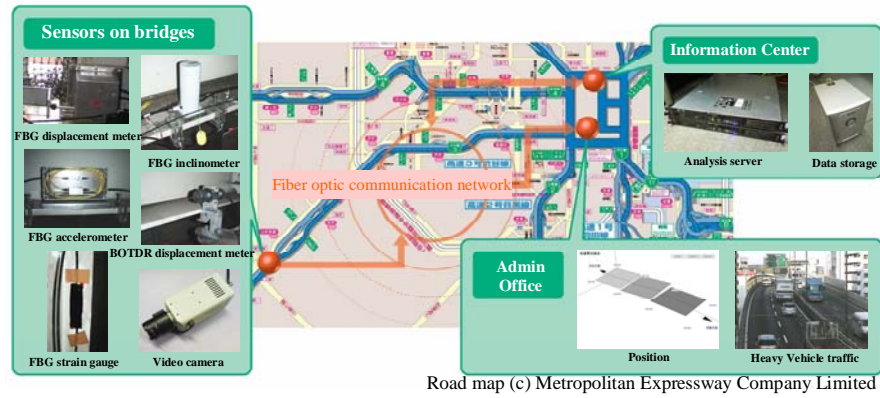


Figure 3: Geographical location of our demonstration system

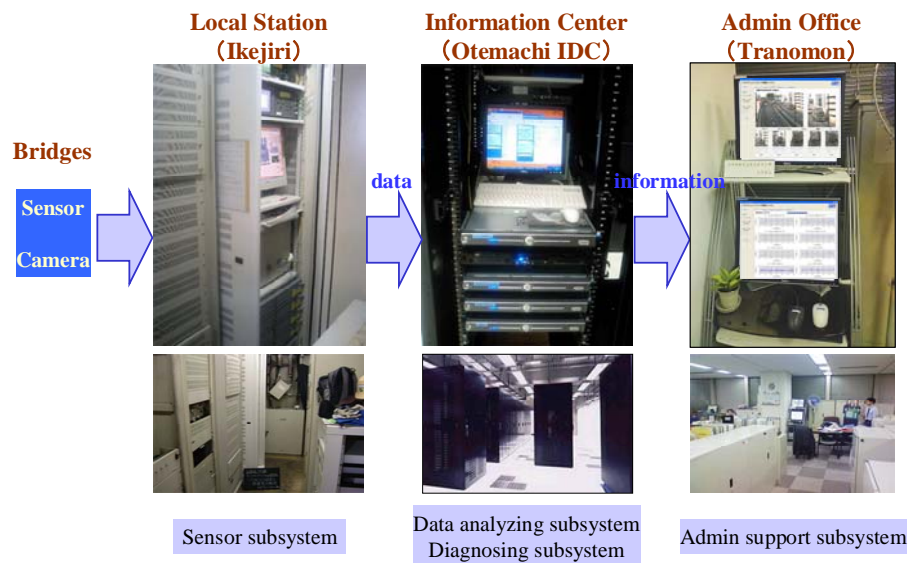


Figure 4: Data and information flow

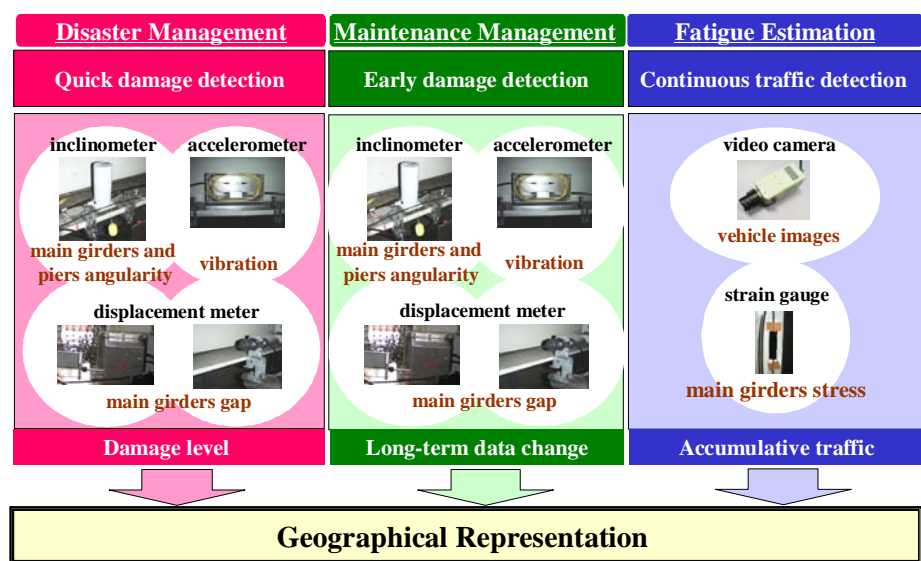


Figure 5: Output information

3.1.3 Measurement items

Figure 5 shows the data and information provided by our demonstration system corresponding to each sensor. As shown in figure 5, we provide them for three purposes, namely the disaster management, the maintenance management and the fatigue estimation, that are indispensable to the bridge management. Only one sensor system is required both for the disaster management and the maintenance management.

3.2 Data and information provision

In this section, some examples of measurement data and diagnosis information provided to the road administrators in our demonstration system are introduced.

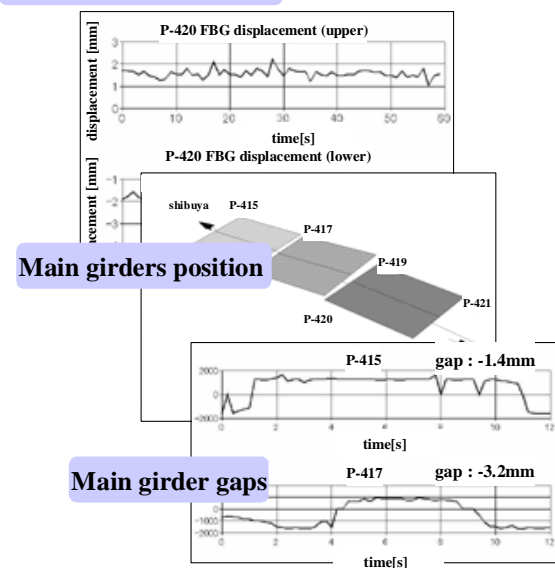
3.2.1 Measurement data provision

Figure 6(a) shows the display representation of measurement data. It is updated corresponding to data collecting cycle, namely 1Hz for FBG displacement meters, every thirty minutes for BOTDR displacement meters and 125Hz for the other sensors. Figure 6(b) shows a result of a real-time detection of heavy vehicles passing thorough our test site, and a histogram of its passing-vehicle number corresponding to its weight levels. These data can be redrawn if only they specify the date and time that they are interested in.

3.2.2 Diagnosis information provision

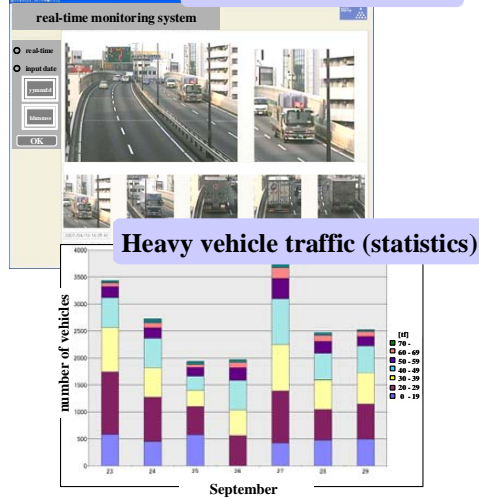
Figure 6(c) shows the display representation of diagnosis information. It is shown on a 2D geographical map using different colors corresponding to each gap level, namely “large”, “small” or “non”.

Real-time Measurement

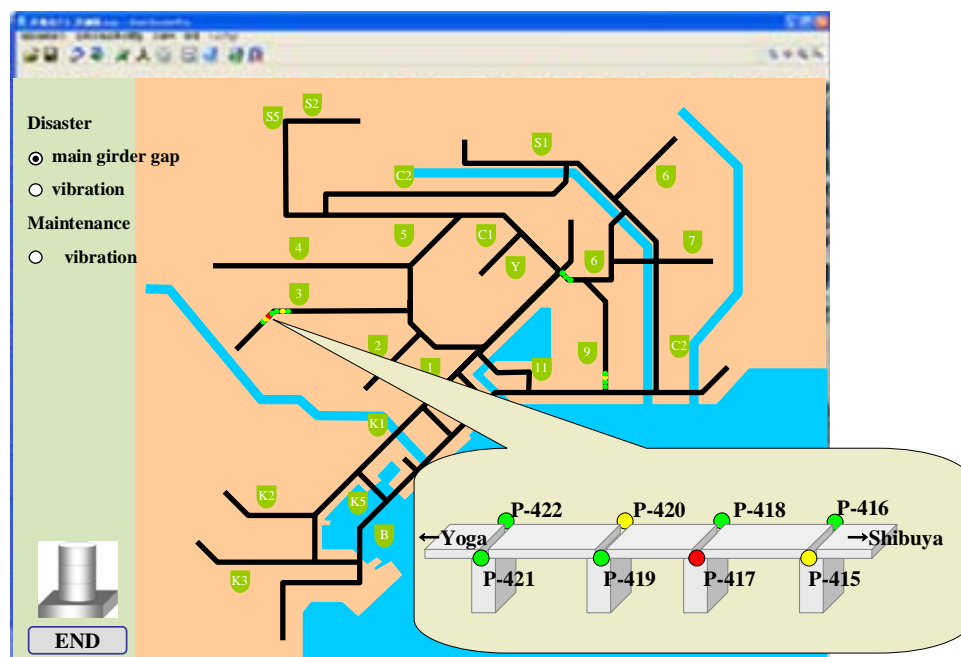


(a) Measurement data

Heavy vehicle detection



(b) Heavy vehicle detection



(c) Example of the diagnoses information

Figure 6: Display representation of the administration support system

4. CONCLUSIONS

We introduce a concept of our real-time bridge remote monitoring system using various sensors for a quick detection of the damage caused by earthquakes and for a reliable measurement of the damage caused by its aging, and also introduce a demonstration system developed on Metropolitan expressway in Tokyo, Japan, for our feasibility study. The system has been in operation since March 2007 without any trouble and failure. In the next step of our research, we will try to establish the reliability and the durability of our system, and to estimate a cost effectiveness for the road administration.

ACKNOWLEDGEMENT

The authors acknowledge to the reviewer for necessary corrections and comments for improving the quality of the paper.

3-D APPLIED ELEMENT METHOD FOR PP-BAND RETROFITTED MASONRY

WORAKANCHANA KAWIN

Project Researcher, ICUS, Institute of Industrial Science,
The University of Tokyo, Japan
kawin@iis.u-tokyo.ac.jp

PAOLA MAYORCA

Project Research Associate, ICUS, Institute of Industrial Science,
The University of Tokyo, Japan
paola@iis.u-tokyo.ac.jp

RAMESH GURAGAIN

Director, Earthquake Engineering and Research,
National Society of Earthquake Technology, Nepal
rguragain@nset.org.np

SATHIPARAN NAVARATNARAJ

Doctoral Student, Meguro Laboratory
The University of Tokyo, Japan
sakthi@iis.u-tokyo.ac.jp

KIMIRO MEGURO

Professor, ICUS, Institute of Industrial Science,
The University of Tokyo, Japan
meguro@iis.u-tokyo.ac.jp

ABSTRACT

Masonry, through its long history, is widespread used around the world and still remains a main building material in many places especially developing countries. However a poorly designed masonry is known as brittle and susceptible to earthquakes. To improve masonry seismic capacity, polypropylene band retrofitting technique was purposed based on economic point of view and local availability of material and skilled labor. In this study, we proposed the 3-D Applied Element Method as an analysis tool to help understanding the polypropylene band retrofitted masonry behavior which will be benefit in the future design process. Unlike the previous version, 3-D Applied Element Method elements can be any rectangular prism which helps reducing the number of elements. Brick and mortar springs are represented by using different spring properties. Nonlinear constitutive law of the mortar spring employed the Gambarotta model which considers the material softening. Polypropylene band is modeled as beam element using conventional plastic constitutive law connected together with the masonry by elastic spring representing the polypropylene band to brick connector. The numerical simulation of non-retrofitted and retrofitted out of plane wallets shows that with the suitable selected parameter the behavior of masonry can be closely reproduced.

1. INTRODUCTION

Masonry along with timber structures are among the oldest structures that are still used nowadays. Masonry structures history can be tracked back as early as 8000-9000 B.C. near Lake Hullen, Israel (Lourenço, 1996). With its long history, abundance of material, ease of construction and the advantages in thermal property, masonry is widespread used around the world. This type of structure still remains a main building material in many places especially in developing countries (Paola, 2003). Despite its advantages as residential structure, masonry is known as brittle and unsuitable for construction of buildings in seismic zones (Tomažević, 1999). The 1997 Umbria-Marche, 1999 Bhuj and 2003 Bam earthquakes shows that masonry is rather susceptible and a huge number of masonry collapses is found especially in the region where the poorly designed masonries are concentrated. Moreover, masonry collapse also results in high casualty because masonry material tends to break into the small debris and left insufficient void which reduce the chance of survival.

In order to improve the current situation, the proper retrofitting method must be invented. Several proposed retrofitting method in the literatures includes grout injection and internal reinforcing, ferrocement coatings, FRP composites and adding of steel elements. These methods were reporting successfully for increasing the seismic capacity of the building. Besides, the recent retrofitting scheme considering economic and availability of material and skilled labor is Polypropylene band (referred later as PP-band) retrofitting technique. The method was first proposed by Paola in 2003. Unlike the former methods, a main objective of this retrofitting technique is to hold the disintegrated elements together and preventing the collapse. In attempt to understand the behavior and to rationalize the design of these retrofitting methods, she carried out the PP-retrofitted masonry wall testing. It was found that the behavior of the retrofitted walls was more stable and larger deformations could be sustained compared to unretrofitted one. Moreover, Paola also proposed the 2-D numerical model based on Applied Element Method (AEM) for simulating PP-band retrofitted wall using constitutive laws provided by Lorencó (1996). In 2005, Sathiparan conducted series of shaking table tests of the $\frac{1}{4}$ scaled single unit masonry models with opening. He found that the retrofitted test models can resist up to 88 mm compared to 7 mm in an unretrofitted case for top displacement without collapse. Later, Guragain (2006) adopted the constitutive laws from Gambarotta (1997) into AEM and succeeded in proposing the model for simulating the in-plane cyclic behavior of PP-band retrofitted masonry.

By considering the damage mechanisms in the masonry structures, the typical damage mechanism in the masonry structure can be identified as 1. cracks between walls and floors 2. cracks at the corners and at wall intersections 3. out-of-plane collapse of perimetral walls 4. cracks in spandrel beams and/or parapets and 5. diagonal cracks in structural walls (Tomažević, 1999). Except the diagonal cracks, most masonry damage behaviors inevitably relate with three dimensional behaviors. With the

proposed PP-band retrofitting, the interaction between each wall will be higher and therefore the seismic resisting mechanism tends to become more important. Therefore, three dimensional behaviors have to be investigated before developing the less complicated two dimension analysis and design process. Moreover, because PP-band stiffness is rather low compared to masonry, the effect of retrofitted PP-band will play more significant role when a structure largely deforms. This is inevitably required the good understanding of three dimensional seismic behavior of masonry structure in the large deformation state. Despite a number of numerical models for structural analysis, few are suitable to simulate masonry in the large deformation range and AEM is one among these. In this study, we proposed the 3-D AEM, based on previous 2-D AEM for masonry and 3-D AEM for concrete, to simulate three dimensional behaviors for PP-band retrofitted masonry structure.

2. 3-DIMENSIONAL APPLIED ELEMENT METHOD

In AEM, the structure is divided in rigid elements, carrying only the system's mass and damping, connected with normal and shear springs representing the material properties (Figure 1). The stress and strain fields are calculated from the spring deformations. 3-D AEM rigid elements with 6 degrees of freedom each are connected through sets of one normal and two shear springs.

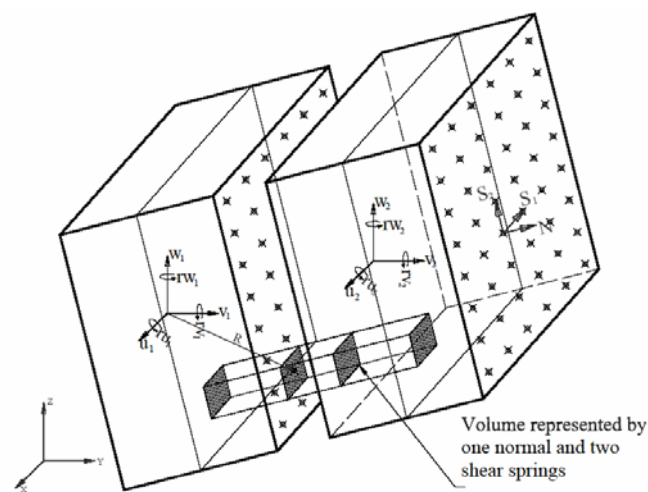


Figure 1: 3-D AEM

3-D AEM used an explicit scheme to solve structural problems therefore it is required to assemble the system stiffness matrix. For this purpose, it is necessary to sum up the contributions of all the springs around one element to the relevant degrees of freedom. Because each element has six degrees of freedom, the stiffness matrix of each spring is a 12 by 12 matrix which its components were generated by direct stiffness method.

Masonry is constituted by two phases: brick and mortar. Therefore,

there are two types of springs: one inside brick units, brick spring, and the other at the joint interface, brick-mortar spring, are defined in 3D-AEM. In this paper, the brick spring stiffness is assumed to be elastic and its stiffness can be calculated as:

$$K_n = \frac{E \times b \times c}{a} \text{ and } K_s = \frac{G \times b \times c}{a} \quad (1)$$

where E and G are Young's and shear modulus of brick, respectively. Other variables are shown in Figure 2. For the brick-mortar springs, an equivalent normal and shear stiffness is calculated by assuming that these springs represent a system of brick and mortar springs arranged in series as shown in Figure 2.

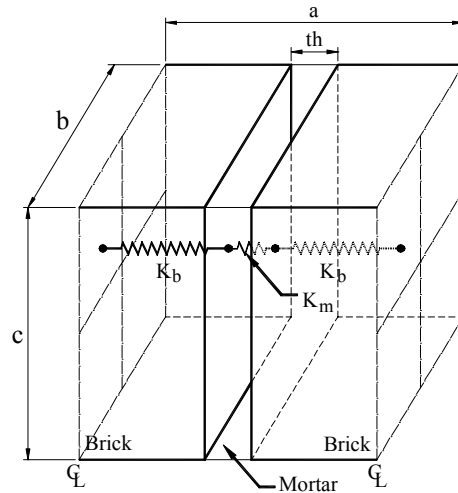


Figure 2: Concept of equivalent brick-mortar spring

The corresponding equivalent stiffness is:

$$\frac{1}{Kn_{eq}} = \frac{a - th}{E_b \times b \times c} + \frac{th}{E_m \times b \times c} \quad (2)$$

$$\frac{1}{K1s_{eq}} = \frac{a - th}{G_b \times b \times c} + \frac{th}{G_m \times b \times c} \quad (3)$$

$$\frac{1}{K2s_{eq}} = \frac{a - th}{G_b \times b \times c} + \frac{th}{G_m \times b \times c} \quad (4)$$

where E_b and G_b are the Young's and shear modulus of brick and E_m and G_m for the mortar. Eigenvalue analysis is also possible with the current version of 3D-AEM. The vector iteration with shifts technique is adopted. This technique is chosen as it provides a practical tool for computing as many pairs of natural vibration frequencies and modes of the structure as desired.

2.1 Masonry Modeling

The material constitutive relation requires spring level stress/strain updating for each loading step in the 3-D AEM. The stiffness changes in accordance to damage that material sustained in local level is required to monitor throughout the loading history. As mentioned earlier, the constitutive law needed to be modified in order to take into account this phenomenon. Such a model should be able to reflect the highly nonlinear

behavior of masonry with the fewest number of parameters so that it results in a simple and stable numerical model. Considering these criteria, the damage model of brick masonry proposed by Gambarotta et al (1996) has been chosen to implement in the 3D-AEM for cyclic behavior of the masonry. This constitutive law is able to reflect the important physical phenomena exhibited by masonry under cyclic loading.

The chosen constitutive model is based on damage mechanics and takes into account both the mortar damage and brick-mortar de-cohesion which is considered to take place when opening and frictional sliding are activated. Constitutive property of joint springs is based on two damage variables representing frictional sliding and mortar joint damage. Those variables are obtained from Mohr-Coulomb's friction surface and damage condition based on fracture mechanics. The damage evolutions in tensile and compression zones as well as the frictional limit criteria are given in Figure 1.

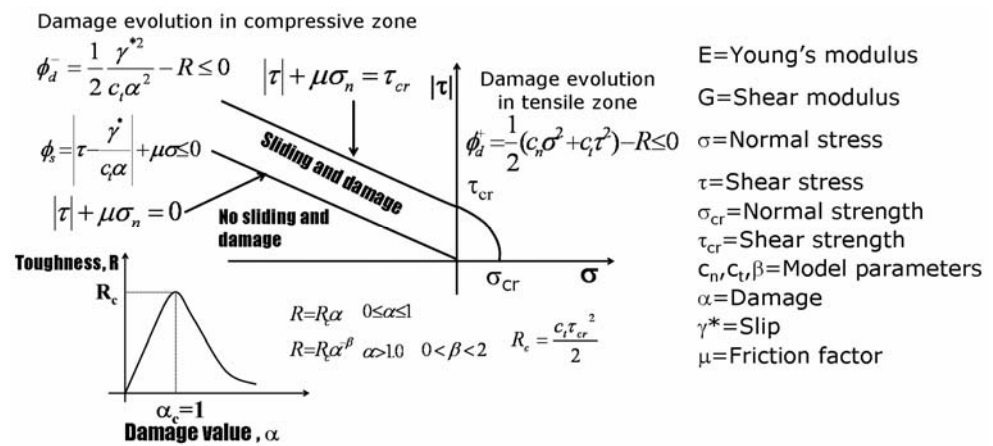


Figure 1: Constitutive relation to model the cyclic behavior of masonry
Stress at any springs can be defined as:

$$\{\sigma\} = [D] \{\varepsilon\} \quad (5)$$

Strain in springs can be split into elastic and plastic strain as:

$$\{\varepsilon\} = [K_e] \{\sigma\} + \{\varepsilon_p\} \quad (6)$$

where, $[K_e]$ is the elastic compliance matrix of the spring. The plastic strain is $\{\varepsilon_p\} = \{\varepsilon_{np}, \gamma_p\}^t$ and is the result of inelastic normal and tangential displacement. Strain components are defined as functions of the damage variable α ,

$$\varepsilon_{np} = h(\alpha) H(\sigma_n) \sigma_n \quad (7)$$

$$\gamma_p = k(\alpha) (\tau \cdot f) \quad (8)$$

where $h(\alpha)$ and $k(\alpha)$ are positive functions representing inelastic compliances in normal and tangential direction. $H(\sigma_n)$ is the heaviside function used to make the expression unilateral in tensile straining action and f is the friction developed at the interface between mortar and brick. Evaluation of the variable α and friction f is made through the limiting

conditions of damage and friction sliding.

The damage condition based on R-curve approach of fracture mechanics is defined on the basis of energy release rate of damage, Y and toughness, R as:

$$\phi_d = Y - R \leq 0$$

$$Y = (1/2) h(\alpha) H(\sigma_n) \sigma_n^2 + (1/2) k(\alpha) (\tau - f)^2 \quad (9)$$

and the compliance functions $h(\alpha)$ and $k(\alpha)$ are assumed linear function of inelastic compliance constants as follows:

$$h(\alpha) = c_n \alpha$$

$$k(\alpha) = c_t \alpha \quad (10)$$

The toughness function, R is related to damage evolution and is defined in terms of damage index α setting to attain its peak value R_c at critical value of $\alpha = \alpha_c (=1)$ and vanishing to zero as α increasing. The friction sliding condition is obtained from Mohr-Coulumb friction condition as:

$$\phi_s = |f| + \mu \sigma_n \leq 0 \quad (11)$$

where, μ is friction coefficient and $|f|$ represents the shear component in surplus to cohesion.

2.2 PP-Band Mesh Modeling

The PP-band mesh is modeled through beam elements spanning between band intersections points as shown in Figure 5. These ends were then connected to the masonry structure through a set of three springs: normal, shear, and rotational. By appropriately setting the properties of these springs, it is possible to consider all possible connecting conditions between mesh and structure. For instance, if there is a wire connector at that particular location, all three springs have values proportional to the connector properties. On the other hand, if there is no connector and no mortar overlay, the normal spring only works in compression, i.e. when the mesh and the structure are in contact. As for the shear and rotation springs, there values are almost zero. This would not be case if there was mortar overlay.

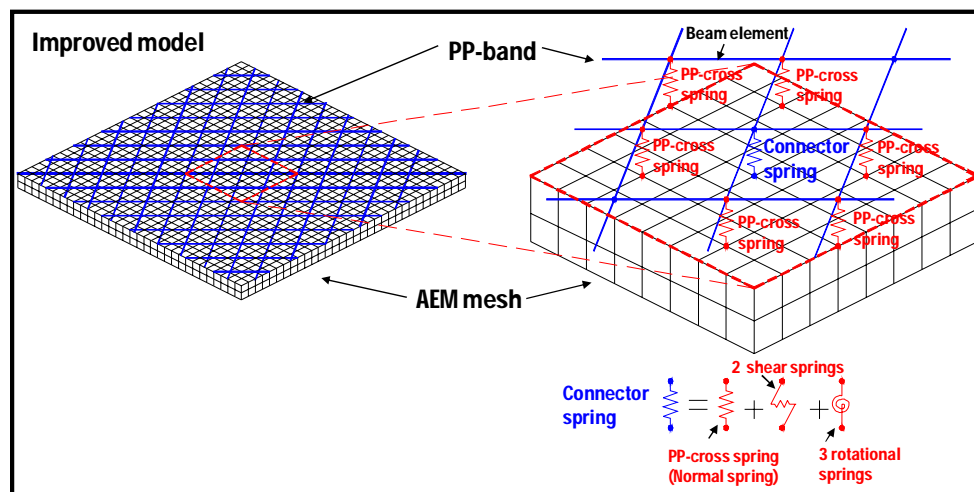


Figure 5: 3D-AEM mesh modeling

The direct implication of a model as the one described above is the considerable increase of degrees of freedom of the system because each intersection point is associated with six more degrees of freedom. A 3-dimensional analysis by itself also involves the solution of systems with large number of degrees of freedom. Therefore, it was absolutely necessary to optimize the algorithms used to solve the equations of motion. This step was successfully implemented.

The material model used for each PP-band beam element was elastic in tension as shown in Figure 6. No compression forces were taken by the beam element. The beam elements were defined so as to have almost no moment resistance at their ends.

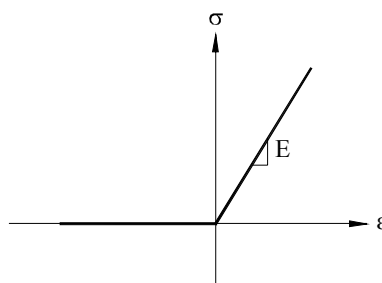


Figure 6: Material model for PP-band beam element

3. MODEL VERIFICATION

The 3D-AEM model was verified using the experimental data obtained by Sathiparan (2005). The non-retrofitted and retrofitted wallettes, shown in Figure 2 and Figure 3, were 475x235x50mm³ and consisted of 6 rows of 6 bricks each. The PP-band mesh was made of 6mm-width, 0.32mm-thick PP-bands placed at 40mm pitch. A total of 6 wire connectors were used to attach the meshes to the wallettes. The wallettes were simply supported by high strength steel rods in both ends. The masonry wallettes were tested under line load using another steel rod of 200mm diameter in the mid span.

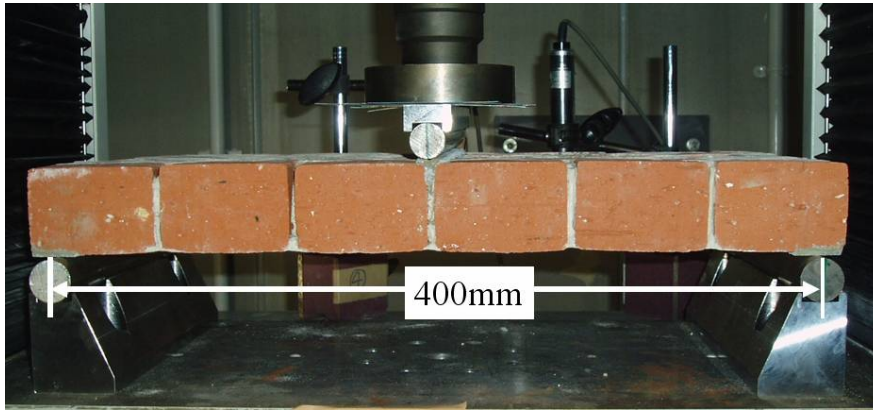


Figure 2: Retrofitted masonry wallet tested for out of plane

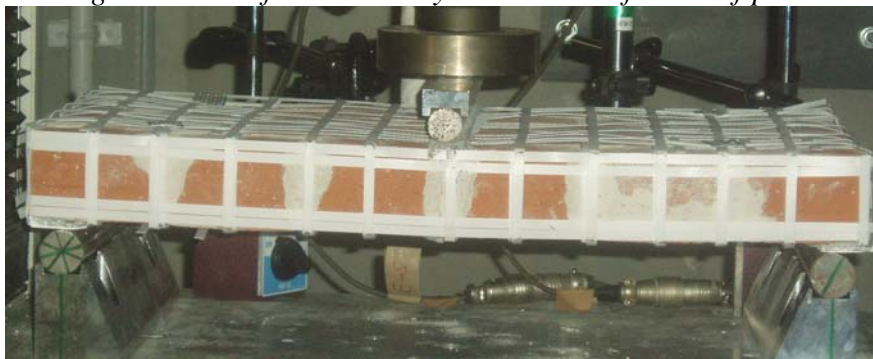


Figure 3: Boundary condition and loading of the masonry wallet for out of plane test

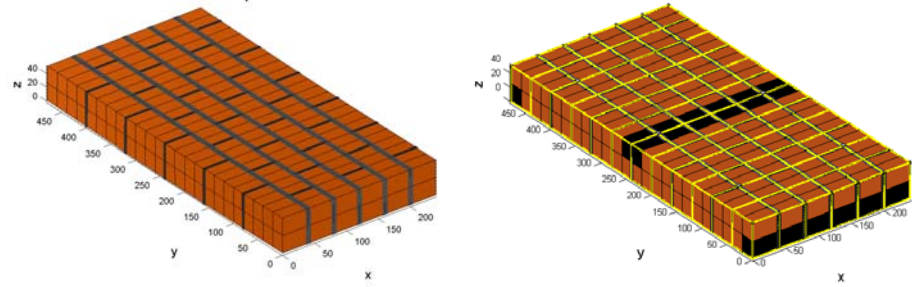
The material properties used for the masonry are summarized in Table 1. The PP-band mesh stiffness was set equal to 9.375 MPa.

Table 5.1: Material properties used for the modeling of out-of-plane masonry wallettes

	Young's modulus E (kN/mm ²)	Shear modulus G (kN/mm ²)	Tensile strength σ_{cr} (kN/mm ²)	Shear strength τ_{cr} (kN/mm ²)	Friction coeff. μ	β	$1/C_{mt}$ (kN/mm ²)
Mortar	0.5	0.25	$0.16e^{-3}$	$0.22e^{-3}$	0.6	0.9	1/30
Brick	15.0	7.5	NA	NA	NA	NA	NA

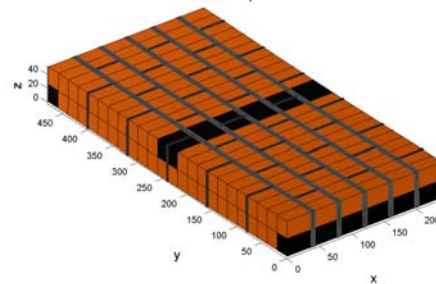
NA: Not applicable

The models used for non-retrofitted and retrofitted models are shown in Figure 4.



(a) Non-retrofitted wallette

(b) Retrofitted wallette



(c) Boundary and loading condition (top dark elements: loading point, bottom dark elements: support)

Figure 4: Boundary condition and loading of the masonry wallette for out of plane test

Figure 5 and Figure 6 show the comparison of numerical and experimental simulations for non-retrofitted and retrofitted wallettes, respectively. It can be seen that in both cases, the model could accurately capture the force-deformation relationships.

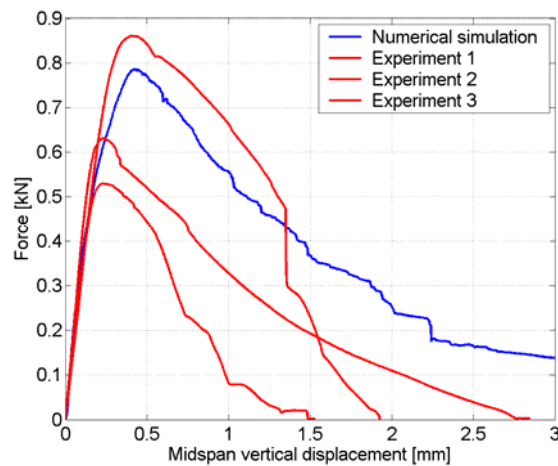


Figure 5: Numerical and experimental force-deformation curves for non-retrofitted wallettes. (Experiments by Sathiparan, 2005)

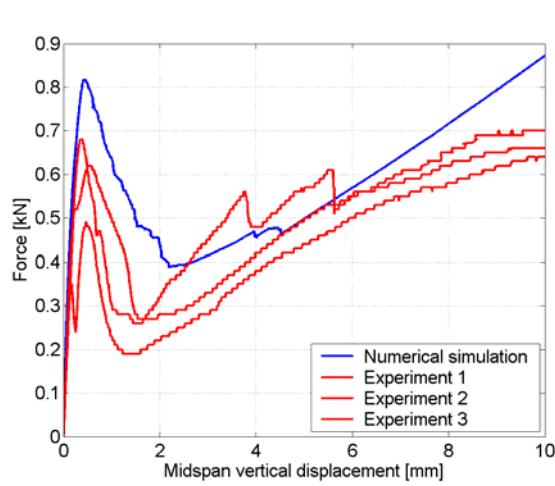
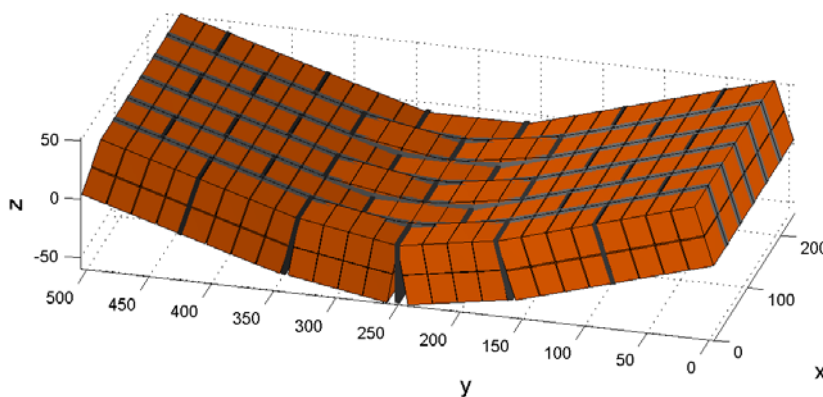


Figure 6: Numerical and experimental force-deformation curves for retrofitted wallettes. (Experiments by Sathiparan, 2005)

The agreement between experiments and numerical simulation can also be observed in the crack patterns and deformed shapes (Figure 13 and 14).

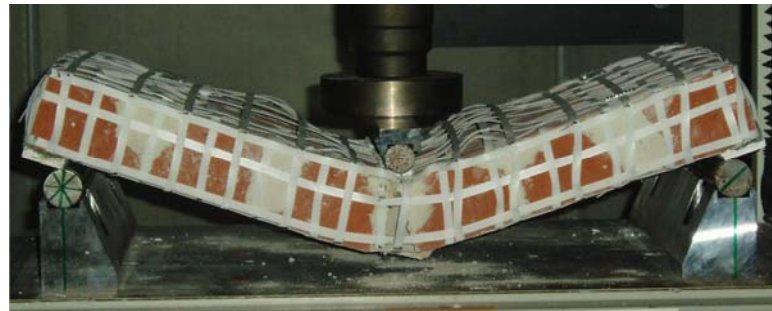


(a) Experiment

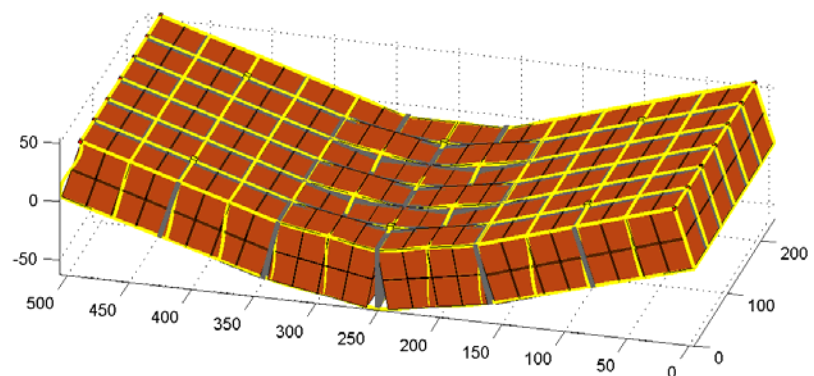


(b) Numerical simulation (scale factor: 20; midspan vertical displacement=3mm)

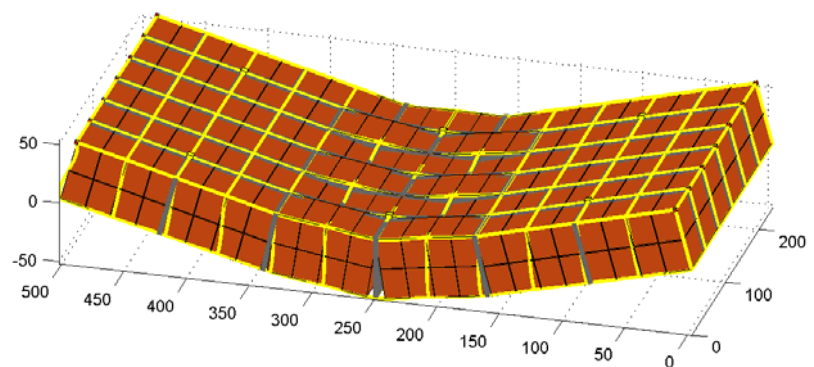
Figure 7: Comparison of numerical simulation and experimental deformed shapes for non-retrofitted masonry.



(a) Experiment



(b) Numerical simulation (scale factor: 20; midspan vertical displacement=3mm)



(c) Numerical simulation (scale factor: 5; midspan vertical displacement=10mm)

Figure 8: Comparison of numerical simulation and experimental deformed shapes for retrofitted masonry

CONCLUSION

The 3-D AEM for simulating static behavior of PP-band retrofitted masonry was developed. The main improvements in this version are the rectangular prism AEM element which helps reducing the element number and the additional beam element and connected spring allowing AEM for simulating PP-band. The verification for 3-D AEM for PP-band retrofitted masonry for the out of plane test was carried out. The verification result shows that with

the suitable selected parameter, the behavior of masonry can be closely reproduced.

REFERENCES

- Gambarotta L. and Lagomarsino S. (1997), "Damage Response for the Seismic Response of Brick Masonry Shear Walls. Part I: The Mortar Joint Model and its Application". *Earthquake Engineering and Structural Dynamics*, 26, 423-439
- Guragain, R. (2006), *Numerical Simulation of Masonry Structures under Cyclic Loading using Applied Element Method*, Master degree thesis, Department of civil engineering, The University of Tokyo.
- Lourenço, P.B. (1996), *Computational Strategies for Masonry Structures*, Delft University Press
- Mayorca, P. (2003), *Strengthening of Unreinforced Masonry Structures in the Earthquake Pone Regions*, Ph.D. thesis, Civil Eng. Dept., the University of Tokyo.
- Tomaževič, M. (1999), *Earthquake-Resistant Design of Masonry Buildings*, Imperial College Press, London
- Sathiparan, N. (2005), *Experimental study of retrofit of masonry building by pp-band mesh*, Master degree thesis, Department of civil engineering, The University of Tokyo

STRUCTURAL HEALTH ASSESSMENT OF INFRASTRUCTURE: THE BANGLADESH PERSPECTIVE

RAIS AHMAD¹, M. KABIRUL ISLAM¹, M. ZAKARIA AHMED¹

¹Department of Civil Engineering,
Bangladesh University of Engineering & Technology, Bangladesh
mzahmed@ce.buet.ac.bd

TRIBIKRAM KUNDU²

²Department of Civil Engineering and Engineering Mechanics
University of Arizona, USA

ABSTRACT

Due to rapid urbanization various multi-storied reinforced concrete buildings are being built in major cities of Bangladesh such as Dhaka and Chittagong. Many of these buildings have soft story in the ground floor and generally have been built without seismic consideration. However these cities as well as most of the region encompassing Bangladesh are located in moderate to severe earthquake zone. In recent years, several earthquakes of magnitude 4.0 to 6.0 have been recorded in Dhaka and Chittagong, which have caused either collapse or damage of concrete and masonry buildings, cyclone shelters, and mud-walled houses. Damages to utilities such as electric transformers have also been recorded. It has been observed in recent times that poor quality or faulty construction and design have also resulted in complete structural collapse of buildings. This paper discusses some of these occurrences and the methods that could be employed to assess the structural health condition of critical buildings and other infrastructure.

1. INTRODUCTION

Rapid urbanization in big cities of Bangladesh, like Dhaka and Chittagong, have been taking place in recent three decades. This thrust has created a demand for multi-storied reinforced concrete (RC) buildings especially of residential type. Many of these apartment complexes are found to have soft stories in the ground floor, which is generally used as parking space. A large number of industrial buildings have also been built throughout Bangladesh during the past decades because of rapid industrialization environment and good government policy.

The epicenters of some of the past (over the last 150 years) major earthquakes measuring greater than 7.0 on the Richter Scale were observed to be located within 150 km from Dhaka city. In recent years several earthquakes with magnitude 4.0 to 6.0 have been recorded. These recent earthquakes (2001-2005) have caused collapse of concrete buildings, damage of cyclone shelters, masonry buildings, electric transformer, mud walled houses in the countryside including loss of human life. Frequent

shaking in the Chittagong region in recent times has raised alarm among the people. It is obvious from these occurrences that Bangladesh is located in a region vulnerable to earthquake hazards. A strong earthquake may strike this country in the future, resulting in huge loss of life and damage to property and infrastructure, and thus can set back the pace of development achieved in this country so far. For ensuring sustainable development of Bangladesh, it is important to take necessary measures for disaster risk reduction.

Some examples of recent building collapse can illustrate the severity and magnitude of disaster management scenario in a post earthquake situation in major cities of Bangladesh. In 2005, a nine storied garment factory building at Savar (located about 30 km from downtown) suddenly collapsed due to gravity load. In this incident, about one hundred workers were killed. It took more than a month to clean the debris from the site even though this building is located in relatively open space compared to other locations and structures in Dhaka city. In February 2006, a five storied building undergoing reconstruction/renovation collapsed without warning at the Tejgaon industrial area of Dhaka city, killing about 20 people. It is reported that this building was being built as a 500 bed specialized hospital in joint collaboration with Mount Elizabeth Hospital, Singapore. Cleaning of the concrete debris took a few days. These are examples of vulnerable buildings that have failed under normal loading. It is quite obvious that in the event of a moderate to severe earthquake, many buildings face a significant risk of collapse as a result of poor quality of construction and due to design without seismic considerations. In densely populated areas of the cities, buildings are located on narrow roads, where it is difficult for fire-fighting and rescue operation vehicles to enter and operate. In addition to inadequate road network, Bangladesh lacks necessary logistic support for rescue and recovery operations. In other words, post earthquake disaster management task for Dhaka and other cities is difficult and cumbersome. A country wide rational structural health assessment is necessary for possible rehabilitation of critically important structures including bridges. The strict enforcement of national building code for the new buildings as well as a strong structural assessment and rehabilitation program for the existing ones with adequate logistic support may help to reduce the extent of devastation during an event of earthquake. From this realization among professionals and academics of this country, and to reduce the risk posed by seismic and man-made hazards, strengthening structural health assessment methods in Bangladesh is evolved.

2. STRUCTURAL HEALTH ASSESSMENT METHODS

Various methods for condition assessment of civil structures are developed. In broader sense, these methods can be categorized into two distinct groups such as Global method and Local method. In Global method the condition of a structure (building, bridge) is evaluated from its global response. On the other hand, in a Local method structure's condition is evaluated based on some of its local response at the critical locations. Brief description of the

methods, which are also known as Non-Destructive Evaluation (NDE) techniques under these two broad categories are presented in the following.

2.1 Global Methods

Global methods are based on changes in their measured dynamic properties such as the stiffness and flexibility measurement, resonance frequency measurement, mode shape measurement or wave velocity measurement of the structure during its vibration. Flexibility and Stiffness of a damaged structure will be different from the good one. Thus in flexibility and stiffness method, displacement at the top of the structure relative to its base (building, long span bridge) or drift ratio of tall buildings is measured during a natural event (earthquake, wind loads), or a man-made event (blasts) using GPS technology. For this purpose, differential Global Positioning Systems (GPS) units are placed at selected locations of the structure (Celebi and Sanli, 2002). The drift ratio can be computed from the measured displacement and story height. Since the drift ratio is related to damage condition of a building, this parameter is employed in an appropriate structural analysis program to predict the stiffness of the structure and its damage level. In this technique, as a reference, drifts for several pre-selected stages of damage are computed using the parameter such as connection types, story height. Measured drift ratios are compared with the pre-computed drift ratios to assess the damage condition of the building. Depending on the damage condition, the building can be alerted by red, yellow or green signals for the users.

GPS technology is also used to monitor the resonance frequency of civil structures that varies when the structure is damaged because of the change in the structural stiffness. In this method, monitoring the resonance frequency of a building or a bridge, the condition of the structure is assessed from the shift in its resonance frequency. The time histories recorded data of different GPS units placed on the roof of a building is used in the spectral analysis to determine peak frequency (Celebi, 2005). The peak frequency shifts when the building is damaged from earthquakes or other events.

In wave propagation method, the condition of a multi-story building is assessed by monitoring the speed of the elastic wave propagating from the bottom to the top of the building (Safak, 1999). For example, accelerometer data were recorded at different floors of the 34 story building in San Francisco during December 2003 San Simeon, California earthquake (Mw = 6.4 with epicentral distance of 258 km). Time shift of a particular peak of the time history curve from lower floors to upper floors was measured from those accelerograms to obtain the velocity of the wave propagating from the ground floor to the top through the building structure. It was observed that the wave propagated from the bottom to the top of the building (80 m high) in 0.5 seconds. This indicates that the wave velocity is 160 m/s (Celebi, 2005). A lower wave velocity will be found if cracks are developed in the building.

2.2 Local Methods

In Local methods, damage condition of critical regions of a structure is assessed by different local techniques based on visual inspection, ultrasonic waves, acoustic emission, electric field, magnetic flux etc. propagation. Among the local methods, Visual inspection is the oldest nondestructive testing method which is fast, simple and economic. Many industries opined that 80 percent of the defects found are located by visual inspection (Bray and McBride, 1992). But a large degree of uncertainty may be associated with the visual inspection technique as small external defects and internal defects cannot be identified by this technique.

Ultrasonic Testing (UT) based on ultrasonic waves are vibrational waves having frequencies usually in the mega hertz range. However, the frequency generally varies from 50 kHz to 20 MHz when detecting most of the defects. These techniques can be used for both the internal flaw detection and the material characterization (Kundu, 2004b). UT can detect defects oriented both in the plane of and normal to the surface of structural components using normal beam or angle beam transducers. By suitable design of ultrasonic transducer, ultrasonic beams can be introduced into a material at almost any angle. There are several forms of ultrasonic waves, the most widely used in NDT being compressional (longitudinal) and transverse (shear) waves. One of advantage of using this method is that for structural element with both surfaces not accessible can also be assessed. In the recent, component with complex geometries are assessed using ultrasonic inspection technique based on guided waves (Lamb waves, Rayleigh waves and cylindrical guided waves). They are different from the bulk ultrasonic waves in that they continue to interact with the boundary of the material in which they travel and require these boundaries to exist. The boundaries confine the waves and allow them to propagate over long distances, which make them attractive for rapid, long screening of different systems. Guided wave ultrasonic inspection as a quality tool has become quite popular and effective in thickness measurement, flaw detection, and material characterization. The guided wave ultrasonics are very effective at detecting anomalies along the sound path. The applications of Guided waves have been shown for inspecting composite-concrete interface (Kundu et al. 1999), pipes (Guo and Kundu, 2000, 2001), concrete beams (Jung et al. 2001, 2002) and interface of concrete and reinforcing bars (Na et al. 2002, 2003).

Eddy Current Method is based on electric field (Figure 1) as developed when an alternating electric current (ac) flows in a coil of many turns of fine. As shown in Figure 1, eddy currents are induced in the material due to placement of an energized coil near the surface of a conducting material that flows in a direction opposite to the current in the coil. Eddy currents are proportional to the electrical conductivity of the material. Magnitude and phase of the induced current depends on the material properties as well as on damage (cracks and voids). Thus analyzing the eddy currents the material conditions of a structure can be assessed. The main advantage of this method is that mechanical contact is not required

between the eddy current transducers and the test object. The other advantage is that eddy current penetration depth can be controlled by adjusting the frequency of energizing current. The penetration depth (mm), α which is related to the material resistivity (micro-ohm-cm), ρ , relative permeability (dimensionless), μ and frequency (Hz), f is given as follow (Bray and McBride, 1992),

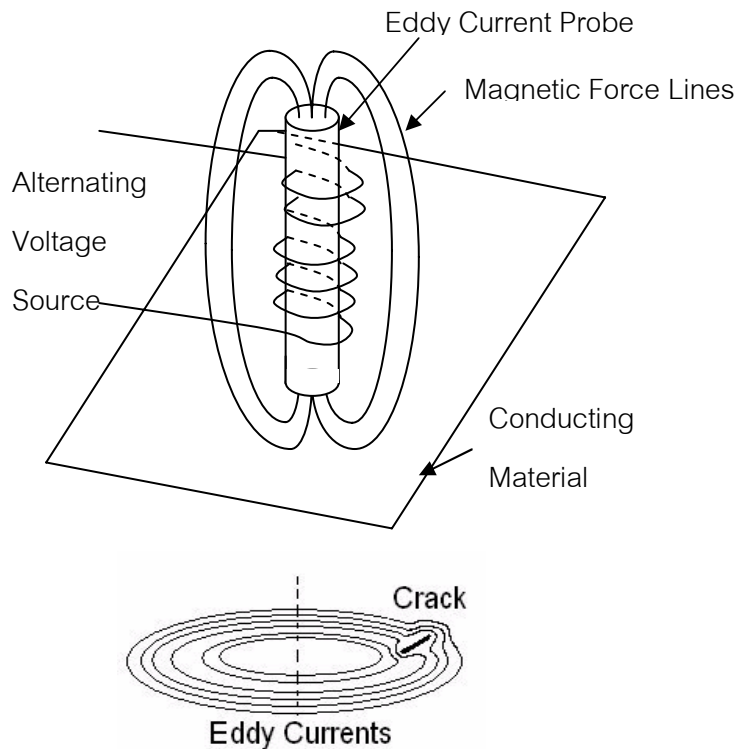


Figure 1: Schematic of an eddy current probe placed near an electrically conductive material.

$$\alpha = 50.3 \left(\frac{\rho}{\mu f} \right)^{\frac{1}{2}} \quad (1)$$

For most applications, instrumentation for eddy current testing is relatively low cost. However, the application of this technique is limited to the electrically conductive materials only.

Acoustic Emission (AE) monitoring is a passive technique where sensors (transducers) are mounted to listen acoustic energy released when cracks are formed inside a material. Acoustic energy is released because of the relaxation of the stress at the point of cracks which propagates through the material to its surface. The source of these emissions in metals is closely associated with the dislocation movement accompanying plastic deformation and with the initiation and extension of cracks in a structure under stress. The AE technique as shown in Figure 2 is based on the detection and conversion of high frequency elastic waves emanating from

the source to electrical signals. This is accomplished by directly coupling piezoelectric transducers on the surface of the structure under test and loading the structure. The output of the piezoelectric sensors (during stimulus) is amplified through a low-noise preamplifier, filtered to remove any extraneous noise and further processed by suitable electronics. The mounted transducers can identify the formation or propagation of cracks inside the material.

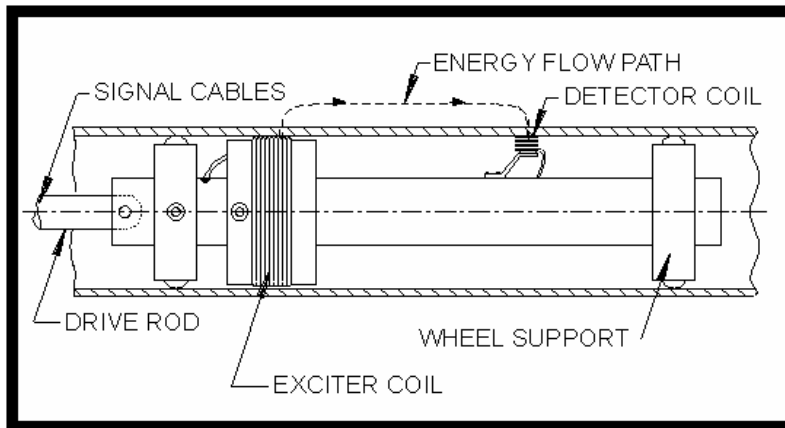


Figure 2: Acoustic emission (AE) testing Sensor

The acoustic emission is also generated due to dislocation movements, fracture of brittle inclusions or surface films, fiber breakage and fiber delamination in composite materials, melting, phase transformation, thermal stresses, cool down cracking and stress build up. Thus one can predict the type of damage created using this technique (Mal et al., 2003). The energy of these disturbances is termed as emission energy. The emission energy in some cases is very small and results in motion of small dislocations in metals. During earthquakes, such emission energy is so large that the resulting disturbances cause major cracking of structural members with consequent catastrophic collapse. The limitation of this method is that it can detect a growing crack and size cannot be determined. The primary advantage of this technique is that no equipment is required to excite a pulse, and hence the instrumentation is relatively simple and inexpensive. Other advantages are that the sensors can be located at remote locations for the object operating in hostile environments and a relatively large volume of material can be inspected at a reasonable cost. Since in most materials, the number and intensity of the released acoustic signal increases significantly near the failure point, AE technique can serve as a good warning tool before the failure. The AE technique has been successfully used to detect leaks in storage tanks located above the ground (Miller, 1990; Nordstrom, 1990). This technique has also been applied to monitor crack initiation and propagation in airplanes during its flight (Martin, 1980).

The magnetic flux leakage (MFL) is one of the most widely used techniques to nondestructively inspect ferromagnetic materials like steel for surface and near-surface defects (Halmshaw, 1987; ASM International, 1989). A magnetic field is applied to steel to magnetically saturate it, so that it can't hold any additional field. In the presence of a flaw, some of the magnetic flux escapes or "leaks" into the surrounding environment, where

magnetic sensors like Hall probes detect it and report a flaw signal. The MFL devices rely on magnetic field perturbation created by imperfections as the means of detecting the anomalies. The distortion in the flux field induces an electric current in one or more groups of coils or detectors located between the poles of the magnet and arrayed around the circumference of the pipe. The resulting electrical signal and its location along the pipeline are recorded on magnetic tape for analysis. MFL is most commonly used for inspecting lifeline structures such as oil and gas pipelines. Magnetic flux leakage method is widely used in industrial inspection. Typical applications of MFL include testing of longitudinal welds in pipe during fabrication, testing of oil-field equipment including oil-well drill pipe, tubing, line pipe and structures. Pipelines are regularly inspected for thin wall using the magnetic flux leakage principle. Internal inspection devices called pigs as shown in Figure 3 are used for inspecting buried pipelines. The structures and piping in chemical plants and petroleum refineries are also tested using this technique.

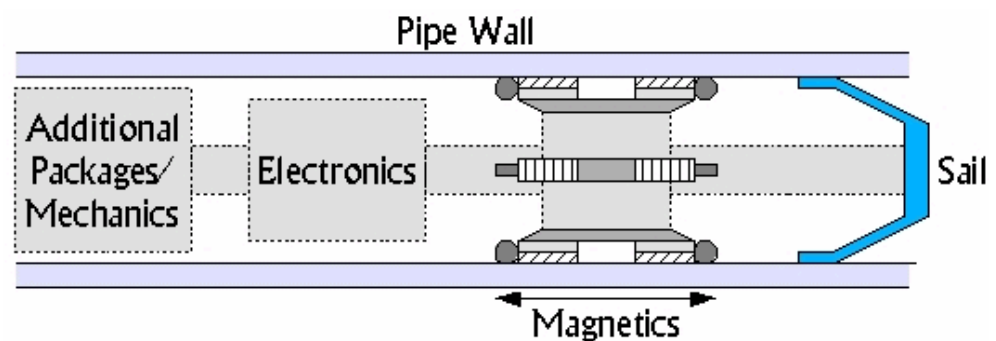


Figure 3: Magnetic Flux Leakage Tests.

3. DEVELOPMENT PLAN FOR CAPACITY UPGRADING:

3.1 Institutional Strengthening

The civil engineering departments of the technical universities of Bangladesh, particularly BUET participate in a large number of national projects yearly where it provides the necessary advisory, consultancy and testing services to the construction industries. Some of those research-cum consultancy projects include structural health assessment, seismic vulnerability evaluation of critical buildings like hospitals and commercial buildings. However at present very primitive methods (such as Schmidt Hammer, core cutting and testing) of evaluation are used due to lack of necessary know-how and logistic facilities, except the recently assessed BUET campus buildings by NDTs (BNUS Report, 2006). To reduce the risk of possible structural collapses in infrastructure, institutional strengthening is essential for providing quality education on structural health assessment techniques to the students and for upgrading knowledge of academics. In this connection, some linkage or collaborative projects need to be

implemented through which our curriculum can be upgraded including procurement of health assessment devices. In addition various training modules can be developed for the practitioners who will be involved in health monitoring of buildings, bridges etc. These linkage projects may also include the provision to provide training to the staff and masons of the construction industries, which is very important for quality and proper construction. Moreover through these projects, young faculty members of the universities can obtain their higher education (MS, PhD) in Non Destructive Evaluation (NDE) of Infrastructures. The financial support for technology transfer on structural health evaluation technologies for the infrastructure can be sought from donors under the framework of International cooperation between Higher Education Institutions.

3.2 Regional Assessment and Rehabilitation Program

The Ministry of Housing and Public works, Ministry of Disaster Management and Relief and other concerned Ministries in joint collaboration with technical universities like BUET should start a step by step structural health assessment program targeting specific regions throughout the country. In this regard, the concerned Ministry can take necessary steps to seek adequate support from international development partners. In the assessment and rehabilitation program, priority should be given in the educational institutions, starting from primary schools to universities as these institution buildings are used as emergency shelters during any disaster e.g., cyclone and earthquake. On the other hand public hospitals of Seismic Zones 2 and 3 of Bangladesh including the buildings where private hospitals, clinics and diagnostics centers are located should be taken care of under the framework of nation-wide assessment and rehabilitation program. Government of Bangladesh should also take necessary steps to execute an investigation regarding the vulnerability of the country's critical facilities like sea port, rail road network, electricity generation and supply systems, gas field and their transmission systems, telecommunication systems, etc.

In addition to above targeted infrastructures and critical facilities of the country, the city government with joint collaboration of the Ministry of Housing and Public could start a seismic assessment program and suggest affordable retrofitting of vulnerable houses. The results of the seismic assessment should be published in pictorial form in the daily newspaper so that house and commercial building owners and the tenants can understand the level of earthquake vulnerability of their respective structures. In this way a fruitful awareness could be developed among the owners and tenants, which in turn would encourage them to undertake appropriate rehabilitation scheme to protect their assets and lives from earthquake disaster

4. CONCLUSIONS

In recent time structural collapse of buildings have occurred in Bangladesh either as a result of seismic activity or due to inadequate ability of the

structures to support occupancy or wind related loads. In both cases the primary reason for such collapse or damage was inadequate design or faulty and poor quality of construction. Appropriate preventive steps such as retrofitting, redesign and partial reconstruction or demolition could have saved life and/or property. For this a thorough structural health assessment of selected or critical structures and utility facilities is necessary. This paper has summarized some of the structural health assessment methods as well as their advantages, limitations and their possible applicability for structures in Bangladesh. A more thorough analysis and comparison of various structural health assessment methods including cost benefit analysis needs to be done in the future. In this regard it is imperative for international and multi-national institutions and organizations to fund extensive research and study of such methods.

ACKNOWLEDGEMENT

The first three authors of this paper express their gratitude to Professor Tribikram Kundu of Civil Engineering and Engineering Mechanics Department of The University of Arizona, USA for his kind consent to be a co-author of this paper.

REFERENCES

- ASM International, 1989. *Metals Handbook*, Vol. 17, 9th ed., ASM International, Materials Park, Ohio
- BNUS Report, 2006, *Evaluation of the Seismic Vulnerability of Bangaldesi Buildings using Non-Destructive Testing - Microtremor Measurements and Fefforscan*, ed. Russel et al. and Yoshimura et al., ICUS, University of Tokyo
- Bray, D. E. and D. McBride, 1992. *Nondestructive Testing Techniques*, John Wiley & Sons, Inc., New York
- Celebi, M., 2005. *Real-time Seismic Monitoring and Functionality Assessment of a Building, Health Monitoring and Smart Nondestructive Evaluation of Structural and Biological Systems, IV*, Proc. of SPIE, Ed. T. Kundu, Vol. 5768, pp. 63-73.
- Celebi, M., and A. Sanli, 2002. *GPS in Pioneering Dynamic Monitoring of Long Period Structures*, Earthquake Spectra, Journal of EERI, Vol. 18, No. 1, pp. 47-61
- Guo, D. and T. Kundu, 2000. *A New Sensor for Pipe Inspection by Lamb Waves*, *Materials Evaluation*, Vol.58(8), pp.991-994
- Guo, D., and T. Kundu, 2001. *A New Transducer Holder Mechanism for Pipe Inspection*, Journal of the Acoustical Society of America, Vol.110, pp.303-309
- Halmshaw, R., 1987. *Non-destructive Testing*, Edward Arnold, London
- Jung, Y. -C., T. Kundu and M. R. Ehsani, 2002. *A New Nondestructive Inspection Technique for Reinforced Concrete Beams*, ACI Materials Journal, Vol.99(3), pp.292-299
- Jung, Y.C., T. Kundu and M. Ehsani, 2001. *Internal Discontinuity Detection in Concrete by Lamb Waves*, *Materials Evaluation*, Vol.59(3), pp.418-

423

- Kundu, T., 2004b. *Ultrasonic Nondestructive Evaluation: Engineering and Biological Material Characterization*, Pub.CRC Press, ISBN 0-8493-1462-3
- Kundu, T., M. Ehsani, K. I. Maslov and D. Guo, 1999. *C-Scan and L-Scan Generated Images of the Concrete/GFRP Composite Interface*, NDT&E International, Vol.32, pp.61-69
- Mal, A. K., F. J. Shih and W. H. Prosser, 2003. *Ultrasonic Methods for Material Characterization*, Special Issue of I2M (Instrumentation, Measurement and Metrology), ed. T. Kundu, Pub. Lavoisier, Paris, Vol. 3, p. 11
- Martin, G. C. , 1980. *In-Flight Acoustic Emission Monitoring*, in *Conf. Proc. Mechanics of Nondestructive Testing*, Blacksburg, VA.
- Miller, R. K., 1990. *Materials Evaluation*, Vol. 48, p. 822, 826, 829
- Na, W. B., T. Kundu and M. Ehsani, 2003. *A Comparison of Steel-Concrete and GFRP-Concrete Interface Inspection by Guided Waves*, *Materials Evaluation*, Vol.61(2), pp.155-161
- Na, W.B., T. Kundu and M. Ehsani, 2003. *Lamb Waves for Detecting Delamination between Steel Bars and Concrete*, *Computer-Aided Civil and Infrastructure Engineering*, Vol.18,pp.57-62
- Na, W.B., T. Kundu and M. Ehsani, 2002. *Ultrasonic Guided Waves for Steel Bar-Concrete Interface Testing*, *Materials Evaluation*, Vol.60(3), pp.437-444
- Safak, E., 1999. *Wave Propagation Formulation of Seismic Response of Multistory Buildings*, *ASCE Journal of Structural Engineering*, Vol. 125, No. 4, pp. 426-437

INVESTIGATION FOR PROMOTING SEISMIC RETROFIT OF CRITICAL FACILITIES - A CASE STUDY OF WAKAYAMA CITY-

REIKO AMANO¹ TAKEYUKI EBI², SHOGO HAYASHI³,
KIMIRO MEGURO⁴ KOUJI UEMATSU⁵, KAZUHISA FUJITA⁶

¹Former Visiting Professor of IIS, University of Tokyo
Kajima Corporation, Tokyo, Japan

²Kajima Corporation

³Former International Center for Urban Safety engineering (ICUS),
Institute of Industrial Science, University of Tokyo, Japan

⁴International Center for Urban Safety Engineering (ICUS),
Institute of Industrial Science, University of Tokyo, Japan

⁵Wakayama city, Japan

⁶Fire and Disaster Management Agency (FDMA) of Ministry of Internal
Affairs and Communications, Japan

amanor@kajima.com

ABSTRACT

There has recently been active interest in municipalities in developing hazard maps of earthquakes, tsunamis, floods, etc. However, the focus of many of these maps is to improve public awareness of these hazards. Thus, maps focusing on other uses are being sought. This report introduces an example in which a data package has been prepared by utilizing an earthquake hazard map to support investigations for prioritizing district disaster-prevention bases for earthquake-resistant conversions.

1. INTRODUCTION

Many large earthquakes are expected to occur in Japan in the future, and relevant authorities of the national government, municipalities, private companies, etc. have planned and executed various measures to minimize damage. Prior measures are considered to be more effective in mitigating the impact of earthquake disasters than post-disaster measures. In particular, it has been reported that the most effective method is to strengthen buildings and structures to make them earthquake resistant (Meguro, 2006). However, it is not easy for municipalities with limited budgets to strengthen their many facilities. As a result, action has been delayed even for disaster-prevention bases.

The paper "Materials for promoting earthquake-resistant strengthening of disaster-prevention bases" was circulated in 2005 for the use of in-charge persons in municipalities. In 2006, this was used as a basis for an investigation aimed at promoting seismic retrofit of disaster-prevention bases in Wakayama city. Damage is anticipated in Wakayama city from

future potential Tonankai and Nankai Earthquakes. The investigation was aimed at prioritizing Wakayama city's many disaster-prevention bases taking into account the structures and earthquake hazard.

This investigation was carried out as an Industry-Government-Education joint project as a continuation from 2005, and was led by the author and her co-workers from Ministry of Internal Affairs and Communications and ICUS, IIS, University of Tokyo.

2. OVERVIEW OF WAKAYAMA CITY

Wakayama city, capital of Wakayama prefecture, is located in the north-western part of the Kii Peninsula, near the border with Osaka-fu. It faces the Izumi Mountains to the north and the Kitan Strait to the west. Figure 1 shows the location map of the city.

The city extends to the mouth of the Kinokawa River, registered as a first-class river in Japan. The coastal area and area along the Kinokawa River are lowlands. The city covers an area of 210km² and its population is about 376,000 as of October 1, 2006, showing a decreasing tendency from its peak of about 403,000 in 1982.



Figure 1: Location map of Wakayama city

3. EARTHQUAKE IN WAKAYAMA CITY

3.1 Past earthquake damage

The observed earthquake occurrence distribution in Wakayama city and its environs is shown in Figure 3-1. Many large and small earthquakes

have been observed in Wakayama prefecture and in neighboring waters, showing that it is a very earthquake-prone area.

During their history, the Kinki and Shikoku regions have experienced many large earthquakes. Including tsunami damage accompanied some of these earthquakes, past records show that several thousand to several tens of thousands of casualties occurred in earthquakes of 1707 Hoei (M8.4), 1854 Ansei Nankai (M8.4), 1944 Tonankai (M7.9), 1946 Nankai-do-oki (M8.0), etc.

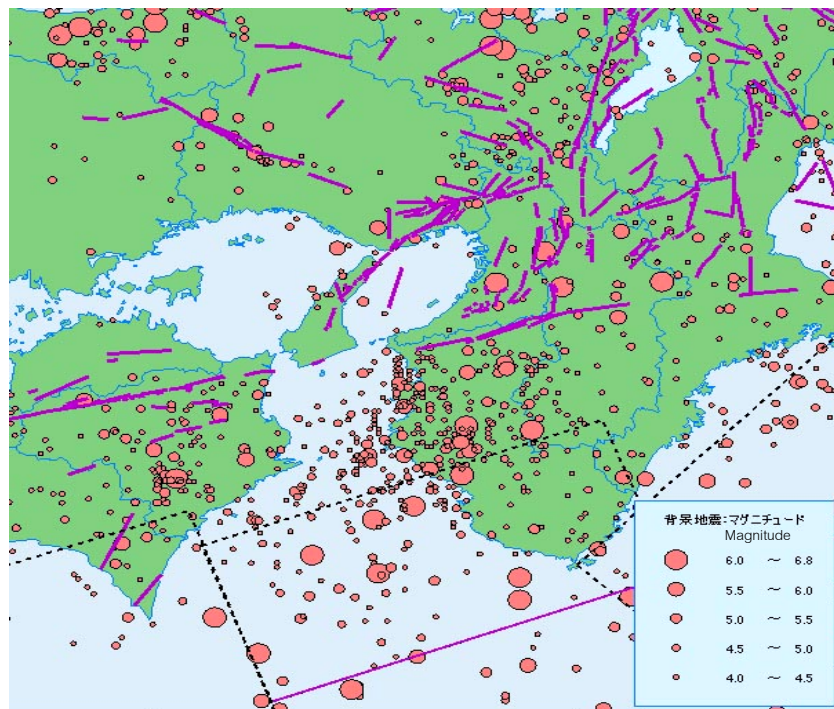


Figure 2: Epicenter distribution in Wakayama city and surroundings (New SEIRA output)

3.2 Future anticipated earthquakes

In 2005, as an aid in development of a future regional disaster prevention plan, Wakayama city conducted an investigation to predict damage caused by two anticipated classes of earthquakes. The first includes the “Tokai, Tonankai and Nankai Earthquakes,” and these are being investigated by the governmental Central Disaster Prevention Conference. The other is the “Chuo Kozo-sen (Central Tectonic Fault)” induced earthquake. This tectonic fault runs directly below Wakayama city. The predicted damage due to these two classes of earthquakes is outlined in Table 1.

Table 3-1: Outline of assumed earthquakes in Wakayama city

	Simultaneous occurrence of Takai, Tonankai and Nankai Earthquakes	Central Tectonic Line Earthquake
Earthquake size	M 8.6 equivalent	M 8.0 equivalent
Location of hypocenter fault	Suruga trough – Nankai trough	Central Tectonic Line (Awaji Island south-easternmost – near Izumi Mountains easternmost)
Depth of hypocenter fault	About 10 – 30km	4 – 14km
Seismic intensity	A little over 6 – a little below 5	7 – a little below 6
Liquefaction	High hazard mainly for filled up land and plain area	High hazard for valley area in mountains in addition to filled up land and plain area
Steep slope /Mountainside slide	72 locations	311 locations
Tsunami	Maximum tsunami height when it hits 1.05 – 3.89m	Tsunami does not occur
Building collapse	Total collapse 4,071 buildings	Total collapse 33,483 buildings
Casualties (as of 18:00 hrs in winter)	2,659 persons	9,094 persons
People of temporarily restricted housing (as of 18:00 hrs in winter)	36,834 persons	201,334 persons
Damaged water works	135 locations	1,305 locations
Probability of earthquake occurrence for coming 30 years	Nankai Earthquake about 50% Tonankai Earthquake about 60 – 70%	0 – 5%

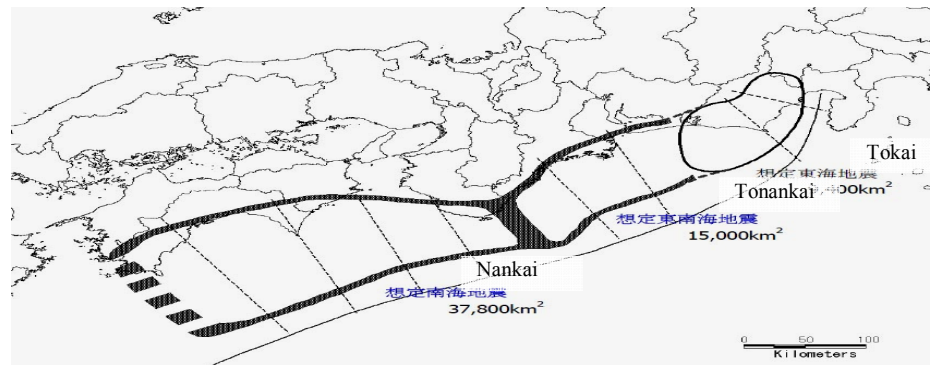


Figure 3: Assumed hypocentral region map of Tokai, Tonankai and Nankai Earthquake

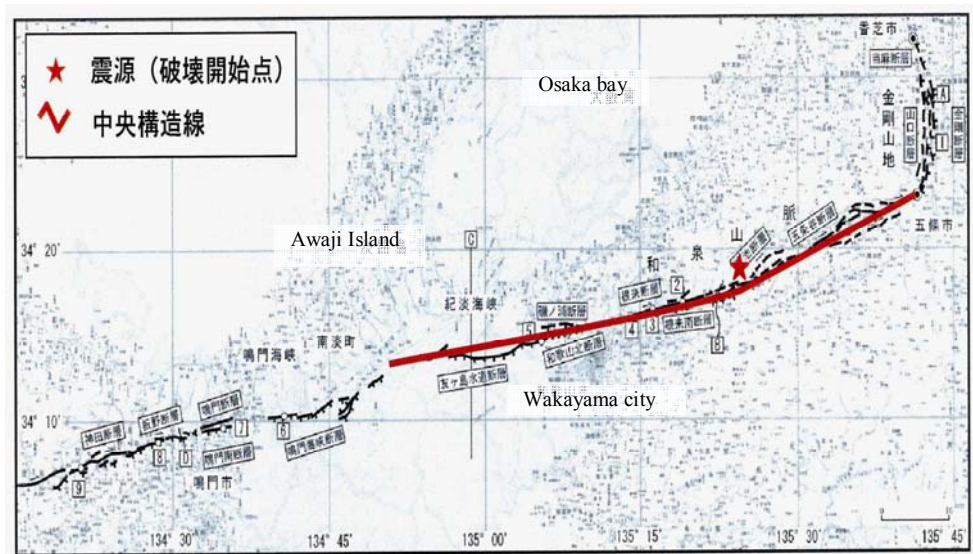


Figure 4: Assumed hypocentral region map of Central Tectonic Fault Earthquake

4. INVESTIGATION TO PRIORITIZE FACILITIES OF DISASTER-PREVENTION BASES FOR SEISMIC RETROFIT

In order to implement seismic retrofit of facilities of disaster-prevention bases, it was necessary to first carry out a seismic diagnosis of them and to assess their health. However, a large budget and a lot of time would have been necessary for detailed seismic diagnosis. Furthermore, it was difficult for Wakayama city to carry out the diagnosis of all of its many facilities at the same time. Thus, for budget phasing, it was necessary to determine priorities that would enable the city to carry out detailed seismic diagnoses in a phased manner over a period of years. It was therefore decided to proceed with the investigation according to the flow chart shown in figure 5.

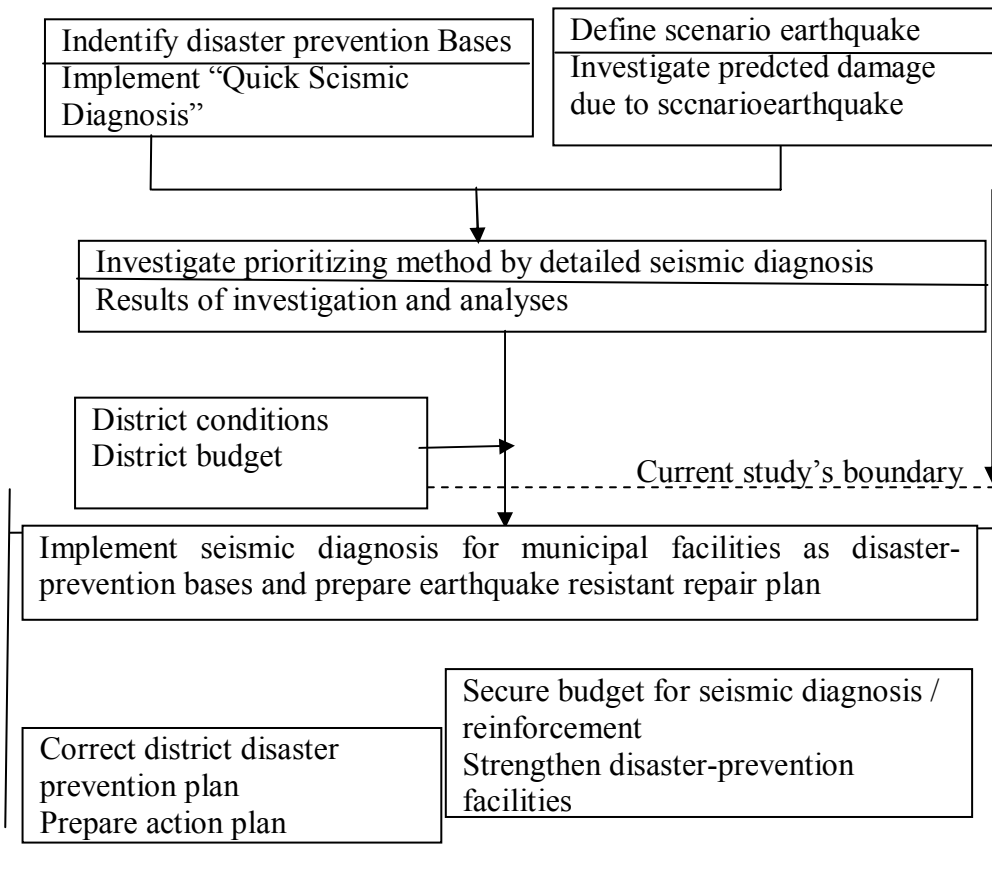


Figure 5: Investigation flow

4.1 Implement quick seismic diagnosis of facilities for disaster-prevention bases

4.1.1 Identify facilities for disaster-prevention bases

A seismic retrofit project was already in progress for schools, etc. in Wakayama city that were planned for use mainly as shelters. In addition, 165 of Wakayama city's facilities for disaster-prevention bases were identified where seismic diagnosis was considered necessary. These facilities are shown in Figure 6.



Figure 6: Part of facilities of disaster-prevention bases in Wakayama city

4.1.2 Implement questionnaire-type “Quick Seismic Diagnosis” (Kajima, 2005)

Quick seismic diagnosis has been developed as a useful tool, based on the results of many detailed seismic diagnoses. A simple questionnaire consisting of 26 questions was prepared. These questions would be easy to answer by persons involved in the building industry, and the results would assist in development of a simplified seismic diagnosis. However, it was not practical for the questionnaire to be answered by only ICUS engineers for all 165 facilities to be used for disaster-prevention bases over the whole area of Wakayama city. Thus, a training course for “Quick Seismic Diagnosis” was held to instruct people how to fill in the questionnaire. This was carried out with the participation of about 25 building engineers of Wakayama city who were familiar with local conditions. These engineers then carried out a site survey of the relevant facilities for about one month, and then answered the questionnaire. The main contents of the questionnaire were as follows:

- What is the number of stories and the total floor area?
- What year was construction of the facility commenced and completed?
- What is the structural type? • Does the facility have pilotis?
- What is the plan configuration of the facility?
- What is the size of the facility’s walls and windows?
- What are the soil conditions at and surrounding the site?

Many of the questions could be simply answered from preset answer options with the help of easy-to-understand figures.

The building engineers of Wakayama city were also requested to attach photos of the facilities with their answers. If they were unsure about some of the questions, ICUS engineers clarified their answers using the provided photos to increase diagnosis accuracy.

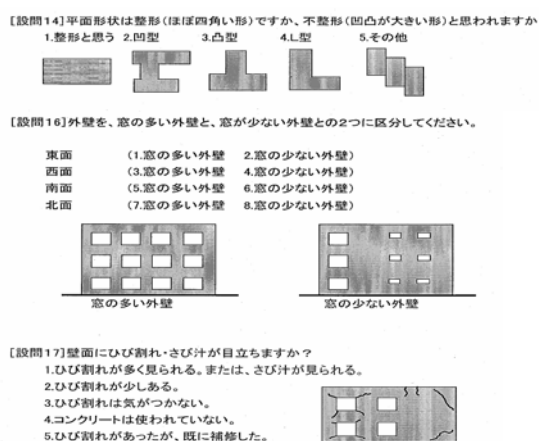


Figure 7: Questionnaire for “Quick Seismic Diagnosis”(part of it)



Figure 8: Training course for “Quick Seismic Diagnosis”

The analysis results for the 165 facilities were assessed as five grades with six indices, i.e. site conditions, building plan configuration, building elevation configuration, seismic standard compliance, deterioration conditions and overall assessment. In addition, the cost of the seismic retrofit for each building was roughly estimated on the basis of similar buildings. The estimated cost covered the cumulative reinforcement cost necessary for the building to satisfy the standard required earthquake resistance defined by the current Construction Standard Act of Japan.

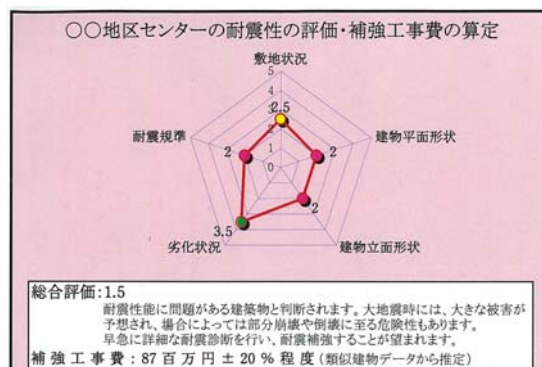


Figure 9: Example of Quick Seismic Diagnosis results

4.2 Investigation of predicted damage

As stated in Section 3 above, two potential classes of earthquakes were identified: the Tokai, Tonankai and Nankai Earthquakes and the Central Tectonic Fault Earthquake. For the scenario-based investigation on prioritizing the facilities for detailed seismic diagnosis, it was necessary to select one of these two earthquake classes. The Central Tectonic Fault Earthquake, whose epicenter is directly below Wakayama city, would cause huge damage but its occurrence probability in the coming 30 years is only 0 to 5%. However, the occurrence probability of the Tokai, Tonankai and Nankai Earthquakes is 50 to 70%. As a result of discussions with the relevant authorities, it was agreed that predicted damage due to the presumed Tokai, Tonankai and Nakai Earthquake would be the priority for the investigation. Then, taking into account the longevity of the facilities

used for disaster-prevention bases and phasing of the budget, it was decided to investigate the subject priority using the above predicted damage.

The utilized predicted damage was based on GIS, and data were extracted by ICUS. The GIS was prepared by Wakayama city as shown in the “Report on results of investigation on predicted earthquake damage as contracted work to develop hazard maps for Wakayama city, etc. (March 2005)” (hereinafter called “Report on predicted damage for Wakayama city”).

4.3 Investigation of prioritization method for detailed seismic diagnosis

4.3.1 Categorization roles of disaster-prevention bases

The roles of the disaster-prevention bases in the event of a disaster vary. For example, in Wakayama city, “Fire Station” takes the roles of controlling / executing measures, dispatching / gathering information, helping / rescuing, etc. “Health Center” takes the roles of dispatching / gathering information and conducting temporary recovery. “Shelter” is a place of refuge for disaster victims. Furthermore, “Branch / Liaison Office” and “Stockpile Storehouse” have their respective roles. However, no roles had been allocated to the 165 facilities for disaster-prevention bases. Prioritization is not practical if the roles are treated equally. As a result, 61 of the 165 facilities that must perform one or more key roles in the event of a disaster were selected for the current investigation. They were identified as “Critical Facilities in Disaster Mode” (key roles are A: control / execute measures, B: dispatch / gather information, C: help / rescue and D: temporary recovery). It is noted that these 61 facilities included those where seismic retrofit was already progressing. This was due to the need to clarify these facilities’ placement conditions to cover the whole district and to assess their resistance to damage.

Table 2: Roles of disaster-prevention bases in Wakayama city

	Disaster prevention bases (roles)	Fire station / office	City hall	Branch / liaison office	Health center	Shelter school	Shelter other than school	Stockpile storehouse	
A	Control and execute measures	○	○	○					
B	Dispatch and gather information	○	○	○	○				
C	help and rescue	○							
D	temporary recovery		○	○	○				
E	Human	Victim				○	○		
F		Injured			○				26 locations: emergency medical organizations
G1	Material	Food				○		○	
G2		Others				○		○	

	Disaster prevention bases (roles)	Fire station /office	City hall	Branch /liaison office	Health center	Shelter - school	Shelter - other than school	Stockpile storehouse	
	Lifeline	Electricity							
		Water							

4.3.2 Kinds of hazards

Many data were incorporated into GIS during the work to produce the “Report on predicted damage for Wakayama city”. These data included not only natural and social conditions but also predicted natural phenomena and a variety of predicted damage to facilities and people. The current investigation predicted direct damage to structures of disaster-prevention base facilities by measuring the severity of hazards predicted to be caused by the presumed Tokai, Tonankai and Nankai Earthquakes. Specifically, three kinds of hazards were studied: seismic intensity, tsunami and landslide. These were supplemented by liquefaction potential values.

4.3.3 Assessment Method

Facilities exposed to large hazards of tsunami or landslide disaster were excluded from the facilities of interest for the current prioritization investigation. This is because they would fail to fulfill their roles as disaster-prevention bases even if their earthquake resistance were improved. It is desirable to study these facilities separately when considering measures for mitigating the impact of hazards or avoiding hazards as well as the application of seismic retrofit.

For facilities of interest, the seismic hazard Z of each facility was obtained from the earthquake ground motion and “overall assessment score X ”, and priority was determined on that basis.

The specific assessment procedures were as follows:

1. Extract numerical data of seismic intensity, tsunami, landslide disaster and liquefaction at the locations of the 61 disaster-prevention base facilities of interest using GIS data obtained from the “Report on predicted damage for Wakayama city”.
2. Exclude facilities exposed to large hazard of tsunami or landslide disaster from facilities of interest. Add supplementary notes on liquefaction for reference only.
3. Derive correction factor α from seismic intensity at each facility location. Assess earthquake resistance taking into account external force or earthquake ground motion. However, seismic intensity is not equal to external force. Thus, acceleration correlatable to seismic intensity was introduced. Acceleration corresponding to seismic intensity slightly below 6 (reference number) was defined as reference acceleration. It is noted that buildings must be resistant to seismic intensity slightly less than 6, according to the current Construction Standard Act of Japan. Then, the ratio of the

- acceleration corresponding to each scenario seismic intensity to the reference acceleration was defined as correction factor α .
4. Obtain seismic hazard Z by dividing correction factor α by overall assessment score X from “Quick Seismic Diagnosis”.
Seismic hazard $Z = \alpha / X$
 5. Give priority in order from large seismic hazard Z obtained above to smaller (the larger the number, the higher the priority).

Table 3: Estimate of correction factor α (relationship between seismic intensity and corresponding acceleration)

Seismic scale	Scenario seismic intensity	Corresponding acceleration cm/s ²	Correction factor α *2)	
A little below 5	4.5	80.0	0.23	
	4.6	94.0	0.27	
	4.7	108.0	0.31	
	4.8	122.0	0.35	
	4.9	136.0	0.39	
Slightly over 5	5.0	150.0	0.43	
	5.1	174.0	0.50	
	5.2	198.0	0.57	
	5.3	222.0	0.63	
	5.4	246.0	0.70	
Slightly under 6	5.5	270.0	0.77	
	5.6	310.2	0.89	
	5.7	350.4	1.00	Reference number *1)
	5.8	390.6	1.11	
	5.9	430.8	1.23	
Slightly over 6	6.0	480.0	1.37	
	6.1	554.0	1.58	
	6.2	628.0	1.79	
	6.3	702.0	2.00	
	6.4	776.0	2.21	
7	6.5	850.0	2.43	

* 1) Reference seismic intensity was defined to be mid-point of seismic intensity scale of “slightly under 6”, which is the current standard earthquake resistance requirement, thus to be 5.7

* 2) Correction factor was defined to be the ratio of the acceleration corresponding to a certain scenario seismic intensity to the reference acceleration 350.4 cm/s² corresponding to the reference seismic intensity 5.7.

4.4 Results of investigation and analysis

4.4.1 Overlay on hazard maps

GIS output and locations / names of facilities of interest are shown in Figures 10. They enabled us to identify the distribution of facilities and

hazards. They should also be useful for subsequent work in developing an action plan, etc.

4.4.2 Results of investigations on priorities of critical facilities in disaster mode

Table 4 shows part of the results of the investigations on priorities of critical facilities in disaster mode, assuming the Tokai, Tonankai and Nankai Earthquakes. No facilities were found where a landslide disaster was anticipated (denoted by “0” in Table 4). Two facilities were found where a tsunami was anticipated (M fire station and T branch office). The other 59 facilities were sorted in order from larger seismic hazard to lower.

In addition, the cost of a detailed seismic diagnosis for each facility was estimated based on similar size and type of buildings.

It is noted that the facilities where questionnaire type “Quick Seismic Diagnosis” was not applied were regarded as no-diagnosis-needed facilities. They were evenly assessed as having an overall assessment score X of 3.5*).

(* Overall assessment score X = 5.0, 4.5 and 4.0 corresponds to a vibration isolation building, a vibration controlled building or a building taller than 60m, and a building taller than 45m, respectively.)

Referring to the current investigation results, it was agreed to start planning for budgeting the detailed seismic diagnosis for seismic retrofit work, taking into account individual circumstances and in line with the municipality budget.

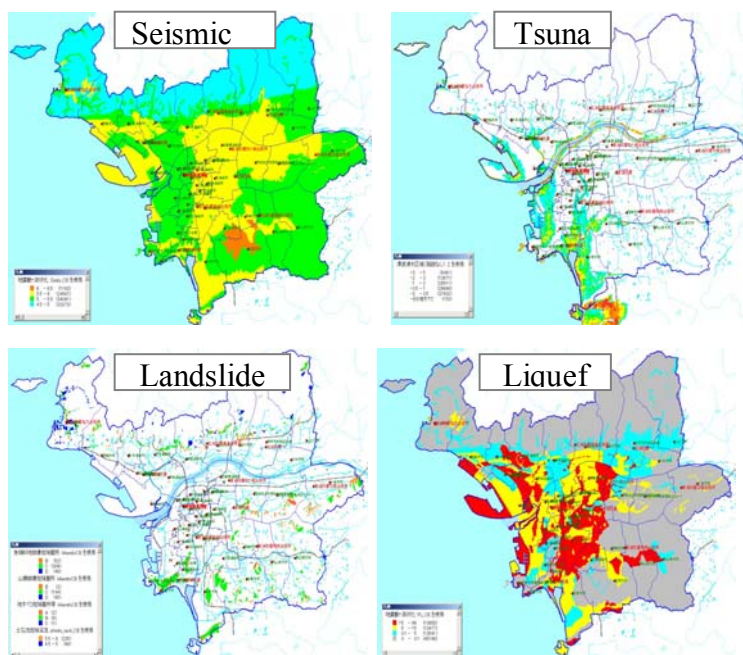


Figure 10: Hazard distribution due to Tokai, Tonankai and Nankai Earthquake and facility location map

also from various factors such as accessibility, sustainability of lifeline function, surrounding population, wooden building ratio, etc.

If the current assessment using seismic hazard Z is regarded as a single-axis assessment, a double-axis assessment would be envisaged as follows. For example, if the seismic hazard Z of the shelter vs. night population, etc. are plotted on a two-axis graph, facilities in a dense population area but with insufficient earthquake resistance become visible. Thus, the assessment method would vary with the facility's role.

The current investigations could utilize "Report on predicted damage for Wakayama city" that Wakayama city worked on in the preceding year. However, even if damage is repeatedly predicted, it can never be reduced (Meguro, 2006). Predicted damage is not useful until it is utilized for disaster impact mitigation measures as in the current investigation. It is planned to further utilize current investigation results in accordance with demand for revision of Wakayama city's disaster prevention plan and development of an action plan.

ICUS expects to contribute to the promotion of seismic retrofit of critical municipal facilities by uploading the current investigation results to the website of the FDMA (Fire and Disaster Management Agency) entitled "Materials for promoting earthquake-resistant strengthening of disaster-prevention bases" and by distributing materials to the relevant authorities through the FDMA.

The authors express their sincere appreciation to the staff of the General Disaster Prevention Office of Wakayama city and to the staff of Kajima Corporation, who provided the authors with a lot of help and advice.

REFERENCES

- Central Disaster Prevention Conference HP (The Cabinet Office)
Kajima Corporation HP, 2005., *KAJIMA Digest*, September
Japan Road Association, 2002. Road and bridge specifications and explanatory note V Seismic design version, March.
Chihokokyodantai tantosha notameno "Bosai kyoten no taishinka sokushin shiryō" ("Materials for promoting earthquake-resistant strengthening of disaster-prevention bases" for in-charge persons in municipalities) HP (FDMA)
Meguro, K., 2006. "Jishin bosaijo no saijuyo kadai dearu kison futekikaku tatemono no taishin kaishu wo suishin suru tameni (In order to implement earthquake resistant repair of existing inadequate buildings that are the most critical task in earthquake disaster prevention)" *Shobo Bosai* Spring Issue vol 5, No. 2
Mapion HP (Cybermap Japan)
Wakayama city HP (Wakayama city)
Ukon, H., 2006. Nagata, S., Miyamura, M.(editors)
"Risukumanejimento notameno jishin kikendo kaiseki sisutemu (Seismic

hazard analysis system for risk management)”*Urban Technology Promotion Conference, 18th Technical Research Meeting*, November 9.

Wakayama city, 2005. “Jishin higai soutei chosa kekka houkokusho (Report on investigation results of earthquake damage supposition)” contracted work to develop Wakayama city tsunami hazard map, etc., *Kokusai Kogyo KK*, March.

Wakayama city, 2005. Wakayama city disaster prevention plan 2005 revision Wakayama city disaster prevention meeting.

FRAGILITY ANALYSIS OF REINFORCED CONCRETE FRAME STRUCTURES

MUNAZ A. NOOR

Bangladesh University of Engineering & Technology

mnoor@ce.buet.ac.bd

M. YASIN

Bangladesh University of Engineering & Technology

yasinbuet96@yahoo.com

ABSTRACT

In this paper fragility curves of low rise reinforced concrete frame structures in Bangladesh is presented. The fragility analysis has been performed using the method proposed by Bazzurro et al. (2004). Uncertainty of three structural parameters, concrete compressive strength, column size and concrete cover have been considered. Fragility curves of different structural limit states of a typical structure have been developed from probabilistic seismic hazard of the site and performance of the structures against the hazard. The uncertainty inherent in building response and capacity for different ground motion levels due to variability in construction and structural evaluation process is used to obtain the desired fragility curves. The main feature of this method is that fragility curves can be drawn very easily.

1. INTRODUCTION

Fragility of structures is obtained from probabilistic seismic hazard of the site and performance of structure or stock of structures against the hazard. Fragility curves of a structure are used to predict the post earthquake functionality. Prediction of the post-earthquake functionality of the important structures such as hospital building, fire brigade building and digester shelter is essential for earthquake digester management. It is very important to identify the vulnerable buildings and estimate the level of damage under a probable earthquake by combining the probabilistic seismic hazard and fragility of the concerning structure or stock of structures.

Noor et al. (2005) developed probabilistic seismic hazard curves for Dhaka, Chittagong and Sylhet city using Boore et al. (1993) and McGuire (1978) acceleration attenuation expression. By using other acceleration attenuation expressions same type of seismic hazard curves with different curvature, can be developed through same procedure, from the same earthquake database. A complex methodology that may be followed to construct fragility curves for reinforced concrete (RC) frame structures in Bangladesh is presented in Noor and Manzur (2005). In the present study seismic hazard analysis is done by using Duggal (1989) acceleration attenuation expression and the earthquake database prepared by Sharfuddin

(2001) and limit-state fragility analysis is done by following the guideline stated in Bazzurro et al. (2004). Duggal (1989) acceleration attenuation expression is developed for the alluvium soil of Japan. The soil of Bangladesh is alluvium. Finally a set of fragility curves for different limit states is prepared for a typical three storey RC frame structure.

2. METHODOLOGY

A limit-state fragility curve provides the conditional probability that the specified limit state will be reached or exceeded as a function of the severity of the future ground motion. Fragility curves involve uncertainties associated with dynamic displacements produced by different ground motion records, material properties, structure geometry, structure modeling and analysis procedure. In Noor and Manzur (2005) a time consuming methodology is used to construct fragility curves for RC frame structures in Bangladesh. In that method a structure is needed to be analyzed many times and the method is time consuming. In this study a structure is needed to be analyzed three times with three percentile values for a particular parameter. Limit-state fragility analysis is done by following the guideline stated in Bazzurro et al. (2004) and considering uncertainty of three major structural parameters, concrete compressive strength, column size and concrete cover. In this research work the limit states in fragilities are related to loss of dynamic capacity.

2.1 Pushover Analysis

For seismic assessment of structures, the knowledge of the nonlinear static behavior of a specific structure subjected to incremental lateral deflection is used and quadrilinear approximation is done to infer its nonlinear dynamic response expected for different levels of ground motion severity. Quantitative measures of the implied degradation in structure safety is used to associate each of several post-earthquake structural damage states with an appropriate post-earthquake structural limit state that may imply some degree of occupancy restrictions. This method of analysis is known as pushover analysis.

2.2 Estimation of Uncertainty

The uncertainty inherent in building response and capacity for different ground motion levels due to variability in construction and structural evaluation process is used to obtain the desired fragility curves for the different structural limit states. Uncertainty is measured from percentile values of parameters and using Equation 1 and the square-root-of-sum-of-squares (SRSS) rule is used to combine the uncertainty (Bazzurro et al. 2004).

$$\Rightarrow \beta = \frac{1}{x} \ln \left(\frac{S_a}{\bar{S}_a^{LS}} \right) \quad (1)$$

where,

β =uncertainty

S_a = percentile spectral acceleration

\tilde{S}_a^{LS} = median spectral acceleration to attain concerning limit state

$x = -0.67, 0.0, 0.67$

for 25 percentile, 50 percentile and 75 percentile value respectively, other values of x can be obtained from table of the Gaussian distribution function.

2.3 Computation of the Fragility Curves

From the median spectral acceleration and corresponding uncertainty (β) the fragility curves associated with onset-of-damage, onset of yellow-tag, onset red-tag, and onset collapse states are plot using Equation 2 (Bazzurro et al. 2004).

$$S_a = \tilde{S}_a^{LS} e^{x\beta} \tag{2}$$

3. DEFINING LIMIT STATES

Seismic hazard analysis of Dhaka is performed by using Duggal (1989) acceleration attenuation expression and the earthquake database prepared by Sharfuddin (2001). Developed seismic hazard curve for Dhaka city is shown in Figure 1. The proposed primary tagging criteria of different limit states are obtained from seismic hazard curve of Dhaka (Figure 1) and displayed in graphical form in Figure 2. The values of the quantities in Figure 2 are proposed for Dhaka city and should be reevaluated for other sites and structures of different importance.

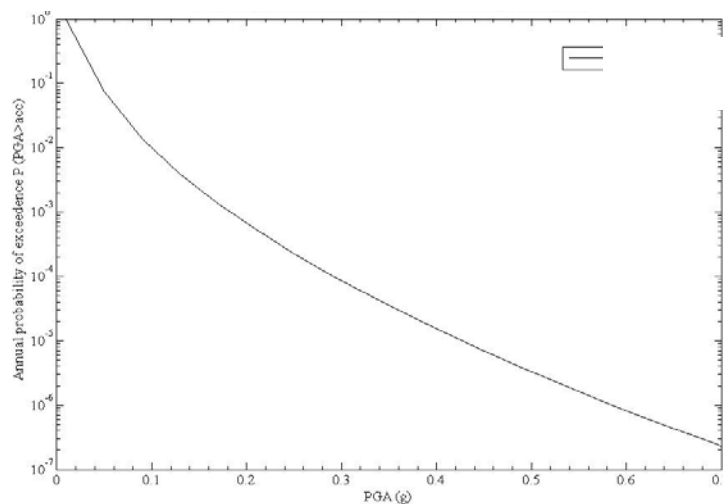


Figure 1: Seismic Hazard Curve for Dhaka city, developed using Duggal (1989) acceleration attenuation expression

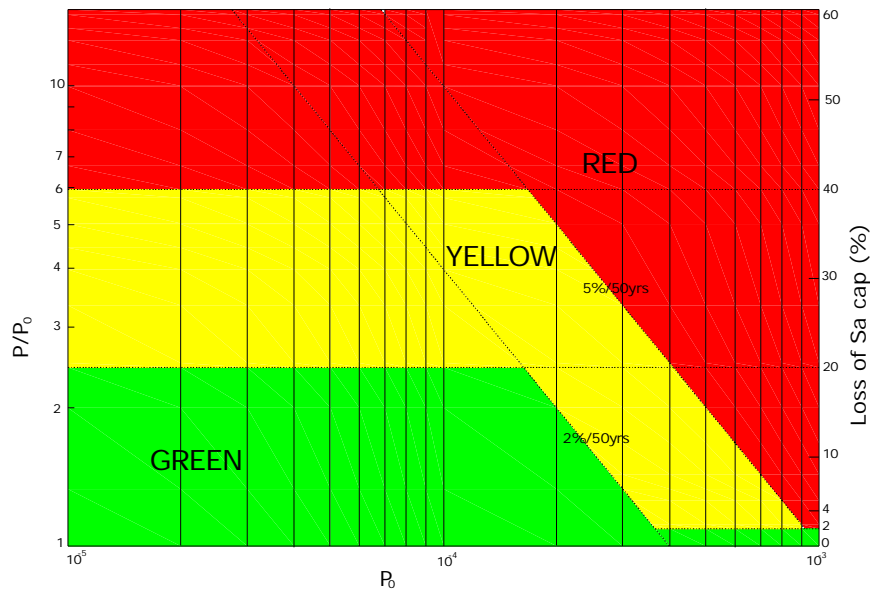


Figure 2: Graphical representation of tagging criteria for Dhaka city

In Figure 2, P_0 is building-site-specific mean annual frequency (MAF) of exceedance of the ground motion corresponding to the dynamic capacity ($\dot{S}_{a, \text{cap}}$) of intact structure and P is building-site-specific MAF of the aftershock ground motion corresponding to the median capacity of the damaged structure. Any building is identified by a particular value of P_0 that can be computed during “peace” time before any earthquake has occurred. A larger value of P_0 implies that the building is either relatively “weak”, or that it is located in an area of higher seismic hazard compared to that considered in the original design, or a combination of both. The opposite is true for lower values of P_0 .

4. FRAGILITY ANALYSIS OF A TYPICAL THREE STOREY REINFORCED CONCRETE FRAME STRUCTURE

A typical three storey reinforced concrete frame is analyzed. The plan and elevation are shown in Figure 3. The building is designed for gravity load. Three dimensional models are created and static displacement controlled pushover analysis is done using Opensees1.6.2 (McKenna and Fenves, 2001).

The solid line in the Figure 4 is static pushover (SPO) curve and dashed line is quadrilinear approximation (Bazzurro et al. 2004). The damage states are identified as on the curve of Figure.4. These choices of damage states are not unique. Any other point relating to a change in any structure properties can be chosen as a damage state. Later, these damage states will be associated to different structural limit states.

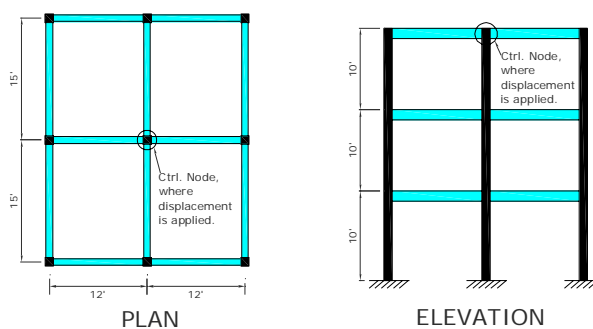


Figure 3: A typical three storey reinforced concrete building frame

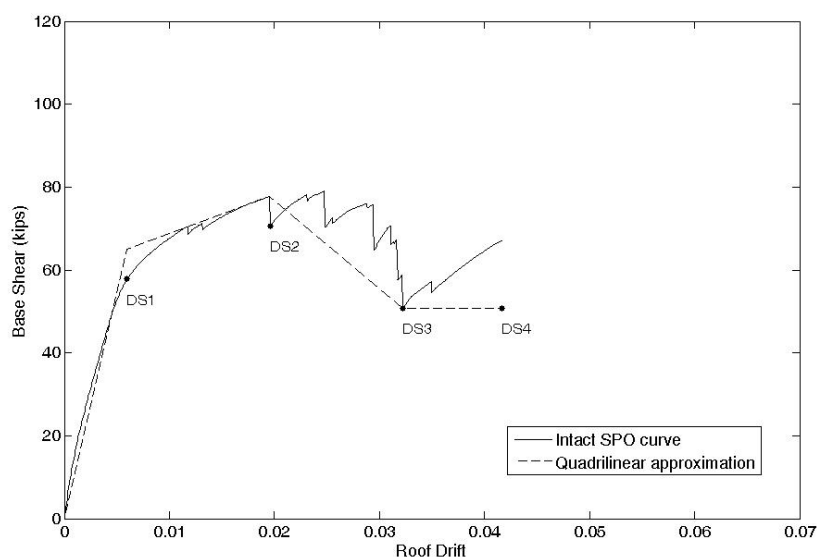


Figure 4: Non linear static pushover curve for the intact structure

The assessment of the residual lateral capacity of the building in a damage state is of interest provided that at the local level every damaged structural member is still capable of carrying vertical loads. If there is loss of local member vertical capacity in the damage state the building will be assigned a structural limit state that corresponds to collapse. The pushover curve for a structure at the onset-of-damage state (DS₁ in Figure 4) coincides with that of the intact structure. Nonlinear Static Pushover (NSP) curves for other damage states are obtained simply by assuming parallel to elastic unloading/re-loading (Figure 5 and Figure 6) that can result in comparable estimates of residual dynamic capacity. Unloading the structure from a damage state may create an initial offset in the damaged-structure NSP curve due to the residual permanent displacement in the structure. The extent of this permanent displacement is somewhat an artifact of applying a static procedure to modeling the dynamic response of the structure subject to ground shaking. The residual displacement obtained from the NSP can be considered as an upper bound because the structure is not allowed to oscillate and therefore return to a residual offset closer to its original upright position. The NSP curves for the structure in the damaged conditions are assumed to start from the origin of the axes (i.e., no permanent displacement). The effects of the expected (or measured) dynamic residual offsets on the residual lateral capacities are accounted to infer dynamic

response. As illustrated in Figure 5, the horizontal shift of the NSP curves for the damaged structures back to the origin does not shift the collapse (e.g., DS₄) displacement.

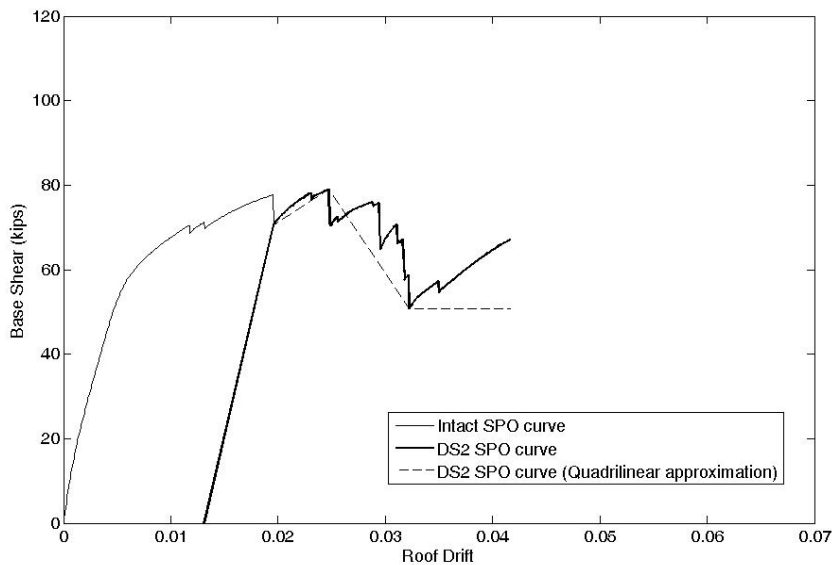


Figure 5: Non linear static pushover curve for damage state DS2

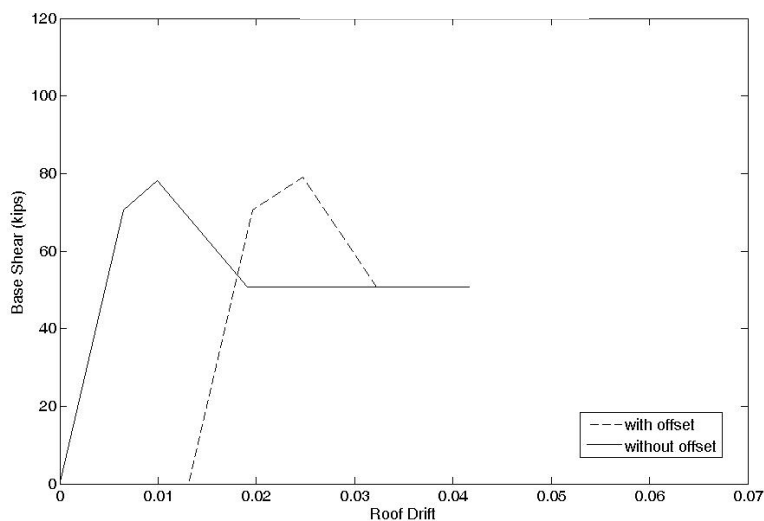


Figure 6: Quadrilinear approximation of DS2 NSP curve, with and without offset

The Incremental dynamic analysis (IDA) curves are obtained from the quadrilinear approximation of NSP curves and shown in Figure 7. For the intact structure four structural damage states are attained at four different spectral accelerations. The capacity of the intact structure and residual capacity of damaged structure are obtained. Figure 8 shows the percent loss of spectral capacity (loss of dynamic capacity) at different spectral acceleration. The input percentile values of those parameters are as in Table 1. The static pushover curves and incremental dynamic analysis curves obtained are shown in Figure 9.

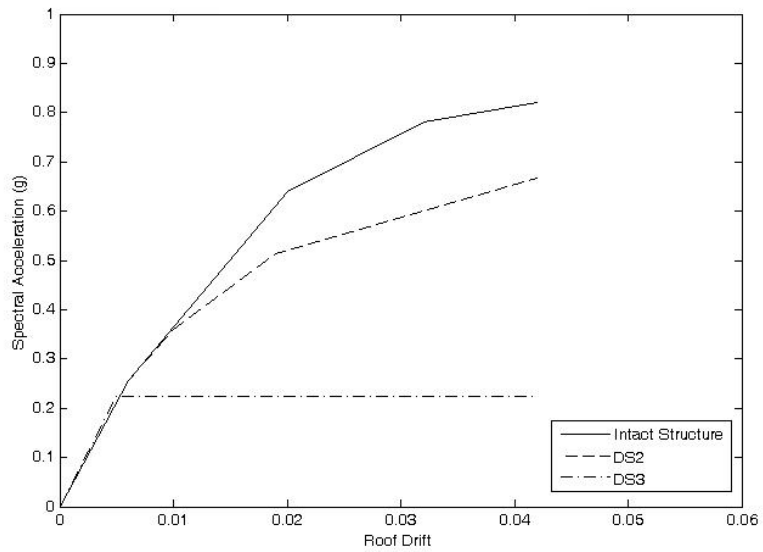


Figure 7: Incremental Dynamic Analysis curves for the structure in different states

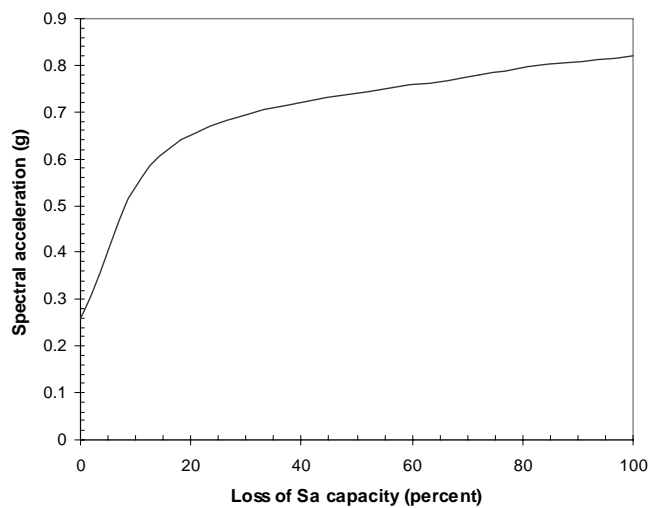
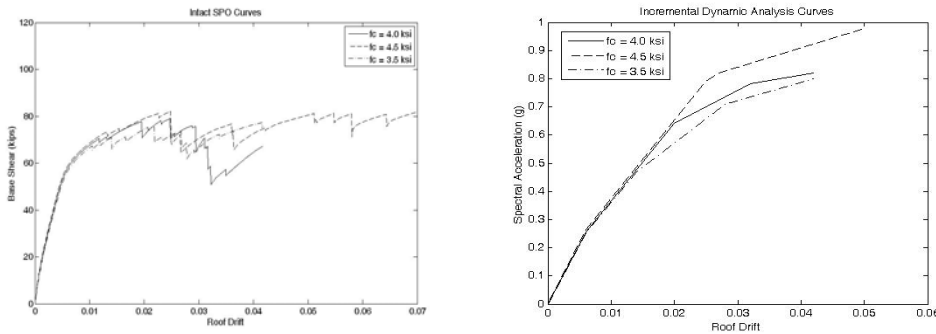


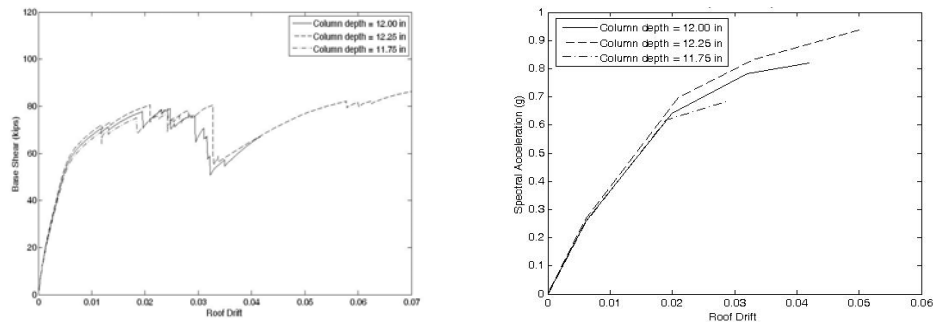
Figure 8: Loss of spectral acceleration capacity at different spectral acceleration

Table 1: Percentile values of three structural parameters

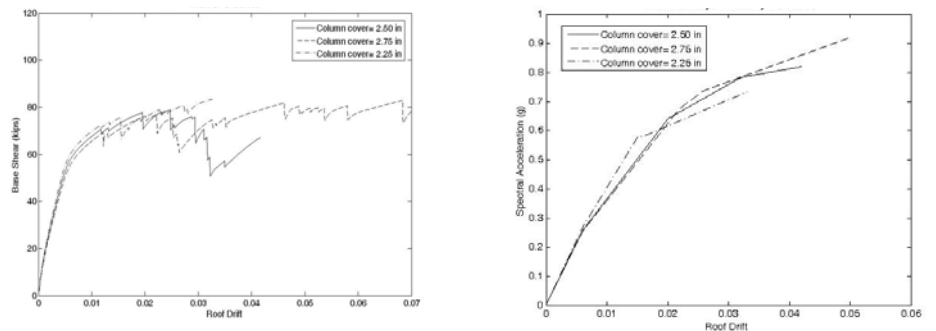
Parameter	Mean value	Percentile value
Concrete compressive strength	4.0 ksi (mean)	50 percentile = 4.0 ksi
		25 percentile = 3.5 ksi
		75 percentile = 4.5 ksi
Column depth	12.00 in	50 percentile = 12.00 in
		25 percentile = 11.75 in
		75 percentile = 12.25 in
Cover	2.50 in	50 percentile = 2.50 in
		25 percentile = 2.25 in
		75 percentile = 2.75 in



(a) for three percentile values of concrete compressive strength



(b) for three percentile values of column size



(c) for three percentile values of concrete cover

Figure 9: Static pushover curves and incremental dynamic analysis curves of the intact structure.

The uncertainty (β) inherent in building response and capacity for different ground motion levels due to variability in construction and structural evaluation process is used to obtain the desired fragility curves for the different structural limit states. Uncertainty (β) is measured from percentile values of parameters and using Equation 1 and the square-root-of-sum-of-squares (SRSS) rule is used to combine the uncertainty.

Computation of the Fragility Curves

From median S_a -values and corresponding β -values of four ground motion levels, the fragility curves associated with onset-of-damage, onset of yellow, onset red, and onset collapse states are plot using Equation 2. The resulting fragility curves are shown in Figure 10.

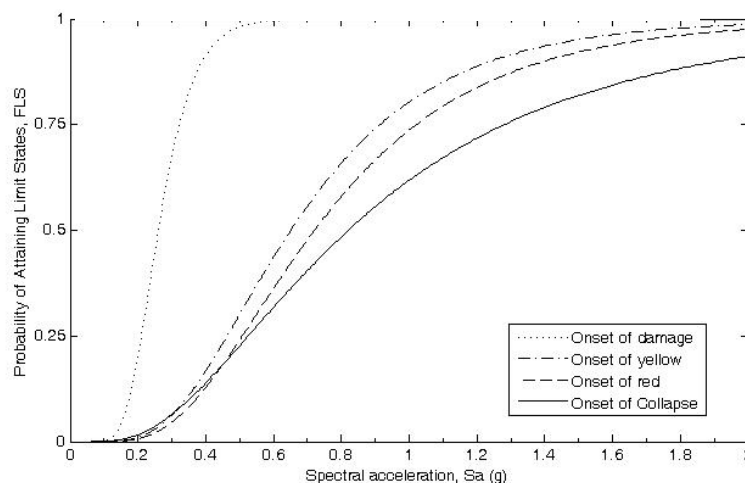


Figure 10: Fragility curves for different limit states of the building

In Figure 10 fragility curve for onset of damage (OD) is the steepest of the four because the value of β is the smallest. The opposite is true for the fragility curve corresponding to the collapse state. The fragility curve corresponding to the green-tag state is equal to unity for all levels of ground motion.

5. CONCLUSION

A methodology is presented to predict post-earthquake functionality of a structure. Coupling the fragility curves with probabilistic seismic hazard analysis will permit assessments of the seismic performance of structures. The procedure developed in this research work is of more general applicability and can be valuable to engineers to assess seismic performance of structure or stock of structure to predict post-earthquake functionality.

REFERENCES

- Bazzurro, P., Cornell, C.A., Menun, C., Luco, N., Motahari, M., 2004. *Advanced Seismic Assessment Guidelines*. Stanford University, Stanford CA, Sep. 30, 2004.
- Boore, D.M., Joyner, W.B., Fumal, T.E., 1993. *Estimation of response spectra and peak accelerations from western North America earthquakes: An interim report*, Open-File-Report 93-509, U.S. Geological Survey, Reston, Virginia, 72 pp.
- Duggal, R., 1989. *Estimation of Seismic Risk and Damage, Their Utilization as Design Criteria*. M Engg. Thesis, University of Tokyo, Japan.
- McGuire, R. K. 1978. Seismic Ground Motion Parameter Relations. *Journal of the Geotechnical Engineering Division*, ASCE, Vol. 104, No. GT4, pp. 481-490.
- McKenna, F. and Fenves, G. (2001). "The OpenSees Command Language Manual: version 1.6.2," *Pacific Earthquake Engineering Center, Univ. of Calif., Berkeley*. (<http://opensees.berkeley.edu>).

NEHRP, 1991. National Earthquake Hazards Reduction Program. *Recommended Provisions for the Development of Seismic Regulations for New Buildings*. Building Seismic Safety Council, Washington, D.C., 1991.

Noor, M.A., Manzur, T., 2005a. *Development of Fragility Curves for R.C.C. Frame Structures: Bangladesh Context*. First Bangladesh Earthquake Symposium (BES-1). Dhaka, Dec. 14-15, 2005.

Noor, M.A., Yasin, M., Ansary, M.A., 2005b. *Seismic Hazard Analysis of Bangladesh*. First Bangladesh Earthquake Symposium (BES-1). Dhaka, Dec. 14-15, 2005.

Sharfuddin, M., 2001. *Earthquake Hazard Analysis for Bangladesh*. M.Sc. Engg. Thesis, BUET, Dhaka.

FLOOD IN BANGLADESH WITH FOCUSES ON 2007 FLOOD

MD. AYNUL KABIR
Flood Forecasting and Warning Centre, BWDB
aynulce@yahoo.com

MD. SAZEDUL KARIM CHOWDHURY
Processing and Flood Forecasting Circle, BWDB
sazed123@gmail.com

ABSTRACT

As a part of climate change over the world, the spatial and temporal distribution of rainfall is changing day by day. And for this, the intensity of floods is increasing nowadays in many countries including Bangladesh with unusual timing. Unlike the past, the 2007 flood in Bangladesh occurred relatively earlier. In this paper, the 2007 flood is extensively analyzed. It reveals that the flood gave less time to the people for taking adequate measures due to its earlier occurrence. At the same time, the flood that had introduced earlier, ended quickly, most perhaps, because of the absence of synchronization of flood peaks at the GBM Rivers. The level of destruction or extent of durations of past flood events (1988, 1998 and 2004) are also found very much co-related with the synchronization of flood peaks at the GBM Rivers. However, the temporal variability has stimulated this year's short duration flood in comparison to the floods in the past. Beside this, a number of people living in flood plains also trigger high flood frequency as well as huge loss. It is marked that breaching of flood protection embankment at Serajganj and Gaibandha has worsened the overall flood situation during the same period.

1. INTRODUCTION

Bangladesh is a part of the world's most dynamic hydrological system. In fact, the country is a fluid landscape framed by three major rivers: the Ganges, the Brahmaputra and the Meghna (GBM). The country is highly prone to natural disasters, especially hydro-meteorological disasters, for its geographic location and topographic composition. Flood is considered here as a regular event, which causes enormous loss of lives and properties almost every year. On an average, 20% area of Bangladesh is affected by flood every year (FFWC 2005). The situation for monsoon river floods is more complex and not fully understood (Khalequzzaman, 1994; Reavill and Rahman, 1995; and Hofer and Messerli, 1997). Many studies, researches, and investigations regarding this issue (e.g. Rasid and Paul, 1987; Khalil, 1990; Haque and Zaman, 1993; Paul, 1997; and Hofer and Messerli, 1997) were conducted over the last few decades. It implies that complete flood control in a country like Bangladesh is neither possible nor feasible. It is no more flood control rather than the flood management. Now it has become

inevitable to develop a plan to live or cope with flood and to take mitigation measures to reduce the damages due to flood.

A Flood Information Cell (FIC) is running at Flood Forecasting and Warning Centre (FFWC) under Bangladesh Water Development board (BWDB) in action to the permanent orders of the Government of the People's Republic of Bangladesh regarding disaster. FFWC presents a model that gives forecast for maximum 72-hour interval. Forecast made by FFWC using model revealed a very satisfactory approximation only in different observation stations. FFWC activities are still limited to macro level applications. Additional efforts are required to reduce the impact of flood hazards in micro level. Flood risk assessment through comprehensive study on past flood events could be an efficient and important tool providing advance planning in flood disaster management for decision makers.

Main objectives of this study include of: (1) Analysis of past flood events (1988, 1998 & 2004) and a comparison with 2007 flood. (2) Pictorial analysis of different flood events (1988, 1998 & 2007) with respect to synchronization of flood peaks at the GBM Rivers. (3) A brief review of nonstructural measurements during 2007 flood. (4) Identification of current flood plain and riverbed status by field observation. (5) A case study on Serajganj with breaching and no breaching of flood protection embankment.

2. RECENT MAJOR FLOODS AND A COMPARISON WITH THE YEAR 2007

Although floods occur every year in Bangladesh, the intensity and magnitude of floods vary from year to year. The extensive flooding in Bangladesh each year is related mainly to the three major rivers in the world – the Ganges, the Brahmaputra (Jamuna) and the Meghna. This section will highlight on the flood events of recent years 1988, 1998, 2004 as well as 2007.

In 1988, the flood peak of the Brahmaputra and Ganges were very high, but most significantly the peaks coincided, with devastating effects on the Padma downstream of the Brahmaputra/Ganges confluence. The huge area along the Brahmaputra, Ganges and Padma were flooded to an unprecedented extent, and Dhaka was seriously affected at that period. 1988 flood established urban flooding as a national issue. The prolong flood in the city caused severe loss of properties and to the business revenue, so interruption to Govt. activities and commercial enterprise. There was an exceptionally high flood on the Meghna basin due to the flood congestion in the Lower Meghna.

The peaks in the Brahmaputra and Ganges again coincided in 1998, causing severe flood and inundating more than half of the country. The Brahmaputra reached its annual peak in July/August from heavy monsoon rainfall. The Ganges started rising in June/July and attained the annual flood peak in late August or early September. The Meghna at Bhairab Bazar

reached the peak during August/September. This resulted in severe flooding in August/September in the three major river basins and periphery of the Dhaka was also seriously affected in 1998. The 1988 and 1998 floods are considered the most severe in recent experience. The main monsoon Aman rice crop in 1998 was severely affected.

Generally the flash floods in the northeast region occur in April/May and in the year 2004, this rapidly rising flood spilled over bank and eventually flew into the main lowland floodplains. Due to high intensity of rainfall in the Meghalaya, the Barak and the Tripura river catchments and great rush of water from the northern hilly region due to vast deforestation, rapidly rising river floods occurred in June-July causing over bank spills, which was aggravated by the backing up of water in the Meghna River resulting in deep flooding throughout the Sylhet depression and Surma-Kushiyara floodplains. The rainfall and high flood level persisted throughout July and reached at recorded highest level due to the backwater effect from the Meghna, which also carried the Brahmaputra flood. This resulted in severe flooding in the Brahmaputra and Meghna basin. Some stations in the major rivers experienced highest ever water levels in July.

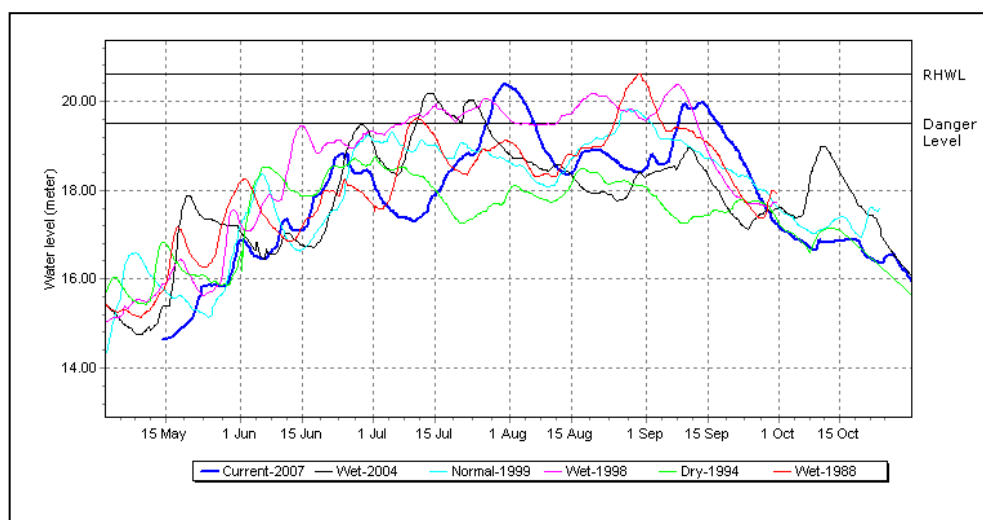
In 2007, Meghna basin experienced moderate magnitude of flash flood during third week of June and Northeast and Southeastern part of the country received approximately 20% above of monthly (June) normal rainfall. July started with relatively dry spell, rainfall intensity rapidly increased from 19th July as monsoon was vigorously active over Assam, Meghalay, Auranachal Pradesh (Brahmaputra basin), Nagaland, Mizoram & Tripura (Meghna basin) and Bihar, East Uttar Pradesh, West Bengal & Nepal (Ganges basin) simultaneously. Floods started in Nepal, Assam, Bihar and Uttar Pradesh from third week of July. In Bangladesh, flash flood hit north-eastern part of the country from 20th July and onrush of floodwater from Assam, Bihar & Nepal has started coming through the Brahmaputra and the Ganges simultaneously from 22nd July. The rate of rise of both the major rivers was very high and northern districts started flooding from 28th July and after then the floodwater spread to central & south-central part of the country. Fortunately, the Ganges was flowing well below from the danger level. In fact, July is not the proper time of Ganges basin flooding. From the 1st week of August, dry spell prevails over the GMB basins and water level started decreasing in the Brahmaputra from 1st August and in the Ganges from 7th August. All the five small rivers in and around Dhaka and Narayanganj crossed danger levels and caused flooding especially in the eastern part and south-western part (outside of BWDB flood embankment) of the Dhaka city. In this spell of flooding, the main Dhaka city was well protected by BWDB flood protection embankment. The flood damage of 2007 has yet to be calculated. According to the thorough investigation by Flood Forecasting and Warning Centre (FFWC), 42% (approximately) area of the country was flooded and 40 districts were affected in different magnitude.

The flood damages in 1988 and 1998 were estimated at US\$ 1.2 billion & 2.8 billion respectively. The damage of 2004 flood has been

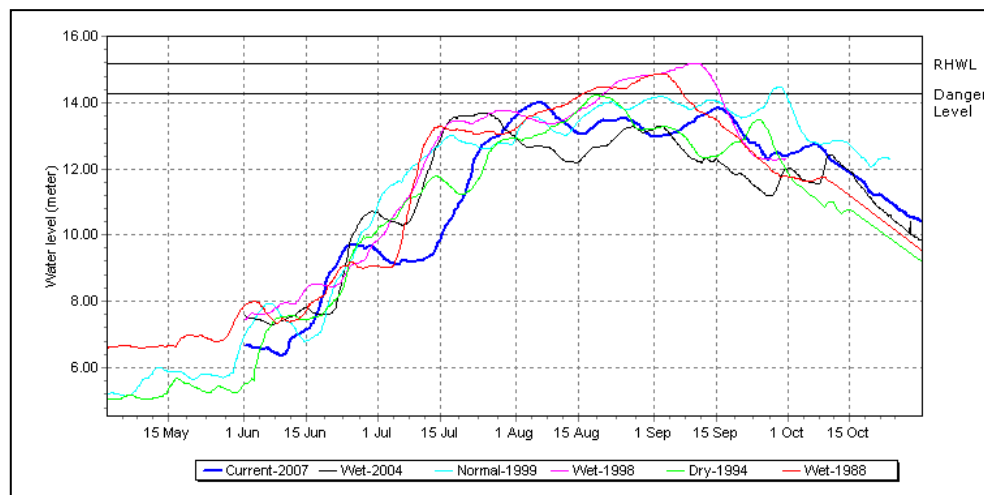
estimated as US\$ 6.6 Billion by UNWFP. The following table (Table 1) provides a comparison of flood duration and flood affected areas of the major floods since 1987 and the figure (Figure 1) illustrate water levels at different stations of the major rivers.

Table 1: Comparison of Flood

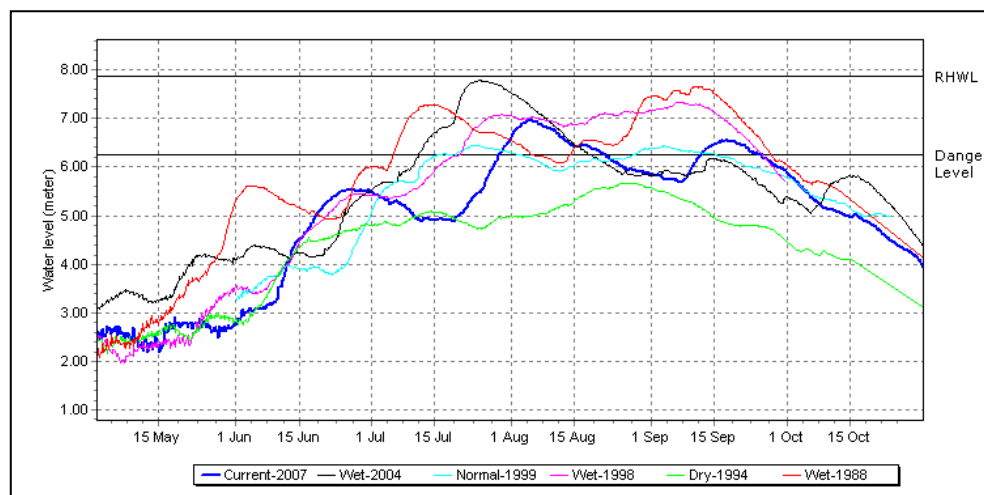
Parameters		Flood Year				
		1987	1988	1998	2004	2007
Flood Duration (days)	a. Bahadurabad (Jamuna)	13	27	66	16	21
	b. Serajganj (Jamuna)	31	44	48	19	31
	c. Hardinge Bridge (Ganges)	55	23	27	0	0
	d. Goalundo (Padma)	54	41	68	23	54
	e. Bhagyakul (Padma)	56	47	72	34	59
	f. Bhairab Bazar (Meghna)	30	68	68	39	37
	g. Chandpur (Meghna)	16	27	49	72	19
Flooded Area in Sq. Km. (% of the country area)		57,300 (39)	89,970 (61)	1,00,250 (68)	56,000 (38)	62,000 (42)
Number of districts affected		50	53	53	39	40



(a) Water Level in Jamuna River at Bahadurabad



(b) Water Level in Ganges River at Hardinge Bridge



(c) Water Level in Meghna River at Bhairab Bazar

Figure 1: Comparison of Water Levels at the GBM Rivers

3. HISTORICAL FLOODS AND THE SYNCHRONIZATION OF FLOOD PEAKS

Flooded area in Bangladesh calculated from the year 1954 to 2007 shown in the figure (Figure 2). It reveals that approximately 37% areas are inundated by floods of 10 years return period. Devastating floods of 1987, 1988, 1998 and 2004 inundated around 40-60% of the country. In fact, the prime cause of flooding was the synchronization of flood peaks of the three major rivers (GBM). Synchronization of flood peaks (especially, the Brahmaputra and the Ganges) triggered large area flooding with relatively longer period in the year 1988 and 1998. Figures (Figure 3a,b) show the synchronization of flood peaks in the year 1988 and 1998 for Bhahadurabad, Hardinge Bridge

and Bhairab Bazar hydrological stations that represents the flow of the Brahmaputra, the Ganges and the Meghna rivers respectively. In 2007, the absence of synchronization in the GBM rivers is pictorial (Figure 3c). As a result, 2007 flood did not last long. But the continued rising of the Brahmaputra river from the middle of July, little bit earlier than that of usual, gave less time to the people to be warned and damaged huge crops.

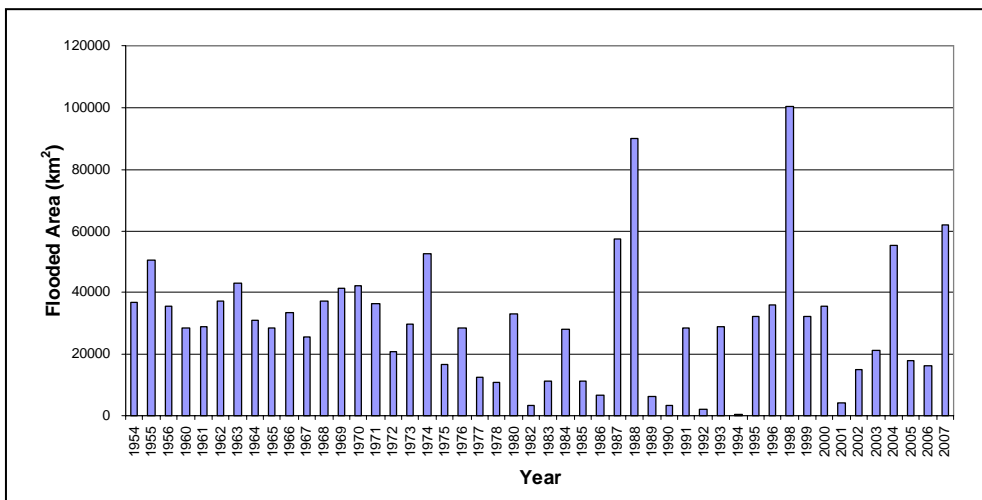
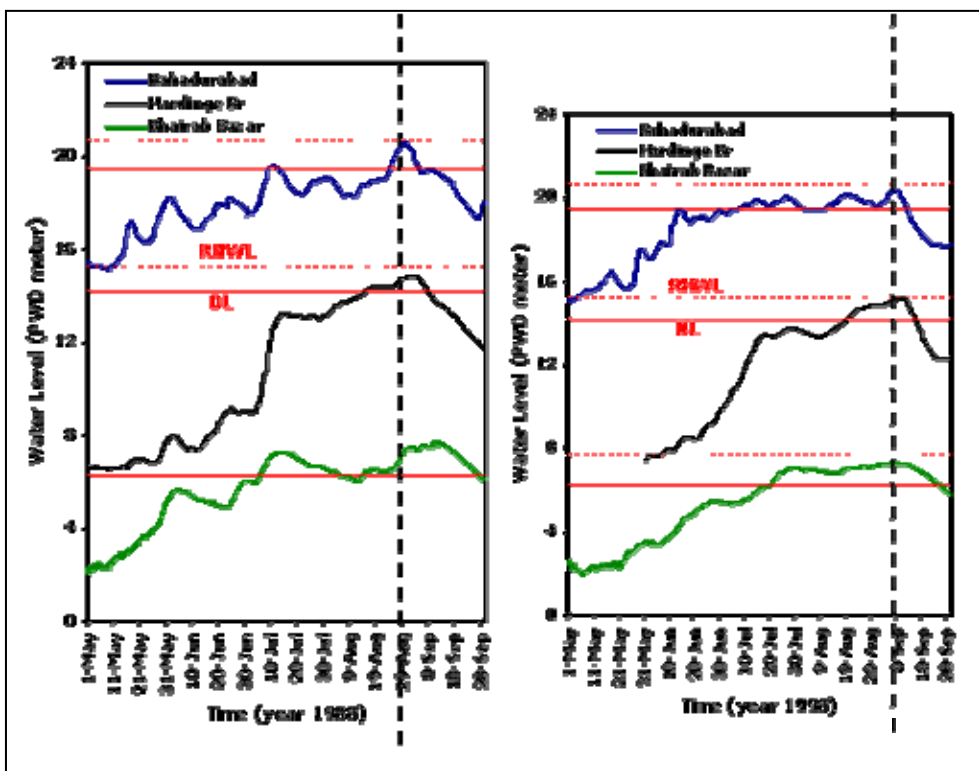


Figure 2: Flooded Area from the year 1954 to 2007



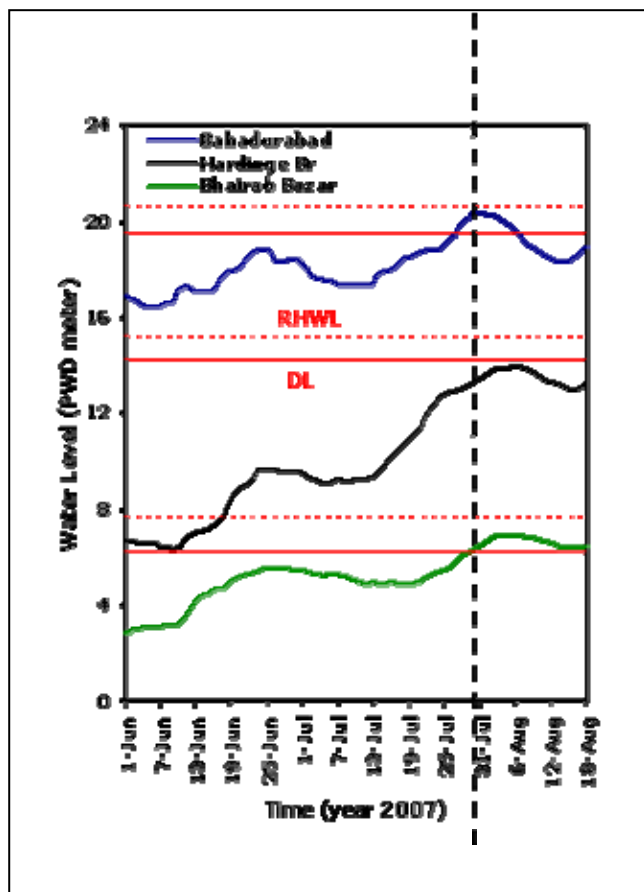
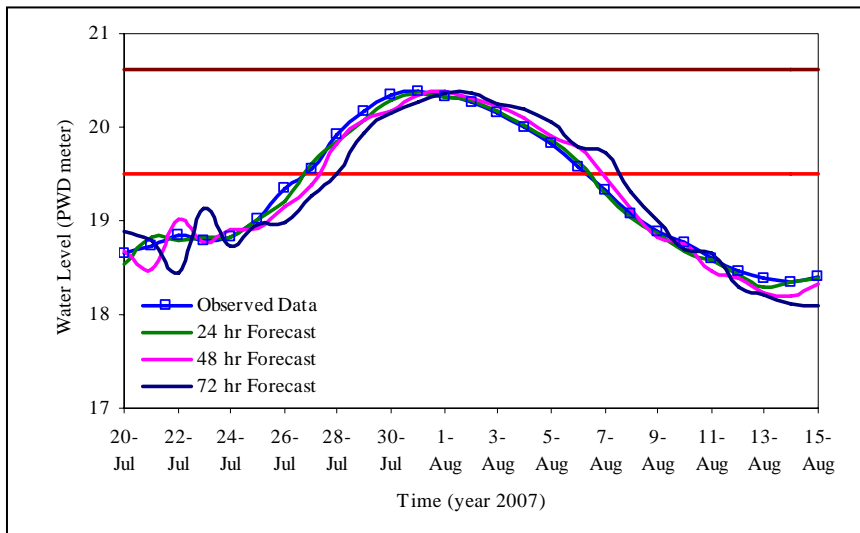


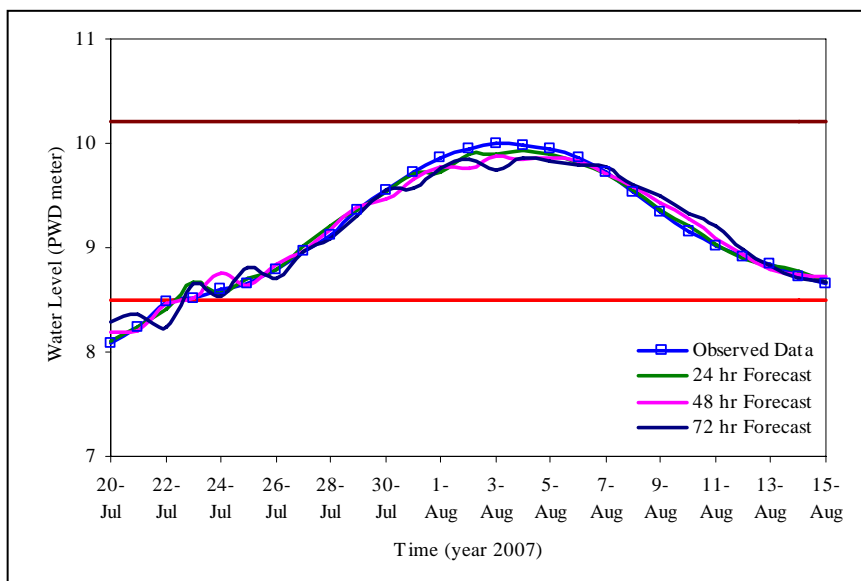
Figure 3: Synchronization of Flood peaks at the GBM Rivers (1988, 1998 & 2007)

4. NONSTRUCTURAL MEASUREMENTS DURING 2007 FLOOD

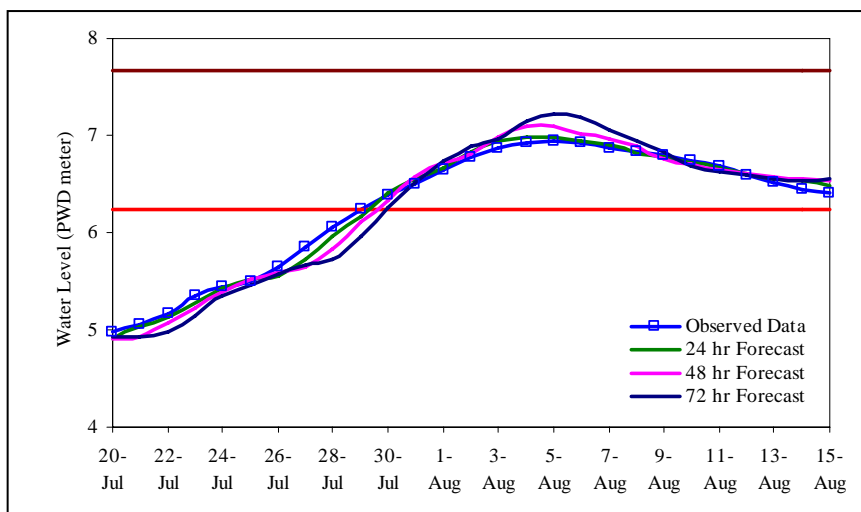
In 1972, Flood Forecasting and Warning Centre (FFWC) formed under the Bangladesh Water Development Board (BWDB). FFWC has been playing key role in flood forecasting since the beginning. The activities of FFWC are very important considering the geography of Bangladesh. And at same time, flood forecasting in Bangladesh is very difficult due to having its complex hydrology. For a long term, FFWC has forecasted the numerical value of water level in different rivers of the country using mathematical model. But in 2007, FFWC tried to explain all the forecasted results in a compressive way. Besides, in some cases, five to seven days qualitative forecast has also been disseminated by FFWC in the same year. Figure (Figure 4) shows a comparison of 24/48/72 hrs forecast with observed data at Bahadurabad, Goalundo and Bhairab Bazar hydrological stations during July 20 to August 15, 2007.



(a) Jamuna River at Bahadurabad



(b) Ganges River at Hardinge Bridge



(b) Meghna River at Bairab Bazar

Figure 4: 24/48/72 hr Forecast Results versus Observed Data (year 2007)

5. RECENT FLOOD PLAIN IN BANGLADESH AND A CASE STUDY ON SERAJGANJ

A number of people living in flood plains is increasing day by day and it triggers high flood frequency as well as huge loss. On the other hand, water carrying capacity of the rivers is decreasing chronologically due to siltation. It is no more obscure that riverbed aggradation on a contrary to substantial compaction of sediments in our delta prevails a critical morphology in which some settlement areas have already gone below the usual water level in the river. Similar phenomena have been observed on 29th July 2007 near the Gangachara thana in adjacent to the river Teesta which is pictorial as shown in the figure (Figure 5).

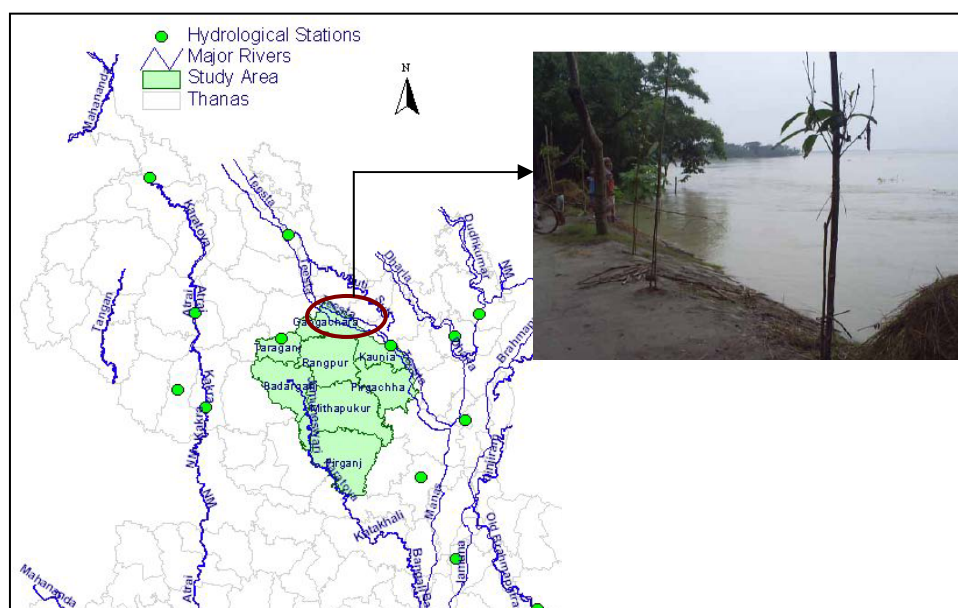
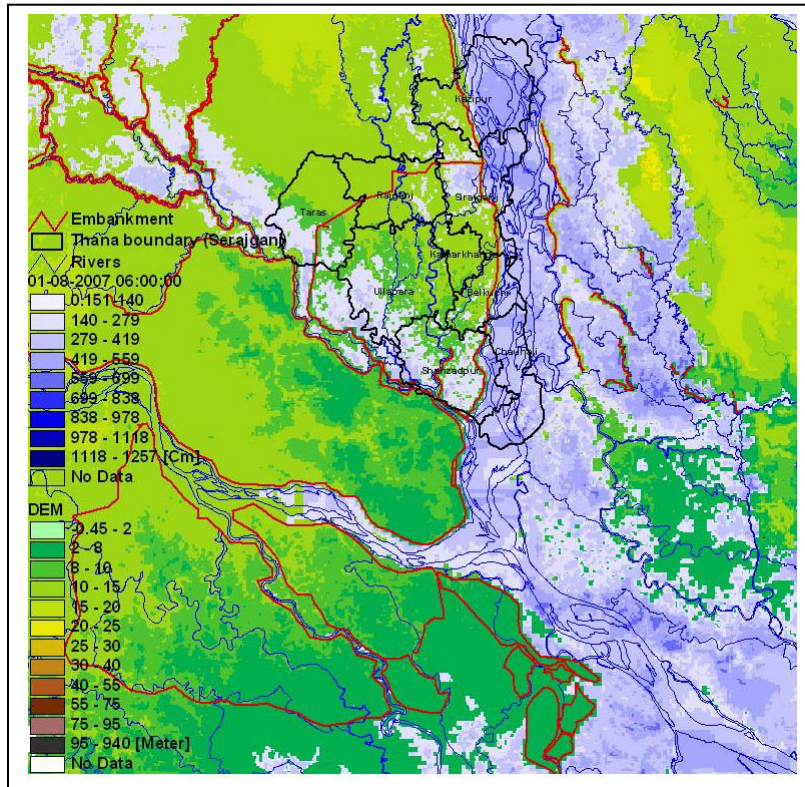
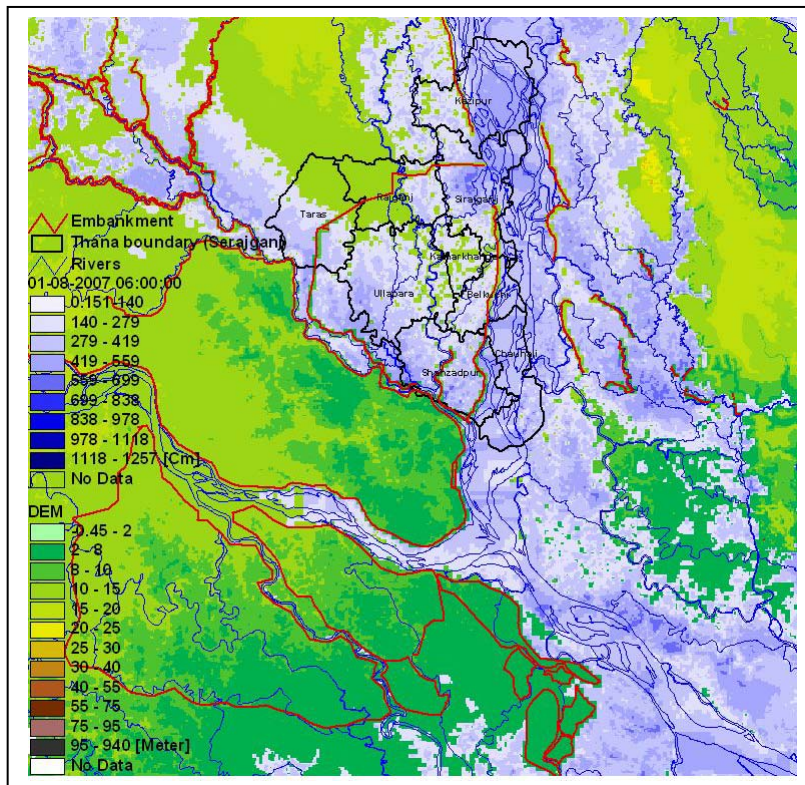


Figure 5: Teesta River State at the Gangachara Thana

For this, the breaching in the flood protection embankment/levees could be a cause of flooding in huge areas. In 2007, breaching in flood protect embankment at Serajganj and Gaibandha has worsened the overall flood situation. Figure 6 shows the inundation areas of Sirajganj district as of August 01, 2007. The inundation maps have been derived using MIKE 11 hydrodynamic model and MIKE 11-GIS. It is worth mentioning here that the Digital Elevation Model (DEM) used to produce inundation maps is coarse (900-meter resolution) and is not sufficient to produce good maps. Rather it is old enough to represent the actual scenario. However, water surface calculated in the embanked area of Serajganj district is around 34.3% of the total area in case of no breaching of embankment as shown in the figure (Figure 6a). But at the same time, the water surface area was found 79.6% of the total area for the case of 20 Km breaching of embankment as shown in the figure (Figure 6b). Similar investigation is undergoing for Dhaka city.



(a) Inundation map considering no breaching



(b) Inundation map considering 20 Km breaching

Figure 6: Inundation maps of Serajganj district as on Aug 01, 2007

6. CONCLUSIONS

The spatial and temporal distributions of rainfall are changing day by day. Beside this, a number of people living in flood plain are decreasing due to not having enough space. For this, flood intensity has increased now a day. Synchronization of the GBM Rivers is still identified the prime cause of major flooding in Bangladesh. Water carrying capacity of the rivers has decreased sufficiently due to siltation. The reduced level of high river-bed elevation with respect to the settlement area has become a great concern for Bangladesh. Breaching of flood protection embankment could be a cause of flooding in huge area. Flood risk assessment and long term flood prediction need to be adopted as a part of non-structural measurement.

In the conclusion, the 2007 Flood although initially seemed to be a lethal one has receded quickly due to lack of synchronization of the Brahmaputra and the Ganges rivers.

REFERENCES

- FFWC, 2005. *Annual Flood Report 2005*. Flood Forecasting & Warning Centre (FFWC), Bangladesh Water Development Board (BWDB).
- Haque, C.E., and M.Q., Zaman, 1993. *Human response to riverine hazards in Bangladesh – A proposal for sustainable floodplain development*. World Development 21, No. 1: 93-107.
- Hofer, T., and B., Messerli, 1997. *Floods in Bangladesh, Process understanding and development strategies*. A synthesis paper prepared for the Swiss agency for development and cooperation. Institute of Geography, University of Berne. 32 pp.
- Khalequzzaman, Md., 1994. *Recent floods in Bangladesh: Possible causes and solutions*. Natural Hazards 9: 65-80.
- Khalil, G.M., 1990. *Floods in Bangladesh: A question of disciplining the rivers*. Natural Hazards 3: 379-401.
- Paul, B.K., 1997. *Flood research in Bangladesh in retrospect and prospect: a review*. Geoforum 28, No. 2: 121-131.
- Rasid, H., and B.K., Paul., 1987. *Flood problems in Bangladesh: Is there any indigenous solution?* Environmental Management 11, No. 2: 155-173.
- Reavill, L.R.P., and T.G., Rahman., 1995. *A systems-science-based analysis of the factors that influence and aggravate the effects of flooding in Bangladesh*. Technological Forecasting and Social Change 49: 89-101.

A STUDY FOR IMPROVING TOTAL DISASTER REDUCTION ABILITY OF NURSERY SCHOOLS AND KINDERGARTENS

MARIKO ABE¹ and KIMIRO MEGURO²
International Center for Urban Safety Engineering
Institute of Industrial Science, The University of Tokyo, Japan
abe@risk-mg.iis.u-tokyo.ac.jp
meguro@iis.u-tokyo.ac.jp

ABSTRACT

In the field of protecting small children in the event of disasters, we have various problems such as many seismic-vulnerable facilities or miscommunication among concerned parties. Improving the disaster-imagination ability is necessary for these people to solve these problems. Therefore, the authors made the disaster situation image-training tool named Meguro-maki from the Meguro-method (Meguro, 1999). Then the authors designed the workshop using Meguro-maki and conducted it at nursery schools among others.

Furthermore, the authors made Meguro-maki stories based on past earthquake disaster cases and expert opinions to support Meguro-maki making and developing disaster mitigation ability. The authors also made a pamphlet for pregnant women and little children's parents using these stories.

1. INTRODUCTION

When small children (in this paper, "small children" means infants and kids under six years old, that is before elementary school age) face unpredictable dangers such as an earthquake, fire or an intruding malicious person, they need adult's help. Today, in Japan, typical places in which small children gather are nursery schools and kindergartens. The former take care of infants who are only several months old. In these groups, because the number of children per adult is larger than that of a regular home, the load on adults when disaster occurs is heavier.

In this study, we propose a system to raise the disaster management ability of these groups by establishing an independent and permanent disaster management cycle starting from "Imagining the disaster situation" up to "Perception of the present state of affairs and problem grasping" and "Design and implementation of countermeasures." In order to "imagine the disaster situation" and "perceive the present state of affairs and grasp the problems", we suggest carrying out disaster management workshops called

“Meguro-maki WS”, in which “Meguro-maki”, a tool to imagine the disaster situation, is used.

An additional positive effect of our proposal is the increase of the disaster management awareness of the whole community. When children’s parents, relatives, and people interacting with them learn about nursery school disaster management activities, they themselves become aware that “disaster management is important” and embrace it even if they did not consider it as their own problem before. Furthermore, focusing on nursery schools and kindergartens creates a disaster mitigation culture among small children that will become a valuable asset for the society in the future.

2. METHODOLOGY

2.1 Importance of disaster-imagination

To deal with the various problems of disaster mitigation appropriately under the severe conditions of the limited members, time, and items, etc, it is necessary to imagine disaster situations. If you don’t have enough imagination about your possible disaster situations, your efforts for disaster mitigation tend to be useless or wrong. When you try to imagine the disaster situation appropriately, it is important to consider various factors on regional characteristics composed of social and natural environmental conditions of the region. Also, as human acts and social activities are strongly dependant on time, time related factor, such as season, weather, day of the week, time of the day etc. on which the earthquake occurs, is important. And of course, your individual conditions such as your family members and living house are important. Moreover, the situation changes according to the passage of time from the hazard occurrence. What and how much you need changes in relation to the elapsed time.

2.2 The Meguro-method

The Meguro-method has been developed in response to these contextual factors. The concept of Meguro-method is "After setting various conditions, imagine your situation and action and feelings, etc. according to the passage of time after the hazard occurrence." In general, the table like Figure 1 is used in the Meguro-method. This table is divided in detail with a vertical and horizontal axis. The vertical axis shows "your typical action pattern along the passage of time during a day". When you fill in these blanks, you should consider the earthquake resistance conditions of the environment around the region where you live and work, conditions of location, and the indoor furniture arrangement, family structures, and each member's action patterns, etc. A horizontal axis is "time passage since the earthquake occurs", like three seconds later, ten seconds later, one minute later, two minutes later, several minutes later, one hour later, one day later, ...one week later, ...one month later, ...one year later, ...ten years later. You may flexibly change a unit of the division length and a final time

passage as this time division responds to your purpose and the writing time limit.

When some people write the Meguro method, the facilitator uses some masses in the table as examples and explains the purpose and “how to image their disaster situations”. For instance, he/she shows the mass "A1a" and makes them imagine "What will your situation be after three seconds when the earthquake happens while sleeping?" Usually a digital worksheet is used to collect and analyze the data easily. Through practices of filling in the Meguro-method, the writer’s disaster imagination ability such as "What happens in my environment as time has passed since the earthquake occurred?" can be improved. After that, the facilitator asks the writers if they could imagine the disaster situation appropriately. For example, the facilitator comments about the possibility of a "situation in which the writer or his/her family members get injured or die." He/she asks “Why are only you are OK in spite many people are killed or injured?” The facilitator uses various pictures and videos of past earthquakes in order to reinforce the writer’s disaster imagination. Because the writers imagine their own situations, they can feel reality. If the writers fill again the tables with different conditions, they will recognize what will change and what will not. Some will drastically change and some will not. Next, the writers think “what can we do to reduce the negative impact?” Based on this, countermeasures can be implemented.

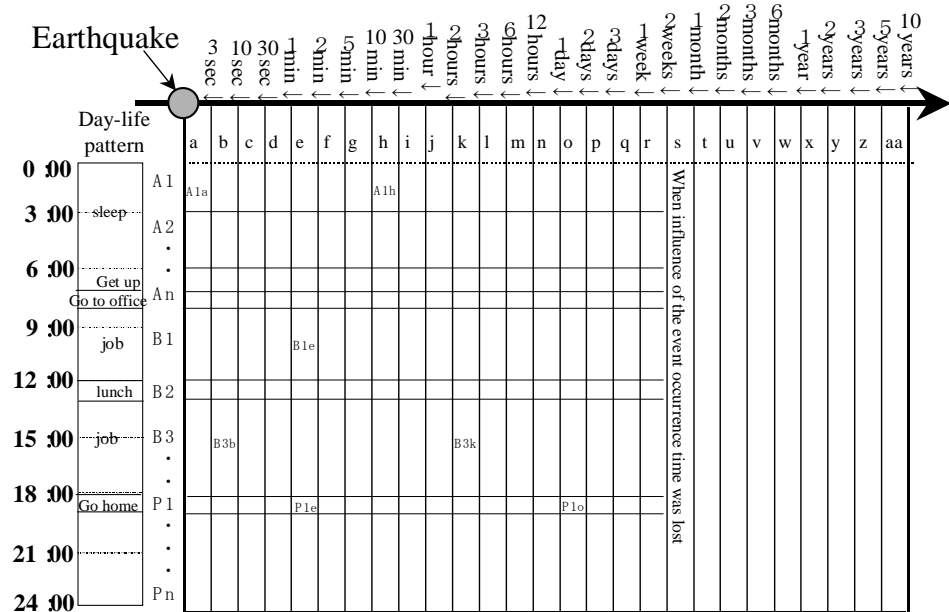


Figure 1: Disaster situation story table

2.3 Meguro-maki & Meguro-maki Workshop

The "Meguro method" is a very effective tool to imagine the disaster situation in detail. However, it is a hard task for beginners and busy people to use the Meguro-method. Therefore, it is necessary to simplify the Meguro method for busy childcare people.

Because nursery teachers do not have a sufficient number of PCs, the tool must be written by hand. Also, because they are very busy, the tool must be written in about 30 minutes. To meet these requirements, the authors prepared “Meguro-maki” from the Meguro-method. “Maki” means “long roll”. The writing board of Meguro-maki is a long paper intended to be lined up on the table and read through the times. The authors made the workshop (WS) using Meguro-maki.

While in Meguro-method several possibilities are considered, Only some conditions and the time axis are on the board. The conditions are the season, the day of the week, time, weather, the writer’s positions at the office or his/her family, and the seismic intensity (in case of the earthquake). First, the writers decide the conditions. While deciding the conditions, there are two important aspects. One is frequency and the other is unpleasantness. After the writers decide the conditions and situations when the disaster occurs, they start writing disaster situations as time passes. The facilitator advises the writer “Please write your own story after the disaster occurs. You are the central figure of the story. What will your situation be and what will you think and do? How about other characters like your family, your neighbors, your coworkers etc.?” Usually, when Meguro-maki WS is held at nursery schools or others, at the first WS the leader and some members do the imagination exercise. At the second WS, the first WS members become the facilitators. The facilitator helps other to imagine the disaster situation if they cannot write smoothly. If the writer becomes aware of the questions and problems, he/she writes down these things on the memo pads. After all the members finish writing, they line up Meguro-maki on the table and read each story. It is interesting for each member to read the other members’ stories.

They compare Meguro-maki stories as time passes. Sometimes the images of each member are different. They can consider the situation and how to manage it through such communication. Through this practice, WS members can share their disaster images and problems. It is important to find and recognize the problems and solve the problems as a group.

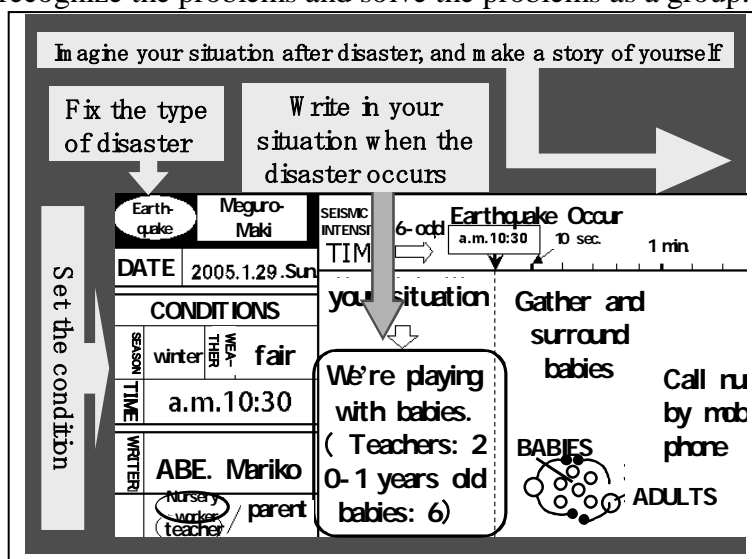


Figure 2: Meguro-maki writing board

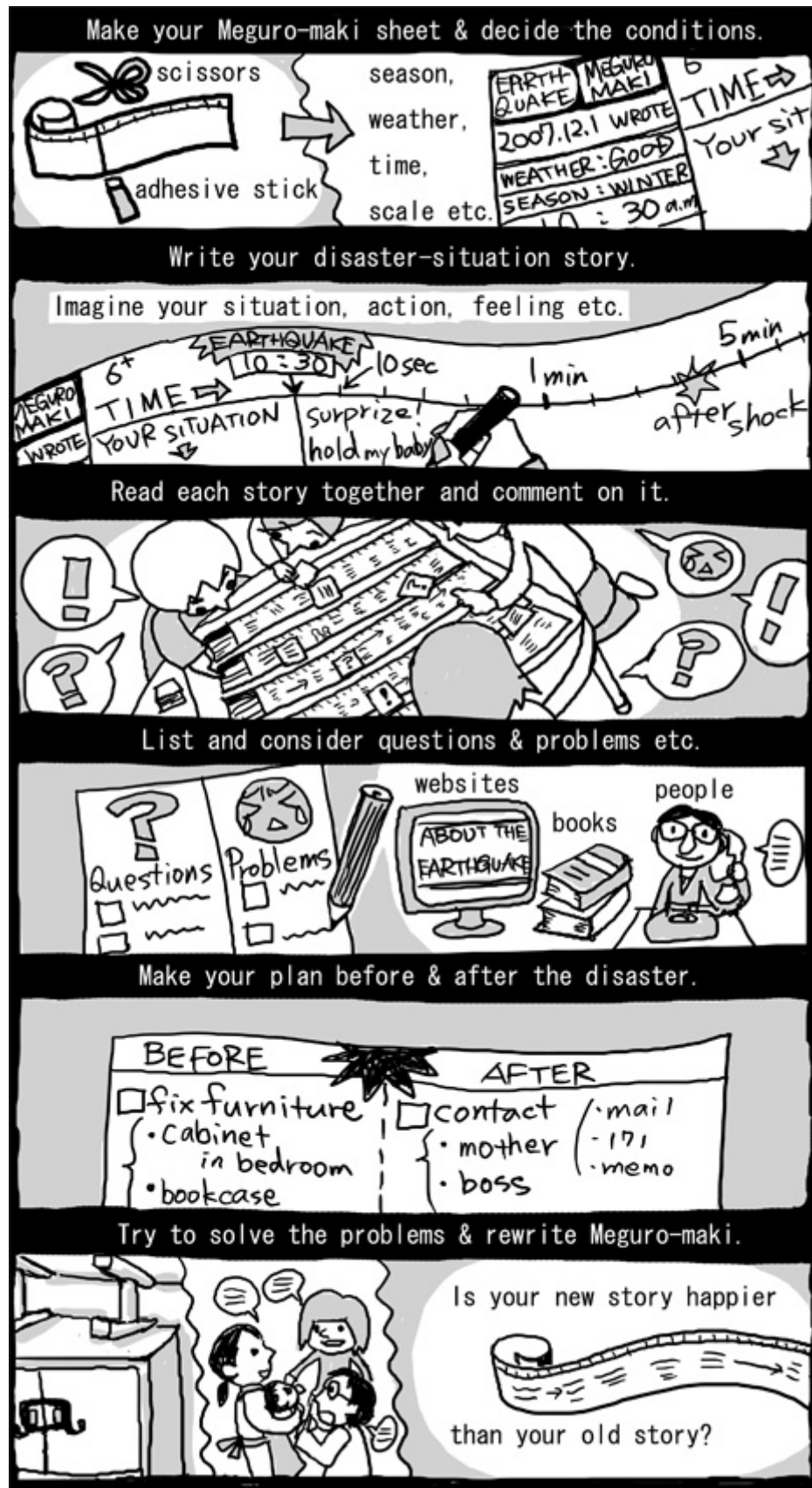


Figure 3: How to use Meguro-maki

3. MEGURO-MAKI WS AT VARIOUS GROUPS

We have held Meguro-maki WSs at nursery schools, kindergartens and other various groups (Fig 4). Through these practices, we found some problems. It is difficult for beginners to imagine the disaster situation without help from the facilitator. And to motivate nursery schools and kindergartens, a combined approach of the government and parents' side is important.

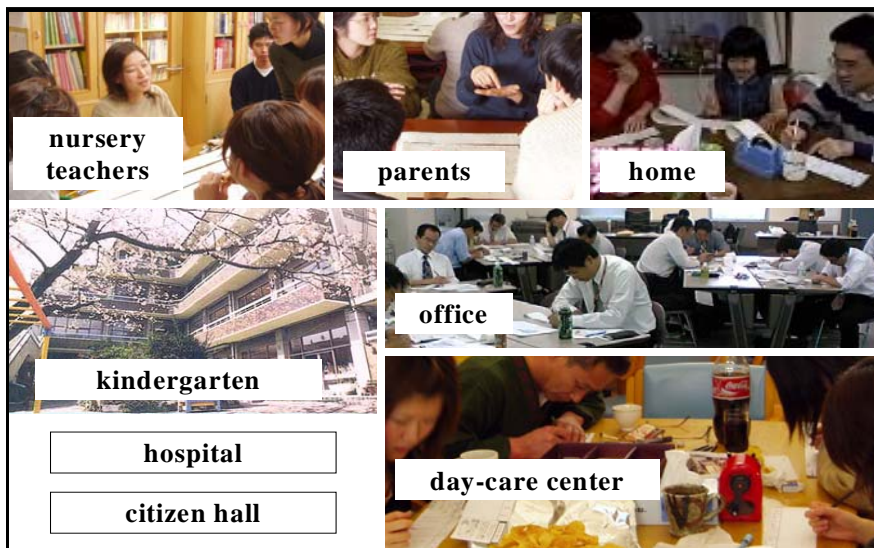


Figure 4: Meguro-maki WS in various situations

4. MAKING DISASTER SITUATION STORIES FOR REFERENCE AND PAMPHLET

To solve these problems, the authors cooperated with Tokyo Metropolitan Government and made Meguro-maki reference stories based on past earthquake disaster cases and expert opinions as the support for making Meguro-maki and having disaster mitigation ability. Then the authors and the Tokyo Metropolitan Government made a pamphlet for pregnant women and little children's parents using these stories.

We conducted a questionnaire survey with the people, mainly little children's guardians, who experienced the Niigata Prefecture Chuetsu Earthquake (M6.8, October 23, 2004). We asked about the situation when the earthquake occurred, their characteristics such as family members and living house, etc. In addition, we asked about their disaster situations, actions and feelings thorough the time passage. Then, we transfer their messages to other pregnant women and little children's guardians who never experienced big earthquakes. After that, we analyzed these data and make disaster situation stories. One main character is a pregnant woman and other is the mother of a baby. Then, we made a pamphlet for pregnant women and little children's guardians in Tokyo.

What we can do for our children before earthquake occurs –
For pregnant women & little children's guardians

Contents

1. Introduction
2. Disaster mitigation before earthquake occurs (house, rooms, items, information & communication)
3. Disaster situation story for reference (2 stories)
4. Your own story (blank story pad)
5. Message by the disaster experienced people
6. Disaster prevention information of Tokyo Metropolitan Government
7. Reference of books & websites



Tokyo Metropolitan Government

Figure 5: Disaster situation story

5. CONCLUSIONS

In the field of saving small children in the event of disasters, we have various problems such as many seismic-vulnerable buildings, or miscommunication among concerned parties. To improve the disaster-imagination ability, it is necessary for those people to solve these problems.

Therefore, the authors made the disaster situation image-training tool Meguro-maki from Meguro-method (Meguro, 1999). Then, the authors designed workshops using Meguro-maki and conducted it at nursery schools among others.

Furthermore, the authors made Meguro-maki stories based on past disaster cases and special findings as the support for making Meguro-maki and developing prevention power. Then, the authors made a pamphlet for pregnant women and little children's parents using these stories.

Using, verifying the case collection, creating a further database, and making other support systems are scheduled to be done in the future.

REFERENCES

Meguro, K., 1999. Lifeline earthquake disaster and its countermeasures, *Comprehensive course on disaster reduction, Urban Disaster Mitigation Part*, Shizuoka Prefecture, pp.33-55 (in Japanese)

SCHOOL EARTHQUAKE SAFETY PROGRAM (SESP) IN OLD DHAKA, BANGLADESH

ISRAT JAHAN
Research Assistant, BNUS, BUET, Bangladesh
sheulyurp@yahoo.com

MEHEDI AHMED ANSARY
Professor, Dept. of Civil Engineering, BUET, Bangladesh
ansary@ce.buet.ac.bd

ABSTRACT

Dhaka as one of the densely populated cities of the world requires hazard risk assessment and needs preparedness to reduce risk. The earthquake risk is more prominent for Dhaka due to its high population density, vulnerable structures, low preparedness, etc. The inhabitants of the city must learn how to reduce risk due to any disaster. To reduce loss the inhabitants of the city must learn what to do to cope with the disaster and minimize the risk at that time. In this perspective the school awareness program is important as the young generation of the country will probably response more eagerly than others and will play a vital role in spreading out the ideas and knowledge among their friends, family and surroundings. Schools are considered as shelter place during any natural hazards in Bangladesh. Schools should be made earthquake resistant and its inhabitants need to know how to cope with any disaster. The structures of Old Dhaka is relatively more vulnerable against earthquakes. To reduce loss in times of any disaster, a school based earthquake safety awareness program has been organized in Govt. High schools in the older part of Dhaka to train the students and spread out the ideas. Earthquake risk reduction and preparedness program in this school covered: (a) seminar to aware about earthquake disaster, (b) short course on First Aid, (c) search and rescue training, and (d) safety drill in Schools.

1. INTRODUCTION

Dhaka, the capital of Bangladesh is the center of economy, commerce, politics and society, with a large population of more or less 12 million. According to a report published by United Nations IDNDR-RADIUS Initiatives, Dhaka and Tehran are the cities with the highest relative earthquake disaster risk (Rahman, 2004). Earthquakes may cause billions of Taka worth of damage (Ansary, 2004). Once a great earthquake occurs, Dhaka will suffer immense losses of life and property. This will have very severe long term consequences for the entire country. This is of particular relevance to Old Dhaka which has large numbers of densely packed very old non-reinforced masonry structures along narrow winding streets. There

is no earthquake disaster management system in Dhaka and with the active involvement of the local community this system will be effective. There is a saying among the earthquake experts: "earthquakes do not kill, what kills is a building that falls, a gas escape or a column". "The human factor changes a natural hazard into a disaster" (Campo, nd). That is why it is very important to reduce human vulnerability through prevention, learning of preventive measures and drills.

The School earthquake awareness program is important as the students are the future generation of the country and their response and contribution in this sector is more far fetching than any other group as a younger generation. They also play a vital role in spreading out the ideas and knowledge on earthquake preparedness among their friends' circle, family level and surrounding locality. Again most often the schools are considered as the Shelter place from any kind of disaster in this country. So it is an emergency task to make the school building safe during and after the occurrence of disaster ensuring the safety of its residing people, i.e. the students. It is of primary importance that the students of the schools should train up to help themselves and provide support to others. To reduce loss the inhabitants must learn what to do to cope with the disaster. If they motivate people, they can play an effective role in risk mitigation, and reduce the impacts of any urban hazard especially earthquakes.

2. PURPOSE OF THE AWARENESS WORKSHOP IN SCHOOL

- To initiate discussions with the school people and the community
- Acknowledge the important role of school buildings within the community as post-disaster shelters.
- To promote earthquake awareness through students and staffs of schools
- To Establish School Earthquake Safety Committee
- To conduct preparedness and mitigation programs like first aid training, search and rescue training and earthquake drills to reduce the loss of lives and properties due to earthquake

3. RATIONALE OF THE STUDY

In Bangladesh, recently due to poor construction quality of buildings, three buildings collapsed. In June 2004 a five storied building collapsed in Sakhari bazar, Old Dhaka that killed 19 people and and injuring several others among it's 30 inhabitants. In April 2005 a nine-storied factory building collapsed in Savar that killed 70 people and injuring around 200 others among its 300 workers. In February 2006 a five storied under construction building collapsed in Tejgaon that killed 18 and injured 40 workers. During an earthquake this will multiply thousand times more. Also due to poor fire preparedness in high-rise buildings of Dhaka city, many buildings may catch fire and people may die due to lack of poor evacuation

facilities. If the people are aware how to cope with the disasters, the losses will be less than what happened in the above cases. Also the trained persons could help in searching the victims and rescue them from the debris. If the local people are trained up they can respond earlier than the outside help such as Fire Service Department, Armed Forces, etc. In emergency case this local trained volunteer group will come handy in reducing the effects of the disaster. So the students should be trained up so that they can carry out rescue work and provide first aid to the injured of their communities and in their schools.

4. SCHOOL EARTHQUAKE SAFETY PROGRAM

Meetings, structured discussions, power point presentations, interviews and an evaluation questionnaire designed to get feedback from the participants are among the tools used during the school awareness workshops. To fulfill the objective, the school awareness-training program covers:

- Brief discussion on earthquake that spreads out the ideas on earthquake, techniques to cope with such an uncertain situation, how to tackle the unwanted situations, how to minimize the losses due to the earthquake disaster, etc.
- First aid training
- Search and Rescue training
- Mock drills

4.1 Surveyed schools under the program

BNUS (Bangladesh Network Office for Urban Safety) has conducted some earthquake safety related programs in several schools in old part of Dhaka city. These schools are situated in the most densely and hazardous area of Old Dhaka, which is the most vulnerable site due to earthquake in this city for its high density and unplanned build-ups. In order to increase the knowledge base and making the students fully aware of their status during and after a disaster, BNUS has undertaken this program. The safety program has been launched in Armenitola Govt. High School (located at Ward 68) in September 2006.

4.2 Open discussion on earthquake vulnerabilities

The earthquake school awareness program in Armenitola Govt. High School has been started with an open discussion on earthquake with the teachers, students and young volunteers of Bangladesh Red Crescent Society and Bangladesh Scout in 21 September 2006. Figures 1 and 2 show glimpses of the seminar. The discussion covered earthquake vulnerabilities, earthquake preparedness and disaster mitigation measures that focuses the outcomes from the participants on how to manage the situation before, during and after earthquake occurs, what are the duties of each individual, what to do to minimize the loss and cope with the casualties due to earthquake, how to provide help to the helpless, what disciplines should be

followed to come out in a safe open place without any injuries, etc. From the discussion it was realized and agreed by the participants that first aid training, search and rescue training and regular mock drill on safety issues is needed to save lives and to minimize the loss due to disasters. Mock drills must be carried out regularly to have a disciplinary technique to be followed during and after disaster occurrence to safeguard against loss.



Figure 1: Prof. Ansary giving his speech on Earthquake awareness



Figure 2: The teachers and the students was present in the program

According to the suggestion that came out from the open discussion BNUS organized training on Earthquake safety awareness that includes short course training on First Aid, Search and Rescue training and final demonstration. The full program concludes with making the students fully aware of their duties in pre, during and post disaster periods.

4.3 Short course on First Aid

First Aid is an initial assistance or treatment given to someone who is injured or suddenly taken ill. First Aid training makes any individuals to remain aware and safe by themselves and provide help to others injured during and after any disasters. In order to make the students fully aware of any disaster especially in case of earthquake, first aid training is of utmost importance to safe lives.

A short course on First Aid has been held in Armenitola Govt. High School from November 30 to December 02, 2006 with 77 students of class VI to IX selected by the school authority. The students are from general groups and the members of Red Crescent and Scout. The general knowledge on primary treatment and special care during injuries especially with casualty due to earthquake was given emphasis in this program. The duration of the training is short to make a person totally capable to manage a first aid required for a person. The training would rather extend help to other first responders such Fire Brigade, Red Crescent members during a disaster to reduce pain and casualty.

4.3.1 Objective of Giving First Aid training to any person

- Train them with the basic principles and practices of the First Aid to provide help during and after any kind of disasters that could save a life and reduce sufferings,
- Make them aware of what they can do in providing first aid to people in emergency care,
- Help people avoid, prepare for and cope with emergencies.

4.3.2 Items covered under First Aid Training

The general knowledge on primary treatment and special care during injuries especially with casualty due to earthquake was given emphasis in this program. The students learned practically all the techniques of giving first aid.

Introductory speech on First Aid Awareness: What is First Aid, general knowledge of the students about First Aid, Objective of First Aid, Principles of First Aid, Responsibilities of a First Aider, etc. Spread out the ideas on:

- Techniques of giving First Aid in case of Airway, Breathing and Circulating (ABC) Disorder
- Major cause of respiratory problems, Artificial Respiration, ways of giving respiration and CPR
- Heatstroke
- Shock, Unconsciousness and Fainting
- How to treat a burn casualty, Burns Scalds and Acid burns
- Bleeding, Wounds, Dressings and Bandages, Pressure bandage and how to dress a fresh wound
- Immobilize the injured part, lower and upper arm sling, chest, leg and skull bandage.
- Fractures, Strains and Sprains
- Poisoning, Bites and Stings
- First Aid materials
- Carrying and transport of casualty
- How to place a casualty in recovery position.

Figures 3 to 8 show different stages of the training.



Figure 3: The ABC Technique of First Aid



Figure 4: Managing the bleeding



Figure 5: Bandage in Chin injury



Figure 6: Bandage in Head injury



Figure 7: Settling down an injured Arm



Figure 8: Make a patient breathe easily and comfortably

4.4 Search and Rescue Training Program

The third step of the program covered Search and Rescue (SAR) training on how to deal with casualty after a disaster. A three days program with 5 hours per day has been organized by BNUS in Armenitola Govt. High School December 11 to 13 2006. The students who got the first aid training are selected for the next step of search and rescue training program

that is the required doings in the after disaster part. There were 33 students from the 77 first aid trainee students.

4.4.1 Topics covered under SAR training

Different Steps in SAR:

- Survey
- Observation
- Information
- Plan
- Actions

General knowledge on different Stage of Search and Rescue (SAR):

Lectures on:

- What is Survey?
- How can they do the survey work?
- Types of Survey:
 - Primary Survey
 - Detailed Survey
 - Specialized Survey
- Ways of observing the damaged part of the area.
- Necessity and methods of collecting information on damaged property?
- Plan to handle the situations perfectly. How to make an appropriate plan with the importance of making appropriate and successful plans? What is the right plan in that moment with details? Ways to develop the plan.
- Finally, why and how an action can take place?

Stage of Rescue:

- 1st Stage: Emergency Rescue
- 2nd Stage: Search in of slightly damaged building.
- 3rd Stage: Immediate rescue
- 4th Stage: selected debris clearance

General Techniques of Rescue:

- Different styles of rescue from a damage sector
- Technique of Stretcher use with casualties
- Casualty leave with fireman using a chair knot
- Technique of Debris cleaning's

Figures 9 to 14 show different stages of SAR training.



Figure 9: Bow line dragging



Figure 10: Toe dragging



Figure 11: Technique of Fireman Lift



Figure 12: Crawling



Figure 13: Stretcher blanketing with rope



Figure 14: Casualty leave using stretcher

4.5 Mock Drill

Finally a mock drill has been organized showing all the techniques of search and rescue, ways of first aid, demonstration showing the duties before, during and after an earthquake to have a clear cut view of the earthquake situation. It is the way of disseminating what they have learnt. The earthquake mock drill was organized by BNUS with assistance of 12 Trainers from Bangladesh Red Crescent Society at Armenitola Govt. High

School, Dhaka on 23 February 2007. The drill lasted for 100 minutes. Total 150 students participated in the drill among them 33 was SAR trainees, rest were first aider and other general students. The program was under the leadership of already SAR trained 33 students. The Guardians of the students and the Schoolteachers were also present in the program in order to spread out the knowledge on earthquake safety. In the program the students presented their duties before, during and after an earthquake. Figures 15 to 19 show different scenes of the mock drill. To increase awareness each school student has given an earthquake awareness poster already made for the Dhaka city (Figure 20).



Figure 15: A Scene of Earthquake Mock drill



Figure 16: Casualty leave using Firemen Chair knot



Figure 17: Casualty leave using Stretcher



Figure 18: First Aid Post

5. SUSTAINABILITY OF THE PROGRAM

The training program is very effective in facing a disaster in respect of reducing the losses. The loss due to any hazard becomes greater if an appropriate measure is not taken in time. The trained up students are themselves a great resource considering the future prospects. They will also work in spreading out the knowledge base in awareness creation. The students will actively take part in reducing the loss from any disaster. Living in the affected or surrounding areas the local community may response most effectively before the outside help reaches in their area. And a trained up community can reduce the loss much more than the untrained. The students will spread out the ideas and knowledge on earthquake safety awareness activities and necessary duties to minimize the sufferings from disasters.

Emergency first aid service and other life saving measures can drastically reduce sufferings and save more lives. These students will work as the leader in their respective classes and guide in tackling any unwanted situation. They will also lead in safety drill in their school. The students who got the search and rescue training and the first aid training will be selected for the next step of earthquake safety drill. Afterwards the safety drill will be undertaken regularly in their school.

The trainee students will work as the following:

- Save lives providing first aid and service to minimize the risk of death and future injury.
- Immediate transfer to minimize the shock and reduce suffering
- First Aid team at local community level.
- The students will actively take part in reducing the loss from any disaster.
- The students will spread out the ideas and knowledge on earthquake safety awareness activities and necessary duties to minimize the sufferings from disasters.
- Emergency first aid service and other life saving measures can drastically reduce sufferings and save more lives.

The Search and Rescue training program is very effective after any disaster occurs in respect of reducing the losses. The loss due to any hazard becomes greater if an appropriate measure is not taken in time. The trained up students are themselves a great resource considering the future prospects. They will also work in spreading out the knowledge base in awareness creation. These 33 students will work as the leader in their respective classes and guide in tackling any unwanted situation. They will also lead in safety drill undertaken in their school. The headmaster of the school wishes to under take safety drill program regularly in their school.

6. CONCLUSIONS

Earthquake risk reduction action plan cannot be successful unless the people at risk in the hazardous zone aware themselves about the risk and considers earthquake safety issues as part of their life and society's culture. The enthusiasm and potential of the school people was exciting and such school community work should be a part of future efforts of any Safety related Project. Schools play a vital role in every community. Schools teach civics, educating citizens of their rights and duties. They foster an appreciation of culture through the study of literature and the arts. Schools are a measure of community well being. Earthquake threatened communities need earthquake-resistant school to protect their teachers and children. In order to reduce Old Dhaka's earthquake risk, the processes started by this project need to be continued for at least several years.

Recommendations for school based disaster management plan

- Emphasize preparedness for natural and technological disasters.
- Prepare charts, outlining who does what in disaster prevention, mitigation, preparedness and response.
- Define the tasks to be fulfilled by the team and the support they need from the authorities.
- Include the BNCC, Red Crescent more fully in support of response to warnings and disasters at all level.
- Reinforce cooperation between different organizations (Fire service, Red Crescent Society) and school.

REFERENCES

- Ansary, M.A., 2004. *Seismic Loss Estimation of Dhaka for an Earthquake of Intensity VII*. Oriental Geographer, Dhaka University.
- Campo, M. A., nd, 2006. *Study of Awareness of Earthquake Risk in the population of Mendoza*. URL: <http://proventionconsortium.org/files>.
- Rahman, M. G. F., 2004. *Seismic Damage Scenerio for Dhaka City*. M.Sc. Engg. Thesis, Department of Civil Engg., BUET, Dhaka

VULNERABILITY RISK AREAS OF BANGLADESH DUE TO MULTIPLE NATURAL HAZARDS

MUSA. SHAMMI AKTHER
Graduate Student, Department of Civil Engineering, BUET, Bangladesh
shammii_bd@yahoo.com

MEHEDI AHMED ANSARY
Professor, Department of Civil Engineering, BUET, Bangladesh
ansary@ce.buet.ac.bd

ABSTRACT

This paper highlights the complete district wise database for natural disasters in Bangladesh and identification of vulnerable areas with reference to different natural hazards. A basic requirement in this regard is to prepare a Vulnerability Atlas, showing specific areas vulnerable to one or more natural disasters. Secondary data and information is collected from the census report as well as from various government and non-government organizations such as Bangladesh Meteorological Department (BMD), SPARSSO, Disaster Management Bureau (DMB) and concerned non-government organizations (NGO). This study is undertaken to identify the historical disaster events, their duration and damage information. GIS is a powerful planning tool, which is used to identify the disaster prone areas in Bangladesh. The existing disaster data and zoning maps are critically reviewed. The location, type, year and damages etc are stored into a database. Based on the available historical data gathered from different sources, the disaster prone area of Bangladesh is identified.

1. INTRODUCTION

Bangladesh is one of the most natural disaster prone areas in the World. The different types of disasters like flood, cyclonic storms, tidal surges, droughts, tornadoes, riverbank erosion, earthquake, etc. occur in Bangladesh regularly and frequently. The most devastating cyclones and floods of the world occurred in Bangladesh. The 1988 flood killed 1517 people and nearly half of the population was affected (Hossain, 2006). The 1970 cyclone killed almost 500,000 people (Karim, 1996). About 1300 people were killed by tornado at Saturia of Manikganj district in Bangladesh in 1989 (EIA, 2004). The 1897 Great Indian Earthquake with a magnitude of 8.7 and considered to be one of the strongest earthquakes in the world killed 1542 and affected almost the whole of Bangladesh (Oldham, 1899). Crop and livestock loss was extremely high. Major factors responsible for disasters in Bangladesh are flat topography, rapid run-off and drainage congestion, low relief of the floods plains, low river gradients, heavy monsoon rainfall, enormous discharge of sediments, funnel shapes and shallow Bay of Bengal etc.

Bangladesh is a developing country with numerous problems like overpopulation, poverty, complex socio economic structure, frequent disasters, low level industrial base, resource constrains, lack of appropriate infrastructural and institutional facilities, dearth of trained manpower, etc. These problems are complicated and compounded with the occurrences of regular and frequent disasters impeding the overall socio-economic development efforts of the country. Exploring the historical disaster database one can imagine the damages that occurred due to natural calamities.

Creating hazard maps will assist us to determine which areas are susceptible to individual hazards or multiple hazards that have been identified. The appropriate decision makers can use maps that depict individual hazards or a combination of hazards. This study identified district wise natural hazards, their hazard risk and finally developed combined hazard map. The multi-hazard maps determine which areas are susceptible to the most destructive hazards in order to determine where to concentrate and fund hazard mitigation measures such as developing property protection ordinances or encouraging development in less hazard-prone areas.

2. METHODOLOGY

In order to locate highest-risk areas, it may be helpful to first develop a risk-prioritization scheme. It is possible to develop such a scheme using publicly available data, although local data — data collected from local agencies — will almost always be more detailed and more accurate. In this study following natural disasters were studied:

- Tornado
- Earthquake
- Cyclone
- Flood

Every community have unique or unusual hazards that need to be considered. Historical records and information from local experts and citizens is used to provide estimates of the zones or locations potentially at risk to such events. As no digital (geographic information systems or GIS) data are available for Bangladesh, it has to construct risk maps showing estimates of hazard extents and magnitudes by using transparencies overlaid on paper maps. Even some paper maps have to be modified to gather data. Following steps were followed for hazard assessment of each district area of Bangladesh:

1. Locate, gather, and process data
2. Assign scores to risk areas (higher rankings should indicate higher risk)
3. Identify high-risk locations (areas with highest scores)
4. Propose a multi hazard map for Bangladesh

2.1 Data Sources

The data were collected from Bangladesh Meteorological Department (BMD), SPARRSO, Disaster Management Bureau (DMB) and concerned non-government organizations (NGO), Cyclone Preparedness Programme (CPP), geological information from the Geological Survey of Bangladesh (GSB). Information from local and environmental organizations, international Journals, local newspapers and many study reports were collected. Personal contacts with experts concerned were also made.

2.2 Hazard Area Scoring Methods

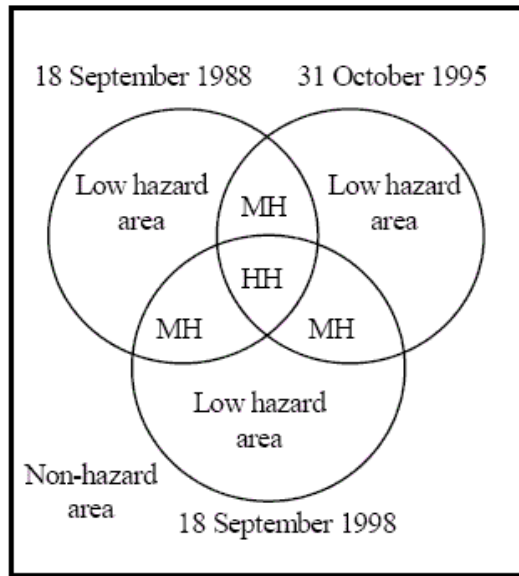
Assign scores within risk areas, where possible. Within risk areas there could be additional boundaries representing varying degrees of risk. These varying degrees of risk should be represented in risk areas both graphically (additional boundaries on the maps) and through some type of relative scoring system (higher scores for higher risk areas). For example, Cyclone maps are generally created for five different categories of storm. Category 1 storms are generally associated with the least severe winds and storm surge while Category 5 storms are considered the most severe for these hazards. Generally, those areas subject to storm surge in the lower category storms are also projected for inundation in all of the higher categories. When developing a relative priority scoring system for storm surge inundation, Category 1 storm surge areas would therefore have the highest risk of being flooded since they are at risk of inundation in all storm events.

The general concept in relative priority scoring system for natural hazard risks is that locations with no consideration for risk will be given a score of 0 and each incremental increase in risk adds 1 point. A multiplier or weighting factor is calculated based on frequency of events (NOAA, 2007).

2.3 Concept of Hazard Affected Frequency

Frequency is the occurrence of a disaster in a particular area. To explain this issue for a particular disaster, occurrence of flood in a particular area per year can be used.

Estimated flooded areas for September 18, 1988, October 31, 1995, and September 18, 1998 are 34.7, 27.7 and 36.1%, respectively, when the drainage network map was superimposed onto the flood season images. Figure 1 shows the concept of the frequency (Islam and Sado, 2000). The flooded area was estimated after subtracting the normal water area (river, lake, pond, etc.) from total inundated area; it was then converted to percentage of land area (non-water area in dry season) of the whole country.



- MH: Medium hazard area
- HH: High hazard area
- : Water area in each image
- : Whole area of Bangladesh

Figure1: Concept for flood-affected frequency (after Islam and Sado, 2000)

The more occurring number indicates more frequency that is expressed by multiplier for a particular risk area for a particular hazard.

2.4 Relative Priority Scoring System for Natural Hazards

For a particular area for the various hazards scores are calculated as follows:

Risk Score (for particular hazard e.g. Cyclone/ Flood/ Tornado/ Earthquake) = Weighting factor (WT(f_r)) × Risk (Potential Damage Magnitude).

$$TR_{(c/f/t/e)} = WT (WT = f(f_r)) \times R \dots\dots\dots(1)$$

For Cyclone:

$$R_{ci} = f(w, h, c_p)$$

Where $i = 0, 1, 2, 3, 4, 5$.
 $w =$ Wind speed, $h =$ Storm Surge, $C_p =$ Central Pressure.

$$WT_{cj} = f(f_r)$$

$f_r =$ Frequency.
 Where $j = 1, 2, 3, 4, 5, 6, 7, 8, 9, 10$.

$$TR_c = R_{ci} \times 0.1WT_{cj} \dots\dots\dots(2)$$

For Tornado:

$$R_{ti} = f(w)$$

Where $i= 0$ and 5 .

$w=$ Wind speed.

$$WT_{ij} = f(f_r)$$

$f_r =$ Frequency.

Where $j= 1, 2, 3, 4, 5, 6, 7, 8, 9, 10$.

$$TR_{ii} = R_{ti} \times 0.1WT_{ij} \dots\dots\dots (3)$$

For Flood:

$$R_{fi} = f(h_w)$$

Where $i= 1, 2, 3, 4, 5$.

$h_w=$ Water level.

$$WT_{fj} = f(f_r)$$

$f_r =$ Frequency.

Where $j= 1, 2, 3, 4, 5, 6, 7, 8, 9, 10$.

$$TR_{ti} = R_{ti} \times 0.1WT_{fj} \dots\dots\dots(4)$$

For Earthquake:

$$R_{ei} = f(m, p)$$

Where $i= 2, 3, 4$.

$m =$ Magnitude, $p=$ Peak Ground Acceleration.

$$WT_{ej} = f(f_r)$$

$f_r =$ Frequency.

Where $j= 1, 2, 3, 4, 5, 6, 7, 8, 9, 10$.

$$TR_{ei} = R_{ei} \times 0.1WT_{ej} \dots\dots\dots(5)$$

Total Risk Score:

$$TR = \sum_{k=1}^n TR_k \dots\dots\dots (6)$$

where

$k= 1$ is for Cyclone.

$k=2$ is for Tornado.

$k=3$ is for Earthquake

$k=4$ is for flood

$k=n$ disaster.

In these equations, two of the hazards have locations with a risk score of 0 (Cyclone and Tornado). In case of Cyclone, the maximum extent of the hazard risk does not realistically include the entire county and is limited to proximity to coastal waters. Tornado may always have high risk, i.e score 5 for all the tornado prone area. For the locations with no consideration of risk for Tornado was given a score of 0. Again earthquake hazard of Bangladesh was expressed as minimum by 2 and as maximum by 4.

The minimum risk score for each of the remaining hazards is 1 since there is some potential that each of these hazards could occur anywhere throughout each county. This scoring system has been used according to our

district-based database. For particular district of Bangladesh the hazard for Earthquake, Tornado, Cyclone and Flood is calculated. Then adding those scores, total risk score for each of the 64 districts was found.

3. LOCATING THE HAZARD

3.1 Tornado

The existing tornado map of DMB, GoB (DMB, 1993), is shown in Figure 2. In the map the areas affected by Tornadoes are identified. The basis of this map is not clear. For this study a new tornado map is digitised based on frequency or number of occurrence from the compiled database, which contains Tornado data from 1875-2007. From the database, the frequency of the tornado is calculated by the occurrence of Tornado. The proposed digitized district wise Tornado map is also shown in Figure 2. Bangladesh is divided into four zones as shown in Figure 2 and Table 1.

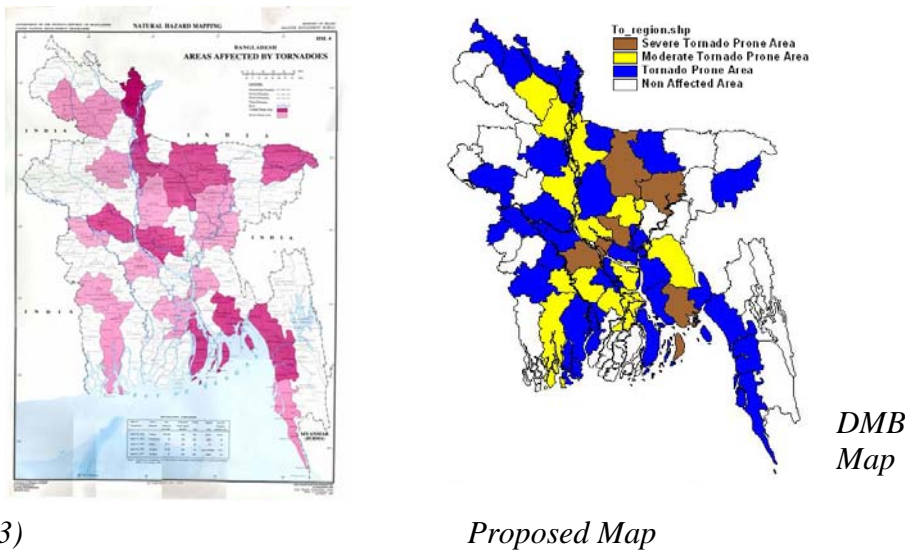


Figure 2: Tornado Hazard Maps of Bangladesh

Table 1: Risk vulnerability Table for Tornado

SL. No.	Area	Occurrence /Frequency	Risk Score
1.	Severe Tornado Prone Area	> 4	5
2.	Moderate Tornado Prone Area	3-2	
3.	Tornado Prone Area	1	
4.	Non Affected Area	0	0

3.2 Earthquake

The peak ground acceleration (PGA), i.e., maximum acceleration experienced by the ground during shaking, is one way of quantifying the severity of the ground shaking. Approximate empirical correlations are

available between the MM intensities and the PGA that may be experienced as Table 2 (Bolt, 1993).

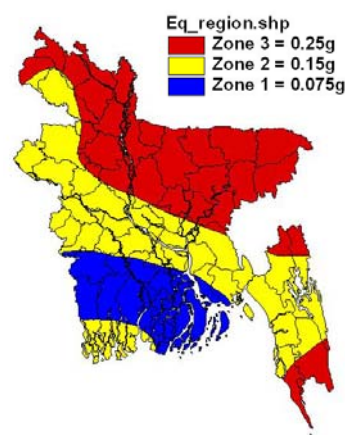
Table 2: PGAs during shaking of different intensities

MMI	V	VI	VII	VIII	IX	X
PGA(g)	0.03-0.04	0.06-0.07	0.10-0.15	0.25-0.30	0.50-0.55	>0.60

The existing seismic zoning map (BNBC, 1993) and the proposed Seismic-zoning map of Bangladesh proposed by Ansary and Sharfuddin (2001) is shown in the Figure 3.



BNBC (1993)



Ansary and Sharfuddin (2001)

Figure 3: Seismic Zoning Map for Bangladesh

Comparing the Table 2 and the seismic zoning map with different Earthquake intensity, a Vulnerability Table for Earthquakes of Bangladesh has been proposed in Table 3.

Table 3: Proposed Vulnerability Table of Earthquake for Bangladesh

SL. No.	Zone	Intensity EMS	PGA	Risk Score
1.	Zone-1	VI	0.075g	2
2.	Zone-2	VII	0.15g	3
3.	Zone-3	VIII	0.25g	4

3.3 Cyclone

From the cyclone affected area map of Bangladesh prepared by SPARRSO, a cyclone risk map of Bangladesh was developed which is shown in Figure 4.

Comparing with the Saffir-Simpson Hurricane Intensity Scale with the damage database of Bangladesh (LGEB, 1991), a cyclone risk area map for Bangladesh was proposed as shown in Table 4.

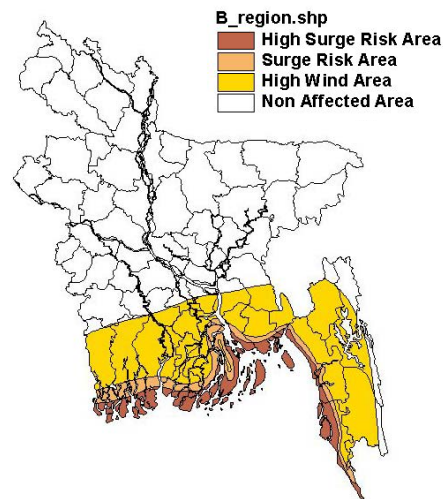


Figure 4: Cyclone Hazard Map of Bangladesh

Table 4: Cyclone Risk Area of Bangladesh

SL No	Risk Area	Category with storm surge		Risk Score
		Storm surge	Category	
1.	High Risk Area	Above 1m	Category 4 and 5	5
			Category 3	4
			Category 2&1	3
2.	Risk Area	Below 1m	-	2
3.	High Wind Area	Storm Surge buffer		1
4.	Non Affected Area	-		0

3.4 Flood

1998 flood is the extreme flooding of Bangladesh. The 1998 flood hazard map prepared by FFWC, BWDB Dhaka, has been used as a reference. According to the hazard map the whole area is divided in four zones based on water level. The map is shown in Figure 5. Table 5 shows different flood level of Bangladesh.

The damage risks for flooding have been developed by the Vulnerability Atlas of India (BMTPC, 1997) based on material behavior under submergence. Comparing with flood water level of Bangladesh with the Vulnerability Atlas of India, a flood risk table for Bangladesh was proposed as shown in Table 6.

Table 5: Flood Water level of Bangladesh

SL. No.	Area	Water Level
1.	Severe Flooding Area	Above 50cm DL
2.	Moderate Flooding Area	Up to 50cm above DL
3.	Normal Flooding Area	Within 50cm DL
4.	Non Flooding Area	Below 50cm DL

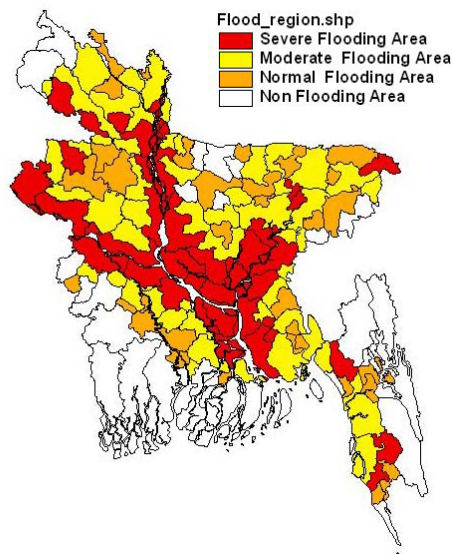


Figure 5: Flood Hazard Map of Bangladesh

Table 6: Flood Risk Table for Bangladesh

SL. No.	Area Type	Water Level	Damage Type	Risk Score
1.	Severe Flooding Area	Above 50cm D.L	Very High Damage Risk (>3m above D.L)	5
			High Damage Risk (<3m above 50cm D.L)	4
2.	Moderate Flooding Area	Up to 50cm Above DL	Moderate Damage Risk	3
3.	Normal Flooding Area	Within 50cm DL	Low Damage Risk	2
4.	No Flooding Area	Below 50cm DL	Very Low Damage Risk	1

3.5 District wise Risk Scores

Total Risk Scores for each of 64 districts were estimated following the above methods. Table 7 summarizes the total risk scores for Districts of Bangladesh.

From the above Table a district risk-ranking map for Bangladesh is proposed which is shown in Figure 6. This map indicates the risky districts of Bangladesh for multi hazard (Cyclone, Flood, Tornado and Earthquake). This Figure shows risk scenario of Bangladesh at a glance.

Table7: Hazard Index and Risk Score

Sl. No.	Hazard Index	Total Risk Score	Hazardous Districts
1.	High	20-30	Dhaka, Bogra, Sirajganj, Feni, Comilla, Cox's bazaar, Lakshmipur, Noakhali, Chittagong, Tangail, Mymensingh, Kishoreganj, Jamalpur, Rangpur, Bhola, Barishal, Kurigram, Gaibandha
2.	Moderate	10-20	Sylhet, Gazipur, Manikganj, Narsingdi, Narayanganj, Munshiganj, Netrokona, Sherpur, Gopalganj, Rajbari, Shariatpur, Madaripur, Sunamganj, Pabana, Bandaban, Faridpur, Naogaon, Natore, Nawabganj, Rajshahi, Brahmanbaria, Joypurhat, Chandpur, Lalmonirhat, Nilphamari, Dinajpur, Magura, Khulna, Satkhira, Bagerhat, Jessore, Panchagarh, Meherpur, kushtia, Habiganj, Narail, Moulvibazar, Potualkali, Pirojpur, Borguna
3.	Low	1-10	Jhalkati, Chuadanga, Rangmati, Thakurgoan, Khgrachari, Jhenaidah

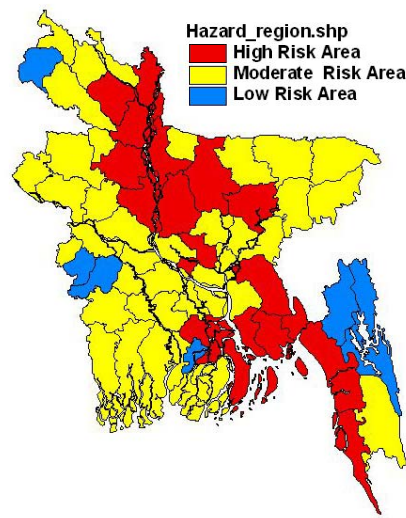


Figure 6: Risk Hazard Map of Bangladesh

4. PROPOSED MULTI HAZARD MAP OF BANGLADESH

Again from the individual digitized maps of Bangladesh for different hazard (Cyclone, Flood, Tornado and Earthquake) and superimposing those, a multi hazard zonation map for Bangladesh is prepared as shown in Figure 7. From this map one can easily identify the hazard area with the hazard type and intensity. This map is comprehensible to everybody.

For identifying multihazard in a district more clearly, the multihazard map of Chittagong District is shown in Figure 8. Table 8 provides explanation for Figure 8.

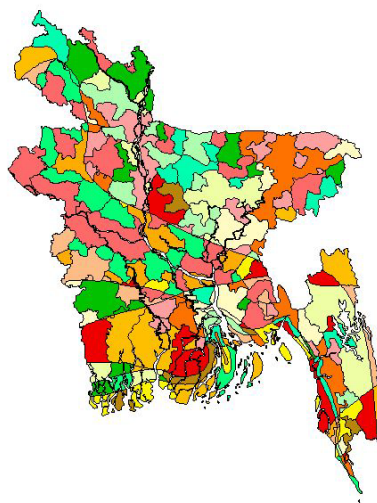


Figure 7: Proposed Multi Hazard Zonation Map of Bangladesh

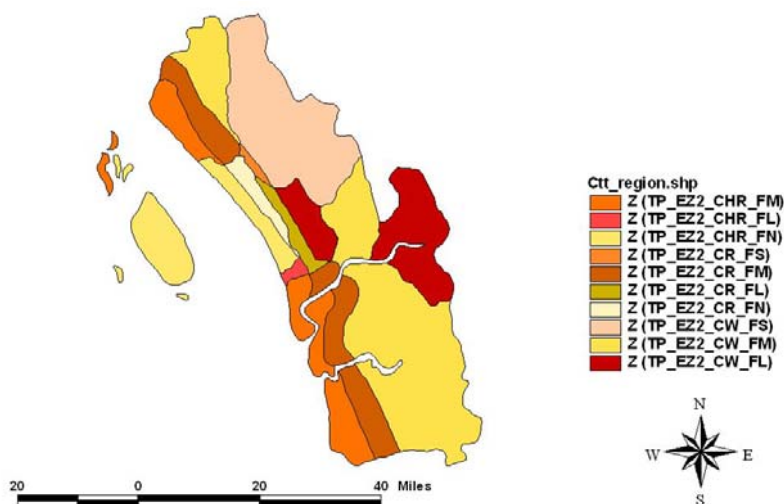


Figure 8: Proposed Multi Hazard Zonation Map of Chittagong

Table 8: Explanation of the multi hazard zonation map of Chittagong

SL. NO.	CODE	Explanation
1.	Z(TP_EZ2_CHR_FM)	Zone: Tornado Prone Area Earthquake Zone 2=0.15g Cyclone High Risk Area Moderate Flooding Area
2.	Z(TP_EZ2_CHR_FL)	Zone: Tornado Prone Area Earthquake Zone 2=0.15g Cyclone High Risk Area Low Flooding Area
3.	Z(TP_EZ2_CHR_FN)	Zone: Tornado Prone Area

SL. NO.	CODE	Explanation
		Earthquake Zone 2=0.15g Cyclone High Risk Area Non Flood Affected Area
4.	Z(TP_EZ2_CR_FS)	Zone: Tornado Prone Area Earthquake Zone 2=0.15g Cyclone Risk Area Severe Flooding Area
5.	Z(TP_EZ2_CR_FM)	Zone: Tornado Prone Area Earthquake Zone 2=0.15g Cyclone Risk Area Moderate Flooding Area
6.	Z(TP_EZ2_CR_FL)	Zone: Tornado Prone Area Earthquake Zone 2=0.15g Cyclone Risk Area Low Flooding Area
7.	Z(TP_EZ2_CR_FN)	Zone: Tornado Prone Area Earthquake Zone 2=0.15g Cyclone Risk Area Non Flood Affected Area
8.	Z(TP_EZ2_CW_FS)	Zone: Tornado Prone Area Earthquake Zone 2=0.15g High Wind Area Severe Flooding Area
9.	Z(TP_EZ2_CW_FM)	Zone: Tornado Prone Area Earthquake Zone 2=0.15g High Wind Area Moderate Flooding Area
10.	Z(TP_EZ2_CW_FL)	Zone: Tornado Prone Area Earthquake Zone 2=0.15g High Wind Area Low Flooding Area

5. CONCLUSIONS

This paper proposes a multihazard Map of Bangladesh based on a recently compiled disaster database. For this purpose initially Tornado, Earthquake, Flood and Cyclone zonation maps were reviewed and updated. This multihazard maps will be used for policy makers to take decision for disaster management and preparedness.

REFERENCES

Ansary M. A. and Sharfuddin, M., 2001. Proposal for a new seismic zoning map for Bangladesh, *Journal of the Civil Engineering, IEB*, No. 30(2), pp. 77-89.

- BMTPC, 1997. *Vulnerability Atlas of India 1997*, Building Materials and Technology Promotion Council, Ministry of Urban Development, Government of India, New Delhi.
- Bolt B.A., 1993. *Earthquakes*, W.H. Freeman and Co., New York, USA.
- DMB, 1993. *Natural Hazard Mapping*, GoB.
- EIA, 2004. *Environmental Informatics Archives, Volume 2 (2004)*, 855-863, EIA04-085, ISEIS Publication #002, © 2004 ISEIS - International Society for Environmental Information Sciences.
- Hossain A. N. H., 2006. *An Overview on Impacts of Flood in Bangladesh and Options for Mitigation*.
- Islam, M. and Sado K., 2007. *Flood Hazard Assessment for the Construction of Flood Hazard Map and Land Development Priority Map Using NOAA/AVHRR Data and GIS - A Case Study in Bangladesh*, Department of Civil Engineering, Kitami Institute of Technology, Japan .
- Karim A.K.M, 1996. *Formation of Planning and Land-Use Policies for Disaster Management in Chittagong Metropolitan Area of Bangladesh*, UNCRD-BUET Joint Research, Department of Urban and Regional Planning, BUET, Bangladesh.
- LGEB, 1991. *Cyclone damage-1991*, Damage Assessment of General Infrastructure, Local Government Engineering Bureau, Final Report, Volume 4, The world Bank, GoB.
- NOAA Coastal Services Center, 2007. *Risk and Vulnerability Assessment Steps, Hazards Analysis Extended Discussion*.
- Oldham, T. 1899. Report on the great India earthquake of 12th June, 1897, *Memoir of Geological Survey of India*, Vol. 19, 1-53.

PROPOSAL OF INTENSITY SCALES FOR DIFFERENT NATURAL HAZARDS IN BANGLADESH

MUSA. SHAMMI AKTHER
Graduate Student, Department of Civil Engineering, BUET, Bangladesh
shammii_bd@yahoo.com

MEHEDI AHMED ANSARY
Professor, Department of Civil Engineering, BUET, Bangladesh
ansary@ce.buet.ac.bd

ABSTRACT

This paper covers topics related to hazard intensity scales for natural disasters like Earthquake, Flood, Cyclone and Tornado for Bangladesh. It also summarizes district-wise housing risk tables based on Earthquakes, Cyclones, Tornados and Floods. All these analyses will be useful to engineers, planners, emergency personnel, government officials, and agencies that may be concerned with hazard mitigation activities in a given region. It will be helpful also to people who will be directly affected by the natural disasters. Secondary data and information was collected from the census report as well as various government and non-government organizations such as Bangladesh Meteorological Department (BMD), SPARSO, Disaster Management Bureau (DMB) and concerned non-government organizations (NGO). For different intensity scale, different models were used. Intensity scales for different disaster of Bangladesh are proposed based on disaster data and worldwide disaster intensity scales. Finally using the census attribute data of housing of different district of Bangladesh a Housing category Table for intensity scales of disaster was prepared.

1. INTRODUCTION

Natural processes such as tropical Cyclones, Floods, Tornadoes, Earthquake, and the like are an enduring condition around the human environment. Natural hazards become disasters when they intersect with the human environment. In Bangladesh, natural disasters have left a profound imprint causing devastating loss of life, property, economy and community.

Bangladesh is one of the most natural disaster prone countries in the World. Floods, cyclonic storms, tidal surges are the major disasters and droughts, tornadoes, riverbank erosion, earthquake are other types of disasters in the country. All these disasters are occurring in Bangladesh regularly and frequently. Intensity scales are subjective and depend upon social condition and construction status of a country, they need revising from time to time. Regional effects must be accounted for. There exists no

individual hazard intensity scale to identify the type of particular hazard for Bangladesh. This paper studied different Bangladeshi disaster and their corresponding scales all over the world, and proposed suitable intensity scales for different disaster in Bangladesh.

2. INTENSITY SCALES AND MODELS

2.1 Tropical Cyclones

Hurricanes, tropical storms and typhoons are collectively known as tropical cyclones. These cyclones are defined as low-pressure areas of closed circulation winds that originate over tropical waters (FEMA, 1997). Figure 1 shows the effect of a cyclone. Tropical storms have sustained surface wind speed that ranges from 39 to < 74 mph and that hurricanes have a minimum sustained surface wind speed of at least 74 mph.



Figure 1: Effect of a Cyclone

In Saffir-Simpson Hurricane Scale, a 1-5 rating based on a hurricane's present intensity, used to give an estimate of the potential property damage and flooding expected along the coast from a hurricane landfall. Wind speed is the determining factor in the scale, as storm surge values are highly dependent on the slope of the continental shelf in the landfall region. Comparing with historical database with the Saffir-Simpson Hurricane Scale and using STP model (Storm Track Prediction) of Cyclone, an intensity Scale for Bangladesh is proposed (Debsarma, 1988).

Also a Storm Surge Forecast (SSF) model (Debsarma, 1993) based on wind speed, central pressure and 200m bathymetric contour for Chittagong, Cox's Bazar, Kutubdia, Sandwip, Hatia, Khulna can be generated. Table 1 presents predicted highest storm surges for those areas based on the SSF model.

Table 1: Predictable Storm surge of Bangladesh by modeling

SL. No.	Wind Speed (kph) Vmax	Expected Central Pressure (ECP)	Location	Storm Surge (m)	
				Above tide level	Above Mean Sea level
1.	153	976	Chittagong	3.04	6.62
			Cox's Bazar	2.28	4.54
			Kutubdia	2.59	6.21
			Sandwip	3.12	7.61
			Hatia	2.98	6.75
			Khulna	2.61	5.53
2.	177	966	Chittagong	3.93	7.51
			Cox's Bazar	2.97	5.23
			Kutubdia	3.36	6.98
			Sandwip	4.03	8.52
			Hatia	3.86	7.63
			Khulna	3.38	6.30
3.	209	948	Chittagong	5.25	8.23
			Cox's Bazar	3.98	6.24
			Kutubdia	4.50	8.12
			Sandwip	5.38	9.87
			Hatia	5.15	8.92
			Khulna	4.52	7.44
4.	220	942	Chittagong	5.73	9.31
			Cox's Bazar	4.35	6.61
			Kutubdia	4.92	8.54
			Sandwip	5.88	10.37
			Hatia	5.63	9.40
			Khulna	4.94	7.86
5.	249	924	Chittagong	7.08	10.66
			Cox's Bazar	5.40	7.66
			Kutubdia	6.09	9.71
			Sandwip	7.25	11.74
			Hatia	6.95	10.72
			Khulna	6.12	9.04
6.	>250	924	Chittagong	7.13	10.71
			Cox's Bazar	5.43	7.69
			Kutubdia	6.13	9.75
			Sandwip	7.30	11.79
			Hatia	7.00	10.77
			Khulna	6.16	9.08

Table 2 presents the proposed Cyclone Intensity Scales for Bangladesh.

Bangladesh needs to develop a damage risk level table from previous damage study. Due to limited data identification of the actual damage risk level is not possible. So Saffir-Simpson Hurricane Scale with some modification suggested by expert based on cyclone damage data of 1991 (LGEB, 1991) is adopted as shown in Table 3.

2.2 Tornadoes

A Tornado is a rapidly rotating vortex of air extending ground-ward from a cumulonimbus cloud. Tornadoes can reach wind speeds in excess of 300 mph causing various intensities of destruction within its path. Often tornadoes are related to larger vortex formations and as a result often form in convective cells. Figure 2 shows a twisting funnel of a tornado (CHCDA, 2005).

Table 2: Cyclone Intensity Scale For Bangladesh

Scale Number (Category)	Expected Central Pressure		Wind Speed		Maximum possible Storm Surge (ATL)	
	(mbar)	(in)	(mph)	(kph)	(m)	(ft)
1	>=976	>=28.94	74-95	119-153	<3.5	<12
2	966-975	28.50-28.91	96-110	154-177	3.5-4.5	12-15
3	948-965	27.91-28.47	111-130	178-209	4.6-5.5	16-18
4	923-947	27.17-27.88	131-155	210-249	5.6-7.5	19-25
5	<924	<27.17	>155	>249	>7.5	>25

ATL = Above Tide Level



Figure 2: The violent, twisting funnel of a tornado

Table 3: Details Cyclone Intensity Scale for Bangladesh

Damage Risk Level	Intensity	Description
Very Low Damage Risk (VL)	Category 1	Winds 74-95 mph (64-82 knots or 119-153 km/hr) - Storm surge maximum below 12 ft above normal. No real damage to building structures. Damage primarily to fishing boats, trees near coastal. Some damage to poorly constructed signs. Also, some coastal road flooding and minor pier damage.
Low Damage Risk (L)	Category 2	Winds 96-110 mph (83-95 knots or 154-177 km/hr) - Storm surge may maximum 12-18 feet above normal. Some roofing material, door, and

Damage Risk Level	Intensity	Description
		window damage of buildings. Considerable damage to trees with some trees blown down. Some fishing boat is missing. Considerable damage to poorly constructed signs, and piers. Small craft in unprotected anchorages break moorings.
Moderate Damage Risk (M)	Category 3	Winds 111-130 mph (96-113 knots or 178-209 km/hr) - Storm surge may reach maximum 16-18 ft above normal. Tin roof, wooden supports blown off. Tin shed cottage industry totally damage. Crack in wall and beam and floor settled of some godown. Some structural damage to small residences and utility buildings with RCC roof and wall crack. Extensive damage to doors and windows of one storey buildings and General damage of doors-windows of some two storey residential buildings. Some damage of boundary wall and steel gate. Some retaining wall washed away and some damage to toe of wall. Wooden jetty totally damage. Some electrical works damage. Major damage to lower floors of structures near the shore.
High Damage Risk (H)	Category 4	Winds 131-155 mph (114-135 knots or 210-249 km/hr) - Storm surge may reach maximum within 18-25 ft above normal. More extensive curtain wall failures with some complete roof structure failures on small residences. Semi pucca tin roof totally destroyed. Roofs blown away and windows-doors damaged of dormitory and community centre. Single storey buildings totally collapse. General damage to interior of cyclone shelter. RCC pillars crack. Doors and windows of two storey cyclone shelter destroy. Complete roof failure of many residential and industrial buildings. Trees and all signs are blown down. Major damage to lower floors of structures near the shore.
Very High Damage Risk (VH)	Category 5	Winds greater than 155 mph (135 knots or 249 km/hr) - Storm surge may maximum greater than 25 ft above normal. Complete roof failure on many residences and industrial buildings. Some complete building failures with small utility buildings blown over or away. All trees and signs blown down. Severe and extensive window and door damage. Stairs, auditorium

Damage Risk Level	Intensity	Description
		and toilet block severely damage. Some one storey buildings and boundary walls collapse. Some two storey buildings destroy.

The Fujita-Pearson Tornado Scale measures the damage severity of a tornado. The historical data of Bangladesh is similar as the Fujita-Pearson Tornado Scale. So for Bangladesh this scale can be adopted. The description of this scale is given in Table 4 (FEMA, 1997).

Table 4: Fujita-Pearson Tornado Scale

Scale Value	Wind Speed (mph)	Intensity	Type of Damage
F0	40-72	Light Damage	Some damage to chimneys; tree branches broken off, shallow-rooted trees pushed over, sign boards damaged.
F1	73-112	Moderate Damage	Roof surfaces peeled off; mobile homes pushed off foundations or overturned; moving automobiles pushed off roads.
F2	113-157	Considerable Damage	Roofs torn from houses, mobile homes demolished; boxcars pushed over; large trees snapped or uprooted; light-object missiles generated.
F3	158-206	Severe Damage	Roofs and some walls torn off well-constructed houses; trains overturned; most trees in forest uprooted; heavy cars lifted off the ground and thrown.
F4	207-260	Devastating Damage	Well-constructed houses levelled; structures with weak foundations blown off some distance; cars thrown; large missiles generated.
F5	261-318	Incredible Damage	Strong frame homes lifted off foundations and carried considerable distances to disintegrate; automobiles-size missiles fly through the air in excess of 100 yards; trees debarked.
F6	>318	Inconceivable Damage	These wind speeds have rarely been recorded. The area of damage would be completely obliterated and unrecognizable. Large missiles would be thrown in excess of 100 yards.

2.3 Flood

Flooding occurs in floodplains when prolonged rainfall over a short period causes rivers or streams to overflow. Flash floods, specifically, occur within six hours of a rain event, after a dam or levee failure or following a sudden release of water held by a debris jam. In addition, development in the flood hazard area can increase the overall height and speed of flooding bringing it to areas that were not originally susceptible.



Figure 3: Typical Flood Damages

Depth classification maps rate also similar to flood depth maps, but instead of using a constant depth increment for showing different depths, depths are grouped into different classes. Depth classification maps can be based on flood depth maps or duration depth maps. Figure 4 shows a depth classification map based on the flood phase categories for the Tangail compartment using the peak flood levels from the 1993 flood.

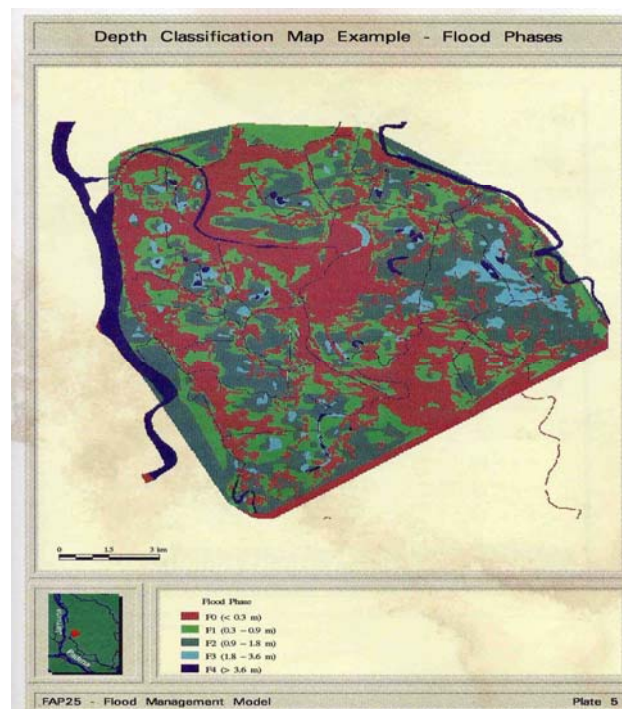


Figure 4: Depth Classification Map (after FAP25, 1994)

Table 5 presents the Bangladesh flood phase classification, which groups flood depths into five classes, F0 to F4 (FAP25, 1994):

Table 5: Bangladesh flood phase classification

SL. No.	Class	Flood Phase	Depth Range
1.	F0	Non-flood	< 0.3m including flood-free ground
2.	F1	Shallow Flood	0.3m to 0.9m
3.	F2	Medium Flood	0.9m to 1.8m
4.	F3	Deep Flood	1.8m to 3.6m
5.	F4	Very Deep Flood	>3.6m

No such data exists for whole Bangladesh. It is not possible for this study to establish such table for whole Bangladesh. For proper identification of hazard area such data of flood for whole Bangladesh is needed.

1998 flood is the extreme flooding in Bangladesh. The flood hazard map prepared by FFWC, BWDB Dhaka, has been used as a reference. According to the hazard map the whole area is divided in four zones based on water level as shown in Figure 5. Table 6 presents four flood water levels of Bangladesh based on 1998 flood:

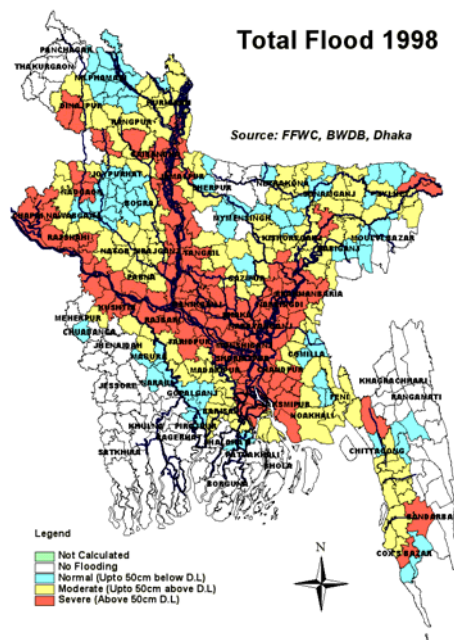


Figure 5: 1998 flood affected area

Table 6: Flood Water level of Bangladesh

SL. No.	Area	Water Level
1.	Severe Flooding Area	Above 50cm DL
2.	Moderate Flooding Area	Up to 50cm above DL
3.	Normal Flooding Area	Within 50cm DL
4.	No Flooding Area	Below 50cm DL

No Detailed building damage reports under flooding was recorded so far. Flood intensities in terms of depth of water velocity of flow or time duration of inundation are not yet defined. In the absence of such data, no definite recommendation about damage risk levels could be made.

The following damage risks have been drafted by the BMPTC (1997) to develop the Vulnerability Atlas of India, based on understanding of material behavior under submergence. Table 7 is used for the intensity of Bangladesh. Comparing the above tables and our historical damage data a intensity table for Bangladesh is proposed as shown in Table 8. If our topographical data, flood level of whole Bangladesh in different flood year, the flood velocity zone etc. are available than it can be made more accurate.

Table 7: Damage Risk Table for Flood

Sl. No.	Damage Type	Description
1.	Very High Damage Risk (VH)	Total collapse of buildings; roof and some walls collapse; floating away of sheets, thatch, etc; erosion of foundation; severe damage to lifeline structures and systems.
2.	High Damage Risk (H)	Gaps in walls; punching of holes through wall by flowing water; parts of buildings may collapse; light roofs float away; erosion of foundation, sinking or tilting; undercutting of floors, partial roof collapse.
3.	Moderate Damage Risk (M)	Large and deep cracks in walls; bulging of walls; loss of belongings; damage to electric fittings.
4.	Low Damage Risk (VL)	Small cracks in walls; fall of fairly large pieces of plaster.
5.	Very Low Damage Risk (L)	Fine cracks in plaster; fall of small pieces of plaster.

Table 8: Flood intensity of Bangladesh

SL. No	Area Type	Water Level	Damage Type	Description
1.	Severe Flooding Area	Above 50cm DL	Very High Damage Risk (>3m above DL)	Total collapse of buildings; roof and some walls collapse; floating away of sheets, thatch, etc; erosion of foundation; severe damage to lifeline structures and systems.
			High Damage Risk (<3m above 50cm DL)	Gaps in walls; punching of holes through wall by flowing water; parts of buildings may collapse; light roofs float away; erosion of foundation, sinking or tilting; undercutting of floors, partial roof collapse.

SL. No	Area Type	Water Level	Damage Type	Description
2.	Moderate Flooding Area	Up to 50cm Above DL	Moderate Damage Risk	Large and deep cracks in walls; bulging of walls; loss of belongings; damage to Electric fittings.
3.	Normal Flooding Area	Within 50cm DL	Low Damage Risk	Small cracks in walls; fall of fairly large pieces of plaster.
4.	No Flooding Area	Below 50cm DL	Very Low Damage Risk	Fine cracks in plaster; fall of small pieces of plaster.

2.4 Earthquakes

Earthquakes are geologic events that involve movement or shaking of the earth's crust. Earthquakes are usually caused by the release of stresses accumulated as a result of the rupture of rocks along opposing fault planes in the earth's outer crust. These fault planes are typically found along borders of the earth's 10 tectonic plates.

The areas of greatest tectonic instability occur at the perimeters of the slowly moving plates, as these locations are subjected to the greatest strains from plates traveling in opposite directions and at different speeds. Deformation along plate boundaries causes strain in the rock and the consequent buildup of stored energy. When the built-up stress exceeds the rocks' strength, a rupture occurs. The rock on both sides of the fracture is snapped, releasing the stored energy and producing seismic waves, generating an earthquake.



Figure 6: Effect of an Earthquake

Earthquakes are measured in terms of their magnitude and intensity. Magnitude is measured using the Richter scale, an open-ended logarithmic scale that describes the energy release of an earthquake through a measure of shock wave amplitude. Each unit increase in magnitude on the Richter scale corresponds to a 10-fold increase in wave amplitude. Intensity is most commonly measured using the Modified Mercalli Intensity (MMI) Scale. It is a 12-level scale based on direct and indirect measurements of seismic effects. There is another seismic Intensity scale name Japanese seismic intensity Scale,

0-VII levels. The MSK 1964 intensity scale is more comprehensive and describes the intensity of earthquake more precisely. EMS 1998 is the updated scale of MSK scale. In this study EMS 98(European Macroseismic Scale) was used. Table 9 shows the different vulnerability class (ESC, 1998).

Table 9: vulnerability classes

Type of Structure		Vulnerability Class					
		A	B	C	D	E	F
MASONRY	rubble stone, fieldstone	○					
	adobe (earth brick)	○	—				
	simple stone	○	—				
	massive stone			○	—		
	unreinforced, with manufactured stone units			○	—		
	unreinforced, with RC floors			○	—		
	reinforced or confined				○	—	
REINFORCED CONCRETE (RC)	frame without earthquake-resistant design (ERD)			○	—		
	frame with moderate level of ERD			○	—		
	frame with high level of ERD				○	—	
	walls without ERD			○	—		
	walls with moderate level of ERD			○	—		
	walls with high level of ERD				○	—	
STEEL	steel structures				○	—	
WOOD	timber structures			○	—		

○ most likely vulnerability class; — probable range;range of less probable, exceptional cases

The masonry types of structures are to be read as, e.g., simple stone masonry, whereas the reinforced concrete (RC) structure types are to be read as, e.g., RC frame or RC wall.

2.4.1 Classification of damage

The way in which a building deforms under earthquake loading depends on the building type. As a broad categorization one can group together types of masonry buildings as well as buildings of reinforced concrete as shown in Table 10 and Table 11.

Table 10: Classification of damage to masonry buildings

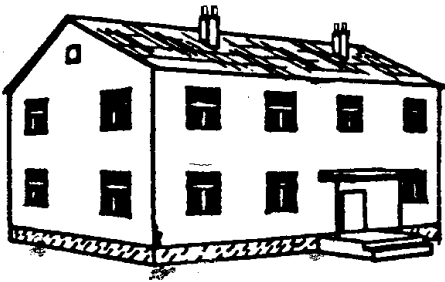
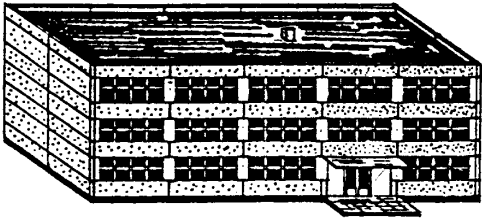
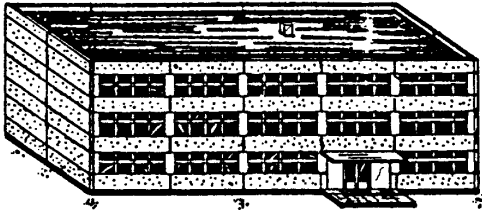
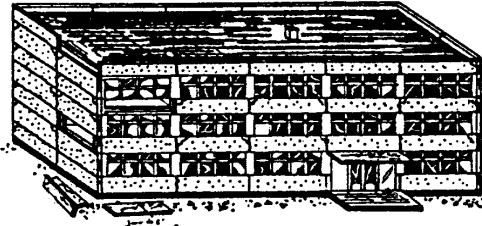
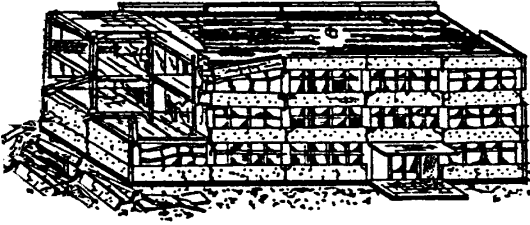
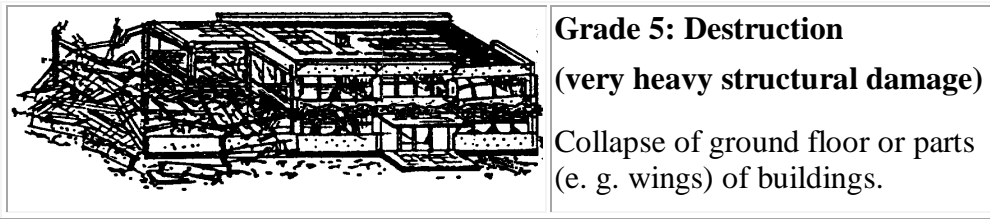
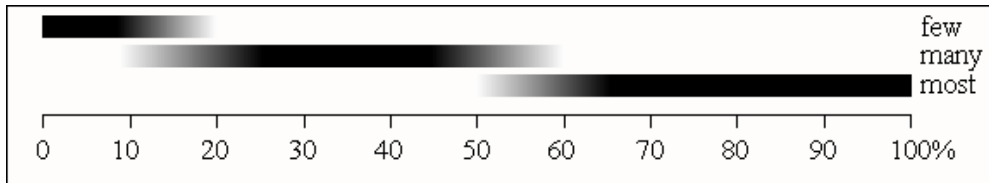
	<p>Grade 1: Negligible to slight damage (no structural damage, slight non-structural damage)</p> <p>Hair-line cracks in very few walls. Fall of small pieces of plaster only. Fall of loose stones from upper parts of buildings in very few cases.</p>
	<p>Grade 2: Moderate damage (slight structural damage, moderate non-structural damage)</p> <p>Cracks in many walls. Fall of fairly large pieces of plaster. Partial collapse of chimneys.</p>
	<p>Grade 3: Substantial to heavy damage (moderate structural damage, heavy non-structural damage)</p> <p>Large and extensive cracks in most walls. Roof tiles detach. Chimneys fracture at the roof line; failure of individual non-structural elements (partitions, gable walls).</p>
	<p>Grade 4: Very heavy damage (heavy structural damage, very heavy non-structural damage)</p> <p>Serious failure of walls; partial structural failure of roofs and floors.</p>
	<p>Grade 5: Destruction (very heavy structural damage)</p> <p>Total or near total collapse.</p>

Table 11: Classification of damage to buildings of reinforced concrete

	<p>Grade 1: Negligible to slight damage (no structural damage, slight non-structural damage)</p> <p>Fine cracks in plaster over frame members or in walls at the base. Fine cracks in partitions and infills.</p>
	<p>Grade 2: Moderate damage (slight structural damage, moderate non-structural damage)</p> <p>Cracks in columns and beams of frames and in structural walls. Cracks in partition and infill walls; fall of brittle cladding and plaster. Falling mortar from the joints of wall panels.</p>
	<p>Grade 3: Substantial to heavy damage (moderate structural damage, heavy non-structural damage)</p> <p>Cracks in columns and beam column joints of frames at the base and at joints of coupled walls. Spalling of concrete cover, buckling of reinforced rods. Large cracks in partition and infill walls, failure of individual infill panels.</p>
	<p>Grade 4: Very heavy damage (heavy structural damage, very heavy non-structural damage)</p> <p>Large cracks in structural elements with compression failure of concrete and fracture of rebars; bond failure of beam reinforced bars; tilting of columns. Collapse of a few columns or of a single upper floor.</p>



Definitions of quantity



2.4.2 Definitions of intensity degrees

Arrangement of the scale:

- a) Effects on humans
- b) Effects on objects and on nature
- c) Damage to buildings

The single intensity degrees can include the effects of shaking of the respective lower intensity degree(s) also, when these effects are not mentioned explicitly.

I. Not felt

- a) Not felt, even under the most favourable circumstances.
- b) No effect. c) No damage.

II. Scarcely felt

- a) The tremor is felt only at isolated instances (<1%) of individuals at rest and in a specially receptive position indoors.
- b) No effect. c) No damage.

III. Weak

- a) The earthquake is felt indoors by a few. People at rest feel a swaying or light trembling.
- b) Hanging objects swing slightly. c) No damage.

IV. Largely observed

a) The earthquake is felt indoors by many and felt outdoors only by very few. A few people are awakened. The level of vibration is not frightening. The vibration is moderate. Observers feel a slight trembling or swaying of the building, room or bed, chair etc.

b) China, glasses, windows and doors rattle. Hanging objects swing. Light furniture shakes visibly in a few cases. Woodwork creaks in a few cases.

- c) No damage.

V. Strong

a) The earthquake is felt indoors by most, outdoors by few. A few people are frightened and run outdoors. Many sleeping people awake. Observers feel a strong shaking or rocking of the whole building, room or furniture.

b) Hanging objects swing considerably. China and glasses clatter together. Small, top-heavy and/or precariously supported objects may be shifted or fall down. Doors and windows swing open or shut. In a few cases windowpanes break. Liquids oscillate and may spill from well-filled containers. Animals indoors may become uneasy.

c) Damage of grade 1 to a few buildings of vulnerability class A and B.

VI. Slightly damaging

a) Felt by most indoors and by many outdoors. A few persons lose their balance. Many people are frightened and run outdoors.

b) Small objects of ordinary stability may fall and furniture may be shifted. In few instances dishes and glassware may break. Farm animals (even outdoors) may be frightened.

c) Damage of grade 1 is sustained by many buildings of vulnerability class A and B; a few of class A and B suffer damage of grade 2; a few of class C suffer damage of grade 1.

VII. Damaging

a) Most people are frightened and try to run outdoors. Many find it difficult to stand, especially on upper floors.

b) Furniture is shifted and top-heavy furniture may be overturned. Objects fall from shelves in large numbers. Water splashes from containers, tanks and pools.

c) Many buildings of vulnerability class A suffer damage of grade 3; a few of grade 4. Many buildings of vulnerability class B suffer damage of grade 2; a few of grade 3. A few buildings of vulnerability class C sustain damage of grade 2. A few buildings of vulnerability class D sustain damage of grade 1.

VIII. Heavily damaging

a) Many people find it difficult to stand, even outdoors.

b) Furniture may be overturned. Objects like TV sets, typewriters etc. fall to the ground. Tombstones may occasionally be displaced, twisted or overturned. Waves may be seen on very soft ground.

c) Many buildings of vulnerability class A suffer damage of grade 4; a few of grade 5. Many buildings of vulnerability class B suffer damage of grade 3; a few of grade 4. Many buildings of vulnerability class C suffer damage of grade 2; a few of grade 3. A few buildings of vulnerability class D sustain damage of grade 2.

IX. Destructive

a) General panic. People may be forcibly thrown to the ground.

b) Many monuments and columns fall or are twisted. Waves are seen on soft ground.

c) Many buildings of vulnerability class A sustain damage of grade 5. Many buildings of vulnerability class B suffer damage of grade 4; a few of grade 5. Many buildings of vulnerability class C suffer damage of grade 3; a few of grade 4. Many buildings of vulnerability class D suffer damage of grade 2; a few of grade 3. A few buildings of vulnerability class E sustain damage of grade 2.

X. Very destructive

c) Most buildings of vulnerability class A sustain damage of grade 5. Many buildings of vulnerability class B sustain damage of grade 5. Many buildings of vulnerability class C suffer damage of grade 4; a few of grade 5. Many buildings of vulnerability class D suffer damage of grade 3; a few of grade 4. Many buildings of vulnerability class E suffer damage of grade 2; a few of grade 3. A few buildings of vulnerability class F sustain damage of grade 2.

XI. Devastating

c) Most buildings of vulnerability class B sustain damage of grade 5. Most buildings of vulnerability class C suffer damage of grade 4; many of grade 5. Many buildings of vulnerability class D suffer damage of grade 4; a few of grade 5. Many buildings of vulnerability class E suffer damage of grade 3; a few of grade 4. Many buildings of vulnerability class F suffer damage of grade 2; a few of grade 3.

XII. Completely devastating

c) All buildings of vulnerability class A, B and practically all of vulnerability class C are destroyed. Most buildings of vulnerability class D, E and F are destroyed. The earthquake effects have reached the maximum conceivable effects.

3. HOUSING IN BANGLADESH

The census of houses (Census, 1991), gives details of houses based on materials of construction for walls and roofs. Table 12 summarized the building types in different category based on Census (1991). This grouping for the whole Bangladesh can be identified by collecting the whole district wise census report of Bangladesh. The census reports generally show the Dwelling Households by Material of Wall and Material of Roof of the Main Structure. The wall and roof combinations are categorized as sloping (Straw/Bamboo/Polythene, Tiles/C.I/Metal Sheet) and Flat (Cement). The vulnerability of different categories of houses can be described according to the intensity scales described in this paper.

Table 12: Category of Housing in Bangladesh

Category A	A1.	Mud wall with all roofs sloping.
	A2.	Unburnt Brick wall with all roofs sloping.
Category B	B1	Burnt Brick wall with sloping roof

	B1	Burnt Brick wall with flat roof
Category C	C1.(a)	Cement Wall with sloping roof
	C1.(b)	Cement Wall with flat roof
	C2.	Wood wall with all roof sloping
Category X	X1.	C.I/Metal Sheet with all roofs sloping
	X2.	Straw/Bamboo with all roofs sloping

4. CONCLUSIONS

This paper is an observation of damage levels in Bangladesh due to multi hazard (e.g. Earthquake, Tornado, Cyclone, Flood). An attempt was made to provide individual intensity scale for different disaster, which occur in Bangladesh. Proper identification of a disaster by intensity scale can provides a more complete understanding of the dangers, thereby easing the initiation of long-term measures within the context of overall development plans for a region.

ACKNOWLEDGEMENT

The authors are grateful to Mr. Sujit Kumar Debsarma, Assistant Director, Bangladesh Metrological Department who helped in analyzing the data.

REFERENCES

- BMTPC, 1997. *Vulnerability Atlas of India 1997*, Building Materials and Technology Promotion Council, Ministry of Urban Development, Government of India, New Delhi.
- BBS, 1991. *Bangladesh Population Census 1991*, December, 1992, Statistics Division, Ministry of Planning, GOB.
- CHCDA, 2005. *Multi Hazard Mitigation Plan*, Country of Hawaii Civil Defense Agency, Country of Hawaii.
- Debsarma, 1995. *Storm Track Prediction (STP) Model*, Storm Warning Centre, Bangladesh Meteorological Department Agargaon, Dhaka-1207.
- ESC, 1998. *European Macroseismic Scale 1998*, European Seismological Commission.
- FEMA, 1997. *Fujita-Pearson Tornado Scale*.
- FAP 25,1994. *FPCO: Flood Modelling and Management*, Final Report, GoB.
- LGEb, 1991. *Cyclone damage-1991*, Damage Assessment of General Infrastructure, Local Government Engineering Bureau, Final Report, Volume 4, The world Bank, GoB.

SOME EMERGING HAZARDS IN METROPOLITAN CITIES OF BANGLADESH

K.M. MANIRUZZAMAN

Professor, Department Of Urban And Regional Planning, BUET
mzaman@urp.buet.ac.bd

MOHAMMAD AMINUR RAHMAN

Teaching Assistant, Postgraduate Programs In Disaster Management,
BRAC University

1. INTRODUCTION

Bangladesh has experienced more than its fair share of natural or human-induced disasters. Floods, oceanic surges, storms have repeatedly ravaged the country, and the people remain braced to face the next onslaught. But when landslides triggered by incessant rain over a period of nearly six hours killed more than 120 people in the port city of Chittagong on 6 June 2007, most Bangladeshis were left awestruck. Bangladeshis are not familiar with landslides, especially those that are serious enough to threaten human lives. In a way, the rude awakening early that morning served as an omen of more surprises that may lie in store in the form of unexpected hazards as rapid urban growth and development test the limits of tolerance of nature and introduce changes into the physical, social and economic landscape.

Changes brought about by the urbanization process are bound to introduce new hazards and vulnerabilities. Urban areas have been called 'crucibles of hazards' (Mitchell, 1999a). As Bangladesh attains a more urbanized character, it is important to assess what other forms of hazards may strike in future, and take necessary precautions accordingly.

Some of the possible emerging hazards are hydro-meteorological in nature but brought about as a result of human interventions in nature. Others are the effects of scarcity of resources and services to meet the demands of the burgeoning urban population. Some potential new hazards arise out of the economic activities concentrated in or around urban areas. Yet others are a result of the increased global connectivity of the metropolitan cities.

2. URBANIZATION IN BANGLADESH

Urbanization in Bangladesh is going on at a very high pace, driven mainly by migrants from rural areas. In 1991, around a fifth of the population lived in urban areas. The share rose to a fourth in 2001 (BBS, 2001). Most of this growth of urban population is absorbed by the capital followed at a distance by Chittagong. Dhaka is experiencing a growth rate between 3 and 4 percent

per annum. Around a tenth of the total population of Bangladesh and almost 40 percent of its urban population reside in Dhaka City. The frenzy of growth and the tremendous pressure it puts on land in these two cities have led to sound practices of planning and construction being flouted and ignored. Resource-strapped city authorities are hard pressed trying to match supply of services with rapidly expanding demand. One of the key consequences of these is the rising threat of hazards that did not exist or were infrequent so far.

3. URBAN FLOODING

The tragedy at Chittagong was a result of indiscriminate cutting of hills by influential and unscrupulous businessmen, to make room for 'development' and to sell the soil removed from the hills, leaving portions of the hill surface devoid of vegetation, often at a precariously steep slope. Under the circumstances, landslides were inevitable. The destruction of hills also clogs up the drainage channels with soil eroded from the hills raising the hazard of urban flooding.

In Dhaka, where there are no hills, the pressure on limited buildable land has resulted in the filling up of wetlands at the fringes and encroachment of waterways. Increased runoff and obstructed drainage channels have exacerbated urban flooding. A few hours' of rain, a common phenomenon in the monsoon season, now inundate large tracts of the city.

4. BUILDING COLLAPSES

The rapid growth of urban economy and population has also resulted in a rising tendency of shoddy construction. A large number of buildings in the cities are not designed or constructed by qualified professionals. High prices of imported construction material motivate people to compromise with quality. Even in buildings erected by corporate bodies who employ professionals, corners are cut in the haste to maximize returns at the cost of structural quality. A number of buildings in Dhaka have collapsed under their own weights in the recent past. The Spectrum Garment building collapse of April 2005 claiming 76 lives, and the Phoenix Garments building collapse of February 2006 killing 22 persons are cases in point. These incidents are stark warnings of what may happen when extreme natural forces inevitably act simultaneously on the urban structures at some point in future.

5. SCARCITY OF WATER

Another form of looming disaster that can be seen on the horizon is the scarcity of water, especially but not exclusively in Dhaka. The Dhaka Water and Sewerage Authority (WASA) is unable to meet the current demand of water and the daily shortfall in supply is around 800 million liters and

increasing. Around 80 percent of the supply is extracted from underground with deep tube wells. The rest comes from the rivers. Environmentalists have been warning against excessive extraction of subsurface water, but the water in the rivers around the city has become polluted beyond treatment in a viable manner. The sources of pollution are untreated sewerage, industrial effluent and spills from marine vessels. Even the subsurface water is now reportedly under threat of contamination from the surface. These are very disturbing signs of an impending water crisis that would have far-reaching and disastrous consequences.

6. TOXIC SPILLS AND EXPLOSIONS

As industrialization takes place in Bangladesh, many of the hazards that the industrial world has faced already are gradually beginning to appear in this country. However, the safeguards against such hazards are not in place, so even at a lower stage of industrialization, the vulnerability is still high. Because of inadequate legal framework and lax supervision, the facilities and process of storing and transporting hazardous material used in industry are less than satisfactory and may lead to disastrous leaks, spills or explosions. Ship breaking yards in Chittagong where scrapped ocean liners, often allegedly containing toxic material, are torn down in primitive fashion without safety precautions posing a constant threat of explosions and toxic contamination.

7. EPIDEMICS

Cities with crowded living conditions and inadequate urban services have been breeding grounds of epidemics throughout history. The bigger cities in Bangladesh fulfill both criteria and are susceptible to outbreaks of diseases spread by water or pests, such as dengue fever, malaria, diarrhea etc. A potentially more serious threat is the outbreak of newer diseases such as Severe Acute Respiratory Syndrome (SARS) or Avian Flu. New diseases may originate in one corner of the globe, but spread very quickly. As the globalizing economy knits countries closer together, increased and more frequent international travel makes it easier for such diseases to spread across national boundaries to far corners away from the site of origin very quickly. For example, a person travelling in China transported SARS to Canada in less than 24 hours (Quarantelli, 2006). The spread of SARS stopped in 2003 and Avian Flu has not attained serious proportions. But there is every possibility that a future disease may be more virulent and lethal. Cities are gateways of international travel and therefore more susceptible to diseases originating in a different region. The most important international airports in Bangladesh are located in Dhaka and Chittagong and the latter is the main seaport of the country. So these cities are the points through which such diseases may make an entry into the country.

8. THE WAY FORWARD

In the face of the situation described above, what measures are being taken and what further measures can be adopted? Bangladesh has a reasonably good body of laws and regulations for protecting the environment. The laws prohibit the cutting of hills and filling of water bodies. Much of the weaknesses in the legal framework for regulating construction have also been removed with the adoption of the Bangladesh National Building Code (BNBC) and the Building Construction Rules (BCR) for Dhaka Metropolitan City. BNBC was formulated in 1993, but the official gazette notification making it mandatory to follow the code was published in November 2006. The Code has extensive provisions to ensure safety against wind, fire and seismic hazards. The rudimentary Building Construction Rules of 1996 was totally revamped for Dhaka City in April 2006. This set of rules incorporates a system of holding responsible designated technical personnel for each phase of design, construction and occupation. The rules not only attempt to assure quality construction, but also ensure that a higher portion of lots is left without construction to reduce runoff and increase recharging of underground water. Similar rules are now being prepared for Chittagong City.

Dhaka Metropolitan Development Plan (1995-2015) has strict directives against building construction in areas delineated as flood flow zones and sub-flood flow zones (RAJUK, 1995). Dhaka WASA has been conducting periodic drives to rid the canals in the city of illegal encroachment. Projects to improve storm water drainage are being implemented. NGOs like the Bangladesh Environmental Lawyers' Association are taking to court organizations that defy the ban on filling up water bodies. This has acted as a deterrent and several 'land development' projects remain suspended. Tanneries in Dhaka, a major source of river pollution, are being rehabilitated at a site away from the city where effluent treatment plants will also be installed.

While Bangladesh has no dearth of legal tools to promote a safe environment, the problem has been with enforcement. Apart from institutional issues such as poor resources, manpower and capacity, endemic corruption has been a hurdle to enforcement of laws. Storage and transportation of hazardous material is one area where laws may be revised and updated. This is an issue that is becoming a matter of serious concern as the country continues on its path to industrialization.

9. CONCLUSION

Bangladesh has earned international acclaim for different aspects of disaster management. However the experience and expertise of Bangladesh lies mainly in dealing with hazards in rural areas. The need to improve preparedness and capacity to meet growing and emerging hazards in urban areas cannot be overemphasized.

Further research is required to assess the degree to which cities can be affected by various types of unprecedented risks such as those associated with climate change, new industrial chemicals or hybrid hazards that combine natural, technological and social risks (Mitchell, 1999b).

REFERENCES

- BBS (2001) Bangladesh Population Census 2001: Preliminary Report, Bangladesh Bureau of Statistics, Dhaka.
- Mitchell, J.K. (1999a) (ed.) *Crucibles of Hazards: Megacities and Disasters in Transition*, United Nations University Press, Tokyo.
- Mitchell, J.K. (1999b) "Megacities and natural disasters: a comparative analysis", *GeoJournal*, vol. 49, pp. 137-142.
- Quarantelli, E.L. (2006) "The Disasters of the 21st Century: A Mixture of New, Old, and Mixed Types", Preliminary Paper #353, Disaster Research Center, University of Delaware.
- RAJUK (1995) Dhaka Metropolitan Area Development Plan (DMDP), Rajdhani Unnayan Karttripakkha, Dhaka.

EARTHQUAKE PREPAREDNESS COMBATS URBAN DISASTERS

WAHIDA BASHAR AHMED
ActionAid Bangladesh
wahida.ahmed@actionaid.org

ABSTRACT

ActionAid, an international non-government organization working in Bangladesh in various development activities as a development partner of the government. ActionAid is doing earthquake preparedness activities in the vulnerable earthquake zone in Bangladesh since the Borkol Earthquake of 2003. As a part of these, ActionAid developed 250 community volunteers to work with community in case of earthquake or other natural disasters. This group received several skill development training as such first aid and search and rescue. This paper will state the effectiveness of their skills, which already applied to the vulnerable community in need.

Chittagong, the second largest metropolitan city in Bangladesh was having heavy rainfall from the early monsoon this year. The hilly city experienced highest rainfall on 11 June and this made several sudden landslides in the city. One of the big ones happened in Kusumbag area where 11 houses were collapsed. ActionAid's developed community volunteers rushed to the spot quickly and started rescuing people. They reached there before the government's search and rescue team reached. The paper will show and analyze the effectiveness of developing community volunteers and their interaction with community in need.

ActionAid developed 200 community volunteers from 6 vulnerable wards of Chittagong City Corporation with aim to work with the community in case of earthquake disasters. They have been provided complete training on earthquake preparedness, participatory vulnerability analysis, first aid and search and rescue.

The community as well as ActionAid found the volunteers proactive just after two disasters, one was fire in slum and another one was landslides in city. The paper will check the preparedness level of the volunteers, their acceptance level to the community, their response initiative and the possibility to work with their community in case of earthquakes and so forth.

1. INTRODUCTION

ActionAid is working in the field of disaster management in Bangladesh for the last two decades. Both preparedness and response were included in ActionAid's intervention. After the Borkol Earthquake of 2003, ActionAid started preparedness work on earthquake in Chittagong City area, which was amongst the second level of vulnerable earthquake zone in the country. One

of the most important components of earthquake preparedness program was developing community volunteers who can work for community in need of disaster and emergency intervention. The following section will illustrate the development of community volunteers, their preparedness for earthquake; and how they intervene in other natural disasters for their community.

2. DEVELOPING COMMUNITY VOLUNTEERS

Primarily 23 vulnerable wards in the city corporation of Chittagong were selected to carry on earthquake preparedness work. Among them, six wards were identified as most vulnerable. Community volunteers were selected from these six wards. Initial criteria for volunteer selection were that the volunteer should come up from that particular community. They should possess strong sense of community and should have acceptance within the community. Total twenty groups of volunteers, each group comprised 10 volunteers, were selected. The selected volunteers have been provided following trainings and orientations to make up their skills, upgrade their attitude, sensitize on earthquake preparedness.

2.1 Foundation Training on Earthquake Preparedness

This was a comprehensive training specially designed for the volunteers to orient them on basic factors of earthquake and earthquake preparedness. They were also interacted on community responsibility, volunteerism, roles and responsibilities of community volunteers. They were oriented on damage and needs assessment and immediate reporting. Though the training objective was to orient community volunteers on earthquake preparedness, it covered several other natural or man made disasters that can hamper normal livelihood of community.

2.2 Training on Participatory Vulnerability Analysis

This was a field-based training with practical demonstration on identifying community's vulnerability. At one stage, community's recommendation is checked to overcome the possible hazard. By this exercise, volunteers demonstrated their ability to analyze community's possible threat to natural disaster or physical vulnerability to a particular disaster. They also learned the technique of bringing recommendations of community to the concerned public representatives or local administrations.

2.3 Training on First Aid

In the process of skill development of the volunteers, training on First Aid was organized. The training covered primarily the casualty situation that can be arising after earthquake or other natural disasters. Volunteers acquainted with the skills of safely shifting of disasters victims to nearby health care centers. They also learned the coordination techniques that can be used in disaster situations.

2.4 Training on Search and Rescue

This was the most important training directly related to volunteer's skill development in earthquake response. The training was designed specially to meet volunteer's need after earthquake situation. In this practical training, volunteers demonstrated skill of rescuing victims from high-rise infrastructure without any heavy equipment.

3. VOLUNTEER PARTICIPATION IN RESPONSE ACTIVITIES

Since there had been no big or devastating earthquake in Chittagong or outside Chittagong for the last couple of years, volunteers could not demonstrate their skills in earthquake situation. However, they demonstrate in other disaster as they took part in some disaster emergency search and rescue or intervention activities initiated by themselves or ActionAid or other actors inside or outside Chittagong. The following two are worth mentioning.

3.1 Fire Response

Fire became a sudden urban disaster that happened in various parts of Chittagong for the last couple of years. The following two cases are worth to mention here as community volunteers actively participated in the search and rescue and demonstrated their ability.

Fire Response in KTS Garments: On the evening of 23 February, 2006 KTS Garments Factory in Chittagong City got fire accident. It was a big one killing 67 and injured 109. Community volunteers rushed the spot immediately but at first they were forbidden to get entered for any search and rescue work. Next morning they opened an information center on the spot. They were collecting and providing information of the distressed to their family members. They Deputy Commissioner of Chittagong appreciated their effort and permit them to get inside the spot to take part in search activity with the government team. They made a quick assessment and opened some mobile medical camp with support of the local medical college. They were able to make coordination with local government and other responding agencies. They conducted final assessment and took part in response activities.

Fire Response in Boubazar Slums: Boubazar is a big slum in Bakolia area in Chittagong City Corporation. A devastating fire broke out here at the early morning of 6 March, 2007. It killed 21 and injured 40 others. Community volunteers quickly rushed the spot and started rescuing people. They brought injured people to Chittagong Medical College Hospital for treatment. They established coordination with the district administration and with all agencies who initiated response activities. They provide constant care to the hospitalized victims. They conducted initial damage and needs assessment survey and informed the concerned agencies for necessary action. On the following day, they conducted detail assessment and

requested for essential relief package distribution. With their active and enthusiastic participation, ActionAid did a huge relief package distribution to the affected victims. They were well taken by the community and administration as well. Their fruitful movement acquainted them within their community and external stakeholders as well.

3.2 Landslide Response

Chittagong was having heavy rainfall for the early monsoon on 11 June 2007. Most of the part of the city gone under knee to throat height water in the early morning. The incessant rainfall caused several sudden landslides in the city. ActionAid's developed community volunteers quickly rushed to some spots and started search and rescuing victims. One of their responses in landslide disaster became widespread as they could rush the spot before the government rescue team arrived. In fact, they were on the spot named Kkusumbag before the landslide happened. ActionAid got the first message from its community volunteer in Kusumbag area while they were in action. The reporter volunteer said,

“We five volunteers were helping the waterlogged people in Kusumbag area from the morning to leave their houses as most of them were drowning by heavy rainwater. We started to work from the early morning as our residences were also in the same area. We learned from ActionAid's training that heavy rainfall may cause landslide in Chittagong. Intact, we were motivating people to evacuate their houses as the heavy rainfall was not stopping and landslide may occur in any time. At about quarter to ten in the morning, we heard a big bang followed by a hue and cry. A landslide happened just on the slopping of the hill. We five quickly rushed near the collapsed houses. Oh, the collapsed houses lost their sign of house, all were mud and mud. People were quite at a loss. We started pulling out the derbies with our hands. We asked the gathered people to help us. Just at this moment, I made a phone call my supervisee organization to inform about the disaster and they reported ActionAid at the same time. It was good that we first started work to search and rescue the victims and then informed our authorities. We could inform them within 20 minutes after the landslide happened.”

When the government's fire brigade rescue worker came, the community volunteers worked with them. They worked like a big team.

4. ACCEPTANCE AND POSSIBILITY

Community volunteers made quick response to the mentioned urban disasters. Though the primary objective of their development was that they

would respond in earthquake disasters, but they proved their ability to respond in any other disaster with the same skill they gained from several training and orientation done by AcitonAid. They made their access within their community. They were accepted by concerned stakeholders. Local government also accepted their existence and appreciated their team work with government rescue workers.

It is evident that community volunteers got skill to respond any sudden disaster in their community. They took part in some other response operation in some other parts of the country, outside their city. They are confident about their capacity and ready to work with less supervision or without supervision in any onset of disasters. So earthquake preparedness is ready to combat with other urban disasters.

5. CONCLUSIONS

ActionAid developed the community volunteers to work with their own community. They were supported to increase their disaster knowledge and improve their capacity and skills to work in earthquake disasters. But it was an added advantage that volunteers were demonstrating in other disaster response within their same capacity. They are owned by their community. They are ready to dedicate their service for their community.

REFERENCES

Several project papers and documents of ActionAid were used as reference.

EARTHQUAKE PREPAREDNESS COMBINED WITH COMMUNITY EFFORTS

MD. FAIZ SHAH
ActionAid Bangladesh
mdfaizshah@yahoo.com

ABSTRACT

ActionAid is doing earthquake preparedness activities in the vulnerable earthquake zone in Bangladesh since the Borkol Earthquake of 2003. ActionAid initiated earthquake preparedness activities in Chittagong, geologically which is situated in the second most vulnerable zone of country. Both institutional and community based preparedness programs were conducted. Institutional based programs comprised: (a) School based programs, (b) Hospital based programs, (c) Garments based programs and (d) Local Government Institution (Ward) based programs. All these programs conducted orientation on earthquake and earthquake preparedness, simulation exercise, sensitization of schoolchildren through puppet show and development of contingency plan. As a result, all these level of beneficiary got their disaster action plan at hand now with the knowledge of preparedness.

Community based activities covered (a) Community sensitization on earthquake through street drama performance, (b) Lokokendra member's orientation on earthquake and other natural disaster preparedness, and doing Participatory Vulnerability Analysis (PVA) exercise to identify the local risks. This community came up with specific recommendation to reduce their vulnerability and they submitted to local government.

ActionAid developed 250 community volunteers to work with community in case of earthquake or other natural disasters. This group received several skill development training such as first aid and search and rescue. This paper reviews the effectiveness of their skills, which can be applicable to the vulnerable community in need.

Finally the paper presents the most important development of ActionAid's preparedness i.e. the development of Earthquake Vulnerability Atlas (EVA). How the concerned stakeholders were sensitized and find the EVA a good preparedness tool – is analyzed.

1. INTRODUCTION

ActionAid Bangladesh has been working in the disaster management sector for more than two decades. During this time, AAB has gained a wealth of experience in the major challenges and crisis prevailing in the sector in Bangladesh. Disaster is now one of AAB's key areas of focus with a clear link to ActionAid international strategy and disaster policy.

2. EARTHQUAKE PREPAREDNESS ACTIVITIES

Earthquake is a new phenomenon in the field of disaster in Bangladesh. The country uses to have small to moderate earthquake every month. Especially people in the southeastern hilly area and adjacent town like Chittagong, felt the jolt almost everyday. The Borkol earthquake in 2003 was big enough to alert people of the area that they should think about the early preparedness. Geologically Bangladesh government identified this part of the country as second most earthquake vulnerable zone. Amongst the towns in the region, Chittagong is the most densely populated, where urbanization is rapid, and land use pattern is diversified. A sudden big earthquake can toll a higher casualty in Chittagong. ActionAid initiated earthquake preparedness activities here to sensitize the community, to build their capacity, and to strengthening institutional capacities.

2.1 Institutional Based Programs

Institutional based programs covered several institutions' preparedness activities. For example, Schools, Hospitals, Garments factories and Ward office of local government was the primary stakeholders under this program.

2.1.1 School Based Programs

Schools are such educational institutions where on an average 200-1500 people stay during the daytime. The objective of school-based program was to sensitize the students, teachers and local community on earthquake and earthquake preparedness, enhance their capacity on evacuation, search and rescue and first aid. First, sensitization session on earthquake and earthquake preparedness was done for all teachers of a school including members of school management committees and selected students. Secondly, evacuation drill was exercised with the participation of all students and teachers. By this exercise school recorded the average evacuation time, identified and marked the safety places for evacuation, demonstrated how to conduct search and how to rescue victims safely after a devastating earthquake hits. After doing this program, every school identified the need for a guided plan or preparedness plan, which may lead them to work effectively for preparedness. They formed school disaster management committees with teachers and members from school management committees, guardians and local community. In some participatory sessions, schools developed their emergency preparedness plan or contingency plan for earthquake preparedness and real time evacuation. ActionAid worked with 12 Schools in Chittagong City including government, private and City Corporation owned. To sensitize the small children on earthquake in an easy way, puppet shows were performed in every school. Being sensitized most of the small children conveyed the earthquake message to their family members and local friends.

2.1.2 Hospital Based Programs

Hospitals are also big public gathering places where 200-500 people stay round the clock and another 500-1000 people gather in the daytime. A sudden earthquake can collapse the hospital system. Hospital itself may be vulnerable. Generally, after a big earthquake, mass casualty situation may arise and people will rush to nearby hospitals. Therefore, hospitals need to be prepared to handle mass casualty situation. Under this program, five hospitals were covered. Sensitization orientation session on earthquake and earthquake preparedness was conducted, hospital disaster management committees were formed, conducted training on mass casualty management, performed simulation exercise on evacuation and mass casualty management, search and rescue and first aid. Triage system was also introduced to the doctors. Hospitals also developed their own contingency plans to prepare and work effectively for preparedness and handle mass casualty situation. Doctors and medical employees of ten health care centers of City Corporation were given sensitization orientation on mass casualty management.

2.1.3 Garments Factory Based Programs

Garments Factories are gathering places of workers who are contributing to the economic development of the country like Bangladesh. Normally factory buildings were not constructed for this type of heavy use. Earthquake shaking can collapse the infrastructure and cause casualty situation, damage and fire. Real time evacuation was the objective of garments based preparedness program. A sensitization session was done at the beginning stating the necessity of such program for garments. Workers took part in safety evacuation and marked the possible gathering places. A disaster management committee was also formed and they developed their preparedness plan or contingency plan.

2.1.4 Ward Based Programs

Ward Offices headed by Ward Commissioners are the lowest tier of City Corporations in metropolitan cities like Chittagong. They have important role in disaster assessment and effective response with decision-making. They are supposed to form disaster management committees to perform their disaster activities effectively. This program supported them to form a balanced disaster management committee, orient the committee and help them to exercise coordination in pre and post disaster situation. ActionAid worked in 23 vulnerable wards in Chittagong City. Among them, most six vulnerable wards were covered by ward-based interventions.

2.2 Community Based Programs

Community based programs mainly focused the low-income urban community in the city corporation area of Chittagong. The selected 23 vulnerable wards of Chittagong City Corporation were densely populated with old houses and infrastructures. People were not aware about their

vulnerability in terms of possible casualty, obstacle for search and rescue work, using open spaces for evacuation and managing fire outbreak.

2.2.1 Community Sensitization

To sensitize this community on earthquake, several street dramas have been performed. The performance made a direct interaction with community people so that they can be sensitized individually on earthquake issues.

2.2.2 Community Sensitization through CBO

Several grouped community people were also covered by the program. People in a vulnerable place formed local CBO named Lokokendara. They have been introduced disaster issues and their vulnerability. They performed participatory vulnerability analysis and came up with specific recommendations. They submitted the result and recommendations to the concerned local ward commissioner for taking necessary steps for safeguard.

3. EARTHQUAKE VULNERABILITY ATLAS (EVA)

One of the most important outcomes of ActionAid's earthquake preparedness activities in Chittagong was developing Earthquake Vulnerability Atlas (EVA) for pre selected 23 vulnerable wards. The EVA was developed by considering the vulnerability by geographic data for example, pattern of land use, infrastructure, population and density, road links etc. The EVA identified vulnerable structures that may be a threat in increasing casualty, marked the narrow streets that may obstacle vehicle movement, found possible landslide locations that may add newer casualty and showed existing open spaces that can be used for evacuation places. The EVA was validated in sessions with concerned Ward offices particularly with the members of ward disaster management committees. Finally it was handed over to ward offices, Chittagong City Corporation and Chittagong Development Authority. These organizations can further develop and improve the atlas and use it as a reference.

4. COMMUNITY VOLUNTEERS

As community can identify their own vulnerability, they can also come in great help in times of disaster. It is evident in every disaster that community offers their first help in real time of need for search and rescue and evacuation work. External support takes time to reach grass root community. If the community knows their possible vulnerability, they can take possible preparedness measures. So a community can be better prepared if they have usable resource in disaster like work force like volunteers. Under the program, ActionAid supported in vulnerable 23 wards to develop a group of young, energetic community volunteers. ActionAid developed total 250 community volunteers most of whom are students. They were given sensitization orientation on earthquake and earthquake preparedness.

Community volunteers also conducted participatory vulnerability analysis involving their neighbors and community. They have been provided skill development training as such training on first aid and search and rescue. They were also provided material for first aid and search and rescue. The volunteers have proven their ability and demonstrated their skills to community. Thus, they have made acceptability within their own community and community possesses the feeling of ownership.

5. LOGICAL ANALYSIS

ActionAid had done preparedness programs for vulnerable institutions and concerned communities. ActionAid's role was like facilitator, identified the need of the community, involve community participation in searching results, making preparedness plan and recommendations. Institutions came up with their own remedy for possible hazards. They are practicing what they evolved. So institutions developed their preparedness. Community related to each institution became the part of the whole effort. For example, school's preparedness efforts are supported by the members of school management committees, guardians and students. Hospitals and garments are also taking local community's support in their preparedness activities. Moreover, community volunteers made a tremendous access to their own community and to these institutions. They are taking part in every institutional preparedness practices. So they are mainly maintaining the bridge between community efforts and institutional initiatives.

6. CONCLUSIONS

ActionAid supported earthquake preparedness activities made a scope for community's participation. Institutions combining related community's presence in regular practices. Community volunteers are combining community with institutions. ActionAid believes if the practices can be maintained and mainstreamed, it will combine community efforts in disaster management.

REFERENCES

Several project papers and documents of ActionAid were used as reference.

SOCIO-ECONOMIC AND ENVIRONMENTAL ASPECTS OF DISASTER RISK REDUCTION MANAGEMENT FOR SUSTAINABLE DEVELOPMENT IN BANGLADESH

MURSHED AHMED
Director (Economics)
Bangladesh Water Development Board, Bangladesh
mahmed_3ch@yahoo.com

ABSTRACT

The main theme of the paper is to provide guidelines for developing a comprehensive approach and appropriate methodology for the mitigation of disasters and the promotion of sustainable development. It aims at designing strategies and plans for mitigating the impact of disaster on social and economic development. Due to the increase of development works, population, rapid urbanization and industrialization with low economic growth the risk and vulnerability of natural disasters is growing in the Asia Pacific region. The main focus of this paper is on identifying and exploring the guiding principles for overcoming the affects of flood disaster and alleviation of their impact for sustained development of Bangladesh. The major challenges are to overcome the urban flood and cyclone hazards by building sustainable communities to live with risk. Historical time series data and records of information provide a wide variety of premises to handle the disaster issue but they are hardly amenable to realistic solutions to the disaster problem nor the flood-prone areas can be changed into flood or disaster free areas in a cost-effective way. Keeping these natural forces in perspective, a long-term disaster mitigation strategy has been tried to be evolved on the basis of sound principles. Effective disaster risk management must take into account not only technical and economic but also social, administrative, environmental, political and legal framework. The paper argues for a more holistic model within a risk management context to address issues of vulnerability. Any solution to be permanent and sustainable for disaster risk management calls for broad political and social consensus enhancing national, regional and international cooperation.

1. BACKGROUND AND RATIONALE

Management of disaster is an emerging need and growing concern of Asian region. The major development challenge in the 21st century is how to ensure effective disaster management. Disaster can be sudden or slow in onset. Sudden onset of disasters like flood, cyclone and storm-surge, drought, river bank erosion and earth quake destroy the country's infrastructures, commercial and industrial activities and environment.

Views expressed herein are exclusively author's own and do not in anyway reflect those of BWDB

Historical statistics suggest that Bangladesh is one of the most disaster prone country in the world with negative consequences of devastating floods, cyclone induced storm surge flooding, river bank erosion, drought, earthquake, groundwater mining, arsenic contamination, chemical pollutants, urban pollution, fire and technological accidents. Although there is limited resources for coping with such calamities, human societies have the capacity to recognize the risks that would lead to manage them with appropriate interventions. It is well recognized fact that it is possible to minimize the destructiveness through mitigation, preparedness, emergency response, rehabilitation and reconstruction.

The future population growth that is predicted in Bangladesh are destined to become more densely populated and thus more vulnerable to hazards. Land use in urban and semi-urban areas need to be planned carefully to minimize the risk due to hazards while maximizing economic development. Over exploitation of land combined with a lack of appropriate mitigation measures will increase the severity of flash floods and the vulnerability to drought (WWC, 2003).

Demand for food is increasing because of growing population. Total population of the country will increase from about 129 million to 181 million by 2025 and 224 million by 2050 (NWMP, 2002).

2. GEO-PHYSICAL SETTING

Bangladesh is located adjacent to seismic belt and one of the largest active delta of the world having a flat topography with very low elevations which is larger than 10 meters from mean sea level. Eighty percent of the country is deltaic floodplains which is criss-crossed by about 230 rivers including 57 transboundary rivers of which 54 is shared with India and three with Myanmar. The river system that flows through Bangladesh is the third largest source of freshwater discharge to the world's ocean. Catchments area of the three major rivers system of the Ganges-Brahmaputra-Meghna (GBM) region is about 1.72 million km², 93% of which lies outside the country. Bangladesh, being a lower riparian country, does not have any control on the flow of these rivers. In GBM region, particularly in Bangladesh, water is distributed unevenly in space and time due to unilateral withdrawal of water by India. This spatial and temporal variations in water distribution creates major concern in relation to water availability. The conditions and challenges of water management in Bangladesh are two folds; scarcity of water during dry season together with water quality deterioration, ground water depletion, salinity intrusion and environmental degradation and too much water during monsoon with devastating flood.

3. MAJOR CHALLENGES

- Lack of political will and political consensus.
- Non-compliance of the international conventions on water sharing
- Lack of legislative and administrative framework for resolution of conflicts
- Lack of conservation storage reservoirs in the Himalayas
- Upstream river basin development beyond the border of the country
- Inter-basin water transfer project/River-linking project of India

To overcome these problems Bangladesh has been persistently trying to negotiate with India since long. But as yet it has not been possible to reach a satisfactory level of solution to the problem (Ahmed, 2007). These challenges are posing threat for the sustainable management of water resources and Poverty Reduction Strategies (PRS). The water resources harnessing and development projects undertaken by the riparian countries could not resolve the problems. The structural measures in isolation done by the respective countries is not the ultimate solution for basin management of the common rivers. It will rather create a severe havoc until and unless the problems are not addressed considering the common interest of the co-riparian countries of the Asia-Pacific region.

The impact of climate change will be more vital to economy and society. The climate change will also affect flows in the transboundary rivers. The Himalayan zone is the climate regulator and also water head of the Indian subcontinent. The role of Himalayas is not only the source of all rivers, they are also the source of the ecological life of the whole region. The problems of water of the Himalayas watershed are a major engineering challenge which can be solved satisfactorily by applying the principles of Integrated Water Resources Management (IWRM). To address the challenges the co-riparian countries should make a paradigm shift and move towards IWRM approaches. The challenge therefore is to:

- Incorporate risk management principles in water resources management
- Prevent flood hazards turning into disasters
- Increase multidisciplinary approaches in flood management
- Improved information on integrated flood management approaches
- Alleviate poverty through preventive and response strategies for vulnerable sections
- Enhance community participation

Priority actions on the above issues are required for achieving the goal-1 of the Millennium Development Goals (MDGs). Implementing country level PRS will need coordinated regional approaches to attaining region's socio-economic challenges.

4. CAUSES OF FLOODING IN URBAN AREAS

Major cities, towns and civilizations are located in floodplains and have grown near to rivers and are vulnerable to flooding. Asian countries like Bangladesh, India, Thailand, China, North Korea, South Korea, Philippines, Malaysia and Indonesia has been inundated this year by unusually heavy and widespread floods. Each and every flood plain is a potential risk area and their intensive use for residential, commercial purposes has resulted in the expenditure of extremely large sums of money for flood protection measures in recent years. Despite the vast expenditures that have been made for flood control works, losses from floods are increasing every year. Due to increase in land price the low lands have been developed which greatly reduced storage facilities for floodwater. Similarly encroachments into drainage facilities increased flooding and water logging. Political leaders, Civil society, City administrators, bureaucrats are responsible for giving permission for land development in urban areas. Urban flood problem in context of Bangladesh can be identified as

- Unplanned housing defying the building codes
- Impeded drainage and water logging
- Over abstraction of ground water
- Reduced ground water recharge
- Ground water mining
- Land subsidence
- Population boom
- Rural to urban migration
- Siltation of rivers
- Free flow of water

The major flood disaster that occurred in Bangladesh are delineated below:

Table-1: Major Floods Affecting Bangladesh

Item	1988	1998	2004	2007
Inundated Area of Bangladesh (%)	60	68	38	30-42
People Affected (million)	45	31	36	14
Total Deaths (people)	2300	1100	750	1071
Livestock Killed (nos.)	172000	26564	8318	40700
Rice Production Losses (million tons)	1.65	2.06	1.00	1.00
Road Damaged (kilometers)	13000	15927	27970	31533
Number of Homes Fully/Partly Damaged (million)	7.20	0.98	4.00	1.10
Total Losses (Tk billion)	83	118	134	-

Source: Ministry of Fisheries and Livestock, ADB and World Bank estimate.

Different development partners provided their continued support services during all natural calamities in the past extraordinary flood and cyclone of 1987, 1988, 1991, 1998 and 2004. Flood damage rehabilitation currently constitutes about 80% of ADB's lending under its emergency assistance facility. ADB will adopt a pro-active approach to reduce the severe economic and social costs of natural disaster by promoting the use of combined structural and non-structural approaches to flood protection including flood-risk insurance (ADB, 2003). It is expected that development partners will further continue their positive cooperation and provide their support in post flood rehabilitation of 2007 for restoring the vital physical and economic activities of the country.

An outcome of the World Conference on Disaster Reduction held in Kobe, Japan in January 2005 was the 'Hyogo Framework for Action 2005-2015'. This Framework calls for all countries of the world including Bangladesh to commit: (DMB, 2005-06).

- To pursue an integrated multi hazard approach for sustainable development to reduce the incidence and intensity of disasters.
- To place disaster risk at the centre of political and economic priorities.
- To integrate disaster risk reduction in development planning.
- To invest substantively in disaster preparedness.
- To enable civil societies actors and affected communities to strengthen their resilience to disasters.

5. ISSUES TO BE CONSIDERED FOR COMPREHENSIVE PLAN FOR DISASTER RISK MANAGEMENT

- The objective of the plan based on the flood management strategy
- Legislative and legal requirements and constraints for the flood plan
- General framework of methodology for formulation of the flood plan including planning criteria
- (e.g. Cost Benefit Analysis, Multi-Criteria Analysis)
- Floodplain mapping to identify the physical location, extent and characteristics of the area
- General setting of the planning area as per NWMP
- Flood hazard mapping both at Macro and Micro levels to determine the severity,
 - frequency, duration and depth of flooding
- Flood risk information and mapping, charts, profiles and graphs
- Hydrological factors and Morphological Characteristics
- hydrological/Hydrometeorological data for the determination of flood frequencies, depth, duration, timing and rapidity
 - river water levels including mean & flood peaks
 - sediment load including bed materials & suspended materials
 - geo-morphological approach based on drainage basin
 - hydrological and hydraulic situation of the basin
- Comprehensive Flood plan and management aspects for flood loss reduction works and measures
- Structural measures:

- large-scale embankments on major rivers
- river training and bank protection
- urban flood protection and drainage
- coastal embankments
- dredging of major channels
- desilting of dead khals and rivers for improved drainage
- Non-structural measures
 - floodplain zoning to reduce flood damage risks
 - flood proofing measures
 - afforestation data required for effective retarding of floods.
 - monitoring system for the purposes of improved disaster warning systems and forecasting
 - better disaster preparedness
- Economic, social, institutional and environmental conditions on existing situations and projections for the future
- Assessment of structural and non structural measures
- Alternative solutions of structural and non structural measures
- Ranking of strategies.

6. INTEGRATED APPROACH TO DISASTER RISK MANAGEMENT

Bangladesh Water Development Board (BWDB) under the Ministry of Water Resources has the primary responsibility for formulating and executing the plan in flood-prone area. BWDB is responsible for water resources management with allied organizations like Water Resources Planning Organization (WARPO), River Research Institute (RRI) under the Ministry of Water Resources (MoWR). Institute of Water Modelling (IWM) and Centre for Environmental and Geographic Information Services (CEGIS) established by GoB provide technical support and environmental management respectively and functions under the aegis of MoWR. IWM has been carrying out modelling activities for improved irrigation management, flood management, flood forecasting, groundwater modelling, morphological assessment and prediction modelling etc. Technical monitoring of environmental parameters are being accomplished by BWDB, IWM, CEGIS. Bangladesh Meteorological Department (BMD), Space Research and Remote Sensing Organization (SPARRSO). Water resources modeling exercises will play vital role for prediction and optimization of trans-boundary water resources. Bangladesh being a disaster prone country, had to concentrate her efforts towards flood loss reduction measures by constructing flood embankment, river training and channel improvement and development of an effective Flood Forecasting and Warning System. The active means of flood management by storage reservoirs is not possible within her territory. Non-structural measures such as flood forecasting and warning is currently performed by the large scale infrastructure like Surface Water Hydrology under BWDB, BMD and SPARRSO.

There had been a renewed awakening nationally as well as internationally over floods and cyclones in Bangladesh and their solution. These recent catastrophic floods have caused a change the attitude of planners and decision makers and the Government of Bangladesh has emphasized that a comprehensive national flood protection programme needs large project aimed at controlling the high discharges that come from the upstream catchment. The strategy is, therefore:

- i) to accord the highest priority to the need for an integrated approach to flood management
- ii) to implement effective flood management programs with emphasis on comprehensive multi sector water development
- iii) to strengthen riparian cooperation leading to a long lasting solution

Disaster Risk management in Bangladesh calls for efforts based on regional (international cooperation) and national (domestic policy) approaches.

6.1 Regional approach (cooperation with upstream nations)

Projects based on international cooperation should be planned, designed and implemented in the following three stages :

Stage 1 : Collection of data from upstream areas to improve flood forecasting and warning systems

Stage 2 : Development of plans to establish an effective flood prevention capability by linking embankments with those in upstream areas. This plan would include an appropriate river training programme.

Stage 3 : Reduction of peak flood inflows under long-term perspective, through construction of dams in upstream areas, management of river basins and afforestation.

6.2 National approach (domestic measures)

Within Bangladesh project should be planned, designed and implemented in the following lines:

- Construction of embankments, implementation of river training, partial dredging of major rivers, removal of silt from minor rivers and distributaries, improvement of existing flood control and drainage facilities, construction of distributary channels or drainage canals, improvement of flood forecasting and warning systems, flood protection and drainage in Dhaka, alleviation of drainage problems caused by banking of roads and railways, controlled flooding of polders, construction of refugee areas, protection of residential areas outside of embankments, amendment of laws concerning irrigation and drainage, reinstatement of river morphology surveys, reestablishment of hydrology training institutes, afforestation, preparation of topographical maps. All these activities need be performed on sound participatory approach through mobilizing water sector institutions at the centres, middle and the peripheries
- Researchers have pointed out any steps to control flooding should emphasise both the structural and non-structural methods. Flood

management programmes will be effective only when the main feature of flood plains are considered. Effective flood management in Bangladesh calls for regional cooperation involving various development options.

Formulating solutions to flooding problems requires a comprehensive understanding of the geologic settings of the region and a better knowledge of hydrodynamic processes that are active in watersheds. Only solutions that take into account the underlying long-term factors contributing to flooding problems can prevail. Such contributing factors are as follows: unplanned urbanization, soil erosion, local relative sea-level rise, inadequate sediment accumulation, subsidence and compaction of sediments, riverbed aggradation, and deforestation. Structural solutions, such as the building of embankments along the rivers and polders in coastal regions in Bangladesh, will not solve the flooding problems but will result in many adverse environmental, hydrologic, economic, ecological, and geologic consequences. Solutions to flooding problems can be achieved by adopting and exercising watershed-scale best management practices that include : floodplain zoning, planned urbanization, restoration of abundant channels and lakes, dredging rivers and streams, increased elevation of roads and village platforms, efficient storm sewer systems, establishing buffer zones along rivers, conservation tillage, controlled runoff at construction sites, good governance, indigenous adjustment of life-style and crop patterns, and improvement on flood warning/preparedness systems.

The most cost effective and efficient way to disaster reduction and management is a co-ordinated approach to the appropriate combination of structural and non-structural measures. The optimum flood mitigation plan for any particular area of Bangladesh region should, therefore, contain several elements of structural and/or non-structural measures. Accordingly, integrated flood management aims to maximise the efficient use of flood plains while minimizing the loss of life from flooding and has five key elements;

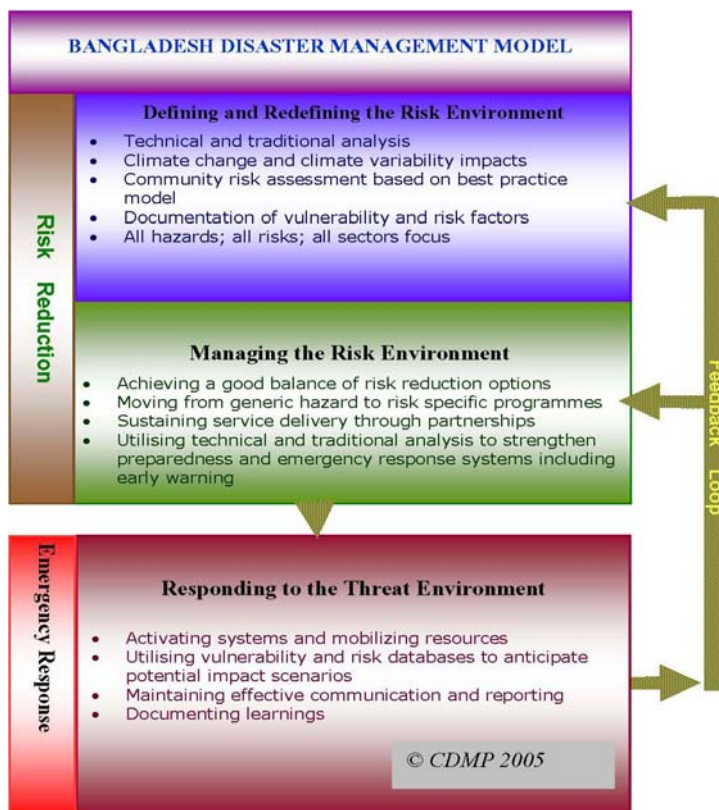
- Adopting a best mix of strategies both structural and non-structural;
- Managing the water cycle as a whole while considering all floods, including both extremes;
- Integrating land and water management, as both have impacts on flood magnitudes and flood risks;
- Adopting integrated hazard management approaches, taking into consideration the risks due to all related hazards such as land slides, mudflows, avalanches, storm surges and tsunamis;
- Ensuring a participatory approach to develop a sense of ownership and reduce vulnerability.

Suggested measures against water management issues and hazards on trans-boundary basins are delineated in Table-2.

Table-2: Development Opportunities and Potentials

Objectives	Diagnostic analysis	Solutions	IWRM through an Apex Body: River Basin Organization
Regional Economic growth and Development	<ul style="list-style-type: none"> ➤ Reduction of damages due to floods, storm surges etc. ➤ Reinforcement of flood plains management 	<ul style="list-style-type: none"> ➤ Flood management modeling ➤ Basin wide management ➤ River basin planning using mathematical modelling ➤ River basin management ➤ Hydro power development ➤ Flood forecasting & warning system 	
Health outcome and Human development	<ul style="list-style-type: none"> ➤ Safe drinking water ➤ Sanitation ➤ Drainage ➤ Cyclone /storm surges etc. 	<ul style="list-style-type: none"> ➤ Water quality monitoring ➤ Managing surface and ground water quality for mainstreaming the environment in the water sector ➤ Urban drainage management 	
Ensure environmental sustainability and bio diversity restoration and protection of eco-system	<ul style="list-style-type: none"> ➤ Improve water quality ➤ Strongly enforce existing legislation related to water ➤ Environmental impact assessment and social impact assessment ➤ Preservation of the aquatic Eco-system 	<ul style="list-style-type: none"> ➤ Balancing supply and future demand ➤ Water quality modeling ➤ Capacity building for integrated management ➤ Developing global partnerships & promoting regional co-operation 	

A disaster management model for Bangladesh and the way forward is shown in Figure-1.



Source: Ministry of Food and Disaster Management

Figure-1: A Holistic Disaster Management Model

Political Economy of Transboundary Water Management

GBM region have experienced long-standing historical disputes around politics of water planning for their common river basins. This has resulted in creating mistrust among the countries of the region. The co-basin states have tried to resolve the disputes but unfortunately because of regional and socio-political controversy these initiatives have largely failed. This failure prevented to capture the great opportunity of social and economic development of the region. It calls for political consensus of the riparian countries. South Asian Association for Regional Co-operation (SAARC) is one of the best forum which could solve the water dispute. But they did not heed to the riparian disputes and consequently the impasse persisted.

Freshwater quality and quantity issues are becoming serious and most critical challenges to the five basin countries. The major factors for freshwater conflicts are human activities like high population growth, agricultural development, rapid rates of industrialization, upstream diversions and abstractions (Figure 2). These factors are affecting water availability both quantitatively and qualitatively which ultimately leads to water dispute among the co-basin states. Human systems depend critically on the state of the environment. Climate change is expected to have a broad

and extensive impacts on the land water system in Bangladesh. The threat of climate changes will become the major regional environmental concern in water disputes in the coming years. There is already clear evidence of escalating conflicts in different parts of the world centered around water quantity and quality issues. While the water quantity crisis is well known in the GBM region freshwater quality will become the principal limiting factor for sustainable development. China for the first time publicly stated that water quality is now limiting economic development. (Stephen, T.T. 1999).

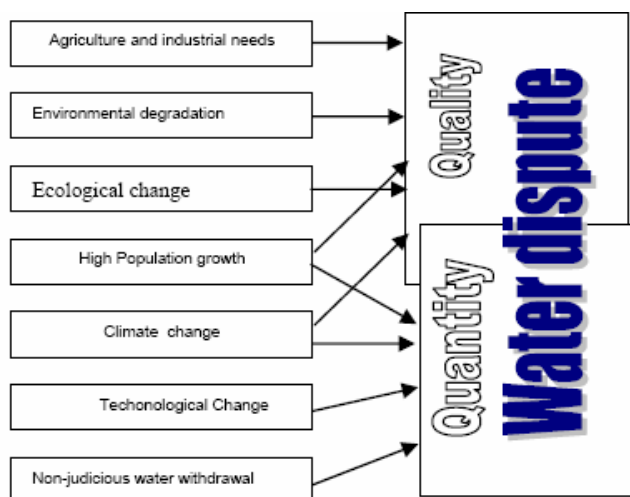


Figure 2: Factors of Freshwater Disputes

7. REGIONAL COOPERATION

Regional cooperation is an important driving force for solidarity in river basin management. One of the options is augmenting the Ganges flows through the construction of a reservoir on the Sunkosh River in Bhutan may be explored. Likewise, the proposed Sapta Kosi High Dam on the Kosi river (a tributary of the Ganges) in Nepal could bring significant benefits to India, Nepal, Bhutan and Bangladesh in terms of flow augmentation. Bangladesh can collaborate with Nepal and India for the construction of this dam for mutual benefits. Basin management in Nepal will conserve soil resources, mitigate flood and augment dry season flow for the areas in the downstream. On the other hand, from economic consideration, the development of the immense hydro-electric potential in Nepal will not only boost up the Nepali economy but can be a cheap source of energy for Bangladesh and India (Rahman, S.M.M et. al, 2003).

Establishing River Basin Organization (RBO) for such regional cooperation in water sector at the macro-level is more essential to make micro-level water resources management sustainable. Network of Asia River Basin Organizations (NARBO) expects to enhance capacity for IWRM, ensure sustainable use of water for effective implementation of IWRM and conflict resolution (4th WWF, 2006). For developing and promoting active collaboration SAARC can patronize the RBO as proposed to harness the potential of the water resources of the GBM region.

8. PRINCIPLES OF SHARED WATER RESOURCES MANAGEMENT

- Act locally but think globally putting people at the centre
- No harm principle: obligation not to cause significant harm (UN, 2005)
- Justice and Equity
- Free flow of data and information
- Notification concerning planned measures
- Political and public awareness.

The convention on the law of the Non-Navigational Uses of International Water courses provides the principles and rules to guide states in negotiating future agreement on specific water courses. All states in the GBM region could adopt and ratify the Convention for future conflict resolution. The Convention was adopted by the United Nations General Assembly on May 21, 1997, following years of work by the International Law Commission, (UN,2005).

9. MULTIPURPOSE RIVER BASIN DEVELOPMENT

Multipurpose River Basin Development (MRD) is fundamental for efficient and dynamic exploitation of water resources over time for irrigation, flood control, erosion prevention, fisheries, industrial water supply, navigation and hydropower generation (World Bank, 1994). The development plan, undertaken so far, had a dominant focus on a single purpose rather than multipurpose development objectives. MRD might be a catalyst for regional growth and sustainable tool for socio-economic and environmental development that will enhance the quality of life shown in Figure 3.

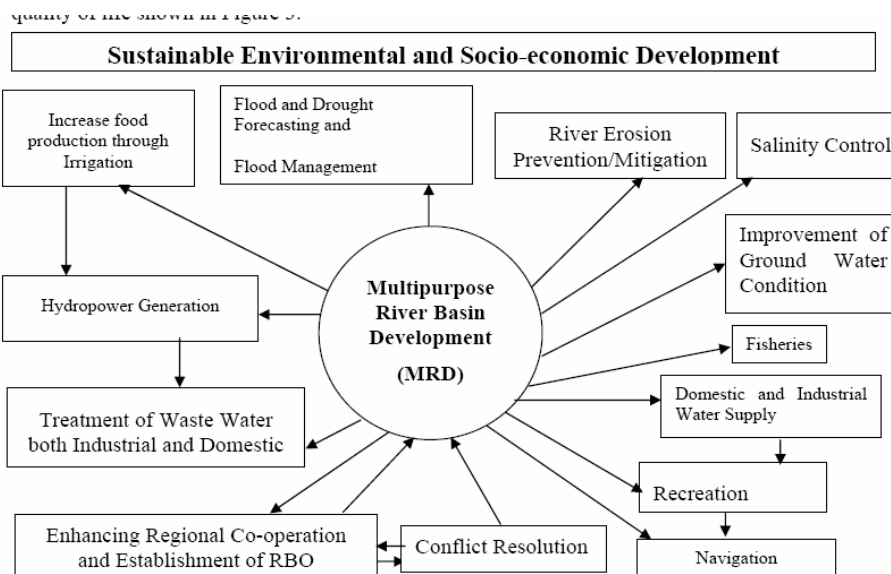


Figure 3: Dynamic and Efficient Exploitation of Water Resources through MRD

MRD concept has not yet been developed for various historical, political and economic reasons. As a result its potential for economic growth and environmental sustenance at the regional and sub-regional level has largely remained unrealized. Although MRD is difficult for accomplishment and full of challenges for Bangladesh alone, nevertheless many problems can be solved with dynamic programming. MRD, a framework for sustainable water use for the countries with predominantly transboundary rivers can help obtain consensus that will decide in a participatory way for undertaking development strategies and investment plans.

10. VISION AND OUTLOOK FOR THE FUTURE

Bangladesh hopes to create a safer environment through effective disaster management, risk reduction management concept and sustainable development. Bangladesh is the role model of cyclone and flood management in the world. The World Meteorological Organization (WMO) has a vision to provide world leadership and expertise in international cooperation to contribute to the safety and wellbeing of the people throughout the world and to the economic benefit of all nations. This vision is being achieved through the strategy of improved protection of life and property through;

- Reduction of the social and economic impacts of natural disasters
- Increased awareness and preparedness of peoples and society
- Improved safety of infrastructures
- Reduced vulnerability of human life and property to water, weather and climate related hazards.

11. RECOMMENDATIONS AND CONCLUSIONS

Recommendations for the Asia Pacific region cover a wide range of issues that require accelerated actions in a concerted manner by strengthening and reinforcing, which are:

- Flood mitigation and drainage facilities should be major determinants of design, planning and development of cities.
- Strong leadership, political commitment, formulation of relevant rules, regulations, laws and principles are urgently needed to avoid sudden release of water retained by constructing barrages on the trans-boundary rivers by upstream countries.
- Regional cooperation on trans-boundary rivers should be ensured for free flow of data exchange and sharing of experiences for forecasting flood incidence
- Long-term research should be undertaken by the national, regional and global experts for capacity building and transfer of latest technology.

However, turning strategies into action will require the following steps:

To develop policy and operational frameworks for stronger coordination, collaboration and information sharing and management across government, development agencies, Universities, NGOs and enabling communities for working together.

To establish and maintain strong regional cooperation and networks and active contribution to national, regional and international urban disaster management agenda.

To pursue the standardisation of disaster management training and systems to align with best practice standards, models and competencies.

To learn from technologically expertise experience and continuous exchange of these experiences.

From the discussion above, it will help towards the achievement and attaining the MDGs of the countries uniformly embodying technological innovations on water related hazards. The reality is that emphasis should be on getting the message right at all the various stages of disaster spectrum in a scientific way.

ACKNOWLEDGEMENTS

The author gratefully acknowledges institutional and support services received from BWDB, Institute of Water Modelling (IWM), Centre for Environmental and Geographic Information Services (CEGIS), Bangladesh University of Engineering and Technology (BUET) and South Asian Disaster Management Centre (SADMC) of International University of Business Agriculture and Technology (IUBAT), Dhaka.

REFERENCES

- ADB,2003, The Water Policy of the Asian Development Bank, Published by ADB, June2003, P.20
- Ahmed, Murshed (2007), Some Reflections on Multipurpose on River Basin Development and Strategies for Achieving Sustainable Solutions in Conflict Management of Water Resources, presented and published in Pre-Conference Paper Volume on International Conference on Water and Flood Management organized by IWFM of BUET, 12-14 March, 2007, Volume-2, Dhaka, Bangladesh. P.680
- DMB, (2005-06), Disaster Management Bureau Strategic Plan, 2005-2006.
- NWMP, (2002), National Water Management Plan, Ministry of Water Resources, Government of Bangladesh, Volume-2, Main Report, Dhaka 2002, P. 23
- Rahman, S.M.M et.al (2003), Conflict management of international river basins: A case study of GBM River Basins, presented in a Regional Conference organized by BUET and sponsored by UNESCO, 2003. P-3,17.
- Stephen, T. T.(1999), et al, Water Quality Processes and Policy (ed.) P.9

- 4th WWF, (2006), Fourth World Water Forum, Asia-Pacific Regional Document, March 16-22, 2006, P. 58
- The World Bank (1994), Multipurpose River Basin Development in China, EDI Seminar Series, (ed.), Peter Sun, October, 1994, P.10.
- UN (2005), The Convention on the Law of the Non-Navigational Uses of International Watercourses 1997, Article 7, P.5.
- WWC (2003), World Water Actions, Forum Edition, March 2003, P.71

URBAN ROAD SAFETY: EFFECTIVE RESCUE OF ACCIDENT VICTIMS USING GIS TECHNOLOGY

DR. MD. MAZHARUL HOQUE
Professor, Department of Civil Engineering,
Director, Accident Research Centre (ARC),
dirarc@arc.buet.ac.bd

KAZI MD. SHIFUN NEWAZ, S. M. SOHEL MAHMUD
Research Assistant
shifunnewaz@yahoo.com; smsohelmahmud@gmail.com,

SABREENA ANOWAR, ARMANA SABIHA HUQ
Junior Research Fellow
Accident Research Centre (ARC),
Bangladesh University of Engineering & Technology (BUET),
Dhaka, Bangladesh

ABSTRACT

Worldwide about 1.2 million people are being killed and up to 30-40 million people are injured or permanently disabled every year due to road traffic accidents. Almost half of this deaths and injuries take place in the countries of Asia and the Pacific region. Whilst deaths are declining in the developed world, significant increases are still taking place in the countries of Asia, including Bangladesh. The rapid increase of urbanization and motor vehicle ownership in Bangladesh in recent years in combination with the wide mixing of vehicle types have resulted in the significant worsening and further aggravating the road safety problems. About 50 percent of road traffic deaths happen within 15 minutes of accidents as a result of injuries to the brain, heart and large blood vessels. A further 35 percent die in the next 1-2 hours of head and chest injuries, and 15 percent over the next 30 days from sepsis and organ failure. After an accident on crowded street of cities, it is difficult to deliver the message to the nearby ambulance service and also it is very much difficult for the ambulance to reach the scene of a crash and transport the victims to the hospital for treatment. The time between injury and initial stabilization is indeed the single most important factor in the victim's survival for which immediate care is of critical importance. Road traffic accidents do have an obvious spatial dimension that can be addressed by Geographic Information System (GIS) which can help in rapid information circulation, prompt emergency assistance and incidence management, subsequently minimizing the road accident deaths. By developing an on line tracking system based on GIS, the urban road safety management system can be enhanced to provide immediate care to the victims and handling the subsequent effects on the overall traffic system. This paper focuses on the GIS based emergency rescuing system of road

traffic accident victims. Detailed aspects of this system are discussed in the context of urban road safety and trauma management.

1. INTRODUCTION

In this era of automobile based personal transportation, road accidents have become of grave concern as a deaths, injuries and suffering. An effective means of accident analysis and road safety management is needed to reduce the number and severity of these accidents. People suffer from Road Traffic Accidents (RTA) due to inadequate prompt casualty handling and absences of Emergency Medical Services (EMS). Survival rates of medical emergencies are dependent on rapid intervention by trained emergency medical personnel. In most cases, the sooner trained emergency medical rescue personnel arrive or vice versa, the greater chance for survival and conservation of life and property. Therefore, time is the critical factor and element for the rescue of occupants and the application of emergency service to minimize the losses when an emergency is reported. Indeed, the time segment between incidence and the start of medical service has a direct relationship to rescue of losses.

After an accident on crowded street of urban areas, it is difficult to identify the nearby ambulance service center and to deliver the message and also it is very much difficult for the ambulance to reach the scene of a crash and transport the victims to the hospital for treatment within a minimum response time. In this paper an attempt has been made to develop a system for Emergency Medical Service (EMS) using principles of GIS tools and technology to ensure prompt and quick response of Emergency Services (ES) for providing the best emergency medical treatment to the accident victims within optimum response time after the incidence. The importance of Emergency Medical Service and the current practices are also discussed. At the very out set of this paper, the safety problem resulting from road traffic accidents with the particular emphasis on urban safety in developing countries like Bangladesh are also highlighted.

2. THE GLOBAL ROAD SAFETY PROBLEM

Latest studies suggest that about 1.2 million people are being killed worldwide every year and up to 30-40 million people are injured or permanently disabled due to road traffic accidents. Around 88 percent of this road traffic deaths and injuries occur in the developing world and almost half of those deaths and injuries take place in the countries of Asia and the Pacific region. This worsening situation in developing countries is particularly noted with a call to accelerate actions through multi-sectoral collaboration, sharing information and knowledge with strong institutional and political will. For every death, there are far greater numbers of injuries- four persons with severe/permanent disabilities, ten persons requiring hospital admission, and thirty persons requiring emergency room treatment (Jacobs, 2006 & Mackay, 2003). Although numerous strategies, programs

and challenges have taken to control the road safety crisis all over the world including developed and developing countries, yet the statistics still paint a bleak picture of both current and predicted trends. The World Health Organization (WHO) predicts that by 2020 road accidents will be the third most important cause of death or disability worldwide. Indeed, they are the second leading cause of death for people aged 5 to 25, with devastating impact on families and communities. The majority of road casualties (injuries and fatalities) in developing countries are not motor vehicle occupants, but pedestrians, motorcyclists, bicyclists and non motorized vehicle occupants.

The economic costs of this epidemic are enormous, is estimated at up to \$100 billion, compared with total bilateral overseas aid amounting to \$106.5 billion in 2005, ranging from 1 to 5 percent of GDP for every nation (IFRTD 2007). Indeed, road traffic injuries are an important obstacle to development and place an enormous strain on a country's health care system, and on the national economy in general (Ban Ki-Moon, 2007).

2.1 The Incidence of High Fatality Index

The road safety in low and middle income countries thus emerges clearly a critical and major public health issue. Many Asian and Pacific countries have an extremely high fatality index (i.e. deaths divided by total casualties [including deaths] expressed as a percentage). The fatality index depends crucially on accurate reporting of death and injuries but can also be influenced by medical facilities (ADB, 1996). Unless prompt medical action can be given to injured people with rapid and efficient emergency scheme, their condition will deteriorate. However, it is clear that emergency medical service and other intervention could do much to reduce the very high fatality indices in the region.

3. ROAD SAFETY PROBLEMS IN BANGLADESH

There is no doubt that road transportation is vitally important to our economic and social welfare and must be so maintained and continually improved with due consideration of safety, minimizing accident hazards and risks. Each year as reported to police, more than 3000 individuals- including from among our peers, our family, our friends and our coworkers- lose their lives in road traffic accidents in Bangladesh and many more sustain disabling injuries. It is estimated that the actual fatalities could well be 10000-12000 each year taking consideration of underreporting and definitional inconsistencies (Hoque, 2005).

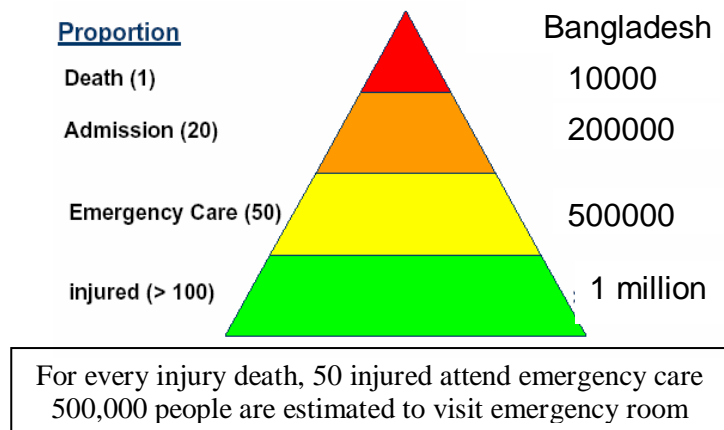


Figure 1: Pyramid of road accident casualties in Bangladesh (Rhaman, 2007)

In economic terms, road accidents in Bangladesh costing community in the order of Tk. 5000 crore (US \$ 850 million) which is nearly 2 percent of GDP. This is, of course, a huge some that the nation can ill afford to loss (Hoque, 2006).

4. ROAD SAFETY ISSUES IN URBAN AREAS OF BANGLADESH

Rapid urbanization in developing countries presents tremendous challenges to the transport systems of expanding cities if they are to meet the access and mobility needs of their communities and provide them with a sustainable, safe and healthy environment. To meet this expansion, many developing world cities are increasing the capacity of their road networks, but often at the expense of the safety of the vulnerable road users. As a result many people die and are injured unnecessarily in road crashes. The situation is critical particularly in metropolitan Dhaka, one of the mega cities of the world today. Statistics reveal that, about 23 percent of country's road accidents occurred in the Dhaka Metropolitan area. The most predominant accident types are hit pedestrians, rear end collisions, side swipes and head on accidents which accounted for around 86 percent of metropolitan accident profile. Accident data also showed that out of the total fatalities, by far the largest proportion constitute the vulnerable road users mostly pedestrians. Pedestrians account for 72 percent of all fatalities in the Dhaka Metropolitan area. The share of pedestrian fatalities is also very high in median size city of Bangladesh viz. Mymensingh 73 percent, Sylhet 63 percent and Bogra 43 percent (Hoque, 1996).



Figure 2: Hospital burden by RTA victim

Typically the principle contributing factors of pedestrian fatalities as well as overall fatalities after accidents in urban areas are improper knowledge of first aid and other life savings skill, miss handling of victims, absence of prompt emergency assistance, inadequate emergency medical and trauma centre, inefficient trauma care management system, lack of rapid response of service center, transportation and communication problem, lack of co-ordination between medical centre and victim manipulators, absence of proper and organized Emergency Medical Services (EMS) etc.

5. THE CONTEXT OF EMERGENCY MEDICAL SERVICE (EMS)

5.1 Importance of Emergency Rescue to Accident Victims

Since 200 years ago, when "flying ambulances" or light horse-drawn carriages were introduced to carry the wounded from the battlefield in Europe, there has been a slow but steady increase in the sophistication of emergency medical services, often accelerated by the requirements of wartime situations. Mortality rates dropped from 4.5 deaths per 100 casualties in World War II to less than one in recent times. This reduction was due, at least in part, to a reduction from hours to minutes in the time required to reach medical care and to the provision of effective care "at the scene" by trained paramedical personnel (ADB, 1996).

About 50 percent of road traffic deaths happen within 15 minutes of the accident as a result of injuries to the brain, heart, and large blood vessels. A further 35 percent die in the next 1-2 hours of head and chest injuries, and 15 percent over the next 30 days from sepsis and organ failure. So, the time between injury and initial stabilization is the single most important factor in patient survival, with the first 30-60 minutes being the most important (ADB, 1996).

The most serious injuries resulting from traffic accidents are head, spinal, and internal soft tissue damage to vital organs. Early treatment and stabilization of these typical accident injuries can enhance a patient's timely and full recovery. Delay or well-intentioned but inappropriate first aid, can result in death or permanent disability. Medical experience around the world has demonstrated that stabilization of the injured person and hospitalization

to a specialist center, within what they describe as the "golden hour," increases the patient's potential for survival and full recovery.

5.2. Generalized Emergency Medical Service System (EMS)

There are two general philosophies in the "formal" provision of emergency medical care. One of these formal approaches is to provide immediate first aid and emergency care at the scene of the incident, then to transport the injured person to the emergency department as fast as possible. It is there to skilled and definitive care, the so-called scoop and run philosophy. This approach is taken in countries such as Australia, New Zealand, United Kingdom (UK), and parts of the US (ADB, 1996).

The alternative is to carry the skilled care to the site of the incident and there provide appropriate treatment. This approach is taken in France, Germany, and Russia, where well equipped vehicles carry skilled doctors to the scene.

A third approach, an "informal system," is found in many situations in countries in the Asian and Pacific region. Since there or passing motorists and carried to the nearest emergency department by whatever transport is available, usually without any treatment or first aid at the scene. This results in rapid transport to the emergency department but without any resuscitation measures. The outcome of this system depends to some extent on the capacity of the emergency department to deal with these severe cases and to provide effective treatment on arrival (ADB, 1996).

Although there is a great diversity in application and practices, there is general agreement on the principles of an effective emergency medical service. The essential functions of such a service are as follows (ADB, 1996):

- the provision of first aid and medical care to the casualties at the roadside;
- the transport of the casualties to a hospital; and
- the subsequent provision of more definitive treatment.

The typical components of an ambulance service in a developed country are as follows:

- a notification and communication system;
- central control and coordination of operations;
- effective rescue and medical aid at the scene; and
- transport to a hospital and the provision of definitive care in an emergency department.

In the light of the above principles, it is important to develop an emergency rescue system to ensure that the accident victims get the best emergency medical treatment practically possible in cognizance of the local situations.

5.3. The Situation in Bangladesh

As indicated earlier, the fatality rates viz. the estimated number of road traffic accident fatalities per 10,000 registered vehicle of Bangladesh (over 100) is very high by international standards, as the fatality rates for motorized countries is usually less than 2. The fatality index in Bangladesh is nearly 40 percent, which is the highest among the developing countries. This signifies probably two important characteristics, viz. the wide spread under reporting of less serious accidents and the lower level of emergency medical services available to accident victims. In Bangladesh with the present level of medical services, there is little scope to provide the prompt and necessary medical attention to injured people, particularly soon after an accident (Hoque, 2003).

Salahuddin and Khandaker (2006) in their study on emergency medical services for road traffic accidents in Bangladesh briefly reviewed the present emergency medical service system in Bangladesh. They point out that, in general public handle improperly the RTA victims without proper knowledge of first aid, Cardio Pulmonary Resuscitation (CPR) and other life saving skills. To avoid the harassment of police cases people usually avoid their involvement in helping someone in RTAs. Though some humanitarian people willingly handle such casualty but they don't know how to do that properly. Usually the rickshaws or auto-rickshaws carry them to the nearest public healthcare providers- more often those are the medical colleges. Nearest hospitals and clinics simply deny giving emergency medical aid that can save many lives. On the way to the hospital 90% casualties come to a fatality because of excessive bleeding. The scenario in first medical response and casualty management in RTA is similar in all over the country.

6. THE POTENTIAL OF GEOGRAPHIC INFORMATION SYSTEM

A brief outline on application and potential of Geographic Information System (GIS) in the field of data analysis, location identification, graphical representation and network analysis are presented by Affum and Taylor (1996), ESRI (2007). They pointed out that in this modern era, GIS is one of the proven and widely used tools for complex incident analysis to display trends, illustrate patterns and identify areas of incidence all over the world. Organizing information so it can be accessed by pointing to a region or a specific location on a map is used in a variety of applications. Systems that support this task are called Geographic Information Systems (GIS). The information available is data that relates to specific locations. GIS can integrate graphic information and data in databases to support the production of geographic information for further arrangement, analysis, and management and maps which are produced and displayed by GIS present excellent visual interpretations of data which are hardly can be achieved by language and letters.

7. APPLICATION OF GIS IN EMS

In the emergency rescue of accident victims, initial response time is a very important factor in determining the quality of pre-hospital EMS. The GIS can assist in emergency rescue operations by identifying where help is needed and helping to direct resources in an efficient manner to reduce the response time by the development and implementation of an emergency medical services (EMS) response system. GIS can quickly analyze and display a route from a station or GPS location to the emergency call. This route (depending on the sophistication of the street file) may be the shortest path (distance) or the quickest path (depending on time of day and traffic patterns). In network analysis, the "optimum path" is derived by considering many criteria. In EMS system, to locate the shortest path, these criteria could be the level of the road, one way or two way transportation, speed limit, congestion period, number of intersections etc. Indeed, emergencies are very dynamic and, as circumstances change, GIS can reflect these changes also.

GIS technology is being deployed in a number of other emergency response areas to increase efficiency and reduce time and provide higher-quality decision support information and data. This includes dispatch, mobile operations, and emergency management. The proposed use of GIS with EMCS will alleviate the damage to life or save life by suggesting first aid location and by admitting the patient to the nearest suitable hospital.

8. A PROPOSED EMS SYSTEM FOR URBAN SAFETY

In the light of the preceding discussions and in the absence of rapid and efficient system of emergency rescuing of accident victims, a framework of effective rescue system using GIS tools for facilitating emergency medical service of accident victims is proposed. The detailed methodology and steps of the system are described in the form of a flow chart in Figure 3. This framework/flowchart essentially provides series of actions and information exchange following the reporting of an accident involving serious casualties for ensuring their proper and timely emergency care. This framework can be applied for any events of public emergency service.

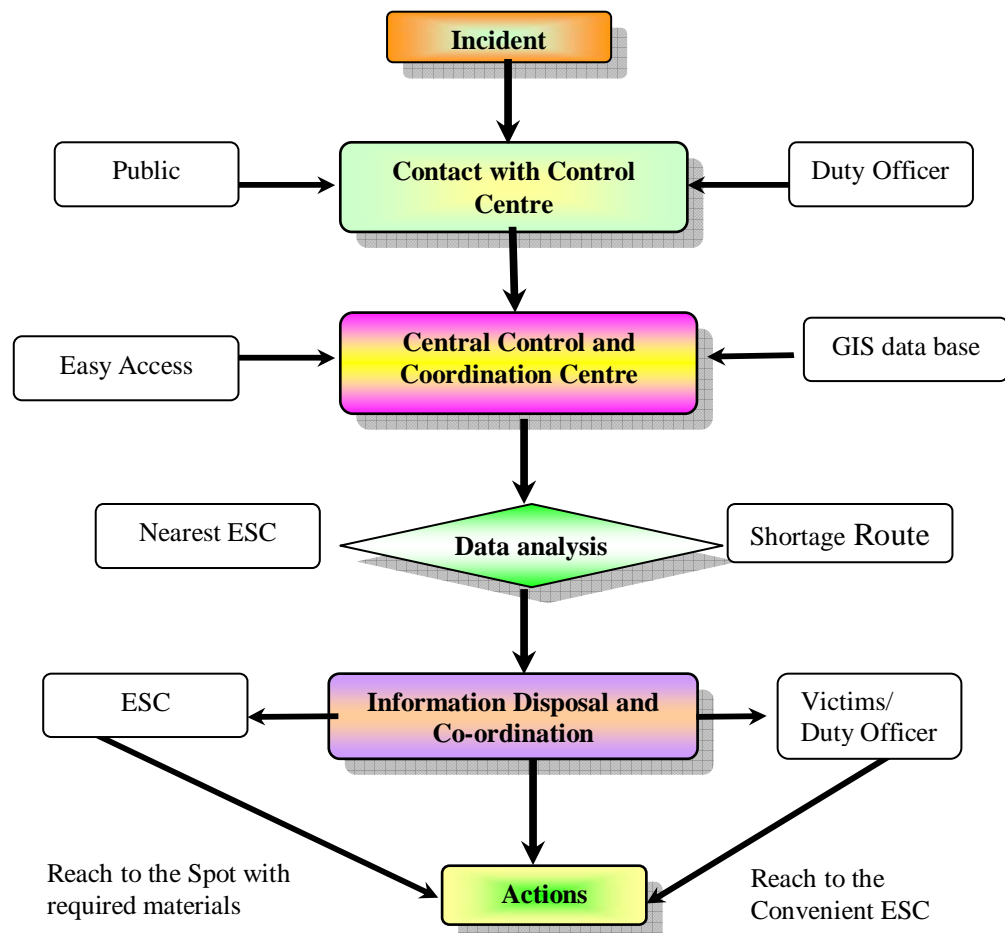


Figure 3: Flow chart of system

8.1 Brief Description of the System Components

- **Events/Incidents:** This refers to any type of event which creates public disturbance, sufferings like road accident, fire, and crime or any other natural hazards and pandemic etc. It may occur anywhere, at any location, at any time, and in various different ways - thus making any one of us susceptible.
- **Contact and Information Exchange:** Of most importance in the system is the immediate contact and information circulation regarding the incidence and victims. This information involves location, incident type, details of injuries and any special medical treatment needed etc. This information will be exchanged by the local viewers of the incidents or local police or duty traffic police to the control center.
- **An Effective Notification and Communication Network:** There should be a single convenient method of notifying the control room about the location and nature of the incidence. In many countries this is a telephone number such as 999, 000, or 111, which operates

throughout the country and provides telephone access to all emergency services, police, fire, and ambulance. Ideally, these calls should also be without charge. An additional requirement for this work is that there must be a way of identifying the exact location of the incident.

The central control center will receive calls from the public and/or duty officers about the incident and dispatch the information to the nearest and competent Emergency Service Center (ESC) (hospital, fire service, police station etc.) and/or to the duty officer to take immediate actions with giving details of injuries and any special medical treatment needed. The control centre will also follow-up and co-ordinate with the ESC to ensure the effective and reliable rescue and emergency incidence management like medical aid after the incidence.

- **Comprehensive GIS data base system:** There should have a comprehensive and details GIS base database of road network, with the information of road name, type, width, traffic characteristics, node id, link id, length of link etc. and location of utility services with the information of name, facilities, location, contact number, land marks etc. The data base information may also includes the location of critical facilities, including hospitals, nursing homes, schools, parks, shopping areas, business areas, manufacturing areas, and transportation routes.
- **Analysis:** After receiving the information, data analyst will locate the incidence location and the required ESC will be identify within a particular radius from the incidence location. Then, the nearest, capable and potential centre is marked out and subsequently finds out the shortage and reliable distance using GIS database by Network Analysis.

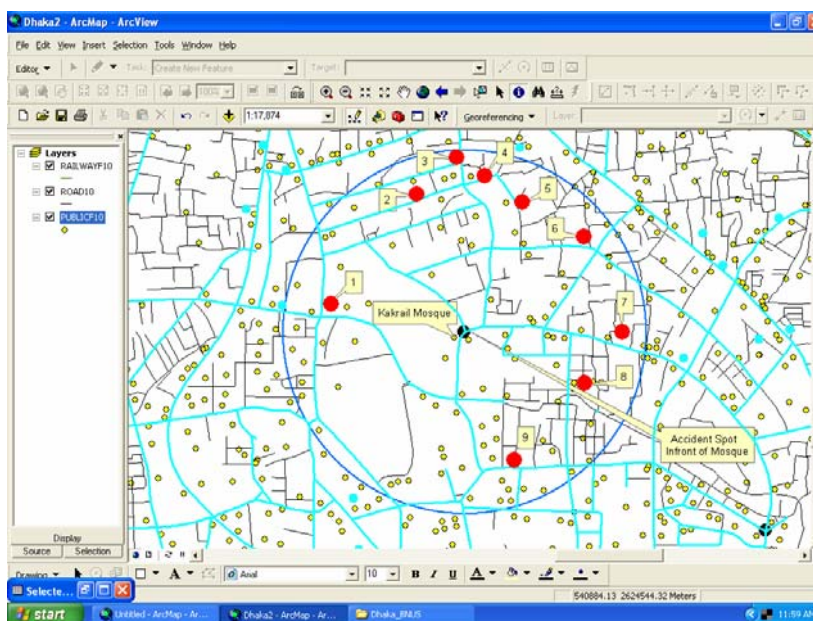


Figure 4: Accident spot and all hospitals within 1 Km radius

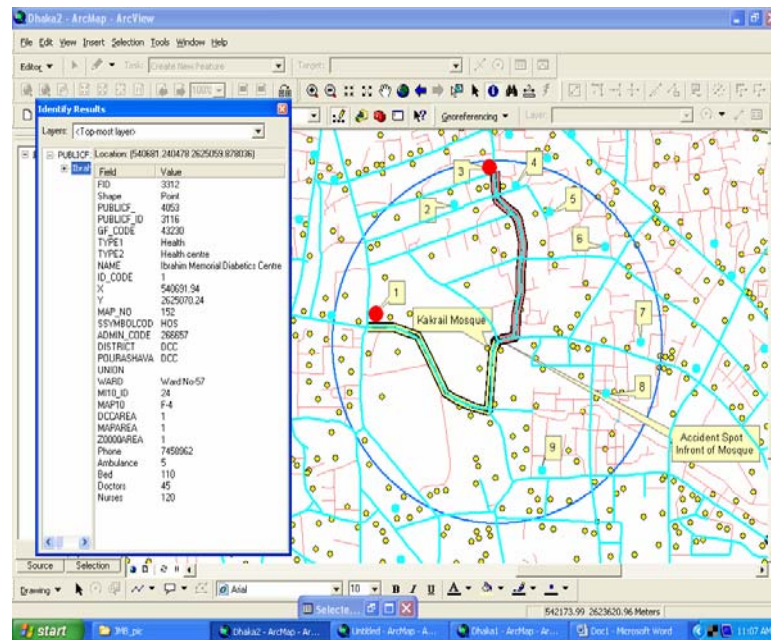


Figure 5: Network analysis to find the nearest and capable hospital.

Figure 4 & 5 is an example of analysis. Figure 4 generated by GIS illustrating the location of the spot and location of hospital within one kilometer radius. This map also shows that there are nine hospitals within that circle which are denoted as chronological number 1 to 9. Figure 5 represent two probable shortage routes to reach the spot from two nearest hospitals with priority 1 and 2 in different color green and red respectively.

- **Information disposal:** Dispatchers have an important responsibility to process emergency calls and send the appropriate public safety resources to the emergency location based on the type and urgency of the incident. According to the data analysis, the information will dispatch to the service centre for immediate action informing about the location, shortage path, nature and severity of injuries or to the local duty officer informing the nearest medical service centre.
- **Actions:** Service centre or victims/duty officer will take immediate action to reach the emergency service team to the spot with required materials or victims will send to the convenient nearest ESC.

9. CONCLUSIONS

In any emergency disastrous situation it is crucial that the right tools are available for operational personnel (viz. fire brigades, emergency service, police or armed forces) at all levels for them to make right decisions for appropriate actions as quickly as possible. GIS is one of such potential tools which have the capability in organizing the extensive amount of spatial data both generated and utilized during an emergency. A properly designed and implemented GIS will allow managers and responders to access critical

location data in a timely manner so that lives and properties can be protected and restored.

The deaths and injuries resulting from road traffic accidents have now emerged as a serious safety problem particularly in urban areas of Bangladesh. In order to minimize the extent of deaths and injuries and their resulting adverse social and economic consequences an effective trauma management system needs to be developed and operated to provide supportive care to the casualties at various stages viz. at the accident scene, pre-hospital and hospital treatment. In this paper a GIS based system of emergency rescuing of accident victims has been described. This system is considered as a vital element to the overall trauma management process and provides opportunity in rendering timely emergency medical services by rapid information circulation and thereby ensures minimum time response for prompt assistance and incidence management. While this system would help minimizing road accident deaths, disabilities and sufferings, it will also alleviate associated traffic congestion and operational hazards. Apart from rescuing road traffic accident victims, the system can be introduced for other emergency and disaster management process in urban areas.

Further research and studies in this regard are underway at the Accident Research Centre (ARC) at BUET to address the requirements viz. equipment/vehicles, software, ITS, management and coordination, enriched and updated database, training of personnel and funding for its full development and subsequent implementation.

REFERENCES

ADB (1996), *Road Safety Guidelines for Asia and Pacific Region*, Regional Technical Assistance Project Draft 2 Report, Asian Development Bank,

Affum J. K., Taylor M. A. P. (1996), *GIS-Based System for the Systematic Determination of Road Accident Problems and Casual Factors*, Proceedings roads 96 conference, Part 5

Askins C., Bresette A. (2006), *Emergency Medical Services: Applying Proven Principles*, Proceedings published on International Conference on Road Safety in Developing Countries, BUET, Dhaka, Bangladesh.

Ki-Moon, B. (2007), *Message on occasion of the First UN Global Road Safety Week*, 23-29 April 2007

ESRI (2007), *GIS for Fire Station Locations and Response Protocol*, White Paper, January 2007, Module 5b

GTZ, *Urban Road Safety*, *Sustainable Transport: A Sourcebook for Policy-makers in Developing Cities*, Deutsche Gesellschaft für Technische Zusammenarbeit (GTZ) GmbH

Hoque, M. M. (2006), *Road Safety in Bangladesh: The Contemporary Issues and Priorities*, Proceedings published on International Conference on Road Safety in Developing Countries, BUET, Dhaka, Bangladesh.

Hoque, M. M. (2005), '*Road Safety Problems and Priorities in Bangladesh*', Published in the Souvenir on occasion of Lunching Highway Police, June 2005

Hoque M. M.; Alam M. J. B.; Habib K.M N., (2003) '*Road Safety Issues and Initiatives in Bangladesh: The Context of Regional Significance.*', 21 ARRB Conference, 2003

Hoque M.M.; Ahmed S.N.U.D.; Choudhury M. A. I., (1996) '*Traffic Management Schemes for Three Medium Sized Cities in Bangladesh*' Proceeding Codatu VII in 12-16 February 1996 in New Delhi (India)

IFRTD (2007), '*Forum news, International Forum for Rural Transport and Development (IFRTD)*', volume 13, Issue 3, February 2007

Jacobs G D (2006), '*Road Safety: the Global Problem*', Proceedings published on International Conference on Road Safety in Developing Countries, BUET, Dhaka, Bangladesh.

Jagadish S, '*The use of GIS for the Emergency Medical Care System, EMCS*' GIS Programmer, Induscorp India PVT Ltd – Bangalore

Khandadar R. M., Salauddin T. (2006), '*Emergency Medical Services for Road Traffic Accidents in Bangladesh*' Proceedings published on International Conference on Road Safety in Developing Countries, BUET, Dhaka, Bangladesh.

Mackay, M. (2003), UN Technical Briefing, "*Global Road Safety Crisis*", May 29, 2003

Peleg K., Pliskin JS., '*A geographic information system simulation model of EMS: reducing ambulance response time*', Trauma and Emergency Medicine Research Unit, The Gertner Institute for Health Policy Research, Sheba Medical Center, Tel-Hashomer, Israel.

Rahman F., '*Community road safety In Bangladesh: a priority social responsibility*', Road Safety Workshop, setting road safety priorities in Rajshahi region, 2006

COMPARATIVE ANALYSIS OF ON-STREET PARKING MANAGEMENT PRACTICES IN DIFFERENT COUNTRIES

SHINJI TANAKA, MASAO KUWAHARA
The University of Tokyo, Japan
stanaka@iis.u-tokyo.ac.jp

ABSTRACT

Illegal on-street parking is one of the major causes of traffic congestions and sometimes traffic accidents in urban streets. Therefore, an appropriate management of on-street parking is very important. In this study, a questionnaire survey was conducted to understand parking management strategies from the practice in 11 different countries. The questions are about institutions in charge of parking management, parking regulations, fees and fines, enforcements, ITS technologies, parking management policies and so on.

In view of the result, one possible parking management strategy for Japanese cities is proposed, that is, modulated parking regulation, utilization of curbside space and so on. The validity of this proposed parking space is evaluated through a simple analysis using traffic simulation.

1. INTRODUCTION

Illegal on-street parking is one of the major causes of traffic congestion in urban area because it reduces the traffic capacity of urban streets significantly. And sometimes, it may cause traffic accidents as an obstacle on a road. From the viewpoint of smoothness and safety, all parking vehicles should be removed from streets and parked in off-street parking garages. However, there are some vehicles, especially commercial ones, which have to repeat short stop for loading / unloading goods in many different locations. If they are forced to park off-street, the efficiency of their business would be largely deteriorated. And urban businesses and activities are supported by these vehicles. Therefore, it may be difficult to employ no parking regulation simply. We need to find more acceptable and realistic solution.

In Japan, on-street parking is prohibited in the most part of urban area in principle, because road is recognized as running space, not for parking. However as there exist vehicles that need to park on-street as mentioned above, there are a lot of illegal parking vehicles on streets in reality due to the shortage of enforcement ability. This gap between the principle and the reality may cause sense of unfairness among road users, and might lead to a kind of moral hazard. It would be meaningful to reconsider the current

system to realize an orderly traffic situation. For this purpose, to survey parking management practices in different countries would be a good way to investigate possible parking management alternatives.

In this study, a questionnaire survey on parking management practices was carried out in 11 countries. Based on the result of a comparative analysis, one possible parking management scheme for Japanese cities is proposed. And the validity of this scheme is evaluated through a simple analysis of traffic simulation.

2. QUESTIONNAIRE SURVEY

2.1 Outline of the survey

A questionnaire survey was designed to understand parking management practices in different countries. The countries and cities answered are shown in Table 1. The questionnaire survey was answered by transportation researchers and engineers in these countries.

Table 1: Surveyed countries and cities

Country	City	Population (ths)
The United States	San Francisco	798
The United Kingdom	Leeds	715
France	Paris	2,150
Germany	Darmstadt	138
The Netherlands	Delft	95
Italy	Turin	902
Switzerland	Geneva	180
Israel	Haifa	300
South Korea	Yeosu	320
Thailand	Bangkok	6,355
Japan	Tokyo	8,520

The questions are about institutions in charge of parking management, laws and ordinances, systems, regulations, charging, enforcement, fine, parking policy, related ITS technologies and so on.

2.2 Result

Representative results are shown in the following sections. Note that in some countries transportation system and regulation is different by cities, therefore the result shown here is not always applicable throughout that country.

2.2.1 Definition of parking

In some countries, “parking” is distinguished from “stopping” or “standing”. For example, it is defined by time duration in Germany and

Switzerland, and by the fact that the driver leaves the vehicle in the United States and France.

Table 2: Definition of parking

Status	Countries
Time duration larger than a certain length	Germany (3 min), Switzerland (15 min)
Driver's absence from the vehicle	The United States, France
Both above	Italy, Japan

2.2.2 Charging measures

Parking meter and pay & display system are the most widely used in many countries. Coupon ticket and manual collection are also seen. As for new technologies, smart card in common with public transportation and mobile phone charging are introduced in some countries. In-vehicle meter which indicates arrival time on the dashboard is used in Germany and Switzerland although it is not a charging measure.

Table 3: Charging measures

	US	UK	France	Germany	Netherlands	Italy	Switzerland	Israel	South Korea	Thailand	Japan
Meter	○	○	○	○	○	○	○	○			○
Pay & display	○	○			○	○	○	○	○		○
Coupon ticket			○	○	○	○	○	○			
Smart card				○			○				
Mobile phone				○		○					
Manual collection										○	
In-vehicle meter				○			○				

2.2.3 Operation of parking meters

As a typical charging measure, way of operating parking meters is asked. Minimum charging unit time is usually 30min or 1 hr, however, 15 / 30 / 60 / 120 min of unit time and sometimes 5 min for loading / unloading vehicles are defined in the United States. This kind of fine unit time seems effective to reduce unnecessary on-street parking and to enhance efficient use of on-street parking spaces.

Table 4: Operation of parking meters

Country	Unit time	Maximum time limit variation	Operation hours	Parking out of operation hours
US	15, 30, 60, 120 min	Day, Time, Location	8-18h	OK
UK	2, 4 hr	Constant	8-18:30	NG
France	N/A	-	-	OK
Germany	30 min - 2 hr	Location	8-20h	OK
Netherlands	2 hr	Day, Location	8-20h	OK
Italy	30 min	Day	8-20h	OK
Switzerland	2 hr	Day, Time, Location	8-12:30, 13:30-19	OK
Israel	N/A	-	7-17h	OK
South Korea	N/A	-	8-21h	OK
Thailand	15 min	Constant	9-17h	OK
Japan	60 min	Constant	8-20h	NG

2.2.4 Charging rate of parking meters

In most countries, charging rate of on-street parking is cheaper than off-street parking except for the United States, where it become possible to induce less necessary vehicles to off-street parking garages. To bring out this effect, charging rate should be different depending on location and time in one city although it is constant in some countries. Some countries employ progressive charging which charges a higher rate for a longer parking and it also has an effect to induce long-term parking to off-street parking garages.

Table 5: Charging rate of parking meters

Country	Off-street (per hr)	On-street (per hr)	Rate variation	Progressive rate
US	2-3 USD	4 USD	Day, Time, Location	No
UK	1.5-3 GBP	1.5-3 GBP	Day, Time, Location	Yes
France	2-3 EUR	1-3 EUR	Day, Time, Location	Yes
Germany	1.5 EUR	1 EUR	Location	No
Netherlands	4 EUR	2-4 EUR	Constant	Yes
Italy	1 EUR	1 EUR	Location	No
Switzerland	2.5 CHF	2.5 CHF	Day, Time, Location	No
Israel	4 USD	1.2 USD	Constant	No
South Korea	1000 KRW	1000 KRW	Location	No
Thailand	50 THB	10 THB	Constant	No
Japan	600 JPY	300 JPY	Constant	No

2.2.5 Institutions of enforcement

In most countries, municipalities and contracted private sectors operate enforcement of illegal parking in addition to the police. In the United States and the Netherlands, specialized parking section is sometimes prepared in a municipal organization. As for the role of municipality / private sector and police, the former issues tickets for normal illegal parking and the latter enforces more serious parking violation, usually.

Table 6: Institutions of enforcement

	US	UK	France	Germany	Netherlands	Italy	Switzerland	Israel	South Korea	Thailand	Japan
Police	○		○		○	○	○	○	○	○	○
Municipality	○	○	○	○	○	○		○	○		
Private sector	○	○				○			○		○

2.2.6 Fine

As for the fine of parking violation, Japanese one is the highest as a whole. However, some countries charge much higher fines in case the violation is serious, e.g. violation in priority space for handicapped people, fire hydrant and dangerous spot which obstruct other traffic. It shows an idea that the amount of fine should be varied depending on the influence.

Table 7: Amount of fine

Country	Fine
US	40-60USD, priority space and fire hydrant: 200USD
UK	50 GBP
France	unpaid: 11EUR, obstruction: 35EUR, priority space: 135EUR
Germany	unpaid: 5EUR, obstruction: 40EUR
Netherlands	-
Italy	54 EUR
Switzerland	overstay: 40-100CHF, unpaid: 40-120CHF
Israel	18 USD
South Korea	40,000 KRW
Thailand	500 THB
Japan	10,000 - 18,000 JPY

2.2.7 Owner's responsibility

All the countries surveyed this time already introduced owner's responsibility of illegal parking vehicle, which means, if the driver of the illegal parking vehicle is not identified, the owner of the vehicle owes the responsibility to pay the fine. And here, one group (the United States, the

Netherlands, South Korea) firstly charges the responsibility to the driver and secondly to the owner if not identified. The other group (the United Kingdom, Germany and Italy) charges to the owner from the first and does not inquire who pay the fine eventually.

2.2.8 Decriminalization

Parking violation is decriminalized together with other traffic violations in many countries, that is, it is treated not as “crime” but as “offense”. This makes possible for municipalities to enforce parking violations.

2.2.9 Role of on-street parking

As for the role of on-street parking in traffic management policy, one group (Italy, Israel, South Korea and Japan) has a principle that parking should be done off-street, whereas the other group (the United States, France, Germany, the Netherlands, Switzerland and Thailand) allows on-street parking depending on necessity. The latter case can be understood that on-street parking is established as an important mode of parking.

3. PROPOSAL OF ON-STREET PARKING MANAGEMENT SCHEME FOR JAPANESE CITIES

Focusing on Japanese on-street parking management scheme, issues of the current system is pointed out based on the result in the previous chapter. Then a new scheme of on-street parking management is proposed.

3.1 Issues in the current system

From the comparative analysis in the chapter 2, it is revealed that there are some issues to be improved in the current Japanese parking management system. The principal ones are as follows.

- On-street parking is regarded as a tentative mode of parking until off-street parking garages are constructed sufficiently.
- A common understanding of priority vehicles which should park on-street is not established.
- Parking regulation is not differentiated depending on location and time.
- Charging rate is constant throughout one city, not time-progressive, and less expensive compared with off-street parking garages nearby.
- Unit time of parking meters is apart from the duration of actual parking behavior.
- Enforcement of parking violation is not strict very much and the fine is not differentiated by the influence.

3.2 New scheme of on-street parking management

Considering these issues, new scheme of on-street parking management should satisfy the following points.

(1) Modulated regulation

The level of parking regulation should be modulated, that is, illegal parking at very influential spots should be strictly prohibited whereas parking at less influential spots can be allowed. Same things can be said in time, duration, vehicle type and fine. This kind of modulated regulation prevents drivers from parking at seriously influential and dangerous spots.

(2) Creation of on-street parking space

Next, it is necessary to create on-street parking space considering on-street parking demand. Here, it is not enough to ensure the amount only. We have to make sure the space is appropriately distributed, e.g. small space in each block, because on-street parking is used for short stop and the distance to the building become critical.

(3) Appropriate enforcement

To ensure the effectiveness of the parking management scheme, a strict enforcement of parking violation is essential. An appropriate enforcement helps to realize an orderly traffic situation.

The important thing is to consider not only parking vehicles but also the relationship with running vehicles. In other words, this is a matter of assignment of limited road resources between traffic function and access function depending on the local situation.

3.3 Design of on-street parking space

Then next issue is how to design on-street parking spaces in existing urban streets. As for traffic congestion in an urban area, the bottleneck is always at a signalized intersection, because the limited amount of green time has to be allocated among different directions of traffic. Therefore, on-street parking around an intersection which reduces the road capacity significantly should be strictly controlled. In other words, there is some room to allow on-street parking at a straight section between intersections.

According to this idea, the authors propose to create on-street parking space between intersections as shown in Figure 1, that is, to make an on-street parking bay at a straight pipe section between two intersections and to keep the maximum capacity at the intersection.

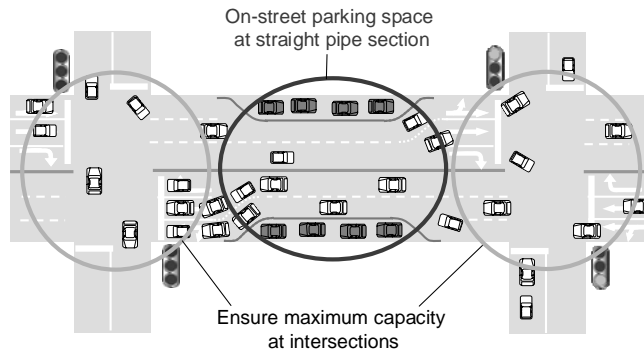


Figure 1: Proposed design of on-street parking space

4. TRAFFIC SIMULATION ANALYSIS

The proposed on-street parking space is designed inside road space, so the road width for passing vehicles has to be narrowed. Therefore, it should be carefully designed not to reduce the capacity at the intersection. If designed appropriately, the congestion level of the network remains the same. To confirm it, a simple simulation analysis was done as follows.

4.1 Setting

The principal design elements of the proposed on-street parking space are the distance from adjacent signalized intersections (named “clearance distance”) and their cycle length. For the simulation, 2 and 3 lanes street with signals on both ends were prepared as shown in Figure 2. We ran several settings of the simulations changing some variables shown in Table 8.

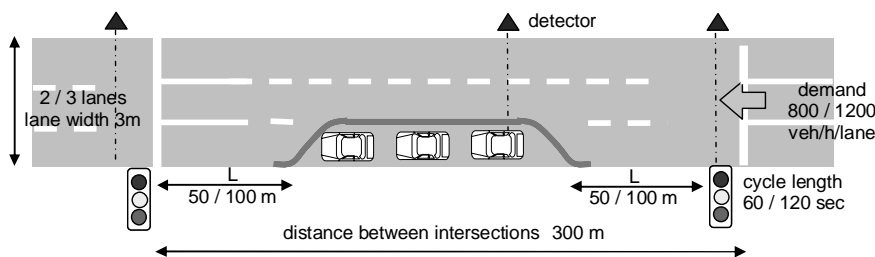


Figure 2: Representation of on-street parking space in the simulation

Table 8: Setting of the simulation

Item	Setting
number of lanes	2, 3 [lanes]
distance between intersections	300 [m]
distance from intersection to parking space (clearance distance) (L)	50, 100 [m]
cycle time (C)	60, 120 [sec]
green time	60% of the cycle time
offset	simultaneous offset
traffic demand (Q)	800, 1200 [veh/h/lane]

4.2 Result

First, let us see the result of 2 lanes simulation with the demand (Q) of 800 [veh/h/lane]. When the cycle time (C) is 120 [sec] and there is no parking space, the throughput of this section is 1447.6 [veh/h]. Here, if parking space is located with clearance distance (L) as 50 [m], the cumulative curve of the passing time of vehicles is shown in Figure 8.

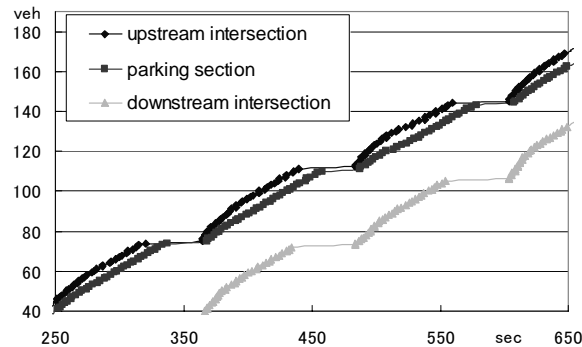


Figure 3: Cumulative curve ($L = 50$ [m], $C = 120$ [sec])

Next, if the clearance distance is set up as 100 [m] and the cycle time is set up as 60 [sec], the cumulative curve becomes as in Figure 4.

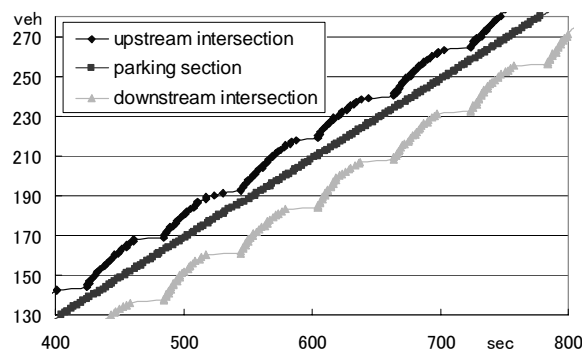


Figure 4: Cumulative curve ($L = 100$ [m], $C = 60$ [sec])

Comparing these two, the latter has a larger gradient, which means it has more ability to process traffic demand. (Note the displayed range of these two graphs is the same.) Actually, the throughput of the latter is 1425.2 [veh/h], which is much larger than that of the former 1102.2 [veh/h] and almost the same as the situation of no parking space (1447.6 [veh/h]).

In the same way, different cases are simulated with the combination of the parameters mentioned above. The results are shown in Table 9 and 10. Of course, no parking space situations have the largest value of the throughput. When the parking space is located with $L = 50$ [m], the value of the throughput is reduced. However, as the cycle time is shortened and the clearance distance is extended, the value of the throughput is improved. Assuming the no parking situation 100%, the throughput rate is improved from 59.5% ($L = 50$ [m], $C = 120$ [sec]) to 77.1% ($L = 100$ [m], $C = 60$ [sec]) in the case of 2 lanes, and from 71.5% ($L = 50$ [m], $C = 120$ [sec]) to

88.6% ($L = 100$ [m], $C = 60$ [sec]) in the case of 3 lanes. From these results, it seems to be possible to keep the enough high throughputs setting appropriate clearance distance and cycle time.

Table 9: Throughput of 2 lanes road [veh/h]

Case	Q=800 [veh/h]	Q=1200 [veh/h]
no parking space (C=120 sec)	1447.6	1856.9
L = 50 m, C = 120sec	1102.0	1105.9
C = 60 sec	1253.3	1238.1
L = 100 m	1247.4	1285.4
L = 100 m, C = 60 sec	1425.2	1431.0

Table 10: Throughput of 3 lanes road [veh/h]

Case	Q=800 [veh/h]	Q=1200 [veh/h]
no parking space (C=120 sec)	2240.9	2758.6
L = 50 m, C = 120sec	1930.0	1973.2
C = 60 sec	2156.9	2180.5
L = 100 m	2045.2	2055.4
L = 100 m, C = 60 sec	2093.6	2445.1

5. CONCLUSIONS

In this study, on-street parking management practices were surveyed and compared through questionnaire survey among 11 countries to find better on-street parking management schemes. From the result, a couple of issues in the current Japanese system were indicated, and one possible management scheme was proposed. The key of the proposal is to make a modulated parking regulation and to create on-street parking space between intersections inside existing streets. Then the feasibility of the proposed parking space was evaluated by a simple analysis of traffic simulation and the result showed a possibility to create on-street parking space without deteriorating traffic smoothness.

All vehicles have to be parked eventually after they are used. Therefore, parking management is one of the most important issues in traffic management policies. And, an appropriate parking management strategy is different depending on the traffic situation in each country. For the next step, we'd like to consider appropriate parking management strategies applicable to Asian mega cities.

REFERENCES

Allison L. C. de Cerreño, 2002. *The Dynamics of On-Street Parking in Large Central Cities*, Rudin Center for Transportation Policy & Management, NYU Robert F. Wagner Graduate School of Public Service

PUBLIC TRANSPORT IN BANGKOK: A CASE OF THE PASSENGER VANS

SHINYA HANAOKA

Department of International Development Engineering
Tokyo Institute of Technology, JAPAN
hanaoka@ide.titech.ac.jp

SUPAPORN KAEWKO LEOPAIRONA

Department of Urban and Environmental Planning
Kasetsart University, THAILAND
supaporn_k@hotmail.com

ABSTRACT

The passenger van services in Bangkok were initiated as informal public transport. Passengers preferred these services to conventional buses due to their speed, comfort and ease of access at affordable fares. The popularity caused public bus operators to judge passenger vans as competitors who affected reduction of their passengers and revenues. Consequently, the government started enforcing passenger van regulations in 1999. According to the regulations entry of the passenger vans and maximum fares are controlled. In this paper, the authors studied background of the passenger van services, and analyzed the passenger van market using data from the supply side, i.e., the passenger van drivers and the demand side, i.e., the passengers on the passenger vans and their competitive modes. Market analysis under the existing regulations showed that there was no price competition at the route and corridor levels. On the route level, the passenger van market was an oligopoly market with implication of collusion. At the corridor level, the market was an oligopoly market with implication of product differentiation.

1. INTRODUCTION

The passenger van services supply 12-seat air-conditioning vans with guaranteed seats. It provides fast and comfortable road-based public transport mode for middle-income passengers who travel between suburbs and city centres. In 2003, passenger vans and bus carried about 3% and 26%, respectively, of daily person trips in Bangkok and the neighbouring provinces (OTP, 2004). The service was initiated illegally as it operated without proper government licenses. Nonetheless, passengers preferred this mode to conventional buses because of its speed, comfort and ease of access at affordable fares. Even though modal share of passenger van was not so high, public bus operators considered passenger vans as competitors and claimed that the competition caused reduction of their passengers and revenues. Consequently, the government started enforcing passenger van regulations to ease competition and to provide legal services to the passengers in 1999 (DLT, 2003). Though the regulations, safety and

qualities of the passenger van services are assured and the entry of number of the passenger vans and maximum fares are controlled.

In this paper, the authors studied background of the passenger van services, and analyzed the passenger van market using data from the supply side, i.e., the passenger van drivers and the demand side, i.e., the passengers on the passenger vans and their competitive modes.



Photo 1: Passenger vans in Bangkok

2. BACKGROUND OF THE PASSENGER VAN SERVICES

2.1 Development of the passenger van services

Passenger van services were started by groups of investors. Since the Land Transport Act B.E. 2522 (1979) states that operating public transport services requires official permission from Department of Land Transport (DLT), the passenger van services were then considered illegal for the reason that they operated without DLT permission. Additionally, the Motor Vehicle Act of B.E. 2522 (1979) prevents drivers from operating the vans as public vehicles when the vans were registered as private vehicles. Furthermore, according to the Royal Decree Establishing Bangkok Mass Transit Authority (BMTA) B.E. 2519 (1976) only BMTA is authorized to provide bus services and other bus operators require BMTA sub-contracts.

Despite existing government policy to eliminate the passenger vans the services kept on expanding in 1990s as suburbs of Bangkok developed to be residential areas and most working places continued to be located in central areas. The passenger vans are preferred by the middle-income passengers because, 1) they charge similar fares to the conventional air-conditioning (a-c) buses but offer more comfort in the form of guaranteed seats, 2) they reduce travel times since their smaller vehicle size enables them to move quickly through congested roads, they have fewer stops, and some of them operate on expressways, and 3) they offer a level of service similar to taxis but lower fares and they give a better sense of safety for female passengers (Leopairojna and Hanaoka, 2005).

The popularity of the passenger vans caused BMTA and its joint-service operators to consider the passenger vans as competitors who affected reduction of their passengers and revenues by interloping the bus routes and “cream skimming”- operating on high demand routes. Furthermore, relationships between the investors and the influential figures

in the passenger van industry led to bribery issues. Therefore, in 1999 the government implemented the policy of “Passenger Van Order” and enforced passenger van regulations to eliminate competitions between the passenger vans and BMTA bus services, ensure good public transport services, and to reduce problems of the influential figures and corruption (DLT, 2003). Government determined number of passenger vans based on the political influence without considering market structure. Market structure of the passenger vans should be studied.

2.2 Regulations regarding the passenger van services

DLT and BMTA are the two main agencies to enforce the passenger van regulations. The regulations under DLT licenses and BMTA contracts are shown in Table 1. As the regulator, DLT provides seven-year license to operate the passenger van services to BMTA, monitors the passenger van services and withdraws license of routes that are below DLT standards. As authorized operator, BMTA distributes its two-year sub-contract rights to operate the passenger van services to the drivers, supervises and discards contracts of the driver, who do not follow BMTA regulations or fail to afford the concession fee, and transfers the contracts to the new driver.

Table 1: Regulation regarding the passenger van services

<p>In the DLT Transport Business Licenses, the following conditions are fixed:</p> <ul style="list-style-type: none"> - Route alignment (total 116 routes), origin and destination - A minimum and maximum range of passenger vans (passenger van quota - total 3,964-5,574 vans) - Type and colour of a passenger van (following DLT standards) and capacity (not more than 12 seats) - Daily work time (head office and local office must be open from 8.30am to 4.30pm on business day) - Operating hours (6.00am to 10.00pm) and minimum total daily trips (detailed timetable and headway are set by a terminal manager of each route) - Maximum Fare (such as, passenger vans on route 1 can charge not more than 15 baht/person/trip) <p>Note: Fares are fixed at not more than 1 baht/km for the first 10 km and not more than 0.60 baht/km for each additional km. An additional fare, not more than 5 baht/person/trip, is allowed for routes operated on expressways and toll way.</p> <p>In the BMTA contracts, the passenger van drivers have to respect the BMTA regulations as follows:</p> <ul style="list-style-type: none"> - Picking up passengers only at origins and drop off them at bus stops along routes or at destinations, asking passengers to get off before arriving at their destinations is prohibited - To operate vans outside regular routes, drivers have to get official permission from DLT and BMTA - To stop temporarily for repairing or for some reasons, drivers have to inform BMTA - Monthly concession fee (1,070 baht) must be paid to BMTA (with no subsidy) - Motor and compulsory third party insurances must be provided to passengers in case of accidents - Drivers have to follow Land Transport Act B.E. 2522 (1979) for driving disciplines

2.3 Stakeholders in the passenger van services

Before the regulations were enforced four stakeholders, i.e., passengers, drivers, investors and influential figures, were involved in the passenger van services. The investors set up terminals, determine routes between city centres and suburbs, and control the services including number of drivers, fare collection, schedules and other general rules. They behaved as unofficial regulators and required supports from the influential figures who received kickbacks in return. Main role of the influential figures was negotiating with government agencies related to bus transport. Drivers were required to pay entry fees (20,000- 100,000 baht) and membership fees (2,000- 4,000 baht/month) to the investors in order to provide services at the terminals (Eamsupawat, 1999). The passengers were not protected in case of accidents and overcharge since the services were not regulated.

After the passenger van regulations were enforced the investors, who registered as passenger van companies, continue to manage the services through terminal managers and the influential figures remained in the industry. The entry fees were changed to 10,000 - 250,000 baht and monthly membership fees were 4,000- 5,000 baht based on number of passengers on the routes (Longji, 2003). Main stakeholders in the passenger van services are the passengers, the drivers, the investors (unofficial regulators), the influential figures and the government agencies, as shown in Figure 1. At present, one passenger van route normally comprises one group of individual drivers (owner, renter and unlicensed drivers) and is unofficially controlled by one investor and influential figures.

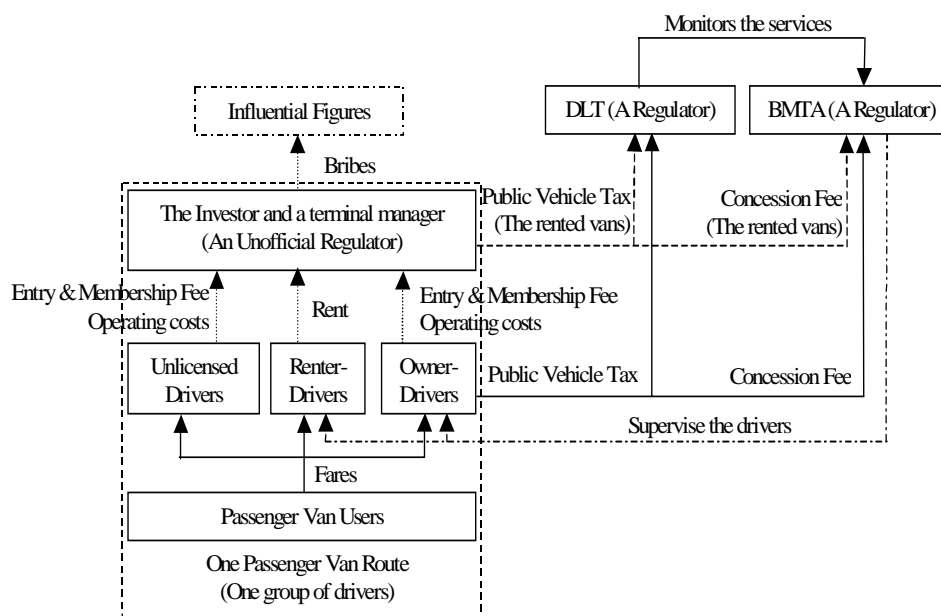


Figure 1: Relationship of the stakeholders in the passenger van services

2.4 Potential competitors of the passenger vans

Competitions in the passenger van services were assumed at two levels, on route level and on corridor level, as presented in Figure 2. On route level, since a passenger van route comprised of several licensed and unlicensed drivers, each driver considered himself as a small enterprise and attempted to balance his costs and revenues to get maximum profits, and then potential competitors of a passenger van driver were other licensed and unlicensed drivers who operated on the same route.

On corridor level, passenger vans provide similar services to other road-based public transport modes. Leopairojna and Hanaoka (2005) compared Bangkok residents data for their household incomes, mode usage, and household vehicle availability with data of respondents on passenger vans in term of their household incomes, and found that the passengers on BMTA a-c buses and on passenger vans had the same levels of household incomes and vehicle availability. The authors concluded that the potential competitors of passenger vans were BMTA a-c buses.

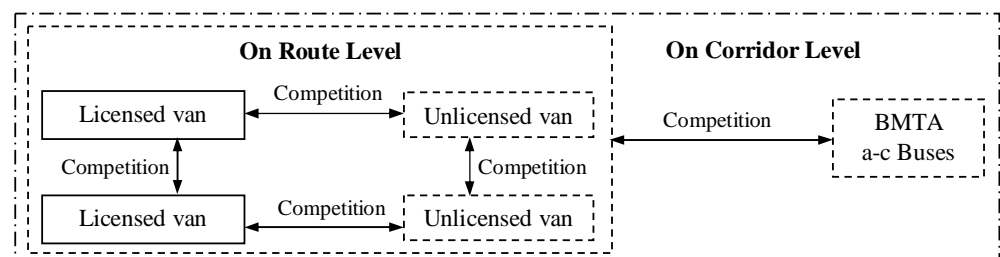


Figure 2: Assumption of Competitions in the Passenger Van Services

3. ANALYSIS OF THE PASSENGER VAN MARKET

To study market structure of passenger vans, the stakeholders were identified as the supply and demand sides. Supply side included the drivers and terminal managers, i.e., representatives of the investors or selected by the drivers, and demand side included the passengers on the passenger vans and a-c buses.

One reason that makes the government judges passenger vans as competitor of the BMTA buses is duplication of routes between both services. To verify competition between the passenger vans and a-c buses, case study areas were selected by comparing alignments of the passenger van and a-c bus routes. There were only three corridors that the two modes have the same origins and destinations and parallel alignments and thus, selected as case study areas.

Questionnaire survey was done to collect information on the supply side in terms of characteristics of the routes, the services and the drivers. Driver opinions related to the existing passenger van regulations and the future deregulated industry were interviewed. On the demand side,

information related to characteristics of the respondents and their trips, mode selections and opinions regarding the passenger van and a-c bus services, and the existing passenger van regulations were obtained. Conjoint analysis was applied to find whether preferences of the respondents on the passenger vans and a-c buses were similar or different.

3.1 Analysis of the supply side

In November 2004, 42 drivers were interviewed on one corridor and it was found that they separated into two groups due to their internal arguments (Leopairojna and Hanaoka, 2005). The two groups agreed to operate on the same route alignment, share the same terminal in the city centre and charge the same fare structure. However, there were conflicts between the two groups due to driver's misbehaviour, such as picking up passengers from bus stops and racing. The conflicts lead to fighting and lawsuits. In April 2005, 29 and 40 drivers on other two corridors were interviewed. There was no conflict among the drivers on the two corridors since they were members of the same groups. Some unlicensed vans were found during the survey.

The drivers preferred this job due to good income, flexibility, comfort and self-employed attribute. In the survey, the drivers were asked about their costs, revenues and incomes. Their incomes were high for their qualification because they earned 300-1,500 baht/day while minimum wage of labours in Bangkok was 170 baht/day and a new graduate earned about 7,000 baht/month in public sector. The data was used for calculating mark-up on cost.

Mark-up on cost is a ratio of price to marginal cost. The formula for the mark-up on cost is expressed as:

$$m = \frac{P - MC}{MC} \quad (1)$$

Where m is the mark-up on cost, P is the product price, and MC is the marginal cost. In this paper, P was revenues that a passenger driver earned from operating one trip and MC was marginal cost that the drivers spent to operate one trip including fuel costs, toll fees, and maintenances. From Table 2, the mark-ups on cost on the three corridors were varied from 63 to 89 percent, which were high values. This indicates that the fare was high and the passenger van services were low elasticity of demand, which means imperfect competitive market such as oligopoly.

Table 2: Mark-up on cost on the three corridors

Corridors	Licensed Passenger Van Drivers	Year
A	89 percent	2004
B	63 percent	2005
C	72 percent	2005

Since the passenger van services had high mark-up on cost, the drivers may reduce the fares but they did not. When oil prices increased to almost double during 2004 to 2006, the regulated fares of the passenger vans on these corridors were slightly changed. In addition, the passenger van drivers receive no subsidy from the government. Conversely, mark-ups on cost of BMTA a-c buses were negative value because of providing cheap fares. Although BMTA is subsidized by the government, BMTA increased the a-c bus fares on many times when oil prices were increased. DLT data shows that the a-c bus fares increased by 3 baht, from 8-16 baht in 2004 to 11-19 baht in 2006, while passenger van fares increased by 2 baht. The increase in a-c bus and passenger van fares were not so different but BMTA earned more revenues per trip due to higher vehicle seat capacity. Passenger vans normally carry 14 passengers, while the a-c buses have regulated capacity of 46 seats and 30 standees.

Passenger van drivers did not consider the BMTA a-c buses as their competitors because they thought their passengers were not the same attributive groups with the a-c bus passengers and they provided different qualities of services. However, BMTA and its joint-operators responded to popularity of the passenger vans by improving their services, such as revising their route alignments, providing better condition buses and giving discount to specific group of passengers to attract more passengers.

During the survey, the authors found that numbers of the passenger vans operating on the three corridors were less than numbers of the passenger vans in the allotted quota. The drivers revealed that some drivers moved to other routes or temporarily stop operating and some passenger vans were under repairing. This finding shows that the drivers observed demand on each route and moved to routes that provided more income to them. However, they did not reduce fares even if it is possible. To get maximum revenues, the drivers wait to occupy full seats before departing the terminals or attempt to get more passengers from bus stops along their routes during off-peak hours. During peak hours, though the frequency was increased, passengers waited in long queues at terminals due to insufficient number of the passenger vans.

The drivers agreed that main problem in operating the passenger van services was unfair competitions with the unlicensed vans. The competitions were unfair since the licensed drivers, who own the passenger vans, had higher costs in paying insurances, BMTA concession fee and DLT taxes. Most of the drivers wanted the unlicensed vans to be eliminated but some drivers recommended solving this problem by licensing the unlicensed vans and allowing them to operate on other new routes to reduce competitions.

3.2 Analysis of the demand side

Questionnaire survey of passenger van and a-c bus passengers was conducted on three corridors between April and May 2005. Total 726 respondents- 348 and 378 respondents boarding on the passenger vans and

a-c buses completed the questionnaires, respectively. Results of the survey showed that majority of the respondents on the passenger vans were females (63%), working adults (51%) and 21- 30 years old (41%). They were middle-income class, household incomes higher than the average of Bangkok (57%) and had private vehicles (83%) but they had no personal vehicles (64%). The main trip purpose was to work or attend schools (51%) and travelling distance was the whole routes (78%).

For the respondents on the a-c buses, percentages of male and female respondents and age groups, that were younger than 20 years old and 21- 30 years old, were not so different. Majority of them had families with household incomes higher than the average of Bangkok (47%) and had private vehicles (82%) but they had no personal vehicles (68%). The larger proportion of them was students (62%) who travelled by the a-c buses to work or attend schools (49%) and travelling distance was shorter than half of the whole routes (50%).

Chi-square test shows that, at 95% confident level, distributions of household incomes, household vehicles and trip purposes of the respondents on the passenger vans and a-c buses were not different. Distributions of genders, age groups, occupations, and frequencies of travel were different but these characteristics were not significant. It was concluded that the respondents on the passenger vans and a-c buses were in the same attribute groups who had household incomes higher than the average household income of Bangkok and had private vehicles in their households but used public transport for commuting or going to school.

In mode selection surveys, under assumption that these passenger van routes stopped operating, 73% of the respondents on the passenger vans would change to the a-c buses. Under assumption that the passenger van fares were increased, 51% would continue travelling by the passenger vans while 37% would change to the a-c buses. For the respondents on the a-c buses, under assumption that these a-c bus routes stopped operating, the respondents would change to the passenger vans (53%) and non a-c buses (29%). Under assumption that the a-c bus fares were increased, 62% of them would continue travelling by the a-c buses while 22% and 10% would change to the passenger vans and non a-c buses, respectively.

The respondents on the passenger vans and a-c buses were asked for their opinions about regulated fares, planned service schedules, consistency of planned and actual schedules, allowing passenger van drivers to pick up passengers from bus stops along routes, and over regulated capacity. Chi-square test shows that, at 95% confident level, distributions of opinions of the respondents on the two modes were not different. Majority of them agreed that new passenger van drivers should be allowed to register for the licenses without limitation of the passenger van quota because number of

the passenger vans need to be increased to meet demand of the passengers, it would provide more alternatives for the passengers, the passengers would be protected and it would lead to competition in terms of fare reduction and quality improvements.

For preferences of the respondents, conjoint analysis showed that the respondents on the two modes had similar preferences. Their major concerns in selecting their modes were comfort (seat availability), convenience (no transfer to other vehicle(s) to complete the trips) and short travelling time while prices (fares) were considered but not of importance. Although their preferences were similar but they selected different modes due to some other reasons, such as they selected the a-c buses when they were travelling only on some parts of the route, their origins or destinations were not served by the passenger vans and they were uncomfortable with narrow space of the passenger vans.

3.3 Market structure of the passenger van services

Based on characteristics of market structures by the view points of Producers (operators), Users (passengers), Entry Barriers, Products and Services, and Relationship of the operators, the market structures of the passenger vans on route and corridor levels were imperfect competitive markets. Comparing characteristics of the passenger van services with the imperfect competitive markets revealed that characteristics of the passenger vans on route level are mixed between oligopoly and monopolistic competition markets, while characteristics of the passenger vans at corridor level are similar to an oligopoly market.

On route level, data from the supply side shows that a passenger van route comprised many drivers and they considered themselves as small firms. They had many middle-income passengers. Their services were separated as licensed and unlicensed services. Entry of driver was controlled by the investor entry fee and the government entry regulation. To get maximum profits, the drivers agreed to charge the same fares, i.e., the maximum regulated fares since they do not want to compete each other. Actions of a driver such as improving vehicle conditions have negligible effects on incomes of other drivers because passengers waited for a passenger van in a queue and boarded on any passenger van without considering vehicle conditions. Data from the demand side shows that the respondents considered the passenger van drivers as the same operator(s) provided similar express services with guaranteed seats. Therefore, market structure of the passenger van services on route level is considered as oligopoly with an implication of collusion, as shown in Figure 3.

On corridor level, data from the supply side shows that one corridor comprised of two main groups of producers, the passenger van drivers and BMTA with its joint-service operators. The passenger van drivers claimed that their passengers were in different attribute group compared to the a-c bus passengers. However, passenger characteristics in this study show that

the respondents on the passenger vans and a-c buses were in the same attribute group and had similar opinions and preferences. The passenger van operators and BMTA provided similar but not identical services, i.e. both services provide vehicles with a-c but the passenger vans offered express services with guaranteed seats and higher fares while BMTA buses provide slow services with not guaranteed seats but cheaper fares. Popularity of the passenger van services encouraged BMTA to improve their services, but there was no price competition. Data from the demand side shows that the respondents selected to travel with either BMTA a-c buses or the passenger vans based on comfort, convenience, travel time and their origins and destinations. Mode selection survey shows that the respondents considered the passenger vans and a-c buses as substitutes. Therefore, market structure of the passenger van services on corridor level is considered as oligopoly with implication of product differentiation, as shown in Figure 3.

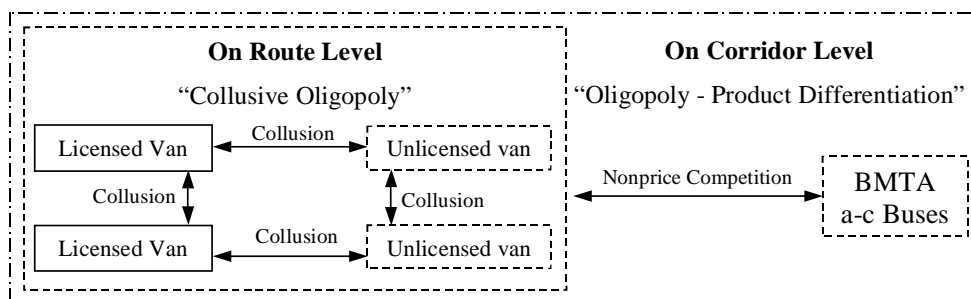


Figure 3: Market structure of the passenger van services

4. CONCLUSION

Market analysis of the passenger van services under the existing regulations showed that there was no price competition at the route and corridor levels. On the route level, the passenger van market was an oligopoly market with implication of collusion. At the corridor level, the market was an oligopoly market with implication of product differentiation. It was observed that the existing entry regulation initiated collusion in the services. Negative impacts of collusion on the passengers of the passenger vans were also observed. The main negative impact was remaining of unlicensed passenger vans. Therefore, removing the passenger van quota, i.e. deregulating only the entry regulation while maintaining maximum prices and safety regulations, was recommended to allow the unlicensed passenger vans to get the licenses and the passengers would be protected in case of accidents.

REFERENCES

- Office of Transport and Traffic Policy and Planning (OTP)., 2004. *Transport data and model center II (TDMC II)*, Bangkok, Thailand.
- Department of Land Transport (DLT)., 2003. *A summary of passenger vans regulating in Bangkok and neighbouring provinces*. Ministry of Transport, Thailand. (In Thai)

Leopairojna, S. and Hanaoka, S. (2005). Market structure of passenger vans in Bangkok. *Journal of the Eastern Asia Society for Transportation Studies* 6, 4192 - 4207.

Eamsupawat, B. (1999). *The factors affecting the transportation pattern of van pooling in Northern Bangkok Metropolis*. CU Master Thesis ISBN 974-334-801-8, Chulalongkorn University (CU), Bangkok, Thailand. (In Thai)

Longji, S. (2003). *A study of bribery in passenger van business*. People's Fund for Exposing Corruption (PFEC), Bangkok, Thailand. (In Thai)

EVALUATION OF EFFECTIVENESS OF PEDESTRIAN OVERPASSES IN DHAKA METROPOLITAN

DR. MD. MIZANUR RAHMAN
Bangladesh University of Engineering and Technology,
Bangladesh

MUHAMMAD ASHIKUL ISLAM
Bangladesh University of Engineering and Technology,
Bangladesh

MD. KAMRUL HASAN RIZVI
Bangladesh University of Engineering and Technology,
Bangladesh

ABSTRACT

A study had been carried out to evaluate the effectiveness of pedestrian overpasses in Dhaka metropolitan, the capital city of Bangladesh. An investigation was carried out on five major overpasses at five different locations of Dhaka metropolitan namely, New Market, Farmgate, Shyamoli, Mirpur-10 and Airport. Data were collected through a questionnaire survey among the overpasses user and also the pedestrian who violated traffic rules and not using the overpasses.

The overpasses of the selected locations were analyzed according to the collected data to evaluate the effectiveness in terms of their usage. The highest percentage of pedestrians, using overpass (85%) was found at Farmgate while the highest percentage of pedestrians not using overpass i.e. violators (65%) was found at Shyamoli. The pedestrian interview data revealed that the reasons for not using the overpasses are as follows: time consuming (54%), hard to climb up (13%), lack of enforcement (6%), not secured at night (7%), obstacle by hawkers (6%). The level of service standard and the capacity of the selected overpasses were also determined in this study.

1. INTRODUCTION

In context of Bangladesh, pedestrians form the largest single road user group. This is primarily because of lack of sufficient transportation facilities and poor economic condition of the people. Increasing urbanization tends to generate, additional traffic volume and hence the pedestrian problems associated with their movement. Many Asian cities have made only 5 to 10% of their urban areas available for transportation facilities, as against 20 to 30% of the urban areas in Western cities. Under this circumstance, there are inadequate transportation facilities for both vehicular traffic and

pedestrian traffic. As a result, the vehicular traffic have had to force their way through narrow, unpaved streets as such the pedestrian traffic have to face different types of difficulties during their movement.

In uncontrolled traffic area it was observed that pedestrians try to cross the roadway across the travel way haphazardly. This type of movement can be reduced to some extent with the provision of pedestrian facilities such as zebra crossing, pedestrian overpass, pedestrian underpass etc. The regulation and control of pedestrians is an important factor that must be considered in the context of overall urban and transportation planning and management process. Being physically unprotected, pedestrians are the most vulnerable group. A large portion of the pedestrian community is either young or elderly each of which has specific problems associated with their respective group. These problems involve either the lack of fully developed facilities or a reduction in optimum facilities due to the aging group.

Hoque (1981), conducted a study on accident type analysis in Dhaka metropolitan and found that, the pedestrian involve accidents constitute the largest category of accident type accounting for about 17% of the total accidents. It is evident that pedestrian accident while crossing the roads is the greatest problem in Dhaka metropolitan. This had clearly indicated that the problem is associated with ignorance of right of pedestrians as well as the lack of road sense of the road users. It was also observed that the pedestrian crosswalks are missing at locations where these are urgently needed because of extensive pedestrian movements. This had necessitated studying the behavior of driver and pedestrian to assess their attitudes towards development of effective measure of safe movements with least interference. Examination of all pedestrian accidents by hour of day disclosed two distinct peaks during 8 a.m. to 10 a.m. with a later peak during 4 p.m. to 8 p.m. This showed the little early peak hour to pedestrian accident in morning compared to that of all accidents. This is primarily due to the reason of greater pedestrian activities at this hour particularly for the generation of trips to schools, markets, as well as to work. The pedestrian movement and characteristics therefore need to be well studied. This task is not so simple and need considerable research towards development of effective devices for the mobility and safety of pedestrians.

The various types of pedestrian facilities that have already been used through out the world are basically to ensure safety and comfort for the pedestrians. These facilities may be classified into three major groups; depending on whether or not pedestrian and vehicle are separated (Victor, 1979). Integrated systems are currently adopted system with side walk provided parallel with the carriageway and cross walks provided at intervals (Zebra crossing, Signalized Zebra crossing, Side walks, Islands). Horizontal separation system located away from the vehicle network accommodates pedestrian movement along pathway that is interdependent on vehicular path (Widened sidewalk, Full malls, Auto free zones, Displaced grids). Vertical separation system is perhaps the most efficient system. The three

primary elements of vertical separation are: Underground, Elevated and At-grade system. In this system conflict with other road users are eliminated.

2. CHARACTERISTICS OF DATA COLLECTION SITES

In the Dhaka metropolitan area a number of overpasses have been installed at different locations on the basis of necessity of pedestrian crossing. All these locations are not equally important according to the volume of the pedestrian. In order to select the locations of the pedestrian overpasses the following factors are considered: importance of the location, amount of pedestrian volume and suitability for the study. In this way five locations were selected for this study (*NewMarket overpass, Shyamoli overpass, Mirpur-10 overpass, Farmgate overpass and Airport overpass*). All these locations are important and busy areas. Different kinds of people move to these place for a lot of purposes. New Market is always filled with a lot of buyers. Farmgate is the center of Dhaka city, where a lot of commercial activities always take place. Shyamoli is newly developed busy region with a mixed land uses area. Mirpur-10 has a very important intersection and Zia International Airport is very important for its air navigation facilities. Amount of pedestrian volumes at these locations are significant as well as suitable for the study. The locations of these overpasses are shown in Figure 1.



Figure 1: Locations of Study Area on Dhaka City's Map

The characteristics of study locations are presented in Table 1.

Table 1: Characteristics of data collection site

Name of Overpass	Location	Width of Overpass (ft)	Height of Overpass (ft)	Pedestrian volume (ped/hr)
New market	Dhanmondi	9.5	18	318
Shyamoli	Mohammedpur	9.5	20.5	179
Mirpur - 10	Mirpur	9.0	21	385
Farmgate	Tejgaon	10.0	20.6	649
Airport	Cantonment	11.0	21	581

Two types of data are collected for this study. To observe the pedestrian behavior pedestrian volume is counted in two groups, using overpass and not using overpass. All data were collected at morning peak (7 AM to 10 AM) and evening peak (4 PM to 7 PM) for three working days. To gather the pedestrian's views a questionnaire survey was conducted at all the selected sites. The pedestrian opinion survey is an important component of this study. The purpose of this is to find out the causes of not using the existing overpasses. For this purpose about 500 pedestrian were interviewed. The method used was random sampling. A prepared questionnaire was used to interview pedestrians.

3. PEDESTRIAN BEHAVIOR

At the selected locations to observe the pedestrian behavior numbers of pedestrians were counted in groups of those using overpass and not using overpass. This data were recorded on hourly and gender basis. Table 2 presents the flow characteristics of pedestrians.

As shown in Table 2, the highest proportion of pedestrians using overpass was at Farmgate location (85%) followed by Airport location (79%) and the maximum number of pedestrians not using overpass was at Shyamoli location (65%) followed by New Market location (57%). At Mirpur-10 location 60% pedestrians were using overpass. From the field observation it was evident that at Farmgate location pedestrians were forced to use overpass as there are fencing all around the roads at this site. At Airport location the average speed of vehicles is too high for pedestrians to cross the road, and the width of the roads at this site is high which forced pedestrians to use the overpass. The maximum number of female pedestrians using overpass was found at New Market, Shyamoli and Mirpur-10 locations. At New Market there are various markets which attracts

women, on the other hand at Shyamoli and Mirpur –10 locations there are a lot of garment factories so garment workers are using the overpass. Also at Mirpur-10 location there are maximum number of female pedestrians who are not using the overpass.

Table 2: Pedestrians Flow Characteristics at Study Sites

Name of overpass	Pedestrians using overpass			Pedestrians not using overpass		
	Male	Female	Total	Male	Female	Total
New Market	1301 (68%)	611 (32%)	1912 (43%)	2143 (85%)	391 (15%)	2534 (57%)
Farmgate	3629 (93%)	263 (7%)	3892 (85%)	657 (93%)	51 (7%)	708 (15%)
Shyamoli	721 (67%)	351 (33%)	1072 (35%)	1805 (91%)	187 (9%)	1992 (65%)
Mirpur -10	1549 (67%)	759 (33%)	2308 (60%)	1186 (79%)	322 (21%)	1508 (40%)
Airport	3097 (89%)	389 (11%)	3486 (79%)	1169 (90%)	137 (10%)	1306 (21%)

4. PEDESTRIAN VIEW

In general, pedestrians tend to walk along a path that represents the shortest distance or most convenient route among several routes. They often cross at mid-block instead of using overpass or underpass. In this study, the pedestrians for different locations have their own point of view for not using the overpass. The reasons are: time consuming, hard to climb up, no median fencing, not so secured specially at night, physically not fit, risky for movement, obstacle by hawkers, vendor and so on. Table 3 presents the causes for not using overpass by pedestrians.

From Table 3 it is found that the highest percentage of pedestrian (54%) is not interested to use overpass just because of more time required to cross the road. Other reasons are: hard to climb up (13%), lack of enforcement (6%), not so secured at night (7%), physically not fit (5%), no median fencing (5%), obstacle due to hawker (6%).

Table 3: Cause for not using the overpass by the pedestrian

Causes	New market	Farm-gate	Shya -moli	Mirpur-10	Air-port	Total	(%)
Time Consuming	50	51	47	79	69	296	54
Hard to climb up	0	37	17	11	6	71	13
Lack of enforcement	0	16	0	11	5	32	6
Not so secured specially at night	7	0	16	13	0	36	7
Far away	0	0	0	0	19	19	3
Physically not fit	5	3	14	5	1	28	5
No median fencing	28	0	0	0	0	28	5

5. CAPACITY OF OVERPASS AND LEVEL OF SERVICE

The actual capacity of an overpass can be determined using the information of pedestrian speed and pedestrian module. The formula established so is given below.

$$\text{Capacity/Hour} = \frac{\text{Width(ft)} * \text{Speed(ft/min)} * 60}{\text{Pedestrian module(ft}^2\text{/ped)}} \quad (\text{HCM, 2000})$$

Table 4: Theoretical Capacity and Level of Service

Location	Width (ft)	Observed Capacity /Hr	Theoretical range of Capacity/Hr	Level of Service	Pedestrian Module (ft ² /ped)
New Market	9.5	318	Below 1140	A	130
Farmgate	10	649	Below 1200	A	130
Shyamoli	9.5	179	Below 1140	A	130
Mirpur-10	9	385	Below 1080	A	130
Airport	11	581	Below 1320	A	130

In this study the flow volume of the pedestrian, those using the overpass and the violators who are not using it were recorded. The level of service standard and capacity were determined to know about the serviceability. These parameters are functions of the width of the overpass.

Therefore, the capacity per hour corresponding to level of service was calculated for different widths of the overpass as found in the study. Observed volume of pedestrian that uses the overpass had been compared with the theoretical capacity to find the level of service and pedestrian module thereafter. The results are presented in Table 4.

Table 4 shows that a level of service standard A is maintained in all five major overpasses during the peak hour. This may be due to the reason that most of the roads do not have continuous median barrier and overpasses are not adjacent to the intersection. Pedestrian get a wide area to cross the road illegally. That's why, a level of service standard A is found, even in the peak hour.

6. FIELD OBSERVATIONS

At New Market, only 43% are using the overpass and the rest 57% are not using it. It reflects that pedestrians at this point tend to cross the road under the overpass since median fencing is not continuous. People prefer the shortcut under the overpass whereas all the stairs to climb up the overpass is heavily crowded. At Farmgate, median fence is continuous and pedestrian have very little opportunity other than using the overpass. At Shyamoli, only 35% pedestrians use the overpass just because of a wider area of crossing. Similarly, some of the pedestrians cross the road by the roundabout at Mirpur-10. Median fencing is continuous at Airport, but people cross through the intersection just in front of the airport. The following images display some scenario and overpass condition of Dhaka City.



Figure 2: Pedestrian crossing the road illegally during green period (Farmgate)



Figure 3: Random crossing interrupts the vehicular flow (Newmarket)



Figure 4: Pedestrians are chasing vehicle under new market overpass



Figure 5: Pedestrians like shortcut rather than using the overpass

7. CONCLUSION

The overpasses of the selected location are analysed according to the collected data to evaluate the effectiveness in terms of their usages. The percentage of pedestrian using the overpass and the number of violators are determined at each location. The investigated regions are NewMarket, Farmgate, Shyamoli, Mirpur-10 and Airport. The result of the studies on the overpasses has been discussed so far. This result on the effectiveness of the overpasses may lead to a better design of the overpass facilities in the future. Based on the study, the following conclusions are made:

- The overpass user is maximum at Farmgate which is around 85%, whereas it is minimum at Shyamoli which is only 35%.
- In most of the location, pedestrians get the opportunity and independence to cross the road according to their wish.
- From the field study, it is evidenced that male pedestrians are more encouraged to use overpass rather than female pedestrians.
- The higher the opportunity to alter the way other than overpass, the lower the number of pedestrian using the overpass.
- It is observed by the study results that reluctance to use the overpass is higher when the amount of time needed to complete the overpass is long.
- Level of service standard is A for all the five overpasses, which showed that the overpasses are flowing less than the capacity

8. RECOMMENDATION

Some drawbacks and limitations were chalked out while carrying out the study. Analyzing the data it was found that the reasons are the absence of median fencing, lack of intention to use the present facilities, less awareness about the safety. From the above viewpoint, to get a better performance from the pedestrian and to make the best possible use of the overpasses the following recommendations are made.

1. Locations of the overpasses have to be eventually distributed. According to the engineers of Dhaka City Corporation, some political and other influence sometimes shifts the overpass from the required location. So the location should be selected as per the necessity of the location.
2. In maximum areas, pedestrians get the opportunity and independence to cross the road according to their wish. So most of them can consider overpass use as time consuming. Therefore, continuous median-barrier is a way to improve the usage of overpass effectively.
3. As we do not have required number of overpasses, the least used overpasses can be shifted to an important location having more demand of an overpass.

4. Road safety education is necessary for every road user to behave better as a pedestrian and to increase the intention to use the existing facilities to be safer.
5. Maintenance work of the overpass should be carried out in a regular manner and cleanliness should be checked daily.
6. Enforcement should be used to wipe out the hawkers and the mobile shops on the overpasses that creates obstacle to the pedestrians.

REFERENCES

Abraham, P.C. (1974), *An Urban Transportation Planning Methodology for Developing Countries: A Thesis*, Asian Institute of Technology, Bangkok, Thailand.

Fruin (1970), *Designing for Pedestrians, A Level of Service Concept*, Dissertation, Polytechnique Institute of Brooklyn, January, 1970.

Hasib, M.M. (1990), *A Study of Mass Transit in Metropolitan Dhaka*, A Thesis, Department of Civil Engineering, Bangladesh University of Engineering and Technology, Dhaka.

Highway Capacity Manual (1985), Transportation Research Board Washington D.C.

Hoque, M.M. (1981), *Traffic Accidents in Dhaka: A Study on Roadway, Safety, Research Report*, Bureau of Research Testing and Consultation, Bangladesh University of Engineering and Technology, Dhaka.

Hoque, M.M. (1981), *Pedestrian Accidents and Road Users Behavior: Some research Findings in Dhaka City*. Paper Presented at the 26th Annual Convention in the Institute of Engineers, Bangladesh.

Paul H. Wright, Radnor J. Paquette (1979), *Highway Engineering*, 4th Edition

Peter J. Moses (1990), *The Vulnerable Road Users- The Pedestrian: 6th Road Engg. Association of Asia and Australia, Conference Proceeding*, Vol. no. 2, 1990.

Victor, D.J. (1979), *Facilities for Pedestrian and Cyclists: Advanced Course on Urban Transportation Management*, Department of Civil engineering, Indian Institute of Technology.

ROAD TRAFFIC ACCIDENTS AND INJURIES: A SERIOUS SAFETY CONCERN IN URBAN AREAS OF BANGLADESH

MD. MAZHARUL HOQUE

Professor, Department of Civil Engineering
and Director, Accident Research Centre (ARC)
dirarc@arc.buet.ac.bd

SHAHNEWAZ HASANAT-E-RABBI¹ and S. M. SOHEL MAHMUD²

Research Assistant, Accident Research Centre (ARC)
romel157@yahoo.com

CHOWDHURY KAWSAR AREFIN SIDDIQUI¹
and SABREENA ANOWAR²

Junior Research Fellow, Accident Research Centre (ARC)
kawsar_arefin@yahoo.com

ABSTRACT

The combination of rapid urbanization and motorization has been a key cause of numerous transport problems in developing cities in Asia. It has resulted in deterioration in accessibility, service levels, safety, comfort, operational efficiency, and the urban environment. This is particularly prevalent in Bangladesh with current urbanization level at around 25 percent. Urban road traffic accidents and resulting deaths has now emerged one of the major safety problems in urban areas all over the world. In 2002 nearly 1.2 million people worldwide died as a result of a road traffic crash. This represents an average of about 3300 persons dying each day around the world. In addition to these deaths, between 20 million and 50 million people globally are estimated to be injured or disabled every year. The majority- around 88 percent- occurs in the so-called developing and emerging countries. Accident rates in developing countries are often 10 to 70 times higher than in developed countries. The vast majority of road accident fatalities comprise vulnerable road user viz. pedestrians, bicyclists and motor cyclists, and they are most prevalent in urban areas. The road safety problems appear to be much more severe than the other violent causes and natural disasters. With the increasing complexities of urban roads and transport problems it is clear that one of the today's biggest challenges of transport engineering professionals is to address the issues of urban road safety with due urgency. This paper presents an overview of the scale and characteristics of the road traffic accident and injury problem in developing countries, with a special reference to the situation in urban areas in Bangladesh. The paper in particular highlights the contemporary road safety issues and the commensurate solution strategies for achieving sustainable and safer urban transportation system in Bangladesh with due regards to the needs and requirements for safety of vulnerable road users, pedestrian in particular.

1. THE PROBLEM OF ROAD TRAFFIC ACCIDENTS AND INJURIES

1.1 The scale of the problem

In 2002 nearly 1.2 million people worldwide died as a result of a road traffic crash. This represents an average of about 3300 persons dying each day around the world. In addition to these deaths, between 20 million and 50 million people globally are estimated to be injured or disabled every year. Around 88 percent of those deaths occur in the developing world (Mackay, 2003), even though these countries only account for 32 percent of the total motor vehicle fleet worldwide (Hoque et al, 2001). For every death, there are far greater numbers of injuries- four persons with severe/permanent disabilities, ten persons requiring hospital admission, and thirty persons requiring emergency room treatment. It is estimated that road traffic injuries will be the third leading cause of life years lost by 2020 (Table 1). Indeed, they are the second leading cause of death for people aged 5 to 25, with devastating impact on families and communities. For all these reasons, road traffic injuries are an important obstacle to development and place an enormous strain on a country's health care system, and on the national economy in general (Ban Ki-Moon, 2007).

Table 1: Change in Rank Order of Disease Burden for 10 Causes (1990-2020)

Ranking	1990 Disease or Injury	2020 (Baseline scenario) Disease or Injury
1.	Lower Respiratory infections	Ischaemic heart disease
2.	Perinatal conditions	Unipolar major depression
3.	Diarrhoeal diseases	Road Traffic Injuries
4.	HIV/AIDS	Cerebrovascular diseases
5.	Unipolar major depression	Chronic obstructive pulmonary diseases
6.	Ischaemic heart disease	Lower Respiratory infections
7.	Cerebrovascular diseases	Tuberculosis
8.	Malaria	War
9.	Road Traffic Injuries	Diarrhoeal diseases
10.	Tuberculosis	HIV/AIDS

Source: WHO. Evidence, information and policy, 2000)

Furthermore, according to World Health Organization (WHO) data for 2002, these road traffic accident deaths accounted for 23 percent of all injury deaths world wide (Figure 1).

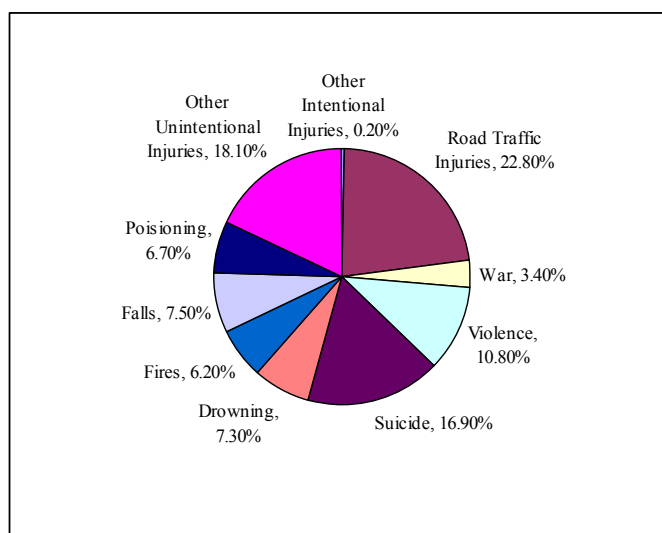


Figure 1: Distribution of global injury mortality by cause (Source: WHO Global Burden of Disease Project, 2002, Version 1)

Even when deaths by various violent causes are considered, road traffic accident is found to be the leading cause accounting for 33 percent, 36 percent and 56 percent of the deaths in developed, developing and Middle-Eastern countries respectively (Table 2).

Table 2: Fatalities by Violent Causes in different regions

Cause	Developing Countries	Developed Countries	Middle Eastern Countries
Fire	2.0	3.0	1.0
Drowning	7.0	2.0	2.0
All other violent causes	20.0	26.0	26.0
Suicide	9.0	33.0	5.0
Homicide	26.0	3.0	10.0
Road Traffic Accident	36.0	33.0	56.0
Total	100%	100%	100%

Source: (Jacobs & Palmer, 1996)

The road safety problem appears to be much more severe compared with other natural disasters such as earthquake, cyclone, tsunami etc. Table 3 shows a list of some of the major disasters and the resulting fatalities. In last 35 years, there were ten major natural disasters which claimed about 1.4 million lives with an average 140,000 deaths per disaster while road traffic accidents alone account for 1.2 million deaths each year of which nearly 50 percent are in the Asia Pacific region with a clear sign of rapid increasing trends. Therefore, it is obvious that road traffic accidents are more serious hazards than other natural disasters.

Table 3: Some major disasters and fatalities in the region

Year	Type of natural disaster	Place	Deaths
1970	Cyclone	Bangladesh	500,000
1976	Earthquake	Tangshan, China	255,000
1988	Earthquake	Spitak, Armenia	25,000
1990	Earthquake	Northwestern Iran	35,000
1991	Cyclone	Bangladesh	140,000
1999	Earthquake	İzmit, Turkey	17,118
2001	Earthquake	Gujrat, India	20,085
2003	Earthquake	Bam, Iran	31,000
2004	Tsunami	Indonesia	283,106
2005	Earthquake	Kashmir	80,000

Source: United States Geological Survey (USGS)

1.2 Road traffic accidents in developing countries

The safety situation in developing countries is rapidly deteriorating with increasing number of road deaths, largely as a direct consequence of rapid growth in population, motorization and urbanization and lack of investment in road safety. While the road accident situation are slowly improving in the industrialized societies (e.g. Australia, UK, USA), most developing countries are experiencing a worsening situation. According to UNESCAP (United Nations Economic and Social Commission for Asia and the Pacific) in 2006 more than half a million people were killed (50 percent of total global fatalities) and 20-30 million injured in road crashes in Asia and the Pacific region at an economic cost of some US\$100 billion. Whereas highly motorized countries' (North America, Australia, New Zealand, Japan and Western Europe) contributes only 12 percent (GRSP). Accident deaths rates in developing countries are often 10 to 70 times higher than in developed countries. The vast majority of road accident fatalities comprise vulnerable road user viz. pedestrians, bicyclists and motor cyclists, and they are most prevalent in urban areas.

It should be noted that road traffic injuries affect mostly the young and the middle age people in the society. In the low and middle income countries and in the South-East Asian region, road traffic injuries are the 6th leading cause of death for all age group (Table 4). From this Figure, it is also found that road traffic injuries ranked the 1st and 3rd leading cause of death for age group 15-29 years and 30-44 years respectively. These age groups represent the main working groups for each country.

Table 4: Leading cause of death in South-East Asian region and other low and middle income countries

Rank	0-4 Years	5-14 Years	15-29 Years	30-44 Years	45-59 Years	≥60 Years	All Ages
1	Lower respiratory infections 176921	Diarrhoeal diseases 18520	Road traffic injuries 53535	Tuberculosis 48762	Ischaemic heart disease 80527	Ischaemic heart disease 316195	Ischaemic heart disease 430062
2	Diarrhoeal diseases 108636	Lower respiratory infections 17790	Tuberculosis 37872	HIV/AIDS 38965	Tuberculosis 70260	Cerebrovascular disease 255251	Cerebrovascular disease 339328
3	Low birth weight 106415	Childhood-cluster diseases 16120	HIV/AIDS 33771	Road traffic injuries 36097	Cerebrovascular disease 55630	Chronic obstructive pulmonary diseases 102826	Lower respiratory infections 332940
4	Childhood-cluster diseases 89015	Road traffic injuries 9451	Fires 15620	Ischaemic heart disease 25369	Cirrhosis of the liver 23607	Lower respiratory infections 102065	Tuberculosis 257614
5	Birth asphyxia and birth trauma 82122	Tuberculosis 8067	Self-inflicted injuries 12521	Cerebrovascular disease 17801	Hypertensive heart disease 22826	Tuberculosis 89129	Diarrhoeal diseases 198178
6	Congenital heart anomalies 43408	Fires 6334	War injuries 12124	Cirrhosis of the liver 16319	Road traffic injuries 18524	Hypertensive heart disease 87439	Road traffic injuries 140405
7	Annencephaly 18009	War injuries 4765	Lower respiratory infections 8337	Diarrhoeal disease 13010	Diabetes mellitus 18224	Diabetes mellitus 66938	Chronic obstructive pulmonary diseases 123881
8	Protein-energy malnutrition 9605	Drowning 3996	Ischaemic heart disease 7278	Lower respiratory infections 12562	Breast cancer 16358	Nephritis and nephrosis 37811	Hypertensive heart disease 120571
9	Endocrine disorders 9252	Nephritis and nephrosis 2500	Rheumatic heart disease 7151	War Injuries 12254	Trachea, bronchus, lung cancers 15292	Diarrhoeal diseases 36857	Childhood-cluster diseases 115110
10	Meningitis 8888	Rheumatic heart disease 2332	Diarrhoeal disease 6731	Fires 10929	Lower respiratory infections 15263	Trachea, bronchus, lung cancers 35203	Low birth weight 106423
11	Road traffic injuries 7891	Congenital heart anomalies 2304	Nephritis and nephrosis 6417	Nephritis and nephrosis 10088	Mouth and oropharynx cancers 14990	Cirrhosis of the liver 25512	Diabetes mellitus 93782
12	Spina bifida 6479	Malaria 1831	Cerebrovascular Disease 6096	Breast cancer 9413	Nephritis and nephrosis 14898	Alzheimer and other dementias 21257	HIV/AIDS 83099
13	Alzheimer and other dementias 5765	Leukaemia 1764	Malaria 5727	Self-inflicted injuries 9394	Chronic obstructive pulmonary diseases 14720	Liver cancer 19982	Birth asphyxia and birth trauma 82562
14	Nephritis and nephrosis 5592	Falls 1753	Interpersonal violence 5431	Hypertensive heart disease 8139	Diarrhoeal diseases 14422	Mouth and oropharynx cancers 19391	Nephritis and nephrosis 77308
15	Drowning 4615	Meningitis 1749	Maternal haemorrhage 4885	Malaria 6782	Liver cancer 12785	Asthma 18867	Cirrhosis of the liver

Source: Global Burden of Disease Project for 2000, Version 1

The traffic safety patterns in developing countries are much more complex than those in developed countries. Among the selected developing countries, Bangladesh has the lowest level of motorization (2.3), but the fatality per 10,000 motor vehicles is the highest. The percent of decreasing trends of fatalities per 10,000 motor vehicles is remarkable in Thailand (-79%) and Malaysia (-89%) within the period of 1996 to 2003 whereas in Bangladesh the same index increases about 15 percent during this period (Table 5). The fatality index (deaths divided by total casualties as a percentage) is also highest in Bangladesh (0.7) among the selected developing countries. It is also revealed that pedestrians are most vulnerable road user group in developing countries, particularly in Bangladesh.

Table 5: Distribution of Road Accident Fatalities of Selected Developing Countries with Bangladesh

Country	Fatalities	Motorization level	Two/three wheelers (% of total)	Fatality per 10,000 MV	% Pedestrian Fatalities	Per capita fatality rate	Fatality index	% change of fatalities / 10,000 MV
India (2003)	85998	63	na	12.8	10	8.1	0.21	-37
Indonesia (2005)	11610	98	75%	5.1	na	9.5	na	-34
Nepal (2001)	1987	20	65%	42.0	50	8.3	0.06	na
Sri Lanka (2005)	2306	133	60%	9.1	32	12.1	0.05	-48
Thailand (2002)	13116	381	68%	5.3	6	20.4	0.14	-79
Myanmar (2003)	1308	22	68%	13.8	na	3.1	0.24	46
Malaysia (2003)	6282	651	48%	4.2	na	27.2	0.02	-89
Bhutan (2005)	23	13	24%	7.7	59	1.0	0.02	-10
Bangladesh (2003)	3334	2.3	67%	116	51	2.7	0.70	15.0

Source: World Bank, TRL, ESCAP road safety statistics

1.3 The urban accident problem

Generally, the road accident problem is disproportionately greater in urban areas than in rural areas (Lundebye 1995). This can be seen with respect to the situation in different cities of developing countries:

- Santiago (Chile): With 35% of Chile's population and 43% of registered vehicles has about 50% of all accidents.
- Sao Paulo (Brazil): With 7% of Brazil's population and 17% of vehicles has about 24% of road traffic injuries.
- Harare (Zimbabwe): Accounted for 43% of road accidents with a population of 12%.
- Metropolitan Dhaka (Bangladesh): Accounted for nearly 23 % of reported road accidents with a population of 7.3%.

Evidence suggested that large proportions of road accidents in cities are concentrated on the main street network. There are still many "blackspots" in urban areas which are amenable to site specific treatments. Up to 70 percent of urban road accident deaths are often pedestrians alone. For example, according to the latest data, Hong Kong had the highest share of pedestrian fatalities, representing 67 percent. Pedestrians were involved in 62 percent of the total fatal accidents reported in Dhaka, 47 percent in the Republic of Korea, 45 percent in Sri Lanka and 43 percent in Fiji (Ross Silcock and TRL 1997). Pedestrian were high in Middle Eastern countries, around 50 percent. The comparable figure for European countries is around 20 percent. Motorcycle accidents also have become or are rapidly becoming a serious problem in some countries, for example in Malaysia, motorcycles accounted for 57 percent of the fatal accidents and 74 percent of the injury accidents in 1994.

2. ROAD TRAFFIC ACCIDENTS AND INJURIES IN BANGLADESH

According to the official statistics, in Bangladesh there were at least 35833 fatalities and 18029 injuries in 32845 reported accidents from 1998 to 2006. The number of fatalities has been increasing from 1009 in 1982 to 3830 in 2006, nearly 3.8 times in 25 years period. It is estimated that the actual fatalities could well be 10000-12000 each year (Hoque 2005).

The statistics revealed that Bangladesh has one of the highest fatality rates in road accidents. As a consequence of these road traffic accidents, the nation is suffering a huge loss of the order of Tk. 5000 crore/US\$ 850 annually, which is nearly 2 percent of country's GDP. Accident victims are mostly young and middle age people (5-44 years) and they are the most economically active and productive group in the society. These tragic losses generate serious consequences for family lives of the victims and the economy particularly affecting the poor people.

The fatality index in Bangladesh is nearly 70 percent, which is one of the highest among the developing countries. The fatality index depends crucially on accurate reporting of deaths and injuries, but can also be influenced by medical facilities. This signifies probably two important characteristics, viz. the wide spread under reporting of injuries and less serious accidents and the lower level of emergency medical services. In Bangladesh, there is little scope to provide the prompt and necessary medical attention to injured people, particularly soon after an accident. In passing, it should be noted that about 50 percent of road traffic deaths happen within 15 minutes of the accident as a result of injuries to the brain, heart and large blood vessels. A further 35 percent die in the next 1-2 hours of head and chest injuries and 15 percent over the next 30 days from sepsis and organ failure. The time between injury and initial stabilization is the single most important factor in patient survival, with the first 30-60 minutes being the most important. Thus prompt emergency assistance and efficient trauma care are clearly important in minimizing the road accident deaths.

Orthopedic hospital reports show that around 56 percent of total patients in the intensive care units are victims of road traffic accidents. Moreover, almost 30 percent of hospital beds are occupied by patients injured by road traffic accidents. During seven days of Eid vacation in October, 2007 a total 668 patients were admitted in the emergency section in Orthopedic hospital. Of these patients 220 (33 percent) were injured from road traffic accidents.

3. ROAD TRAFFIC ACCIDENT SCENERIO IN URBAN AREAS OF BANGLADESH

During eight years period, from 1998 to 2006, at least 11459 accidents occurred in urban areas contributing 35 percent of total accidents occurred within this country. More than 8250 fatalities and almost 6700 injuries occurred in these accidents which represent around 28 percent of the total casualties (MAAP 5). Some striking road accident characteristics in urban areas are briefly discussed in the following sections.

3.1 Pedestrians-the most vulnerable road user group

In Bangladesh, with a low level of motorization, the role of walk mode is quite significant. Pedestrians have received far less attention than vehicular traffic. Up to 70 percent of urban road accident deaths are pedestrians alone. Their involvement varied between 43 and 73 percent of the road accident fatalities in the medium sized cities. Pedestrians accounted for 53 percent of all reported fatalities in the accident database in urban areas (Figure 2).

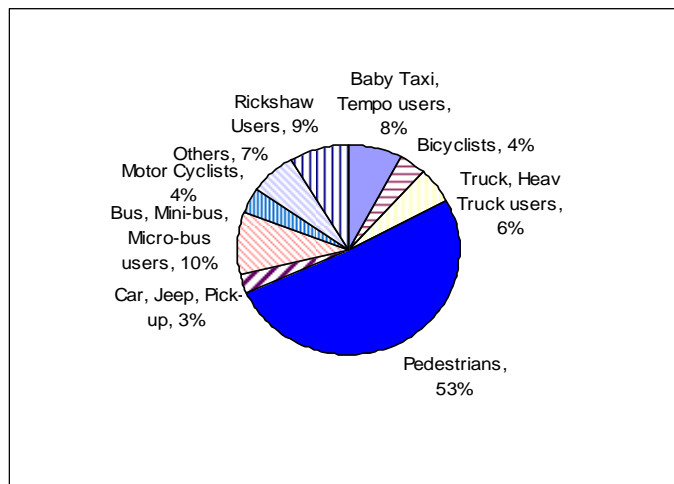


Figure 2: Distribution of road fatalities in urban areas of Bangladesh



Figure 3: Pedestrians-the most vulnerable road user

3.2 Predominant accident types

Event specified accident type analysis showed ‘hit pedestrian’ as the dominant accident type in urban areas, 62 percent involvement in fatal accidents. Other common accident types are: rear end collision (15%) and head on collision (8%). These three accident types account for nearly 85 percent of the fatal accidents.

3.3 Accidents at intersections

A large number of accidents occur at intersections. These intersection locations often become accident black spots. Analysis showed that 31 percent road accidents occur at intersections in urban areas. Of these intersection accidents 72 percent occurred in Dhaka. In the analysis, a site experiencing a total number of 10 or more accidents of all severities during the study period (1998-2003) was classified as hazardous. A total of 313 intersections (with 2040 accidents) were found where at least one accident took place during 1998 and 2003. Out of these 313 intersections, 54 intersections were identified having 10 or more accidents. These 54 intersections accounted for nearly 79 percent of all intersection accidents and almost 78 percent of total pedestrian accidents at intersections.



Figure 4: Unregulated pedestrian movements and High intensity pedestrian flow at a major intersection in Dhaka

3.4 Over involvement of trucks and buses

Studies of road accidents revealed that heavy vehicles such as trucks and buses including minibuses are major contributors to road accidents. This group of vehicles is particularly over involved in pedestrian accidents accounting for about 65 percent (trucks 28%, buses 22% and minibuses 15%).

3.5 Involvement of children in road accidents

The national road accidents statistics in Bangladesh revealed a serious threat to the children. The incidence of overall child involvement in road accident fatalities in Bangladesh is found to be very high, accounting for about 22 percent. In urban areas, the proportion is about 12 percent. This involvement of children under 15 years of age in road accident fatalities is much higher than those in other developing countries.

3.6 Accident factors

The principal contributing factors of accidents are adverse roadway roadside environment, poor detailed design of junctions and road sections, excessive speeding, overloading, dangerous overtaking, reckless driving, carelessness of road users, failure to obey mandatory traffic regulations, variety of vehicle characteristics and defects in vehicles such as worn out tyres, loose wheels, overloaded axle, faulty brake and indicator lighting system etc. and conflicting use of roads. Incompetent drivers and driving with open and widespread use of fake licenses appear to be a major concern to safety on our roads. Others include a low level of awareness of the safety problems, inadequate and unsatisfactory education, safety rules and regulations and traffic law enforcement and sanctions.

4. SOME STRATEGIES FOR SAFETY IMPROVEMENT IN URBAN AREAS

Considerable safety improvements can be made through road safety engineering strategies. Strategies for reducing and preventing road traffic accidents and injuries are many and varied. More common strategies are exposure control (restrict certain travel and deny access to hazardous situation), accident prevention (design, construction and maintenance of vehicles and road system), behavior modification (road user education, the law and its enforcement and sanctions), injury control (vehicle design, road side hazard management) and post-injury management (recovery, treatment and rehabilitation measures). All of those strategies played a major part in achieving greater safety on the road network. For the future, it is important to maintain the impetus in such strategies by the introduction of newly developed measures, approaches as well as technologies.

With particular regard to urban road safety in developing countries, Bangladesh, in particular, pedestrian vehicle conflicts are clearly the

greatest problem with significant involvement of trucks and buses. There is specific need and much scope for road environment improvements aimed at correcting the most common deficiencies through wider application of traffic engineering approaches. It is argued that priorities be placed on the principles like traffic segregation to provide facilities and road space for the most vulnerable users particularly pedestrians and non-motorised vehicles, force correct road user behaviour (self enforcing measures) via channelisation, speed reduction measures etc. With resource constraints the greater emphasis should be placed on low cost improvement schemes. Implementation of such measures should take place at hazardous road locations (accident blackspots) identified by systematic accident investigation (rather than in an ad-hoc manner). To promote enhanced road safety, developing countries like Bangladesh should have programs to implement well known engineering measures, leading to larger and longer lasting effects at fewer expenses, widely and systematically. Importantly systematic application of road safety audit- a powerful tool for accident prevention is considered to be extremely useful and effective in alleviating the deteriorated safety situation.

4.1 New innovative high-tech solution options

Improved and innovative solutions are vital to reduce road traffic accidents and casualties. Such as safety barriers and crash cushioning (energy absorption system) at increased impact speeds are highly effective in saving lives. Improved road markings could guide motorists and reduce casualties. Advanced road side management system (fixed objects, trees, poles etc.) and high-tech solutions such as Intelligent Transport System (ITS) can reduce overall hazards by a big margin. The ITS is intended for advances in navigation systems, assistance for safe driving, optimization of traffic management and increasing efficiency in road management by building an integrated system of people, roads and vehicles utilizing advanced data communication technologies. While providing users with quick information required for their safe and comfortable travel in ways easy to understand, ITS makes it possible for users to enjoy a high level transportation system and thus reduce much of the workload commonly associate with driving and thereby accomplish a major improvement in road transport safety. A recent study on ITS application for Bangladesh revealed that with 100 percent deployment of ITS technology, the fatal and injury related accidents could be reduced as much as 26 percent and 30 percent respectively (Hoque 2001).

5. CONCLUDING COMMENTS

With the recurrent losses of lives and properties, road traffic accidents have loomed as a serious and growing problem in urban areas of Bangladesh. The road safety situation is very severe by international standards as well. The global forecast has indicated that over the next 10 years developing countries like Bangladesh will experience the alarming increase in urban road accidents and casualties. This paper has highlighted the scale and

characteristics of the road safety problem in urban areas in Bangladesh. It also discusses the strategies for improving safety. There is urgent need and scope for improving the road safety situation by implementing an effective and coordinated safety policy and actions which require significant improvements in the relevant sectors. Intensified efforts are needed to bring about changes in the attitudes of road users including drivers towards safe operations. The opportunities and need for road environmental and engineering improvements by incorporation of new approaches and methods are particularly discussed in the paper.

REFERENCES

Hoque, M. M. Ahsan, HM, & McDonald, M., 1997, *Traffic Congestion and Safety : Some Contemporary Issues and Options in Bangladesh*, ASCE Conference on Traffic Congestion and Traffic Safety in the 21st Century, Chicago, Illinois, USA, June 8-11, 1997.

Hoque, M. M., McDonald, M. & Hall, RD., 1998, *Relevance and introduction of road safety audit in developing countries*, First AUSTROADS International Road Safety Audit Forum, Melbourne 11-12 May 1998

Hoque, M. M., 2001, *Road Safety Improvements in Developing Countries: Priority Issues and options*, Proceedings of 20th Australian Road Research Board (ARRB) Conference.

Hoque, M.M., 2004, Editor of Booklet *Understanding Road Safety*, Published by Accident Research Centre (ARC), Bangladesh University of Engineering and Technology (BUET), Dhaka-1000, Bangladesh, July 2004

Hoque, M.M., 2005, *Road Safety Problems and Priorities in Bangladesh*, Publication on the eve of establishment day of Highway Police, Dhaka, 11 June, 2005.

Hoque, M.M. (edited), 2006, *Road Safety in Developing Countries*, Proceedings of International Conference on Road Safety in Developing Countries, BUET, Dhaka, 22-24 August, 2006.

Mahmud, S. M. S., Rahman M. F., Hoque, M. M., Hoque, S., *A Preliminary Comparison of Road Safety Situation in Selected Countries*, Proceedings of International Conference on Road Safety in Developing Countries, BUET, Dhaka, 22-24 August, 2006.

Report and Workshop Paper on 'On Improving Road Safety on the Asian Highway', UNESCAP (United Nations Economic and Social Commission for Asia and the Pacific) Publication, June, 2007

World Report on Road Traffic Injury Prevention, World Health Organization (WHO) Publication, 2004

Authors' Index

AUTHORS' INDEX

A		H	
Ansary, Mehedi Ansary	79, 103, 113, 191, 231, 265, 287, 529, 541, 555	Hug, Mohammad Sajedul	103
Anam, Iftekhar	91	Haque, Md. Nafiul	103
Ahmad, Monsur	183	Hossain, Muhammad Shahadat	147
Akand, Md. Shah Aziz	243	Horri, Toshiyuki	173
Anam, Iftekhar	243	Henry, Michael	201
Ahsan, Raquib	265, 275	Hossain, Tahsin R.	287
Ahmed, Syed Ishtiaq	307	Hossain, Md. Raquibul	307
Amin, Md. Sohel Reza	397	Hsu, Kai-Lin	333
Ahmad, Rais	473	Huang, Hong	343, 441
Ahmed, M. Zakaria	473	Hussain, Mohammad Asad	357
Amano, R	483	Hossain, Md. Motaher	357
Abe, Mariko	521	Herath, Srikantha	367
Akther, M. S.	541, 555	Hayami, H.	441
Ahmed, Wahida Bashar	579	Hayashi, Shogo	483
Ahmed, Murshed	591	Hoque, Md. Mazharul	607
Anowar, Sabreena	607, 653	Hung, Armana Sabiha	607
Anjuman, Tahera	653	Hanoka, Shinya	631
		Hossain, Md. Zakir	653
		Hassanat-E-Rabbi, Shahnewaz	653
B		I	
Byun, Keun Joo		Ishihara, Kenji	11
Begum, Mahbuba	127	Imtiaz, A. B. Afifa	79, 191
		Iwanami, Mitsuyasu	211, 221
C		Islam, Md. Shahabul	375
Choi, Ho	253	Ishikawa, Yuji	453
Chang, Tai-Ping	311	Izumi, Kimihiko	453
		Islam, M. Kabirul	473
D		Islam, Muhammad Ashikul	643
Dhar, Ashutosh Sutra	79, 191		
Das, Rubel	183, 417	J	
Deng, Zhihua	343	Joshi, Ranjeet	161
Dutta, Dushmanta	385	Johansen, Jorgen	275
		Johan, Israt	529
E		K	
Endo, Takahiro	409	Katayama, Tsuneo	1
Eicker, Ursula	425	Kanok-Nukulchai, Worsak	41
Ebi, Takeyuki	483	Khan, Aftab Alam	147
		Kumar, Ramancharla Pradeep	161
F		Kuwano, Reiko	173
Fujita, Kazuhisa	483	Kohashi, Hidetoshi	173
		Kato, Yoshitaka	201
G			
Grzmil, Toby			
Guragain, Ramesh	461		

K		R	
Kato, Ema	211, 221	Roy, Himadree	91
Kanada, Hisashi	231	Rizvi, Mohammad Salahuddin	103
Konagai, Kazuo	275	Rahman, Syed Zillur	231
Kato, Shinsuke	343	Reza, Samy Muhammad	265
Kawasaki, Akiyuki	367	Rahman, Md. Musur	357
Khiem, M. V.	441	Rahman, Md. Mafizur	375
Kunda, Tribikram	473	Rahman, MA	573
Kabir, Md. Aynual	509	Rahman, Md. Mizanur	643
Kuwahara, Masao	621	Rizvi, Md. Kamrul Hasan	643
L		S	
Liu, Naian	343	Shamim, Mahfuza	79
Leopairojna, Supaporn Kaewko	631	Sadat, Mohammad Rafat	103
M		Saha, Rajan	113, 231
Meguro, Kimiro	61, 139, 231, 297, 367, 461, 483,521	Sutradhar, Ashutosh	113
Murao, Osamu	67	Siddiqui, Md. Ziya Ur Rahman	161
Miyamoto, Atsushi	67	Siddiquee, Md. Zahid Hasan	183, 417, 425
Mayorca, Paola	297, 461	Shimomura, Takumi	221
Miyazaki, Sanae	453	Siddiquee, Mohammed Saiful Alam	307
Maniruzzaman, KM	573	Sarker, Maminul Haque	357
Mahmud, S M Sohel	607	Schroder, Dietrich	425
N		Sasaki, Eiichi	453
Noor, Munaz A.	231, 287, 499	Shah, Md. Faiz	585
Nakano, Yoshiaki	253	Siddiquii, Chowdhury Kawsar Arefin	653
Navaratnaraj, Sathiparan	461	T	
Newaz, Kazi Md. Shifun	607	Tsukamoto, Yoshimichi	11
Nag, Dilip		Takashima, Masasuke	61
Nam, Jin-Won		Tanaka, Hidetaki	275
Nakano, Yoshiaki		Tamima, Umma	397
O		Takeuchi, Wataru	435
Ooka, Ryoza	343, 441	Tanaka, Shinji	621
Okubo, Takahide	453	U	
P		Uomoto, Taketo	51, 231
Prathuchai, Kul	375	Uddin, M. Moslam	287
Phonekeo, Vibarad	435	Uddin, Mohammad Nazim	357
Q		Uematsu, Kouji	483
Quader, Mohammad Abdul	417		

W

Wenguo, Weng 321
Worakanchana, Kawin 435, 461

Y

Yasuoka, Yoshifumi 409, 435
Yokota, Hiroshi 211, 221
Yamaji, Toru 211
Yoshimura, Miho 139, 231
Yasin, M. 499

Z

Zobair, Mohammad
Zhang, Linhe